frontiers | Research Topics

Case reports in pediatric cardiology 2022

Edited by
Alvise Guariento, Estela Azeka, Cecile Tissot, Utpal S. Bhalala and Elena Cervi

Published in
Frontiers in Cardiovascular Medicine
Frontiers in Pediatrics

ISSN 1664-8714
ISBN 978-2-8325-3812-8
DOI 10.3389/978-2-8325-3812-8

About Frontiers

Frontiers is more than just an open access publisher of scholarly articles: it is a pioneering approach to the world of academia, radically improving the way scholarly research is managed. The grand vision of Frontiers is a world where all people have an equal opportunity to seek, share and generate knowledge. Frontiers provides immediate and permanent online open access to all its publications, but this alone is not enough to realize our grand goals.

Frontiers journal series

The Frontiers journal series is a multi-tier and interdisciplinary set of open-access, online journals, promising a paradigm shift from the current review, selection and dissemination processes in academic publishing. All Frontiers journals are driven by researchers for researchers; therefore, they constitute a service to the scholarly community. At the same time, the *Frontiers journal series* operates on a revolutionary invention, the tiered publishing system, initially addressing specific communities of scholars, and gradually climbing up to broader public understanding, thus serving the interests of the lay society, too.

Dedication to quality

Each Frontiers article is a landmark of the highest quality, thanks to genuinely collaborative interactions between authors and review editors, who include some of the world's best academicians. Research must be certified by peers before entering a stream of knowledge that may eventually reach the public - and shape society; therefore, Frontiers only applies the most rigorous and unbiased reviews. Frontiers revolutionizes research publishing by freely delivering the most outstanding research, evaluated with no bias from both the academic and social point of view. By applying the most advanced information technologies, Frontiers is catapulting scholarly publishing into a new generation.

What are Frontiers Research Topics?

Frontiers Research Topics are very popular trademarks of the *Frontiers journals series*: they are collections of at least ten articles, all centered on a particular subject. With their unique mix of varied contributions from Original Research to Review Articles, Frontiers Research Topics unify the most influential researchers, the latest key findings and historical advances in a hot research area.

Find out more on how to host your own Frontiers Research Topic or contribute to one as an author by contacting the Frontiers editorial office: frontiersin.org/about/contact

Case reports in pediatric cardiology: 2022

Topic editors

Alvise Guariento — University of Toronto, Canada
Estela Azeka — University of São Paulo, Brazil
Cecile Tissot — Clinique des Grangettes, Switzerland
Utpal S. Bhalala — Driscoll Children's Hospital, United States
Elena Cervi — Great Ormond Street Hospital for Children NHS Foundation Trust, United Kingdom

Citation

Guariento, A., Azeka, E., Tissot, C., Bhalala, U. S., Cervi, E., eds. (2023). *Case reports in pediatric cardiology: 2022*. Lausanne: Frontiers Media SA. doi: 10.3389/978-2-8325-3812-8

Table of contents

frontiers | Frontiers in Pediatrics

TYPE Editorial
PUBLISHED 13 October 2023
DOI 10.3389/fped.2023.1298526

OPEN ACCESS

EDITED AND REVIEWED BY
Ruth Heying,
University Hospital Leuven, Belgium

*CORRESPONDENCE
Alvise Guariento
✉ alvise.guariento@unipd.it

RECEIVED 21 September 2023
ACCEPTED 29 September 2023
PUBLISHED 13 October 2023

CITATION
Guariento A, Bertelli F and Vida VL (2023) Editorial: Case reports in pediatric cardiology 2022.
Front. Pediatr. 11:1298526.
doi: 10.3389/fped.2023.1298526

Editorial: Case reports in pediatric cardiology 2022

Alvise Guariento*, Francesco Bertelli and Vladimiro L. Vida

Pediatric Cardiac Surgery, Department of Cardiac, Thoracic, Vascular Sciences and Public Health, University of Padua, Padua, Italy

KEYWORDS

pediatric cardiology, congenital heart disease, editorial, research topic, congenital cardiac surgery

Editorial on the Research Topic
Case reports in pediatric cardiology 2022

Pediatric cardiology stands as a distinctive subset within the field of cardiology, which typically brings to mind cardiovascular issues prevalent among older individuals. Yet, the truth is that the heart is an incredibly resilient organ, capable of allowing years of relatively symptom-free survival even when significantly damaged. Regrettably, children can and do encounter cardiovascular problems, although their occurrence remains considerably lower compared to the adult population. This reality carries numerous implications. Firstly, due to social and economic factors, scientific and clinical research predominantly focuses on diseases with higher prevalence. Consequently, pediatric cardiology remains, and likely always will be, an area of study that receives less attention. Secondly, as children grow and naturally outgrow surgically implanted prosthetic devices or tissues, this presents unique challenges in their treatment.

One of the most captivating facets of pediatric cardiology lies in its close connection to the intriguing realm of congenital heart disease (CHD). This umbrella term encompasses structural or functional abnormalities of the heart or major blood vessels that originate before birth. While most CHD occur independently of other diseases, severe and complex forms often coexist with additional medical conditions.

It is essential to acknowledge how CHD can sometimes manifest in unconventional ways, resembling conditions such as ischemic heart disease. A noteworthy example is a case reported by Fallah et al. involving a 2-year-old child with left main coronary artery atresia. This child exhibited classical features of ischemic heart failure, including failure to thrive, a significantly dilated left ventricle, an ejection fraction of 20%–25%, and severe functional mitral regurgitation. The diagnosis was initially suspected due to cardiac magnetic resonance findings, which indicated ischemic heart disease through extensive scarring of the left ventricle.

Another intriguing case is presented by Wu et al. involving a term female newborn who presented with congestive heart failure and a grade 4/6 continuous heart murmur in the left upper sternal border. This child was diagnosed with a giant fistula between the right coronary artery and the right ventricle, with an orifice of approximately 2 mm. What makes this case remarkable is the successful percutaneous closure of the fistula using an Amplatzer Duct Occluder II, originally designed for patent ductus arteriosus (PDA) closure. This was possible due to the severe aneurysmatic dilatation of the proximal right coronary artery, which could accommodate both the guidewire and the device itself.

In some instances, coronary artery anomalies can be challenging to diagnose, as demonstrated in the case reported by Hu et al. In this case, a seven-year-old male child experienced sudden, sharp chest pain and syncope during high-intensity exercise. While cardiac ultrasound initially showed a normal right coronary artery, the left coronary artery exhibited non-continuous blood flow, raising suspicion of a coronary artery anomaly. Subsequent electrocardiogram (EKG)-gated computed tomography (CT) angiography revealed an abnormal origin of the left coronary artery from the upper portion of the non-coronary sinus, with a lengthy stenotic intra-mural course. This case highlights the importance of advanced imaging when there is a high clinical suspicion of a coronary artery anomaly.

Anomalous aortic origin of a coronary artery (AAOCA) is a prevalent congenital coronary artery anomaly that can lead to syncope in children. In fact, AAOCA is the second most common cause of sudden cardiac death in young athletes (1), as reported by Gao et al. in a case series of pediatric patients admitted to their hospital due to syncope. Namely, the stories of a total of eight patients with an average age of 12.5 years were described. However, not all cardiovascular problems in children are congenital; various other causes, including trauma, are possible, as documented by Ai et al. Their case involved an eight-month-old female child who underwent elective corrective surgery for Tetralogy of Fallot but experienced a life-threatening right coronary artery rupture as a result of cardiopulmonary resuscitation (CPR). This case highlights that coronary artery rupture can occur as a complication of CPR, an occurrence documented in limited literature.

While pediatric cardiologists predominantly focus on CHD, acquired cardiovascular issues commonly seen in adults can also affect previously healthy children. This includes both common conditions like myocarditis and acute myocardial ischemia, as well as exceptionally rare conditions such as pulmonary artery dissection (PAD). Most cases of PAD arise due to medial degeneration, characterized by the fragmentation of elastic fibers and the widespread enlargement of pulmonary arterial branches, typically resulting from chronic pulmonary hypertension. However, Ren et al. reported two infant patients with PAD who lacked pulmonary hypertension and underlying medical conditions. Notably, these patients presented with recurrent pneumonias, lacking the typical symptoms of chest pain and hemoptysis seen in adults.

While many CHDs lack a clearly defined genetic basis, some genetic diseases directly or indirectly affect cardiovascular and pulmonary physiology. Lin et al. reported the case of a newborn boy who suffered from severe dyspnea, extreme anemia, skin pallor, and hypoxemia due to severe pulmonary hypertension. Whole-exome sequencing revealed a novel compound heterozygous mutation in the gene encoding the Pyruvate Kinase enzyme, leading to a diagnosis of pyruvate kinase deficiency (PKD). Treatment of the underlying condition also resolved the pulmonary hypertension, highlighting the importance of precise diagnosis, even when a genetic component may not be immediately apparent.

Liu et al. described the case of a 21-year-old man diagnosed with arrhythmic-dilated cardiomyopathy secondary to Duchenne muscular dystrophy, primarily treated with steroids. This case underscores the significance of cardiological follow-up in all patients at risk of developing heart problems, even if such cases are rare. Another example comes from Feng et al. who reported the case of a 17-year-old girl with Axenfeld-Rieger syndrome (ARS), an autosomal dominant disorder linked to disruption of the development of neural crest cells. While cardiac defects associated with ARS have been reported, this patient presented with a range of cardiac malformations not previously described. This suggests the need for echocardiography in patients with characteristic clinical manifestations of ARS or specific genetic alterations.

Generalized arterial calcification of infancy (GACI) is an autosomal recessive condition characterized by extensive calcification and intimal proliferation of the large and medium arteries, including the aorta, coronary arteries, and renal arteries (2). This leads to vascular stenosis and a range of complications, such as severe systemic hypertension and heart failure. Făgărăşan et al. presented a case of successful surgical treatment of severe aortic arch obstruction caused by calcified plaques mimicking severe coarctation of the aorta. Additionally, Lu et al. reported a case of GACI in an 8-month-old boy who presented with hypertension, hypertrophic cardiomyopathy, and heart failure, ultimately leading to his demise before bisphosphonate treatment could be initiated.

Mitochondrial diseases (MDs) are exceedingly rare (3), characterized by oxidative phosphorylation dysfunction due to nuclear and/or mitochondrial DNA variations (4). Wang et al. described the case of an 8-month-old male with MD, initially presenting with severe lactic acidemia and respiratory distress, along with echocardiographic features suggesting hypertrophic cardiomyopathy. The importance of this case lies in the correlation between MD and cardiac manifestations, highlighting the need for a comprehensive investigation in such patients.

Chromosomal defects, particularly Turner syndrome, are strongly associated with CHDs. Lin et al. reported a case involving a patient with Turner syndrome who had severe aortic coarctation. They successfully deployed a Cheatam-Platinum stent to address this condition, offering an alternative treatment method.

The integrity and configuration of vascular stents can easily be compromised with aggressive manipulation, making percutaneous interventions more challenging and technically intricate. Currently, there are no established protocols for reclaiming embolized strutted stents through percutaneous means. Prakoso et al. recounted their experience in retrieving a strutted stent from the abdominal inferior vena cava of a three-month-old boy scheduled for femoral transvenous ductal stenting (DS). Due to complex angulation, inserting the stent into the PDA proved technically unfeasible. However, they successfully recaptured the stent using a gooseneck snare through a right atrial appendage (RAA) hybrid access, all without the need for cardiopulmonary bypass support.

Patients with Fontan circulation present distinct challenges related to their cardiopulmonary function. As a result, ongoing research seeks to determine whether COVID-19 poses an increased risk to this specific population. Wen et al. detailed the case of a nine-year-old male child who underwent Fontan palliation and later contracted COVID-19 during the pandemic. This case prompted investigations into the unique therapeutic needs of Fontan patients. While complications were not uncommon in this population, thrombotic complications were the most frequent. However, these complications did not appear to be specific to Fontan circulation, and most patients ultimately improved and fully recovered. Notably, worse physiological conditions like cyanosis and pulmonary hypertension were associated with higher mortality rates.

At the outset of the COVID-19 outbreak, children were minimally affected, accounting for only 1.7% of cases and often presenting as asymptomatic carriers. Nevertheless, as the pandemic progressed, a growing number of children exposed to the virus developed Multisystem Inflammatory Syndrome in Children (MIS-C). Di Filippo et al. provided an extensive case series shedding light on cardiac manifestations observed during COVID-19 in children and highlighting the significance of elevated troponin levels. Among their cases, 13.6% exhibited various forms of cardiac involvement, and 9.6% showed elevated troponin levels. Given the ongoing COVID-19 pandemic that has persisted in recent years and the widespread vaccination efforts, it is unsurprising that adverse reactions to vaccination, even in children, have been reported. The use of COVID-19 vaccines is now recommended for the pediatric population. Lu et al. presented a noteworthy case series detailing their experience with adverse reactions to the hepatitis B vaccine, aiming to provide insights into the general mechanisms underlying vaccine adverse reactions. Of the adverse events documented, three were cases of myocarditis, two were meningitis, and two were interstitial pneumonia. A similar case of adverse reaction to an RNA COVID-19 vaccine in a pediatric patient was described by Han et al. They presented the medical history of a 17-year-old female patient who experienced chest pain and syncope following her initial dose of the messenger RNA COVID-19 vaccine. Subsequent cardiac magnetic resonance imaging confirmed the diagnosis of myocarditis based on established criteria.

Dilated cardiomyopathy (DCM) stands as one of the primary causes of heart failure in children, with heart failure often being the initial presentation, though clinical manifestations can vary. Wang et al. reported the first documented case of marked right atrial (RA) enlargement as the initial presentation of DCM. Genetic analysis revealed a heterozygous mutation associated with cardiomyopathies. Further sequencing identified the same variant in Pkp2 in the patient's asymptomatic mother, whose echocardiography showed an enlarged left atrium (LA) and left ventricle (LV), mild to moderate mitral regurgitation, and a reduced left ventricular ejection fraction (LVEF) of 48%. Thus, she was also diagnosed with DCM, establishing a familial DCM diagnosis based on the patient's and mother's features.

Zhang et al. presented another unique case: the first instance of fetal non-compaction cardiomyopathy occurring simultaneously in both ventricles, coupled with the identification of a mutation in the calmodulin gene (CALM2). Prenatal echocardiography initially detected biventricular non-compaction cardiomyopathy alongside sinus bradycardia. Following the termination of the pregnancy, autopsy and histopathological examination confirmed the diagnosis of fetal biventricular non-compaction cardiomyopathy.

Torsades de pointes (Tdp) represents a life-threatening ventricular tachyarrhythmia characterized by a constantly shifting QRS complex morphology, twisting the electrical axis around the isoelectric line. Wang et al. conducted a study to document the diagnosis and management of a rare case involving frequent Tdp in a child with a novel genetic mutation. The patient was successfully treated with a cardioverter-defibrillator (ICD) implantation and optimization of antiarrhythmic therapy.

Atrial tachycardia (AT) originating from the atrial appendage (AA) is clinically characterized by palpitations, chest discomfort, dyspnea, and other nonspecific symptoms. In children, AT originating from the AA accounts for approximately 30%–50% of AT cases, a higher incidence than in adults (5). Liu et al. reported three cases of AT originating from the AA, treated with a combination of three-dimensional electroanatomic mapping and ablation, and surgical atrial appendage resection performed in conjunction with cardiac surgery. Atrial fibrillation (AF) is an uncommon occurrence among children, especially in the absence of underlying congenital heart disease (6). Pediatric epidemiological data on AF are limited, often relying on findings from studies conducted in the adult population. When AF is diagnosed in a young patient with a structurally normal heart, a comprehensive investigation into its underlying cause becomes essential. Hubrechts et al. presented a rare and potentially life-threatening origin of AF: intrathoracic non-Hodgkin lymphoma with cardiac involvement, as revealed by cardiac magnetic resonance imaging (CMR). This represents the first documented pediatric case attributing new-onset AF to neoplastic infiltration of the left atrial wall.

Catecholamine-induced cardiomyopathy is a rare and challenging complication associated with phaeochromocytoma-paraganglioma, more commonly observed in pheochromocytoma but less common in neuroblastoma (NB). Xu et al. presented the case of a 5-year-old girl with NB who developed catecholamine cardiomyopathy, specifically hypertrophic cardiomyopathy (HCM), leading to ventricular hypertrophy, hypertension, and heart failure. Surgical removal of the tumor resulted in the normalization of blood pressure and urinary catecholamine levels. A 7-month follow-up revealed the resolution of ventricular hypertrophy and the restoration of normal ventricular function.

Restrictive cardiomyopathy (RCM) represents the least common phenotype among pediatric heart muscle diseases, accounting for approximately 5% of all diagnosed cardiomyopathies, and is associated with a poor prognosis in children (7). Ji et al. reported a case of RCM that initially manifested with ventricular fibrillation in a 7-year-old boy who was successfully resuscitated by an automated external defibrillator (AED) outside the hospital. At present, the boy is being treated with oral diuretics and metoprolol tartrate tablets,

as his parents declined an ICD implantation, and he is undergoing outpatient follow-up.

Heart–lung transplantation (HLT) remains the sole viable treatment for certain advanced cardiopulmonary diseases. However, the scarcity of donors, the necessity for intricate surgical coordination, and the demanding post-operative care limit the number of such procedures performed in children worldwide. Post-transplantation challenges persist, including rejection, infections, renal issues, tumors, and other complications that can adversely impact patients' quality of life. Zhuang et al. documented a case of cerebral aspergillosis in a 10-year-old child that developed three months after HLT. Fortunately, the patient responded well to treatment, and there were no recurrences of the disease during the 3-year follow-up period.

Idiopathic pulmonary arterial hypertension (PAH) is a rare and progressively debilitating condition affecting the pulmonary arteries. Epoprostenol, a synthetic prostaglandin analog, stands out as the most potent pharmaceutical option for treating PAH. Chida-Nagai et al. shared their experience with an adolescent female patient who successfully transitioned from continuous intravenous epoprostenol therapy to gradual oral selexipag administration over an extended period. Encouragingly, this shift proved effective, suggesting that oral selexipag can offer comparable efficacy to epoprostenol, especially for managing PAH in young patients.

Lian et al. presented a case involving an eight-year-old child with an exceedingly rare combination of right aortic arch, right patent ductus arteriosus (PDA), and right tracheal bronchus, a condition known since birth. Interestingly, the patient later developed symptoms of airway compression, prompting surgical intervention involving the ligation and division of the PDA through a standard midline sternotomy. This case is remarkable not only for its unprecedented combination but also because the patient remained asymptomatic for many years despite the congenital anomaly being known since birth.

Hypoplastic left heart complex (HLHC), which also encompasses Shone's syndrome, constitutes a rare congenital heart disease (CHD) characterized by severe obstructive lesions in the left-sided inflow and outflow tracts (8). While supramitral fibroelastic membranes contributing to mitral valve (MV) obstruction are common in this disease entity, left ventricular endocardial fibroelastosis (EFE) has not typically been considered a major factor in Shone's variant HLHC. Diaz-Gil et al. provided the first description of active clinical manifestation of EFE and remodeling of the endocardium through endothelial-to-mesenchymal transformation (EndMT) in an adolescent with Shone's variant HLHC and a genetic heterozygous ABL1 variant. This case highlights the need for novel therapeutic approaches for EFE, potentially focusing on molecular factors influenced by intrinsic and extrinsic stimuli of EndMT.

Surgery is the standard approach to correct ventricular septal defects (VSDs), especially in complex cases involving individuals with pulmonary hypertension and multiple defects. In recent years, transcatheter percutaneous closure has gained favor, particularly for muscular VSDs located in challenging surgical sites. However, repairing multiple defects often involves using multiple devices and typically relies on fluoroscopy guidance (9). Siagian et al. detailed their experience with the closure of multiple VSDs using a single device and a zero-fluoroscopy technique in a 7-year-old patient who had experienced shortness of breath for a year prior to admission. They employed a jugular vein approach to successfully perform percutaneous transcatheter VSD closure. Remarkably, 1.5 years after the procedure, any visible signs of pulmonary hypertension had resolved, leading to the discontinuation of pulmonary artery dilator treatment.

In conclusion, it is crucial to raise awareness of pediatric cardiology among healthcare professionals, and the objective of these case series is precisely that. Through the sharing of a collection of rare case reports, we aimed to foster an understanding of the various conditions' potential manifestations and their corresponding treatments. This knowledge can significantly enhance clinical practices, diagnostics, and therapeutic interventions.

Author contributions

AG: Writing – review & editing. FB: Writing – original draft. VV: Writing – review & editing.

Conflict of interest

The authors declare that the research was conducted in the absence of any commercial or financial relationships that could be construed as a potential conflict of interest.

Publisher's note

References

1. Basso C, Maron BJ, Corrado D, Thiene G. Clinical profile of congenital coronary artery anomalies with origin from the wrong aortic sinus leading to sudden death in young competitive athletes. *J Am Coll Cardiol.* (2000) 35(6):1493–501. doi: 10.1016/S0735-1097(00)00566-0

2. Mulcahy CH, Mone F, McAuliffe FM, Mooney E, McParland P, Mc Mahon CJ. Antenatal diagnosis of idiopathic infantile arterial calcification (IIAC): a single centre experience and review of the literature. *J Congenit Cardiol*. (2019) 3(1):1. doi: 10.1186/s40949-018-0022-1

3. Mazzaccara C, Mirra B, Barretta F, Caiazza M, Lombardo B, Scudiero O, et al. Molecular epidemiology of mitochondrial cardiomyopathy: a search among mitochondrial and nuclear genes. *Int J Mol Sci*. (2021) 22(11):5742. doi: 10.3390/ijms22115742

4. Meyers DE, Basha HI, Koenig MK. Mitochondrial cardiomyopathy: pathophysiology, diagnosis, and management. *Texas Hear Inst J*. (2013) 40(4):385–94.

5. Martin CA, Lambiase PD. Pathophysiology, diagnosis and treatment of tachycardiomyopathy. *Heart*. (2017) 103(19):1543–52. doi: 10.1136/heartjnl-2016-310391

6. Kopecky SL, Gersh BJ, McGoon MD, Whisnant JP, Holmes DR, Ilstrup DM, et al. The natural history of lone atrial fibrillation. *N Engl J Med*. (1987) 317(11):669–74. doi: 10.1056/NEJM198709103171104

7. Ditaranto R, Caponetti AG, Ferrara V, Parisi V, Minnucci M, Chiti C, et al. Pediatric restrictive cardiomyopathies. *Front Pediatr*. (2022) 9:745365. doi: 10.3389/fped.2021.745365

8. Shone JD, Sellers RD, Anderson RC, Adams P Jr., Lillehei CW, Edwards JE. The developmental complex of "parachute mitral valve," supravalvular ring of left atrium, subaortic stenosis, and coarctation of aorta. *Am J Cardiol*. (1963) 11(6):714–25. doi: 10.1016/0002-9149(63)90098-5

9. Felice H, Chandran S, Bhamra-Ariza P, Brecker S. Transcatheter closure of multiple defects of the atrial septum: technique and follow-up. *Int J Clin Med*. (2015) 06(09):591–6. doi: 10.4236/ijcm.2015.69079

frontiers in Cardiovascular Medicine

CASE REPORT
published: 25 March 2022
doi: 10.3389/fcvm.2022.872049

Case Report: Two Cases of Pulmonary Artery Dissection in Young Infants

*Chunnian Ren, Libing Zhang, Huan Yan and Zhengbing Yang**

Department of Cardiothoracic Surgery, School of Medicine, Chengdu Women's and Children's Central Hospital, University of Electronic Science and Technology of China, Chengdu, China

Pulmonary artery dissection (PAD) is a rare disease. This article reports the treatment of PAD in young infants for the first time. Both cases of the infants were treated with surgery. Different surgical methods achieve different results, which provide ideas for treating PAD in young infants.

Keywords: pulmonary artery dissection, young infants, treatment, surgery, case report

INTRODUCTION

Helmbrecht et al. was the first to report a case of pulmonary artery dissection (PAD) in 1842 (1). A recent literature review reported 150 cases of patients with PAD (1), but all were concentrated on adults. Here, we report two cases of young infants diagnosed with PAD. Surgical treatment was performed concurrently, and good results were achieved.

CLINICAL SUMMARY

Case 1

Male, 57 days old, admitted to hospital because of pneumonia; there was no abnormality in the pregnancy checkup of the mother. No other deformities were found. On admission, the measured weight was 5.2 kg, length was 57 cm, and a grade 3/6 systolic murmur in the pulmonary valve area was heard, but no thrill was heard. Cardiac color Doppler ultrasound showed a space-occupying lesion in the trunk of the pulmonary artery to the start of the left pulmonary artery. The space-occupying lesion causes obvious stenosis of the left pulmonary artery lumen (**Figure 1A**), the diameter of the left pulmonary artery is 1.8 mm, and maximum blood flow velocity is 2.3 m/s. Cardiac CT (computed tomography) examination revealed space-occupying lesions in the trunk of the pulmonary artery and the start of the left pulmonary artery area, but the nature of the lesions is unclear (**Figures 2A,B**). Cardiac MRI (magnetic resonance imaging) showed space-occupying lesions in the trunk of the pulmonary artery and the start of the left pulmonary artery area; therefore, the possibility of hematoma or mural thrombosis was considered (**Figure 2C**).

After anesthesia, a median incision was made to open the chest, and cardiopulmonary bypass was established. During the operation, the pulmonary artery was significantly dilated, and local bulging was observed. A thrombotic tissue was seen in the anterior wall of the trunk of the pulmonary artery extending to the start of the left pulmonary artery, and the thrombus-like tissue is about 2 cm long and 1 cm in diameter (**Figures 3A,B**). The aortic end of the ductus arteriosus was closed and fibrotic. The abnormal anterior wall of the pulmonary artery was removed, the aortic end of the arterial duct was sutured and ligated, and pulmonary angioplasty was performed with an autologous pericardial patch up to the start of the left pulmonary artery. No full-segment left pulmonary artery patch widening was performed.

OPEN ACCESS

Edited by:
Alvise Guariento,
University of Toronto, Canada

Reviewed by:
Claudia Cattapan,
University of Padua, Italy
Omar R. J. Tamimi,
King Fahd Medical City, Saudi Arabia

****Correspondence:***
Zhengbing Yang
Yangzhengbing0@163.com

Specialty section:
This article was submitted to Pediatric Cardiology, a section of the journal Frontiers in Cardiovascular Medicine

Received: *09 February 2022*
Accepted: *28 February 2022*
Published: *25 March 2022*

Citation:
Ren C, Zhang L, Yan H and Yang Z (2022) Case Report: Two Cases of Pulmonary Artery Dissection in Young Infants. Front. Cardiovasc. Med. 9:872049. doi: 10.3389/fcvm.2022.872049

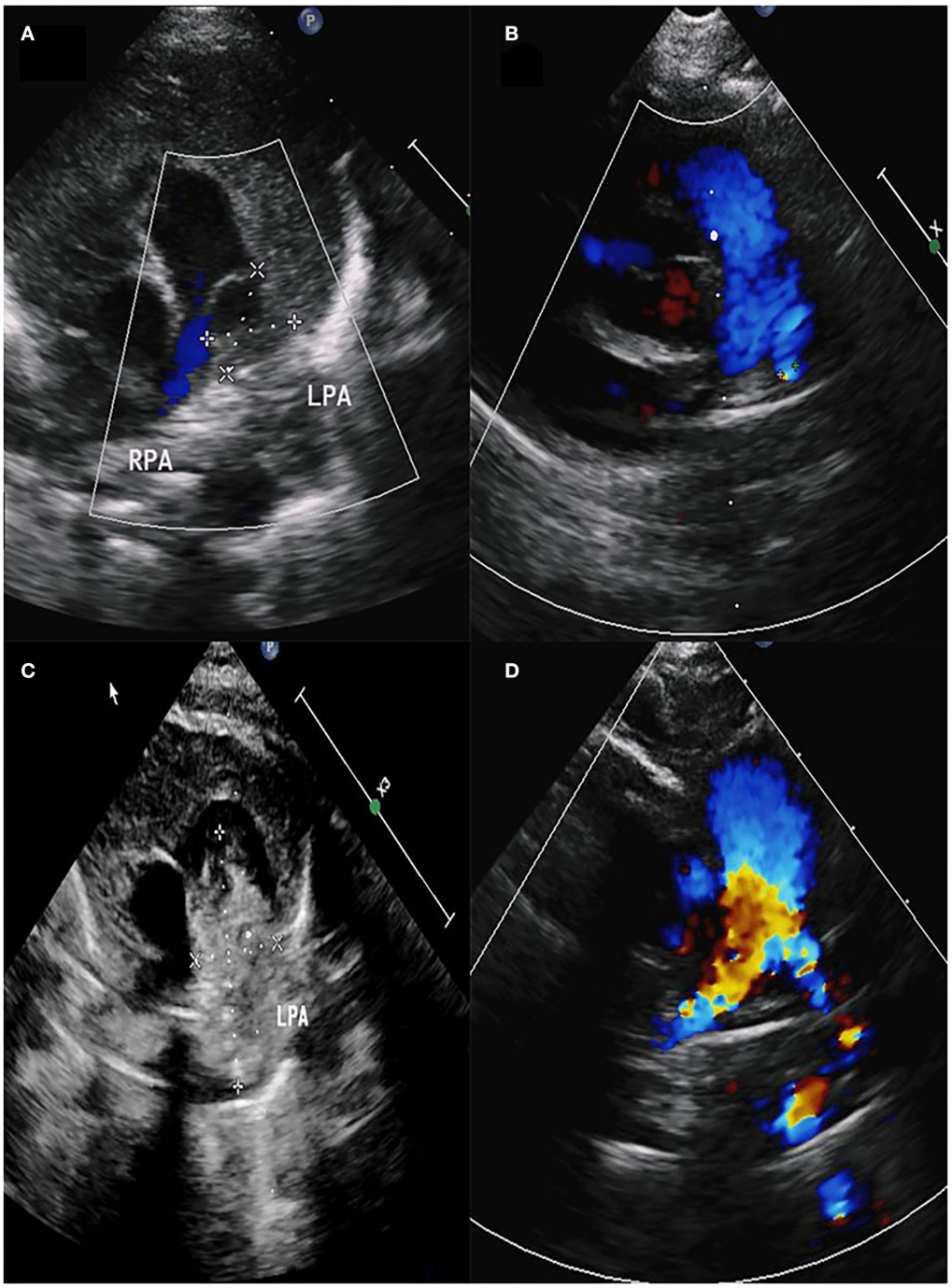

FIGURE 1 | (A) Space-occupying lesion with a size of 11.6 × 10.5 mm in the pulmonary artery. **(B)** Diameter of the left pulmonary artery was 2.2 mm. **(C)** Space-occupying lesion with a size of 31.9 × 15.7 mm in the pulmonary artery. **(D)** Diameter of the left pulmonary artery was 3.9 mm.

Postoperative pathological findings: PAD, mural thrombus was seen, and membrane separation was seen (**Figure 3D**). The pathological section showed presence of hemosiderin and calcification in the diseased tissue (**Figure 3C**). Cardiac color Doppler ultrasound was reviewed 3 months after the operation. The diameter of the right pulmonary artery was 4 mm, the diameter of the left pulmonary artery was 2.2 mm, and the maximum velocity of blood flow was 1.84 m/s (**Figure 1B**).

Abbreviations: PAD, pulmonary artery dissection; CT, computed tomography; MRI, magnetic resonance imaging; PDA, patent ductus arteriosus.

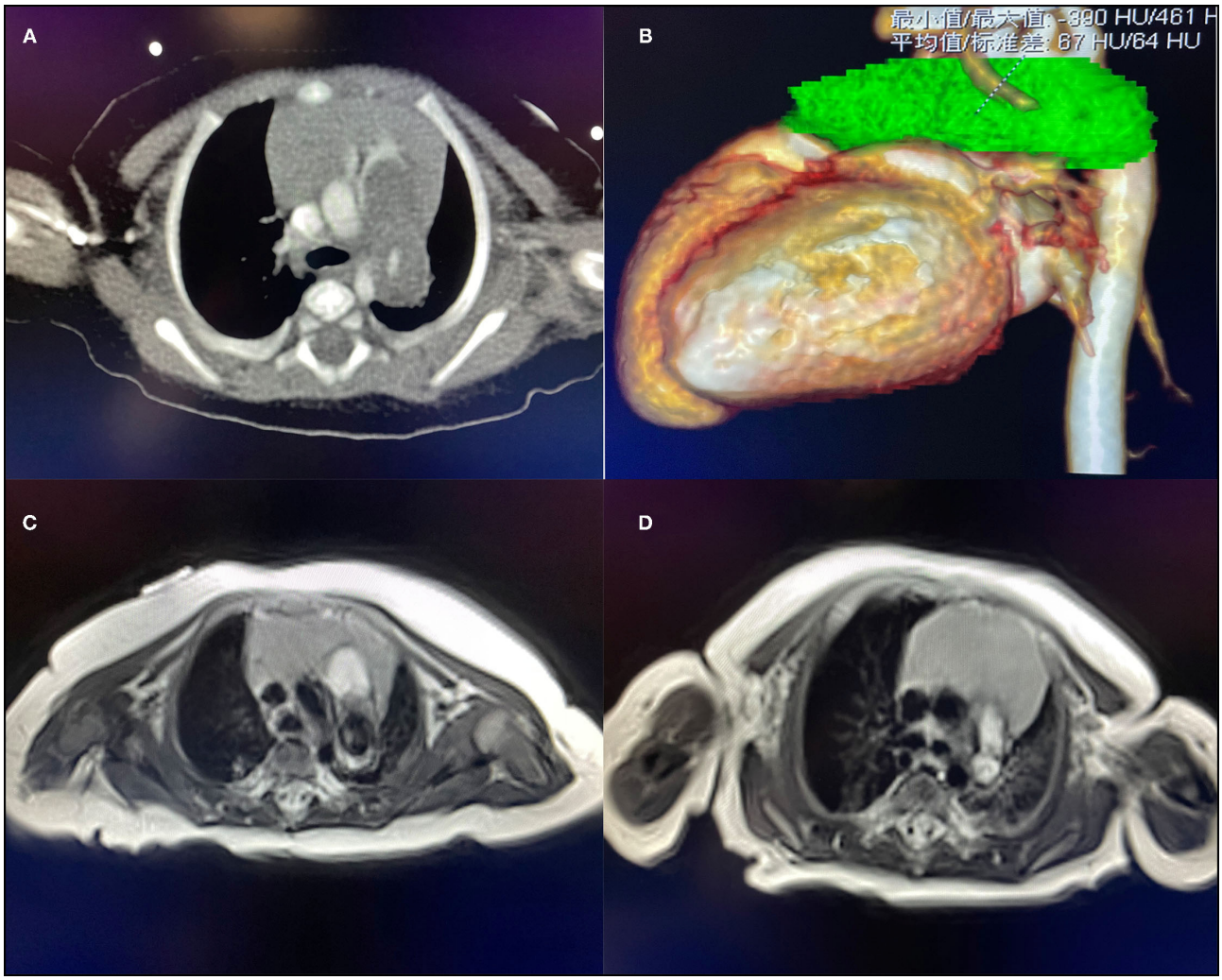

FIGURE 2 | (A) CT suggests space-occupying lesions of the pulmonary artery. **(B)** The green part is the three-dimensional imaging of the lesion. **(C)** T1 image of the MRI of case 1 found a pulmonary artery space-occupying lesion. **(D)** T1 image of the MRI of case 2 found a pulmonary artery space-occupying lesion.

Case 2

Female, 60 days old, measured weight was 5 kg, and length was 55 cm. She was admitted to hospital because of recurring pneumonia. A grade 3/6 systolic murmur in the pulmonary valve area was heard on admission, but no thrill was heard. No other deformities were found. Cardiac color Doppler ultrasound screening revealed a space-occupying lesion in the trunk of the pulmonary artery to the start of the left pulmonary artery (**Figure 1C**), filamentous blood flow was seen in the left pulmonary artery, and maximum blood flow velocity was 3.06 m/s. Cardiac MRI showed space-occupying lesions in the trunk of the pulmonary artery and the start of the left pulmonary artery area (**Figure 2D**). PAD was seen during surgery, and a thrombotic tissue was seen in the anterior wall of the trunk of the pulmonary artery extending to the start of the left pulmonary artery. The thrombus-like tissue is about 2 cm long and 1.2 cm in diameter, the aortic end of the ductus arteriosus was closed and fibrotic. Unlike case 1, the pericardial patch expanded the trunk of the pulmonary artery up to the start of the left pulmonary artery; therefore, an autologous pericardium patch was used to widen the left pulmonary artery to the hilum. The color Doppler ultrasound was rechecked 3 months after the operation. The right pulmonary artery diameter was 4.9 mm, the diameter of the left pulmonary artery was 3.9 mm, and the maximum velocity of blood flow was 2.19 m/s (**Figure 1D**).

DISCUSSION

PAD was once considered to be a rare disease with a high fatality rate (2). However, reports were all concentrated among adults r, and there was no specific report on PAD in young infants.

The majority of PADs occurs in the presence of medial degeneration with fragmentation of elastic fibers and generalized

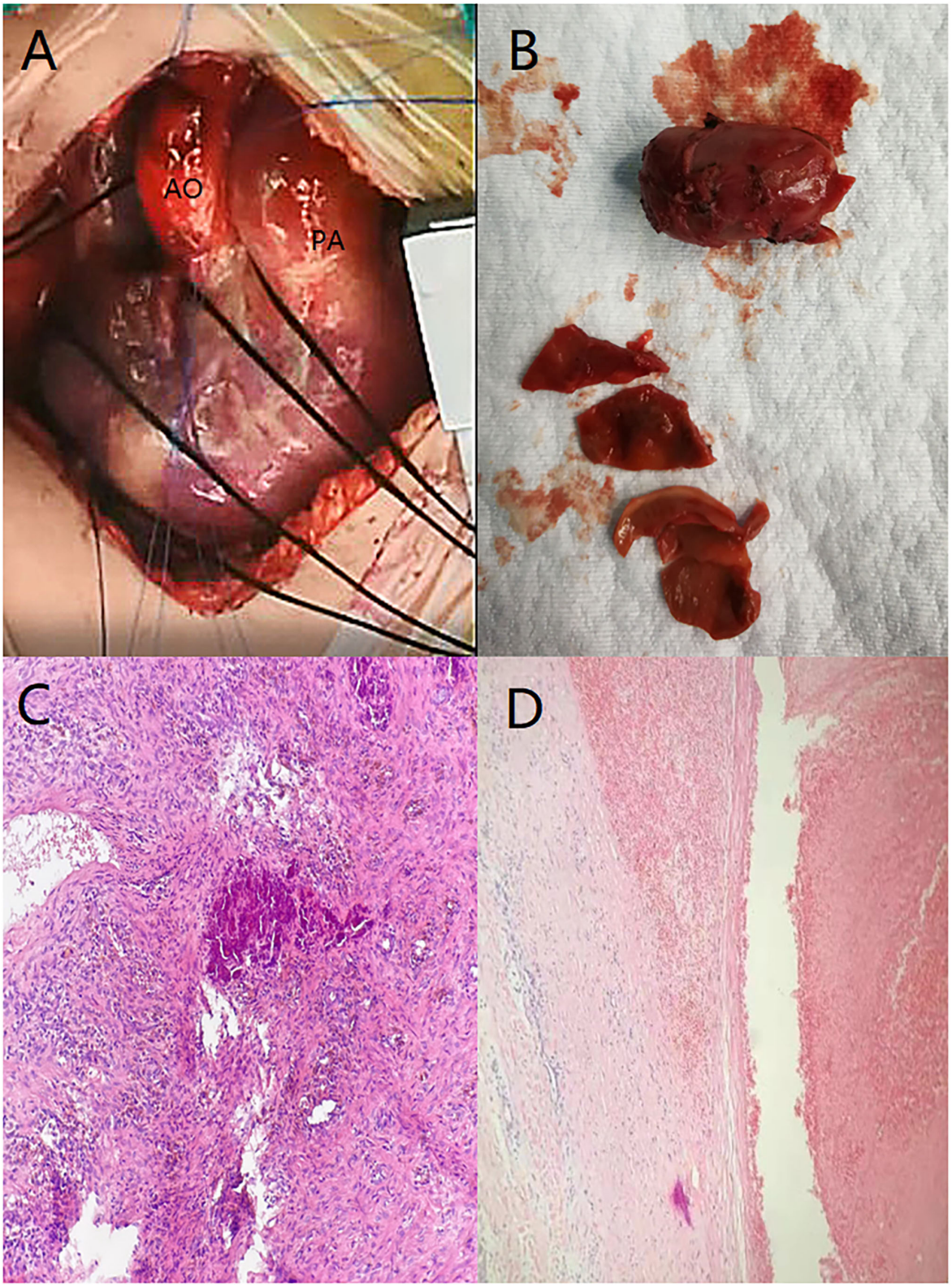

FIGURE 3 | (A) Anterior wall of the trunk of the pulmonary artery was enlarged. **(B)** Thrombus-like tissue was removed during the operation, the color is darker, and the blood vessel wall is visible. **(C)** Visible dark calcification and surrounding brown-yellow hemosiderin changes. **(D)** Static image shows that the membrane is separating.

dilatation of the pulmonary arterial tree caused by chronic pulmonary hypertension (3). In a small number of cases, PAD may occur in the site of local aneurysm formation. Aneurysms are most commonly associated with congenital heart disease that causes persistently high pulmonary flow velocity and pulmonary hypertension, and, especially, hemodynamic changes caused by persistent arterial ducts, leading to increased pulmonary blood flow, increased intravascular pressure, and increased wall stress (3). We reported two patients who were both infants and had no pulmonary hypertension and other underlying diseases. Closed ductus arteriosus was seen during the operation, considering that PAD may be related to continuous acceleration of blood flow at the ductus arteriosus during the fetal period that led to increased intravascular pressure and tearing of the intima. The postoperative pathology shows that the membrane is separating and further confirms this conjecture. The pathological section showed presence of hemosiderin and calcification in the diseased tissue, indicating that the formation of the diseased tissue took a long time. It is further speculated that the formation of PAD may be related to PDA during the fetal period.

Adults with PAD most often present with chest pain, dyspnea, and hemoptysis (2). Unlike in adults, PAD in young infants usually manifests as recurring pneumonia. The two patients we reported came to the hospital for recurring pneumonia. The first infant we reported underwent CT examination. However, because of rare experience in diagnosing PAD in young infants, radiologists finally considered it as a space-occupying lesion, but the nature of the lesion is unclear. At the same time, an MRI examination was also performed to confirm the diagnosis. The final diagnosis of the MRI was hematoma or mural thrombus. However, in the end, the patient was diagnosed with PAD, which was further confirmed by intraoperative findings and postoperative pathology. Although CT is considered the best method for diagnosing PAD (2), for PAD in young infants, MRI can provide more information through a multi-level comparison. At the same time, compared to CT examinations, MRI examinations can avoid the use of contrast agents on young infants.

In our report, the lesions in the two infants were present in the trunk of the pulmonary artery to the start of the left pulmonary artery. For the first infant, the anterior wall of the diseased pulmonary artery was removed, and an autologous pericardial patch was used for pulmonary angioplasty. Although the postoperative review showed that the operation was good, the left pulmonary artery was still narrower than usual. Considering that infants are in the stage of growth and development, PAD compresses the left pulmonary artery, resulting in long-term obstruction of blood flow to the left pulmonary artery, which further affects the development of pulmonary blood vessels. Eventually, it causes irreversible stenosis of the left pulmonary artery. The same procedure used for the first infant was adopted for the second infant. At the same time, we completely freed the left pulmonary artery and used a pericardial patch to expand the left pulmonary artery to the left hilum. The postoperative review revealed that the second patient had no left pulmonary artery stenosis. Because there is no previous report on surgical methods for infants with PAD, our center has reported on a surgical procedure for infants with PAD. We suggest that using an autologous pericardium patch is feasible to expand the pulmonary artery for PAD in young infants. At the same time, for the left and right pulmonary artery branches with lesions, although lesions only exist at the start of the left or the right pulmonary artery, full-segment expansion of the pulmonary artery branch should be performed during surgery to avoid left or right pulmonary stenosis.

DATA AVAILABILITY STATEMENT

The original contributions presented in the study are included in the article/**Supplementary Material**, further inquiries can be directed to the corresponding author.

AUTHOR CONTRIBUTIONS

CR wrote the manuscript. ZY, HY, and LZ helped in the clinical case analysis. All the authors contributed in the care, diagnosis, and treatment of the patients.

SUPPLEMENTARY MATERIAL

The Supplementary Material for this article can be found online at: https://www.frontiersin.org/articles/10.3389/fcvm.2022.872049/full#supplementary-material

REFERENCES

1. Fernando DMG, Thilakarathne SMNK, Wickramasinghe CU. Pulmonary artery dissection-a review of 150 cases. *Heart Lung.* (2019) 48:428–35. doi: 10.1016/j.hrtlng.2019.02.007
2. Adodo DK, Kloeckner M, Bergoend E, Couëtil JP. Pulmonary artery dissection: a case treated by homograft replacement. *Ann Thorac Surg.* (2017) 103:e47. doi: 10.1016/j.athoracsur.2016.06.052
3. Lopez-Candales A, Kleiger RE, Aleman-Gomez J, Kouchoukos NT, Botney MD. Pulmonary artery aneurysm: review and case report. *Clin Cardiol.* (2010) 18:738–40. doi: 10.1002/clc.4960181211

Conflict of Interest: The authors declare that the research was conducted in the absence of any commercial or financial relationships that could be construed as a potential conflict of interest.

frontiers | Frontiers in Cardiovascular Medicine

CASE REPORT
published: 26 April 2022
doi: 10.3389/fcvm.2022.872172

Novel Compound Heterozygous *PKLR* Mutation Induced Pyruvate Kinase Deficiency With Persistent Pulmonary Hypertension in a Neonate: A Case Report

Sha Lin†, Xintian Hua†, Jinrong Li and Yifei Li**

Key Laboratory of Birth Defects and Related Diseases of Women and Children of MOE, Department of Pediatrics, West China Second University Hospital, Sichuan University, Chengdu, China

Background: Pulmonary hypertension could be associated with pyruvate kinase deficiency (PKD). There are few reported cases of PPHN as the first clinical manifestation of PKD. Herein we report a rare case of PKD in which the patient exhibited persistent pulmonary hypertension in the neonate (PPHN), and genetic testing helped to rapidly identify an potential association.

Case presentation: The patient was a newborn boy who suffered from severe dyspnea, extreme anemia, skin pallor, and hypoxemia. Repeated echocardiography indicated persistent severe pulmonary hypertension with a calculated pulmonary artery pressure of 75 mmHg, and right ventricular hypertrophy. The administration of nitric oxide significantly reduced the pulmonary artery pressure. Whole-exome sequencing revealed a compound heterozygous mutation consisting of c.707T > G and c.826_827insAGGAGCATGGGG. PolyPhen_2 and MutationTaster indicated that both the c.707T > G (probability 0.999) and c.826_827insAGGAGCATGGGG (probability 0.998) mutations were disease causing. PROVEAN protein batch analysis indicated that the associated p.L236R region was deleterious (score −4.71) and damaging (SIFT prediction 0.00), and this was also the case for p.G275_V276insEEHG (deleterious score −12.00, SIFT prediction 0.00). Substantial structural changes in the transport domain of the protein were predicted using SWISS-MODEL, and indicated that both mutations led to an unstable protein structure. Thus, a novel compound heterozygous mutation of PKLR-induced PKD with PPHN was diagnosed.

Conclusion: The current study suggests that molecular genetic screening is useful for identifying PPHN, particularly in children with metabolic disorders. In patients exhibiting unexplained hyperbilirubinemia combined with severe pulmonary hypertension, PKD might be a potential possible alternative explanation. Genetic screening is helpful for identifying genetic causes of pulmonary hypertension, especially in patients with PPHN. This report expands the mutation spectrum of the *PKLR* gene, and contributes to the genotype-phenotype map of PKD.

Keywords: case report, genomic sequence, persistent pulmonary hypertension in the neonate, *PKLR*, pyruvate kinase deficiency

OPEN ACCESS

Edited by:
Angela Bates,
University of Alberta, Canada

Reviewed by:
Sachin Gajanan Damke,
Datta Meghe Institute of Medical Sciences, India
Omar R. J. Tamimi,
King Fahd Medical City, Saudi Arabia

****Correspondence:***
Jinrong Li
lijinrong224@163.com
Yifei Li
liyfwcsh@scu.edu.cn

† These authors have contributed equally to this work

Specialty section:
This article was submitted to Pediatric Cardiology, a section of the journal Frontiers in Cardiovascular Medicine

Received: *09 February 2022*
Accepted: *04 April 2022*
Published: *26 April 2022*

Citation:
Lin S, Hua X, Li J and Li Y (2022) Novel Compound Heterozygous PKLR Mutation Induced Pyruvate Kinase Deficiency With Persistent Pulmonary Hypertension in a Neonate: A Case Report. Front. Cardiovasc. Med. 9:872172. doi: 10.3389/fcvm.2022.872172

INTRODUCTION

Persistent pulmonary hypertension in the neonate (PPHN) is a severe condition. Generally, life – threatening infection, developmental disorders, and cardiac malformation are considered the main causes of PPHN. Notably, however, metabolic disorders are increasingly being identified as involved in the development of PPHN. Genetic abnormalities have been reported in association with refractory PPHN, such as mutations in surfactant protein B and the ATP-binding cassette protein A3. Such mutations may lead to insufficient surfactant function, and induce PPHN. Beyond pulmonary disease, several inherited systemic hematological and metabolic disorders are reportedly associated with pulmonary hypertension, including primary thrombocytosis, polycythemia vera, Gaucher disease, glycogen storage disease, and pyruvate kinase deficiency (PKD). Notably, however, few patients with hematological diseases have been identified with pulmonary hypertension in the neonatal period. Due to hypoxia and hemolysis, PPHN may present as a severe complication with hyperbilirubinemia.

Pyruvate kinase deficiency is the most common defect affected by the glycolytic pathway, and it can result in severe congenital hemolytic anemia (1). With the development of genetic sequencing, mutations in the pyruvate kinase L/R (*PKLR*) gene located on chromosome 1q21 have been identified as genetic causes of PKD (2, 3). To date > 300 mutations have been reported. Differences in residual red blood cell (RBC) enzyme between homozygotes (>25%) and heterozygotes (40–60%) of *PKLR* mutations have also been described (1). PKD has been regarded as a heterogeneous disease caused by reduced PK activity and PKLR variants (4–6). PKLR participates in glycolysis as a catalyst involved in the transphosphorylation of phosphoenolpyruvate into pyruvate and ATP, which is an irreversible component of glycolysis. Previous reports suggest that the generation of ATP in RBCs contributes to maintaining their structural and functional integrity throughout their lifecycle, and deficiency of pyruvate kinase activity could result in failure of ATP production. Potential consequences include membrane plasticity loss, cellular dehydration, and the premature destruction of RBCs in the spleen or liver, leading to severe refractory hyperbilirubinemia and anemia in neonates.

In most reported cases of PKD the crucial clinical symptoms were severe anemic phenomena and substantial elevation of indirect bilirubin (IDIL) (5). Pulmonary hypertension is considered a rare and life-threatening complication of PKD, while PPHN has been seldom reported. Recent reports indicate that the incidence of pulmonary hypertension in PKD patients is relatively low, and that it is predominantly observed in adolescents (>3%) and adults (>5%). Hitherto there have been no reported cases in newborns, but a statement provided limited evidence on pulmonary hypertension during neonatal period (5). Herein we describe a case of severe hyperbilirubinemia and PPHN diagnosed soon after birth. Metabolic screening and genetic testing helped to identify a novel heterozygous mutation of *PKLD*, guiding further optimal therapeutic strategies. This is the first report of PKD with PPHN, and expands the known mutations associated with PKLD, and it also suggests that rapid genetic testing to distinguish between potential causes of PPHN in complex situations would be beneficial.

CASE PRESENTATION

Ethics Compliance

The study was approved by the ethics committee of the West China Second Hospital of Sichuan University (approval number 2014-034). Written informed consent was obtained from the patient's parents prior to performing WES, and for the inclusion of the patient's clinical and imaging details in publications.

History of Illness and Physical Examination

The patient was a newborn boy who was admitted to our hospital 5 h after birth suffering severe dyspnea, extreme anemia, skin pallor, and hypoxemia. He was born at 37 + 6 gestational weeks, and his birth weight was 2.4 kg. Due to substantial intrauterine distress, meconium-stained amniotic fluid, and torsion of umbilical cord a cesarean had been performed to prevent further injuries. The respective Apgar scores were 7, 8, and 9 at the 1st, 5th, and 10th minutes after birth. Physical examination revealed mild jaundice, weak breath sounds in bilateral lungs, and dull cardiac sound. An enlarged liver was evident 5.0 cm under the lower rib and 3.5 cm below the xiphoid process, with a blunt edge, and the spleen was 3.0 cm under the rib. He had hypomyotonia of limbs, decreased primary reflex, and cold extremities with a capillary refill time of 3 s.

Laboratory and Radiological Results

The patient demonstrated severe anemia within a short time postnatally (hemoglobin 56 g/L, n.v. > 170 g/L), and reduced platelets (67×10^9/L, n.v. > 292×10^9/L). White blood cells were elevated (92.6×10^9/L, n.v $9.0–30.0 \times 10^9$/L), as was C-reactive protein (12.9 mg/L, n.v. < 8.0 mg/L). Natriuretic peptide was 4379.8 pg/mL, indicating heart failure. Biochemistry tests demonstrated an elevation of total bilirubin (216.4 μmol/L, n.v. < 210.0 μmol/L), IDIL of 200.1 μmol/L (n.v < 193.0 μmol/L), and direct bilirubin (DBIL) of 16.3 μmol/L (n.v. < 10.0 μmol/L). IDIL dropped to approximately 50–80 μmol/L from the 3rd postnatal day (**Figure 1A**), but DBIL had increased to 193.4 μmol/L by the 15th postnatal day (**Figure 1A**). In tests for specific pathogens, quantitative polymerase chain reaction (qPCR) to detect pathogenic bacteria, viruses, and fungi, TORCH IgM antibody screening, group B *Streptococcus* testing were negative. Besides, the aerobic or anaerobic culture cultures of blood, septum, urine and cerebral spinal fluid were all negative. So that, non-specific pathogen had been identified.

Repeated echocardiography indicated persistent severe pulmonary hypertension with a highest calculated pulmonary artery pressure of 75 mmHg, with right ventricular hypertrophy at the 3rd day after birth. X-rays depicted patchy shadows in the lungs. Hepatic ultrasound indicated normal liver density (**Figure 1B**) and normal gallbladder morphology (**Figure 1C**), thus liver fibrosis and biliary atresia were ruled out as causes

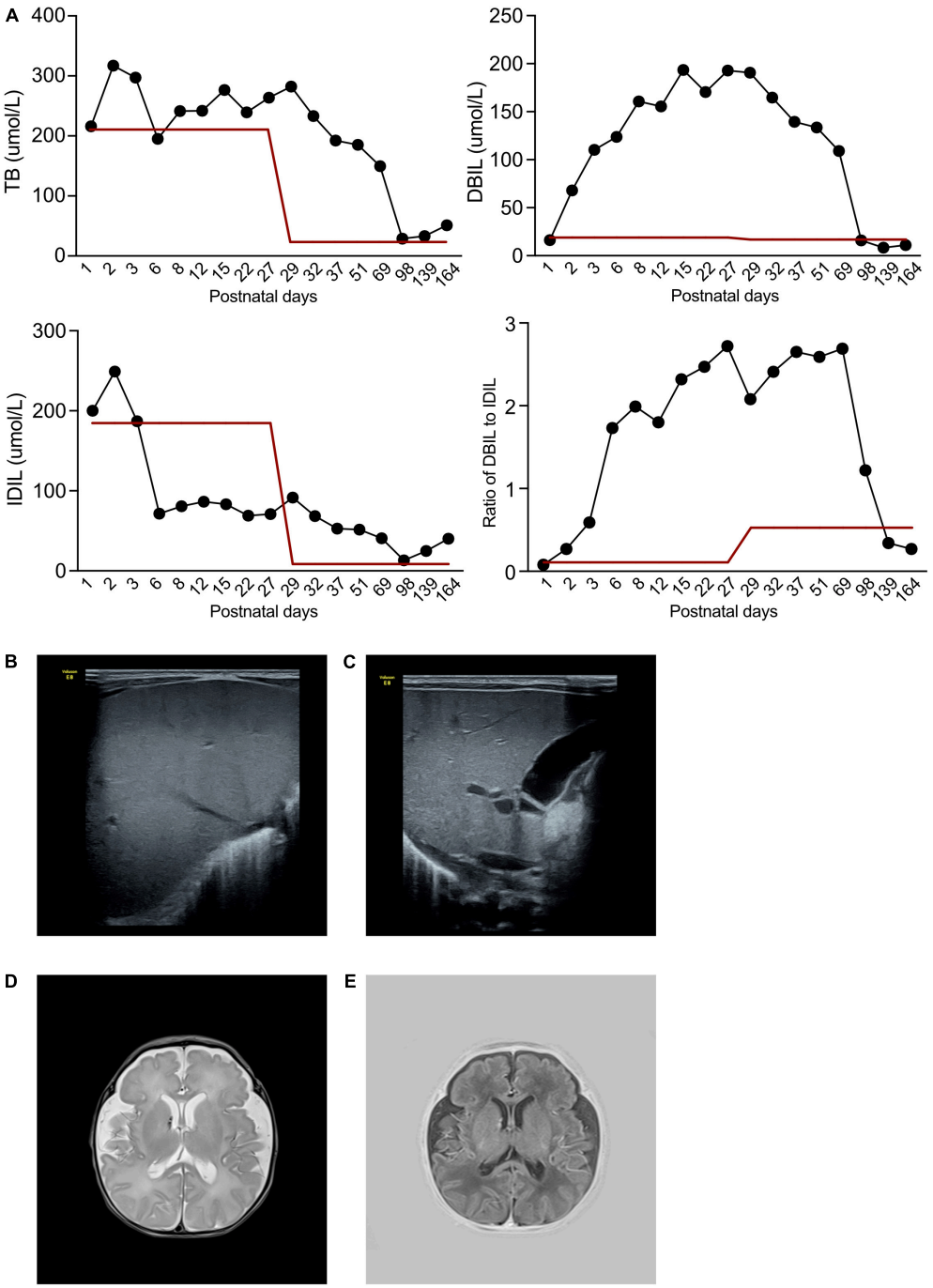

FIGURE 1 | Clinical and radiology manifestation in the current proband. **(A)** The patient exhibited abnormal bilirubin in plasma, while the total bilirubin remained high during his illness. At the beginning, DBIL elevated rapidly to a high level, while IDIL remained normal. However, after 3 months follow-up, DBIL dropped to normal level, and IDIL increased. **(B)** Hepatic ultrasound demonstrated a normal density of liver. **(C)** Gallbladder demonstrated a normal morphology. **(D,E)** The cerebral MRI identified hematoma near right cerebral ventricle.

of the elevated DBIL. Cerebral magnetic resonance imaging revealed hematoma signs in the right cerebral ventricle (T2 image in **Figure 1D** and T1 image in **Figure 1E**).

Given the above laboratory and radiological results in conjunction with his clinical manifestations, the dominant concerns were PPHN and unexplained continuously elevated DBIL. Thus, metabolic disorder was highly suspected. Comprehensive metabolic function profiling analyzing organic acids in urine revealed large proportions of α-keto-b-methylvaleric acid, methylglutaric acid, hydroxyphenylacetic

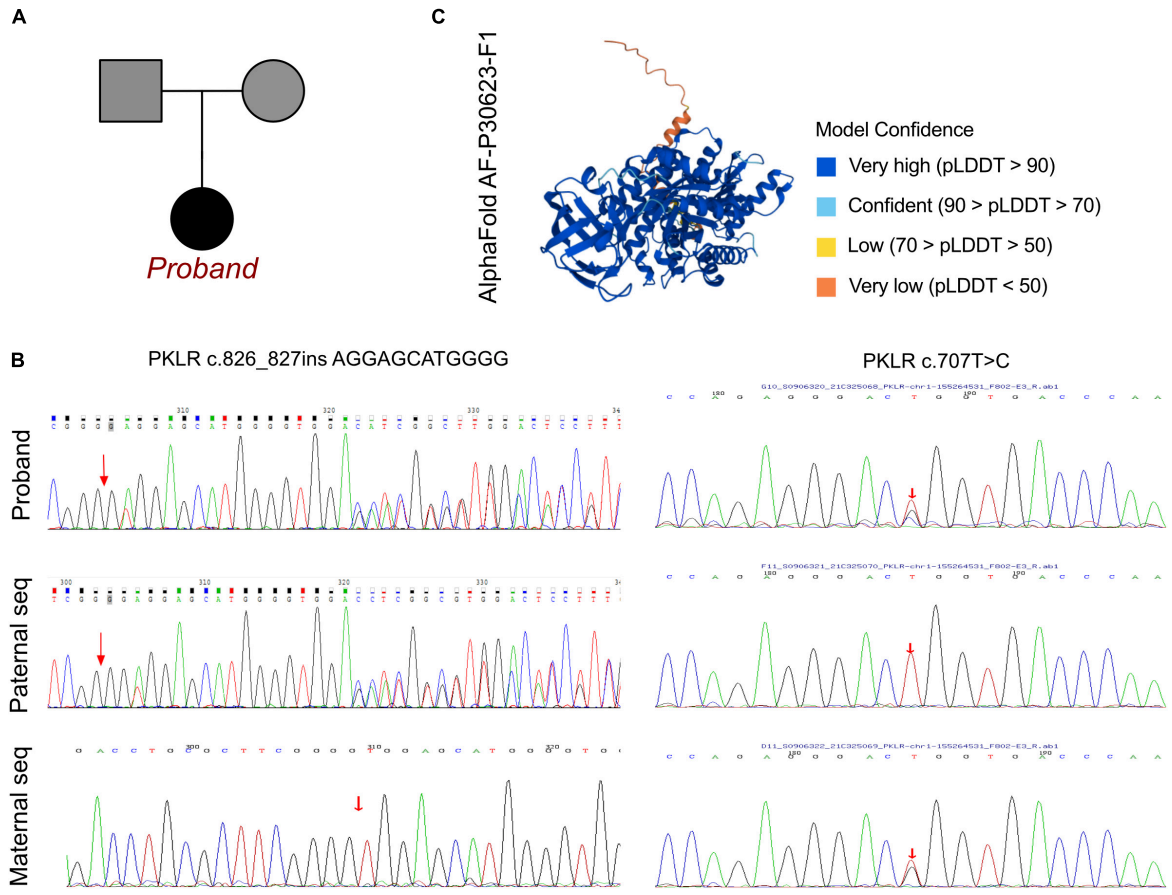

FIGURE 2 | The *PKLR* mutations in this family. **(A)** Family pedigree in the current proband. **(B)** Sanger sequencing validation of the current proband and his parents, revealing the maternal carrier of *PKLR* c.707T > C (p.L236R) and his paternal carrier of *PKLR* c.826_827insAGGAGCATGGGG. The current proband exhibited PPHN and metabolic disorder in neonatal period and congenital non-spherocytic hemolytic anemia with a novel compound heterozygous mutation of *PKLR*. **(C)** The crystal structure of full length of AA sequence built by AlphaFold 2.0.

acid, fumarate, acetoacetic acid, and ketoisocarproate, which were strongly indicative of a metabolic disorder.

Molecular Results

A peripheral blood sample was obtained from the patient in an ethylenediaminetetraacetic acid anticoagulant blood sample tube then stored at 4°C for less than 6 h. DNA was extracted using the Blood Genome Column Medium Extraction Kit (Tiangen Biotech, Beijing, China) in accordance with the manufacturer's instructions. Protein-coding exome enrichment was performed using the xGen Exome Research Panel v1.0. WES was performed using the NovaSeq 6000 platform (Illumina, San Diego, CA, United States). The patient's parents reported that there was no known family history of pulmonary hypertension or PKD, and no other relatives in his family exhibited any potential symptoms (**Figure 2A**). PPHN was the primary consideration in this patient, as well as substantial elevations in total bilirubin, DBIL, and IDIL, consistent with metabolic disorder. Therefore, after ruling out other possible causes a genetic metabolic disorder was strongly suspected. WES was performed using the Illumina NovaSeq 6000 platform, followed by analysis of the variable genes involved in metabolic diseases, and a compound heterozygous mutation of c.707T > G and c.826_827insAGGAGCATGGGG were identified, both located in exon 6 of the *PKLR* gene. These data were confirmed by Sanger sequencing, and the patient's mother carried the heterozygous variant of c.707T > G, and his father carried the c.826_827insAGGAGCATGGGG frame insertion as a heterozygous variant (**Figure 2B**).

To elucidate the molecular architecture of the human *PKLR* gene, MutationTaster with R software was used to predict the pathogenicity of *PKLR* c.707T > C and c.826_827insAGGAGCATGGGG. The effects of these mutations on protein structure were also assessed via PROVEAN protein batch with Provean score and SIFT prediction. A crystal structure was built based on amino acids 47–574, and formatting of the complex of pyruvate kinase isoform L-type with phosphorylated Ser113 (pS113). The AlphaFold protein structure database[1] tool was used to predict a protein crystal structure containing amino acids 1–574. The protein structure of PKLR has been built and named AF-P30623-F1 (7, 8). Modeling analysis was performed

[1]https://alphafold.ebi.ac.uk/

using the online software SWISS-MODEL[2] to visualize and analyze the altered amino acid sequence and stability of PKLR with the 6eck.1.A template. The capability of the protein structure was estimated using Ramachandran Plots. The signature vector that was ultimately generated was used to train the predictive classification and regression model for calculating the change in Gibbs folding free energy ($\Delta\Delta G$) induced by the mutations shown in the ensemble variance figures.

The crystal structure of the full amino acid sequence is shown in **Figure 2C**. According to updated data in ExAC and 1000G neither of the mutations had been reported, indicating that they were novel variants (**Figure 3A**). Verification via Rare Exome Variant Ensemble Learner, SIFT, PolyPhen_2, and MutationTaster indicated that both the c.707T > G (probability 0.999) and c.826_827insAGGAGCATGGGG (probability 0.998) mutations were disease causing (**Figure 3A**). PROVEAN protein batch indicated that the p.L236R protein was deleterious (Provean score −4.71) and damaging (SIFT prediction 0.00), as was the p.G275_V276insEEHG protein (deleterious Provean score −12.00, damaging SIFT prediction 0.00) (**Figure 3A**). According to the American College of Medical Genetics the genetic variant of c.826_827 ins AGGAGCATGGGG was a frameshift with uncertain pathogenicity (PM2 + PM4), and the c.707T > G mutation was a missense mutation with uncertain pathogenicity (PM2 + PP3), and both were related to PKD.

SWISS-Model was used to assess the crystal structure of PKLR due to the identified mutations. The altered crystal structures of PLKR complexes are shown in **Figure 3B**. Generally there were no significant changes in crystal structure in the PKLR p.L236R complex, and an additional loop was identified in the PKLR p.G275_V276insEEHG complex (**Figure 3B**). Notably, however, differences in Ramachandran plots were observed in both PKLR p.L236R and PKLR p.G275_V276insEEHG compared to wild-type (**Figure 3C**). Detailed structures including changes in positions in p.L276R and p.G275_V276insEEHG are shown in **Figure 3D**. Structural comparisons were completed for both mutations, and are shown in **Figure 3E**. Ensemble variance revealed free energy changes due to the two mutations. The above analyses indicated that both of the mutations identified could alter the transcription of the *PKLR* gene, and damage the functional protein structures of the PKLR complex. Thus, a compound heterozygous mutation that was the likely cause of PKD was identified in the patient.

Treatment and Clinical Outcome

During the neonatal period the patient was administered antibiotic therapy including ceftazidime and ampicillin. Mechanical ventilation, recurrent red blood cell and plasma transfusions, catecholamine, and nutritional support were administrated to save his life. After a series of positive treatments had been administrated to correct his severe anemia, alleviate hypoxia stress, and control infection, echocardiography still recorded pulmonary hypertension with a relative reduced pressure around 55–60 mmHg, which was different from other PPHNs induced by intrauterine stress and significant infection. So that, we considered the development of PPHN might be related with PKD, and nitric oxide inhalation had been provided to relieve PPHN. After the nitric oxide therapy, the pulmonary artery pressure dropped to 30–35 mmHg at the end of neonatal period. Furthermore, the pulmonary artery pressure decreased to normal of 20–25 mmHg at the age of 6 months postnatally.

IDIL increased again, however, whereas DBIL dropped to a normal level during 3 months of follow-up. The patient required RBC transfusions once a month, consistent with the classic clinical manifestation of PKD. The present case included PKD onset with PPHN and severe metabolic disorder, intrauterine distress, and perinatal extreme hypoxia. The typical clinical symptoms of congenital non-spherocytic hemolytic anemia appeared during follow-up. This case indicates that perinatal exposure to adverse environments may induce the onset of PKD with genetic deficiency of *PKLR*, resulting in various manifestations. Thus, early metabolic screening and WES may help to distinguish the disease based on molecular diagnosis, which could distinguish between truly positive and false positive PKD.

At present, the patient has been carefully followed by almost 18 months without any significant complications. And there was no obviously developmental retardation, cognitive function and motor movement delay. He received blood transfusion every 1.5 month, and 2 times blood test had been provided. To monitor the status of his cardiovascular function and pulmonary artery pressure, echocardiography had been involved every 2 months. After fully informed the patient's parents, the patient would receive allogeneic hematopoietic stem cell transplantation around 3–5 years age.

DISCUSSION

The *PKLR* gene encodes RBC isoenzymes, and associated clinical symptoms are usually limited in RBCs. *PKLR* mutation leads to PKD. Hepatic enzyme activity is protected in hepatocytes, or compensated by the PK-M2 isoenzyme encoded by the *PKM* gene, which provides an explanation for degrees of diversity of anemia. Zanella et al. (9) reported that the clinical presentation is not entirely dependent on molecular variants, but reflects a combination of genetic background, concomitant functional polymorphisms of other enzymes, and ineffective erythropoiesis. (3) reported that *PKLR* variants did not contribute to intrauterine lesions. Surgical effects, infection, and hypoxia attacks may enhance the severity of PKD (10). PKD could be misdiagnosed due to its various clinical manifestations. In some patients the phenotype is nearly normal, whereas others exhibit extreme anemia and hyperbilirubinemia. Cardiopulmonary dysfunction is a life - threatening complication associated with PKD. PKD management guidelines usually recommend cardiovascular screening for outcome evaluation. In general, pulmonary hypertension is observed in 3% of adolescent PKD patients, but the incidence increases to 5% in adults (11). Several reviews indicate that pulmonary hypertension occurs in the neonatal phase, but none of them provide a convincing incidence rate. The average age that PKD-related pulmonary hypertension is

[2]https://swissmodel.expasy.org/

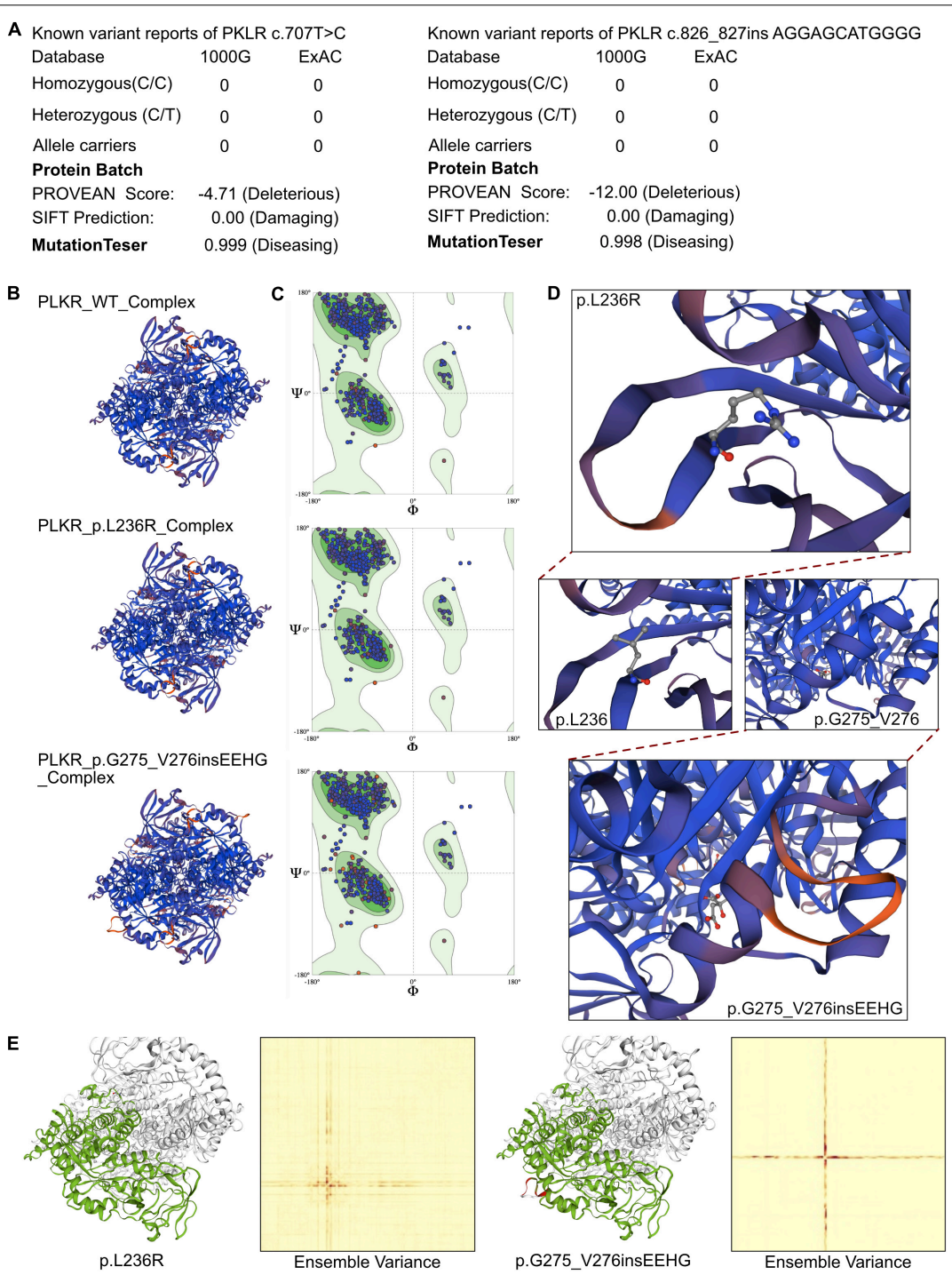

FIGURE 3 | The effects of *PKLR* c.707T > C and c.826_827insAGGAGCATGGG mutations on the molecular structure of the protein. **(A)** The reported cases of the identified mutations in database 1000G and ExAC. And the PROVEAN protein batch and MutationTaster scores revealed the two newly identified mutations would be protein damaging and diseasing causing variants. **(B)** Individual crystal structures of wild type, p.L236R and p.G275_V276insEEHG according to the 36eck.1.A model template. **(C)** Ramachandran plots of AA with wild type, p.L236R and p.G275_V276insEEHG. **(D)** The detailed space structure between wild type and mutant proteins. **(E)** The comparisons of free energy on crystal structure of wild type sequence and p.L236R and p.G275_V276insEEHG variants, respectively.

diagnosed is 39.2 years (11). Thus, PPHN is seldom considered as the first clinical manifestation of PKD. In the current patient it was initially difficult to distinguish PKD from PPHN. Timely metabolic screening facilitated identification of the disorder, however, and prompted genetic testing, which resulted in a diagnosis of PKD at very early stage postnatally. PKD and

other hemolytic anemia would lead to pulmonary hypertension in long term due to nitric oxide deficiency, oxidative stress, and hypercoagulability (12). And, the PPHN could be mainly induced by anemia, infection, intrauterine stress and meconium stained liquor. To this patients, we detected PPHN by routine echocardiography after birth and the highest pulmonary artery pressure was 75 mmHg. However, pulmonary pressure only reduced to 55–60 mmHg after anemia and infection had been controlled. Thus, nitric oxide inhalation had been provided, and the pulmonary artery pressure went down to 30–35 mmHg. Finally, the pulmonary artery pressure decreased to normal at 6 months old during follow-up. According to previous statement from Rachael F. Grace and Wilma Barcellini (5) indicated that PKD could induce critical anemia intrauterine, which would lead to evidence of neonatal pulmonary hypertension or stroke. So that we attempt to associated the presentation of PPHN with PKD based on the following reasons: (1) the patient suffered significantly severe anemia prenatally; (2) the pulmonary hypertension still remained after the anemia, infection and other conditions controlled; (3) the administration of nitric oxide significantly reduced the pulmonary hypertension; and (4) the pulmonary hypertension remained beyond neonatal period.

With respect to PKD's etiology, perinatal hypoxia and infection could result in insufficient intracellular ATP supplementation. Elevation of arachidonic acid cyclase enhances the production of prostaglandins such as TXA2 and PGF2α, and increased lipoxygenase promotes the formation of leukotriene (13). Production of endothelium-derived contraction factor increases, in conjunction with a reduction in endothelium-derived relaxing factor, promoting pulmonary vasoconstriction. Histamine, angiotensin, and the consumption of nitric oxide caused by hemolysis are also involved in the generation of PPHN in neonatal PKD with hypoxia. Proliferation of vascular smooth muscle would contribute to PPHN.

Hyperbilirubinemia reportedly has some protective effects in patients with physiological jaundice and early-onset neonatal sepsis (14), but the sustained reversal of IDIL and DBIL elevation is also thought-provoking. Identifying the causes of persistent hyperbilirubinemia is critical in such patients. In the present patient substantially increased DBIL in the early phase was considered a consequence of PKD. Elevated IDIL was the major contributor to hyperbilirubinemia, however, which is the opposite of the classic clinical PKD manifestation. Based on genetic testing and molecular diagnosis, PKD was considered a confirmed diagnosis. An optimal therapeutic strategy was continuously provided to the patient. Integrated treatment to reduce IDIL was administered after excluding biliary atresia. During follow-up the IDIL level dropped to normal, and continuous hemolysis became the dominant concern, and also indicated the accuracy of the diagnosis of PKD. Severe perinatal hemolysis and hypoxia can evidently induce hepatic injury and damage intralobular canaliculi, which can result in elevated IDIL (15).

Neonatal jaundice and hyperbilirubinemia are commonly seen in infants with PKD, and can rapidly progress to hepatocellular damage and synthetic dysfunction. Early diagnosis is therefore crucial, but it is not easy to achieve. In the current patient WES was performed to facilitate an early molecular diagnosis. With the development of genetic sequencing, more than 300 *PKLR* gene mutations located on chromosome 1q21 have been confirmed to induce PKD. Thus, PKD could be definitively diagnosed even in neonates only exhibiting partial PKD-related symptoms. Compared to traditional analysis, WES helps to identify the radical fact of common symptom, such as hyperbilirubinemia and pulmonary hypertension. Molecular diagnosis contributes to identifying rare diseases, and providing targeted therapeutic strategies. To date the present patient has been given regular transfusions, and has not suffered iron overload, heart failure due to extreme anemia, or other complications, demonstrating the advantages of early genetic testing to identify rare diseases.

CONCLUSION

In conclusion, there are few reported cases of PKD presenting with PPHN. In patients exhibiting unexplained hyperbilirubinemia combined with severe pulmonary hypertension, WES should be considered as a possible approach to reach a molecular diagnosis. Molecular genetic screening is helpful for identifying the genetic causes of pulmonary hypertension with metabolic disorders. The current report expands the mutation spectrum of the *PKLR* gene, and contributes to the genotype-phenotype map of PKD.

DATA AVAILABILITY STATEMENT

The original contributions presented in the study are included in the article/supplementary material, further inquiries can be directed to the corresponding authors.

ETHICS STATEMENT

The studies involving human participants were reviewed and approved by the Ethics Committee of West China Second Hospital of Sichuan University (2014-034). Written informed consent to participate in this study was provided by the participants' legal guardian/next of kin. Written informed consent was obtained from the individual(s), and minor(s)' legal guardian/next of kin, for the publication of any potentially identifiable images or data included in this article.

AUTHOR CONTRIBUTIONS

YL and JL were the patient's physicians. SL and XH reviewed the literature and contributed to manuscript drafting. YL conceptualized and designed the study, coordinated and supervised data collection, and critically reviewed the manuscript for important intellectual content. SL, YL, and JL were responsible for the revision of the manuscript for important intellectual content. All authors issued final approval for the version to be submitted.

FUNDING

This work was supported by grants from the National Natural Science Foundation of China (No. 81700360), Technology Project of Sichuan Province of China (2020YFS0102), and Central Government Funds of Guiding Local Scientific and Technological Development for Sichuan Province (2021ZYD0105).

REFERENCES

1. Bianchi P, Fermo E, Glader B, Kanno H, Agarwal A, Barcellini W, et al. Addressing the diagnostic gaps in pyruvate kinase deficiency: consensus recommendations on the diagnosis of pyruvate kinase deficiency. *Am J Hematol.* (2019) 94:149–61. doi: 10.1002/ajh.25325
2. Bianchi P, Fermo E. Molecular heterogeneity of pyruvate kinase deficiency. *Haematologica.* (2020) 105:2218–28. doi: 10.3324/haematol.2019.241141
3. Bianchi P, Fermo E, Lezon-Geyda K, van Beers EJ, Morton HD, Barcellini W, et al. Genotype-phenotype correlation and molecular heterogeneity in pyruvate kinase deficiency. *Am J Hematol.* (2020) 95:472–82. doi: 10.1002/ajh.25753
4. Chonat S, Eber SW, Holzhauer S, Kollmar N, Morton DH, Glader B, et al. Pyruvate kinase deficiency in children. *Pediatr Blood Cancer.* (2021) 68:e29148. doi: 10.1002/pbc.29148
5. Grace RF, Barcellini W. Management of pyruvate kinase deficiency in children and adults. *Blood.* (2020) 136:1241–9. doi: 10.1182/blood.2019000945
6. van Beers EJ, van Straaten S, Morton DH, Barcellini W, Eber SW, Glader B, et al. Prevalence and management of iron overload in pyruvate kinase deficiency: report from the Pyruvate Kinase Deficiency Natural History Study. *Haematologica.* (2019) 104:e51–3. doi: 10.3324/haematol.2018.196295
7. Jumper J, Evans R, Pritzel A, Green T, Figurnov M, Ronneberger O, et al. Highly accurate protein structure prediction with AlphaFold. *Nature.* (2021) 596:583–9. doi: 10.1038/s41586-021-03819-2
8. Tunyasuvunakool K, Adler J, Wu Z, Green T, Zielinski M, Žídek A, et al. Highly accurate protein structure prediction for the human proteome. *Nature.* (2021) 596:590–6. doi: 10.1038/s41586-021-03828-1
9. Zanella A, Fermo E, Bianchi P, Chiarelli LR, Valentini G. Pyruvate kinase deficiency: the genotype-phenotype association. *Blood Rev.* (2007) 21:217–31. doi: 10.1016/j.blre.2007.01.001
10. Minucci A, Ricerca BM, Tripodi D, Matarazzo L, De Michele T, Giardina B, et al. Worsening of the clinical-hematological picture in a patient with a rare PK-LR compound heterozygosis after mitral replacement. *Clin Biochem.* (2011) 44:1261–3. doi: 10.1016/j.clinbiochem.2011.07.007
11. Grace RF, Bianchi P, van Beers EJ, Eber SW, Glader B, Yaish HM, et al. Clinical spectrum of pyruvate kinase deficiency: data from the Pyruvate Kinase Deficiency Natural History Study. *Blood.* (2018) 131:2183–92. doi: 10.1182/blood-2017-10-810796
12. Wahl S, Vichinsky E. Pulmonary hypertension in hemolytic anemias. *F1000 Med Rep.* (2010) 2:10. doi: 10.3410/m2-10
13. Delannoy E, Courtois A, Freund-Michel V, Leblais V, Marthan R, Muller B. Hypoxia-induced hyperreactivity of pulmonary arteries: role of cyclooxygenase-2, isoprostanes, and thromboxane receptors. *Cardiovasc Res.* (2010) 85:582–92. doi: 10.1093/cvr/cvp292
14. Hansen R, Gibson S, De Paiva Alves E, Goddard M, MacLaren A, Karcher AM, et al. Adaptive response of neonatal sepsis-derived Group B *Streptococcus* to bilirubin. *Sci Rep.* (2018) 8:6470. doi: 10.1038/s41598-018-24811-3
15. Raphaël MF, Van Wijk R, Schweizer JJ, Schouten-van Meeteren NA, Kindermann A, van Solinge WW, et al. Pyruvate kinase deficiency associated with severe liver dysfunction in the newborn. *Am J Hematol.* (2007) 82:1025–8. doi: 10.1002/ajh.20942

Conflict of Interest: The authors declare that the research was conducted in the absence of any commercial or financial relationships that could be construed as a potential conflict of interest.

Publisher's Note: All claims expressed in this article are solely those of the authors and do not necessarily represent those of their affiliated organizations, or those of the publisher, the editors and the reviewers. Any product that may be evaluated in this article, or claim that may be made by its manufacturer, is not guaranteed or endorsed by the publisher.

frontiers | Frontiers in Cardiovascular Medicine

CASE REPORT
published: 09 June 2022
doi: 10.3389/fcvm.2022.918832

An Atypical Anomalous Aortic Origin of the Left Coronary Artery With Intra-Arterial Wall Course Pretending a Normal Migration on Imaging Screening: A Case Report

Fan Hu†, Xinyue Wang†, Jiaojiao Wan†, Yifei Li†, Tao Wang, Kaiyu Zhou, Xiaoqing Shi, Zhongqiang Liu, Jie Fang and Yimin Hua**

Key Laboratory of Birth Defects and Related Diseases of Women and Children of MOE, State Key Laboratory of Oral Diseases, Department of Pediatrics, National Clinical Research Center for Oral Diseases, West China Second University Hospital, West China Hospital of Stomatology, Sichuan University, Chengdu, China

OPEN ACCESS

Edited by:
Alvise Guariento,
University of Toronto, Canada

Reviewed by:
Shagun Sachdeva,
Baylor College of Medicine, United States
Yi-Gang Li,
Shanghai Jiao Tong University, China

***Correspondence:**
Jie Fang
jiefangscu@qq.com
Yimin Hua
Nathan_hua@163.com

† These authors have contributed equally to this work

Specialty section:
This article was submitted to Pediatric Cardiology, a section of the journal Frontiers in Cardiovascular Medicine

Received: *12 April 2022*
Accepted: *26 May 2022*
Published: *09 June 2022*

Citation:
Hu F, Wang X, Wan J, Li Y, Wang T, Zhou K, Shi X, Liu Z, Fang J and Hua Y (2022) An Atypical Anomalous Aortic Origin of the Left Coronary Artery With Intra-Arterial Wall Course Pretending a Normal Migration on Imaging Screening: A Case Report. Front. Cardiovasc. Med. 9:918832. doi: 10.3389/fcvm.2022.918832

Background: An anomalous aortic origin of a coronary artery (AAOCA) has been considered as a dominant cause of sudden cardiac death (SCD) among young age children. Therefore, it is critical to identify AAOCA timely to avoid lethal events. Recently, accumulating cases of right or left coronary arteries originating from inappropriate locations at the sinus of Valsalva have been identified. Here, we report a rare case of AAOCA with an intra-arterial wall course pretending normal migration on imaging screening in a patient who suffered from syncope.

Case summary: A 7-year-old male without a previous history of cardiovascular and cerebrovascular diseases suddenly suffered from sharp chest pain and syncope after intensive exercise. The electrocardiogram showed that the ST segment of multiple leads was depressed by more than 0.05 mV, and biomarkers indicated severe myocardial injuries. The left ventricular ejection fraction (LVEF) decreased dramatically to 23%. Fulminant myocarditis and cardiomyopathy were therefore excluded. However, a relatively normal coronary artery origin, which arose from the left coronary sinus, presented on echocardiography and cardiac CT angiography (CTA). It is difficult to draw an association between severe clinical manifestations and slight malformations on echocardiography and CTA. Furthermore, selective coronary angiography revealed that an anomalous left coronary artery arose from the superior margin of the inappropriate sinus, developed an intramural wall course and finally exits the left sinus of Valsalva and migrated between the aorta and the pulmonary artery, which induced severe myocardial infarction during exercise. Then, the patient received surgical correction with a modified unroofing procedure. After 2 months of intensive treatment, the patient was discharged and remained asymptomatic through 18 months of follow-up.

Conclusion: AAOCA, especially anomalous left coronary artery (ALCA), represents a major potential risk of SCD. We reported an atypical manifestation of ALCA arising from

the inappropriate sinus of Valsalva and merging into the intra-arterial wall to develop a strange course and then sprout between the aorta and the pulmonary artery. The diversity of AAOCA might present as a relatively normal course under non-invasive radiological imaging scanning.

Keywords: anomalous aortic origin of a coronary artery, non-coronary sinus of valsalva, intra-arterial wall course, syncope, case report

INTRODUCTION

Congenital anatomical variation of the coronary artery can be classified as abnormalities of coronary artery origin, course, destination, and various vessels (1). Due to the complex phenotypes of congenital coronary artery malformation, various clinical manifestations can be observed. Some types of malformations can be recognized as benign variations, as coronary artery perfusion and circulation maintain physiological function. Adverse outcomes occur at a low incidence. However, in some cases of coronary artery malformation lead to severe myocardial ischemia and result in recurrent syncope and even sudden cardiac death (SCD) (2, 3). Moreover, anomalous aortic origin of a coronary artery (AAOCA) has been considered as a dominant cause of SCD at a young age (4–6). Therefore, it is critical to identify AAOCA timely to avoid lethal events.

Recently, several cases of right or left coronary arteries originating from inappropriate locations at the sinus of Valsalva have been reported. Generally, the majority of patients with anomalous left coronary artery (ALCA), which originates from the sinus of Valsalva, demonstrated poor prognosis, especially for those patients who suffered from an interarterial segment coursing between the aorta and the pulmonary artery, predicting a relatively high incidence of syncope, myocardial infarction and SCD (7, 8). With the application of CT angiography (CTA) and cardiac MRI scanning, a greater proportion of ALCA can be identified with non-invasive protocols (9). The guidelines for adult treatment of congenital heart disease issued by the American Cardiology Association (ACC) and the American Heart Association (AHA) point out that the treatment for all patients with left coronary arteries originating from the inappropriate coronary sinus and abnormal course between the aorta and the pulmonary artery should be surgical revascularization as early as possible (10). Unfortunately, AAOCA is often misdiagnosed as fulminant myocarditis or cardiomyopathy. Therefore, the rapid and accurate diagnosis of AAOCA is associated with advanced prognosis for such patients to avoid SCD.

Here, we report a rare case of AAOCA with an intramural course pretending normal migration on imaging screening who suffered syncope and SCD. This patient presented a relatively normal coronary artery migration on echocardiography. Furthermore, CTA demonstrated significant dysplasia of the left coronary artery, but it remained in the typical course. Besides, electrocardiogram (EKG) and cardiac MRI revealed severe myocardial ischemia. Finally, transcatheter angiography for the coronary artery was performed to identify an intramural course of left coronary artery and exits the left sinus of Valsalva, giving the impression of normal origin by echocardiography.

CASE PRESENTATION

Ethical Compliance

This report was approved by the Ethics Committee of the West China Second Hospital of Sichuan University (approval number 2014-034). Informed consent was obtained from the patient's parents prior to performing whole exon sequencing and for the inclusion of the patient's clinical and imaging details in subsequent publications.

History of Illness

A 7-year-old boy suddenly suffered sharp chest pain and syncope during athletic training of fast-running for 5 min. Timely cardiopulmonary resuscitation (CPR) was performed by the coach before the arrival of ambulance. The patient was transferred to our cardiac intensive care unit within 30 min. The patient denied any history of past cardiovascular and cerebrovascular illness. His parents also had no positive and related family history of arrhythmia, cardiomyopathy, congenital heart disease or coronary artery diseases. However, when systematically reviewing his past illness history, we found several transient manifestations of dizziness and amaurosis during exercise in the most recent year.

Physical, Laboratory, Imaging Examination, and Surgical Treatment

The patient presented with severe cardiac dysfunction with NYHA class IV heart function. The initial EKG measurement at hospital administration showed global ST segment depression of leads II, III, aVF, and V3-V6 of more than 0.05 mV and abnormal Q waves (**Figure 1**), which revealed myocardial ischemia. In addition, the serum level of cardiac troponin I (cTnI) was greater than the upper threshold ($>$50.00 μg/L, n.v. $<$0.06 μg/L) and significantly elevated B-type natriuretic peptide (BNP) at 1157.14 pg/mL (n.v. $<$100 pg/mL). Fulminant myocarditis was ruled out based on negative results for all tests for suspected virus and EKG changes. Echocardiography demonstrated a normal cardiac structure with a mildly enlarged left ventricle. However, his left ventricular ejection fraction (LVEF) decreased dramatically to 23% (**Figure 2A**). Unfortunately, there was no evidence of myocardial hypertrophy, pathological ventricular dilatation, or restriction of cardiac diastolic movements. Therefore, there was no convincing evidence for a diagnosis of cardiomyopathy.

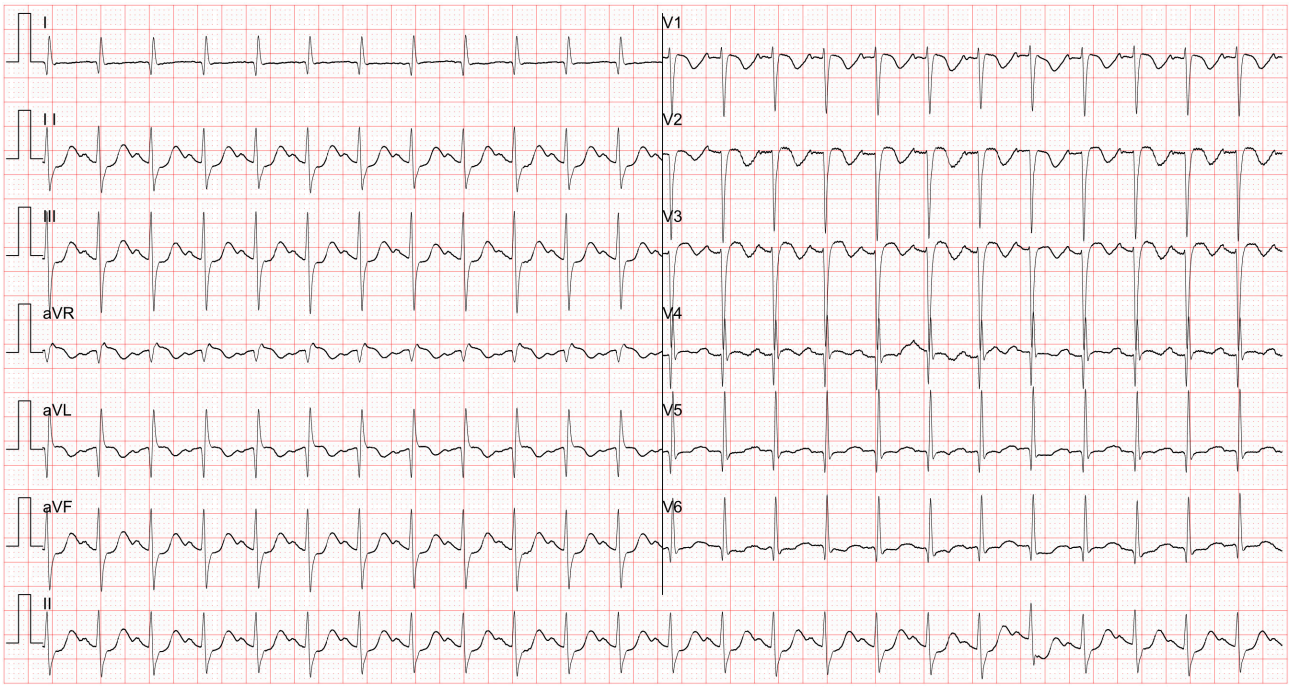

FIGURE 1 | The electrocardiogram global ST segment depression of leads II, III, aVF and V3-V6 was more than 0.05 mV, and abnormal Q waves were observed.

According to the diagnostic flow chart for SCD and myocardial ischemia, any malformation of the coronary artery was suspected. Therefore, echocardiography was used to scan the origins of the right and left coronary arteries. In these images, the right coronary artery clearly presented with normal formation and lumen diameter (**Figure 2B**). The origin and course of the left coronary artery seemed to be normal, presenting a slightly narrowed lumen diameter (**Figure 2C**). However, Doppler demonstrated non-continuous blood flow in the left coronary artery (**Figure 2D**), which indicated dysfunction of the left coronary artery. Vasculitis or dysplasia of coronary arteries was carefully reviewed. Laboratory tests demonstrated normal levels of C-reactive protein, ESR, anti-O-streptolysin, cytokines (including IL2, IL-6, IL-12, and TNF-α) and autoimmune antibodies, which excluded a diagnosis of vasculitis. CTA was performed to determine the overall shape of the left coronary artery. The results of CTA from diverse sections of the heart revealed that the left coronary artery originated from an abnormal location at the superior and posterior sites in the left coronary sinus (**Figure 3A**). Importantly, the CTA images presented dysplasia of the left coronary artery (**Figures 3B–D**). So that, ALCA-induced coronary artery dysplasia had been suspected. Furthermore, cardiac MRI demonstrated significant myocardial ischemia and fibrosis in the left ventricular wall (**Figure 3E**).

To further validate the results obtained from CTA, transcatheter angiography was performed. Angiography at the root of the aorta showed that the right coronary artery could be perfused with contrast agent, but the left coronary artery was missing (**Figure 4A**). Selective right coronary artery angiography demonstrated a dilated right coronary artery (**Figure 4B**). Delay radiological exposure revealed that the left ventricle could be supplied by the right coronary artery, which was considered right coronary artery-dependent left coronary artery circulation (**Figure 4C**). Compared to the CTA images, angiography illustrated the left coronary artery originated from the non-coronary sinus (**Figure 4D**). However, a strange curve, such as migration of the origin of the left coronary artery, was observed by angiography at a superior location (**Figure 4E**). Then, the left coronary artery could be perfused as an extremely low volume (**Figure 4F**). Thus, we suspected that the left coronary artery originated from the non-coronary sinus with a long intramural course exits the left sinus of Valsalva, giving the impression of normal origin by echocardiography.

After that, the patient immediately received surgical correction with a modified unroofing procedure. AAOCA from the non-coronary sinus of Valsalva with an initial intramural segment was diagnosed intraoperatively as well, which matched our suspicion based on angiography. The intramural wall segment finally exited from the margin of the left-right-coronary sinus, generated a sharp angle and coursed between the aorta and the pulmonary artery with general severe stenosis, resulting in severe coronary artery dysplasia (**Figure 4G**). After surgery, aspirin, diuretics and angiotensin-converting enzyme inhibitors were administered for a long time. Cardiac MRI post-surgery presented a normal myocardial perfusion (**Figure 3F**).

Molecular Results

To exclude any genetic mutation-induced cardiomyopathy or syndrome, whole exon sequencing (WES) was performed.

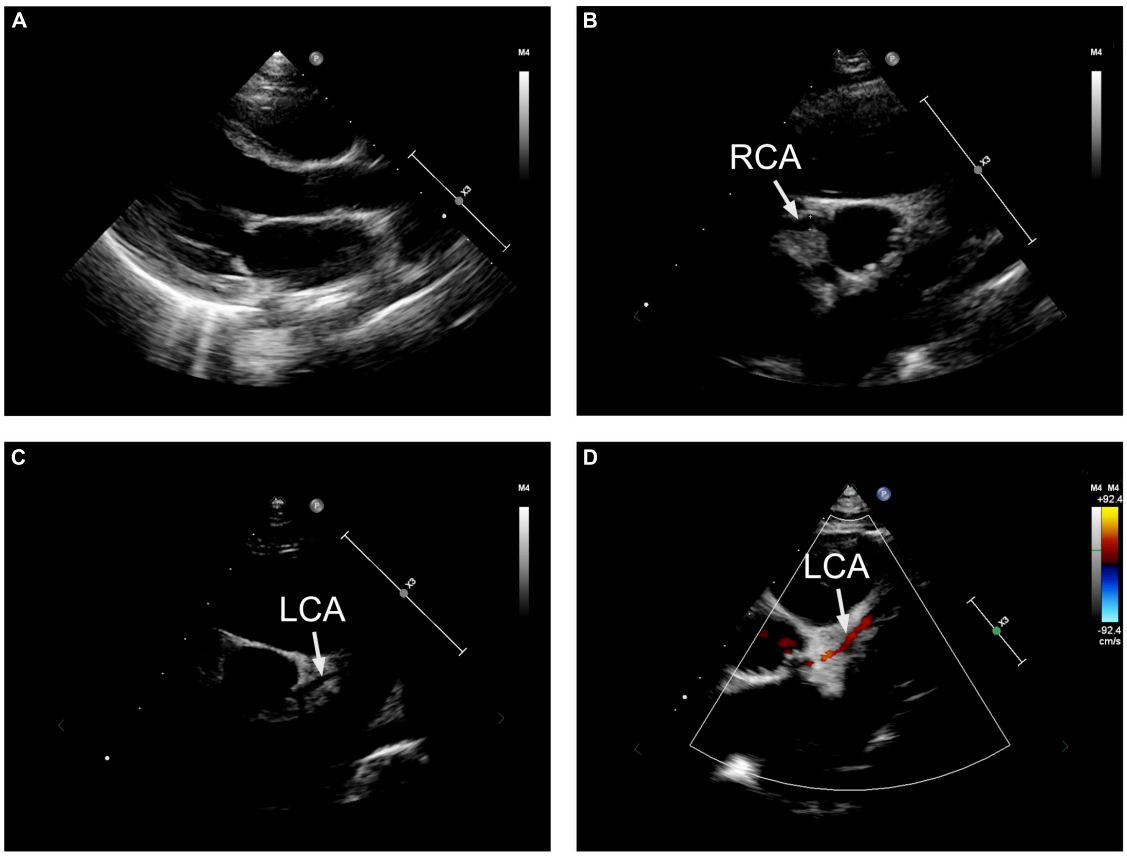

FIGURE 2 | The echocardiographic presentation. **(A)** Left ventricular ejection fraction (LVEF) decreased dramatically to 23%. **(B)** The right coronary artery presented clearly with normal formation and lumen diameter. **(C)** The origin and course of the left coronary artery seemed to be normal, with a related narrowed lumen diameter. **(D)** Doppler demonstrated a non-continuous blood flow in the left coronary artery. RCA, right coronary artery; LCA, left coronary artery.

A peripheral blood sample was obtained from the patient in an ethylenediaminetetraacetic acid anticoagulant blood sample tube and then stored at 4°C for less than 6 h. DNA was extracted using the Blood Genome Column Medium Extraction Kit (Tiangen Biotech, Beijing, China) in accordance with the manufacturer's instructions. Protein-coding exome enrichment was performed using the xGen Exome Research Panel v.1.0. Whole exon sequencing was performed using the NovaSeq 6000 platform (Illumina, San Diego, CA, United States), and the raw data were processed using FastP to remove adapters and filter out low-quality reads. Paired-end reads were aligned to the Ensembl GRCh38/hg38 reference genome using the Burrows–Wheeler Aligner. Variant annotation was performed in accordance with database-sourced minor allele frequencies (MAFs) and practical guidelines on pathogenicity issued by the American College of Medical Genetics. The annotation of MAFs was performed based on the 1,000 Genomes, dbSNP, ESP, ExAC, Provean, Sift, Polypen2_hdiv, Polypen2_hvar, and Chigene in-house MAF databases using R software (R Foundation for Statistical Computing, Vienna, Austria). After retrieving all the potential variants based on WES, there was no identical genic mutation related to his clinical phenotype identified, and the patient was negative for any proven cardiomyopathy or familial inheritance of arrhythmia-associated mutations. Additionally, potential metabolic disorders were also excluded by the WES analysis.

Outcome and Follow-Up

After 1 month of intensive care and positive treatment, the patient was discharged and remained asymptomatic for myocardial ischemia. However, cardiac function could not recover to normal levels, and follow-up echocardiography demonstrated a drop in LVEF of 40–45%. During his 18-month follow-up, the patient was engaged in slight and mild exercise only. The markers of myocardial injuries recovered gradually, and the ST segment of EKG returned to baseline level. Furthermore, myocardial fibrosis was terminated according to the cardiac MRI scanning at 1 year post operation.

DISCUSSION

Cardiogenic syncope is one of the most dangerous presentations, which leads to high potential onset of SCD, threatening healthy outcomes among high-risk populations. Genetic and environmental factors are identified to be involved in

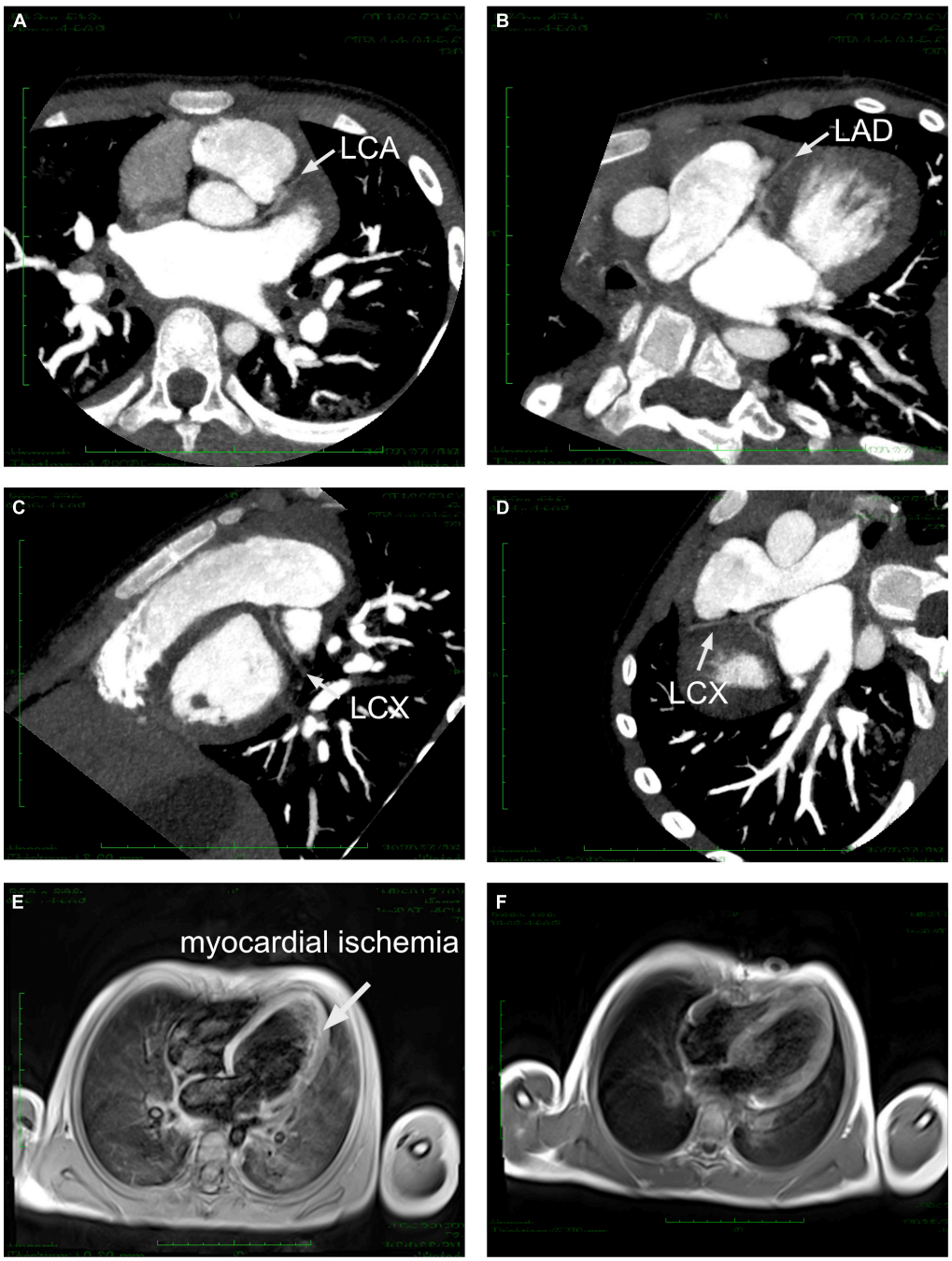

FIGURE 3 | Cardiac CTA and MRI imaging. **(A)** Left coronary artery originated from an abnormal location at the superior and posterior sites in the left coronary sinus. **(B–D)** LAD and LCX demonstrated severe dysplasia under several sections of CTA. **(E)** Cardiac MRI demonstrated significant myocardial ischemia and fibrosis in the left ventricular wall before surgical correction. **(F)** Cardiac MRI image after surgical correction revealed a normal perfusion. LCA, left coronary artery; LAD, left anterior descending; LCX, left circumflex.

the events of syncope or SCD attacks. Typically, critical arrhythmia, hypertrophic cardiomyopathy, congenital heart malformation and congenital or required coronary artery disease are significantly associated with attacks of SCD (11). In an autopsy study of college athletes who suffered SCD, congenital coronary artery malformation was the top identified reason responding for this adverse event (12). Therefore, AAOCA should be considered in young patients with unexplained as the top cause.

Traditionally, congenital anatomical variation of the coronary artery can be classified as abnormalities of coronary artery origin, course, destination, and various vessels. AAOCA generally

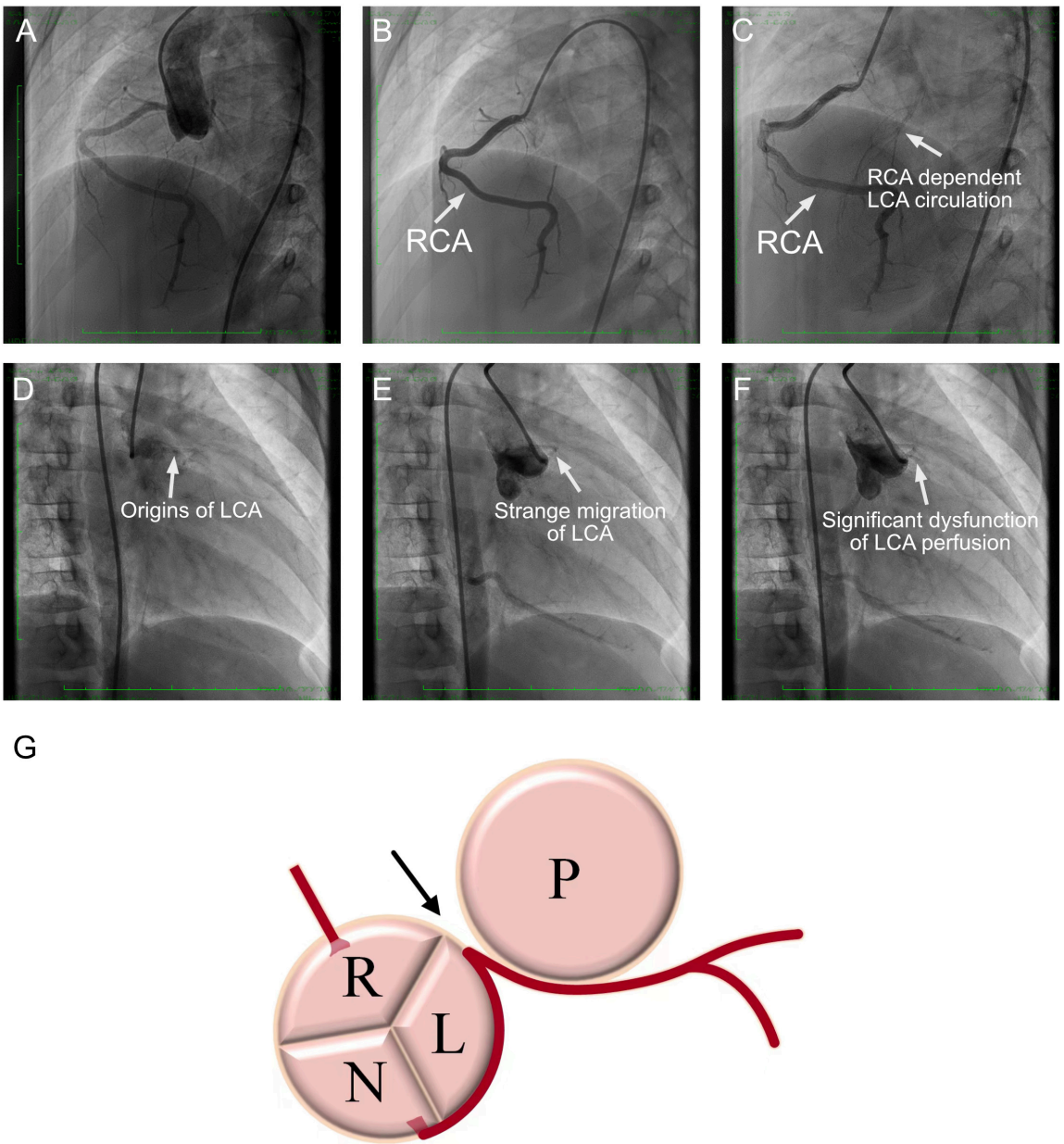

FIGURE 4 | Coronary angiography images. **(A)** Angiography at the root of the aorta. The right coronary artery could be perfused with contrast agent, but the left coronary artery was missing. **(B)** Selective right coronary artery angiography demonstrated a dilated right coronary artery. **(C)** Delay radiological exposure revealed that the left ventricle could be supplied by the right coronary artery, which was considered the right coronary artery-dependent left coronary artery circulation. **(D)** The angiography failed to illustrate the left coronary artery in the left coronary sinus. **(E)** A strange curve-like migration of the origin of the left coronary artery by angiography at a superior location. **(F)** Then, the left coronary artery could be perfused at an extremely low volume. **(G)** Anatomic aspect of the axial section of aortic and pulmonary valves and left coronary artery arising from the non-coronary sinus of Valsalva with an intramural segment course. RCA, right coronary artery; LCA, left coronary artery; R, right coronary sinus; L, left coronary sinus; N, non-coronary sinus; P, pulmonary artery.

refers to a kind of congenital coronary artery malformation in which the left or right coronary artery fails to originate normally from the corresponding aortic sinus, with or without an intramural course (13). AAOCA is caused by the deviation of the arterial trunk separation in the embryonic stage and the abnormal development or incomplete development of the coronary artery (14). While most coronary anomalies are benign, among AAOCA subtypes, ALCA arising at or above the right sinus of Valsalva with an intramural course between the aorta and the pulmonary artery has been commonly considered the most fatal type in prior studies (15–17). In addition, the existing angle between the coronary ostium and proximal segment has also been emphasized as a crucial risk factor in SCDs (18). The most common pathogenic mechanisms of coronary dysfunction

related to the intramural coronary course are identified as variable lateral compression and stenosis inside the aortic tunica media (19). This compression can present at the rest stage or display when performing intensive exercise. However, the formation of lateral branches that originate from the "right" coronary artery can improve compensatory circulation, rescue the ischemic regions, and relieve symptoms. Sometimes, functional compensation for a healthy coronary artery causes delayed diagnosis and surgical treatment for AAOCA. The failure to diagnose AAOCA leads to recurrent attacks of syncope, resulting in irreversible myocardial ischemia and SCD. Moreover, AAOCA can be easily misdiagnosed as fulminant myocarditis or cardiomyopathy without detailed coronary artery-based radiographic examination. Therefore, it is challenging to identify AAOCA patients early.

Currently, individuals who are suspected with AAOCA are recommended to undergo transthoracic echocardiography, non-invasive coronary CTA and cardiac MRI. The combination of several imaging strategies is reasonable to better screen the coronary artery anatomy and to achieve an accurate diagnosis in children (20). In most cases, coronary CTA can identify the location of the anomalous origin, details of the intra-arterial segment, and the angle between the coronary ostium and proximal segment (21, 22). Cardiac MRI has the advantages of providing coronary artery and functional imaging, particularly in evaluating the area and severity of myocardial infarction, and illustrating the course of coronary arteries in most patients (23). Moreover, transcatheter angiography could provide an adjunct to determine the detailed coronary artery anomalies. However, it is an invasive examination, which limits its application as a routine method, as CTA and cardiac MRI might achieve the imaging goal in most cases. In this case, the combination of coronary CTA and cardiac MRI (non-invasive protocol) failed to demonstrate the accurate origin and course of the left coronary artery due to the extreme severity of intramural stenosis and the unique coronary existing. Therefore, non-invasive examination could not identify the real reason for myocardial ischemic attack. On this occasion, more reliable measurements of intramural segments were obtained by transcatheter angiography (invasive protocol), which is the most recommended method of classifying the anatomical structure and severity of AAOCA, and benefit the strategy design for surgical treatment.

Therefore, proper selection for non-invasive and invasive protocols is critical for coronary anatomic and functional evaluation. Early recognition and intervention could reduce malignant events. The unroofing technique has been confirmed as a safe and reliable surgical method for ALCA (24, 25). However, how to treat asymptomatic patients with incidental findings of ALCA from the opposite sinus with an inter-arterial course is still controversial. Avoiding strenuous activity is recommended in all left coronary arteries originating from the inappropriate coronary sinus, and surgical revascularization should be performed as early as possible in symptomatic cases before transient dizziness and amaurosis frequently appear during exercise, as these symptoms imply an intramural or inter-arterial course between the aorta and the pulmonary artery, with or without a narrow angle between the coronary ostium and proximal segment.

CONCLUSION

In summary, AAOCA, especially ALCA, presented a major potential risk of SCD. Here, we report an atypical manifestation of ALCA arising from the inappropriate sinus of Valsalva and merging into the intramural to develop a strange course and then sprouting between the aorta and the pulmonary artery. However, normal echocardiography and CTA failed to reveal malformation of the left coronary artery. Finally, angiography and observation during surgical treatment both confirmed this diagnosis. Therefore, the diversity of AAOCA might result in a relatively normal course under non-invasive radiological imaging scanning. Further angiography would be necessary for significant separation between clinical manifestations and imaging tests.

DATA AVAILABILITY STATEMENT

The datasets for this article are not publicly available due to concerns regarding participant/patient anonymity. Requests to access the datasets should be directed to the corresponding authors.

ETHICS STATEMENT

This study was approved by the Ethics Committee of West China Second Hospital of Sichuan University (2014-034). Written informed consent to participate in this study was provided by the participants' legal guardian/next of kin. Written informed consent was obtained from the individual(s), and minor(s)' legal guardian/next of kin, for the publication of any potentially identifiable images or data included in this article.

AUTHOR CONTRIBUTIONS

YL, FH, YH, KZ, XS, ZL, and TW were the patient's physicians. JW and JF reviewed the literature and contributed to manuscript drafting. YL and JF performed the mutation analysis. JF and YH conceptualized and designed the study, coordinated and supervised the data collection, and critically reviewed the manuscript for important intellectual content, were responsible for the revision of the manuscript for important intellectual content. All authors issued final approval for the version to be submitted.

FUNDING

This work was supported by grants from the Technology Project of Sichuan Province of China (2019YFS0241, 2020YFS0102, 2020YFS0110, and 2021YFQ0061) and the Central Government Funds of Guiding Local Scientific and Technological Development for Sichuan Province (2021ZYD0105).

REFERENCES

1. Jacobs ML, Mavroudis C. Anomalies of the coronary arteries: nomenclature and classification. *Cardiol Young.* (2010) 20:15–9. doi: 10.1017/S1047951110001046
2. Poynter JA, Williams WG, McIntyre S, Brothers JA, Jacobs ML, Congenital Heart Surgeons Society AAOCA Working Group. Anomalous aortic origin of a coronary artery: a report from the congenital heart surgeons society registry. *World J Pediatr Congenit Heart Surg.* (2014) 5:22–30. doi: 10.1177/2150135113516984
3. Alsalehi M, Jeewa A, Wan A, Contreras J, Yoo SJ, Laks JA. A case series of left main coronary artery ostial atresia and a review of the literature. *Congenit Heart Dis.* (2019) 14:901–23. doi: 10.1111/chd.12842
4. Meyer L, Stubbs B, Fahrenbruch C, Maeda C, Harmon K, Eisenberg M, et al. Incidence, causes, and survival trends from cardiovascular-related sudden cardiac arrest in children and young adults 0 to 35 years of age: a 30-year review. *Circulation.* (2012) 126:1363–72. doi: 10.1161/CIRCULATIONAHA.111.076810
5. Pilmer CM, Kirsh JA, Hildebrandt D, Krahn AD, Gow RM. Sudden cardiac death in children and adolescents between 1 and 19 years of age. *Heart Rhythm.* (2014) 11:239–45. doi: 10.1016/j.hrthm.2013.11.006
6. Maron BJ, Haas TS, Ahluwalia A, Rutten-Ramos SC. Incidence of cardiovascular sudden deaths in Minnesota high school athletes. *Heart Rhythm.* (2013) 10:374–7. doi: 10.1016/j.hrthm.2012.11.024
7. Garcia-Arribas D, Olmos C, Higueras J, Marcos-Alberca P, de la Pedraja I, Garcia-Bouza M. Anomalous origin of left coronary artery with intramural aortic course causing symptoms in a teenaged athlete. *Texas Heart Inst J.* (2020) 47:165–7. doi: 10.14503/THIJ-16-5771
8. Doan TT, Zea-Vera R, Agrawal H, Mery CM, Masand P, Reaves-O'Neal DL, et al. Myocardial ischemia in children with anomalous aortic origin of a coronary artery with intraseptal course. *Circ Cardiovasc Interv.* (2020) 13:e008375. doi: 10.1161/CIRCINTERVENTIONS.119.008375
9. Cheezum MK, Liberthson RR, Shah NR, Villines TC, O'Gara PT, Landzberg MJ, et al. Anomalous aortic origin of a coronary artery from the inappropriate sinus of Valsalva. *J Am Coll Cardiol.* (2017) 69:1592–608.
10. Stout KK, Daniels CJ, Aboulhosn JA, Bozkurt B, Broberg CS, Colman JM, et al. 2018 AHA/ACC guideline for the management of adults with congenital heart disease: executive summary: a report of the American college of cardiology/American heart association task force on clinical practice guidelines. *J Am Coll Cardiol.* (2019) 73:1494–563.
11. Dalal A, Czosek RJ, Kovach J, von Alvensleben JC, Valdes S, Etheridge SP, et al. Clinical presentation of pediatric patients at risk for sudden cardiac arrest. *J Pediatr.* (2016) 177:191–6. doi: 10.1016/j.jpeds.2016.06.088
12. Harmon KG, Drezner JA, Maleszewski JJ, Lopez-Anderson M, Owens D, Prutkin JM, et al. Pathogeneses of sudden cardiac death in national collegiate athletic association athletes. *Circ Arrhythm Electrophysiol.* (2014) 7:198–204. doi: 10.1161/CIRCEP.113.001376
13. Finocchiaro G, Behr ER, Tanzarella G, Papadakis M, Malhotra A, Dhutia H, et al. Anomalous coronary artery origin and sudden cardiac death: clinical and pathological insights from a national pathology registry. *JACC Clin Electrophysiol.* (2019) 5:516–22. doi: 10.1016/j.jacep.2018.11.015
14. Pérez-Pomares JM, de la Pompa JL, Franco D, Henderson D, Ho SY, Houyel L, et al. Congenital coronary artery anomalies: a bridge from embryology to anatomy and pathophysiology–a position statement of the development, anatomy, and pathology ESC working group. *Cardiovasc Res.* (2016) 109:204–16. doi: 10.1093/cvr/cvv251
15. Osaki M, McCrindle B, Van Arsdell G, Dipchand A. Anomalous origin of a coronary artery from the opposite sinus of Valsalva with an interarterial course: clinical profile and approach to management in the pediatric population. *Pediatr Cardiol.* (2008) 29:24–30. doi: 10.1007/s00246-007-9054-6
16. Opolski MP, Pregowski J, Kruk M, Witkowski A, Kwiecinska S, Lubienska E, et al. Prevalence and characteristics of coronary anomalies originating from the opposite sinus of Valsalva in 8,522 patients referred for coronary computed tomography angiography. *Am J Cardiol.* (2013) 111:1361–7. doi: 10.1016/j.amjcard.2013.01.280
17. Angelini P. Congenital coronary artery ostial disease: a spectrum of anatomic variants with different pathophysiologies and prognoses. *Texas Heart Inst J.* (2012) 39:55–9.
18. Kaushal S, Backer CL, Popescu AR, Walker BL, Russell HM, Koenig PR, et al. Intramural coronary length correlates with symptoms in patients with anomalous aortic origin of the coronary artery. *Ann Thorac Surg.* (2011) 92:986–92. doi: 10.1016/j.athoracsur.2011.04.112
19. Angelini P, Uribe C. Anatomic spectrum of left coronary artery anomalies and associated mechanisms of coronary insufficiency. *Catheter Cardiovasc Interv.* (2018) 92:313–21. doi: 10.1002/ccd.27656
20. Brothers JA, Frommelt MA, Jaquiss RD, Myerburg RJ, Fraser CD, Tweddell JS. Expert consensus guidelines: anomalous aortic origin of a coronary artery. *J Thorac Cardiovasc Surg.* (2017) 153:1440–57. doi: 10.1016/j.jtcvs.2016.06.066
21. Frommelt P, Lopez L, Dimas VV, Eidem B, Han BK, Ko HH, et al. Recommendations for multimodality assessment of congenital coronary anomalies: a guide from the American society of echocardiography: developed in collaboration with the society for cardiovascular angiography and interventions, Japanese society of echocardiography, and society for cardiovascular magnetic resonance. *J Am Soc Echocardiogr.* (2020) 33:259–94. doi: 10.1016/j.echo.2019.10.011
22. Malone LJ, Morin CE, Browne LP. Coronary computed tomography angiography in children. *Pediatr Radiol.* (2021). [Epub ahead of print]. doi: 10.1007/s00247-021-05209-2
23. Rajiah P, Setser RM, Desai MY, Flamm SD, Arruda JL. Utility of free-breathing, whole-heart, three-dimensional magnetic resonance imaging in the assessment of coronary anatomy for congenital heart disease. *Pediatr Cardiol.* (2011) 32:418–25. doi: 10.1007/s00246-010-9871-x
24. Sachdeva S, Frommelt MA, Mitchell ME, Tweddell JS, Frommelt PC. Surgical unroofing of intramural anomalous aortic origin of a coronary artery in pediatric patients: single-center perspective. *J Thorac Cardiovasc Surg.* (2018) 155:1760–8. doi: 10.1016/j.jtcvs.2017.11.003
25. Mery CM, De León LE, Molossi S, Sexson-Tejtel SK, Agrawal H, Krishnamurthy R, et al. Outcomes of surgical intervention for anomalous aortic origin of a coronary artery: a large contemporary prospective cohort study. *J Thorac Cardiovasc Surg.* (2018) 155:305–19.e4. doi: 10.1016/j.jtcvs.2017.08.116

Conflict of Interest: The authors declare that the research was conducted in the absence of any commercial or financial relationships that could be construed as a potential conflict of interest.

frontiers | Frontiers in Pediatrics

CASE REPORT
published: 17 June 2022
doi: 10.3389/fped.2022.909595

An Adolescent Patient With Idiopathic Pulmonary Arterial Hypertension Weaned Off Intravenous Epoprostenol Following Treatment With Selexipag: A Case Report

*Ayako Chida-Nagai, Takao Tsujioka, Daisuke Sasaki, Gaku Izumi, Hirokuni Yamazawa and Atsuhito Takeda**

Department of Pediatrics, Hokkaido University Hospital, Sapporo, Japan

Idiopathic pulmonary arterial hypertension (PAH) is a rare, progressive disease affecting the pulmonary arteries. Epoprostenol, a synthetic prostaglandin analog, is the most potent pharmacological treatment modality used in patients with PAH. However, it requires continuous intravenous infusion, which negatively impacts the patient's quality of life and frequently results in complications, such as catheter-related bloodstream infection. We weaned an adolescent female patient off epoprostenol by gradually introducing oral selexipag over a sustained period, following many years of continuous intravenous epoprostenol use alone. Oral selexipag might have an efficacy comparable to epoprostenol in young patients with PAH.

Keywords: pulmonary arterial hypertension, epoprostenol, drug transition, adolescence, selexipag

OPEN ACCESS

Edited by:
Cecile Tissot,
Clinique des Grangettes, Switzerland

Reviewed by:
Martin Koestenberger,
Medical University of Graz, Austria
Omar R. J. Tamimi,
King Fahd Medical City, Saudi Arabia

***Correspondence:**
Atsuhito Takeda
a-takeda@med.hokudai.ac.jp

Specialty section:
This article was submitted to Pediatric Cardiology, a section of the journal Frontiers in Pediatrics

Received: *31 March 2022*
Accepted: *25 May 2022*
Published: *17 June 2022*

Citation:
Chida-Nagai A, Tsujioka T, Sasaki D, Izumi G, Yamazawa H and Takeda A (2022) An Adolescent Patient With Idiopathic Pulmonary Arterial Hypertension Weaned Off Intravenous Epoprostenol Following Treatment With Selexipag: A Case Report. Front. Pediatr. 10:909595. doi: 10.3389/fped.2022.909595

INTRODUCTION

An adolescent female patient with idiopathic pulmonary arterial hypertension (PAH) was being treated with epoprostenol; however, the PAH remained severe. When she was 14 years of age, oral selexipag was added to her regimen of epoprostenol, and her condition improved. At the age of 17 years, the patient was weaned off epoprostenol. This method of switching and weaning off has the potential to improve the quality of life of young patients with idiopathic PAH.

CASE PRESENTATION

The patient was born at 41 weeks fetal age by normal vaginal delivery; her birth weight was 3,200 g, and there was no history of neonatal asphyxia. She was apparentlyasymptomatic until the age of 5 years, when, after crying, her face went pale and her level of consciousness transiently decreased. A heart murmur and cough were noted during a medical check-up performed immediately after the event, and she was admitted to our hospital for further investigation. After a thorough examination, including ultrasound cardiography and cardiac catheterization (**Table 1**), she was diagnosed with

TABLE 1 | Cardiac catheterization result at 5 years of age.

PA pressure (mmHg)	85/58 (77)
PA wedge pressure (mmHg)	8
LV (mmHg)	97/EDP11
RV (mmHg)	86/EDP18
RpI (Woods units·m^2)	40.7
C.I. (l/min·m^2)	2.2

EDP, end-diastolic pressure.

idiopathic PAH. She had no family history of PAH. Genetic testing revealed no pathological variants in *BMPR2, ACVRL1, ENG, SMAD9, CAV1, KCNK3,* and *EIF2AK4*, which are the genes responsible for heritable PAH. Although beraprost, sildenafil, and bosentan were administered, her dyspnoea continued to worsen, and she developed pulmonary hypertensive (PH) crisis. Three months after the initial diagnosis, she underwent cardiac catheterization to facilitate the initiation of epoprostenol therapy. When intravenous anesthesia was administered prior to the insertion of the cardiac catheter, she suffered an acute PH crisis again and went into cardiopulmonary arrest. Two days after she was weaned off cardiopulmonary support, a computed tomography scan of the head revealed extensive cerebral infarction. Hypoxic encephalopathy was confirmed, and tracheostomy, central venous (CV) catheter implantation, gastrostomy, as well as Nissen fundoplication were subsequently performed. Thereafter, the patient was transferred to a long-term care facility, where she was followed up with increasing doses of epoprostenol, bosentan, and sildenafil. At the age of 6 years, beraprost was discontinued.

At 11 years of age, she had a catheter-related bloodstream infection and was treated by antibiotics. At 13 years of age, she was switched from sildenafil to tadalafil, owing to tadalafil's longer half-life in comparison to sildenafil and its once-daily-dose effectiveness. Even after increasing the dose of epoprostenol during subsequent outpatient visits, the estimated systolic right ventricular pressure on ultrasound cardiography was comparable to the systolic left ventricular pressure. Therefore, when she was 14 years of age, she was admitted to our hospital, and treatment with selexipag was initiated. After titration of selexipag to 0.8 mg/day, ultrasound cardiography showed that the estimated systolic right ventricular pressure improved to approximately 50% of the systolic left ventricular pressure (**Figure 1**). At the age of 15 years, her CV catheter broke and had to be replaced. At 17 years of age, we increased the dose of selexipag to 2.8 mg/day and decreased the dose of epoprostenol from 31 to 10 ng/kg/min (**Figure 2**). Shortly thereafter, there were two more instances of catheter-related bloodstream infection; thus, we decided to begin the process of weaning her off epoprostenol. After increasing the dose of selexipag to the maximum daily dose (3.2 mg/day), epoprostenol was tapered and discontinued over a period of 2 weeks. After the discontinuation of epoprostenol, the estimated right ventricular pressure as perultrasound cardiography was approximately 60% of the left ventricular pressure (**Figure 2**). The patient had hypoxic encephalopathy and was, thus, unable to complain of headache, jaw pain, or other symptoms. Therefore, it was difficult to

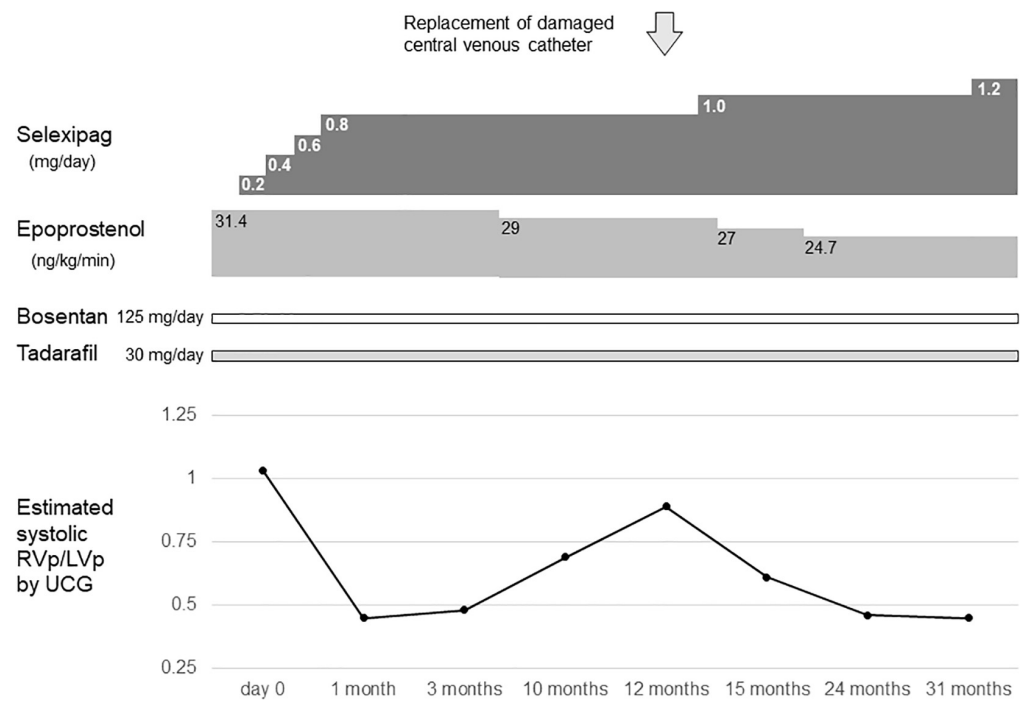

FIGURE 1 | Timeline of selexipag initiation at the age of 14–16 years. Day 0 indicates the day on which selexipag was initiated. RVp, right ventricular pressure; LVp, left ventricular pressure; UCG, ultrasoundcardiography.

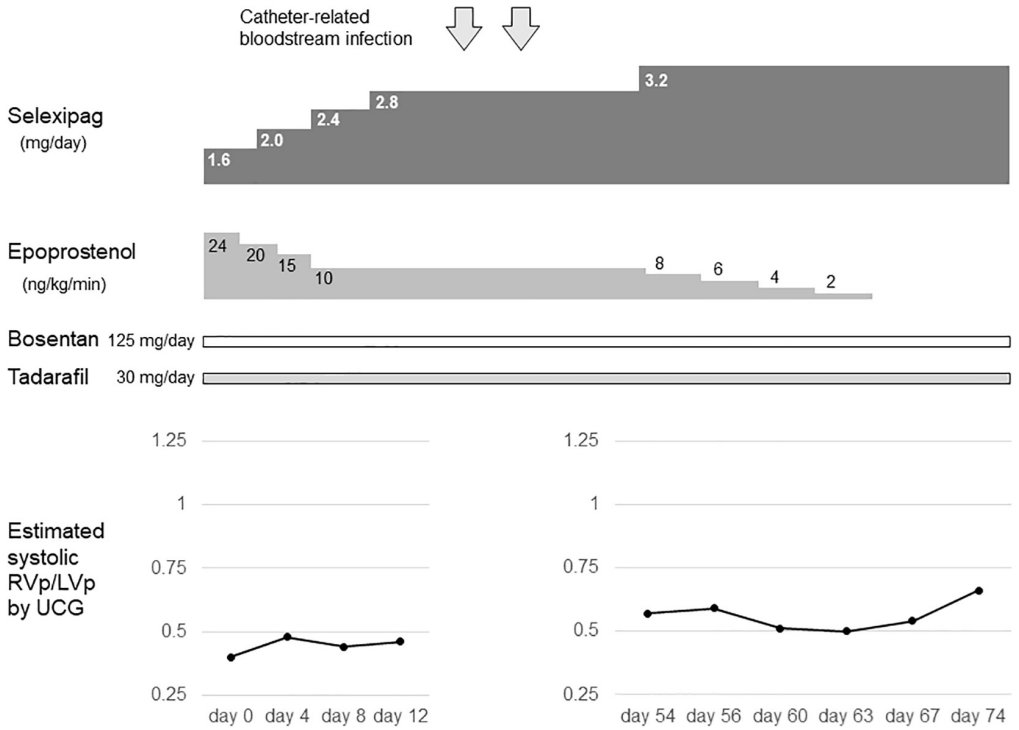

FIGURE 2 | The drug transition timeline at the age of 17 years. Day 0 indicates the day on which the dose of selexipag was increased to 1.6 mg/day. RVp, right ventricular pressure; LVp, left ventricular pressure; UCG, ultrasoundcardiography.

determine whether there were any adverse side effects from increasing the dose of selexipag. However, we proceeded with the drug transition while monitoring her facial expressions, pulse rate, blood pressure, and sleep status, and determined that there were no severe adverse reactions. Brain natriuretic peptide levels in the blood remained below detectable ranges throughout the clinical course.

DISCUSSION

Pulmonary vasodilators used to treat PAH are classified into three types based on their pathway of action: the endothelin pathway, the nitric oxide pathway, and the prostacyclin pathway (1). Epoprostenol was the first prostanoid to be approved as a PAH-specific drug, and many patients have benefited from its use (2). However, due to its short half-life, it requires continuous intravenous infusion. This makes its use restrictive in daily life and, as seen in this case, can lead to complications, such as CV catheter breakage and catheter-related bloodstream infections. Thus, the development of an effective oral PH treatment comparable to epoprostenol is the need of the hour.

Selexipag is a relatively new oral prostacyclin receptor agonist, which was approved for use in Japan in 2016. Its safety and efficacy have been established in pediatric patients with PAH (3, 4).

To our knowledge, our patient is the first adolescent with PAH who was successfully weaned off epoprostenol with the addition of selexipag over a prolonged duration of time. There have been several recent reports regarding this drug transition in adults with PAH (5, 6). We took an extended period of time to carefully transition this patient from her regimen of epoprostenol to stand-alone treatment with selexipag, given that she was a child and suffered from hypoxic encephalopathy. The long-term course of this patient, who has only recently been transitioned to stand-alone selexipag, will need to be closely monitored in the future.

A concern in this case report is that no cardiac catheterization was performed before or after the transition from epoprostenol to selexipag. This is because cardiac catheterization in this patient was prohibited, following the cardiopulmonary arrest that occurred during cardiac catheterization at the age of 5 years; however, frequent ultrasound cardiography was used to safely monitor drug transition.

Herein, the estimated systemic right ventricular pressure on ultrasound cardiography decreased from the time of initial selexipag induction (0.8 mg/day), indicating a sensitive response. It is expected that there will be variability in the response of patients to selexipag. Further investigation is warranted in larger populations, besides the two available pediatric studies (3, 4) to assess the efficacy across a more diverse sample size.

In conclusion, we demonstrated that the transition from epoprostenol to selexipag can be safely performed in an adolescent patient with PAH. The extended duration of transition helps better analyze potential complications and drug response. Individualized assessment of cases is critical to identify patients with PAH in whom this transition is feasible.

DATA AVAILABILITY STATEMENT

The raw data supporting the conclusions of this article will be made available by the authors, without undue reservation.

ETHICS STATEMENT

Ethical review and approval were not required for the study on human participants in accordance with the local legislation and institutional requirements. Written informed consent to participate in this study was provided by the patient's legal guardian. Written informed consent was obtained from the minor' legal guardian for the publication of any potentially identifiable images or data included in this article.

AUTHOR CONTRIBUTIONS

AC-N drafted the manuscript. All authors listed have contributed to the clinical care and management of the patient.

REFERENCES

1. Seferian A, Simonneau G. Therapies for pulmonary arterial hypertension: where are we today, where do we go tomorrow? *Eur Respir Rev.* (2013) 22:217–26. doi: 10.1183/09059180.00001713
2. Sitbon O, VonkNoordegraaf A. Epoprostenol and pulmonary arterial hypertension: 20 years of clinical experience. *Eur Respir Rev.* (2017) 26:160055. doi: 10.1183/16000617.0055-2016
3. Hansmann G, Meinel K, Bukova M, Chouvarine P, Wåhlander H, Koestenberger M. Selexipag for the treatment of children with pulmonary arterial hypertension: first multicenter experience in drug safety and efficacy. *J Heart Lung Transplant.* (2020) 39:695–706. doi: 10.1016/j.healun.2020.03.029
4. Rothman A, Cruz G, Evans WN, Restrepo H. Hemodynamic and clinical effects of selexipag in children with pulmonary hypertension. *Pulm Circ.* (2020) 10:2045894019876545. doi: 10.1177/2045894019876545
5. Saiki C, Kashiwado Y, Yokoyama T, Ayano M, Imabayashi K, Kawano S, et al. Successful transition from intravenous epoprostenol to oral selexipag and inhaled iloprost in a case of severe pulmonary arterial hypertension associated with systemic lupus erythematosus. *Mod Rheumatol Case Rep.* (2022). doi: 10.1093/mrcr/rxac009 [Epub ahead of print].
6. Yanaka K, Guillien A, Soumagne T, Benet J, Piliero N, Picard F, et al. Transition from intravenous epoprostenol to selexipag in pulmonary arterial hypertension: a word of caution. *Eur Respir J.* (2020) 55:1902418 doi: 10.1183/13993003.02418-2019

Conflict of Interest: The authors declare that the research was conducted in the absence of any commercial or financial relationships that could be construed as a potential conflict of interest.

Publisher's Note: All claims expressed in this article are solely those of the authors and do not necessarily represent those of their affiliated organizations, or those of the publisher, the editors and the reviewers. Any product that may be evaluated in this article, or claim that may be made by its manufacturer, is not guaranteed or endorsed by the publisher.

frontiers | Frontiers in Pediatrics

ORIGINAL RESEARCH
published: 05 July 2022
doi: 10.3389/fped.2022.879753

Congenital Anomalous Origin of Coronary Artery Disease in Children With Syncope: A Case Series

*Yumeng Gao†, Qingyou Zhang†, Yan Sun and Junbao Du**

Department of Pediatrics, Peking University First Hospital, Beijing, China

Objective: This study is aimed to analyze the characteristics of congenital anomalous origin of coronary artery in pediatric patients with syncope.

Methods: A total of eight patients were retrospectively analyzed from August 2018 to August 2020 who were admitted to the Peking University First Hospital with the complaint of syncope and were diagnosed with congenital coronary artery disease.

Results: In total, eight patients were included in the study with a median age of 12.5 ± 2.7 (8–16) years. In total, four of them were males, and four were females. Six of the eight patients were diagnosed with right anomalous coronary artery from the opposite sinus (R-ACAOS), while two patients were diagnosed with left anomalous coronary artery from the opposite sinus (L-ACAOS). The most frequent inducement was exercise, and the commonest prodromes were dizziness and blurred vision. Serum cardiac markers and exercise electrocardiography test (EET) were normal in seven of the patients. The majority of cases had abnormal electrocardiograms (ECGs), but only two of them manifested elevated/depressed ST-T segments. In total, seven patients had positive head-up tilt test (HUT). Echocardiography and coronary artery computed tomography angiography (CTA) were performed to aid the diagnosis. Coronary unroofing procedures were conducted in four patients, and none of them reported syncope after the surgery. The other four patients received routine medical treatment for vasovagal-like syncope. In total, two patients out of them became asymptomatic, and in the other two patients, episodes of syncope were reduced, but they still required medical treatment.

Conclusion: Congenital coronary artery anomalies in children with syncope need prompt attention. Though ECG and echocardiography are the common methods for investigating cardiac syncope, they have limited ability to find coronary artery anomalies. When coronary artery anomalies are suspected, coronary CTA should be considered.

Keywords: syncope, pediatric, coronary artery disease, anomalous aortic origin of a coronary artery, bezold-jarisch reflex

OPEN ACCESS

Edited by:
Alvise Guariento,
University of Toronto, Canada

Reviewed by:
Régis Guieu,
Aix Marseille Université, France
Dorota Zyśko,
Wroclaw Medical University, Poland

***Correspondence:**
Junbao Du
junbaodu1@126.com

†These authors have contributed equally to this work and share first authorship

Specialty section:
This article was submitted to Pediatric Cardiology, a section of the journal Frontiers in Pediatrics

Received: *20 February 2022*
Accepted: *06 June 2022*
Published: *05 July 2022*

Citation:
Gao Y, Zhang Q, Sun Y and Du J (2022) Congenital Anomalous Origin of Coronary Artery Disease in Children With Syncope: A Case Series. Front. Pediatr. 10:879753. doi: 10.3389/fped.2022.879753

INTRODUCTION

Syncope is defined as a sudden loss of consciousness caused by global hypoperfusion of the brain (1, 2). Its incidence is 15–25% in children, predominantly occurring in female child (3). The relapse rate of syncope is as high as 33–51% within 5 years (3). Etiologies of transient loss of consciousness in the young include vasovagal syncope (70–80%), psychogenic and unexplained diseases (20%), and cardiovascular diseases (2–3%) (4). Though cardiac syncope comprises a small proportion of

the pediatric syncope, it is often associated with high mortality due to sudden cardiac death (SCD), and hence requires urgent assessment and treatment (5). Cardiac diseases leading to syncope include arrhythmias, cardiac tumors, and structural heart diseases. Structural heart disease is classified into coronary artery anomalies, valvular heart disease, hypertrophic obstructive cardiomyopathy, idiopathic pulmonary hypertension, etc (6, 7). After combining thorough history, physical examination, and ECGs, nearly 50% of the cases can be diagnosed (5). Moreover, echocardiography and Holter-monitoring can contribute to confirming the etiological diagnosis of cardiac syncope. However, some coronary artery anomalies with no special medical history or abnormal imaging results may be difficult to diagnose through a routine approach. To improve the evaluation and management of the disease, we present the case series of eight children suffering from congenital coronary artery disease with syncope.

MATERIALS AND METHODS

We retrospectively reviewed all the 371 pediatric patients hospitalized with the chief complaint of syncope from August 2018 to August 2020 and found that eight (2.2%) patients were diagnosed with congenital coronary artery disease through coronary CTA or coronary angiography. Criteria used for coronary CTA were (1) high probability of cardiogenic syncopes, such as exercise-related syncope and syncope with a previous history of Kawasaki disease; (2) children with symptoms suggestive of coronary artery disease, such as syncope with chest pain. Personal details and clinical history of the patients were recorded, including age, gender, clinical manifestations, laboratory examinations (e.g., serum CK–MB, cTnI, and BNP), ECG, echocardiography, coronary CTA, etc. The follow-up period was 12–34 months (**Table 2**). Descriptive analysis was used to analyze the data.

RESULTS

Clinical Characteristics

In total, eight patients were included in the study with a median age of 12.5 ± 2.7 (8–16) years. In total, four of them were men, and four were women. Six of them were diagnosed with the right anomalous coronary artery from the opposite sinus (R-ACAOS), while two were diagnosed with the left anomalous coronary artery from the opposite sinus (L-ACAOS). The clinical history and manifestations are shown in **Table 1**. The triggers of syncope were exercise (three cases) and postural change (three cases). However, no obvious trigger was found in four patients. Six children complained of prodromes before syncope, predominantly dizziness and blurred vision. Concomitant symptoms such as incontinence and limb twitching were not reported. The duration of syncope was usually short, lasting from a few seconds to 3 min. A family history for syncope was present in one patient.

Serum Cardiac Markers

Myocardial necrosis biomarkers were measured routinely in all the 371 patients admitted to our hospital. The serum measurements were done 0–2 days after the syncope in all the eight patients. Serum cardiac markers (CK, CK–MB, and cTnI) were normal in seven patients. Myocardial necrosis biomarkers were significantly elevated in one patient (CK 1789IU/l, CK-MB 140IU/l, and cTnI 9.92 ng/ml).

Electrocardiograms

All the patients underwent routine 12-lead ECG and 24-h ambulatory electrocardiogram (Holter), and abnormal ECGs were recorded in most patients (**Figure 1** and **Table 2**). The abnormalities included single premature ventricular contraction in two cases, ST-T changes in two cases, sinus arrest in one case, prolonged QT interval in one case, and axis deviation in 1 case. EET was conducted in six cases revealed no other abnormal results except abnormal ECG at rest.

Head-Up Tilt Test

Head-up tilt test was conducted on seven patients. They were placed in the upright position, tilted upward at an angle of 60° and supine position, with simultaneous monitoring of heart rate, blood pressure, and ECG (8). All of the seven cases had positive findings. In total, five cases were found to have postural tachycardia syndrome (POTS), one case had orthostatic

TABLE 1 | Clinical history and manifestations.

Patient number	Gender	Age (year)	Course of illness (month)	Number of episode	Syncope during exercise	Syncope after postural change	Precursor	Duration of syncope (min)	Family history
1	F	10	24	1	-	+	+	1	-
2	M	14	4	5	-	-	+	<1	-
3	F	15	12	2	+	+	+	2	-
4	M	11	84	20	-	-	+	<1	+
5	M	14	6	3	-	-	-	<1	-
6	F	16	72	2	+	+	+	<1	-
7	M	8	2	1	-	-	-	<1	-
8	F	10	12	2	+	-	+	3	-

Gender: F, female, M, male.

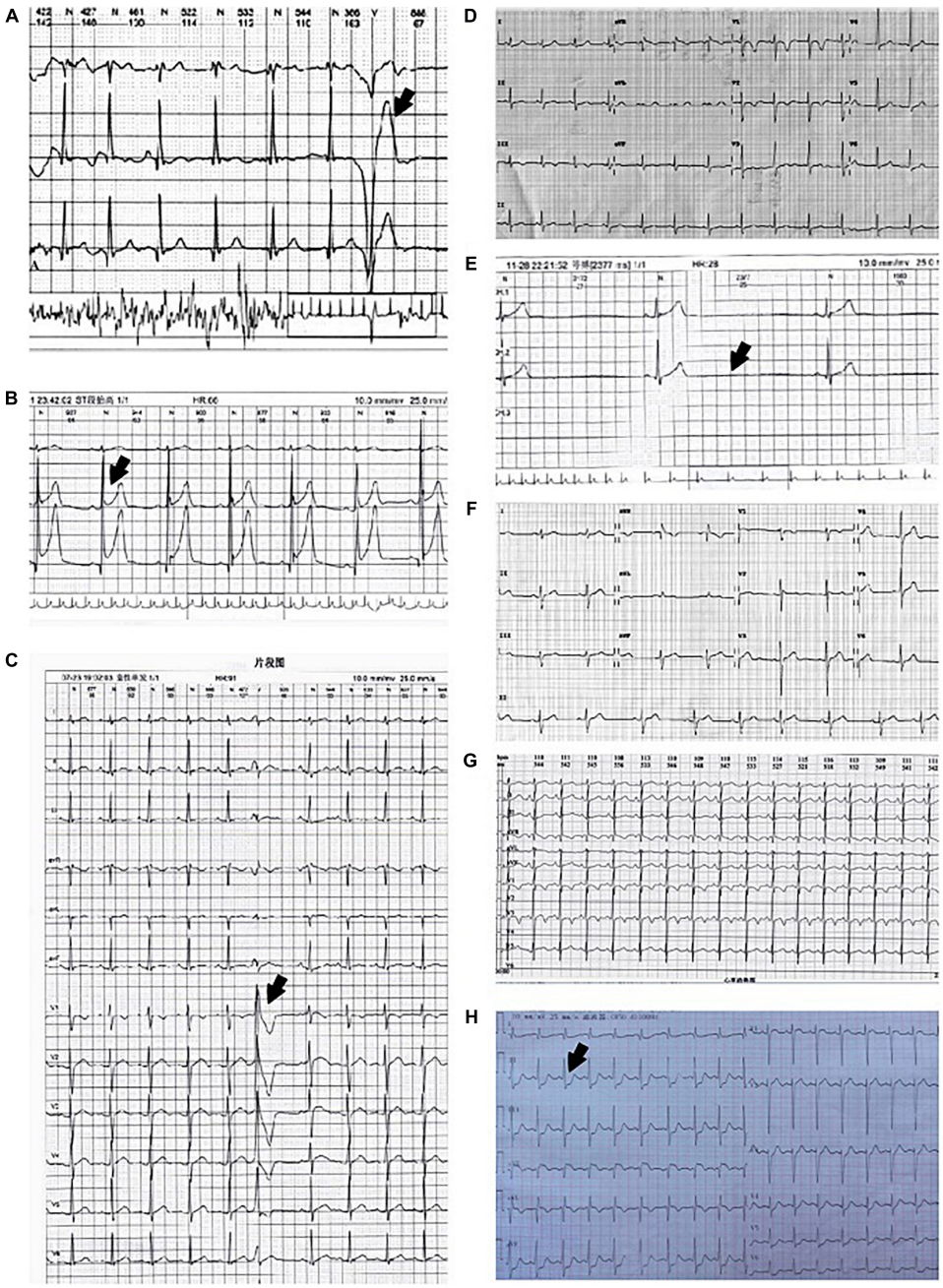

FIGURE 1 | Electrocardiogram (ECG)/Holter ECG of eight patients. **(A)** Single premature ventricular contraction in Patient 1. **(B)** ST-T elevated in patient 2. **(C)** Single premature ventricular contraction in patient 3. **(D)** Normal ECG of patient 4. **(E)** Sinus arrest in patient 5. **(F)** Left axis deviation in patient 6. **(G)** QTc 0.50 s in patient 7. **(H)** ST-T depressed in patient 8.

hypertension, and one case had vasovagal-like syncope (vasoinhibitory type) (**Table 2**).

Echocardiography

Echocardiography was done in all the cases, two of them were found to have coronary artery anomalies, and two had left atrium and/or ventricle enlargement.

Coronary Computed Tomography Angiography

Coronary CTA was conducted to characterize coronary artery disease and detect coronary artery stenosis. From 1 August 2018 to 1 August 2020, coronary CTAs were performed on 74 patients in our hospital, and eight of them were diagnosed with AAOCA. We found that all the eight patients had intramural segments

TABLE 2 | Laboratory and imaging findings, treatment, and prognosis.

Patient number	Myocardial necrosis biomarkers	ECG/Holter ECG	HUT	Echo	Coronary artery CTA/Angiography	Treatment	Follow-up period (month)	Prognosis
1	-	Single premature ventricular contraction	POTS	Tiny branch of coronary artery	Interarterial R-ACAOS with no obvious stenosis	Beta-blocker	21	Less syncope
2	-	ST-T elevated	POTS	Tricuspid regurgitation	Interarterial R-ACAOS with proximal RCA stenosis	Coronary unroofing surgery	34	No symptom
3	-	Single premature ventricular contraction	POTS	L-ACAOS	Interarterial L-ACAOS with proximal LCA stenosis	Coronary unroofing surgery	27	No symptom
4	-	Normal	POTS	Left superior vena cava	Interarterial R-ACAOS with no obvious stenosis	Functional exercise, ORS	24	No symptom
5	-	Sinus arrest	OHT	Left atrium and ventricle enlargement	Interarterial R-ACAOS with proximal RCA stenosis	Functional exercise, ORS	23	No symptom
6	-	Left axis deviation	VVS	Tricuspid regurgitation	Interarterial R-ACAOS with proximal RCA stenosis	Alpha-1 adrenergic agonist	26	Less syncope
7	-	QTc 0.50 s	POTS	Normal	Interarterial R-ACAOS with proximal RCA stenosis	Coronary unroofing surgery	22	No symptom
8	+	ST-T depressed	/	Left atrium enlargement	Interarterial L-ACAOS with proximal LCA stenosis	Coronary unroofing surgery	12	No symptom

ECGs, electrocardiograms; HUT, head-up tilt test; CTA, computed tomography angiography; POTS, postural tachycardia syndrome; OHT, orthostatic hypertension; VVS, vasovagal-like syncope; R-ACAOS, right anomalous coronary artery from the opposite sinus; L-ACAOS, left anomalous coronary artery from the opposite sinus; Echo, echocardiography; RCA, right coronary artery; LCA, left coronary artery; ORS, oral rehydration salt.

and different degrees of coronary artery narrowing (**Figure 2** and **Table 3**). The ostial type was a separate ostium, and the take-off angle was less than 45° in all the cases (**Table 3**).

Treatment and Prognosis

Coronary unroofing procedures were performed on four patients (patient number 2, 3, 7, and 8), and none of the patients complained of syncope after the surgery. The rest of the four patients received treatment, such as functional exercise, oral rehydration salts (ORSs), beta-blocker, and alpha-1 adrenergic agonists. All the symptoms resolved in two patients (patient number 4 and 5), and they stopped treatment. The other two patients (patient number 1 and 6) suffered from fewer syncopal episodes than before and still needed medication (**Table 2**).

DISCUSSION

Though syncope caused by coronary artery disease among children has a low incidence, it poses a significant risk to their health. Anomalous aortic origin of a coronary artery (AAOCA) is one of the most common congenital coronary artery anomalies and can manifest as syncope in children. AAOCA is the second most common cause of sudden cardiac death (SCD) in young athletes (9). From 1 August 2018 to 1 August 2020, there were 371 children admitted to our hospital with syncope as the chief complaint, and 8 (2.2%) were diagnosed with congenital coronary artery disease. All of them were found to have AAOCA, and the incidence is higher than in the newborns (0.64%) (10) or in the asymptomatic children (0.17%) (11). Thus, syncope is an important clinical symptom of congenital coronary disease in children.

Anomalous aortic origin of a coronary artery can further be classified into five subtypes: interarterial, subpulmonic (intraconal or intraseptal), pre-pulmonic, retroaortic, and retrocardiac (12). L-ACAOS is generally associated with a high risk of SCD, and the benefits of revascularization in L-ACAOS patients likely outweigh the risks (12, 13). The study by Cheezum reported that R-ACAOS patients with interarterial compression suffered from more frequent syncopal episodes and chest pain than AAOCA without interarterial compression (3, 12). In another study by Kaushal (13), symptomatic patients with AAOCA had a longer intramural course than asymptomatic patients with AAOCA. These findings suggest that the appearance of symptoms is affected by the degree to which the ectopic artery is compressed. In total, eight patients in our study were diagnosed with AAOCA (interarterial type) with different levels of interarterial compression. Moreover, all of them were symptomatic. Studies have revealed that clinical manifestations of AAOCA vary from asymptomatic, palpitation, chest discomfort, cardiac syncope, and acute myocardial infarction to sudden death (12, 14). Whether there is a positive correlation between the severity of symptoms and the degree of coronary compression has not been elucidated.

Exercise stimulates myocardial contraction, thus, compressing the intramural vessels. Compressed coronary artery leads to

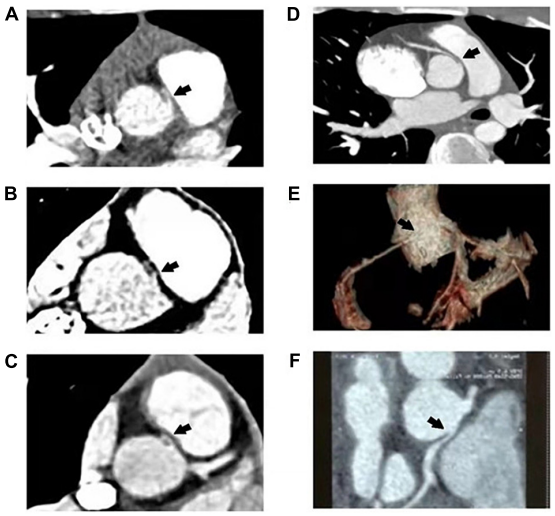

FIGURE 2 | Computed tomography angiography (CTA) of six patients. Black arrows indicate the interarterial course between the aorta and pulmonary artery. **(A)** Interarterial R-ACAOS with no obvious stenosis (Patient 1). **(B)** Interarterial R-ACAOS with proximal RCA stenosis (Patient 2). **(C)** Interarterial R-ACAOS with no obvious stenosis (Patient 4). **(D)** Interarterial R-ACAOS with proximal RCA stenosis (Patient 6). **(E)** Interarterial R-ACAOS with proximal RCA stenosis (Patient 7). **(F)** Interarterial L-ACAOS with proximal LCA stenosis (Patient 8).

ischemia of the heart conduction system and cardiomyocytes, resulting in arrhythmia and decreased myocardial contractility, respectively. Consequently, cardiac ejection fraction decreases, and hence, blood flow to the brain is diminished. This results in a syncopal attack. This pathogenesis may be accountable for the syncope during the exercise in three of the patients in our study. Syncope during exercise is an indicator of coronary disease.

However, three patients suffered from syncope after a sudden postural change, and seven patients had positive HUT findings, suggestive of vasovagal-like syncope. Although clinical features suggest vasovagal-like syncope, it is essential to rule out cardiac syncope before the diagnosis is confirmed. Further investigation and follow-up are essential in such cases (15–17).

Electrocardiogram changes in AAOCA are also significant in diagnosing interarterial compression. There may be no typical characteristics at rest, while short-lived myocardial ischemia caused by compressed coronary artery after exercise may appear as the abnormal QRS wave and the change of ST-T in ECG. Severe or continued compression also results in the elevation of myocardial necrosis biomarkers. So, when increased myocardial necrosis biomarkers or depressed/elevated ST-T in ECG are observed, especially after exercise in a child with syncope and AAOCA, it is strongly suggestive of syncope due to AAOCA. But even in the absence of the elevated myocardial necrosis biomarkers or changed ST-T in ECGs, the possibility of cardiac syncope cannot be excluded. The normal levels of myocardial necrosis biomarkers and the normal EET findings in our study may be due to very mild coronary artery compression, transient coronary stenosis, and the fact that these tests were not conducted during the ischemia. Two patients (the third and eighth) suffered from syncope during exercise, and we found that both of them suffered from interarterial L-ACAOS with proximal LCA stenosis. Considering the potential risks associated with EET, we did not recommend EET in these two cases. Some studies demonstrate that a normal EET result can not preclude SCDs (18). For those cases with strong evidence of cardiac ischemia, more sensitive and specific methods such as stress echocardiography or nuclear myocardial perfusion imaging may be necessary. Echocardiography is a common modality to evaluate suspected or confirmed cardiac disease as an inexpensive, efficient, non-invasive, and widely available modality. However, echocardiography plays a limited

TABLE 3 | Coronary artery computed tomography angiography (CTA).

Patient number	Coronary artery CTA	Intramural segment length (mm)	Proximal vessel morphology	Take off angle	Ostial type
1	Interarterial R-ACAOS with no obvious stenosis	2	Normal	<45°	Separate ostium
2	Interarterial R-ACAOS with proximal RCA stenosis	5	Oval	<45°	Separate ostium
3	Interarterial L-ACAOS with proximal LCA stenosis	3	Oval	<45°	Separate ostium
4	Interarterial R-ACAOS with no obvious stenosis	2	Normal	<45°	Separate ostium
5	Interarterial R-ACAOS with proximal RCA stenosis	5	Oval	<45°	Separate ostium
6	Interarterial R-ACAOS with proximal RCA stenosis	8	Oval	<45°	Separate ostium
7	Interarterial R-ACAOS with proximal RCA stenosis	3	Slit-like	<45°	Separate ostium
8	Interarterial L-ACAOS with proximal LCA stenosis	2	Oval	<45°	Separate ostium

CTA, computed tomography angiography; R-ACAOS, right anomalous coronary artery from the opposite sinus; L-ACAOS, left anomalous coronary artery from the opposite sinus; RCA, right coronary artery; LCA, left coronary artery.

role in evaluating AAOCA due to its minimal ability to visualize surrounding structures, limited dynamic imaging, low-spatial resolution, dependence on body habitus, and operator competence (12). CTA, which is the Class I-indicated test used to image AAOCA, is still a preferred modality (18). Coronary CTAs were performed on 74 patients in our hospital, and eight (10.8%) of them were diagnosed with AAOCA. It signifies that coronary CTA plays a vital role in diagnosing syncope caused by coronary disease.

The management of AAOCA depends on the symptoms or diagnostic evidence of coronary ischemia due to the anomalous coronary artery. Surgery is the Class I-indicated treatment in such cases in R-ACAOS or L-ACAOS (18–20). In L-ACAOS, even without ischemic symptoms or diagnostic evidence, surgery is recommended (Class IIa) because it is associated with a higher risk of SCD (18–20). However, in patients with R-ACAOS without ischemic symptoms or diagnostic evidence, surgical intervention is not proven to alter the risk of SCD. Thus, the management option for these patients is still controversial and watchful waiting, and also surgery is Class IIb-indicated (18–20). In our study, two patients with L-ACAOS and two patients with symptomatic R-ACAOS underwent coronary unroofing surgery and were relieved of syncope after the surgery. The other four patients with symptomatic R-ACAOS also had the indication for surgical treatment, but they denied surgery. These patients were observed on follow-up visits and received conservative treatment, though the possibility of opting for surgery in the future was explained to them. We observed that BJR activation, one of the main mechanisms for vasovagal syncope, could also exist in AAOCA. Thus, the syncope attributable to AAOCA might be associated not only with decreased coronary flow but also with vasovagal-like syncope. In our study, two patients of AAOCA with proximal coronary stenosis receiving treatment for vasovagal-like syncope reported reduced or no syncopal episodes during the follow-up period. This suggests that vasovagal response may also be an etiology for syncope.

There are also some limitations in our study. AAOCA may be underestimated in our study due to a limited number of patients undergoing echocardiography and CT scan. We propose that the reason for the low-diagnosis rate of echocardiography is that the routine echocardiography does not include coronary examination in some hospitals of China. One of the primary significances of this study is to emphasize that in addition to routine echocardiography, further attention should be paid to the detection of coronary malformations in children with syncope, and pediatricians and sonographers should be vigilant about it. In addition, another limitation is that we could not provide the cross-sectional imaging of all the patients with relative 3D reconstruction. Moreover, the follow-up period in our study was not long enough for a valid long-term assessment. The increased frequency of the presence of AAOCA is very low. Therefore the sample size of the cases in the study group should be much larger to obtain statistically significant differences in comparison with the historical group of other authors. Furthermore, it should be stressed that the patients with the greatest risk of death with the left main artery coming from the pulmonary trunk were not observed in the study likely due to the small sample size.

Therefore, we conclude that more attention should be paid to congenital coronary disease in children with syncope. ECG and echocardiography, as the common methods for investigating cardiac syncope, may have limited ability to find coronary artery anomalies. Patients with positive HUT results should not be simply diagnosed with vasovagal syncope. In the cases of suspected cardiac syncope, ruling out coronary artery anomalies through coronary CTA is imperative. In AAOCA, L-ACAOS can be symptomatic and need close monitoring and even surgery, but in R-ACAOS, the etiology of syncope needs to be thoroughly evaluated.

DATA AVAILABILITY STATEMENT

The original contributions presented in this study are included in the article/supplementary material, further inquiries can be directed to the corresponding author.

ETHICS STATEMENT

The studies involving human participants were reviewed and approved by the Peking University First Hospital Ethics Committee. Written informed consent to participate in this study was provided by the participants' legal guardian/next of kin. Written informed consent was obtained from the legal guardian/next of kin for the publication of any potentially identifiable images or data included in this article.

AUTHOR CONTRIBUTIONS

YG: design and implementation of experiments, data collection and analysis, statistical analysis, and drafting of the article. QZ: design of experiments, data interpretation and analysis, statistical analysis, guidance of the article drafting, and critical review. YS: implementation of experiments, data collection and analysis, statistical analysis, drafting of the article, and supporting contribution. JD: design of experiments, data interpretation and analysis, statistical analysis, guidance of the article drafting, critical review, and supporting contribution. All authors contributed to the article and approved the submitted version.

FUNDING

This study was supported by the National High Level Hospital Clinical Research Funding (Multi-center Clinical Research Project of Peking University First Hospital) (No. 2022CR59).

ACKNOWLEDGMENTS

We thank all the subjects taking part in our research.

REFERENCES

1. Feit LR. Syncope in the pediatric patient: diagnosis, pathophysiology, and treatment. *Adv Pediatr.* (1996) 43:469–94.
2. Singhi P, Saini AG. Syncope in pediatric practice. *Indian J Pediatr.* (2018) 85:636–40. doi: 10.1007/s12098-017-2488-9
3. Friedman NR, Ghosh D, Moodley M. Syncope and paroxysmal disorders other than epilepsy. 5th Edn. In: Swaiman KF editor. *Swaiman's Pediatric Neurology: Principles and Practice*. Philadelphia: Elsevier Saunders (2012). p. 906–25. doi: 10.1016/B978-1-4377-0435-8.00065-2
4. Zhang Q, Du J, Wang C, Du Z, Wang L, Tang C. The diagnostic protocol in children and adolescents with syncope: a multi-centre prospective study. *Acta Paediatr.* (2009) 98:879–84. doi: 10.1111/j.1651-2227.2008.01195.x
5. Zhang Q, Zhu L, Wang C, Du Z, Hu X, Tian H, et al. Value of history taking in children and adolescents with cardiac syncope. *Cardiol Young.* (2013) 23:54–60. doi: 10.1017/S1047951112000303
6. Kanjwal K, Calkins H. Syncope in children and adolescents. *Cardiol Clin.* (2015) 33:397–409. doi: 10.1016/j.ccl.2015.04.008
7. Jacobs ML, Mavroudis C. Anomalies of the coronary arteries: nomenclature and classification. *Cardiol Young.* (2010) 20:15–9. doi: 10.1017/S1047951110001046
8. Wang C, Li Y, Liao Y, Tian H, Huang M, Dong X, et al. 2018 Chinese Pediatric Cardiology Society (CPCS) guideline for diagnosis and treatment of syncope in children and adolescents. *Sci Bull.* (2018) 63:1558–64.
9. Basso C, Maron BJ, Corrado D, Thiene G. Clinical profile of congenital coronary artery anomalies with origin from the wrong aortic sinus leading to sudden death in young competitive athletes. *J Am Coll Cardiol.* (2000) 35:1493–501. doi: 10.1016/S0735-1097(00)00566-0
10. Kimbiris D, Iskandrian AS, Segal BL, Bemis CE. Anomalous aortic origin of coronary arteries. *Circulation.* (1978) 58:606–15. doi: 10.1161/01.CIR.58.4.606
11. Davis JA, Cecchin F, Jones TK, Portman MA. Major coronary artery anomalies in a pediatric population: incidence and clinical importance. *J Am Coll Cardiol.* (2001) 37:593–7. doi: 10.1016/S0735-1097(00)01136-0
12. Cheezum MK, Liberthson RR, Shah NR, Villines TC, O'Gara PT, Landzberg MJ, et al. Anomalous aortic origin of a coronary artery from the inappropriate sinus of valsalva. *J Am Coll Cardiol.* (2017) 69:1592–608. doi: 10.1016/j.jacc.2017.01.031
13. Kaushal S, Backer CL, Popescu AR, Walker BL, Russell HM, Koenig PR, et al. Intramural coronary length correlates with symptoms in patients with anomalous aortic origin of the coronary artery. *Ann Thorac Surg.* (2011) 92:986–92. doi: 10.1016/j.athoracsur.2011.04.112
14. Jegatheeswaran A, Devlin PJ, McCrindle BW, Williams WG, Jacobs ML, Blackstone EH, et al. Features associated with myocardial ischemia in anomalous aortic origin of a coronary artery: a congenital heart surgons' society study. *J Thorac Cardiovasc Surg.* (2019) 158:822–34. doi: 10.1016/j.jtcvs.2019.02.122
15. Arya S, Belwal S, Uniyal B, Tiwari B, Sharma P. Bezold Jarisch reflex- new interest, old phenomenon. *Am J Intern Med.* (2020) 8:24–9. doi: 10.11648/j.ajim.20200801.15
16. Sakai C, Kawasaki T, Sugihara H, Matoba S. The Bezold-Jarisch reflex in a patient with coronary spastic angina. *Ann Noninvasive Electrocardiol.* (2020) 25:e12759. doi: 10.1111/anec.12759
17. Veelken R, Sawin LL, DiBona GF. Epicardial serotonin receptors in circulatory control in conscious Sprague-Dawley rats. *Am J Physiol.* (1990) 258:H466–72. doi: 10.1152/ajpheart.1990.258.2.H466
18. Stout KK, Daniels CJ, Aboulhosn JA, Bozkurt B, Broberg CS, Colman JM, et al. 2018 AHA/ACC guideline for the management of adults with congenital heart disease: a report of the American College of Cardiology/American Heart Association task force on clinical practice guidelines. *J Am Coll Cardiol.* (2019) 73:e81–192. doi: 10.1161/CIR.0000000000000602
19. Krasuski RA, Magyar D, Hart S, Kalahasti V, Lorber R, Hobbs R, et al. Long-term outcome and impact of surgery on adults with coronary arteries originating from the opposite coronary cusp. *Circulation.* (2011) 123:154–62. doi: 10.1161/CIRCULATIONAHA.109.921106
20. Frommelt PC, Sheridan DC, Berger S, Frommelt MA, Tweddell JS. Ten-year experience with surgical unroofing of anomalous aortic origin of a coronary artery from the opposite sinus with an interarterial course. *J Thorac Cardiovasc Surg.* (2011) 142:1046–51. doi: 10.1016/j.jtcvs.2011.02.004

Conflict of Interest: The authors declare that the research was conducted in the absence of any commercial or financial relationships that could be construed as a potential conflict of interest.

frontiers | Frontiers in Cardiovascular Medicine

CASE REPORT
published: 06 July 2022
doi: 10.3389/fcvm.2022.937111

COVID-19 in a Child With Transposition of the Great Arteries S/P Fontan Palliation: A Case Report and Literature Review

Chen Wen[1†], *Guocheng Shi*[1†], *Wei Liu*[1], *Hao Zhang*[1], *Gangxi Lin*[2,3,4,5,6*] *and Huiwen Chen*[1*]

[1] *Department of Cardiothoracic Surgery, Shanghai Children's Medical Center, School of Medicine, Shanghai Jiao Tong University, Shanghai, China,* [2] *Department of Pediatrics, The First Affiliated Hospital of Xiamen University, Xiamen, China,* [3] *Pediatric Key Laboratory of Xiamen, Xiamen, China,* [4] *Institute of Pediatrics, School of Medicine, Xiamen University, Xiamen, China,* [5] *The School of Clinical Medicine, Fujian Medical University, Fuzhou, China,* [6] *The Third Clinical Medical College, Fujian Medical University, Fuzhou, China*

OPEN ACCESS

Edited by:
Hongfang Jin,
Peking University, China

Reviewed by:
Yanqiu Ou,
Guangdong Academy of Medical Sciences, China
Tianli Zhao,
Central South University, China
Atsuhito Takeda,
Hokkaido University Hospital, Japan

***Correspondence:**
Gangxi Lin
lingangxi@qq.com
Huiwen Chen
chenhuiwen@scmc.com.cn

[†]*These authors have contributed equally to this work and share first authorship*

Specialty section:
This article was submitted to Pediatric Cardiology, a section of the journal Frontiers in Cardiovascular Medicine

Received: *05 May 2022*
Accepted: *10 June 2022*
Published: *06 July 2022*

Citation:
Wen C, Shi G, Liu W, Zhang H, Lin G and Chen H (2022) COVID-19 in a Child With Transposition of the Great Arteries S/P Fontan Palliation: A Case Report and Literature Review. Front. Cardiovasc. Med. 9:937111. doi: 10.3389/fcvm.2022.937111

Background: Although adult patients with cardiovascular disease are at higher risk of adverse outcomes such as death or severe infection, limited data exist regarding pediatric patients with congenital heart disease. We would like to report our experience with COVID-19 in a pediatric patient with Fontan circulation. Furthermore, we present a review of patients with Fontan palliation and COVID-19 previously reported in the literature to summarize the clinical characteristics of this population.

Case Presentation: A 9-year-old boy with dextro-transposition of the great arteries, ventricular septal defect, pulmonary stenosis, patent foramen ovale, and borderline left ventricle post bidirectional Glenn shunt and Fontan palliation presented with paroxysmal cough in the context of COVID-19. The coagulation profile was beyond the normal limits, and the patient began to receive anticoagulant aspirin. On the 5th day, the patient presented with fever, sore throat, and fatigue. The oxygen saturations dropped to 93%, and he received nasal catheter oxygen inhalation. On the 7th day, computed tomography of the chest revealed little emerging flaky exudation in the posterior basal segment of the left lower lobe. Nasal cannula was removed on the 12th day, and the coagulation profile returned to normal on the 16th day. After two consecutively negative SARS-CoV-2 viral RNA tests (on the 18th and 19th days, interval $\geq$ 24 h), he was discharged from the hospital on the 21st day. Literature review indicated that COVID-19 with Fontan palliation seemed to be more common in male adults. Disease presentation varied from mild upper respiratory tract infection to severe pneumonia. Complications were not uncommon in this population. The treatments varied depending on the specific factors. Fortunately, most patients reported a favorable prognosis.

Conclusion: Although patients with COVID-19 and Fontan circulation might have the risk of adverse outcomes due to multiple mechanisms, most patients have a favorable prognosis.

Keywords: congenital heart disease, COVID-19, Fontan procedure, SARS-CoV-2, case report

INTRODUCTION

Coronavirus disease 2019 (COVID-19) caused by severe acute respiratory syndrome virus 2 (SARS-CoV-2) has become a global pandemic. Although adult patients with cardiovascular disease are at higher risk of adverse outcomes, such as death or severe infection, limited data exist regarding pediatric patients with congenital heart disease (CHD). Furthermore, children have a lower risk of infection and a milder course than adults (1). Some experts believe that patients with univentricular circulation are susceptible to COVID-19 (2, 3). However, anatomic complexity does not predict infection severity of adult patients with CHD (4). There is a dearth of literature regarding the impact of Fontan circulation on COVID-19, with data mostly based on case reports or series. In this study, we presented the diagnosis and management of COVID-19 in a 9-year-old boy after Fontan palliation. Furthermore, we conducted a review of patients with COVID-19 and Fontan palliation previously reported in the literature to summarize the clinical characteristics of this population.

CASE DESCRIPTION

This boy with a background of dextro-transposition of the great arteries, ventricular septal defects, pulmonary stenosis, patent foramen ovale, and borderline left ventricle presented to our hospital at 3 months of life due to cyanosis. He underwent a bidirectional Glenn procedure at 5 months old. Subsequently, he underwent collateral closure with two embolization coils and enlargement angioplasty of pulmonary arteries with bovine pericardial patch at 4 years old, and completed an extracardiac fenestrated Fontan procedure with a 19 # Gore-Tex conduit at $5^1/_2$ years old. At the last outpatient visit, his temperature was 37°C; heart rate, 85 beats/min; blood pressure, 110/70 mm Hg; and respiratory rate, 19 breaths/min with oxygen saturation (SpO_2) 98%. No abnormality was seen in routine blood test, liver and renal function, and the coagulation profile. The echocardiography demonstrated good Fontan circulation, involving a blood flow velocity of 0.58 m/s in the conduit, 0.68 m/s in the inferior vena cava, 0.98 m/s in the cavopulmonary anastomosis, 1.8 m/s at the level of fenestration, and only mild mitral valve regurgitation.

This 9-year-old patient initially presented with paroxysmal cough (**Figure 1**). Physical examination revealed pharyngeal congestion and coarse breath sounds in both lungs. Vital signs revealed a temperature of 36°C; heart rate, 102 beats/min; blood pressure, 82/69 mm Hg; and respiratory rate, 20 breaths/min, with SpO_2 97%. We informed the patient that the ideal SpO_2 after Fontan was generally 90–95%. The drop in SpO_2 caused by COVID-19 would be lower than usual. An electrocardiogram showed a sinus tachycardia with ST-T change and clockwise rotation (**Supplementary Figure 1**). Computed tomography showed slight inflammation in the middle lobe of the right lung and the upper lobe of the left lung (**Figure 2A**), which could rule out happy hypoxia. The monocyte count and proportion, and C-reactive protein were elevated. The coagulation profile was beyond the normal limits, including elevated fibrinogen, fibrin degradation products, and D-dimer. Cytokine interleukin (IL)-6 was normal on admission and rose to a peak value on hospital Day 6. Liver and renal functions were normal. Cardiac markers, including creatine kinase and creatine kinase-myocardial band, were within normal limits. The nasopharyngeal swab specimens of the patient, his parents, and older sister were positive for SARS-CoV-2. The strain was the delta variant determined by sequencing. The patient had not been vaccinated against SARS-CoV-2. The prevalent strain was the delta variant at that time.

On HD 2, the patient had fever and complained of sore throat the next day. On HD 5, the patient had a transient low fever, and he presented with sore throat and fatigue. The oxygen saturations dropped to 93%, and he received 1 L/min of oxygen *via* a nasal cannula, which improved the oxygen saturations to 94–96%. Arterial blood gas tests showed decreased CO_2 partial pressure, O_2 partial pressure, HCO_3^-, and SpO_2. The oxygen flow rate was adjusted to 2 L/min, and the oxygen saturations were maintained at 96%. On HD 6, the echocardiography revealed

Hospital day	1	2	3	4	5	6	7	8	9	10	11	12	13	14	15	16	17	18	19	20	21
Temperature (°C)	36	38	37.8	36.5	37.6	36.6	38	36.9	36.9	36.8	36.4	36.6	36.4	36.5	36.4	36.1	36.7	36.3	36.3	36.3	36.2
SaO_2 min (%)	97	99	94	94	94	94	94	92	92	92	94	91	89	90	90	90	91	91	91	90	93
SaO_2 max (%)	97	98	95	95	98	98	98	98	98	98	97	98	97	96	95	94	93	94	94	92	93
Cough																					
Sore throat																					
Fatigue																					
Respiratory support																					

FIGURE 1 | A timeline of the symptoms and managements.

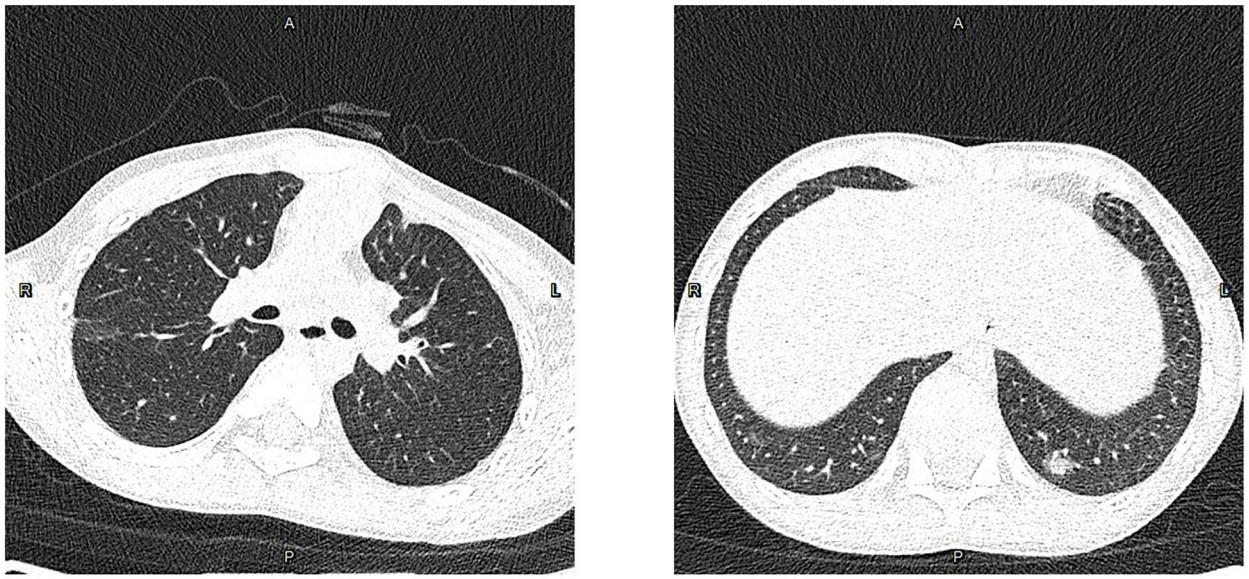

FIGURE 2 | Computed tomography of the chest in the axial plane. **(A)** On hospital Day (HD) 1, showing slight inflammation in the middle lobe of the right lung and upper lobe of the left lung. **(B)** On HD 7, showing little emerging flaky exudation in the posterior basal segment of the left lower lobe.

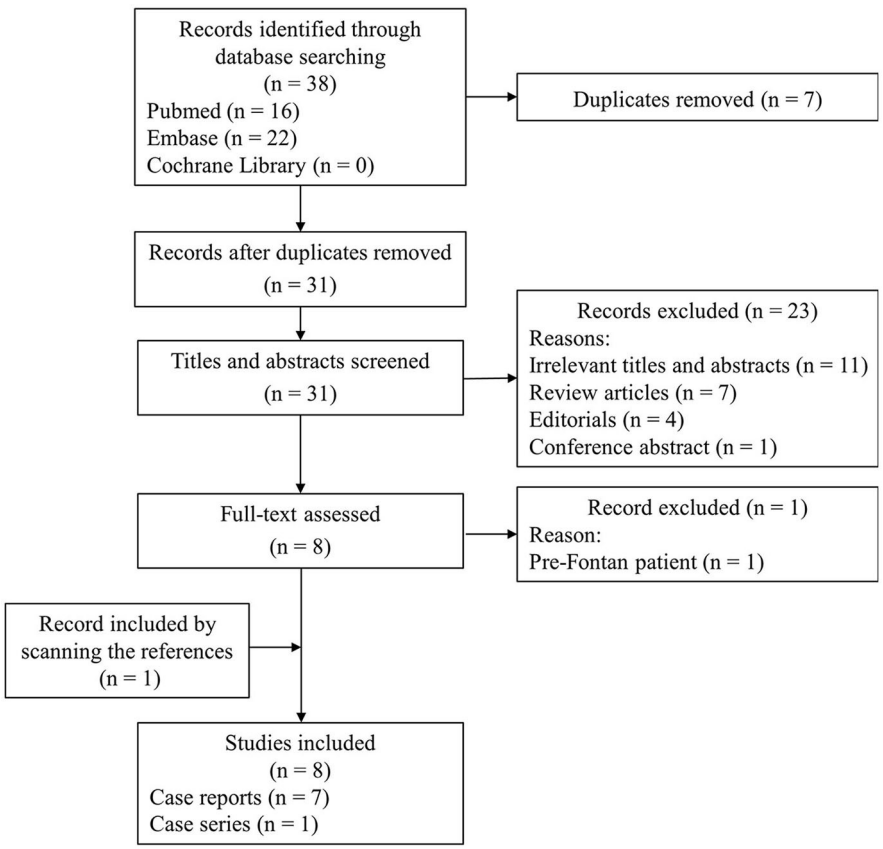

FIGURE 3 | The flow chart of the literature screening process for patients with COVID-19 and Fontan palliation.

TABLE 1 | A summary of articles describing patients with Fontan palliation and COVID-19.

Study	Age	Gender	Diagnosis	Type of Fontan	Previous interventions	Other comorbidities	Signs and symptoms	Complications	Managements	Outcomes
Vaikunth et al. (6)	40 y	M	TA	Lateral tunnel	Glenn, Fontan	HIV, gout	Fever, shortness of breath, diarrhea	Pneumothorax	Evacuating the pneumothorax, oxygen, nitric oxide, solumedrol, remdesivir, convalescent plasma, draining blood, red cells	Discharged on day 20
Linnane et al. (7)	10 y	M	DILV, PA, ASD, RAA	Extracardiac conduit	Glenn, Fontan	None	Fever, red eyes, lethargy, mild cough	None	Oxygen, cephalosporin, macrolide antibiotics	Discharged on day 14
Bezerra et al. (8)	35 mo	F	HLHS	Extracardiac conduit	Fontan	None	Dyspnea, dry cough	Complete atrioventricular block	Metamizole, heparin, enoxaparin, pleural drain, pacing, pacemaker implantion, milrinone, diuretics, sildenafil, vancomycin, cefepime, oxygen	Discharged on postoperative day 24
Ahluwalia et al. (9)	29 y	M	TA	Lateral tunnel	BT shunt, Glenn, Fontan, device closure of a venovenous collateral, balloon dilation and stent placement of IVC	Fontan Associated Liver Disease under investigation	Low-grade fevers, nonproductive cough, easy fatigability, progressive shortness of breath	None	Oxygen, hydroxychloroquine, azithromycin, furosemide, sildenafil, heparin, lovenox, aspirin	Discharged on day 10
Jicinska et al. (10)	6 y	M	HLHS, dextrocardia	Extracardiac conduit	Fontan	None	Shortness of breath during exercise, increased fatigue during daily activities, newly acquired hepatomegaly	Multiple thrombi	Underwent a thrombectomy, left pulmonary artery plasty, atrial communication enlargement	There were no post-operative thrombotic complications
Jamshidi et al. (11)	51 y	M	TA	Extracardiac Fontan	Atriopulmonary Fontan, extracardiac Fontan	None	Cough, diarrhea	Phlegmasia cerulea dolens	Bilevel positive airway pressure and vasopressor support, remdesivir, tadalafil, warfarin, heparin, convalescent plasma, thrombectomy, left below-the-knee amputation	Discharged to an acute rehabilitation unit
Fusco et al. (5)	1) 24 y 2) 27 y 3) 40 y 4) 39 y 5) 56 y 6) 28 y 7) 23 y	1) M 2) F 3) F 4) M 5) M 6) M 7) F	1) PA IVS 2) AVSD 3) TA 4) DILV with TGA 5) Dextrocardia, TA with TGA 6) TA 7) TA	1) Extracardiac conduit 2) Extracardiac conduit 3) Bjork Fontan 4) Extracardiac conduit 5) Extracardiac conduit 6) Lateral tunnel 7) Extracardiac conduit	1) BT shunt, Glenn, Fontan 2) PA banding, Glenn, Damus-Kaye, Fenestrated Fontan, Fenestration closure 3) Atrial septostomy, BT shunt, Fontan 4) BT shunt, Fontan 5) BT shunt (x2), Glenn, Fontan 6) BT shunt, Glenn, Fontan, stenting of Fontan conduit 7) Glenn, Fontan, stenting of Fontan conduit	1) None 2) None 3) Dysthyroidis, hepatitis C 4) None 5) Restrictive lung disease 6) None 7) PLE, acute kidney injury currently on dialysis, recent hemoperitoneum	1) Malaise, fatigue, sore throat, cough 2) Fever, sore throat, loss of smell, cough 3) Fever, fatigue, myalgia, diarrhoea, cough 4) Fever, fatigue 5) Fever, cough, dyspnoea 6) Fever, cough,myalgia, headache 7) Fever, malaise, fatigue, cough, dyspnoea	1) None 2) None 3) None 4) None 5) None 6) None 7) Desaturation	1) Azithromycin 2) None 3) Azithromycin 4) None 5) Azithromycin 6) Azithromycin 7) Oxygen, steroids, azithromycin	1) Full recovery 2) Full recovery 3) Full recovery 4) Full recovery 5) Full recovery 6) Full recovery 7) Hospitalization required
Chun et al. (12)	51 y	M	TA, PS	-	Fontan	None	Cough, fever, shortness of breath	Phlegmasia cerulea dolens	Vitamin K, convalescent plasma, heparin, enoxaparin sodium, thrombectomy, left below-the-knee amputation, warfarin	Discharged on day 48

F, female; ASD, atrial septal defect; AVSD, atrioventricular septal defect; DILV, double inlet left ventricle; HLHS, hypoplastic left heart syndrome; IVC, inferior vena cava; M, male; PA, pulmonary atresia; PA IVS, pulmonary atresia with intact ventricular septum; PLE, protein losing enteropathy; PS, pulmonary stenosis; RAA, right aortic arch; TA, tricuspid atresia; TGA, transposition of the great arteries.

a normal diameter and no filling defect of the inferior vena cava, a blood flow velocity of 0.23 m/s in the portal vein, and only traced mitral valve regurgitation (**Supplementary Figure 2**). On HD 7, computed tomography of the chest showed little emerging flaky exudation in the posterior basal segment of the left lower lobe (**Figure 2B**). The patient had a transient low fever at night. On HD 12, nasal cannula was removed. The patient began to receive anticoagulant aspirin on HD 1. Symptoms were observed and related indicators were detected; heparin was not used due to no-significant deterioration. The coagulation profile returned to normal on HD 16. After two consecutively negative SARS-CoV-2 viral RNA tests (on HD 18 and HD 19, interval $\geq$ 24 h), he was discharged from the hospital on HD 21. We would continue to follow up this patient closely at least for 1 year, including rechecking his clinical manifestations, electrocardiogram, chest computed tomography, and echocardiography.

DISCUSSION

Although Fontan palliation with COVID-19 is less common, it has gradually attracted the attention of clinicians. A literature search process using search strategies, comprising a subject word and a free word, was conducted in PubMed, Embase, and Cochrane Library databases (**Supplementary Table 1**) until April 10, 2022. References of relevant articles were also scanned. The flow chart of the literature screening process is presented in **Figure 3**. A total of 8 articles involving 14 patients were analyzed. Most pieces of literature are case reports, and Fusco et al. (5) published a case series, describing 7 adult patients. For each case, we extracted the patient's demographics, diagnosis, symptoms, comorbidities, managements, and outcomes (**Table 1**).

Studies from different countries reporting cases revealed mild-to-severe disease presentation in this population. The virus types were not mentioned in the reviewed cases. In reported cases, COVID-19 with Fontan palliation seemed to be more common in male adults. Different from the demographic data in the literature review, the patient in this report was 9 years old. The symptoms were diverse, with fever and cough being most common. More than half of all the cases were diagnosed with tricuspid atresia. Extracardiac conduit Fontan was mostly common. Our case was diagnosed with transposition of the great arteries and underwent extracardiac fenestrated Fontan. Complications were not uncommon in this population, with thrombotic complications being the most common. No complications were specific to Fontan circulation. No late complications were reported in the reviewed cases. It is worth noting that patients with phlegmasia cerulea dolens were at risk for amputation. Our case had no complications. The treatments varied, depending on the specific factors. More than half of the patients received antibiotics. Fortunately, most patients reported a favorable prognosis. Our patient received anticoagulant and oxygen therapy, and was discharged with full recovery.

There is a need to recognize the potential of SARS-CoV-2 infection in the subpopulation after CHD surgery during the pandemic, particularly when patients present with cough, fever, and hypoxemia that can usually be postoperative morbidities. Since SARS-CoV-2 nucleic acid test was widely carried out in tertiary hospitals, our patient was diagnosed on admission and isolated immediately. It is worth noting that a minority of patients are asymptomatic; the diagnosis is made accidentally before a procedure. As the pandemic continues to evolve, the access to test should be increased, allowing for confirming cases.

When a patient with the Fontan circulation is infected by SARS-CoV-2, the prognosis may be worrying. Owing to the lack of sub-pulmonary ventricular pump, the blood flow through the pulmonary arteries in patients with Fontan physiology is materially driven by the negative intrathoracic pressure and systemic blood pressure. Therefore, patients with Fontan physiology are at increased risk for complications related to coronavirus infection, given the following potential reasons. Any acute respiratory infection may contribute to increased pulmonary vascular resistance, therefore affecting the Fontan circulation. Furthermore, if intubation is required, management for this subgroup of patients is challenging because positive pressure ventilation can cause deleterious effects on the intrapulmonary and intracardiac hemodynamics. Patients with Fontan circulation are likely to have dysfunction of the pulmonary arterial endothelium, which results in impaired NO availability and concomitant increased release of IL-6 (13). Pieces of evidence have indicated that SARS-CoV-2 could determine a more severe cytokines storm in those whose base levels of cytokines are higher and NO levels are lower. Patients with Fontan circulation can have associated liver disease (hepatic fibrosis). The prior study has revealed that patients with liver disease are vulnerable to infection or a severe course of COVID-19 (14). Long-term anticoagulation is usually required in patients with Fontan circulation. Of note, abnormal coagulation is an important aspect of COVID-19, which can result in microthrombus. COVID-19 can lead to myocardial injury, which is a serious complication in patients with univentricular circulation. In addition, myocardial injury and systemic inflammation due to COVID-19 may easily trigger arrhythmia in this susceptible population.

Most patients did not present severe manifestations as expected and were managed routinely. A previous multicenter study also suggested that Fontan palliation did not appear to increase the risk of adverse outcomes (4). Many patients with Fontan palliation were younger, which might explain the favorable results. However, the worse physiological stage, such as cyanosis and pulmonary hypertension, was a predictor for mortality in patients with CHD (4); therefore, Fontan patients with unstable hemodynamics might have adverse outcomes.

CONCLUSION

Although patients with COVID-19 and Fontan circulation might have the risk of adverse outcomes due to multiple mechanisms, most patients have a favorable prognosis.

DATA AVAILABILITY STATEMENT

The original contributions presented in the study are included in the article/**Supplementary Material**, further inquiries can be directed to the corresponding authors.

ETHICS STATEMENT

The Institutional Review Board of Shanghai Children's Medical Center approved the present case report (approval number SCMCIRB-W2022001; date of approval 7 January 2022). A formal written consent was obtained from the patient's parents for the publication of any potentially identifiable images or data included in this article.

AUTHOR CONTRIBUTIONS

CW and GS were responsible for the literature research and the manuscript drafting. GL and HC revised the manuscript for important intellectual content. WL and HZ collected the clinical data. All authors contributed to the article and approved the submitted version.

FUNDING

This study is supported by the Chinese National Natural Science Foundation of China (Grant Nos. 82170307, 81801777, and 81970267), Shanghai Jiao Tong University School of Medicine (Grant No. YG2022QN094), and Science and Technology Commission of Shanghai Municipality (Grant Nos. 19411964000 and 20025800300).

SUPPLEMENTARY MATERIAL

The Supplementary Material for this article can be found online at: https://www.frontiersin.org/articles/10.3389/fcvm.2022.937111/full#supplementary-material

Supplementary Figure 1 | 12-lead electrocardiogram. Sinus tachycardia, ST-T change.

Supplementary Figure 2 | Transthoracic echocardiogram showing **(A)** normal flow in the Fontan circulation and **(B)** mild mitral valve regurgitation.

REFERENCES

1. Dong Y, Mo X, Hu Y, Qi X, Jiang F, Jiang Z, et al. Epidemiology of COVID-19 among children in China. *Pediatrics.* (2020) 145:e20200702. doi: 10.1542/peds.2020-0702
2. Alsaied T, Aboulhosn JA, Cotts TB, Daniels CJ, Etheridge SP, Feltes TF, et al. Coronavirus disease 2019 (COVID-19) pandemic implications in pediatric and adult congenital heart disease. *J Am Heart Assoc.* (2020) 9:e017224. doi: 10.1161/JAHA.120.017224
3. Radke RM, Frenzel T, Baumgartner H, Diller GP. Adult congenital heart disease and the COVID-19 pandemic. *Heart.* (2020) 106:1302–9. doi: 10.1136/heartjnl-2020-317258
4. Broberg CS, Kovacs AH, Sadeghi S, Rosenbaum MS, Lewis MJ, Carazo MR, et al. COVID-19 in adults with congenital heart disease. *J Am Coll Cardiol.* (2021) 77:1644–55. doi: 10.1016/j.jacc.2021.02.023
5. Fusco F, Scognamiglio G, Merola A, Palma M, Correra A, Borrelli N, et al. Coronavirus disease 2019 in patients with Fontan circulation. *Int J Cardiol Congenit Heart Dis.* (2021) 3:100126. doi: 10.1016/j.ijcchd.2021.100126
6. Vaikunth SS, Bykhovsky MR, Romfh AW, Haeffele CL, Rogers IS, Dong E, et al. A 40-year-old man with tricuspid atresia, status post-Fontan, with severe COVID-19 pneumonia and pneumothorax. *JACC Case Rep.* (2021) 3:187–91. doi: 10.1016/j.jaccas.2020.10.032
7. Linnane N, Cox DW, James A. A case of COVID-19 in a patient with a univentricular heart post total cavopulmonary connection (Fontan) surgery. *Cardiol Young.* (2020) 30:1350–2. doi: 10.1017/S1047951120001882
8. Bezerra RF, Franchi SM, Khader H, Castro RM, Liguori GR, da Fonseca da Silva L, et al. COVID-19 as a confounding factor in a child submitted to staged surgical palliation of hypoplastic left heart syndrome: one of the first reports of SARS-CoV-2 infection in patients with congenital heart disease. *J Thoracic Cardiovasc Surg.* (2021) 161:e97–e101. doi: 10.1016/j.jtcvs.2020.05.081
9. Ahluwalia N, Love B, Chan A, Zaidi AN. COVID-19 in an adult with tricuspid atresia s/p Fontan palliation. *JACC Case Rep.* (2020) 2:1261–6. doi: 10.1016/j.jaccas.2020.05.013
10. Jicinska D, Jicinsky M, Koubsky K. Does COVID-19 pose a threat for patients after univentricular palliation? Thrombosis of the Fontan tunnel. *Cardiol Young.* (2022) 1–3. doi: 10.1017/S1047951122000348
11. Jamshidi N, Tan W, Foote D, Reardon L, Lluri G, Aboulhosn J, et al. Mechanical thrombectomy of COVID-19 DVT with congenital heart disease leading to phlegmasia cerulea dolens: a case report. *BMC Cardiovasc Disord.* (2021) 21:592. doi: 10.1186/s12872-021-02403-w
12. Chun TT, Jimenez JC, Pantoja JL, Moriarty JM, Freeman S. Phlegmasia cerulea dolens associated with acute coronavirus disease 2019 pneumonia despite supratherapeutic warfarin anticoagulation. *J Vascular Surg Cases Innovat Techn.* (2020) 6:653–6. doi: 10.1016/j.jvscit.2020.10.002
13. Calo L, Semplicini A, Davis PA, Bonvicini P, Cantaro S, Rigotti P, et al. Cyclosporin-induced endothelial dysfunction and hypertension: are nitric oxide system abnormality and oxidative stress involved? *Transpl Int.* (2000) 13 Suppl 1:S413–8. doi: 10.1111/j.1432-2277.2000.tb02073.x
14. Boettler T, Newsome PN, Mondelli MU, Maticic M, Cordero E, Cornberg M, et al. Care of patients with liver disease during the COVID-19 pandemic: EASL-ESCMID position paper. *JHEP Rep.* (2020) 2:100113. doi: 10.1016/j.jhepr.2020.100113

Conflict of Interest: The authors declare that the research was conducted in the absence of any commercial or financial relationships that could be construed as a potential conflict of interest.

Publisher's Note: All claims expressed in this article are solely those of the authors and do not necessarily represent those of their affiliated organizations, or those of the publisher, the editors and the reviewers. Any product that may be evaluated in this article, or claim that may be made by its manufacturer, is not guaranteed or endorsed by the publisher.

frontiers | Frontiers in Cardiovascular Medicine

TYPE Case Report
PUBLISHED 05 August 2022
DOI 10.3389/fcvm.2022.915111

OPEN ACCESS

EDITED BY
Elaine L. Shelton,
Vanderbilt University Medical Center,
United States

REVIEWED BY
Michael Hofmann,
University of Zurich, Switzerland
Su-Zhen Dong,
Shanghai Jiao Tong University, China

*CORRESPONDENCE
Yuhang Liu
15524709667@163.com

†These authors have contributed equally to this work

SPECIALTY SECTION
This article was submitted to Pediatric Cardiology, a section of the journal Frontiers in Cardiovascular Medicine

RECEIVED 07 April 2022
ACCEPTED 13 July 2022
PUBLISHED 05 August 2022

CITATION
Lian X, Wang N, Bai C, Wen P and Liu Y (2022) Case report: A rare combination of right aortic arch with right patent ductus arteriosus and right tracheal bronchus causing impaired respiratory function.
Front. Cardiovasc. Med. 9:915111.
doi: 10.3389/fcvm.2022.915111

Case report: A rare combination of right aortic arch with right patent ductus arteriosus and right tracheal bronchus causing impaired respiratory function

Xingchen Lian[1,2†], Ning Wang[1,2†], Chuan Bai[1], Ping Wen[1†] and Yuhang Liu[1,2*†]

[1]Department of Cardiothoracic Surgery, Dalian Municipal Women and Children's Medical Center (Group), Dalian, China, [2]Graduate School, Dalian Medical University, Dalian, China

A right aortic arch with concomitant right patent ductus arteriosus and right tracheal bronchus is a rare congenital anomaly. Herein, the respiratory and circulatory functions of the child were normal at early ages, and imaging examination indicated that conservative treatment was suitable. However, with the growth and development of the child, the right tracheal bronchus was oppressed by the right arterial duct. We performed a cut and ligation of the right patent ductus arteriosus to relieve the pressure on the right tracheal bronchus. At the 6-month follow-up, the child had recovered well and exhibited no symptoms of respiratory restriction. Therefore, we believe that early interventions should be considered for this rare anatomic presentation to benefit the patient's respiratory and circulatory systems. Our experience provides a foundational reference for future cases.

KEYWORDS

right aortic arch, right patent ductus arteriosus, right tracheal bronchus, case report, tracheobronchial stenosis

Introduction

A right aortic arch with a left patent ductus arteriosus is likely to generate a clinically significant vascular ring that narrows the airway. However, a right aortic arch with a right patent arterial duct, as part of a normal anatomic variation, is associated with a relatively low risk of extracardiac anomalies or surgery (1). In this case, compression of the right tracheal bronchus by the right aortic arch with the right patent ductus arteriosus was identified by computed tomography angiography (CTA). We performed surgical ligation of the right patent ductus arteriosus to relieve

airway compression in the patient. At the 6-month follow-up, no aberrant clinical symptoms were noted.

Case description

During the prenatal phase, echocardiographs revealed that the fetus had a right aortic arch with a right patent ductus arteriosus (≤1 mm). Hepatitis B, human immunodeficiency virus, syphilis, and rubella tests were all negative in maternal prenatal tests. After birth, the infant performed well, with Apgar scores of 8 and 9 at 1 and 5 min, respectively. Transthoracic echocardiography and CTA were conducted after delivery to validate the findings of prenatal echocardiography and confirmed the right aortic arch with the right patent ductus arteriosus and the right tracheal bronchus. No interventions were carried out, considering that the infant did not exhibit any respiratory symptoms; however, follow-up after delivery was proposed. At the subsequent follow-up, transthoracic echocardiography showed that the right patent ductus arteriosus (≤1 mm) persisted. Family members were disinclined to surgical intervention, so further follow-up and observation were recommended.

Years later, the parents brought their 8-year-old child to our hospital under the mistaken assumption of pneumonia. Physical examination revealed hyperresonance in the right upper lung, and chest CT showed that the right upper lung had enhanced transmittance (**Figure 1**). Echocardiographs showed that the intra-cardiac anatomy was otherwise normal, in addition to good cardiac function, normal pulmonary artery, and right aortic arch with right patent ductus arteriosus (≤1 mm). On CTA, we found that the right aortic arch, right patent ductus arteriosus, and right pulmonary artery formed an "H-shaped" loop in conjunction with the right tracheal bronchus, which was "clamped" in it (**Figure 2**).

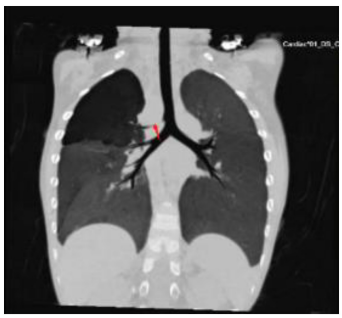

FIGURE 1
Computed tomography of the chest showed that the right upper lung had enhanced transmittance due to the right tracheal bronchus' oppression (arrow).

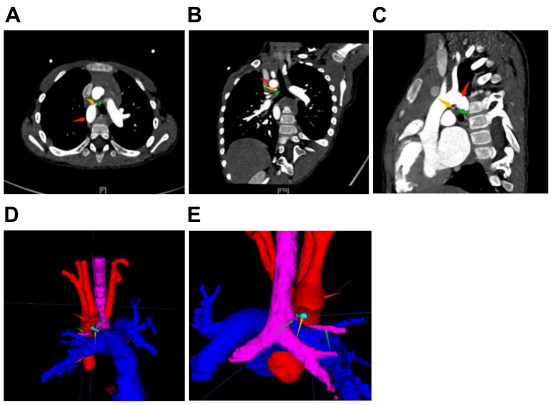

FIGURE 2
Computed tomography angiography [CTA, **(A–C)** horizontal, coronal, and sagittal] and [3-D reconstruction **(D,E)** front, back] show the right aortic arch (red arrow) and right ductus arteriosus (yellow arrow) with right tracheal bronchus (green arrow). The aorta and pulmonary artery are located in an anteroposterior relationship. In a normal conformation, even with the right aortic arch, the aorta is located to the right of the pulmonary artery. In addition, the left brachiocephalic artery and the right common carotid artery have a common trunk. This is the so-called bovine arch, a normal variant. The right tracheal bronchus, from the tracheal wall above the carina, runs in the "H"-shaped structure formed by the right aortic arch, right patent ductus, and right pulmonary artery.

After informing the parents of the patient's condition and related risks in detail, they requested urgent surgical intervention. Cut and ligation of the right patent ductus arteriosus through midline sternotomy without cardiopulmonary bypass was performed. At the 6-month follow-up, the patient had recovered well without any respiratory or cardiovascular symptoms. **Table 1** summarizes the clinical presentation and management of the patient.

Discussion

The right aortic arch can be defined as an anatomic anomaly, wherein the aorta arches over the right side of the bronchus instead of the left. The right aortic arch grows from the right fourth pharyngeal arch artery and the right dorsal aorta embryologically. The prevalence of the right aortic arch is approximately 0.1% in the general population and 13–34% in the tetralogy of Fallot (2, 3). Bronchus suis, also known as pig bronchus or tracheal bronchus, is usually an asymptomatic abnormal bronchus that arises from the tracheal wall above the carina. The incidence of bronchus suis in humans is 0.1–3.0% (4). During early embryogenesis, an aberrant bronchus is normally the result of additional tracheal outgrowth (5).

Right-sided ductus arteriosus occurs in 10% of fetuses with a right aortic arch and is usually asymptomatic (6). However, to the best of our knowledge, the combination of the right

TABLE 1 Timeline of events.

Timeline	Events
2011	A male infant was born who had a right aortic arch with a right patent ductus arteriosus (≤1 mm).
2011∼2021.09	The child was regularly followed up in the hospital and no abnormal manifestations were observed.
2021.09	Imaging revealed the child's airway obstruction and surgery was performed.
2021.09∼2022.03	On a follow-up of 6 months, the child recovered well without any symptoms of respiratory or cardiovascular problems.

tracheal bronchus compressed by the right aortic arch with the right patent ductus arteriosus was reported herein for the first time. In our case, the right tracheal bronchus runs in an "H-shaped" conformation formed by the right aortic arch, right patent ductus, and right pulmonary artery (**Figure 3**). These anatomic variants are usually not clinically significant when they are present alone.

As the patient grew and developed, the tracheal bronchus became compressed and narrowed. At the early follow-up, we were inclined toward conservative treatment as the patient did not exhibit any symptoms. In addition, the follow-up observation was recommended in accordance with the families' desire for conservative treatment. After the patient developed symptoms of airway obstruction, the family requested urgent treatment resolution. Post-case evaluation, the recommended treatment, included dissecting the ductus arteriosus or the arterial ligament and dissociating the surrounding tracheobronchial tissue to release the compression of the tracheal bronchus. The patient exhibited good postoperative recovery that confirmed our treatment strategy. However, further research is needed to determine whether earlier surgical intervention is warranted. In general, we should pay greater attention to the existence of airway blockages in patients when confronted with this unique anatomic combination.

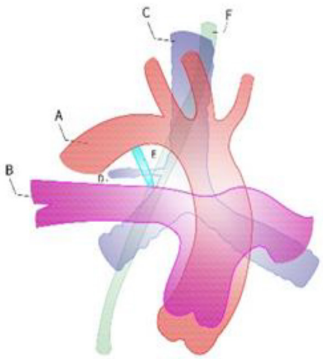

FIGURE 3
Right aortic arch with the right ductus against the right tracheal bronchus. A: descending aorta, B: right pulmonary artery, C: trachea, D: tracheal bronchus, E: right patent ductus, F: esophageal.

Data availability statement

The original contributions presented in the study are included in the article/supplementary material, further inquiries can be directed to the corresponding author.

Ethics statement

The studies involving human participants were reviewed and approved by the Medical Ethics Committee of the Dalian Municipal Women and Children's Medical Center (Group). Written informed consent to participate in this study was provided by the participants' legal guardian/next of kin.

Author contributions

XL and YL designed the study, performed the experiments, and were major contributors to write the manuscript. XL, NW, CB, PW, and YL performed the experiments, analyzed the data, and wrote the manuscript. All authors contributed to the article and approved the submitted version.

Acknowledgments

We would like to thank all of the doctors, nurses, and patients enrolled in the study in the Heart Center and Ultrasound Department at the Dalian Municipal Women and Children's Medical Center (Group) for their support.

Conflict of interest

The authors declare that the research was conducted in the absence of any commercial or financial relationships that could be construed as a potential conflict of interest.

Publisher's note

References

1. Cavoretto PI, Sotiriadis A, Girardelli S, Spinillo S, Candiani M, Amodeo S, et al. Postnatal outcome and associated anomalies of prenatally diagnosed right aortic arch with concomitant right ductal arch: A systematic review and meta-analysis. *Diagnostics.* (2020) 10:831. doi: 10.3390/diagnostics10100831

2. Liechty JD, Shields TW, Anson BJ. Variations pertaining to the aortic arches and their branches; with comments on surgically important types. *Q Bull Northwest Univ Med Sch.* (1957) 31:136–43.

3. Hastreiter AR, D'Cruz IA, Cantez T, Namin EP, Licata R. Right-sided aorta. I. Occurrence of right aortic arch in various types of congenital heartdisease. II. Right aortic arch, right descending aorta, and associated anoma-lies. *Br Heart J.* (1966) 28:722–39. doi: 10.1136/hrt.28.6.722

4. Ikeno S, Mitsuhata H, Saito K, Hirabayashi Y, Akazawa S, Kasuda H, et al. Airway management for patients with a tracheal bronchus. *Br J Anaesthesia.* (1996) 76:573–5. doi: 10.1093/bja/76.4.573

5. Dosi RA, Jain A, Joshi P, Motiwale S, Songara A. A rare case of a tracheal bronchus. *JACP.* (2018) 6:76–9. doi: 10.4103/jacp.jacp_28_17

6. Bronshtein M, Zimmer EZ, Blazer S, Blumenfeld Z. Right ductus arteriosus: Facts and theory. *Eur J Obstet Gynecol Reprod Biol.* (2011) 159:282–8. doi: 10.1016/j.ejogrb.2011.07.047

frontiers | Frontiers in Cardiovascular Medicine

TYPE Case Report
PUBLISHED 08 August 2022
DOI 10.3389/fcvm.2022.898914

OPEN ACCESS

EDITED BY
Utpal S. Bhalala,
Driscoll Children's Hospital,
United States

REVIEWED BY
Maruti Haranal,
U N Mehta Institute of Cardiology and Research Centre, India
Sabarinath Menon,
Sree Chitra Tirunal Institute for Medical Sciences and Technology (SCTIMST), India
Hari Gourabathini,
Indiana University South Bend,
United States

*CORRESPONDENCE
Jong-Hau Hsu
jhh936@yahoo.com.tw

SPECIALTY SECTION
This article was submitted to Pediatric Cardiology, a section of the journal Frontiers in Cardiovascular Medicine

RECEIVED 18 March 2022
ACCEPTED 18 July 2022
PUBLISHED 08 August 2022

CITATION
Wu Y-H, Liu Y-C, Chao M-F, Dai Z-K, Chen I-C, Lo S-H and Hsu J-H (2022) Case report: Transcatheter closure of a giant and tortuous right coronary artery to right ventricle fistula in an infant.
Front. Cardiovasc. Med. 9:898914.
doi: 10.3389/fcvm.2022.898914

Case report: Transcatheter closure of a giant and tortuous right coronary artery to right ventricle fistula in an infant

Yen-Hsien Wu[1], Yi-Ching Liu[1], Min-Fang Chao[2], Zen-Kong Dai[1,3], I-Chen Chen[1,3], Shih-Hsing Lo[1] and Jong-Hau Hsu[1,3]*

[1]Department of Pediatrics, Kaohsiung Medical University Hospital, Kaohsiung, Taiwan, [2]Department of Medical Imaging, Kaohsiung Medical University Hospital, Kaohsiung, Taiwan, [3]Department of Pediatrics, School of Medicine, College of Medicine, Kaohsiung Medical University, Kaohsiung, Taiwan

Congenital coronary artery fistulas (CAFs) are an uncommon congenital anomaly. While most patients are asymptomatic, life-threatening events including sudden death, myocardial ischemia, heart failure, infective endocarditis, and rupture of aneurysm may occur. Surgical ligation was once the standard choice of management of CAFs in the past. However, transcatheter closure of CAFs has become an emerging alternative to surgery in patients with suitable anatomy. We reported a 7-month-old infant with a giant and tortuous CAF that originated from the distal right coronary artery and drained into the right ventricle, and was successfully treated by transcatheter closure with an Amplatzer ductus occluder.

KEYWORDS

coronary artery fistula (CAF), transcatheter closure (TCC), ADO II, pediatric (infant), right ventricle (RV)

Introduction

Congenital coronary artery fistulas (CAFs) are abnormal connections between either or both coronary arteries and a cardiac chamber or a great vessel. It is a rare disease, and the incidence is around 0.002% of the general population (1). The natural history of CAFs is highly variable depending on their size. Those with small CAFs are often asymptomatic with incidental heart murmurs. Spontaneous closure has also been reported (2). However, patients with large CAFs may be complicated by acute myocardial ischemia, heart failure, infective endocarditis, and cardiac tamponade if there is a rupture of the fistula (3).

Coronary artery fistulas can be classified according to their origin or complexity. Sakakibara et al. suggested that a CAF can be classified as a proximal or distal type based on its origin (4). In the proximal type, the proximal native feeding arteries tend to be dilated, while the coronary arteries distal to the CAF remain normal. In contrast, in the distal type, the entire vessel is dilated. Based on the complexity of the morphology,

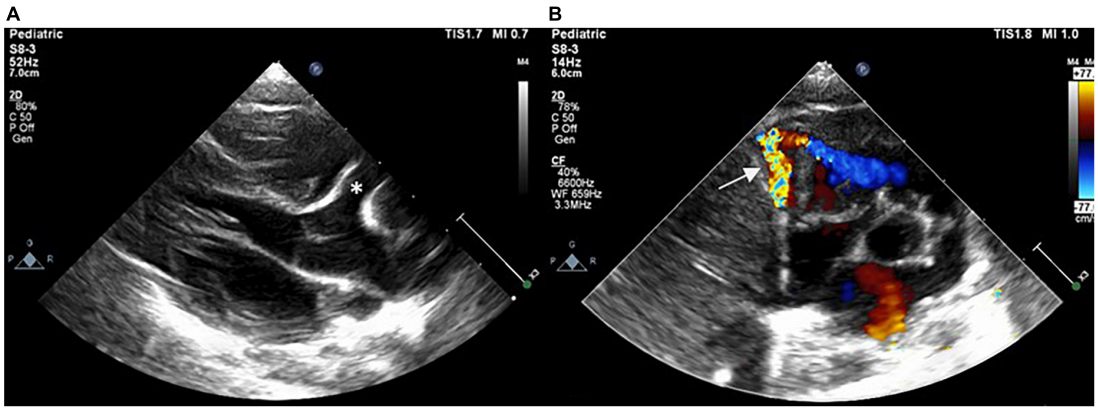

FIGURE 1
Postnatal echocardiogram showing dilated RCA (asterisk) with a fistula (arrow) drained into the RV in **(A)** parasternal long-axis view and **(B)** short-axis view. RCA, right coronary artery; RV, right ventricle.

a simple CAF has a single origin and drainage site through a single fistulous tract, whereas a complex CAF is composed of multiple origins or drainage sites with multiple fistulous structures (5).

Conventionally, surgical ligation was the standard option for management. Nevertheless, transcatheter closure of CAFs has recently become a potential alternative (3). In general, the favorable anatomies for transcatheter closure of CAFs include non-tortuous vessels, a single narrow drainage site, and a proximal origin. Herein, we report a 7-month-old infant with a large coronary artery (RCA) to the right ventricle (RV) fistula with a distal origin and tortuous right coronary artery. In this infant, the CAF was successfully obliterated by transcatheter closure with an Amplatzer ductus occluder II device.

Case report

A term female neonate was brought to our newborn intensive care unit with mild tachypnea 1 week after birth and a grade 4/6 continuous heart murmur in the left upper sternal border. Oxygen saturation was 100% under nasal cannula with a 1 L/min oxygen supply. Laboratory data revealed elevated serum B-type natriuretic peptide (BNP) (695 pg/ml) and normal troponin-I level (0.01 ng/ml). Electrocardiography showed sinus tachycardia with no evidence of myocardial ischemia, and her chest x-ray showed mild cardiomegaly with a cardiothoracic ratio of 0.58. Echocardiogram revealed a giant right coronary RCA to RV fistula with normal left ventricular systolic function. The orifice of the fistula on the RV side was about 2 mm (**Figure 1**). The fistula was found with a lageniform aneurysm arising from the distal RCA drained into the inferior wall of RV in the computed tomography angiography (CTA; **Figure 2**). Oral medications including furosemide and digoxin were administered, and the condition of congestive heart failure improved.

However, due to mild tachypnea and poor body weight gain (6.7 kg, 3 percentile), transcatheter closure of the fistula was performed at the age of 7 months old. The Qp/Qs was 1.2 while performing cardiac catheterization. However, a high mean pulmonary artery pressure of 23 mmHg was measured. RCA angiography revealed a giant and tortuous fistula that originated from the distal RCA and drained into the inferior RV, with an aneurysmal tract proximal to the drainage site (**Figure 3**). The size of the aneurysm was 6 mm, and the narrowest diameter of the drainage site was 1.5 mm. After delineating the morphology of the CAF, a 0.025-inch, 260-cm Terumo guidewire was first inserted from the RCA through the tortuous fistula to the RV, and then it was advanced to the pulmonary artery and snared to establish an arteriovenous wire loop. Based on the morphology of the aneurysmal tract and the width of the drainage site (1.5 mm), the Amplatzer Duct Occluder II (ADO II, 9-PDA2-04-04) with a 4-mm waist was chosen and the strategy for sizing the device for closure of patent ductus arteriosus was followed, that is, the occluder should be at least 2 mm greater than the narrowest drainage site. The ADO II device was then

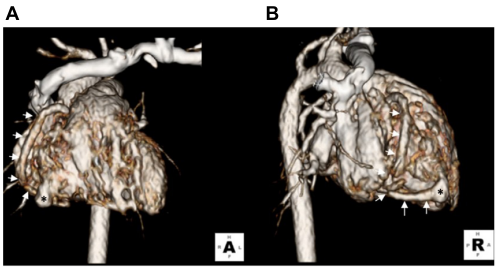

FIGURE 2
Three-dimensional computed tomography showing a lageniform coronary artery fistula (asterisks) arising from the RCA (arrows) drained into the inferior wall of the RV. **(A)** Anterior-posterior view. **(B)** Right lateral view.

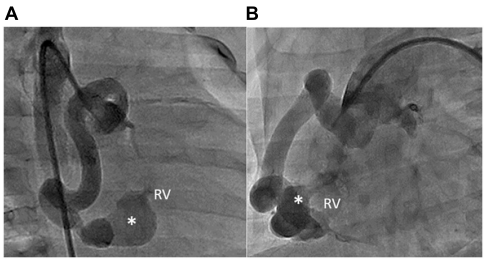

FIGURE 3
RCA angiography revealing that the aneurysmal fistula (asterisks) had arisen from the distal RCA and drained into the inferior wall of the RV. The shape of the fistula was lageniform. The aneurysmal tract of the fistula was 6 mm wide. The narrowest diameter of the drainage site was 1.5 mm. **(A)** RAO 30° and **(B)** LAO 60°.

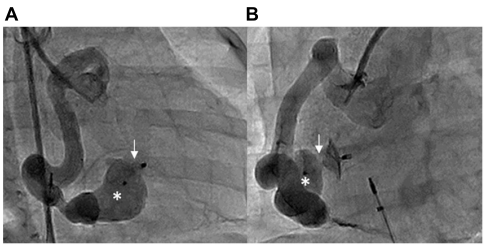

FIGURE 4
Post-procedural RCA angiography showing that the ADO II device (arrows) occluded the fistula with minimal residual shunt, with one disk in the aneurysmal tract (asterisks). **(A)** RAO 30° and **(B)** LAO 60°.

deployed through a low-profile 4 French delivery sheath and placed to occlude the fistula by antegrade approach from the femoral vein into the RV. After implantation of the device into the fistula and before releasing the device, a repeated RCA angiogram revealed a good device position with a minimal residual shunt. No ST segment change was noted in ECG, and no native coronary artery was involved by the device. After confirming the device's proper size and positioning, the ADO II was released smoothly (**Figure 4**). No complications such as heart ischemia and atrioventricular block were noted. The post-procedural echocardiogram showed a proper position of the device without a residual shunt. The patient was discharged the next day with medications of aspirin (5 mg/kg/day) and clopidogrel (1 mg/kg/day) for 12 months. The follow-up CTA 12 months after the procedure showed good device position without residual shunt or recanalization of the fistula. There was a slow flow state in the aneurysmal tract of the fistula due to thrombosis; however, the flow in the native vessels was normal. Therefore, clopidogrel alone was continued to prevent potential thrombus extension proximally into the native coronary artery. After the procedure, her dyspnea disappeared, and she regained normal body weight after follow-up for 2 years.

Discussion

Coronary artery fistulas are a rare disease accounting for 0.2–0.4% of congenital cardiac anomalies (6). CAFs arise most commonly from the RCA (55%), followed by the left coronary artery (35%), and rarely, 5% of fistulas are bilateral. Meanwhile, CAFs terminate mostly in the RV (45%), followed by the right atrium (25%), the pulmonary artery (15%), and less commonly the coronary sinus (7%) (3). An incomplete degeneration of sinusoidal connection between the lumens of primitive tubular heart in the early embryonic period may result in the formation of CAFs. The main hemodynamic drawback of abnormal shunts is coronary steal phenomenon and left-to-right shunt (6). Symptoms of CAFs depend on their size and severity of the shunt. Continuous heart murmur may be the only symptom in small shunts. However, large CAFs can result in heart failure, infective endocarditis, and myocardial ischemia (7).

The diagnosis of CAFs is confirmed by two-dimensional echocardiography and color Doppler sonography. Coronary artery dilatation is an important reminder of this disease as shown in our case (**Figure 1A**). Even though coronary angiography is essential to delineate the anatomy of CAFs, CTA can assist in non-invasive evaluation of CAFs before transcatheter intervention, especially in infants, to minimize the risk of catheterization. ECG and troponin tests are also helpful to detect myocardial ischemia.

The management of CAFs in children depends on the size and anatomy of the fistula and the presence of symptoms. According to American College of Cardiology/American Heart Association guidelines (8), treatment of small CAFs in asymptomatic patients is not suggested. Nonetheless, an intervention is recommended for large CAFs without symptoms and small to moderate-size fistulas with evidence of myocardial ischemia, arrhythmia, ventricular dysfunction, ventricular enlargement, or endarteritis (8). In our case, even though the Qp/Qs was small, this fistula is classified as large in size, since that fistulas, at any point larger than three times the expected proximate normal coronary artery diameter, or associated with similar ranges of dilation of the proximal associated coronary artery, are considered to be large size fistulas (9). In addition, coronary artery dilation and aneurysmal tract are often associated with stasis, which could lead to acute myocardial ischemia and aneurysmal rupture, respectively (10). After evaluating her clinical symptoms and fistula size and to prevent potential complications, we decided to perform percutaneous closure. As expected, her symptoms improved after the intervention.

In 1947, Biork et al. completed the first CAFs surgical closure (11). Since that procedure, surgical closure became the standard choice for closing CAFs. Even though the general outcome of surgical closure of CAFs is good, there is surgical mortality of 0–4% (12). CAF surgery is an invasive procedure that requires median sternotomy, and half of patients

undergo cardiopulmonary bypass. Postoperative complications including bleeding, infections, myocardial infarctions, and arrhythmias were reported (11). The first CAF transcatheter closure was reported in 1983 by Reidy et al. Since then, transcatheter closure became an alternative option for closing a simple CAF, but surgery remains the only option for complex CAFs. The advantages of transcatheter closure of CAF over surgery are avoidance of cardiopulmonary bypass and median sternotomy, lower cost of the procedure, and shorter recovery time. The procedural complications of CAF transcatheter closure include device displacement, fistula dissection, myocardial infarction, and transient atrial arrhythmia (6). Recently, numerous reports of transcatheter closure have been described, with the successful closure rate of CAFs being around 75–87% (6). In general, the favorable anatomies for transcatheter closure of CAFs were single fistula, non-tortuous vessels, single narrow drainage site, and proximal origin of the fistula (13). Notwithstanding, in our case, the CAF drained into the RV in the distal part of the RCA, and the fistula was tortuous.

There are several important procedural aspects to be addressed in this case. First, the main challenge was to place the occluder with the antegrade approach from the RV *via* the femoral vein. In our patient, the retrograde approach of from the aorta to the RCA carried a high risk of complications such as myocardial ischemia, thrombosis, and aneurysmal rupture during occluder device delivery due to the tortuosity of the RCA and the distal drainage site. Thus, the antegrade method was chosen, and we established an arteriovenous wire loop from the tortuous RCA, through the aneurysmal fistula, to the RV. Then, a snare technique was used to catch the wire, and then the CAF was occluded. Second, procedures of occluding a CAF are more challenging in an infant because of the risk of vascular damage by the delivery sheath or the occluder device. In this context, we suggest that choosing a low-profile delivery system and a soft device has an important role to minimize potential complications. Various devices are used to close CAFs, such as coils, Amplatzer vascular plugs, ADO, and Rashkind double-umbrella devices (7, 14, 15). Among these devices, the ADO II has the following advantages in the context of CAFs with a narrow drainage site and an aneurysmal tract, especially in infants. The ADO II is made of a fabric-free fine nitinol wire resulting in its soft texture and can be delivered through a low-profile sheath. These features make it easier to pass through a narrow drainage site and safer to advance into the aneurysmal tract in the RV wall, with minimized risk of aneurysmal rupture or RV injury in an infant as shown in our case. Finally, the morphology of fistula in our patient was in a lageniform shape near the RV drainage site, which is also a favorable factor for using ADO II since it has two disks clamping both the RV wall and aneurysm, thus could have less chance of device dislodgement (11, 16, 17).

Anticoagulation after intervention was controversial. Low-dose aspirin (3–5 mg/kg/day) for at least 6 months was mentioned in most literature (18), and severe coronary artery dilatation (> 10 mm) may warrant anticoagulation with warfarin (19). In our case, we prescribed a dual antiplatelet combination of aspirin and clopidogrel for 12 months followed by clopidogrel alone to prevent thrombosis in the dilated native RCA.

Long-term outcomes of transcatheter CAF closure from a limited case series demonstrate that this procedure is effective in most patients. However, complications can be found in certain patients at long-term follow-up, such as myocardial infarction and recanalization (20). Myocardial infarction can occur because of thrombus formation in the aneurysmal coronary artery or device thrombosis. In a case series, recanalization of a fistulous tract was found in 4 of 27 fistulas on repeat angiography at a median of 423 days after transcatheter closure (21). Thus, they recommended follow-up imaging study with coronary CT angiography or angiography for all patients who underwent successful CAF closure at 1–5 years to evaluate for recanalization.

Conclusion

Transcatheter closure is an effective management for infants with large RCA to RV fistula with suitable anatomy. ADO II can be considered as the device of choice for infants with tortuous CAF.

Data availability statement

The original contributions presented in the study are included in the article/supplementary material, further inquiries can be directed to the corresponding author.

Author contributions

J-HH carried out the studies. Y-CL, Z-KD, and I-CC participated in collecting the data. S-HL drafted the manuscript. Y-HW helped to draft the manuscript. All authors contributed to the article and approved the submitted version.

Acknowledgments

We appreciate Lorraine Tong for English editing of the manuscript.

Conflict of interest

The authors declare that the research was conducted in the absence of any commercial or financial relationships that could be construed as a potential conflict of interest.

Publisher's note

References

1. Buccheri D, Chirco PR, Geraci S, Caramanno G, Cortese B. Coronary artery fistulae: anatomy, diagnosis and management strategies. *Heart Lung Circ.* (2018) 27:940–51.

2. Yamanaka O, Hobbs RE. Coronary artery anomalies in 126,595 patients undergoing coronary arteriography. *Cathet Cardiovasc Diagn.* (1990) 21:28–40. doi: 10.1002/ccd.1810210110

3. Yun G, Nam TH, Chun EJ. Coronary artery fistulas: pathophysiology, imaging findings, and management. *Radiographics.* (2018) 38:688–703.

4. Sakakibara S, Yokoyama M, Takao A, Nogi M, Gomi H. Coronary arteriovenous fistula. nine operated cases. *Am Heart J.* (1966) 72:307–14.

5. Agarwal PP, Dennie C, Pena E, Nguyen E, LaBounty T, Yang B, et al. Anomalous coronary arteries that need intervention: review of pre- and postoperative imaging appearances. *Radiographics.* (2017) 37:740–57. doi: 10.1148/rg.2017160124

6. Challoumas D, Pericleous A, Dimitrakaki IA, Danelatos C, Dimitrakakis G. Coronary arteriovenous fistulae: a review. *Int J Angiol.* (2014) 23:1–10.

7. Zhu XY, Zhang DZ, Han XM, Cui CS, Sheng XT, Wang QG, et al. Transcatheter closure of congenital coronary artery fistulae: immediate and long-term follow-up results. *Clin Cardiol.* (2009) 32:506–12.

8. Warnes CA, Williams RG, Bashore TM, Child JS, Connolly HM, Dearani JA, et al. ACC/AHA 2008 guidelines for the management of adults with congenital heart disease: a report of the american college of cardiology/american heart association task force on practice guidelines (writing committee to develop guidelines on the management of adults with congenital heart disease). *Circulation.* (2008) 118:e714–833.

9. Latson LA. Coronary artery fistulas: how to manage them. *Catheter Cardiovasc Interv.* (2007) 70:110–6.

10. Li Y, Wu C, Liu W. Coronary artery ectasia presenting with thrombus embolization and acute myocardial infarction: a case report. *Medicine (Baltimore).* (2017) 96:e5976.

11. Gribaa R, Slim M, Ouali S, Neffati E, Boughzela E. Transcatheter closure of a congenital coronary artery to right ventricle fistula: a case report. *J Med Case Rep.* (2014) 8:432.

12. Waqar T, Farhan Ali Rizvi HM, Ahmed Ansari MZ. Surgical repair of congenital coronary artery fistula: a case report. *J Pak Med Assoc.* (2018) 68:804–6.

13. Wang X, Pang C, Liu X, Wang S, Zhang Z, Chen J, et al. Congenital coronary artery fistula in pediatric patients: transcatheter versus surgical closure. *BMC Cardiovasc Disord.* (2020) 20:484. doi: 10.1186/s12872-020-01769-7

14. Atik E, Leal F, Arrieta R. Case 2 / 2018 – coronary-cavitary fistula of right ventricular coronary artery 5 years after its occlusion by interventional catheterization. *Arq Bras Cardiol.* (2018) 110:289–91. doi: 10.5935/abc.20180048

15. De Santis A, Cifarelli A, Violini R. Transcatheter closure of coronary artery fistula using the new Amplatzer vascular plug and a telescoping catheter technique. *J Cardiovasc Med (Hagerstown).* (2010) 11:605–9. doi: 10.2459/JCM.0b013e3283313504

16. Zhao T, Lu M, So A, Wu W, Wang C, Xu Z, et al. Transcatheter closure of coronary artery fistulae: initial human experience with the Amplatzer Duct Occluder II. *J Interv Cardiol.* (2013) 26:359–65. doi: 10.1111/joic.12039

17. Wongwaitaweewong K, Roymanee S, Jarutach J. Transcatheter closure of an aortic-right ventricular fistula with an amplatzer duct occluder II (ADO II). *J Health Sci Med Res.* (2020) 38:331–5.

18. Amoozgar H, Edraki MR, Naghshzan A, Mehdizadegan N, Mohammadi H, Ajami G, et al. Midterm follow up of transcatheter closure of coronary artery fistula with Nit-Occlud® patent ductus arteriosus coil. *BMC Cardiovasc Disord.* (2021) 21:192. doi: 10.1186/s12872-021-01999-3

19. McMahon CJ, Nihill MR, Kovalchin JP, Mullins CE, Grifka RG, et al. Coronary artery fistula. management and intermediate-term outcome after transcatheter coil occlusion. *Tex Heart Inst J.* (2001) 28:21–5.

20. Al-Hijji M, El Sabbagh A, El Hajj S, AlKhouli M, El Sabawi B, Cabalka A, et al. Coronary artery fistulas: indications, techniques, outcomes, and complications of transcatheter fistula closure. *JACC Cardiovasc Interv.* (2021) 14:1393–406.

21. El-Sabawi B, Al-Hijji MA, Eleid MF, Cabalka AK, Ammash NM, Dearani JA, et al. Transcatheter closure of coronary artery fistula: A 21-year experience. *Catheter Cardiovasc Interv.* (2020) 96:311–9. doi: 10.1002/ccd.28721

frontiers | Frontiers in Pediatrics

TYPE Brief Research Report
PUBLISHED 23 September 2022
DOI 10.3389/fped.2022.888686

OPEN ACCESS

EDITED BY
Utpal S. Bhalala,
Driscoll Children's Hospital,
United States

REVIEWED BY
Omar R. J. Tamimi,
King Fahd Medical City, Saudi Arabia
Hsiuying Wang,
National Yang Ming Chiao Tung University, Taiwan

*CORRESPONDENCE
Hong Xu
hxu@shmu.edu.cn
Zhiping Li
zpli@fudan.edu.cn

SPECIALTY SECTION
This article was submitted to Pediatric Cardiology, a section of the journal Frontiers in Pediatrics

RECEIVED 03 March 2022
ACCEPTED 08 September 2022
PUBLISHED 23 September 2022

CITATION
Lu J, Zhang X, Xu H and Li Z (2022) Inspiration to mRNA-based COVID-19 vaccination: Serious adverse case reports with hepatitis B vaccine in real-world. *Front. Pediatr.* 10:888686. doi: 10.3389/fped.2022.888686

Inspiration to mRNA-based COVID-19 vaccination: Serious adverse case reports with hepatitis B vaccine in real-world

Jinmiao Lu [1], Xunjie Zhang[1], Hong Xu[2]* and Zhiping Li [2]*

[1]Department of Clinical Pharmacy, National Children's Medical Center, Children's Hospital of Fudan University, Shanghai, China, [2]Department of Nephrology, National Children's Medical Center, Children's Hospital of Fudan University, Shanghai, China

Objectives: The hepatitis B vaccine comprises hepatitis B surface antigen (HBsAg) produced by transgenic yeast cells. There are few serious adverse events (SAE) reports after Hepatitis B vaccination.

Methods: The authors searched the Chinese legal documents database for all SAE with Hepatitis B vaccination from January 2010 to January 2022.

Results: All seven patients received yeast-derived recombinant hepatitis B vaccine. Three cases of myocarditis (death), 2 cases of interstitial pneumonia (death), and 2 cases of encephalitis. The mean time of onset of SAE was 8.3 ± 4.3 h after vaccination.

Conclusion: The mechanism of vaccine-induced myocarditis may come from immune protein reactions. Based on the experience of Hepatitis B vaccine adverse events, we present new insights into the mechanism of myocarditis caused by the COVID-19 vaccine.

KEYWORDS

hepatitis B, safety, vaccine, myocarditis, COVID-19

Introduction

More than 800,000 people die from the Hepatitis B virus each year, and vaccination is the most cost-effective way to prevent the spread of the virus (1, 2). About 10% of the Chinese population carries the hepatitis B virus, and the Chinese government has implemented universal free hepatitis B vaccination since 2002 (3). Five enterprises in China produce hepatitis B vaccines, all recombinant hepatitis B vaccines. Hepatitis B vaccine is a milky suspension composed of purified virus surface antigen (HBsAg) and an aluminum adjuvant. And these vaccine preparations include sodium hydroxide, aluminum chloride, Disodium phosphate, sodium dihydrogen phosphate, and sodium chloride. Since 1999, thiomersal has been removed as a preservative from the Hepatitis B vaccine used in infant vaccinations (4). HBsAg is a hepatitis B virus capsid protein produced by recombinant yeast or CHO cells. HBsAg does not contain genetic material and pathogenicity. Recombinant hepatitis B vaccine can stimulate the body to produce protective antibodies and can be used to prevent all hepatitis B virus subtypes. The Hepatitis B vaccine showed well-established safety and effectiveness (5, 6). Clinical

studies have shown that the most common adverse events are local pain, fever, and rash. These symptoms will subside within 3 days (7).

The whole course of Hepatitis B vaccination requires three doses given within a few days of birth, 1 month later, and 6 months later. Some rare serious adverse events (SAE) are associated with Hepatitis B vaccination. Besides, China still lacks a separate database for adverse events and data collection on serious adverse events related to vaccines. And serious adverse events are rarely reported for complex reasons (8). Therefore, it is a feasible supplementary method to obtain the vaccine adverse reaction from the public legal dispute database. We analyzed the available legal cases related to the hepatitis B vaccine and SAE from an open legal document database. The data from the real world may expand current public knowledge and improve patient safety with the hepatitis B vaccine.

Methods

The data in this study came from the website database of China's court, https://wenshu.court.gov.cn. The authors searched the database from January 2010 to January 2022. Legal disputes include death after vaccination, prolonged hospitalization, and permanent disability. A panel of five experts evaluated the cause-and-effect relationship between vaccines and adverse reactions. The experts were senior specialists who have worked in clinical medicine, epidemiology, clinical laboratory, pharmacy, and forensic medicine for at least 3 years. The panel members evaluated causality by considering seven factors: time sequence, medicine information, dose-effect relationship, response pattern to drugs, reactivation, etiology, and combination of drugs. Then, this method evaluated outcomes as highly possible, possible, indeterminate, or impossible.

Results

Seven severe adverse events related to the hepatitis B vaccine were retrieved from the database, five males and two females, with a ratio of 2.5:1. Six infants, were under 1 year of age, and one was an adult of 19 years. All were healthy before vaccination and had no hepatitis B or history of hepatitis B infection in their family history. Of all adverse events, 3 were myocarditis, 2 were meningitis, and 2 were interstitial pneumonia (Table 1).

Four infants and one adult died after the second vaccination. There were 3 cases of myocarditis and 2 cases of interstitial pneumonia. Their median time of death was 9 h after vaccination, ranging from 2 to 13 h. The onset of the adverse events was rapid, and there was no course of treatment in all the cases. The deceased patients had previously been in good health and had no heart disease or pneumonia history. The meeting of a panel of five senior medical experts (requested by the court) concluded that three cases of myocarditis were directly related to hepatitis B vaccination. Two patients could not determine the cause and effect of vaccine adverse reactions, which may be due to the long treatment time and slow progress of the disease.

Case 1: Less than 1 year-old. After his third dose of the hepatitis B vaccine, he had a fever for 3 days and hematuria for 2 days. He was diagnosed with myocarditis complicated by the hemolytic uremic syndrome. He died of multiple organ dysfunction syndromes 5 days later.

Case 2: Less than 1 year-old. She developed a fever and rash 3 h after her third vaccination. She was admitted to the hospital for myocarditis, but the parents refused the patient to be hospitalized. Two days later, she became sicker at home and died in the emergency room.

Case 3: Twelve hours after his fourth hepatitis B vaccination, he collapsed and died at home. At autopsy, the cardiac blood tests were myoglobin >3,000 μg/L, creatine kinase isoenzyme >300 μg/L, and troponin >10 μg/L.

Case 4: Less than 1 year-old. On the way home, he died 2 h after his second hepatitis B vaccination. The death was diagnosed as a result of acute respiratory failure caused by bilateral lung bronchopneumonia.

Case 5: Less than 1 year-old. She died 11 h after returning home after her third hepatitis B vaccination. The death was diagnosed as respiratory and circulatory failure due to interstitial pneumonia.

Case 6: Less than 1 year-old. He developed fever, cough, vomiting, diarrhea, and convulsions 8 h after the third dose. He was hospitalized for 3 months with focal brain atrophy, encephalomalacia, and gliosis. His final diagnosis was encephalitis sequelae and disability.

Case 7: Less than 1 year-old. He developed fever 9 h after the third dose. Oral ibuprofen was not practical, and he had one convulsion. After 4 months in hospital, he was diagnosed with epilepsy, and cerebral palsy, which resulted in a disability.

Discussion

The smallpox vaccine is recognized to induce myocarditis with an incidence of 16 cases per 100,000 (9). Our study reported three cases of myocarditis induced by hepatitis B vaccination to raise the attention of this potential severe adverse event after vaccination. According to the China Health Statistics Yearbook, 185 million babies were vaccinated against the Hepatitis B vaccine. Therefore, seven severe cases represented the incidence of serious adverse events was 4 per 1 million. We may underestimate the incidence rate, but it is consistent with the phenomenon that only some adverse events cause legal controversy.

Why does myocarditis cause rapid infant death in a short period? We think there are three possible reasons. First, fulminant myocarditis is a hazardous disease, with a

TABLE 1 Summary of severe adverse reactions due to hepatitis B vaccine ($n = 7$).

Gender	Age (years)	Vaccination times	Patient presentation/Diagnostic procedure	Diagnose	Prognosis	Causality
Male	0.5	3	He developed a fever on the day of vaccination and was hospitalized for 2 days before being diagnosed with myocarditis and hemolytic uremic syndrome. He died 5 days later. The autopsy showed that the child died of myocarditis.	Myocarditis	Death	Highly possible
Female	0.6	3	She developed a fever and Rash 3 h after vaccination. The diagnosis was myocarditis. The patient's family refused to be hospitalized. Two days later, she died at home. The autopsy showed that the child died of myocarditis.	Myocarditis	Death	Highly possible
Male	19	4	He finished his vaccination in the morning and there was nothing abnormal after the vaccination. At night, he collapsed and died. The blood from his heart at autopsy was found: Myoglobin >3,000 μg/L, Creatine kinase isoenzyme > 300 μg/ L, Troponin> 10 μg/L.	Myocarditis	Death	Highly possible
Male	0.3	2	Two hours after he finished his vaccination, the parents found the child dead.	Interstitial pneumonia	Death	Highly possible
Female	0.5	3	She died in her sleep 11 h after being vaccinated.	Interstitial pneumonia	Death	Highly possible
Male	0.6	3	He developed fever, seizures, and other symptoms 8 h after the inoculation. After 3 months of hospitalization, the diagnosis was focal cerebral atrophy, encephalomalacia, gliosis, and cerebral palsy.	Encephalitis	Disability	Indeterminate
Male	0.6	3	He developed fever and febrile convulsion 9 h after vaccination. After 4 months of treatment, the diagnosis was: 1. Epilepsy: 2. Encephalitis: 3. Cerebral palsy.	Encephalitis	Disability	Indeterminate

pediatric patient's mortality rate of more than 48% (10). The Pathophysiology of heart failure in children is markedly different from that in adults (11). Second, the patient is too late to be rescued in time. The cardiovascular adverse effects of the vaccine do not occur immediately after the injection. Third, early adverse events (crying, shortness of breath) in infants who received subsequent vaccinations were ignored based on the excellent safety of the first dose. In addition, our study showed a higher incidence of myocarditis in men than in women (2:1). This appearance may be related to the physiological characteristics of a male. Men also have a higher incidence of other myocarditis, with more severe heart symptoms (12).

Hepatitis B vaccine myocarditis is associated with allergic vasculitis and may subside with corticosteroid therapy (13). In all of the cases in our study, adverse events occurred immediately after the second dose of the vaccine. It is suggested that hepatitis B vaccine-induced myocarditis may be a drug-induced allergic syndrome. Accordingly, severe autoimmune adverse events following Hepatitis B vaccine vaccination have been reported in the literature (14). There is a causal relationship between the hepatitis B vaccine and autoimmune diseases, including rheumatoid arthritis, myelitis, optic neuritis, and nephritis (15). And the Hepatitis B vaccine is positively associated with an increased incidence of child arthritis (16). Two cases in this study with childhood encephalitis caused by the hepatitis B vaccine may also be related to autoimmune disease.

The mRNA-Based COVID-19 vaccine is similar to the hepatitis B vaccine in the following perspectives. First, both

vaccine's substrates induce human immune responses and are partly identical in structure (HBsAg protein *vs.* SARS-CoV-2 S protein). For example, hepatitis B proteins presented antigenic properties that can cause a putative protective effect against COVID-19 (17). Second, all the adverse occurs after the second dose, regardless of the vaccine source (18, 19). Recently, many studies have shown that multiple mRNA-Based COVID-19 vaccines can cause myocarditis (20, 21). On the myocarditis reports of 1,626 cases, 82% occurred after the second vaccination dose (20). Another study showed that all instances of juvenile myocarditis occurred 4 days after the second injection (22). Third, the cases in this study were all sudden myocarditis deaths, similar to those caused by SARS-CoV-2. Therefore, we hypothesized that the first vaccine established immune system memory, and then the second vaccine caused acute allergies, including myocarditis or other autoimmune diseases. Interestingly, a new COVID-19 Vaccine, Novavax, is clearly stated in its specifications: Clinical trials data provide evidence for increased risks of myocarditis (23).

Rare heart death cases were reported in patients after their mRNA COVID-19 vaccination (21). We suspected that the mild symptoms of the mRNA vaccine might be related to the slow release of SARS-CoV-2 S protein with mRNA vaccines. The Hepatitis B vaccine contains protein injected directly into the body and can induce acute allergies. In contrast, mRNA-Based COVID-19 vaccine takes a while to translate the mRNA into virus protein, which acts as a "slow-release" process, resulting in milder symptoms and few sudden deaths. The limitation of this study is that our legal documents only report a small number of cases and may have missed other patients.

Conclusion

In this report, we summarize each patient's clinical course and evaluation. Despite these rare adverse events, the benefit of universal vaccination against hepatitis B still outweighs the risk at this point. Hepatitis B vaccine-induced serious adverse events are rare, and myocarditis may be related to an autoimmune reaction. The vaccination after the first dose is associated with a higher risk of SAE than the first dose. The similarity between the hepatitis B vaccine protein and the COVID-19 vaccine-derived protein, we should pay close attention to the vaccine autoimmune response, especially myocarditis.

Data availability statement

The raw data supporting the conclusions of this article will be made available by the authors, without undue reservation.

Ethics statement

The studies involving human participants were approved by Medical Ethics Committee of Children's hospital of Fudan University in Shanghai, China (No. 2020-187). Written informed consent from the participants' legal guardian/next of kin was not required to participate in this study in accordance with the national legislation and the institutional requirements.

Author contributions

JL and XZ requested the data sets and drafted the manuscript. HX and ZL were involved in the study conception and design and critically reviewed the draft manuscript. All authors approved the final manuscript as submitted and agreed to be accountable for all aspects of the work.

Funding

This work was supported by National Natural Science Foundation (grant number 81874325) and the Scientific Research Project of Science and Technology Commission of Shanghai Municipality (grant numbers 19DZ1910604, 19XD1400900, and 18DZ1910604).

Conflict of interest

The authors declare that the research was conducted in the absence of any commercial or financial relationships that could be construed as a potential conflict of interest.

Publisher's note

References

1. Lavanchy D, Kane M. Global epidemiology of hepatitis B virus infection. In: Liaw Y-F, Zoulim F, editors. *Hepatitis B Virus in Human Diseases*. Springer. (2016). p. 187–203. doi: 10.1007/978-3-319-22330-8_9

2. Kim WR. Emerging therapies toward a functional cure for hepatitis B virus infection. *Gastroenterol Hepatol.* (2018) 14:439–42.

3. Tang J, Luo Y-Q, Zhou Y-H. Elimination of hepatitis B virus infection in children: experience and challenge in China. *Chin Med J.* (2021) 134:2818–24. doi: 10.1097/CM9.0000000000001791

4. Centers for Disease Control and Prevention (CDC). Availability of hepatitis B vaccine that does not contain thimerosal as a preservative. *MMWR Morb Mortal Wkly Rep*. (1999) 48:780–82.

5. Weng MK, Doshani M, Khan MA, Frey S, Ault K, Moore KL, et al. Universal hepatitis B vaccination in adults aged 19–59 years: updated recommendations of the advisory committee on immunization practices—United States, 2022. *Morb Mortal Wkly Rep.* (2022) 71:477. doi: 10.15585/mmwr.mm7113a1

6. Poland GA, Jacobson RM. Prevention of hepatitis B with the hepatitis B vaccine. *N Engl J Med.* (2004) 351:2832–8. doi: 10.1056/NEJMcp041507

7. Nency YM, Rahmadi FA, Mulyono DTA, Farhanah N, Hapsari R, Farida H, et al. Protectivity and safety following recombinant hepatitis B vaccine with different source of bulk compared to hepatitis B (Bio Farma) vaccine in Indonesia. *Clin Exp Vaccine Res.* (2022) 11:43. doi: 10.7774/cevr.2022.11.1.43

8. Lopez-Gonzalez E, Herdeiro MT, Figueiras A. Determinants of under-reporting of adverse drug reactions. *Drug Saf.* (2009) 32:19–31. doi: 10.2165/00002018-200932010-00002

9. Dudley MZ, Halsey NA, Omer SB, Orenstein WA, O'Leary ST, Limaye RJ, et al. The state of vaccine safety science: systematic reviews of the evidence. *Lancet Infect Dis.* (2020) 20:e80–9. doi: 10.1016/S1473-3099(20)30130-4

10. Matsuura H, Ichida F, Saji T, Ogawa S, Waki K, Kaneko M, et al. Clinical features of acute and fulminant myocarditis in children – 2nd nationwide survey by Japanese Society of Pediatric Cardiology and Cardiac Surgery. *Circ J.* (2016) 80:2362–8. doi: 10.1253/circj.CJ-16-0234

11. Kaski JP. Paediatric cardiology - Not just small hearts in small bodies!: An editorial by the section editor of the new section on pediatric cardiology. *Int J Cardiol*. (2022) 366:88–9. doi: 10.1016/j.ijcard.2022.07.002

12. Fairweather D, Cooper LT Jr., Blauwet LA. Sex and gender differences in myocarditis and dilated cardiomyopathy. *Curr Probl Cardiol.* (2013) 38:7–46. doi: 10.1016/j.cpcardiol.2012.07.003

13. Barton M, Finkelstein Y, Opavsky MA, Ito S, Ho T, Ford-Jones LE, et al. Eosinophilic myocarditis temporally associated with conjugate meningococcal C and hepatitis B vaccines in children. *Pediatr Infect Dis J.* (2008) 27:831–5. doi: 10.1097/INF.0b013e31816ff7b2

14. Grotto I, Mandel Y, Ephros M, Ashkenazi I, Shemer J. Major adverse reactions to yeast-derived hepatitis B vaccines—a review. *Vaccine.* (1998) 16:329–34. doi: 10.1016/S0264-410X(97)00214-4

15. Geier MR, Geier DA. A case-series of adverse events, positive re-challenge of symptoms, and events in identical twins following hepatitis B vaccination: analysis of the Vaccine Adverse Event Reporting System (VAERS) database and literature review. *Clin Exp Rheumatol.* (2004) 22:749–55.

16. Fisher MA, Eklund SA, James SA, Lin X. Adverse events associated with hepatitis B vaccine in U.S. children less than six years of age, 1993 and 1994. *Ann Epidemiol*. (2001) 11:13–21. doi: 10.1016/S1047-2797(00)00078-8

17. Haddad-Boubaker S, Othman H, Touati R, Ayouni K, Lakhal M, Ben Mustapha I, et al. *In silico* comparative study of SARS-CoV-2 proteins and antigenic proteins in BCG, OPV, MMR and other vaccines: evidence of a possible putative protective effect. *BMC Bioinform.* (2021) 22:1–14. doi: 10.1186/s12859-021-04045-3

18. Kim HW, Jenista ER, Wendell DC, Azevedo CF, Campbell MJ, Darty SN, et al. Patients with acute myocarditis following mRNA COVID-19 vaccination. *JAMA Cardiol.* (2021) 6:1196–201. doi: 10.1001/jamacardio.2021.2828

19. Salah HM, Mehta JL. COVID-19 vaccine and myocarditis. *Am J Cardiol.* (2021) 157:146–8. doi: 10.1016/j.amjcard.2021.07.009

20. Oster ME, Shay DK, Su JR, Gee J, Creech CB, Broder KR, et al. Myocarditis cases reported after mRNA-based COVID-19 vaccination in the US from December 2020 to August 2021. *JAMA*. (2022) 327:331–40. doi: 10.1001/jama.2021.24110

21. Habib MB, Hamamyh T, Elyas A, Altermanini M, Elhassan M. Acute myocarditis following administration of BNT162b2 vaccine. *IDCases.* (2021) 25:e01197. doi: 10.1016/j.idcr.2021.e01197

22. Marshall M, Ferguson ID, Lewis P, Jaggi P, Gagliardo C, Collins JS, et al. Symptomatic acute myocarditis in 7 adolescents after Pfizer-BioNTech COVID-19 vaccination. *Pediatrics.* (2021) 148:e2021052478. doi: 10.1542/peds.2021-052478

23. Heath PT, Galiza EP, Baxter DN, Boffito M, Browne D, Burns F, et al. Safety and efficacy of NVX-CoV2373 covid-19 vaccine. *N Engl J Med.* (2021) 385:1172–83. doi: 10.1056/NEJMoa2107659

frontiers | Frontiers in Cardiovascular Medicine

TYPE Case Report
PUBLISHED 23 September 2022
DOI 10.3389/fcvm.2022.977432

OPEN ACCESS

EDITED BY
Alvise Guariento,
University of Toronto, Canada

REVIEWED BY
Sathish Srinivasan,
Oklahoma Medical Research Foundation, United States
Antionette Latrece Williams,
Ann & Robert H. Lurie Children's Hospital of Chicago, United States

*CORRESPONDENCE
Chaoji Zhang
chaojizhang@163.com

†These authors have contributed equally to this work and share first authorship

SPECIALTY SECTION
This article was submitted to Pediatric Cardiology, a section of the journal Frontiers in Cardiovascular Medicine

RECEIVED 28 June 2022
ACCEPTED 29 August 2022
PUBLISHED 23 September 2022

CITATION
Feng J, Wang Y, Cheng S, Liu Z, Lan L, Miao Q and Zhang C (2022) Case report: Congenital mitral and tricuspid valve insufficiency in a patient with Axenfeld-Rieger syndrome. *Front. Cardiovasc. Med.* 9:977432. doi: 10.3389/fcvm.2022.977432

Case report: Congenital mitral and tricuspid valve insufficiency in a patient with Axenfeld-Rieger syndrome

Jingwei Feng[1†], Yingjiao Wang[1†], Shiyu Cheng[2], Zishuo Liu[3], Ling Lan[4], Qi Miao[5] and Chaoji Zhang[5*]

[1]Department of Surgery, Peking Union Medical College Hospital, Peking Union Medical College, Chinese Academy of Medical Sciences, Beijing, China, [2]Department of Ophthalmology, Peking Union Medical College Hospital, Peking Union Medical College, Chinese Academy of Medical Sciences, Beijing, China, [3]Department of Ultrasound, Beijing Hospital, National Center of Gerontology, Institute of Geriatric Medicine, Chinese Academy of Medical Sciences, Beijing, China, [4]Department of Anesthesiology, Peking Union Medical College Hospital, Peking Union Medical College, Chinese Academy of Medical Sciences, Beijing, China, [5]Department of Cardiac Surgery, Peking Union Medical College Hospital, Peking Union Medical College, Chinese Academy of Medical Sciences, Beijing, China

Axenfeld-Rieger syndrome (ARS) is an autosomal dominant disorder that is primarily due to disruption of the development of neural crest cells. The onset of associated symptoms in both eyes accompanied by extraocular developmental defects is referred to as ARS. Cardiac defects associated with ARS have been reported, but the extent of the cardiac defects has yet to be defined. We report a case of a 17-year-old girl with ARS with typical facial malformations and severe mitral and tricuspid valve insufficiency. The patient was diagnosed with secondary glaucoma detected on ophthalmologic examination. Echocardiography showed severe mitral and tricuspid valve insufficiency. This case provides further evidence of the association of ARS with cardiac malformations and extends the reported range of cardiac malformations in patients with ARS.

KEYWORDS

Axenfeld-Rieger syndrome (ARS), mitral valve insufficiency, tricuspid valve insufficiency, glaucoma, cardiac malformations

Background

Axenfeld-Rieger anomaly (ARA) is an ocular condition characterized by extensive defects of the anterior chamber of the eye, mainly affecting the corneal structures. Anterior chamber defects include Axenfeld anomaly, characterized by prominent and anteriorly displaced Schwalbe lines and iris-corneal adhesions, and Rieger anomaly, which manifests as iris hypoplasia and pupil malformation (1). These ocular changes may lead to secondary glaucoma. Secondary glaucoma occurs due to ocular or systemic diseases that affect or destroy the normal aqueous humor circulation, block aqueous humor discharge, and cause intraocular pressure elevation. The presence of anomalies in the anterior chamber angle and drainage structures of the eye contributes to a

10.3389/fcvm.2022.977432

lifetime risk of glaucoma and can lead to irreversible blindness (2). ARA can occur as an isolated defect, be episodic, an autosomal dominant trait, or part of a syndrome. ARA is sometimes associated with extraocular developmental defects, particularly of the teeth, facial bones, and periaqueductal skin (3). The combination of ocular and extraocular malformations is known as Axenfeld-Rieger syndrome (ARS) (4). The disorders that make up ARS are complex, inherited in a dominant manner, have a high ectopic rate, and are genetically heterogeneous (5). ARS is classified into three types based on systemic manifestations. Patients with ARS type 1 typically present with dental anomalies, craniofacial anomalies, and umbilical anomalies; patients with ARS type 2 usually present with oligodontia and microdontia, but craniofacial and umbilical anomalies are less common; patients with ARS type 3 rarely present with significant dental or facial anomalies, but may have hearing loss and heart defects (6–8). Herein, we report a rare case of a patient with ARS with both distinctive facial malformations and mitral and tricuspid valve dysplasia.

Case presentation

A 17-year-old girl was admitted to the hospital 1 year ago for shortness of breath after activity, dyspnea, weakness, and generalized swelling with no apparent reason. The patient then visited us for investigation of bilateral secondary glaucoma. The patient had poor vision in her left eye and could only see the optometrist's hand moving at 30 cm from her face. Ocular examination revealed visual acuity of 0.5 in the right eye, intraocular pressure of 28.2 mmHg in the right eye and 39.8 mmHg in the left eye; the left eye had 15 degrees of exotropia, a corneal diameter of 13 mm, slight edema, partial anterior adhesion of the atrial angle, iris atrophy, and localized hole formation (Figure 1). She had a distorted and deviated left pupil, clear right cornea, round right pupil, clear lens in both eyes, cup-to-disc ratio of 0.9 in the left eye and 0.3 in the right eye, pale and well-defined optic disc in the left eye, and normal retinas (Figure 2). Atrial angle examination revealed extensive anterior adhesions of the iris in both eyes, anterior displacement of Schwalbe's ring, and striated tissue across the atrial angle in the peripheral part Bof the iris, adhering to Schwalbe's line and pulling on the iris. The midface was flattened and the eyes were widely spaced (Figure 3A). The dentition was still regular, with a sharp crown and poorly developed permanent teeth, of which there were currently only four (Figure 3B). The heart borders were enlarged on percussion. On auscultation, the heart rate was 87 beats/min without arrhythmia, with systolic murmurs (grade 3/6) in the mitral and tricuspid valve areas.

The patient was diagnosed with ARS and secondary glaucoma in both eyes, and anti-glaucoma surgery was recommended. Considering the patient's young age, advanced glaucoma, and the risk of non-compliance during awake surgery, anti-glaucoma surgery under general anesthesia was proposed to reduce the intraoperative stimulation of the optic nerve. Preoperative echocardiography showed a left ventricular ejection fraction of 58%, mitral valve thickening and severe mitral valve closure incompetence (Figure 4A), total heart enlargement, severe tricuspid valve closure incompetence (Figure 4B), and reduced right ventricular systolic function. These findings showed that the patient had poor cardiac function and was potentially unable to tolerate ocular surgery.

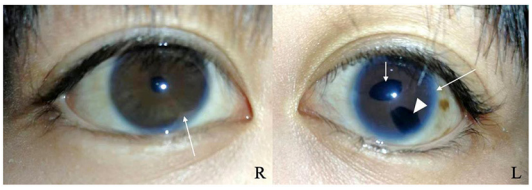

FIGURE 1
Slit-lamp photographs of the right and left eyes. Both eyes show anterior synechia (long arrows). The left eye shows pupil deformation and deviation (short arrow), iris atrophy causing the formation of a localized pore (arrowhead).

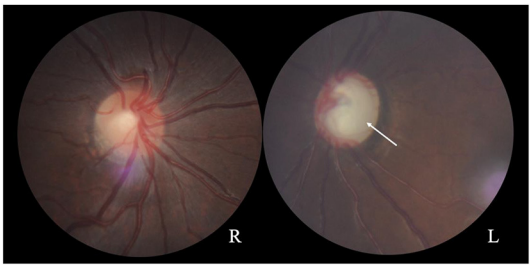

FIGURE 2
Fundus photographs showing a normal optic disc in the right eye and a pale optic disc with a clear border in the left eye (arrow). The cup-to-disc ratio is 0.3 for the right eye and 0.9 for the left eye.

FIGURE 3
(A) The patient has a wide flat nasal bridge, increased distance between the medial canthi, and flat cheeks. **(B)** The patient has fairly normal dentition with a sharp crown and poorly developed permanent teeth.

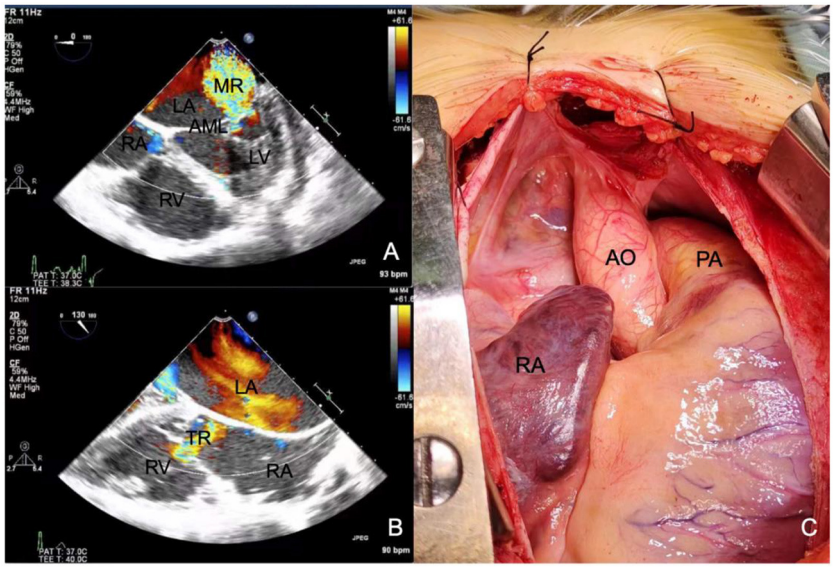

FIGURE 4
Echocardiography shows **(A)** severe mitral regurgitation and **(B)** severe tricuspid regurgitation. **(C)** Intraoperative photographs show that the aorta is 1.5 cm in diameter, which is significantly smaller than normal. RA, right atrium; RV, right ventricle; LA, left atrium; LV, left ventricle; AML, anterior mitral leaflet; MR, mitral regurgitation; TR, tricuspid regurgitation; AO, aorta; PA, pulmonary artery.

Therefore, she was treated with diuretics to lower the intraocular pressure and underwent cardiac surgery to improve her cardiac function. The patient underwent mitral and tricuspid valvuloplasty with a #28 Sovering band in the mitral valve and a #27 Sovering band in the tricuspid valve. Intraoperatively, the patient was also found to have a hypoplastic aorta with a significantly smaller aortic diameter than normal for her age (Figure 4C). The patient recovered well postoperatively, and postoperative echocardiography showed normal valve function.

Discussion

There are previous reports of ARS in association with congenital cardiac anomalies such as mitral, aortic, and pulmonary valve lesions, atrial septal defects, ventricular septal defects, and arterial trunk malformations (9–14). Gripp et al. (10) reported a 21-month-old patient with glaucoma who had congestive heart failure due to a dysplastic arched mitral valve and a mildly dysplastic left ventricular outflow tract and aortic valve. Grosso et al. (15) reported a patient with both mitral valve prolapse and tricuspid stenosis who presented with mitral and tricuspid valve insufficiency after two valvuloplasty procedures. Their patient's father underwent echocardiography for recurrent dyspnea, which was suggestive of mitral valve prolapse and tricuspid valve insufficiency (15). The family reported by Grosso et al. (15) is unusual in that they had no characteristic facial features of ARS, such as widely spaced eyes, a wide flat nasal bridge, flat cheeks, an acutely protruding lower jaw, an underbite, missing teeth, sparse teeth, a sharp crown, a central notch in the crown of the tooth, or degenerated periungual skin (16). Grosso et al. (15) concluded that the genetic characteristics of the family members were interrelated and not coincidental, and suggested that their findings might further support the hypothesis of a new genetic syndrome as proposed by Cunningham et al. (17). In the present case, we reported a 17-year-old girl with ARS with secondary glaucoma who had characteristic significant facial deformities and dental hypoplasia. Our patient also presented with severe mitral and tricuspid valve insufficiency, and had a small aortic diameter. Leaflet plication and repair were successful and well-tolerated intraoperatively.

Numerous studies have shown that the ocular and extra-ocular manifestations of ARS are associated with neural crest dysplasia. Besides, some researchers have suggested that neural crest dysplasia is related to the pathogenesis of aortic constriction and mitral aortic valve disease, as neural crest cells are also present in the heart valves (11, 18). Similarly, we believe that the heart valve defects observed in our patient were attributable to a developmental disorder of the neural crest tissue. To date, three loci associated with ARS have been identified on chromosomes 4q25, 6p25, and 13q14 (19–21). Genes for 4q25 and 6p25 have been cloned and are known as *PITX2* and *FOXC1*, respectively (3, 22, 23). *PITX2* is a pair of homologous frameshift genes that regulate the expression of other genes during embryonic development. Lu et al. (24). suggested that the *PITX2* product may be an effector from the early embryo stage to the formation of the left

and right axes of each organ. Expression of the homologous frame gene *PITX2* in the neural crest is required for the development of the optic stalk and preoptic ganglion. Studies have demonstrated a direct link between *PITX2* deficiency and abnormal development of cardiac structures, including the atrioventricular valve (25, 26). Although *PITX2c* is a major transcript in mouse and human embryonic and adult hearts and is primarily responsible for cardiogenesis, *PITX2a* and *PITX2b* are expressed simultaneously during heart development and play an essential role in the development of the heart (27–29).

The presence of congenital heart malformations in ARS is reportedly associated with *FOXC1* mutations (30–32). Swiderski et al. (33) showed that the mouse homolog of *FOXC1*, *Mf1*, contributes not only to cardiac neural crest cell-derived structures but also to a range of embryonic tissue-derived structures, including the endocardial cushion cells that form the mitral and tricuspid valves; they also referenced cases with mitral and tricuspid valve insufficiency that support the possibility that the *FOXC1* gene may have an important effect on mitral and tricuspid valve insufficiency in ARS (33). The existing evidence suggests that individuals with the *FOXC1* variant are generally more likely to exhibit an isolated ocular phenotype or to exhibit a range of systemic features, of which heart defects, hearing loss, and growth delay are the most common. In contrast, the *PITX2* variant is closely associated with the ocular phenotype with dental anomalies (microdontia, hypodontia) and cord defects (periumbilical skin, umbilical hernia) (30, 31, 34, 35).

Conclusion

The present patient had the distinct ocular phenotype, dental anomalies, and mitral and tricuspid valve manifestations of ARS. The findings in this patient expand the range of cardiac malformations reported in ARS patients. We believe that echocardiography should be performed in patients with characteristic clinical manifestations of ARS or with alterations in the *PITX2* and *FOXC1* genes.

Data availability statement

The original contributions presented in the study are included in the article/supplementary material, further inquiries can be directed to the corresponding author.

Author contributions

JF and YW wrote the manuscript. SC collected the patient information and data. ZL, LL, and QM participated in the formulation and management of the patient's perioperative treatment plan. CZ designed and reviewed the manuscript. All authors were involved in the revision of the manuscript and approved the submitted version.

Acknowledgments

We thank the patient and her families for sharing this valuable information.

Conflict of interest

The authors declare that the research was conducted in the absence of any commercial or financial relationships that could be construed as a potential conflict of interest.

Publisher's note

References

1. Mears AJ, Jordan T, Mirzayans F, Dubois S, Kume T, Parlee M, et al. Mutations of the forkhead/winged-helix gene, FKHL7, in patients with Axenfeld-Rieger anomaly. *Am J Hum Genet.* (1998) 63:1316–28. doi: 10.1086/302109

2. Shields MB. Axenfeld-Rieger syndrome: a theory of mechanism and distinctions from the iridocorneal endothelial syndrome. *Trans Am Ophthalmol Soc.* (1983) 81:736–84.

3. Kulak SC, Kozlowski K, Semina EV, Pearce WG, Walter MA. Mutation in the RIEG1 gene in patients with iridogoniodysgenesis syndrome. *Hum Mol Genet.* (1998) 7:1113–7. doi: 10.1093/hmg/7.7.1113

4. Shields MB, Buckley E, Klintworth GK, Thresher R. Axenfeld-Rieger syndrome. A spectrum of developmental disorders. *Surv Ophthalmol.* (1985) 29:387–409. doi: 10.1016/0039-6257(85)90205-X

5. Alward WLM. Axenfeld-Rieger syndrome in the age of molecular genetics. *Am J Ophthalmol.* (2000) 130:107–15. doi: 10.1016/S0002-9394(00)00525-0

6. Seifi M, Walter MA. Axenfeld-Rieger syndrome. *Clin Genet.* (2018) 93:1123–30. doi: 10.1111/cge.13148

7. Weegerink NJ, Swinnen FK, Vanakker OM, Casselman JW, Dhooge IJ. Phenotype of a Belgian family with 6p25 deletion syndrome. *Ann Otol Rhinol Laryngol.* (2016) 125:734–45. doi: 10.1177/00034894166 50687

8. Yamazaki H, Nakamura T, Hosono K, Yamaguchi T, Hiratsuka Y, Hotta Y, et al. Sensorineural hearing loss and hypoplastic cochlea in Axenfeld-Rieger syndrome with FOXC1 mutation. *Auris Nasus Larynx.* (2021) 48:1204–8. doi: 10.1016/j.anl.2020.07.006

9. Gürbüz-Köz O, Atalay T, Köz C, Ilgin-Ruhi H, Yarangümeli A, Kural G. Axenfeld-Rieger syndrome associated with truncus arteriosus: a case report. *Turkish J Pediatr.* (2007) V49N4:444–7.

10. Gripp KW, Hopkins E, Jenny K, Thacker D, Salvin J. Cardiac anomalies in Axenfeld-Rieger syndrome due to a novel FOXC1 mutation. *Am J Med Genet A.* (2013) 161A:114–9. doi: 10.1002/ajmg.a.35697

11. Tsai JC, Grajewski AL. Cardiac Valvular Disease and Axenfeld-Rieger syndrome. *Am J Ophthalmol.* (1994) 118:255–6. doi: 10.1016/S0002-9394(14)72910-1

12. Sanchez Ferrer F, Grima Murcia MD. Progressive moderate mitral regurgitation in a children with Axenfeld-Rieger syndrome. The importance of cardiologic follow up. *Arch Argent Pediatr.* (2016) 114:e417–e20. doi: 10.5546/aap.2016.e417

13. Chrystal PW, French CR, Jean F, Havrylov S, van Baarle S, Peturson AM, et al. The Axenfeld-Rieger syndrome gene FOXC1 contributes to left-right patterning. *Genes.* (2021) 12:170. doi: 10.3390/genes12020170

14. Chang TC, Summers CG, Schimmenti LA, Grajewski AL. Axenfeld-Rieger syndrome: new perspectives. *Br J Ophthalmol.* (2012) 96:318–22. doi: 10.1136/bjophthalmol-2011-300801

15. Grosso S, Farnetani MA, Berardi R, Vivarelli R, Vanni M, Morgese G, et al. Familial Axenfeld-Rieger anomaly, cardiac malformations, and sensorineural hearing loss: a provisionally unique genetic syndrome? *Am J Med Genet.* (2002) 111:182–6. doi: 10.1002/ajmg.10493

16. O'Dwyer EM, Jones DC. Dental anomalies in Axenfeld-Rieger syndrome. *Int J Paediatr Dent.* (2005) 15:459–63. doi: 10.1111/j.1365-263X.2005.00639.x

17. Cunningham ET, Eliott D, Miller NR, Maumenee IH, Green WR. Familial Axenfeld-Rieger anomaly, atrial septal defect, and sensorineural hearing loss: a possible new genetic syndrome. *Arch Ophthalmol.* (1998) 116:78–82. doi: 10.1001/archopht.116.1.78

18. Nakamura T, Colbert MC, Robbins J. Neural crest cells retain multipotential characteristics in the developing valves and label the cardiac conduction system. *Circ Res.* (2006) 98:1547–54. doi: 10.1161/01.RES.0000227505.19472.69

19. Murray JC, Bennett SR, Kwitek AE, Small KW, Schinzel A, Alward WL, et al. Linkage of Rieger syndrome to the region of the epidermal growth factor gene on chromosome 4. *Nat Genet.* (1992) 2:46–9. doi: 10.1038/ng0992-46

20. Gould DB, Mears AJ, Pearce WG, Walter MA. Autosomal dominant Axenfeld-Rieger anomaly maps to 6p25. *Am J Hum Genet.* (1997) 61:765–8. doi: 10.1016/S0002-9297(07)64340-7

21. Phillips JC, del Bono EA, Haines JL, Pralea AM, Cohen JS, Greff LJ, et al. A second locus for Rieger syndrome maps to chromosome 13q14. *Am J Hum Genet.* (1996) 59:613–9.

22. Nishimura DY, Swiderski RE, Alward WL, Searby CC, Patil SR, Bennet SR, et al. The forkhead transcription factor gene FKHL7 is responsible for glaucoma phenotypes which map to 6p25. *Nat Genet.* (1998) 19:140–7. doi: 10.1038/493

23. Mirzayans F, Gould DB, Heon E, Billingsley GD, Cheung JC, Mears AJ, et al. Axenfeld-Rieger syndrome resulting from mutation of the FKHL7 gene on chromosome 6p25. *Eur J Hum Genet.* (2000) 8:71–4. doi: 10.1038/sj.ejhg.5200354

24. Lu MF, Pressman C, Dyer R, Johnson RL, Martin JF. Function of Rieger syndrome gene in left-right asymmetry and craniofacial development. *Nature.* (1999) 401:276–8. doi: 10.1038/45797

25. Liu C, Liu W, Palie J, Lu MF, Brown NA, Martin JF. Pitx2c patterns anterior myocardium and aortic arch vessels and is required for local cell movement into atrioventricular cushions. *Development.* (2002) 129:5081–91. doi: 10.1242/dev.129.21.5081

26. Zhao CM, Peng LY Li L, Liu XY, Wang J, Zhang XL, et al. PITX2 loss-of-function mutation contributes to congenital endocardial cushion defect and Axenfeld-Rieger syndrome. *PLoS ONE.* (2015) 10:e0124409. doi: 10.1371/journal.pone.0124409

27. Hernandez-Torres F, Franco D, Aranega AE, Navarro F. Expression patterns and immunohistochemical localization of PITX2B transcription factor in the developing mouse heart. *Int J Dev Biol.* (2015) 59:247–54. doi: 10.1387/ijdb.140224fh

28. Torrado M, Franco D, Hernández-Torres F, Crespo-Leiro MG, Iglesias-Gil C, Castro-Beiras A, et al. Pitx2c is reactivated in the failing myocardium and stimulates myf5 expression in cultured cardiomyocytes. *PLoS ONE.* (2014) 9:e90561. doi: 10.1371/journal.pone.0090561

29. Kahr PC, Piccini I, Fabritz L, Greber B, Schöler H, Scheld HH, et al. Systematic analysis of gene expression differences between left and right atria in different mouse strains and in human atrial tissue. *PLoS ONE.* (2011) 6:e26389. doi: 10.1371/journal.pone.0026389

30. Souzeau E, Siggs OM, Zhou T, Galanopoulos A, Hodson T, Taranath D, et al. Glaucoma spectrum and age-related prevalence of individuals with FOXC1 and PITX2 variants. *Eur J Hum Genet.* (2017) 25:839–47. doi: 10.1038/ejhg.2017.59

31. Reis LM, Tyler RC, Volkmann Kloss BA, Schilter KF, Levin AV, Lowry RB, et al. PITX2 and FOXC1 spectrum of mutations in ocular syndromes. *Eur J Hum Genet.* (2012) 20:1224–33. doi: 10.1038/ejhg.2012.80

32. Chrystal PW, Walter MA. Aniridia and Axenfeld-Rieger Syndrome: Clinical presentations, molecular genetics and current/emerging therapies. *Exp Eye Res.* (2019) 189:107815. doi: 10.1016/j.exer.2019.107815

33. Swiderski RE, Reiter RS, Nishimura DY, Alward WLM, Kalenak JW, Searby CS, et al. Expression of theMf1 gene in developing mouse hearts: Implication in the development of human congenital heart defects. *Develop Dynam.* (1999) 216:16–27. doi: 10.1002/(SICI)1097-0177(199909)216:1<16::AID-DVDY4>3.0.CO;2-1

34. D'Haene B, Meire F, Claerhout I, Kroes HY, Plomp A, Arens YH, et al. Expanding the spectrum of FOXC1 and PITX2 mutations and copy number changes in patients with anterior segment malformations. *Invest Ophthalmol Vis Sci.* (2011) 52:324–33. doi: 10.1167/iovs.10-5309

35. Strungaru MH, Dinu I, Walter MA. Genotype-phenotype correlations in Axenfeld-Rieger malformation and glaucoma patients with FOXC1 and PITX2 mutations. *Invest Ophthalmol Vis Sci.* (2007) 48:228–37. doi: 10.1167/iovs.06-0472

frontiers | Frontiers in Cardiovascular Medicine

TYPE Case Report
PUBLISHED 18 October 2022
DOI 10.3389/fcvm.2022.990325

OPEN ACCESS

EDITED BY
Utpal S. Bhalala,
Driscoll Children's Hospital,
United States

REVIEWED BY
Yun Gi Kim,
Korea University Anam Hospital,
South Korea
Juan-Miguel Gil-Jaurena,
Gregorio Marañón Hospital, Spain
Guohua Fu,
Ningbo First Hospital, China

*CORRESPONDENCE
Yong Zhang
zhangyong1@zgwhfe.com

†These authors have contributed equally to this work and share first authorship

SPECIALTY SECTION
This article was submitted to Pediatric Cardiology, a section of the journal Frontiers in Cardiovascular Medicine

RECEIVED 09 July 2022
ACCEPTED 21 September 2022
PUBLISHED 18 October 2022

CITATION
Liu J, Cao X, Li C, Feng X, Sun D and Zhang Y (2022) Case report: Efficacy analysis of radiofrequency catheter ablation combined with atrial appendage resection for atrial tachycardia originating from the atrial appendage in children. *Front. Cardiovasc. Med.* 9:990325. doi: 10.3389/fcvm.2022.990325

Case report: Efficacy analysis of radiofrequency catheter ablation combined with atrial appendage resection for atrial tachycardia originating from the atrial appendage in children

Jing Liu[1†], Xiaoxiao Cao[1†], Changjian Li[1], Xiaoyuan Feng[2], Dongming Sun[1] and Yong Zhang[1*]

[1]Department of Cardiology, Wuhan Children's Hospital (Wuhan Maternal and Child Healthcare Hospital), Tongji Medical College, Huazhong University of Science and Technology, Wuhan, China, [2]Department of Cardiac Ultrasound, Wuhan Children's Hospital (Wuhan Maternal and Child Healthcare Hospital), Tongji Medical College, Huazhong University of Science and Technology, Wuhan, China

Objective: The aim of this study was to investigate the efficacy of radiofrequency catheter ablation (RFCA) combined with atrial appendage (AA) resection to treat atrial tachycardia (AT) originating from the AA in children.

Materials and methods: Using the Ensite three-dimensional electroanatomic mapping system, three children with AT originating from the AA were diagnosed. Clinical features and electrocardiographic (ECG) manifestations were analyzed. Ablations were performed using a cold saline-infused catheter at appendages targeting loci of AT origin under the guidance of the Ensite system. Atrial appendage resection was performed in combination with cardiac surgery, and the curative effect was evaluated.

Results: The ages of the three patients were 3.5, 5.75, and 12.9 years. Two cases originated from the right atrial appendage (RAA) and one originated from the left atrial appendage (LAA). The ECG characteristics of AT from the RAA were as follows: (1) negative P waves in lead V1; (2) positive P waves in leads II, III, and aVF; (3) positive P wave in lead I with varying shapes in lead aVL; and (4) prolonged PR interval with no QRS wave after some P waves. The ECG of the LAA was characterized by (1) positive P waves in lead V1 with a bimodal pattern; (2) positive P waves in leads II, III, and aVF; and (3) negative P waves in leads I and aVL. Preoperative echocardiography showed cardiac enlargement and a decreased left ventricular ejection fraction (LVEF) in all three cases. One case was cured after RFCA, and the remaining two cases required AA resection after RFCA. No recurrence was detected at 1–18 months of follow-up, and the left ventricular end-diastolic diameter and LVEF returned to normal.

Conclusion: Atrial tachycardia originating from the AA in children showed a characteristic P-wave presentation on ECG, and sustained episodes of AT resulted in tachycardia-induced cardiomyopathy. Children who are not successfully controlled by RFCA or who have a recurrence after RFCA could benefit from AA resection.

KEYWORDS

case report, heart surgery, cardiology, atrial tachycardia, atrial appendage, tachycardia-induced cardiomyopathy, radiofrequency catheter ablation, atrial appendage resection

Introduction

Atrial tachycardia (AT) originating from the atrial appendage (AA) is clinically characterized by palpitation, chest distress, dyspnea, and other non-specific manifestations. Persistent AT is the electrocardiographic (ECG) characteristic of AT originating from the AA, and approximately 25–50% develops tachycardia-induced cardiomyopathy (TIC), which is characterized by increased left ventricular end-diastolic diameter (LVEDD) and decreased left ventricular ejection fraction (LVEF) (1, 2). Atrial tachycardia originating from the AA in children accounts for approximately 30–50% of AT cases (3), which is higher than that in adults. In a study of 60 children with AT by Gulhan et al., AT originating from the left atrial appendage (LAA) and right atrial appendage (RAA) accounted for 15.8 and 15.5% of cases, respectively (4).

Antiarrhythmic drugs do not adequately mitigate AT, and catheter radiofrequency ablation (RFCA) is often used to treat AT. The success rate of RFCA is variable. Freixa (5) reported that 15 patients with RAA tachycardia had no recurrence after RFCA, whereas Yamada (6) reported that 13 patients with LAA tachycardia had no recurrence after RFCA. The recurrence of AT following RFCA maybe 10–20% (7). In cases of recurrence, a second ablation or other treatments were needed (8). For cases of ablation failure or recurrence after ablation, AA resection was an option (9).

In this report, three children were diagnosed with AT using surface ECG and were determined to have originated from the AA using Ensite's three-dimensional mapping system. Each of the patients was treated using RFCA. Notably, one patient was successfully ablated immediately, one patient experienced ablation failure, and one patient underwent successful ablation but experienced recurrence. In the latter two cases, small incision LAA and thoracoscopic RAA resection were performed during cardiothoracic surgery.

Subjects and materials and methods

General information

In this study, three children with AT who were admitted to the Department of Cardiovascular Medicine, Wuhan Children's Hospital for RFCA to treat AT that originated from the AA were included. The ages were 3.5, 5.75, and 12.9 years, with two girls and one boy. Antiarrhythmic drugs failed to convert the patients to sinus rhythm. Atrial tachycardia was determined to originate from the LAA in one case and from the RAA in two cases, as determined by intracardiac mapping and RFCA.

Diagnostic criteria

Atrial tachycardia was diagnosed based on the following surface ECG criteria (10): (1) narrow QRS tachycardia and (2) P waves present in the front of the QRS waves or hidden in the QRS or T waves, resulting in differences from sinus P shape.

Surgical protocol

Electrophysiological examination

Before surgical procedures, children stopped using antiarrhythmic drugs for more than 5 half-lives. During the operation, 100°U/kg of intravenous heparin was given for anticoagulation. Aspirin (3–5 mg/kg/day) was administered orally for 1°month after any operation involving the LAA. The electrophysiological examination was performed under general anesthesia without intubation. After the puncture through the left subclavian vein, a 6F vascular sheath was inserted, and the coronary sinus mapping electrode was inserted. After the puncture through the left femoral vein, a 6F vascular sheath was placed near the right ventricular electrode. The ablation catheter was delivered after inserting an 8F vascular sheath through the right femoral vein puncture.

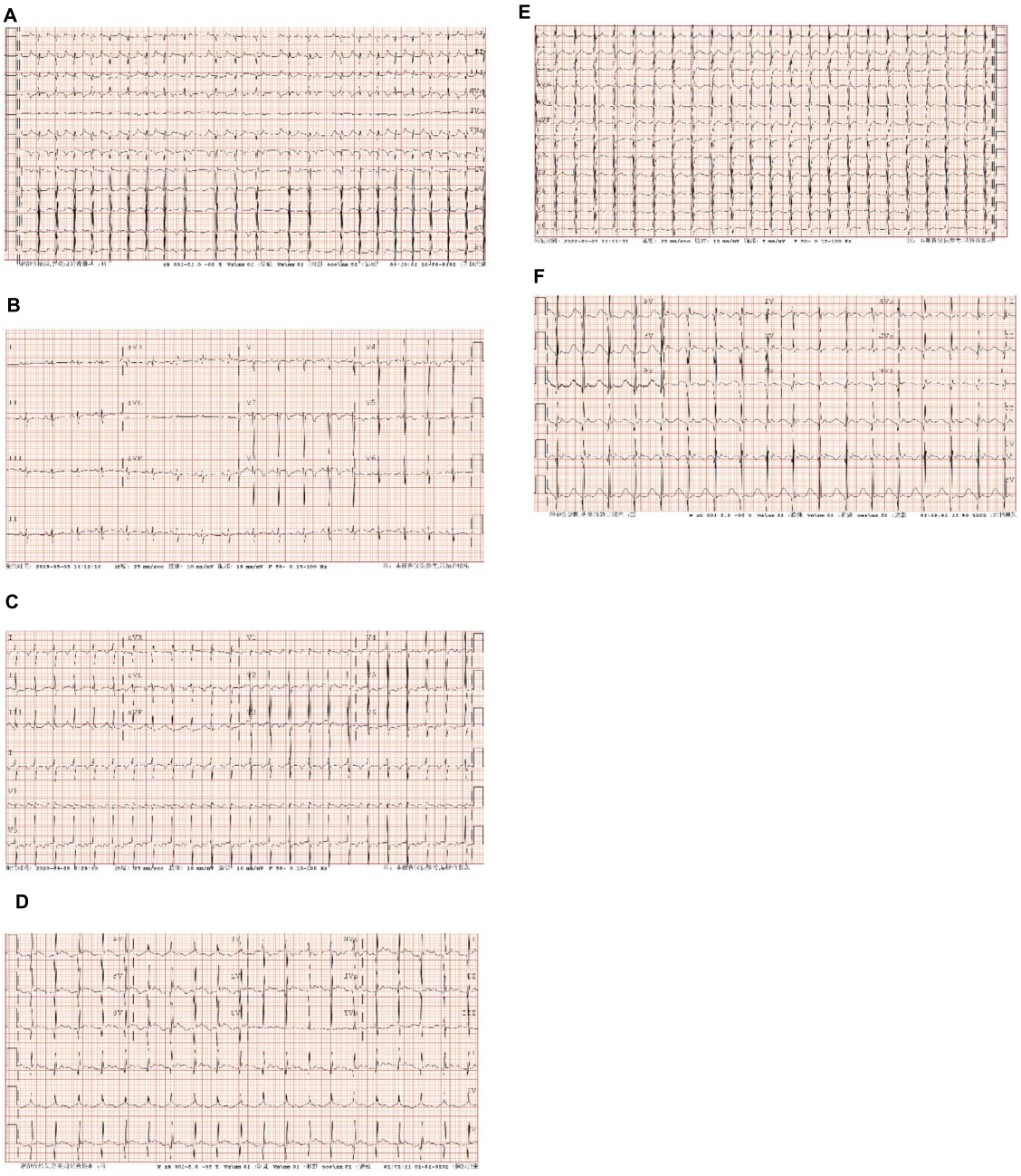

FIGURE 1

Preoperative and postoperative electrocardiographic (ECG) of atrial tachycardia (AT) from atrial appendage (AA). **(A)** Case 1: persistent AT. The ventricular rate was 137–200 bpm; P waves in lead V1 were negative, and P waves in V3–V6 gradually moved in the positive direction; P waves in leads I, II, III, and aVF were positive, and P waves in lead aVL were negative; the PR interval was prolonged, with no QRS wave after partial P wave. **(B)** Case 1: ECG after radiofrequency catheter ablation (RFCA). Sinus rhythm; P waves in leads I, II, III, aVF, and V1–V6 were positive, and the HR was 110 bpm. **(C)** Case 2: persistent AT. The ventricular rate was 142 bpm; P waves in lead V1 were positive and bimodal; P waves in leads II, III, and aVF were positive; P waves in leads I and aVL were negative. **(D)** Case 2: ECG after left atrial appendage (LAA) resection. sinus rhythm; P waves in leads I and aVL were positive, and the HR was 120 bpm. **(E)** Case 3: persistent AT. The ventricular rate was 145 bpm; P waves in lead V1 were negative, and P waves in leads V2–V6 gradually moved in the positive direction; P waves in leads I, II, III, aVF, and aVL were positive; the PR interval was prolonged. **(F)** Case 3: ECG after RAA resection. Sinus rhythm; P waves in leads I, II, III, aVF, and V1–V6 were positive, and the HR was 108 bpm. AT, atrial tachycardia; bpm, beats per minute; RFCA, radiofrequency catheter ablation; ECG, electrocardiogram; LAA, left atrial appendage; RAA, right atrial appendage; HR, heart rate.

Radiofrequency ablation

(1) Using the Ensite system, atrial modeling and AT activation mapping were performed, and three-dimensional images of the anatomy and activation sequence of the atrium and AA were constructed. If AT originated from the left atrium, a puncture was performed through the atrial septum, and the ablation catheter was introduced into the left atrium through the long sheath for mapping. Each part of the cardiac chamber was marked using different colors based on excitation times. Red was the earliest excitation point, and purple was the last. The earliest excitation point was identified through accurate mapping of the red area. If the rough mark showed the origin of the deep part of the AA or the special shape of the AA, it was necessary to perform radiography first, and then perform fine mapping after clearly showing the shape of the AA.

(2) A cold saline infusion catheter or a pressure cold saline infusion catheter was selected, and 17 ml/min of cold saline was introduced to maintain a temperature of 43°C and a power of 20–35 W. If the ablation was effective, the ablation was consolidated for 60 s (s) per point. AT was not observed 20 min after ablation. Atrial program stimulation after intravenous isoprenaline drip and regular atrial program stimulation did not induce AT.

Atrial appendage resection

Atrial tachycardia originating from the AA that was not controlled by RFCA was treated by AA resection as follows. (1) Thoracoscopic RAA resection. Incisions were made among the eighth intercostal space of the right posterior axillary line, the fourth intercostal space of the middle axillary line, and the fifth intercostal space of the anterior axillary line. A thoracoscope, operating forceps, and electrocoagulation hook were placed in the Trocar. The right pericardium was opened to expose the right atrium and RAA. Using non-invasive forceps, the RAA was pulled open and removed using an endoscopic cutting stapler. (2) LAA resection. A posterolateral incision was made in the left chest, and the pericardium was opened to expose the left atrium and LAA. The root of the LAA was clamped with a C-clamp, and

TABLE 1 Clinical features and efficacy analysis of three cases of atrial tachycardia originating from the atrial appendage.

		Case 1	Case 2	Case 3
Gender		female	female	male
Age		3.5 years	5.75 years	12.9 years
Body mass (kg)		15	23	34
Chief complaint		Tachycardia was found for 5 days	Syncope once 3 days ago	Palpitation for 2 years
AT frequency (bpm)		200	160	145
CK-MB (U/L)		26	17	17
Troponin T (ng/ml)		0.068	0.113	0.066
BNP (pg/ml)		> 9000	2768\	181
Preoperative ECG		Sustained AT	Sustained AT	Sustained AT
The orgin of AT		RAA	LAA	RAA
Preoperative LVEDD (mm)		40	45.8	45
Preoperative LVEF (%)		42	29	45
antiarrhythmic agents		amiodarone	cedilanid, amiodarone	propafenone, amiodarone, digoxin, betaloc
treatment		RFCA	RFCA combined with LAA resection	RFCA combined with thoracoscopic RAA resection
Postoperation of RFCA	ECG	sinus rhythm	paroxysmal AT	AT
	LVEDD (mm)	39	-	-
	LVEF (%)	50	-	-
Postoperation of AA resection	ECG	-	sinus rhythm	sinus rhythm
	LVEDD (mm)		42.6	44
	LVEF (%)		33	52
1°month after the operation	ECG	sinus rhythm	sinus rhythm	sinus rhythm
	LVEDD (mm)	36	37	42
	LVEF (%)	53	46	56
1°year after the operation	ECG	sinus rhythm	sinus rhythm	-
	LVEDD (mm)	35	35	
	LVEF (%)	65	60	

bpm, beats per minute; CK-MB, creatine kinase-MB; BNP, brain natriuretic peptide; ECG, electrocardiogram; AT, atrial tachycardia; RAA, right atrial appendage; LAA, left atrial appendage; LVEDD, left ventricular end-diastolic diameter; LVEF, left ventricular ejection fraction; RFCA, radiofrequency catheter ablation; AA, atrial appendage.

the LAA was completely removed. The excised left and right AA was sent for pathological examination.

Follow-up

All patients underwent continuous 12-lead ECG, 24-h ambulatory ECG, and echocardiography before discharge. The patients were followed up using 12-lead ECG and echocardiography, and if necessary, a 24-h ambulatory ECG, at 1, 3, 6, and 12 months, and every year thereafter.

Results

In this study, three cases of AT originating from the AA were included, with a history of 3 days to 2 years of persistent AT that failed to respond to antiarrhythmic drugs. Echocardiography showed an enlarged heart with LVEDDs of 40, 45.8, and 45 mm, and LVEFs of 42, 29, and 45%, respectively (**Table 1**).

Electrocardiogram characteristics of AT originating from the RAA in 2 cases included the following: (1) P waves in lead V1 were negative, and the precordial lead gradually moved in the positive direction; (2) P waves in leads II, III, and aVF were positive; (3) P waves in lead I were positive; and (4) the PR interval was prolonged, with no QRS waves after some P waves (**Figure 1**).

Electrocardiogram characteristics of AT originating from the LAA in 1 case were as follows: (1) P waves in lead V1 were positive and double-peaked; (2) P waves in leads II, III, and aVF were positive; and (3) P waves in lead I and aVL were negative (**Figure 1**).

Three children with AT from the AA were treated by RFCA. In case 1, the earliest excitation point was marked at the peak of RAA during the operation. The catheter was perfused with cold saline, and the ablation parameters (43°, 35 W, 17 ml/min) were selected, and the pressure was controlled at 5–10 g. Atrial tachycardia was terminated after acceleration, and consolidation ablation was performed four times for 60 s. Atrial tachycardia could not be induced by regular atrial programed stimulation or atrial programed stimulation following intravenous isoprenaline drip. In case 2, the A wave at the apex of the LAA occurred earliest during the operation. The catheter was perfused with cold saline, and the ablation parameters (43°, 20–30 W, 17 ml/min) were selected, with the pressure controlled at 5 g. Atrial tachycardia converted to sinus rhythm temporarily but returned to AT after a few seconds. Sinus rhythm and AT appeared alternately in the child after 40 s × 5 times consolidation ablation around this area. Because the best target was located at the apex of the LAA and the ablation risk was high, resection of the LAA was performed through the posterior lateral incision of the left chest combined with cardiothoracic surgery. In case 3, meticulous mapping was performed from outside to inside along the RAA. The earliest excitation

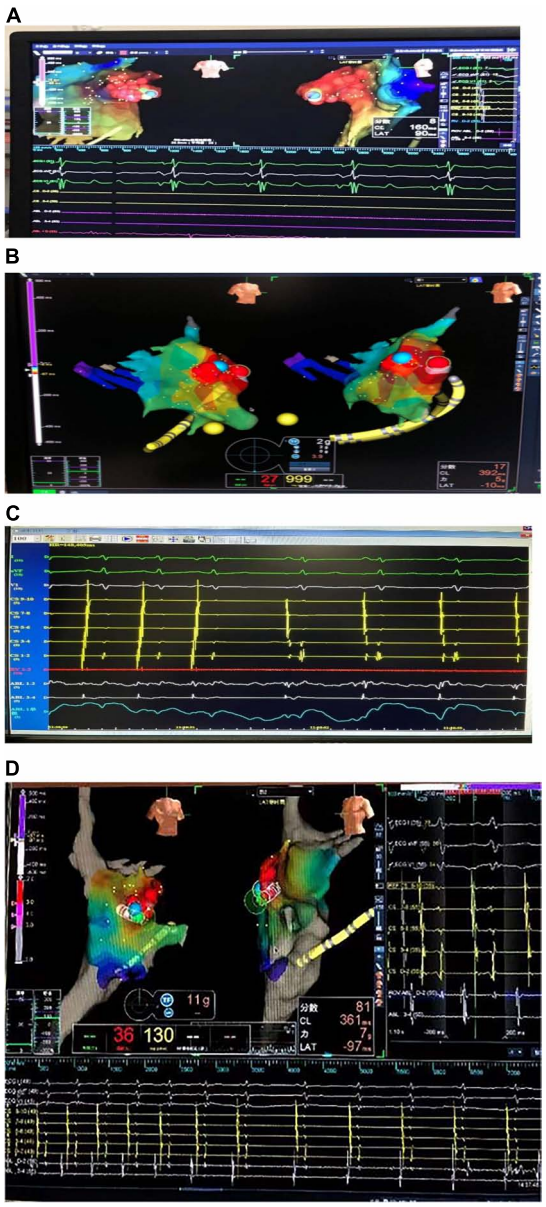

FIGURE 2
Three-dimensional electroanatomical mapping.
(A) Three-dimensional electroanatomical mapping of case 1 showed the atrial tachycardia (AT) from right atrial appendage (RAA): the earliest excitation point in the red area is the RAA, the red circle is the ablation target, and the blue circle is the best ablation target. **(B)** Three-dimensional electroanatomical mapping of case 2 showed the AT from left atrial appendage (LAA): the earliest excitation point in the red area is LAA, the red circle is the ablation target, and the blue circle is the best ablation target. **(C)** The electrogram of the target site of case 2: during the ablation, the atrial activation sequence was changed from CS1-2 to CS9-10 to CS9-10 to CS1-2.
(D) Three-dimensional electroanatomical mapping of case 3 showed the AT from RAA: the earliest excitation point in the red area is the RAA, the red circle is the ablation target, and the blue circle is the best ablation target. The sequence of atrial activation did not change significantly, but the shape of the A wave and the AA interval was changed. AT, atrial tachycardia; LAA, left atrial appendage; RAA, right atrial appendage.

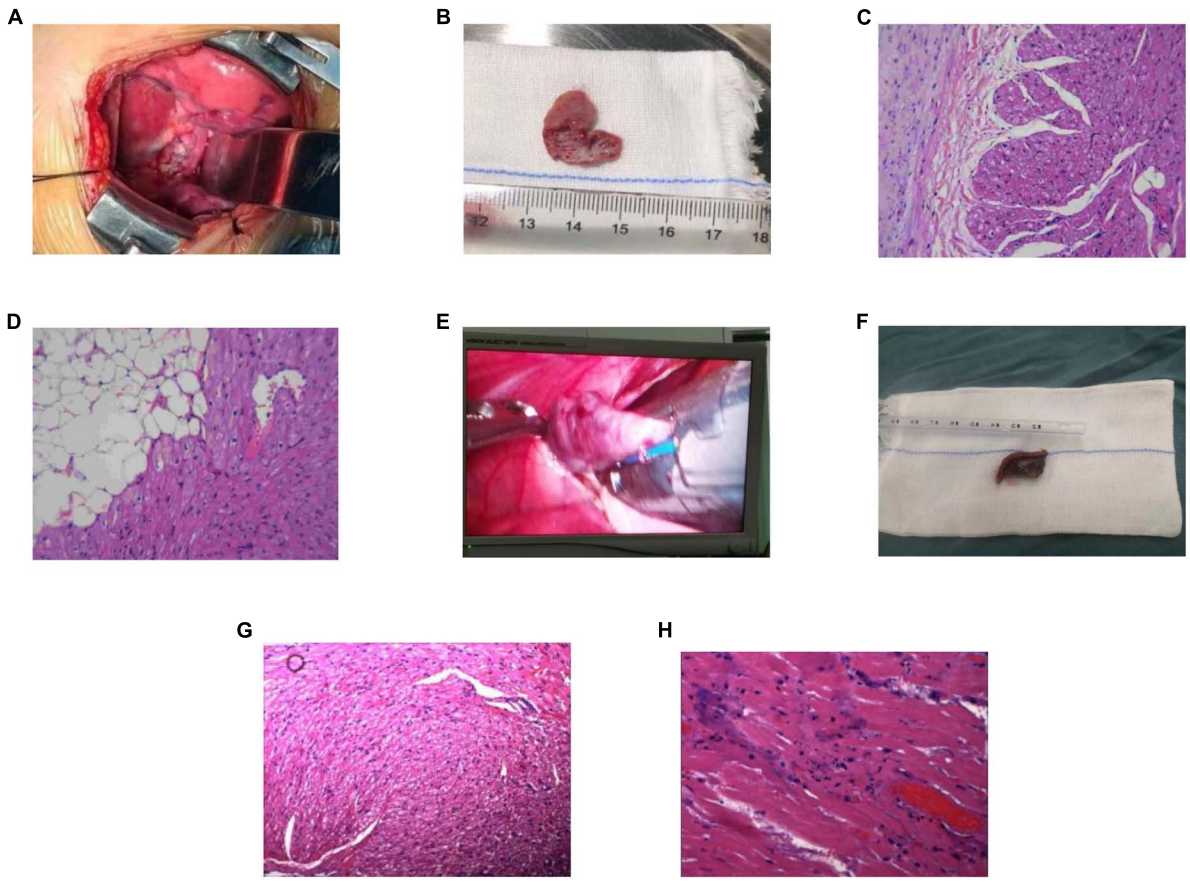

FIGURE 3
Excised atrial appendage and pathology (200×). **(A)** Case 2: the image of the left atrial appendage (LAA) during the operation. **(B)** Case 2: the excised LAA. **(C,D)** Case 2: postoperative pathology. Striated muscle and fibrous adipose tissue of LAA, local tissue degeneration. **(E)** Case 3: the image of the right atrial appendage (RAA) during the operation. **(F)** Case 3: the excised RAA. **(G,H)** Case 3: postoperative pathology. The arrangement of myocardial fibers in the RAA was disordered, some myocardial nuclei were enlarged, some muscle fibers showed granular degeneration and vacuoles, and tiny necrosis foci could be seen locally. LAA, left atrial appendage; RAA, right atrial appendage.

point was marked at the tip of the middle part of the RAA, the ablation parameters (43°, 25–35 W, 17 ml/min) were selected, and the pressure was controlled around 5–10 g. Atrial tachycardia was terminated after acceleration, and consolidation ablation was performed for 60 s. After the operation, AT recurred, and thoracoscopic RAA resection was performed in combination with cardiothoracic surgery. During the atrial appendectomy, ECG monitoring suggested that atrial tachycardia was terminated after the atrial appendage was clamped. **Figure 2** shows three-dimensional mapping shown in, and **Figure 3** shows postoperative pathology.

After the operation, all three children recovered sinus rhythm (**Figure 1**). Follow-up from 1°month to 1.5 years showed no recurrence of AT, and heart size and ejection fraction gradually recovered (**Figures 1**, **4** and **Table 1**).

The time line of the three cases showed in **Figure 5**.

Discussion

Atrial tachycardia originating from the AA shows characteristic P wave changes on ECG. Electrocardiograms of AT originating from the RAA showed the following: (1) P waves in lead V1 were negative, some of which included notches, and the other precordial leads gradually move in a positive direction; (2) P waves in leads II, III, and aVF were positive; and (3) P waves in lead I were positive or on the equipotential line, were positive or negative in lead aVL, and were negative or on the equipotential line in lead aVR (11–13). In contrast, the ECG of AT from LAA showed the following: (1) P waves in lead V1 are positive; (2) P waves in leads II, III, and aVF were positive; and (3) P waves in leads I and aVL were negative (11, 14, 15). In this report, the P waves in the ECGs of 2 cases of AT from the RAA and 1 case of AT from the LAA were consistent with these characteristics.

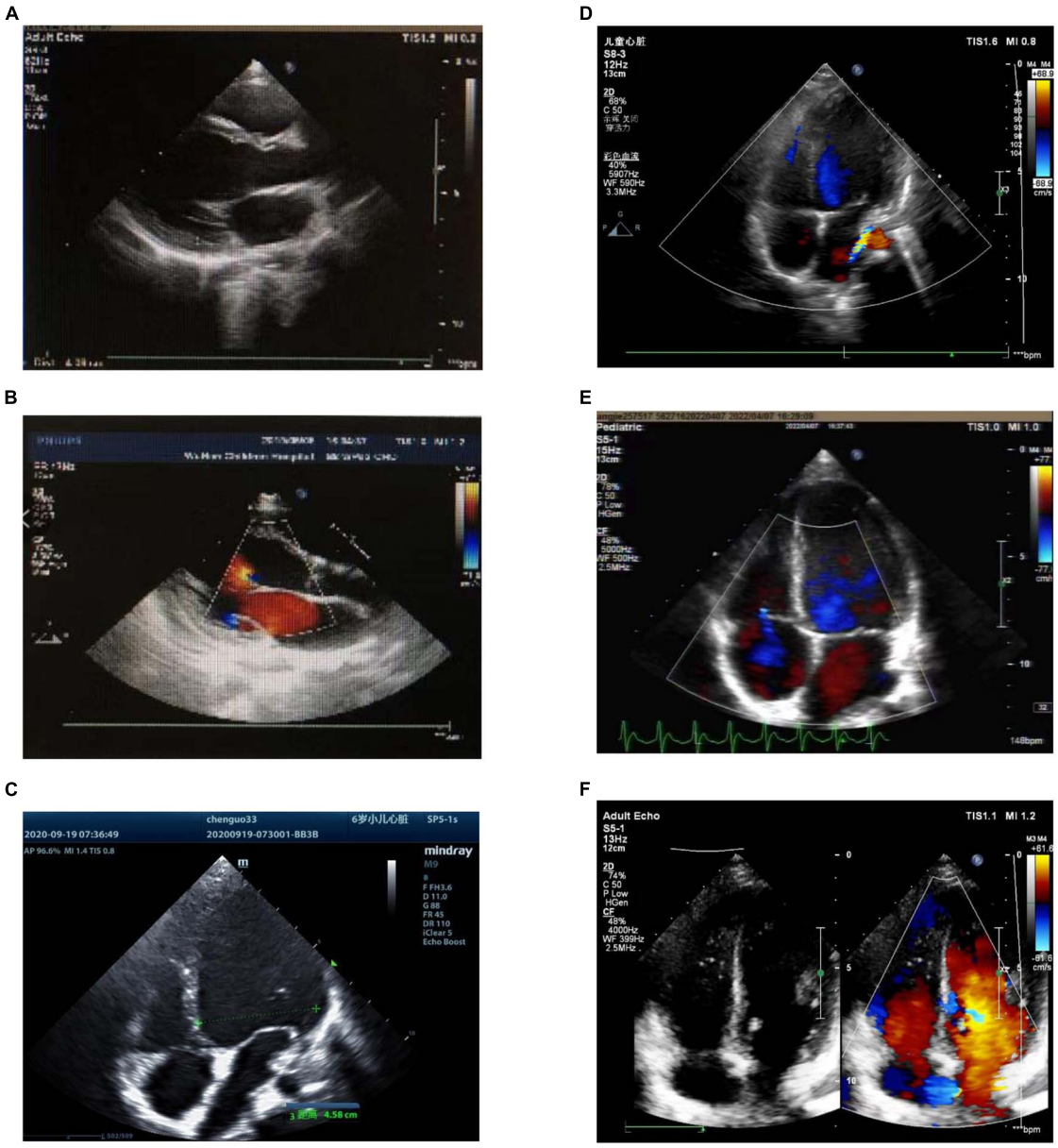

FIGURE 4
Preoperative and postoperative echocardiography of atrial tachycardia (AT) from the atrial appendage. **(A)** Case 1: preoperative echocardiography. Left ventricular end-diastolic diameter (LVEDD) 40 mm, left ventricular ejection fraction (LVEF) = 42%. **(B)** Case 1: echocardiography 1°month after radiofrequency catheter ablation (RFCA). LVEDD 37 mm, LVEF = 53%. **(C)** Case 2: preoperative echocardiography. LVEDD 45.8 mm, LVEF = 29%. **(D)** Case 2: echocardiography 1°month after LAA resection. LVEDD 37 mm, LVEF = 46%. **(E)** Case 3: the left picture shows preoperative echocardiography. LVEDD 45 mm, LVEF = 45%. **(F)** Case 3: echocardiography 1°month after RAA resection. LVEDD 42 mm, LVEF = 56%. LVEDD, left ventricular end-diastolic diameter; LVEF, left ventricular ejection fraction; RFCA, radiofrequency catheter ablation; LAA, left atrial appendage; RAA, right atrial appendage.

The comb muscles on the inner wall of the AA are developed and have differing thicknesses. Atrial tachycardia originating from this site may have multiple excitation loci and may radiate in all directions, resulting in a low success rate of RFCA (8). Due to the thin myocardial tissue between the pectinate muscles of the AA, RFCA in this area can cause the perforation of the AA, resulting in pericardial tamponade. Therefore, AT originating from the AA is easily mapped and difficult to ablate, resulting in a high rate of recurrence (16). In the three cases in our study, we used the Ensite three-dimensional mapping system to guide mapping and ablation. Ablations were performed *via* a cold saline-infused catheter, and the pressure and ablation temperature were controlled. A contrast agent was introduced through the catheter to allow for better mapping

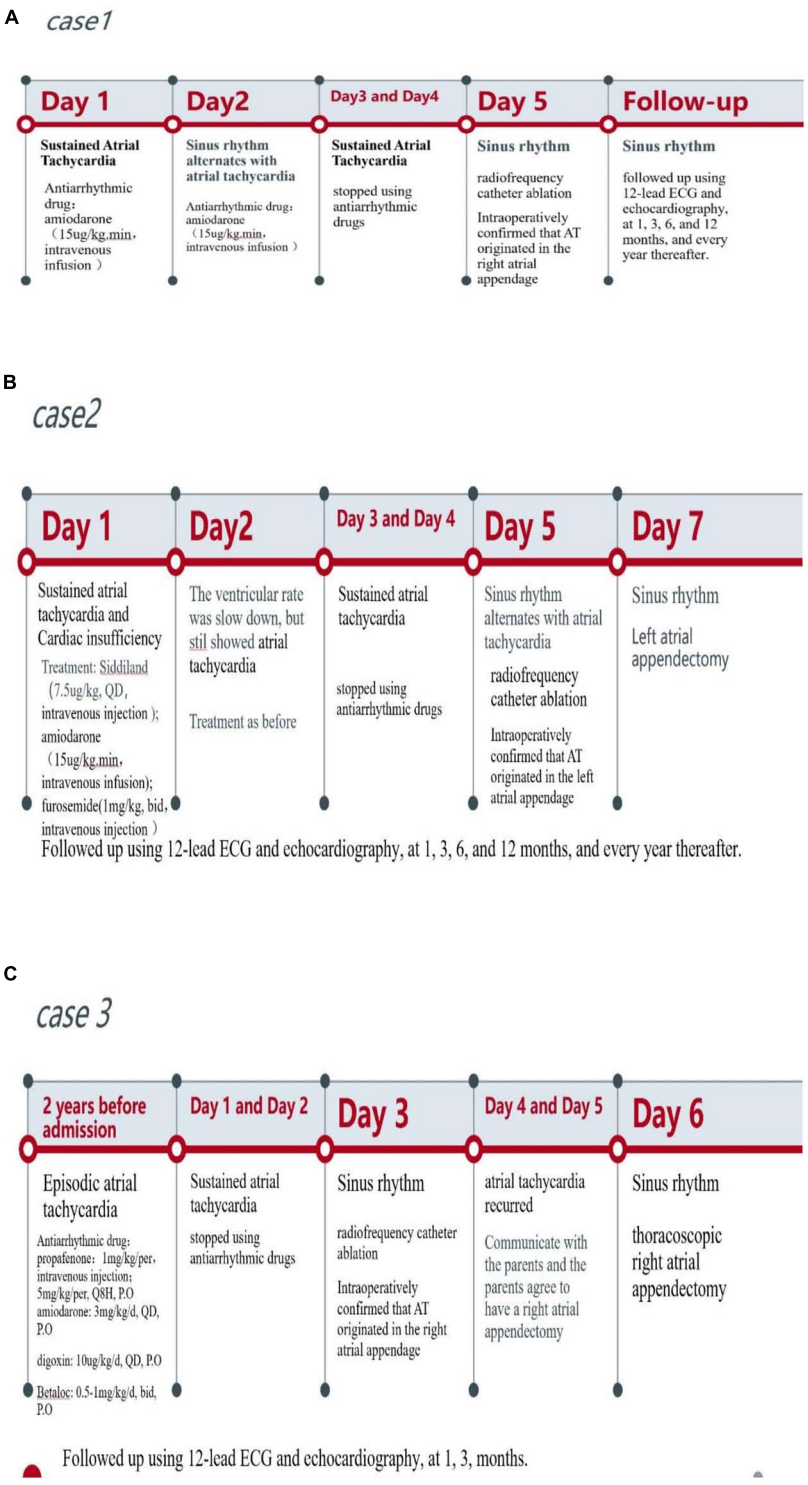

FIGURE 5
The timeline of the three cases. **(A)** The timeline of case 1. **(B)** The timeline of case 2. **(C)** the timeline of case 3.

of the earliest excitation point (17). Catheter introduction was carefully performed to reduce the risk of pericardial perforation and AA thrombosis. Successful ablation occurred immediately in one patient, one case could not be successfully ablated, and one case was successfully ablated, but AT recurred. In the last two cases, small incision LAA resection and thoracoscopic RAA resection were performed during cardiothoracic surgery, respectively. For failed ablation or postoperative recurrence of

AT, AA resection resulted in less trauma, longer-lasting curative effects, and a better long-term prognosis (11, 18).

Compared with traditional transthoracic incision surgery, video-assisted thoracoscopic surgery results in less bleeding during the operation, faster recovery, and less scarring. However, only one case of video-assisted thoracoscopic surgery has been reported in a child (19). In addition, there was a report of a 13-year-old boy who underwent thoracoscopic clamp RFCA to treat AT that originated from the RAA following the failure of catheter ablation (20). Losantos reported a 21-year-old woman with LAA tachycardia who underwent successful ablation in the epicardium following two failed endocardial ablation procedures (21). Combined ablation and exclusion of the LAA were reported in a 10-year-old boy for treatment of AT using video-assisted thoracoscopic surgery (22). These cases provided valuable information regarding the treatment of AT originating from the AA.

Histopathological examination found that there were local degenerative and necrotic foci in the excised atrial appendage specimens, which were considered the ablation target. The myocardial cells showed granular degeneration, vacuolar degeneration, fibrous tissue proliferation, and inflammatory cell infiltration.

In our three cases, AT lasted from 3 days to 2 years, and each case resulted in TIC, which was characterized by increased LVEDD and decreased LVEF. Each of the three patients was treated with several antiarrhythmic drugs before undergoing RFCA, but no therapeutic effects were observed. After RFCA and AA resection, the ECGs showed recovery of sinus rhythm, and LVEDD and LVEF gradually recovered in each patient. These findings showed that cardiomyopathy caused by tachycardia was reversible. Studies have shown that the median duration required for LVEF to return to normal in children with TIC caused by AT was 1.5 months, while reverse ventricular remodeling required several months to years to complete (23, 24). In this report, two cases returned to normal LVEDD and LVEF at 1-year follow-up, and one case improved on the second day after surgery. However, long-term data were not available due to the short follow-up period. Additional follow-up appointments will be scheduled to monitor these patients.

In summary, AT originating from AA in children showed characteristic P-wave manifestations on ECG, and persistent AT resulted in TIC. For children who cannot be cured using RFCA or who relapse after an operation, AA resection may be a reliable therapeutic approach.

Data availability statement

The original contributions presented in this study are included in the article/**Supplementary material**, further inquiries can be directed to the corresponding author.

Ethics statement

The studies involving human participants were reviewed and approved by Wuhan Children's Hospital. Written informed consent to participate in this study was provided by the participants' legal guardian/next of kin.

Author contributions

JL and XC proposed case ideas and participated in discussions. XF and DS assisted in collecting and summarizing cases. JL and CL wrote the original manuscript. YZ critically reviewed and proofread the manuscript. All authors contributed to the article and approved the submitted version.

Funding

This study was supported by the Wuhan Science and Technology Project (No. 2019CFB783).

Acknowledgments

We thank the patient for participating in this study.

Conflict of interest

The authors declare that the research was conducted in the absence of any commercial or financial relationships that could be construed as a potential conflict of interest.

Publisher's note

Supplementary material

The Supplementary Material for this article can be found online at: https://www.frontiersin.org/articles/10.3389/fcvm.2022.990325/full#supplementary-material

References

1. Lau DH, Thiyagarajah A, Willems S, Rostock T, Linz D, Stiles MK, et al. Device therapy for rate control: pacing, resynchronisation and AV node ablation. *Heart Lung Circ.* (2017) 26:934–40. doi: 10.1016/j.hlc.2017.05.124

2. Martin, CA, Lambiase PD. Pathophysiology, diagnosis and treatment of tachycardiomyopathy. *Heart.* (2017) 103:1543–52. doi: 10.1136/heartjnl-2016-310391

3. Toyohara K, Fukuhara H, Yoshimoto J, Ozaki N, Nakamura Y. Electrophysiologic studies and radiofrequency catheter ablation of ectopic atrial tachycardia in children. *Pediatr Cardiol.* (2011) 32:40–6. doi: 10.1007/s00246-010-9809-3

4. Sahin GT, Kafali HC, Ozturk E, Guzeltas A, Ergul Y. Catheter ablation of focal atrial tachycardia in children using three-dimensional electroanatomic mapping system: a 6-year single-centre experience. *Cardiol Young.* (2021) 31:744–50. doi: 10.1017/S1047951120004527

5. Freixa X, Berruezo A, Mont L, Magnani S, Benito B, Tolosana JM, et al. Characterization of focal right atrial appendage tachycardia. *Europace.* (2008) 10:105–9. doi: 10.1093/europace/eum264

6. Yamada T, Murakami Y, Yoshida Y, Okada T, Yoshida N, Toyama J, et al. Electrophysiologic and electrocardiographic characteristics and radio frequency catheter ablation of focal atrial tachycardia originating from the left atrial appendage. *Heart Rhythm.* (2007) 4:1284–91. doi: 10.1016/j.hrthm.2007.06.008

7. Guo XG, Zhang JL, Ma J, Jia YH, Zheng Z, Wang HY, et al. Management of focal atrial tachycardia originating from the atrial appendage with the combination of radio frequency catheter ablation and minimally invasive atrial appendectomy. *Heart Rhythm.* (2014) 11:17–25. doi: 10.1016/j.hrthm.2013.10.017

8. Roshan J, Gizurarson S, Das M, Chauhan VS. Successful cryoablation of an incessant atrial tachycardia arising from the right atrial appendage. *Indian Pacing Electrophysiol.* (2015) 15:168–71. doi: 10.1016/j.ipej.2015.09.005

9. Xu Z, Li X, Wu Q, Li H, Pan G. Surgical treatment of focal atrial tachycardia originating from an atrial appendage in children. *Chin Med J.* (2014) 127:3507–9. doi: 10.3760/cma.j.issn.0366-6999.20140253

10. Katritsis DG, Boriani G, Cosio FG, Hindricks G, Jaïs P, Josephson ME, et al. European Heart Rhythm Association (EHRA) consensus document on the management of supraventricular arrhythmias, endorsed by Heart Rhythm Society (HRS), Asia-Pacific Heart Rhythm Society (APHRS), and Sociedad Latinoamericana de Estimulacion Cardiaca y Electrofisiologia (SOLAECE). *Europace.* (2016) 11:17–9. doi: 10.1093/europace/euw301

11. Li XM, Liu HJ, Wu QY, Pan GY, Li YH, Zhang Y. Radiofrequency catheter ablation combined with appendectomy to cure pediatric atrial tachycardia originating from atrial appendages. *Chin J Cardiac Arrhyth.* (2013) 1:31–5. doi: 10.3760/cma.j.issn.1007-6638.2013.01.009

12. Zhang T, Li XB, Wang YL, Yin JX, Zhang P, Zhang HC, et al. Focal atrial tachycardia arising from the right atrial appendage: electrophysiologic and electrocardiographic characteristics and catheter ablation. *Int J Clin Prac.* (2009) 63:417–24. doi: 10.1111/j.1742-1241.2007.01489.x

13. Wang Z, Chen YW, Jiang YH, Sun LP, Chen XJ, Tao HL, et al. Electrophysiological characteristics and therapeutic efficacy of radiofrequency ablation of focal atrial tachycardia originating from the right atrial appendage during pregnancy. *Chin J Cardiol.* (2020) 48:859–65. doi: 10.3760/cma.j.cn112148-20191104-00683

14. Yang Q, Ma J, Zhang S, Hu JQ, Liao ZL. Focal atrial tachycardia originating from the distal portion of the left atrial appendage: characteristics and long-term outcomes of radiofrequency ablation. *Europace.* (2012) 14:254–60. doi: 10.1093/europace/eur302

15. Wang YL, Guo JH, Li XB, Ren XJ, Han ZH, Chen F. Electrophysiological characterization and efficacy of radiofrequency ablation of focal atrial tachycardia originating from the left atrial appendage. *Chin J Cardiol.* (2010) 38:493–6. doi: 10.3760/cma.j.issn.0253-3758.2010.06.004

16. Wei HQ, Sun Q, Guo XG, Yang JD, Ma J. Successful ablation of focal atrial tachycardia originating from the left atrial appendage using 23-mm second-generation cryoballoon. *Heart Rhythm Case Rep.* (2019) 5:325–8. doi: 10.1016/j.hrcr.2019.03.006

17. Nishizaki K, Itoh T, Kimura M, Tomita H. Contrast injection into the right atrial appendage apex using an external irrigation catheter for focal atrial tachycardia ablation. *J Arrhythm.* (2022) 38:157–9. doi: 10.1002/joa3.12664

18. Combes S, Albenque JP, Combes N, Boveda S, Cardin C, Ciobotaru V, et al. An original management of focal atrial tachycardia originating from a giant left atrial appendage. *Heart Rhythm Case Rep.* (2018) 4:135–7. doi: 10.1016/j.hrcr.2017.10.016

19. Kwon HW, Bae EJ, Kwak JG, Seo JW. Successful video-assisted thoracoscopic atrial appendectomy in a 4-year-old child with intractable atrial tachycardia and tachycardia-induced cardiomyopathy. *Cardiol Young.* (2020) 30:869–72. doi: 10.1017/S1047951119002580

20. Luo L, Qin Z, Shi R, Ge L. Case report: application of thoracoscopic clamp radiofrequency ablation on atrial tachycardia originating from right atrial appendage after catheter ablation failure. *Front Cardiovasc Med.* (2021) 8:659821. doi: 10.3389/fcvm.2021.659821

21. Losantos C, Barrón D, Márquez MF, Gómez J, Levinstein M, Nava S. Epicardial ablation of incessant left atrial appendage tachycardia in a case with tachycardiomyopathy. *J Intrev Card Electr.* (2021) 62:495–7. doi: 10.1007/s10840-021-01015-w

22. Pérez-Caballero-Martínez R, Pita-Fernández A, González-López MT, Gil-Jaurena JM, Gil-Jaurena JM. Combined ablation and exclusion of the left atrial appendage in a pediatric patient: a minimally invasive simplified approach. *Ann Thorac Sugr.* (2016) 101:2379–82. doi: 10.1016/j.athoracsur.2015.08.056

23. Dohain AM, Lotfy W, Abdelmohsen G, Sobhy R, Abdelaziz O, Elsaadany M, et al. Functional recovery of cardiomyopathy induced by atrial tachycardia in children: insight from cardiac strain imaging. *Pacing Clin Electrophysiol.* (2021) 44:442–50. doi: 10.1111/pace.14186

24. Moore JP, Patel PA, Shannon KM, Albers EL, Salerno JC, Stein MA, et al. Predictors of myocardial recovery in pediatric tachycardia-induced cardiomyopathy. *Heart Rhythm.* (2014) 11:1163–9. doi: 10.1016/j.hrthm.2014.04.023

frontiers | Frontiers in Cardiovascular Medicine

TYPE Case Report
PUBLISHED 21 October 2022
DOI 10.3389/fcvm.2022.898467

OPEN ACCESS

EDITED BY
Cecile Tissot,
Clinique des Grangettes, Switzerland

REVIEWED BY
Kai Ma,
Chinese Academy of Medical Sciences and Peking Union Medical College, China
Natallia Maroz-Vadalazhskaya,
Belarusian State Medical University, Belarus

*CORRESPONDENCE
Kiara Rezaei-Kalantari
rkkiara@gmail.com

SPECIALTY SECTION
This article was submitted to Pediatric Cardiology, a section of the journal Frontiers in Cardiovascular Medicine

RECEIVED 17 March 2022
ACCEPTED 11 August 2022
PUBLISHED 21 October 2022

CITATION
Asl Fallah S, Mahdavi M, Rezaei-Kalantari K, Qanadli SD and Mirsadraee S (2022) Left main coronary artery atresia in a 2-year-old toddler with *de novo* heart failure: Case report and review of the literature. *Front. Cardiovasc. Med.* 9:898467. doi: 10.3389/fcvm.2022.898467

Left main coronary artery atresia in a 2-year-old toddler with *de novo* heart failure: Case report and review of the literature

Sahar Asl Fallah[1], Mohammad Mahdavi[2], Kiara Rezaei-Kalantari[2]*, Salah D. Qanadli[3] and Saeed Mirsadraee[4,5]

[1]Tehran Heart Center, Tehran University of Medical Sciences, Tehran, Iran, [2]Rajaie Cardiovascular Medical and Research Center, Iran University of Medical Sciences, Tehran, Iran, [3]Cardiothoracic and Vascular Division, Department of Diagnostic and Interventional Radiology, Lausanne University Hospital and University of Lausanne, Lausanne, Switzerland, [4]Department of Radiology, Royal Bromton Hospital, London, United Kingdom, [5]National Heart and Lung Institute, Imperial College London, London, United Kingdom

Congenital coronary anomalies are among the rare disorders of the otherwise normal heart. A 2-year-old toddler was evaluated for *de novo* heart failure after a flu-like event 2 months before being suspicious of post-Covid-19 dilated cardiomyopathy. The cardiac magnetic resonance (CMR) technique displayed the basal to mid subendocardial to transmural scar, suggestive of an ischemic etiology. Further assessment with CT and invasive angiography confirmed the very uncommon left main coronary artery atresia (LMCAA) as the main cause of the patient's heart failure. This is not only the first reported LMCAA case that had undergone a CMR study but was also initially suspected with characteristic CMR findings.

KEYWORDS

cardiac magnetic resonance (CMR), *de novo* heart failure, congenital coronary anomaly, left main artery atresia, anomalous left coronary artery from the pulmonary artery (ALCAPA)

Introduction

Congenital coronary anomalies are rare disorders with a reported prevalence of 0.6–1.3% in angiographic series (1). Left main coronary artery atresia (LMCAA) is one of the least prevalent anomalies where the ostium of the left main (LM) artery is absent and the left anterior descending artery (LAD) and the left circumflex artery (LCX) connect blindly without direct origin from other vessels or cardiac chambers (2). While CT angiography (CTA) is the preferred method for the anatomic evaluation of coronary arteries (3), cardiac magnetic resonance (CMR) also plays an important role in myocardial tissue characterization for treatment strategy. We reported a case of LMCAA referred for CMR due to recent symptoms of heart failure. Written informed consent was obtained from the father of the patient for the publication of any potentially identifiable images or data included in this article.

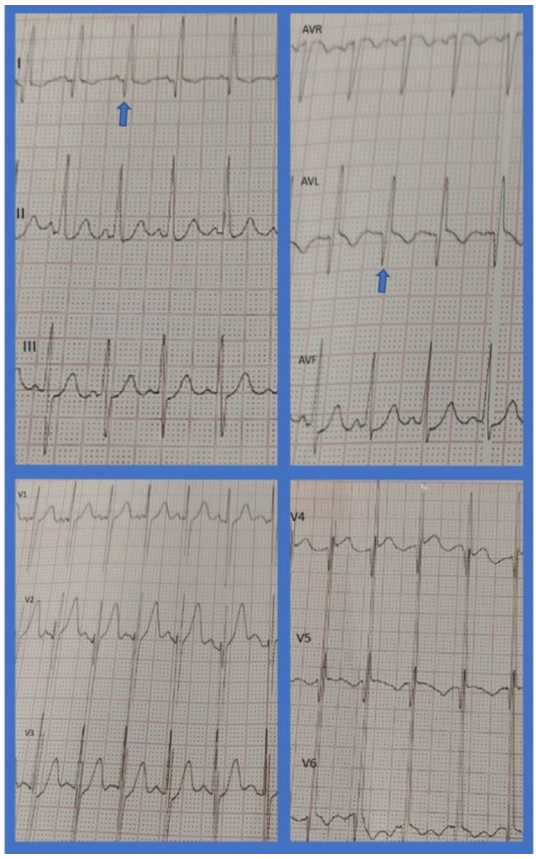

FIGURE 1
ECG demonstrating sinus tachycardia, pathologic Q waves in leads I, AVL, and V4–V6.

Case report

A 2-year-old toddler presented to a clinic with recent onset of abdominal pain, irritation, and failure to thrive. The patient had experienced flu-like symptoms 2 months before being suspicious of the COVID-19 infection. Outpatient workup revealed significantly dilated left ventricle (LV) and impaired systolic LV function with an EF of 20–25% and severe functional mitral regurgitation (MR). On physical examination, S1, S2, and S3 were audible with an early systolic grade 4 murmur. The patient's lungs were clear. Electrocardiography showed sinus tachycardia (150 bpm) and deep Q waves in leads I, AVL, V4, V5, and V6 in favor of chronic LV myocardial injury (Figure 1). Cardiac troponin, ESR, and CRP levels were normal. The ProBNP level increased (1,950 pg/ml) and COVID-19 PCR was tested negative.

Cardiac magnetic resonance was performed to investigate the possible underlying pathology, which confirmed severe LV dilation, severely reduced systolic function (LVEF: 22%), and severe MR (Figure 2). Late gadolinium enhancement (LGE) sequence demonstrated subendocardial to transmural scar in the basal and especially at the mid anterior and anteroseptal segments, raising suspicion of an ischemic insult. Gated CT coronary angiography (Figure 3) demonstrated an absent LM stem with a centripetal filling of the small caliber confluent LAD and circumflex, likely from collaterals from a dilated right coronary artery. Angiography confirmed the LM atresia with a retrograde collateral filling of LAD and LCX arteries from a dominant RCA. There was no connection to the pulmonary arterial branches (Figure 4; Supplementary Videos 1, 2). Considering the extent of myocardial fibrosis, small-sized coronary arteries and LV remodeling were required, and according to the decision of heart team specialists, the patient underwent medical treatment for heart failure and was scheduled for a heart transplant.

Discussion

To our knowledge, this is the first LMCAA case suspected initially from the findings of CMR of characteristic ischemic LGE pattern and further confirmed by the CTA and invasive angiography.

The left main coronary artery atresia is one of the rarest congenital coronary anomalies with <100 reported cases, in which an enlarged RCA is responsible to provide perfusion for the left system *via* collaterals. The clinical presentation depends mostly on the capacity and size of collateral arteries and the site of their connection to the left system and is variable from asymptomatic to congestive heart failure, syncope, and sudden cardiac death (SCD) (2, 4). Small and distally connected collaterals are indicative of poor outcomes compared to larger, more prominent, and proximally connected ones (1).

A case series study with a review of the literature, which was published in 2019, analyzed previously reported cases of 50 pediatric patients and 45 adult patients with LMCAA. In total, 88% of the pediatric group was symptomatic while 79% of the adult group was symptomatic. Heart failure was reported to be the most common finding in pediatric patients occurring in 44%, followed by syncope (28%). In the adult group, angina was the most prevalent symptom (48.8%) followed by exertional dyspnea (14%). Sudden cardiac death was reported in 10 and 7% of the pediatric and adult groups, respectively (2).

The coronary artery anatomy and anomalous origins are best visualized with multislice CTA due to its high spatial resolution and reconstruction techniques (3). Invasive angiography is used to help confirm the diagnosis (1, 2).

Differentiating LMCAA from other conflicting diagnoses such as absent LM with a single coronary artery, an anomalous left coronary artery from the pulmonary artery (ALCAPA), and secondary occlusion of LM coronary artery is crucial (Supplementary Table 1).

The left main coronary artery atresia is completely different from absent LM with a single coronary artery, which occurs in <1% of congenital coronary anomalies (5). It is a condition

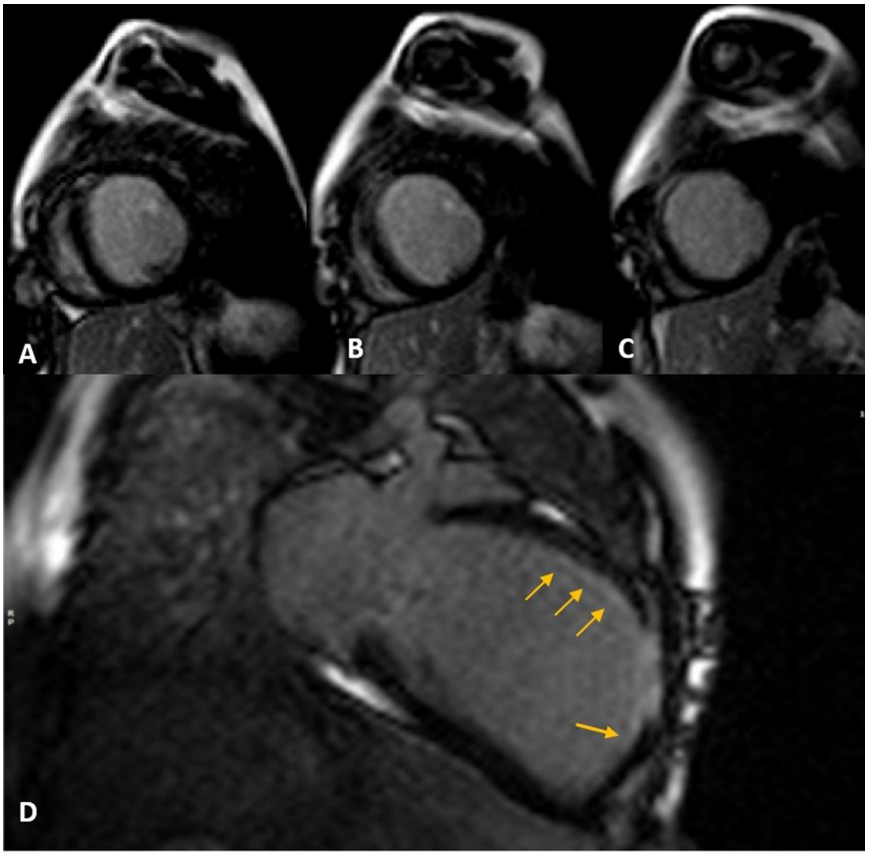

FIGURE 2
Late gadolinium enhancement (LGE) sequence images in short **(A–C)** and long **(D)** axis views show subendocardial (thin arrows) to transmural scar concentrated in mid-anteroseptal and anterior LV segments.

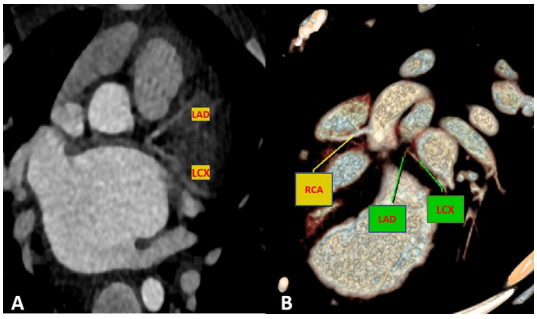

FIGURE 3
Maximum intensity projection **(A)** and volume rendered **(B)** CT images demonstrate an absence of the LM artery with proximally connected left anterior descending artery (LAD) and left circumflex artery (LCX).

where a single ostium coronary artery from the aortic trunk may have either RCA or LM origin and divides proximally to take a normal RCA/LCA course or a totally different coronary tree with the antegrade flow (6). This is mostly taken as a normal variation since it rarely causes symptoms (7). In both LMCAA and single coronary with right coronary cusp origin, RCA is dilated; however, in LMCAA, the blood supply to the left system is retrogradely perfused by collaterals (1).

Another common misdiagnosis for LMCAA is ALCAPA occurring in 1 in 300,000 live births (3). A total of 26% of pediatric patients reported in Alsalehi et al.'s (2) review were first misdiagnosed with ALCAPA. In both ALCAPA and LMCAA, RCA is dilated; however, in ALCAPA, the proximal part of the left system finally drains to the pulmonary artery. An accurate diagnosis of LMCAA from ALCAPAS is important for preoperative planning and pulmonary artery division (2, 6).

An anomalous left coronary artery from the pulmonary artery causes chronic ongoing myocardial hypoperfusion leading to myocardial hibernation, which dramatically improves after coronary reimplantation (6, 8). CMR has the advantage of distinguishing hibernated from irreversibly infarcted myocardium (9). In a case series of patients with ALCAPA undergoing CMR, only 25% of patients with ALCAPA showed scar in their LGE sequence, which validated the

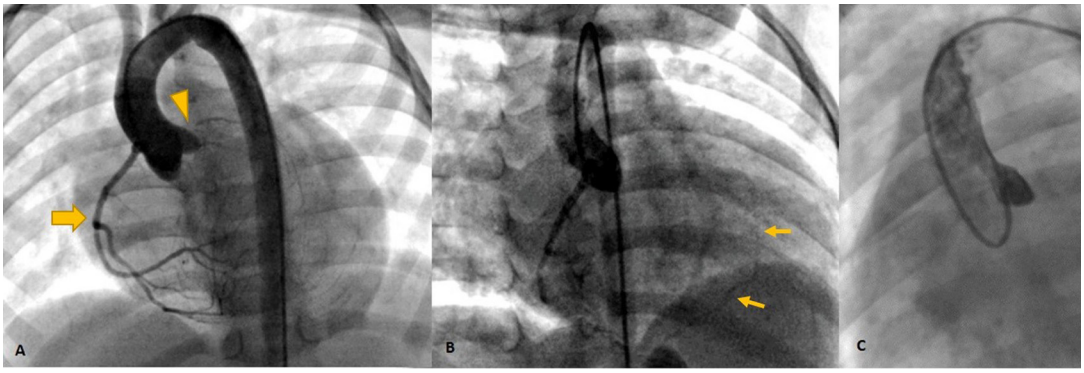

FIGURE 4
Invasive angiography **(A–C)** showing the dominant RCA [Thick arrow in **(A)**] retrogradely filling the left system *via* collaterals [Thin arrows in **(B)**] and no antegrade flow in left cusp injection **(C)** confirming left main atresia (arrowhead).

fact that myocardium is mainly viable despite depressed ventricular function (8). Nonetheless, no CMR or clinical data in patients with LMCAA on myocardial viability or functional reversibility after revascularization have been reported to this date. Regarding the retrograde flow dynamic pattern of coronary arteries in both LMCAA and ALCAPA, the ischemic scar might have basal/mid LV segment predilection due to more downstream locations in the retrograde perfusion pathway. However, further investigation is required for a thorough assessment.

Total occlusion of the LM has a relatively similar manifestation to LMCAA as demonstrated in reported cases of arteritis by Takayasu (10) and Kawasaki (11); Cross-sectional imaging often reveals the occluded portion, sometimes accompanied by adjacent aortic wall thickening.

Patients with LMCAA should undergo surgical correction with the restoration of the antegrade flow to the left coronary system either by osteoplasty or bypass grafting. Otherwise, the condition deteriorates gradually with a poor outcome. In instances in which reperfusion is not possible (due to small coronary artery diameter) or not effective (due to extensive transmural myocardial scar), the treatment strategy will focus on heart failure management till the provision of condition for heart transplantation as the last remaining option.

Data availability statement

The original contributions presented in the study are included in the article/Supplementary material, further inquiries can be directed to the corresponding author.

Ethics statement

Ethical review and approval was not required for the study on human participants in accordance with the local legislation and institutional requirements. Written informed consent to participate in this study was provided by the participants' legal guardian/next of kin. Written informed consent was obtained from patient father for the publication of any potentially identifiable images or data included in this article.

Author contributions

SA, KR-K, and MM contributed to gathering data and writing the original draft. SQ and SM contributed to editing and reviewing the manuscript. All authors contributed to the article and approved the submitted version.

Conflict of interest

The authors declare that the research was conducted in the absence of any commercial or financial relationships that could be construed as a potential conflict of interest.

Publisher's note

All claims expressed in this article are solely those of the authors and do not necessarily represent those of their affiliated organizations, or those of the publisher, the editors and the reviewers. Any product that may be evaluated in this article, or claim that may be made by its manufacturer, is not guaranteed or endorsed by the publisher.

Supplementary material

The Supplementary Material for this article can be found online at: https://www.frontiersin.org/articles/10.3389/fcvm.2022.898467/full#supplementary-material

References

1. Tanawuttiwat T, O'Neill BP, Schob AH, Alfonso CE. Left main coronary atresia. *J Card Surg Include Mech Biol Supp Heart Lungs.* (2013) 28:37–46. doi: 10.1111/jocs.12044

2. Alsalehi M, Jeewa A, Wan A, Contreras J, Yoo SJ, Laks JA, et al. case series of left main coronary artery ostial atresia and a review of the literature. *Cong Heart Dis.* (2019) 14:901–23. doi: 10.1111/chd.12842

3. Heermann P, Heindel W, Schuelke C. Coronary artery anomalies: diagnosis and classification based on cardiac CT and MRI (CMR)-from ALCAPA to anomalies of termination. *RoFo: Fortschritte auf dem Gebiete der Rontgenstrahlen und der Nuklearmedizin.* (2016) 189:29–38. doi: 10.1055/s-0042-119452

4. Angelini P. Coronary artery anomalies: an entity in search of an identity. *Circulation.* (2007) 115:1296–305. doi: 10.1161/CIRCULATIONAHA.106.618082

5. Yturralde F, Nesto R, Wald C. Congenital single coronary artery with an absent left main coronary artery. *J Cardiovasc Comput Tomogr.* (2008) 1:50–1. doi: 10.1016/j.jcct.2007.11.002

6. Pandey NN, Sinha M, Sharma A, Rajagopal R, Bhambri K, Kumar S. Anomalies of coronary artery origin: evaluation on multidetector CT angiography. *Clin Imag.* (2019) 57:87–98. doi: 10.1016/j.clinimag.2019.05.010

7. Chou M, Chen C. Left main coronary artery atresia. *Acta Cardiol Sin.* (2007) 23:273.

8. Latus H, Gummel K, Rupp S, Mueller M, Jux C, Kerst G, et al. Cardiovascular magnetic resonance assessment of ventricular function and myocardial scarring before and early after repair of anomalous left coronary artery from the pulmonary artery. *J Cardiovasc Magn Reson.* (2014) 16:1–9. doi: 10.1186/1532-429X-16-3

9. Bhalgat P, Naik A, Salvi P, Bhadane N, Shah K, Paunipagar B, et al. Cardiac magnetic resonance imaging, myocardial scar and coronary flow pattern in anomalous origin of left coronary artery from the pulmonary artery. *Indian Heart J.* (2018) 70:303–7. doi: 10.1016/j.ihj.2017.08.004

10. Limsuwan A, Khowsathit P, Pienvichit P. Left main coronary occlusion from Takayasu arteritis in an 8-year-old child. *Pediatric Cardiol.* (2007) 28:234–7. doi: 10.1007/s00246-006-0080-6

11. Madhavan S, Sathish G. Left main coronary artery ostial occlusion in a young man: late sequelae of Kawasaki's disease? *Heart Asia.* (2015) 7:15. doi: 10.1136/heartasia-2014-010598

frontiers | Frontiers in Cardiovascular Medicine

TYPE Case Report
PUBLISHED 07 November 2022
DOI 10.3389/fcvm.2022.1042593

OPEN ACCESS

EDITED BY
Utpal S. Bhalala,
Driscoll Children's Hospital,
United States

REVIEWED BY
Hari Gourabathini,
Indiana University South Bend,
United States
Suresh Kumar Angurana,
Post Graduate Institute of Medical Education and Research (PGIMER), India

*CORRESPONDENCE
Hanbo Tang
tanghanbo75@163.com

SPECIALTY SECTION
This article was submitted to Pediatric Cardiology, a section of the journal Frontiers in Cardiovascular Medicine

RECEIVED 12 September 2022
ACCEPTED 21 October 2022
PUBLISHED 07 November 2022

CITATION
Ai C, Lv X, Qi X and Tang H (2022) Case report: Right coronary artery rupture—A rare complication of cardiopulmonary resuscitation. *Front. Cardiovasc. Med.* 9:1042593. doi: 10.3389/fcvm.2022.1042593

Case report: Right coronary artery rupture—A rare complication of cardiopulmonary resuscitation

Chenchen Ai, Xiaobo Lv, Xuehong Qi and Hanbo Tang*

Cardiovascular Center, Gansu Provincial Maternity and Child-Care Hospital, Lanzhou, China

An 8-month-old female experienced a life-threatening right coronary artery rupture resulting from cardiopulmonary resuscitation (CPR) 1 week after corrective surgery for Tetralogy of Fallot (TOF). Emergency exploratory thoracotomy was performed due to uncorrectable hemorrhagic shock. During exploration, active bleeding was detected in the anterior branch of the right ventricular coronary artery. After the repair, the patient's condition improved. Coronary artery rupture is an extremely rare complication of CPR. Here, we present a case that provides new reflections and warnings to clinicians.

KEYWORDS

cardiovascular injury, coronary artery rupture, hemorrhagic shock, chest compression, cardiopulmonary resuscitation

Introduction

Effective chest compression is the key to successful cardiopulmonary resuscitation (CPR). Reports of cardiovascular injury secondary to chest compression are limited. Among these, coronary artery lacerations have rarely been reported. Owing to the absence of awareness of this type of complication, CPR-associated coronary injury may not be identified in a timely fashion. In particular, in this case, we present that some misleading information inhibited accurate judgement of the condition in time. Coronary artery rupture has a high risk of mortality and, once identified, timely surgical intervention is warranted. Here, we describe a case of rupture of the right coronary artery secondary to CPR in an infant patient who underwent corrective surgery for Tetralogy of Fallot (TOF).

Case description

An 8-month-old female patient with TOF was admitted to our heart center. The patient underwent corrective surgery for TOF after completion of the relevant examination, and written informed consent was obtained from parents. The procedure was performed smoothly. Postoperatively, a bedside transthoracic echocardiogram demonstrated that the patient's cardiac function had improved noticeably. Owing to the small amount of drainage liquid, the pericardial drainage tube was removed

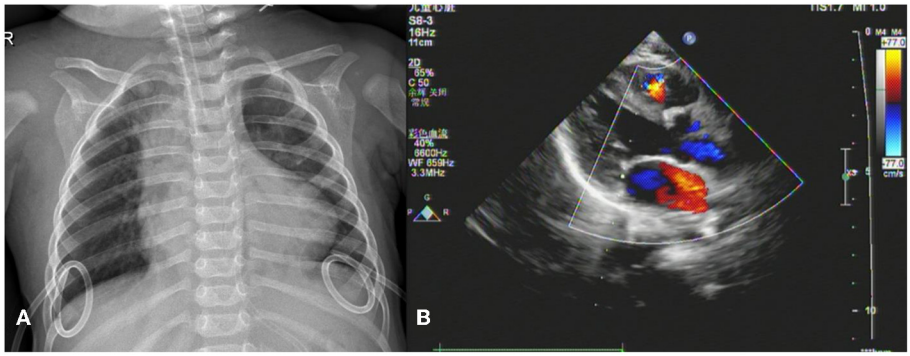

FIGURE 1
Imaging findings. **(A)** Chest X-ray shows bilateral drainage tubes and no obvious signs of pleural effusion. **(B)** No signs of pericardial tamponade or pericardial effusion on echocardiogram in left ventricular long-axis view.

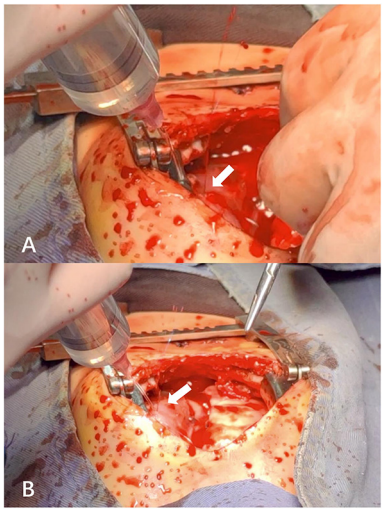

FIGURE 2
(A,B) Active bleeding from the anterior right ventricular branch (a branch of the right coronary artery) observed at different angles in the same operative field during exploratory thoracotomy.

on postoperative day three. However, the patient developed a pulmonary infection postoperatively, thus the tracheal intubation was left in place. Chest radiography indicated bilateral pleural effusion; therefore, closed thoracic drainage was performed. Light yellow clear fluid was observed in the left drainage tube, and light bloody clear fluid was observed in the right drainage tube. Laboratory examination of the pleural effusion suggested an exudative pleural effusion.

Thereafter, the vital signs were stable. There was no fever and the infection indicators were not high. The infant's circulatory and respiratory conditions were stable, and tracheal intubation was expected to be removed if there was no change in condition. An acute alteration occurred in the patient's condition on postoperative day seven after chest radiography. The patient developed an unstable condition with a reduced heart rate, hypotension, and hypoxemia that progressed rapidly to cardiac arrest. Effective CPR was initiated and the possible causes of cardiac arrest were evaluated. Unplanned extubation was identified as the most probable cause of cardiac arrest. After 10 min uninterrupted resuscitation, spontaneous respiratory and normal circulation returned. However, clinical observation revealed that the pre-existing thoracic drainage tube on the right side continuously drained hemorrhagic fluid, which was complicated by decreasing hemoglobin and blood pressure. The patient presented with progressive anemia and hypovolemic shock. After aggressive fluid resuscitation, hemorrhagic shock persisted. A bedside ultrasound was performed, and pericardial tamponade and effusion were not found. In addition, no significant pleural effusion was observed on repeat chest radiography (Figure 1). Therefore, emergency exploratory thoracotomy was required, given that intercostal vessel injury or intrathoracic injury during the rescue process might be possible reasons for persistent thoracic cavity bleeding. After informed consent was obtained from the immediate family, exploratory surgery was performed. The chest was entered through the original median sternal incision, and a small number of blood clots and fresh bleeding were observed in the mediastinum. After cleaning the accumulated blood, exploration continued to reveal active bleeding in the anterior branch of the right ventricular coronary artery which had a half a millimeter long tear (Figure 2). Because the tear was small, we repaired it directly using a 7-0 Prolene suture. The bleeding stopped immediately, and the patient's condition gradually stabilized. In addition, a 1 cm tear was found in the right pleura that communicated with the anterior mediastinum. Opening of the right pleura and continued exploration of the right thoracic cavity revealed no active bleeding. During 30 min observation, no ST segment changes were observed on electrocardiography. After sternal closure, the patient was returned to the cardiac

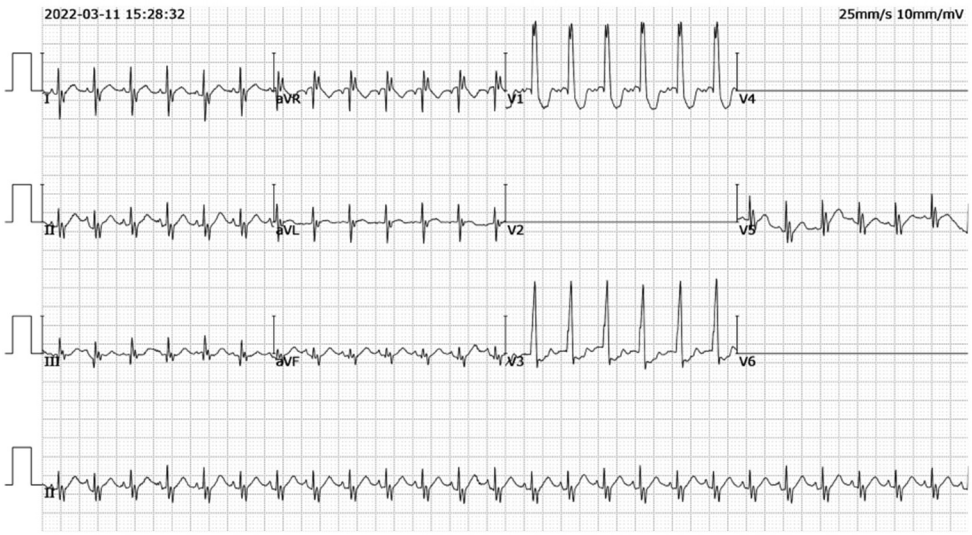

FIGURE 3
Postoperative electrocardiogram findings. No significant ST-T changes on postoperative electrocardiogram.

intensive care unit (CCU). The patient's postoperative ECG showed no significant ST-T changes (Figure 3). The patient subsequently recovered successfully and was extubated on day three after exploratory thoracotomy and coronary repair surgery, transferred out of the CCU on day six, and discharged on day 15. At the follow-up 3 months after discharge, the patient's cardiac function had recovered well and blood indicators were normal.

Discussion

High-quality external chest compression is the cornerstone of successful CPR. In some circumstances, this urgent medical process is accompanied by iatrogenic injuries, such as closed injuries or fractures of the chest and abdomen. Rib and sternal fractures are the most common complications of chest compression (1). However, vital internal organs, including the heart and vessels, can also be injured during this medical maneuver (2, 3).

Coronary artery rupture is often closely linked to percutaneous coronary intervention (PCI). It is also associated with macrovascular diseases such as dissection and artery aneurysms (4). However, coronary artery rupture as a complication of CPR has rarely been reported. To date, published data on CPR-associated cardiovascular injuries have been limited. Miller et al. reported an atrial rupture secondary to standard CPR, confirmed by echocardiography, and performed bedside thoracotomy to repair the breakage (5). In another study, a left coronary artery perforation was identified as a complication of CPR in a middle-aged man who had a cardiac arrest following laparoscopic inguinal herniorrhaphy (6). Early recognition and prompt therapy are crucial for CPR-associated cardiac injury, which has significant mortality, to avoid catastrophic consequences.

In the case presented here, where a female infant experienced hemorrhagic shock due to right coronary artery rupture secondary to standard manual chest compression, emergency exploratory thoracotomy was required for diagnosis. Ultimately, the patient's urgent condition was successfully relieved by prompt surgical intervention. This rare case provides unique insights regarding the cardiovascular complications of CPR. First, the strategy of chest compression in the pediatric age group differs from adults, emphasizing the "two-thumbs" encircling technique to reduce the incidence of injury to infants. Consequently, the intensity and energy of chest compression is much lower than in adults. In our case, we performed a standard CPR procedure according to the latest pediatric CPR guidelines (7). Regardless, CPR-associated cardiovascular injuries occurred in this case. Second, in regard to sternal closure in cardiac surgery, surgeons typically partially suture the pericardium to provide a protective effect. We sutured sections of the pericardium in the patient, but the post-sutured pericardium failed to completely cover the region of coronary artery distribution, which left some vessels unprotected, likely contributing to the occurrence of injuries. In addition, the tear on the right pleura caused communication between the anterior mediastinum and thoracic cavity, which was the direct reason for thoracic hemorrhage. Owing to continuous drainage of the right chest drainage

tube, no obvious signs of pleural effusion were observed on chest radiography. In addition, the change in the patient's condition occurred on day seven after TOF corrective surgery, when a slight adhesion formed in the pericardial cavity, which was one of the reasons for the absence of pericardial effusion.

Early detection and evaluation of the condition of patients with CPR-related coronary artery injury are essential for effective intervention. Bedside ultrasound is a non-invasive imaging examination that aids in the assessment and diagnosis of critical patients. The main signs of coronary artery rupture on echocardiography are pericardial effusion and tamponade. However, in this case, echocardiography did not provide valuable clues for a definitive diagnosis. It also inhibited our early judgement that the source of bleeding originated from the heart vessels. Volume evaluation and fluid resuscitation are critical for hypovolemic shock. Once anemia refractory to transfusion is verified, the cause of hemorrhage must be identified as quickly as possible. In the context of an unknown etiology, prompt surgical exploration merits consideration. In our case, the solution to the critical situation of the infant benefited from a timely exploratory thoracotomy.

Conclusion

In conclusion, cardiovascular injuries after external chest compression are rare in clinical practice. In particular, rupture of the right coronary artery is an exceptionally rare complication of CPR. Our case provides insights for clinicians based on actual practice regarding when this rare complication may occur and what clinicians can monitor to avoid fatal consequences from this rare occurrence.

Data availability statement

The original contributions presented in the study are included in the article/Supplementary material, further inquiries can be directed to the corresponding author/s.

Ethics statement

Written informed consent was obtained from the minor's legal guardian for the publication of any potentially identifiable images or data included in this article.

Author contributions

CA drafted this manuscript. XL prepared the figures. XQ collected the data. HT revised the manuscript. All authors read and approved the manuscript.

Funding

This work was supported by the Lanzhou Science and Technology Development Guiding Plan Project Grant Number: 2019-ZD-126.

Conflict of interest

The authors declare that the research was conducted in the absence of any commercial or financial relationships that could be construed as a potential conflict of interest.

Publisher's note

All claims expressed in this article are solely those of the authors and do not necessarily represent those of their affiliated organizations, or those of the publisher, the editors and the reviewers. Any product that may be evaluated in this article, or claim that may be made by its manufacturer, is not guaranteed or endorsed by the publisher.

Supplementary material

The Supplementary Material for this article can be found online at: https://www.frontiersin.org/articles/10.3389/fcvm.2022.1042593/full#supplementary-material

References

1. Buschmann CT, Tsokos M. Frequent and rare complications of resuscitation attempts. *Intensive Care Med.* (2009) 35:397–404. doi: 10.1007/s00134-008-1255-9

2. Diop S, Gautier A, Moussa N, Legriel S. Cardiopulmonary resuscitation-related left gastric artery laceration. *Intensive Care Med.* (2019) 45:1307–8. doi: 10.1007/s00134-019-05603-3

3. Hickey TB, Gill GG, Seidman MA, Webber DL. CPR-associated right ventricular rupture in the setting of pulmonary embolism. *CJEM.* (2016) 18:484–7. doi: 10.1017/cem.2016.327

4. Cheng ST, Liu CJ, Huang HL, Ko YL. Rescue coilization for spontaneous coronary artery rupture. *JACC Cardiovasc Interv.* (2021) 14:e149–50. doi: 10.1016/j.jcin.2021.04.005

5. Miller AC, Rosati SF, Suffredini AF, Schrump DS. A systematic review and pooled analysis of CPR-associated cardiovascular and thoracic injuries. *Resuscitation.* (2014) 85:724–31. doi: 10.1016/j.resuscitation.2014.01.028

6. Wiemer M, Horstkotte D, Schultheiss HP. Non-surgical management of a perforated left anterior descending coronary artery following cardiopulmonary resuscitation. *Z Kardiol.* (1999) 88:675–80. doi: 10.1007/s003920050344

7. Topjian AA, Raymond TT, Atkins D, Chan M, Duff JP, Joyner BL, et al. Part 4: pediatric basic and advanced life support: 2020 American heart association guidelines for cardiopulmonary resuscitation and emergency cardiovascular Care. *Circulation.* (2020) 142:S469–523. doi: 10.1161/CIR.0000000000000901

frontiers | Frontiers in Cardiovascular Medicine

TYPE Case Report
PUBLISHED 09 November 2022
DOI 10.3389/fcvm.2022.974843

OPEN ACCESS

EDITED BY
Cecile Tissot,
Clinique des Grangettes, Switzerland

REVIEWED BY
Yusheng Pang,
Guangxi Medical University, China
Abdallah Fayssoil,
Hôpital Raymond-Poincaré, France

*CORRESPONDENCE
Weihua Zhang
weihua@jlu.edu.cn

SPECIALTY SECTION
This article was submitted to Pediatric Cardiology, a section of the journal Frontiers in Cardiovascular Medicine

RECEIVED 21 June 2022
ACCEPTED 24 October 2022
PUBLISHED 09 November 2022

CITATION
Liu X, Zhao W, Shu S and Zhang W (2022) Duchenne muscular dystrophy involves the myocardium and causes arrhythmia: Case report. *Front. Cardiovasc. Med.* 9:974843. doi: 10.3389/fcvm.2022.974843

Duchenne muscular dystrophy involves the myocardium and causes arrhythmia: Case report

Xuhan Liu, Wei Zhao, Shangzhi Shu and Weihua Zhang*

Department of Cardiovascular Medicine, The First Hospital of Jilin University, Changchun, China

Background: Patients with muscular dystrophy have mutations in the gene that can lead to severe muscle wasting, respiratory issues or heart failure between ages 30 and 40. Currently, there is no effective treatment for DMD-induced heart failure.

Case presentation: We report a patient with recurrent unexplained fever and muscle soreness was definitely diagnosed with DMD. An analysis of the patient's genetics revealed a nonsense mutation (C.1207G > T). His DMD was treated with hormones. Also, the patient's fever is under control because of hormone therapy. However, as the disease progresses, the heart structure and function gradually change, and eventually malignant arrhythmias occur.

Conclusion: We report a rare case of DMD involving the heart causing heart failure and malignant arrhythmia. Currently, no complete treatment is available for these patients, but our treatment regimen may benefit our patient and improve his outcomes.

KEYWORDS

heart failure, arrhythmia, duchenne and baker muscular dystrophies, myocardial damage, ARNI

Background

Duchenne Muscular Dystrophy (DMD) is genetic or caused by mutations of motor function proteins (1). It is often diagnosed in childhood, contributing to life-long disabilities and shorter lifespans (1). Mutations of the Duchenne gene, located on chromosome Xp21.2, are the cause of most Duchenne muscular dystrophies in children (2). Mutations in the dystrophin gene lead to serious muscle wasting, respiratory or cardiac failure by the age of 30 (3). It is estimated to be 1/5,000 in the population (1). The disease progresses rapidly, with wheelchair dependence occurring in the teens (4) and usually progresses to a severe cardiomyopathic condition. Here we present a case of a patient with DMD and a nonsense mutation (C.1207G > T), faced intermittent fever and muscle pain all over the body repeatedly that eventually advanced to heart failure and arrhythmia.

Case presentation

A 21-year-old Chinese man was diagnosed in June 2002 with muscular dystrophy. His genetic test and muscle biopsy revealed a diagnosis of DMD. The data of that time are no longer accessible due to distance in time.

A ten-day period of intermittent fever occurred in October 2018, when he was 18 years old. During the past 2 years, he suffered from liver disease, suspected brucella infection, and obesity. One year later, he fell ill with sepsis. Despite the fact that fevers had a fairly clear cause of infection, DMD had no concomitant symptoms except weakness of the lower limbs. Accordingly, systematic treatment hadn't been applied. At admission, the body temperature was 38°C, the heart rate was 90 beats/min, blood pressure was 110/72 mmHg, and breathing was 20 beats/min. Laboratory findings are as followed: creatine kinase (CK) 664 U/L, creatine kinase isoenzymes (CK-MB) 35.9 U/L, C-reaction protein (CRP) 29.66 mg/L, lactate dehydrogenase (LDH) 273 U/L, α-hydroxybutyrate dehydrogenase (αHBDH) 190 U/L, mycoplasma antibody: 1:160 positive. This patient was discharged after undergoing effective antiviral therapy (ganciclovir 0.25 g iv. Bid), mannatide (20 mg iv. Qd2) and creatine phosphate sodium (1g iv. Qd2). Because he did not have heart symptoms at that time, he did not have cardiac echocardiography test.

He was admitted to the hospital with a high fever and numerous joint pains throughout his body for 4 days, with a temperature of up to 39°C in January 2020. At admission, his body temperature was 36.8°C, his heart rate was 84 beats per min, his blood pressure was 126/69 mmHg, and he was unable to walk upright. He is 175 cm tall and weighs 97 kg. His BMI is 31.67 kg/m2, which is overweight. Laboratory findings are as followed: CK 514U/L, CRP 43.41 mg/L, Interleukin-4 (IL-4) 3.42 pg/ml, IL-6 10.17 pg/ml, IL-10 8.13 pg/ml, tumor necrosis factor-α(TNF-α) 3.16 pg/ml. CT scan of the lungs revealed a small amount of inflammation in the left lower lobe and in the right lower lobe. After anti-infection treatment, he was discharged. After half a year, he was hospitalized again for a fever and muscle pain. Laboratory findings are as followed: CK 411 U/L, CK-MB 7.40 ng/ml, troponin I (Tn I) 0.067 ng/ml, N-terminal pro-B type natriuretic peptide (NT-pro BNP) 1250.0 pg/ml, CRP 45.67 mg/L, LDH 257U/L, mycoplasma antibody: positive. The lung CT was similar to the last one. In the abdominal CT, it was found that the patient had fatty liver, multiple enlarged lymph nodes around the abdominal aorta, and less muscle density on both sides of his back and buttocks, which should consider the possibility of fat infiltration. During echocardiography (Figure 1), the left ventricular ejection fraction (EF) was 39%, and left ventricle were enlarged (left ventricle endomesosomal diameter was 63 mm), abnormal ventricular movement, decreased left ventricular systolic and diastolic function, weak mitral regurgitation and trace pericardial effusion. The ECG showed

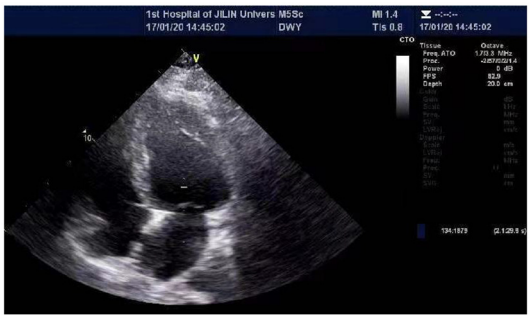

FIGURE 1
Echocardiographic of the patient's heart. The echocardiography revealed EF 29%, left atrial and left ventricle enlargement (left ventricular endomesosomal diameter 63 mm), reduced ventricular wall pulsation diffusion, decreased left ventricular systolic and diastolic function, and trace pericardial effusion.

sinus rhythm, a normal ECG. This time his cardiac function was level III and was placed on hormone therapy. He was discharged when his condition improved.

In order to test if his heart disease was related to DMD, he and his family had another genetic test 2 months later. The results of sequencing suggested a nonsense mutation (c.1207G > T) in the exon eleven region of the DMD (Muscular dustrophy, Duchenne) gene, encoding amino acid p.G403X (guanine > thymine). It was found that neither his parents nor his sister carried heterozygous variation of this locus, and neither of them exhibited any clinical signs of muscular dystrophy (Figure 2).

In April 2021, again, he suffered from a fever and aching muscles. However, his heart function deteriorated. ECG showed left anterior branch block. The echocardiography revealed EF 29%, left atrial and left ventricle enlargement (left ventricular endomesosomal diameter 63 mm), reduced ventricular wall pulsation diffusion, decreased left ventricular systolic and diastolic function, and trace pericardial effusion. Diuretics, nitrates, and beta blockers are taken orally following discharge. His heart function was Grade III at that time. The hormone dose was reduced because his fever was controlled. Hormone should not be stopped immediately and should be reduced gradually. Even though he had another fever 8 months later, his heart function improved significantly, with his EF reaching 42%. The lung CT shows atrophy of the chest and back muscles and an increase in fat. His medication regimen was changed to oral beta blockers, coenzyme Q10, and hormones.

Palpitations began in June 2022, becoming more frequent over the following month. He developed acute myocardial injury. A rise of 0.18 ng/mL in TnI, a normal creatine kinase level, and 44% in EF were observed. The myocardial injury was persistent and troponin did not increase or decrease significantly. 24-h Holter electrocardiography showed a mean heart rate of 86 BPM, occasional premature ventricular

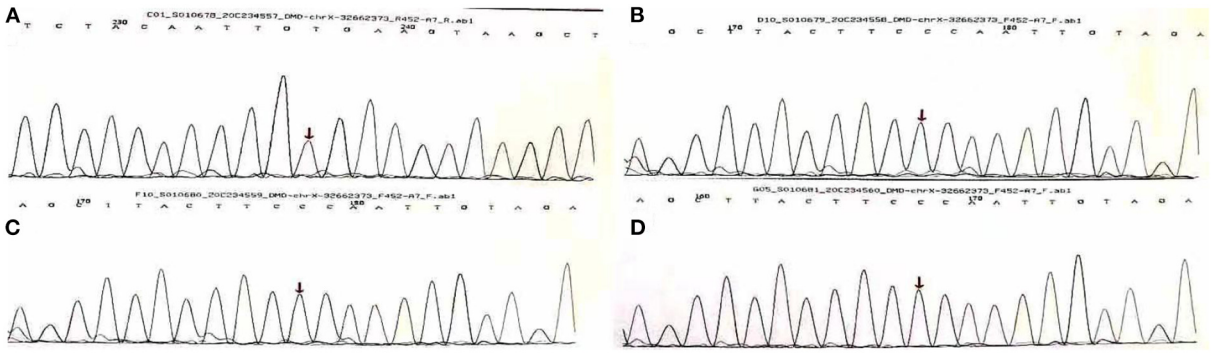

FIGURE 2
Gene sequencing results of Sanger method of Duchenne gene mutation in A family [Missense mutation occurred at the 1,207 base of the 11th exon of Duchenne gene in **(A)** (C.1207 G > T, P.G403x), arrows are the mutation sites, **(B–D)** are normal phenotypes].

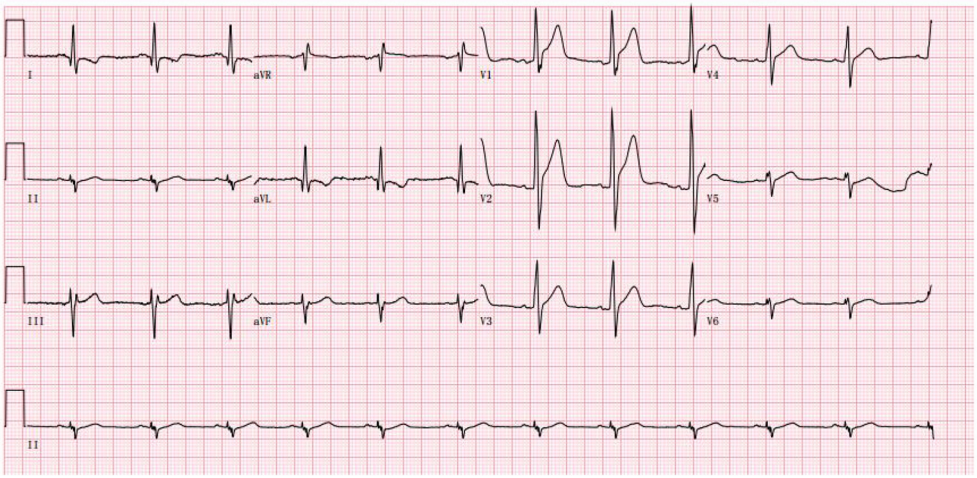

FIGURE 3
The abnormal ECG at the admission in June 2022 (Sinus rhythm and tall R wave in V1V2V3, left anterior branch block).

contractions in pairs (673), occasional premature atrial contractions, and paroxysmal atrial tachycardia (total > 100 BPM, 283, maximum 6 min) (Figure 3). To treat the condition, the oral drugs were adjusted as hormone (in reduction), coenzyme Q10, trimetazidine and ARNI. Afterwards, the patient improved, and he was discharged (Table 1).

Discussion and conclusions

DMD is a condition caused by a mutation in the dystrophin gene, which results in critical muscle wasting and death by age 30 (1). Children usually show symptoms in early childhood, and if untreated with corticosteroids by the age of 12 years, they will probably lose their abilities to walk (2). In the patient's case, his parents discovered that the patient had weakness in both lower limbs and could not walk independently at age 3, which coincided with DMD's symptoms.

DMD is a recessive autosomal-recessive disorder that results from mutations in the dystrophin gene that cause the absence of dystrophin protein (NIH U.S., 2020 National Library of Medicine) (1). The patient has a nonsense mutation (c.1207G > T) in exon eleven of the DMD (Muscular Dystrophy, Duchenne) gene, encoding amino acid p.G403X (guanine > thymine), which is one of the rarest type of genetic mutation. In the skeletal muscle cells, DMD encodes the dystrophin protein, which functions as a link between the intracellular cytoskeleton, the extracellular matrix, and the dystrophin–glycoprotein complex (2). Dystrophin-producing gene mutations cause a reduction in muscle ragility and result in contraction-induced injuries (5).

A diagnosis of DMD was determined based on clinical symptoms, age of onset, creatine kinase test, muscle biopsy

TABLE 1 The patient's timeline of admission, diagnosis and treatment.

Symptoms	Age	Treatment
Bilateral lower limb weakness	3 years old	
Intermittent fever for 10 days	18 years old	Antiviral
High fever and numerous joint pains throughout his body for 4 days	19 years old	Anti-infection
High fever and numerous joint pains throughout his body for 5 days	20 years old	Hormone therapy (oral 12 mg methylprednisolone twice a day)
High fever and numerous joint pains throughout his body for 4 days	20 years old and a half	Oral beta blockers, diuretics, nitrates, and hormones(16 mg methylprednisolone once a day)
High fever and numerous joint pains throughout his body for 4 days	21 years old	Oral beta blockers, coenzyme Q10, and hormones(16 mg methylprednisolone once a day)
Palpitations for 3 months	21 years old and a half	Hormone (5 mg methylprednisolone once a day), coenzyme Q10, trimetazidine, and ARNI

analysis, and dystrophin mutation genetic testing (1). The current examination results show that the patient's chest, bilateral back, and gluteal floor muscles have been involved, which has resulted in fat infiltration and effected his overall motor function. Laboratory tests for patients with advanced DMD showed that creatine kinase levels were normal, which matched the patient's clinical findings.

Corticosteroids remain among one of the best methods for managing complications and have significantly increased the longevity of these patients (6). Evidence-based benefits of corticosteroids include a longer period of disease progression (7). Prednisone/prednisolone and deflazacort are the two most commonly used corticosteroids (7). Patients with DMD may benefit from taking 0.3 to 1.5 mg/kg/d of prednisone (8). In this case, the patient weighed 100 kg and took 5 mg of methylprednisolone orally daily, which is equivalent to 6.25 mg of ponisone, which is consistent with the dose required to benefit from ponisone treatment. He took corticosteroids as standard of care. Besides these medications, the FDA has approved other drugs as well, including eteplirsen (EXONDYS 51®), golodirsen (VYONDYS 53TM), and viltolarsen (VILTEPSO®) (1).

It is recommended to detect and treat cardiomyopathy in DMD patients early, as it can prolong survival (9). As the dystrophin protein is absent throughout life span, fibrofatty infiltration begins in the left ventricle's posterobasal wall (10). Infiltration of the ventricular wall can lead to fibrosis, thinning, dilation, and progressive decline of ejection fraction (11). According to the heart failure guidelines (12), this patient was Stage B HF. In spite of asymptomatic heart failure, there are structural and functional abnormalities that pose a greater risk for symptomatic heart failure (13). Yet for patients without myocardial infarction, there is no complete routine diagnosis or treatment. The pre-clinical stage of heart failure is treated with ARNI. ARNI is the abbreviation of Angiotensin receptor blocker Neprilysin. It is an anti-heart failure drug. After entering the body, it is hydrolyzed into valsartan and sacubitril. Valsartan is an ARB, which is a RAAS system inhibitor. Sacubitril can inhibit the degradation of various peptides including BNP and improve the level of endogenous BNP. Currently, in clinical guidelines (12), the efficacy evaluation of ARNI for heart failure with preserved ejection fraction and heart failure due to muscle metabolic diseases is limited. This patient's cardiac function improved after the application of ARNI, suggesting that such patients could benefit from the treatment of ARNI. The use of coenzyme Q10 and trimetazidine was also used to nourish the heart and improve its metabolism. The mechanism of trimetazidine is through inhibition of fatty acid β-oxidation. The metabolism of myocardial fat can be changed into oxidation using GLU, and the efficiency of oxygen utilization can be improved, so as to improve myocardial energy metabolism. The patient's palpitation symptoms improved after discharge, which indicated that the treatment was effective, but closer observation was still required.

DMD guidelines suggest baseline assessments of cardiac function consisting of an electrocardiogram, non-invasive imaging with echocardiography, or magnetic resonance imaging (CMR) at time of diagnosis (14). Individuals with asymptomatic disease should be re-examined annually (14). With progression of the disease, cardiac arrhythmia is more likely, which leads to further surveillance during the late ambulatory stage and the use of periodic 24-h Holter monitoring, as is directed by the specialist (1). Although ECG, echocardiography, and a 24-h holter ECG were performed on this patient, it was relatively late in the process. By the time myocardial involvement is detected, the ejection fraction has already decreased significantly and the myocardium has already been remodeled. As patients with

DMD and other genetic metabolic diseases affecting the heart, we should remind them to regularly review electrocardiograms and echocardiograms. The prognosis of patients can greatly be improved by early diagnosis.

Data availability statement

The original contributions presented in the study are included in the article/supplementary material, further inquiries can be directed to the corresponding author.

Ethics statement

Written informed consent was obtained from the individual(s) for the publication of any potentially identifiable images or data included in this article.

Author contributions

XL: methodology, investigation, formal analysis, and writing-original draft. WZhao: conceptualization, methodology, and visualization. SS: investigation, formal analysis, and writing-review and editing. WZhan: project administration and supervision. All authors contributed to the article and approved the submitted version.

Conflict of interest

The authors declare that the research was conducted in the absence of any commercial or financial relationships that could be construed as a potential conflict of interest.

Publisher's note

All claims expressed in this article are solely those of the authors and do not necessarily represent those of their affiliated organizations, or those of the publisher, the editors and the reviewers. Any product that may be evaluated in this article, or claim that may be made by its manufacturer, is not guaranteed or endorsed by the publisher.

References

1. Iftikhar M, Frey J, Shohan MJ, Malek S, Mousa SA. Current and emerging therapies for Duchenne muscular dystrophy and spinal muscular atrophy. *Pharmacol Ther.* (2021) 220:107719. doi: 10.1016/j.pharmthera.2020.107719

2. James KA, Gralla J, Ridall LA, Do TN, Czaja AS, Mourani PM, et al. Left ventricular dysfunction in Duchenne muscular dystrophy. *Cardiol Young.* (2020) 30:171–6. doi: 10.1017/S1047951119002610

3. Findlay AR, Wein N, Kaminoh Y, Taylor LE, Dunn DM, Mendell JR, et al. Clinical phenotypes as predictors of the outcome of skipping around DMD exon 45. *Ann Neurol.* (2015) 77:668–74. doi: 10.1002/ana.24365

4. Wu B, Cloer C, Lu P, Milazi S, Shaban M, Shah SN, et al. Exon skipping restores dystrophin expression, but fails to prevent disease progression in later stage dystrophic dko mice. *Gene Ther.* (2014) 21:785–93. doi: 10.1038/gt.2014.53

5. Hamada S, Ishikawa Y, Aoyagi T, Ishikawa Y, Minami R, Bach JR. Indicators for ventilator use in Duchenne muscular dystrophy. *Respir Med.* (2011) 105:625–9. doi: 10.1016/j.rmed.2010.12.005

6. Falzarano MS, Scotton C, Passarelli C, Ferlini A. Duchenne muscular dystrophy: from diagnosis to therapy. *Molecules.* (2015) 20:18168–84. doi: 10.3390/molecules201018168

7. Birnkrant DJ, Bushby K, Bann CM, Alman BA, Apkon SD, Blackwell A, et al. Diagnosis and management of Duchenne muscular dystrophy, part 2: respiratory, cardiac, bone health, and orthopaedic management. *Lancet Neurol.* (2018) 17:347–61. doi: 10.1016/S1474-4422(18)30025-5

8. Evans NP, Misyak SA, Robertson JL, Bassaganya-Riera J, Grange RW. Dysregulated intracellular signaling and inflammatory gene expression during initial disease onset in Duchenne muscular dystrophy. *Am J Phys Med Rehabil.* (2009) 88:502–22. doi: 10.1097/PHM.0b013e3181a5a24f

9. Birnkrant DJ, Bushby K, Bann CM, Apkon SD, Blackwell A, Brumbaugh D, et al. Diagnosis and management of Duchenne muscular dystrophy, part 1: diagnosis, and neuromuscular, rehabilitation, endocrine, and gastrointestinal and nutritional management. *Lancet Neurol.* (2018) 17:251–67. doi: 10.1016/S1474-4422(18)30024-3

10. Wein N, Alfano L, Flanigan KM. Genetics and emerging treatments for Duchenne and Becker muscular dystrophy. *Pediatr Clin North Am.* (2015) 62:723–42. doi: 10.1016/j.pcl.2015.03.008

11. Escolar DM, Hache LP, Clemens PR, Cnaan A, McDonald CM, Viswanathan V, et al. Randomized, blinded trial of weekend vs daily prednisone in Duchenne muscular dystrophy. *Neurology.* (2011) 77:444–52. doi: 10.1212/WNL.0b013e318227b164

12. McDonagh TA, Metra M, Adamo M, Gardner RS, Baumbach A, Böhm M, et al. 2021 ESC Guidelines for the diagnosis and treatment of acute and chronic heart failure. *Eur Heart J.* (2021) 42:3599–726. doi: 10.1093/eurheartj/ehab368

13. Topaloglu H, Gloss D, Moxley RT, Ashwal S, Oskoui M. Practice guideline update summary: corticosteroid treatment of Duchenne muscular dystrophy: report of the guideline development subcommittee of the American academy of neurology. *Neurology.* (2016) 87:238. doi: 10.1212/01.wnl.0000489553.99227.18

14. McNally EM, Kaltman JR, Benson DW, Canter CE, Cripe LH, Duan D, et al. Contemporary cardiac issues in Duchenne muscular dystrophy. working group of the national heart, lung, and blood institute in collaboration with parent project muscular dystrophy. *Circulation.* (2015) 131:1590–8. doi: 10.1161/CIRCULATIONAHA.114.015151

frontiers | Frontiers in Cardiovascular Medicine

TYPE Case Report
PUBLISHED 11 November 2022
DOI 10.3389/fcvm.2022.1058341

OPEN ACCESS

EDITED BY
Inga Voges,
University Medical Center
Schleswig-Holstein, Germany

REVIEWED BY
Andreas Brodehl,
Heart and Diabetes Center North
Rhine-Westphalia, Germany
Emanuele Micaglio,
IRCCS San Donato Polyclinic, Italy

*CORRESPONDENCE
Shiwei Yang
jrdoctoryang@163.com

†These authors have contributed
equally to this work

SPECIALTY SECTION
This article was submitted to
Pediatric Cardiology,
a section of the journal
Frontiers in Cardiovascular Medicine

RECEIVED 30 September 2022
ACCEPTED 31 October 2022
PUBLISHED 11 November 2022

CITATION
Ji L, Chen J, Qin Y and Yang S (2022)
Case report: Rare restrictive
cardiomyopathy with ventricular
fibrillation as initial symptom rescued
by automatic external defibrillator in a
pediatric patient.
Front. Cardiovasc. Med. 9:1058341.
doi: 10.3389/fcvm.2022.1058341

Case report: Rare restrictive cardiomyopathy with ventricular fibrillation as initial symptom rescued by automatic external defibrillator in a pediatric patient

Lianfu Ji†, Jinlong Chen†, Yuming Qin and Shiwei Yang*

Department of Cardiology, Children's Hospital of Nanjing Medical University, Nanjing, China

Restrictive cardiomyopathy (RCM) is a rare form of heart muscle disease with poor prognosis. Its primary manifestations were caused by systemic or pulmonary circulation congestion. Here, we reported a case of RCM with ventricular fibrillation as initial symptom in a 7-year-old boy. The child suffered cardiac and respiratory arrest suddenly while exercising at school and immediately was given external chest compression and defibrillation by the school's equipped automatic external defibrillator (AED). The rescue was successful. At the time of the AED discharge, his electrocardiogram (ECG) indicated ventricular fibrillation. Upon further examination, the echocardiogram revealed enlarged bilateral atria, decreased diastolic function and normal ventricular thickness. Genetic analysis identified a heterozygous missense mutation [c.611(exon8)G>A,p.R204H] of *TNNI3* in the proband boy. This case contributes to our understanding of RCM in children and emphasizes the importance of having AEDs available in public places.

KEYWORDS

restrictive cardiomyopathy, ventricular fibrillation, *TNNI3*, AED, constrictive pericarditis

Introduction

Restrictive cardiomyopathy (RCM), a rare type of cardiomyopathy, is characterized by diastolic dysfunction, enlargement of the left atrium or bilateral atria and normal or nearly normal ventricular thickness (1–3). Typically, systolic function is normal or nearly normal, but in advanced stages of RCM, it may decrease (4). The clinical manifestations of RCM which were primarily caused by systemic or pulmonary circulation congestion were non-specific and varied. Pediatric patients with RCM may suffer dyspnea, distended jugular veins, large liver, respiratory rales, ascites, lower limb edema, and even syncope (1, 3). Syncope may be a sign of low cardiac output ischemic, arrhythmias or sudden death (5).

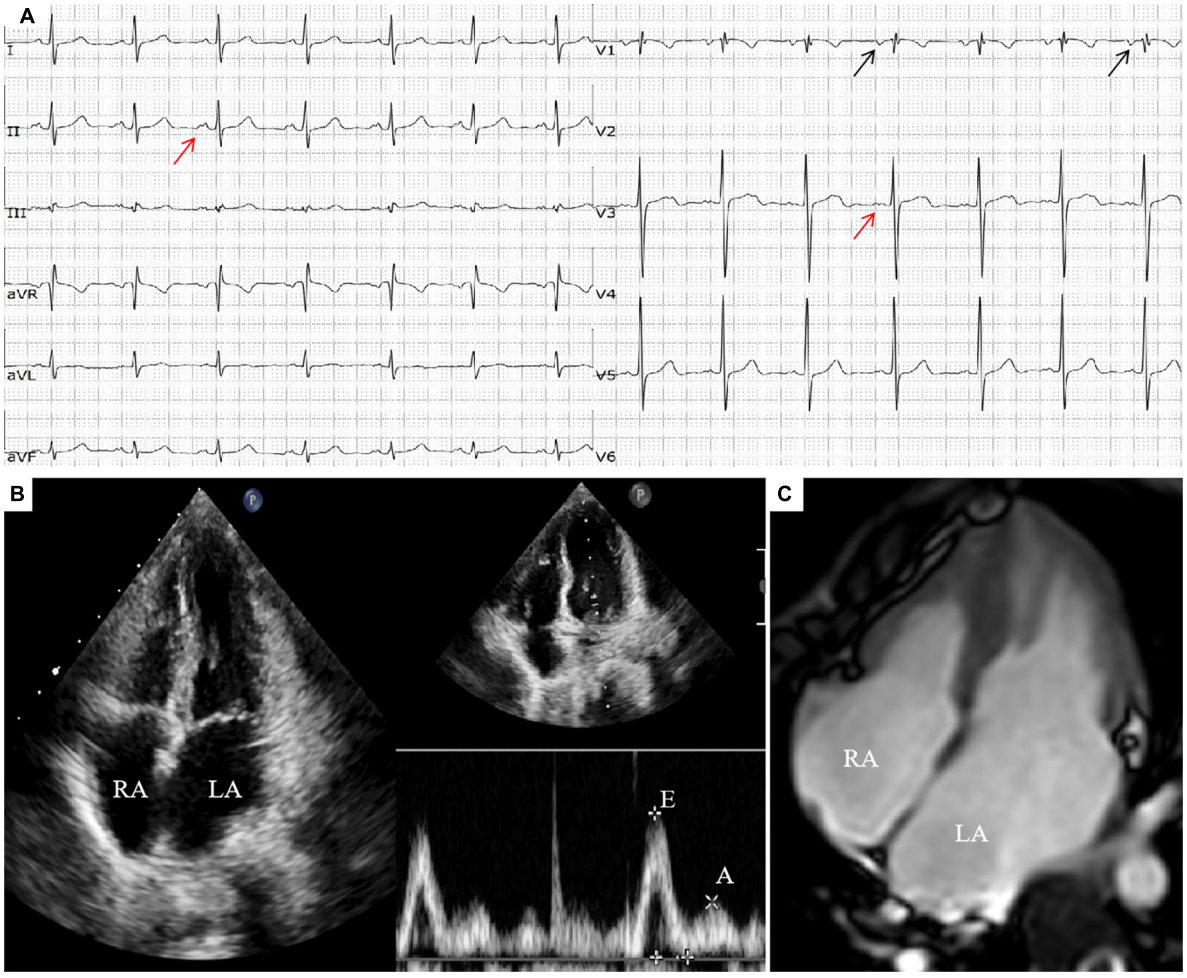

FIGURE 1
(A) ECG showed sinus rhythm, incomplete right bundle branch block, Ptf-V_1 < −0.04 mm·s (the black arrow) and biphasic P waves (the red arrow). **(B)** Echocardiogram showed biatrial enlargement, left atrium obvious (LA: 32 mm, RA: 30 mm) and decreased diastolic function (E/A = 2.6). **(C)** Transverse section of CMR showed biatrial enlargement slightly.

Genetic and non-genetic factors contribute to RCM. Pathogenic mutations in over 19 different genes related to RCM have been identified (6). The major mutations are found in genes encoding for sarcomere proteins, such as cardiac troponins I (*TNNI3*), alpha tropomyosin (*TPM1*), titin (*TTN*), and so on (7). Mutations in non-sarcomeric genes are also relevant, for example in the filamin-C (*FLNC*), αB-crystallin (*CRYAB*), and desmin (*DES*) (8–11). Here we reported a case of RCM with ventricular fibrillation in a 7-year-old boy who was successfully rescued by AED outside the hospital.

Clinical presentation

A 7-year-old boy was admitted to our emergency department after losing consciousness for an hour. The boy suffered a sudden cardiac and respiratory arrest 1 h ago while exercising at school. He was immediately given external chest compression and defibrillation used AED equipped in the school. As a result, his heartbeat and respiration recovered. When the boy was sent to our hospital, he was conscious and agitated which was alleviated by sedation and intracranial pressure reduction. His vital signs were measured: heart rate 124/min; respiratory rate 25/min; blood pressure 102/55 mmHg. On his physical examination, the liver and spleen were not touched under the ribs and there was no edema in the lower limbs. The boy and his parents were in generally good health and other family members denied a history of syncope, sudden death or cardiomyopathy.

There were no obvious abnormalities in the brain MRI and video electroencephalogram (VEEG). The electrocardiogram (ECG) revealed Ptf-V_1 < −0.04 mm·s and biphasic P waves, indicating left atrial enlargement and the chest X-ray revealed an enlarged heart shadow. The echocardiogram showed biatrial

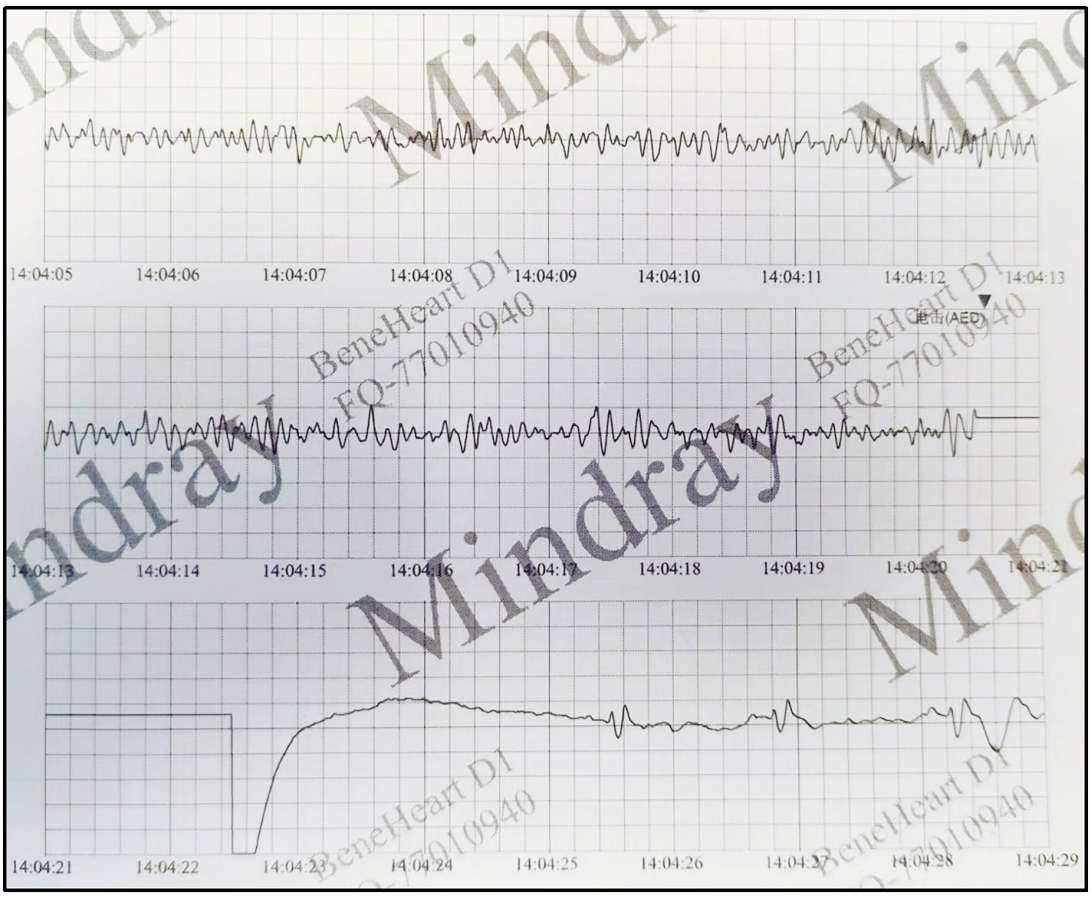

FIGURE 2
The ECG at the time of the AED discharge indicated ventricular fibrillation.

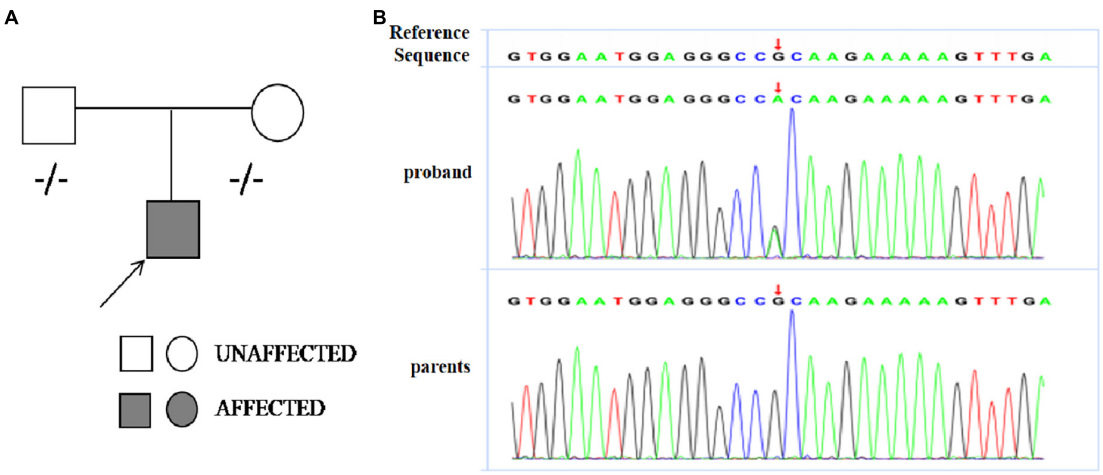

FIGURE 3
(A) Pedigree analysis of the family of patient. The arrow points out the proband. Circles correspond to female. Squares correspond to male. The mutation was indicated −/− if negative. **(B)** Sanger sequencing revealed a heterozygous missense mutation [c.611(exon8)G>A,p.R204H] of *TNNI3* in the proband boy and his parents did not carry the mutation.

enlargement, especially in the left atrium (LA: 32 mm, RA: 30 mm), decreased diastolic function (E/A = 2.6; E Peak deceleration time 130 ms; Constant volume diastolic time 49 ms), moderate mitral valve regurgitation and left ventricular ejection fraction of 51.8%. Except for bilateral enlargement, cardiac magnetic resonance (CMR) indicated no abnormalities (see **Figure 1**). The ECG at the time of the AED discharge indicated ventricular fibrillation (see **Figure 2**). Troponin T and brain natriuretic peptide (BNP) levels were normal.

Genetic analysis revealed the boy had a heterozygous missense mutation [c.611(exon8)G>A,p.R204H] of *TNNI3* which was not detected in his biological parents and *de novo* (see **Figure 3**). This mutation located in exon 19 of *TNNI3* which was conserved. We analyzed the mutation using bioinformatics protein function prediction software PolyPhen_2 and Mutation Taster and found the variant is possibly detrimental. Common genetic mutations in arrhythmias such as *SCN5A*, *KCNH2*, *KCNQ1*, *CACNA1C*, *RYR2*, and *LMNA* (12) were not found in the family members.

According to the results above, we concluded that the boy was a patient of primary RCM. At present, the vital signs of the boy are stable. We communicated with the parents and suggested installing an implantable cardioverter defibrillator (ICD) for the boy, but the parents refused. We have informed his parents that a heart transplant may be required if the disease progresses further. At present, the boy is being treated with oral diuretics and metoprolol tartrate tablets and he is in outpatient follow-up.

Discussion

Restrictive cardiomyopathy (RCM) is the least common phenotype among pediatric heart muscle diseases. Despite accounting for only about 5% of all diagnosed cardiomyopathies, RCM has the worst prognosis. In children, half of all deaths occurred within 2 years after diagnosis and heart transplantation is frequently the only treatment (1, 3).

To confirm the diagnosis of RCM, a series of examinations should be performed in addition to the relevant clinical manifestations. Echocardiography showed left atrial or biatrial enlargement and decreased ventricular diastolic function identified by increased parameters of early diastolic velocity (E wave) and low late filling velocity (A wave), mitral inflow E/A ratio > 2.5 (13). Atrial enlargement and restrictive filling may cause mitral or tricuspid regurgitation. CMR can reflect the changes of cardiac structure and function in children with RCM, and clearly show the extent and scope of lesions. It is a specific and sensitive non-invasive examination method for the diagnosis of RCM at present (14). With the development of molecular genetics, more and more studies have found that genetic factors play an important role in cardiomyopathy (15). *TNNI3* gene is the first gene identified to be associated with RCM. The gene is a conserved sequence of cardiac troponin I gene, whose mutation can affect the function of troponin (16). As research advances, more and more genes related to RCM have been discovered, such as cardiac actin (*ACTC1*), cardiac myosin binding protein C (*MYBPC3*), β-myosin heavy chain (*MYH7*), titin *(TTN*), troponin T (*TNNT2*), filamin-C (*FLNC*), αB-crystallin (*CRYAB*), desmin (*DES*), etc. (7–11, 17–19). In this boy, we found no other variants in genes associated with RCM, except for *TNNI3*.

Restrictive cardiomyopathy must be distinguished from constrictive pericarditis (CP), for they have several similarities in clinical symptoms and hemodynamic changes. In addition, pediatric patients with sudden malignant ventricular arrhythmia, syncope attack, adams-stokes syndrome or sudden cardiac death should be alert to cardiac ion channel disease, such as long Q-T syndrome (LQTS), brugada syndrome, catecholaminergic polymorphic ventricular tachycardia(CPVT), etc. (1, 3). The boy had no history of infection, no pericardial thickening or calcification was observed on CMR and multiple QTc measurements were normal. Combined with the results of echocardiogram, ECG, CMR, and genetic analysis, the diagnosis of primary RCM was clear.

The boy had never felt discomfortable before and his first symptom was ventricular fibrillation which is rare in RCM. Biatrial enlargement and left ventricular stiffness may contribute to the arrhythmias (20). This case not only deepens our understanding of RCM in children, but also highlights the importance of AED placing in public places. Timely defibrillation with an AED was the key to saving his life when the boy suffered a sudden cardiac and respiratory arrest in school. AEDs, also known as "life-saving devices," are portable medical devices that can be used by non-medical personnel to restore the heart rhythm of patients experiencing cardiac arrest or ventricular fibrillation and prevent sudden cardiac death. In recent years, there have been an increasing number of reports about saving lives in airports, schools, and railway stations by AED which reflects the effectiveness of strengthening the installation and training of AED in public places in China.

Data availability statement

The raw data supporting the conclusions of this article will be made available by the authors, without undue reservation.

Ethics statement

The studies involving human participants were reviewed and approved by the Ethics Committee of Children's Hospital Affiliated to Nanjing Medical University. Written informed

consent to participate in this study was provided by the participants' legal guardian/next of kin. Written informed consent was obtained from the minor(s)' legal guardian/next of kin for the publication of any potentially identifiable images or data included in this article.

Author contributions

LJ edited the manuscript. JC contributed to samples collection. YQ and SY revised the manuscript. All authors contributed to the article and approved the submitted version.

Funding

This study was supported by Nanjing Medical Science and Technology Development Fund (YKK19109/ZKX20041/QRX17024), Medical Research Project of Jiangsu Commission of Health (ZD2021058), and Jiangsu Maternal and Child Health Research Project (F202023).

Conflict of interest

The authors declare that the research was conducted in the absence of any commercial or financial relationships that could be construed as a potential conflict of interest.

Publisher's note

All claims expressed in this article are solely those of the authors and do not necessarily represent those of their affiliated organizations, or those of the publisher, the editors and the reviewers. Any product that may be evaluated in this article, or claim that may be made by its manufacturer, is not guaranteed or endorsed by the publisher.

References

1. Chintanaphol M, Orgil BO, Alberson NR, Towbin JA, Purevjav E. Restrictive cardiomyopathy: from genetics and clinical overview to animal modeling. *Rev Cardiovasc Med.* (2022) 23:108. doi: 10.31083/j.rcm2303108

2. Dadson K, Hauck L, Billia F. Molecular mechanisms in cardiomyopathy. *Clin Sci.* (2017) 131:1375–92. doi: 10.1042/cs20160170

3. Ditaranto R, Caponetti AG, Ferrara V, Parisi V, Minnucci M, Chiti C, et al. Pediatric restrictive cardiomyopathies. *Front Pediatr.* (2021) 9:745365. doi: 10.3389/fped.2021.745365

4. Webber SA, Lipshultz SE, Sleeper LA, Lu M, Wilkinson JD, Addonizio LJ, et al. Outcomes of restrictive cardiomyopathy in childhood and the influence of phenotype: a report from the pediatric cardiomyopathy registry. *Circulation.* (2012) 126:1237–44. doi: 10.1161/circulationaha.112.104638

5. Rivenes SM, Kearney DL, Smith EO, Towbin JA, Denfield SW. Sudden death and cardiovascular collapse in children with restrictive cardiomyopathy. *Circulation.* (2000) 102:876–82. doi: 10.1161/01.cir.102.8.876

6. Brodehl A, Gerull B. Genetic insights into primary restrictive cardiomyopathy. *J Clin Med.* (2022) 11:2094. doi: 10.3390/jcm11082094

7. Kaski JP, Syrris P, Burch M, Tomé-Esteban MT, Fenton M, Christiansen M, et al. Idiopathic restrictive cardiomyopathy in children is caused by mutations in cardiac sarcomere protein genes. *Heart.* (2008) 94:1478–84. doi: 10.1136/hrt.2007.134684

8. Brodehl A, Ferrier RA, Hamilton SJ, Greenway SC, Brundler MA, Yu W, et al. Mutations in FLNC are associated with familial restrictive cardiomyopathy. *Hum Mutat.* (2016) 37:269–79. doi: 10.1002/humu.22942

9. Bermúdez-Jiménez FJ, Carriel V, Santos-Mateo JJ, Fernández A, García-Hernández S, Ramos KA, et al. ROD2 domain filamin C missense mutations exhibit a distinctive cardiac phenotype with restrictive/hypertrophic cardiomyopathy and saw-tooth myocardium. *Rev Esp Cardiol.* (2022). [Epub ahead of print]. doi: 10.1016/j.rec.2022.08.002

10. Brodehl A, Gaertner-Rommel A, Klauke B, Grewe SA, Schirmer I, Peterschröder A, et al. The novel αB-crystallin (CRYAB) mutation p.D109G causes restrictive cardiomyopathy. *Hum Mutat.* (2017) 38:947–52. doi: 10.1002/humu.23248

11. Brodehl A, Hain C, Flottmann F, Ratnavadivel S, Gaertner A, Klauke B, et al. The desmin mutation DES-c.735G>C causes severe restrictive cardiomyopathy by inducing in-frame skipping of exon-3. *Biomedicines.* (2021) 9:1400. doi: 10.3390/biomedicines9101400

12. Zhang L, Cheng X, Chen J, Zhou M, Qian T, Zhang Z, et al. left bundle pacing for left bundle branch block and intermittent third-degree atrioventricular block in a MYH7 mutation-related hypertrophic cardiomyopathy with restrictive phenotype in a child. *Front Pediatr.* (2020) 8:312. doi: 10.3389/fped.2020.00312

13. Nagueh SF, Smiseth OA, Appleton CP, Byrd BF III, Dokainish H, Edvardsen T, et al. Recommendations for the evaluation of left ventricular diastolic function by echocardiography: an update from the American society of echocardiography and the European association of cardiovascular imaging. *J Am Soc Echocardiogr.* (2016) 29:277–314. doi: 10.1016/j.echo.2016.01.011

14. Galea N, Polizzi G, Gatti M, Cundari G, Figuera M, Faletti R. Cardiovascular magnetic resonance (CMR) in restrictive cardiomyopathies. *Radiol Med.* (2020) 125:1072–86. doi: 10.1007/s11547-020-01287-8

15. Ware SM, Wilkinson JD, Tariq M, Schubert JA, Sridhar A, Colan SD, et al. Genetic causes of cardiomyopathy in children: first results from the pediatric cardiomyopathy genes study. *J Am Heart Assoc.* (2021) 10:e017731. doi: 10.1161/jaha.120.017731

16. Mogensen J, Kubo T, Duque M, Uribe W, Shaw A, Murphy R, et al. Idiopathic restrictive cardiomyopathy is part of the clinical expression of cardiac troponin I mutations. *J Clin Invest.* (2003) 111:209–16. doi: 10.1172/jci16336

17. Ware SM, Quinn ME, Ballard ET, Miller E, Uzark K, Spicer RL. Pediatric restrictive cardiomyopathy associated with a mutation in beta-myosin heavy chain. *Clin Genet.* (2008) 73:165–70. doi: 10.1111/j.1399-0004.2007.00939.x

18. Peled Y, Gramlich M, Yoskovitz G, Feinberg MS, Afek A, Polak-Charcon S, et al. Titin mutation in familial restrictive cardiomyopathy. *Int J Cardiol.* (2014) 171:24–30. doi: 10.1016/j.ijcard.2013.11.037

19. Ezekian JE, Clippinger SR, Garcia JM, Yang Q, Denfield S, Jeewa A, et al. Variant R94C in TNNT2-encoded troponin T predisposes to pediatric restrictive cardiomyopathy and sudden death through impaired thin filament relaxation resulting in myocardial diastolic dysfunction. *J Am Heart Assoc.* (2020) 9:e015111. doi: 10.1161/jaha.119.015111

20. Pereira NL, Grogan M, Dec GW. Spectrum of restrictive and infiltrative cardiomyopathies: part 1 of a 2-part series. *J Am Coll Cardiol.* (2018) 71:1130–48. doi: 10.1016/j.jacc.2018.01.016

frontiers | Frontiers in Pediatrics

TYPE Case Report
PUBLISHED 21 November 2022
DOI 10.3389/fped.2022.995167

OPEN ACCESS

EDITED BY
Elena Cervi,
Great Ormond Street Hospital for Children NHS Foundation Trust, United Kingdom

REVIEWED BY
Tamas Alexy,
University of Minnesota Twin Cities, United States
Ashraf Hamdan,
Rabin Medical Center, Israel

*CORRESPONDENCE
Joowon Lee
jwlee04@gmail.com

SPECIALTY SECTION
This article was submitted to Pediatric Cardiology, a section of the journal Frontiers in Pediatrics

RECEIVED 15 July 2022
ACCEPTED 03 November 2022
PUBLISHED 21 November 2022

CITATION
Han J, Lee J, Choi S, Lee H and Song YH (2022) Case report: Myocarditis with nonsustained ventricular tachycardia following COVID-19 mRNA vaccination in a female adolescent. Front. Pediatr. 10:995167. doi: 10.3389/fped.2022.995167

Case report: Myocarditis with nonsustained ventricular tachycardia following COVID-19 mRNA vaccination in a female adolescent

Jeongho Han[1], Joowon Lee[2]*, Sujin Choi[2], Hyunju Lee[2,3] and Young Hwan Song[2]

[1]Department of Pediatrics, Seoul National University Children's Hospital, Seoul, South Korea, [2]Department of Pediatrics, Seoul National University Bundang Hospital, Seongnam, South Korea, [3]Department of Pediatrics, Seoul National University College of Medicine, Seoul, South Korea

Children with underlying medical conditions potentially develop severe illness from Coronavirus disease 2019 (COVID-19). The use of vaccines against COVID-19 is currently recommended for the pediatric population. The COVID-19 vaccine has a temporal association with the occurrence of myocarditis. Although most patients with COVID-19 vaccination-associated myocarditis (C-VAM) exhibit a mild clinical course and rapid recovery, C-VAM potentially causes electrical instability and sudden cardiac death. Herein, we report the case of a 17-year-old woman who presented with chest pain and syncope following the first dose of the messenger RNA COVID-19 vaccine. The patient's heart function was impaired, and nonsustained ventricular tachycardia was frequent. Cardiac magnetic resonance (CMR) imaging satisfied the criteria for myocarditis. Despite the administration of immunomodulatory drugs, the patient's heart function was not fully restored, and the concentration of cardiac enzymes remained above the normal range. Persistence of late gadolinium enhancement was observed on short-term follow-up CMR imaging. Although most patients with C-VAM exhibit mild symptoms, significant cardiac arrhythmias potentially occur. Furthermore, some patients with C-VAM demonstrate prolonged impaired heart function and sustained late gadolinium enhancement on follow-up CMR imaging. Therefore, monitoring of electrical and functional cardiac abnormalities in patients with C-VAM is crucial and the long-term outcomes and prognosis of patients with C-VAM require further investigation.

KEYWORDS

adolescent, myocarditis, COVID-19, vaccine, case report

Abbreviations

CMR, Cardiac magnetic resonance; CDC, Centers for Disease Control and Prevention; COVID-19, Coronavirus disease 2019; C-VAM, COVID-19 vaccination-associated myocarditis; EMB, Endomyocardial biopsy; LGE, Late gadolinium enhancement; PCR, Polymerase chain reaction

Introduction

Coronavirus disease 2019 (COVID-19) is a worldwide health problem, as it has reached pandemic level and caused multiple outbreaks globally. Although COVID-19 infection in children is typically asymptomatic or mild, it potentially progresses to severe illness in children with underlying medical conditions (1). Multisystem inflammatory syndrome in children, which is associated with high morbidity and mortality, can develop after COVID-19 infection (2). The use of vaccines against COVID-19 has increased among children and adolescents. Both the Pfizer-BioNTech BNT162b2 and Moderna mRNA-1273 vaccines have exhibited excellent efficacy and safety in the pediatric population (3, 4). The Centers for Disease Control and Prevention (CDC) recommended the use of the vaccine for adolescents aged ≥12

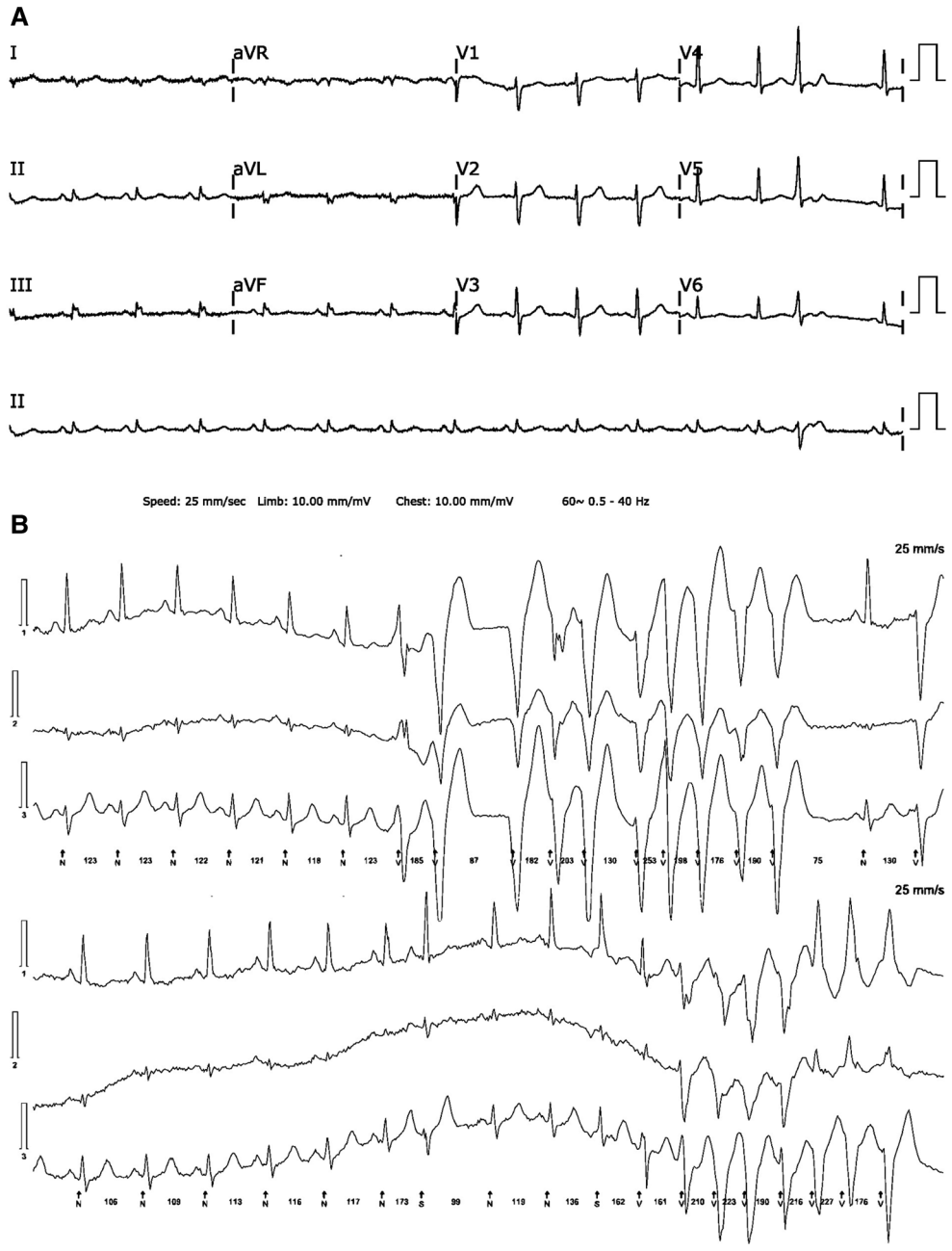

FIGURE 1
(A) A 12-lead electrocardiogram reveals low QRS voltage in limb leads and isolated ventricular premature beat. (B) Ambulatory 24-hour Holter monitoring reveals several runs of nonsustained polymorphic ventricular tachycardia.

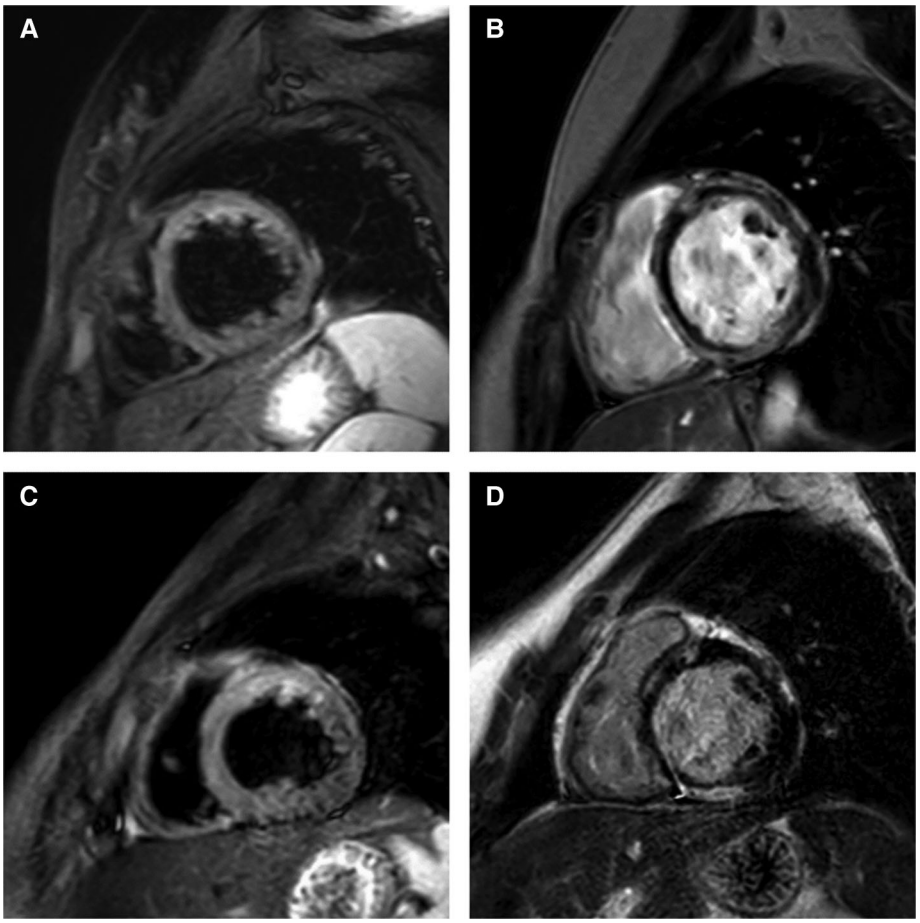

FIGURE 2
Short-axis cardiac magnetic resonance imaging on days 2 (**A**,**B**) and 18 (**C**,**D**) after the patient's presentation. (**A**) High signal intensity in anterior wall of left ventricle on T2-weighted image. (**B**) Diffuse multifocal patchy late gadolinium enhancement (LGE). (**C**) Sustained high signal intensity in anterior wall of left ventricle on T2-weighted image. (**D**) Persistent multifocal patchy LGE.

years on May 12, 2021, and for children aged 5–11 years on November 2, 2021 (5). The Korea Advisory Committee on Immunization Practices also recommended extending the use of the vaccine to persons aged ≥12 years on August 25, 2021.

Myocarditis and pericarditis are complications that potentially occur after COVID-19 vaccination (6–16). In most cases of COVID-19 vaccination-associated myocarditis (C-VAM) after BNT162b2 or mRNA-1273 vaccination, symptoms developed within a few days after the second vaccine dose, and the clinical course usually appeared mild with resolution of symptoms and signs within 1 week. However, fulminant myocarditis and sudden death after vaccination have also been reported (17, 18).

Herein, we describe the case of a 17-year-old woman with myocarditis after the first dose of the BNT162b2 vaccine. This patient, who presented with syncope and experienced several episodes of polymorphic nonsustained ventricular tachycardia, exhibited a chronic clinical course, which is an uncommon finding in other patients with C-VAM.

Case description

A previously healthy 17-year-old woman presented with syncope 7 days after her first BNT162b vaccine dose. The patient was obese, with a body mass index of 26.6 kg/m^2 (above the 95 percentile for their age and sex). Two days after the vaccination, the patient started experiencing generalized malaise, headache, chest pain, and dyspnea on exertion. Three days later, the patient experienced palpitations, and the intensity of her chest pain increased. The patient visited the emergency department of our hospital. The patient's electrocardiogram exhibited low voltage in the limb leads, and her troponin I concentration was within the normal range (0.032 ng/ml; normal: 0–0.045 ng/ml). The patient's symptoms were improved slightly, resulting in her subsequent discharge. The next day, the patient lost consciousness for several minutes while sitting in a restaurant.

The patient's vital signs on arrival were as follows: blood pressure, 102/60 mmHg; heart rate, 92 beats/min; respiratory rate, 19 breaths/min; temperature, 37.7 °C; and oxygen

saturation, 100%. Physical examination revealed no remarkable findings. Neither audible murmurs nor signs of congestion were observed. Laboratory blood tests revealed myocardial injury without systemic inflammation. The level of high-sensitivity cardiac troponin I was 0.072 ng/ml (normal: 0–0.045 ng/ml). The patient's white blood cell count was elevated (10,960/uL; normal: 4,000–10,000/ul), and eosinophilia was absent. The C-reactive protein concentration (<0.40 mg/dl; normal: 0–0.5 mg/dl) and erythrocyte sedimentation rate (17 mm/h; normal: 0–20 mm/h) were not elevated. The patient's nasopharyngeal polymerase chain reaction (PCR) test result was negative for COVID-19. PCR tests for other viruses using nasopharyngeal swabs, blood, and stool samples were negative. Although serum neutralizing antibody titers against adenovirus types 2 and 5 were 1:180 and 1:256, respectively, nasopharyngeal PCR tests were negative for adenovirus.

Electrocardiography revealed low voltage in the limb leads and premature ventricular contraction (**Figure 1**). There was no abnormal finding on the chest radiograph. Transthoracic echocardiography revealed left ventricular dilatation with a reduced ejection fraction of 45.1% (biplane Simpson's method). Ambulatory Holter monitoring exhibited repeated episodes of nonsustained polymorphic ventricular tachycardia. Cardiac magnetic resonance (CMR) imaging 2 days after presentation revealed global left ventricular dysfunction with an ejection fraction of 41%, marked hypokinesia, high T2 values in the apical to mid portion of the anterior wall, and diffuse multifocal patchy late gadolinium enhancement (LGE) (**Figure 2**).

The patient was admitted to the intensive care unit for the monitoring of hemodynamic and electrical instability and treated with 1 g/kg of intravenous immunoglobulin for two consecutive days as well as 2 mg/kg/day of intravenous methylprednisolone. Ibuprofen use was discontinued after severe myocardial inflammation was identified using CMR imaging. The patient was administered intravenous milrinone and furosemide for a brief period in consideration of the possibility of progressive deterioration of hemodynamic status. Therapy with an angiotensin-converting enzyme inhibitor and beta blocker was initiated after discontinuation of intravenous milrinone.

The troponin I concentration peaked 2 days after presentation (0.689 ng/ml); subsequently, it gradually declined and reached its nadir 9 days after presentation (0.153 ng/ml). Thereafter, it resumed its rising trend, and the patient was administered 1 g/kg of pulsed methylprednisolone therapy for three consecutive days, followed by a planned oral prednisolone taper. CMR imaging 18 days after presentation continued to demonstrate high T2 values in the apical to mid portion of the anterior wall and a slightly decreased extent of diffuse multifocal patchy LGE. A right ventricular endomyocardial biopsy was performed to exclude other etiologies of myocarditis, including giant cell myocarditis. Histological examination of the biopsy specimen revealed focal myocardial degeneration and interstitial edema without significant inflammatory cell infiltration. The patient was discharged 31 days after presentation due to the reduced burden of ventricular tachycardia, improved symptoms, and partial recovery of ventricular function.

Nine days later, the patient was re-hospitalized for *Campylobacter* colitis and treated with intravenous antibiotics, a stress dose of intravenous hydrocortisone, and an intravenous vasopressor during hospitalization. On follow-up 1 month later, a repeat echocardiography revealed left ventricular dilatation with a reduced ejection fraction of 49.1% (biplane Simpson's method), and the troponin I concentration remained above the normal range (0.137 ng/ml). Follow-up CMR imaging was scheduled two months after hospital discharge (**Table 1**).

TABLE 1 Timeline of case.

Time	Event
October 18, 2021	First dose of BNT162b vaccine
October 20, 2021	Generalized malaise, headache, chest pain, dyspnea on exertion
October 23, 2021	Palpitation, increased intensity of chest pain
October 24, 2021	The patients visited the emergency department of our hospital Low voltage in the limb leads on electrocardiogram Troponin I level 0.032 ng/ml (normal: 0–0.045 ng/ml)
October 25, 2021	Loss of consciousness for several minutes
October 26, 2021	The patient was admitted to the intensive care unit Echocardiography revealed left ventricular dilatation and dysfunction Holter monitoring showed nonsustained polymorphic ventricular tachycardia 1 g/kg IVIG for two consecutive days, 2 mg/kg methylprednisolone, intravenous milrinone
October 27, 2021	CMR imaging findings satisfied with criteria for myocarditis ACE inhibitor and beta blocker initiated after discontinuation of milrinone
November 3, 2021	Troponin I level 0.153 ng/ml (nadir)
November 10, 2021	1 g/kg of pulsed methylprednisolone therapy for three consecutive days because of increased cardia
November 12, 2021	CMR imaging showed persistent late gadolinium enhancement
November 18, 2021	Endomyocardial biopsy showed focal myocardial degeneration and interstitial edema
November 25, 2021	Discharge
December 4–7, 2021	Re-hospitalized for *Campylobacter* colitis and treated with intravenous antibiotics, a stress dose of intravenous hydrocortisone, and an intravenous vasopressor
December 24, 2021	Echocardiography revealed sustained left ventricular dysfunction Troponin I level 0.137 ng/ml

IVIG, Intravenous immunoglobulin; CMR, Cardiac Magnetic Resonance; ACE, Angiotensin-converting enzyme.

TABLE 2 Case series and retrospective studies of coronavirus disease 2019 vaccination-associated myocarditis and myopericarditis in children.

Study	Truong	Jain	Chua[a]	Das[b]	Schauer[c]	Dionne	Nygaard[d]	Tano[e]	Marshall	Snapiri	Puchalski
Reference	(16)	(9)	(6)	(7)	(13)	(8)	(11)	(15)	(10)	(14)	(12)
Cases, *n*	139	63	33	25	16	15	12	8	7	7	5
Company											
BNT162b2	131	59	33	25	16	15	12	8	7	7	5
mRNA-1273	5	4									
JNJ-78436735	1										
Unknown	2										
Age, y	15.8 (12.1–20.3)	15.6 ± 1.8	15.2 (12.7–17.8)	15 (12–17)	15 (12–17)	15 (12–18)	16 (13–17)	16.7 (15.2–17.9)	17 (14–19)	16.8 (16.2–17.6)	17 (15–17)
Male Sex, *n* (%)	126 (91)	58 (92)	28 (85)	22 (88)	15 (94)	14 (93)	10 (83)	8 (100)	7 (100)	7 (100)	5 (100)
Patients presenting after second vaccination, *n* (%)	128 (92)	62 (98)	27 (82)	22 (88)	16 (100)	14 (93)	6 (50)	7 (88)	7 (100)	6 (86)	2 (40)
Time between symptom onset and last vaccine, *d*	2 (0–22)	2.1 ± 1.3	2 (1–26)	2 (0–20)	3 (2–4)	3 (1–6)	4 (1–39)	2.5 (1–4)	2 (2–4)	2 (1–3)	2 (2–23)
Chest pain, *n* (%)	138 (99)	63 (100)	32 (97)	25 (100)	16 (100)	15 (100)	12 (100)	8 (100)	7 (100)	7 (100)	5 (100)
Fever, *n* (%)	43 (31)	28 (44)	9 (27)	6 (24)	6 (37.5)	10 (67)	N/A	1 (12.5)	5 (71)	1 (14.3)	4 (80)
Elevated troponin level, *n* (%)	139 (100)	63 (100)	32 (97)	25 (100)	16 (100)	15 (100)	12 (100)	8 (100)	7 (100)	7 (100)	5 (100)
Reduced left ventricular ejection fraction, *n* (%)	26 (19)	9 (14)	0	2 (8)	2 (2)	3 (20)	3 (25)	0	1 (14)	0	0
Ventricular tachycardia, *n* (%)	7 (5)	3 (5)	0	3 (12)	N/A	1 (7)	N/A	2 (25)	0	0	0
Complete atrioventricular block, *n* (%)	1 (1)	1 (2)	0	0	N/A	0	N/A	0	0	0	0
Cardiac magnetic resonance, *n*	97	56	32	16	16	15	10	3	7	0	5
Late gadolinum enhancement, *n* (%)	74 (76)	49 (88)	18 (56)	15 (94)	15 (94)	12 (80)	N/A	3 (100)	7 (100)		5 (100)
Hospital stay, *d*	2 (0–10)	3.0 ± 1.4	N/A	3 (2–7)	2 (1–4)	2 (1–5)	4 (3–10)	56.5 (34–95) h	4 (2–6)	5 (3–6)	12 (10–16)
Intensive care unit admission, *n* (%)	26 (19)	27 (43)	0	0	0	0	1 (8)	0	0	4	0
Inotropic/vasoactive support, *n* (%)	2 (1)	0	0	0	0	0	N/A	0	0	0	0
Mechanical circulatory support, *n* (%)	0	0	0	0	0	0	N/A	0	0	0	0
Intravenous immunoglobulin, *n* (%)	30 (22)	17 (27)	0	2 (8)	3 (19)	7 (47)	1 (8)	1 (13)	4 (57)	0	0
Steroid, *n* (%)	30 (22)	15 (24)	0	1 (4)	2 (13)	7 (47)	1 (8)	2 (25)	4 (57)	0	0
Death	0	0	0	0	0	0	0	0	0	0	0

Data are presented as number (%), median (range), or mean ± standard deviation.
N/A; Not applicable.
[a]Two patients with definite pericarditis were excluded and two patients presented >14 days after vaccination were included.
[b]Three patients did not require hospitalization.
[c]This study only included patients with myocarditis following the second dose of the BNT162b2 vaccine.
[d]Three patients with pericarditis were excluded.
[e]One patient was diagnosed with perimyocarditis after the first and second dose of the BNT162b2 vaccine, respectively.

10.3389/fped.2022.995167

Discussion

The patient in this report, who developed myocarditis after the first BNT162b vaccine dose, presented with syncope. Since her ventricular function was impaired, and nonsustained ventricular tachycardia was frequent, the patient required electrical and hemodynamic monitoring in the intensive care unit. The patient's cardiac function did not fully recover, with the persistence of elevated cardiac enzymes and residual LGE on CMR imaging.

A large proportion of patients with myocarditis have experienced cardiac arrhythmia at any stage of the disease. The most serious types of arrhythmias have been ventricular tachycardia and ventricular fibrillation. Ventricular arrhythmia has been associated with poor patient outcomes, including the use of mechanical circulatory support and death (19, 20). This arrhythmia potentially manifests as cardiopulmonary arrest and sudden cardiac death. Therefore, current guidelines recommend mandatory close monitoring of cardiovascular status (including heart rhythm) in the early phase in the management of patients with myocarditis (21, 22). Although no deaths have been attributed to arrhythmia in patients with C-VAM, some patients had nonsustained ventricular tachycardia (**Table 2**) (7–9, 15, 16). Moreover, a case of sudden cardiac death due to C-VAM have been reported (18). Therefore, electrical monitoring is crucial in the management of pediatric patients with C-VAM.

Although endomyocardial biopsy (EMB) is the gold standard for the diagnosis of myocarditis, CMR imaging is currently adopted for the confirmation of myocarditis (21). The CMR imaging findings of the patient in this report satisfied the updated Lake Louise criteria, and the patient's condition was consistent with the CDC's definition of confirmed myocarditis. However, the EMB results did not reveal significant inflammatory cell infiltration. These findings possibly resulted from sampling errors associated with the focal distribution of inflammatory infiltrates. The sites of inflammatory infiltrates were sometimes inaccessible to the bioptomes. The false negative rates of EMB were 45% for the left ventricle and 37% for the right ventricle in 38 autopsied hearts with lymphocytic myocarditis (23). The sampling error also occurred due to difference between biopsy sites and involved regions on CMR imaging (24). The biopsy site was usually the right ventricle, while CMR imaging demonstrated predominant left ventricular involvement.

A few case reports and case series showed the histopathologic findings in C-VAM (18, 25–30). The marked inflammatory infiltrates with a predominance of T-cells and macrophages, occasionally admixed with eosinophils, B cells, and plasma cells, and multifocal cardiomyocyte damages were demonstrated in patients with C-VAM (27–30). The autopsied heart with sudden death after COVID-19 vaccination revealed diffuse inflammatory infiltrates predominantly composed of macrophages and neutrophils and the existence of contraction band necrosis (18, 26). However, similar to the findings of the patient in this report, the results of endomyocardial biopsy in patients with C-VAM occasionally demonstrated no inflammatory infiltrates or findings incompatible with classic histopathologic criteria of myocarditis (25, 30–32).

The heart function of the patient in this report was persistently impaired, and LGE was sustained on short-term follow-up CMR imaging. LGE was an independent predictor of mortality and major adverse cardiac events in adult patients with myocarditis (33, 34). The midwall septal pattern of LGE has been associated with late progressive deterioration of left ventricular function (35). Recent studies investigating changes in CMR imaging findings in patients with C-VAM have demonstrated sustained and decreased LGE on follow-up CMR imaging (13, 36, 37). Persistent LGE was observed in a considerable proportion of adult and pediatric patients with myocarditis on follow-up CMR imaging at 3–6 months, even after normalization of inflammatory and cardiac markers (38, 39). Although LGE without edema at 6-month follow-up CMR imaging was associated with a worse outcome in adult patients with acute myocarditis, the clinical significance of LGE and longitudinal changes in heart function in C-VAM require further investigation (40).

Conclusion

We described an adolescent woman with myocarditis after BNT162b2 mRNA vaccination, who exhibited frequent episodes of nonsustained ventricular tachycardia and persistent left ventricular dysfunction with sustained LGE. Monitoring the electrical and functional cardiac abnormalities in patients with C-VAM is crucial. Further studies focusing on the long-term outcomes and prognosis of patients with C-VAM are warranted.

Data availability statement

The original contributions presented in the study are included in the article, further inquiries can be directed to the corresponding author.

Ethics statement

This report was reviewed and approved by the Institutional Review Board of Seoul National University Bundang Hospital (IRB No. B-2205-757-701). The requirement for informed consent was waived.

Author contributions

JL and YS contributed to the formation of the research idea. JH and JL collected data and wrote the original draft. JH, JL, SC, HL, and YS participated in patient care, and contributed to manuscript review and editing. All authors contributed to the article and approved the submitted version.

Conflict of interest

The authors declare that the research was conducted in the absence of any commercial or financial relationships that could be construed as a potential conflict of interest.

Publisher's note

All claims expressed in this article are solely those of the authors and do not necessarily represent those of their affiliated organizations, or those of the publisher, the editors and the reviewers. Any product that may be evaluated in this article, or claim that may be made by its manufacturer, is not guaranteed or endorsed by the publisher.

References

1. Preston LE, Chevinsky JR, Kompaniyets L, Lavery AM, Kimball A, Boehmer TK, et al. Characteristics and disease severity of US children and adolescents diagnosed with COVID-19. *JAMA Netw Open*. (2021) 4(4):e215298. doi: 10.1001/jamanetworkopen.2021.5298

2. Son MBF, Murray N, Friedman K, Young CC, Newhams MM, Feldstein LR, et al. Multisystem inflammatory syndrome in children—initial therapy and outcomes. *N Engl J Med*. (2021) 385(1):23–34. doi: 10.1056/NEJMoa2102605

3. Creech CB, Anderson E, Berthaud V, Yildirim I, Atz AM, Melendez Baez I, et al. Evaluation of mRNA-1273 COVID-19 vaccine in children 6 to 11 years of age. *N Engl J Med*. (2022) 386(21):2011–23. doi: 10.1056/NEJMoa2203315

4. Walter EB, Talaat KR, Sabharwal C, Gurtman A, Lockhart S, Paulsen GC, et al. Evaluation of the BNT162b2 COVID-19 vaccine in children 5 to 11 years of age. *N Engl J Med*. (2022) 386(1):35–46. doi: 10.1056/NEJMoa2116298

5. Woodworth KR, Moulia D, Collins JP, Hadler SC, Jones JM, Reddy SC, et al. The advisory committee on immunization practices' interim recommendation for use of pfizer-BioNTech COVID-19 vaccine in children aged 5–11 years—United States, november 2021. *MMWR Morb Mortal Wkly Rep*. (2021) 70(45):1579–83. doi: 10.15585/mmwr.mm7045e1

6. Chua GT, Kwan MYW, Chui CSL, Smith RD, Cheung EC, Tian T, et al. Epidemiology of acute myocarditis/pericarditis in Hong Kong adolescents following comirnaty vaccination. *Clin Infect Dis*. (2022) 75(4):673–81. doi: 10.1093/cid/ciab989

7. Das BB, Kohli U, Ramachandran P, Nguyen HH, Greil G, Hussain T, et al. Myopericarditis after messenger RNA coronavirus disease 2019 vaccination in adolescents 12 to 18 years of age. *J Pediatr*. (2021) 238:26–32.e1. doi: 10.1016/j.jpeds.2021.07.044

8. Dionne A, Sperotto F, Chamberlain S, Baker AL, Powell AJ, Prakash A, et al. Association of myocarditis with BNT162b2 messenger RNA COVID-19 vaccine in a case series of children. *JAMA Cardiol*. (2021) 6(12):1446–50. doi: 10.1001/jamacardio.2021.3471

9. Jain SS, Steele JM, Fonseca B, Huang S, Shah S, Maskatia SA, et al. COVID-19 vaccination-associated myocarditis in adolescents. *Pediatrics*. (2021) 148(5):e2021053427. doi: 10.1542/peds.2021-053427

10. Marshall M, Ferguson ID, Lewis P, Jaggi P, Gagliardo C, Collins JS, et al. Symptomatic acute myocarditis in 7 adolescents after pfizer-BioNTech COVID-19 vaccination. *Pediatrics*. (2021) 148(3):e2021052478. doi: 10.1542/peds.2021-052478

11. Nygaard U, Holm M, Bohnstedt C, Chai Q, Schmidt LS, Hartling UB, et al. Population-based incidence of myopericarditis after COVID-19 vaccination in danish adolescents. *Pediatr Infect Dis J*. (2022) 41(1):e25–e8. doi: 10.1097/INF.0000000000003389

12. Puchalski M, Kaminska H, Bartoszek M, Brzewski M, Werner B. COVID-19-vaccination-induced myocarditis in teenagers: case series with further follow-up. *Int J Environ Res Public Health*. (2022) 19(6):3456. doi: 10.3390/ijerph19063456

13. Schauer J, Buddhe S, Gulhane A, Sagiv E, Studer M, Colyer J, et al. Persistent cardiac magnetic resonance imaging findings in a cohort of adolescents with post-coronavirus disease 2019 mRNA vaccine myopericarditis. *J Pediatr*. (2022) 245:233–7. doi: 10.1016/j.jpeds.2022.03.032

14. Snapiri O, Rosenberg Danziger C, Shirman N, Weissbach A, Lowenthal A, Ayalon I, et al. Transient cardiac injury in adolescents receiving the BNT162b2 mRNA COVID-19 vaccine. *Pediatr Infect Dis J*. (2021) 40(10):e360–e3. doi: 10.1097/INF.0000000000003235

15. Tano E, San Martin S, Girgis S, Martinez-Fernandez Y, Sanchez Vegas C. Perimyocarditis in adolescents after pfizer-BioNTech COVID-19 vaccine. *J Pediatric Infect Dis Soc*. (2021) 10(10):962–6. doi: 10.1093/jpids/piab060

16. Truong DT, Dionne A, Muniz JC, McHugh KE, Portman MA, Lambert LM, et al. Clinically suspected myocarditis temporally related to COVID-19 vaccination in adolescents and young adults: suspected myocarditis after COVID-19 vaccination. *Circulation*. (2022) 145(5):345–56. doi: 10.1161/CIRCULATIONAHA.121.056583

17. Abbate A, Gavin J, Madanchi N, Kim C, Shah PR, Klein K, et al. Fulminant myocarditis and systemic hyperinflammation temporally associated with BNT162b2 mRNA COVID-19 vaccination in two patients. *Int J Cardiol*. (2021) 340:119–21. doi: 10.1016/j.ijcard.2021.08.018

18. Choi S, Lee S, Seo JW, Kim MJ, Jeon YH, Park JH, et al. Myocarditis-induced sudden death after BNT162b2 mRNA COVID-19 vaccination in Korea: case report focusing on histopathological findings. *J Korean Med Sci*. (2021) 36(40):e286. doi: 10.3346/jkms.2021.36.e286

19. Miyake CY, Teele SA, Chen L, Motonaga KS, Dubin AM, Balasubramanian S, et al. In-hospital arrhythmia development and outcomes in pediatric patients with acute myocarditis. *Am J Cardiol*. (2014) 113(3):535–40. doi: 10.1016/j.amjcard.2013.10.021

20. Othman HF, Byrnes J, Elsamny E, Hamzah M. Impact of ventricular arrhythmias on outcomes in children with myocarditis. *Eur J Pediatr*. (2020) 179(11):1779–86. doi: 10.1007/s00431-020-03687-4

21. Law YM, Lal AK, Chen S, Cihakova D, Cooper Jr. LT, Deshpande S, et al. Diagnosis and management of myocarditis in children: a scientific statement from the American heart association. *Circulation*. (2021) 144(6):e123–e35. doi: 10.1161/CIR.0000000000001001

22. Kociol RD, Cooper LT, Fang JC, Moslehi JJ, Pang PS, Sabe MA, et al. Recognition and initial management of fulminant myocarditis: a scientific statement from the American heart association. *Circulation*. (2020) 141(6):e69–92. doi: 10.1161/CIR.0000000000000745

23. Hauck AJ, Kearney DL, Edwards WD. Evaluation of postmortem endomyocardial biopsy specimens from 38 patients with lymphocytic myocarditis: implications for role of sampling error. *Mayo Clin Proc*. (1989) 64(10):1235–45. doi: 10.1016/S0025-6196(12)61286-5

24. Chow LH, Radio SJ, Sears TD, McManus BM. Insensitivity of right ventricular endomyocardial biopsy in the diagnosis of myocarditis. *J Am Coll Cardiol*. (1989) 14(4):915–20. doi: 10.1016/0735-1097(89)90465-8

25. Amemiya K, Kobayashi T, Kataoka Y, Iwai T, Nakagawa S, Morita Y, et al. Myocarditis after COVID-19 mRNA vaccination in three young adult males:

significance of biopsy in vaccine-associated myocarditis. *Pathol Int*. (2022) 72 (7):385–7. doi: 10.1111/pin.13234

26. Gill JR, Tashjian R, Duncanson E. Autopsy histopathologic cardiac findings in 2 adolescents following the second COVID-19 vaccine dose. *Arch Pathol Lab Med*. (2022) 146(8):925–9. doi: 10.5858/arpa.2021-0435-SA

27. Kazama S, Okumura T, Kimura Y, Ito R, Araki T, Mizutani T, et al. Biopsy-proven fulminant myocarditis requiring mechanical circulatory support following COVID-19 mRNA vaccination. *CJC Open*. (2022) 4(5):501–5. doi: 10.1016/j.cjco.2022.02.004

28. Lim Y, Kim MC, Kim KH, Jeong IS, Cho YS, Choi YD, et al. Case report: acute fulminant myocarditis and cardiogenic shock after messenger RNA coronavirus disease 2019 vaccination requiring extracorporeal cardiopulmonary resuscitation. *Front Cardiovasc Med*. (2021) 8:758996. doi: 10.3389/fcvm.2021.758996

29. Verma AK, Lavine KJ, Lin CY. Myocarditis after COVID-19 mRNA vaccination. *N Engl J Med*. (2021) 385(14):1332–4. doi: 10.1056/NEJMc2109975

30. Yamamoto M, Tajiri K, Ayuzawa S, Ieda M. Pathological findings of clinically suspected myocarditis temporally associated with COVID-19 vaccination. *Eur J Heart Fail*. (2022) 24(6):1132–8. doi: 10.1002/ejhf.2523

31. Larson KF, Ammirati E, Adler ED, Cooper Jr. LT, Hong KN, Saponara G, et al. Myocarditis after BNT162b2 and mRNA-1273 vaccination. *Circulation*. (2021) 144(6):506–8. doi: 10.1161/CIRCULATIONAHA.121.055913

32. Rosner CM, Genovese L, Tehrani BN, Atkins M, Bakhshi H, Chaudhri S, et al. Myocarditis temporally associated with COVID-19 vaccination. *Circulation*. (2021) 144(6):502–5. doi: 10.1161/CIRCULATIONAHA.121.055891

33. Grun S, Schumm J, Greulich S, Wagner A, Schneider S, Bruder O, et al. Long-term follow-up of biopsy-proven viral myocarditis: predictors of mortality and incomplete recovery. *J Am Coll Cardiol*. (2012) 59(18):1604–15. doi: 10.1016/j.jacc.2012.01.007

34. Grani C, Eichhorn C, Biere L, Murthy VL, Agarwal V, Kaneko K, et al. Prognostic value of cardiac magnetic resonance tissue characterization in risk stratifying patients with suspected myocarditis. *J Am Coll Cardiol*. (2017) 70 (16):1964–76. doi: 10.1016/j.jacc.2017.08.050

35. Aquaro GD, Perfetti M, Camastra G, Monti L, Dellegrottaglie S, Moro C, et al. Cardiac MR with late gadolinium enhancement in acute myocarditis with preserved systolic function: ITAMY study. *J Am Coll Cardiol*. (2017) 70 (16):1977–87. doi: 10.1016/j.jacc.2017.08.044

36. Amir G, Rotstein A, Razon Y, Beyersdorf GB, Barak-Corren Y, Godfrey ME, et al. CMR imaging 6 months after myocarditis associated with the BNT162b2 mRNA COVID-19 vaccine. *Pediatr Cardiol*. (2022) 43(7):1522–29. doi: 10.1007/s00246-022-02878-0

37. Hadley SM, Prakash A, Baker AL, de Ferranti SD, Newburger JW, Friedman KG, et al. Follow-up cardiac magnetic resonance in children with vaccine-associated myocarditis. *Eur J Pediatr*. (2022) 181(7):2879–83. doi: 10.1007/s00431-022-04482-z

38. Berg J, Kottwitz J, Baltensperger N, Kissel CK, Lovrinovic M, Mehra T, et al. Cardiac magnetic resonance imaging in myocarditis reveals persistent disease activity despite normalization of cardiac enzymes and inflammatory parameters at 3-month follow-up. *Circ Heart Fail*. (2017) 10(11):e004262. doi: 10.1161/CIRCHEARTFAILURE.117.004262

39. Dubey S, Agarwal A, Nguyen S, Adebo D. Persistence of late gadolinium enhancement on follow-up CMR imaging in children with acute myocarditis. *Pediatr Cardiol*. (2020) 41(8):1777–82. doi: 10.1007/s00246-020-02445-5

40. Aquaro GD, Ghebru Habtemicael Y, Camastra G, Monti L, Dellegrottaglie S, Moro C, et al. Prognostic value of repeating cardiac magnetic resonance in patients with acute myocarditis. *J Am Coll Cardiol*. (2019) 74(20):2439–48. doi: 10.1016/j.jacc.2019.08.1061

frontiers | Frontiers in Pediatrics

TYPE Case Report
PUBLISHED 23 November 2022
DOI 10.3389/fped.2022.1012600

OPEN ACCESS

EDITED BY
Cecile Tissot,
Clinique des Grangettes, Switzerland

REVIEWED BY
Edward George Jones,
Baylor College of Medicine, United States
Shiwei Yang,
Children's Hospital of Nanjing Medical University, China

*CORRESPONDENCE
Jiao Chen
chenjiao@scu.edu.cn

†These authors have contributed equally to this work and share first authorship

SPECIALTY SECTION
This article was submitted to Pediatric Cardiology, a section of the journal Frontiers in Pediatrics

RECEIVED 05 August 2022
ACCEPTED 24 October 2022
PUBLISHED 23 November 2022

CITATION
Zhang W, Dai X, Liu H, Li L, Zhou S, Zhu Q and Chen J (2022) Case report: Prenatal diagnosis of fetal non-compaction cardiomyopathy with bradycardia accompanied by *de novo CALM2* mutation.
Front. Pediatr. 10:1012600.
doi: 10.3389/fped.2022.1012600

Case report: Prenatal diagnosis of fetal non-compaction cardiomyopathy with bradycardia accompanied by *de novo CALM2* mutation

Wen Zhang[1,2†], Xiaohui Dai[1,2†], Hanmin Liu[2,3], Lei Li[2,4], Shu Zhou[2,5], Qi Zhu[1,2] and Jiao Chen[1,2*]

[1]Department of Ultrasonic Medicine, West China Second University Hospital of Sichuan University, Chengdu, China, [2]Key Laboratory of Birth Defects and Related Diseases of Women and Children, Ministry of Education, Sichuan University, Chengdu, China, [3]Department of Pediatrics, West China Second University Hospital of Sichuan University, Chengdu, China, [4]Department of Pathology, West China Second University Hospital of Sichuan University, Chengdu, China, [5]Department of Obstetrics, West China Second University Hospital of Sichuan University, Chengdu, China

We herein report what appears to be the first case of fetal non-compaction cardiomyopathy in both ventricles accompanied by a mutation in the calmodulin gene (*CALM2*). A 25-year-old woman was referred to our hospital at 25^{+1} weeks of gestation for evaluation of fetal defects. Prenatal echocardiography showed biventricular non-compaction cardiomyopathy with sinus bradycardia. After termination of the pregnancy, fetal biventricular non-compaction cardiomyopathy was confirmed by autopsy and histopathologic examination. Additionally, whole-exome sequencing of genomic DNA demonstrated a *de novo* heterozygous mutation (c.389A > G; p.D130G) in *CALM2*, whereas the parents were normal. In this case report, we highlight the importance of prenatal ultrasound and genetic testing in fetal non-compaction cardiomyopathy with arrhythmia.

KEYWORDS

prenatal, ultrasound, non-compaction cardiomyopathy, bradycardia, CALM2 mutation

Introduction

Non-compaction cardiomyopathy (NCCM) is a rare disorder that frequently manifests as monogenic diseases, especially neuromuscular disorders and chromosomal defects, and it was first reported on autopsy in 1969 (1). The incidence of NCCM in the general population ranges from 0.05% to 0.25%, whereas the incidence in children may reach 9.2% (2). NCCM is characterized by increased numbers of prominent trabeculations and deep intertrabecular spaces. Additionally, NCCM combined with arrhythmia has been rarely reported during the prenatal period. With the development of medical imaging techniques, the detection rate of NCCM has increased. Prenatal ultrasound is the primary and most convenient modality and can be used to recognize fetal arrhythmias. Thus, it is possible to identify NCCM with arrhythmia as early as the fetal period. As a rare genetic cardiomyopathy, NCCM is regulated by various genes that are

involved in encoding ion channels, sarcomeres, and chaperone proteins. The related ion channel genes mainly include *SCN5A*, *RYR2*, *KCNQ1*, and *HCN4* (3). However, involvement of the calmodulin gene (*CALM2*) in fetal NCCM has been rarely reported. *CALM2* is a Ca^{2+}-signaling gene that encodes for calmodulin, which is a multifunctional Ca^{2+}-binding protein (4). Calmodulin is also an important calcium-sensitive signal transduction protein involved in regulating almost every cardiac ion channel through calcium/calmodulin-dependent protein kinase II (5, 6), and calmodulin may simultaneously contribute to cardiomyopathy and arrhythmia. We herein present the first case of fetal NCCM in both ventricles combined with sinus bradycardia and *CALM2* mutation at 25^{+1} weeks of gestation.

Case description

A 25-year-old woman (gravida 1, para 0) was referred to our hospital at 25^{+1} weeks of gestation for evaluation of fetal defects. The patient was allergic to penicillin. Both parents were healthy, and there was no family history of birth defects or exposure to any specific teratogenic agents. A prenatal two-dimensional ultrasonographic investigation (3.0–5.0 MHz) (Voluson E10; GE Healthcare, Chicago, IL, United States) showed dilated ventricles (*Z*-score of left ventricular end-diastolic dimension: 2.51, Z-score of right ventricular end-diastolic dimension: 2.32), an increased cardiac area/thoracic area ratio (0.56), slight pericardial effusion, and extensive trabeculations in both ventricles. We found that in the left ventricle, the compacted layer became thinner (2 mm) and the non-compacted layer became thicker (6 mm), and in the right ventricle, the compacted layer became thinner (1.5 mm) and the intertrabecular space reached deeply into the epicardium. The ratio of non-compacted to compacted myocardium (N/C ratio) in the left and right ventricle was 3 and 2, respectively (**Figure 1A**). Color Doppler revealed blood perfusion to the intertrabecular recesses (**Figure 1B**). The heart rate was 101 bpm, and the atrioventricular (AV) interval was 133 ms. Therefore, the prenatal ultrasound diagnosis was biventricular NCCM with sinus bradycardia and pericardial effusion. Two weeks later, the fetal heart showed no significant improvement. The parents opted for pregnancy termination at 28 weeks' gestation after prenatal counseling, and heart autopsy and whole-exome sequencing (WES) were performed after obtaining the parents' informed consent. At autopsy, the biventricular wall contained increased numbers of prominent trabeculae and deep intertrabecular recesses (**Figure 2**). Histopathologic examination confirmed fetal NCCM (**Figure 3**). Genomic DNA was extracted from the muscle of the fetus to perform WES. The result demonstrated a *de novo* heterozygous mutation (c.389A > G; p. D130G) in *CALM2* (**Figure 4**). According to the current American College of Medical Genetics guidelines, the *CALM2* mutation was preliminarily determined to be the pathogenic variant (PS2 + PS4 + PM1 + PM2 + PM5 + PP3). The filtering cascades for the WES data of other variant genes are listed in **Supplementary Table S1**. The sequencing results of the parents were normal. The *CALM2* variant was not found in either the largest

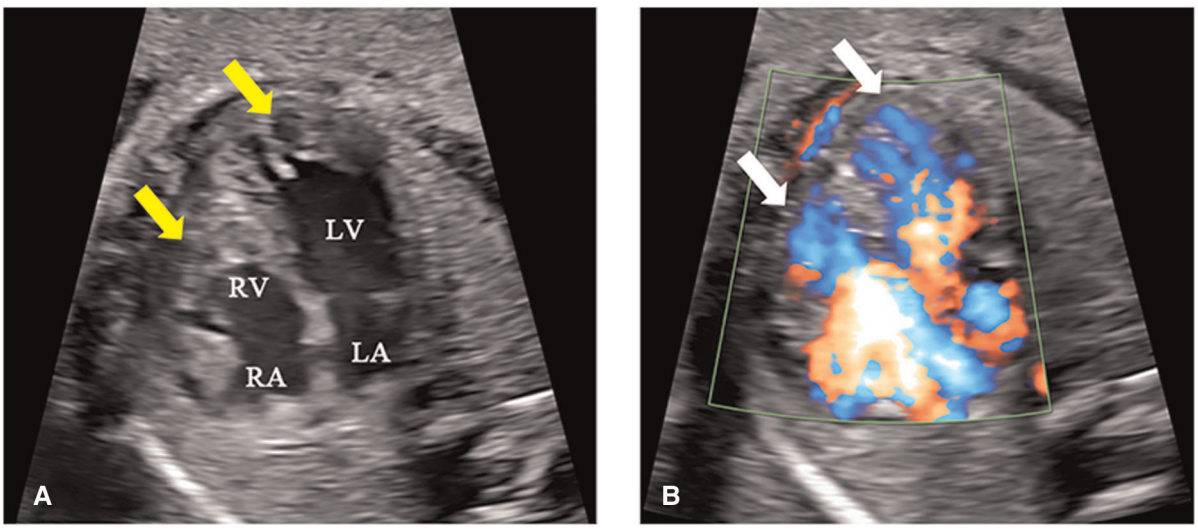

FIGURE 1
Fetal echocardiography at 25^{+1} weeks of gestation. (A) The two-dimensional ultrasound image shows increased numbers of prominent trabeculations and deep intertrabecular spaces in both ventricles (yellow arrow), especially at the left ventricular apex. The ratio of non-compaction (6 mm) to compaction (2 mm) was 3:1. (B) The color Doppler ultrasound image shows blood perfusing the intertrabecular recesses (white arrow). LA, left atrium; LV, left ventricle; RA, right atrium; RV, right ventricle.

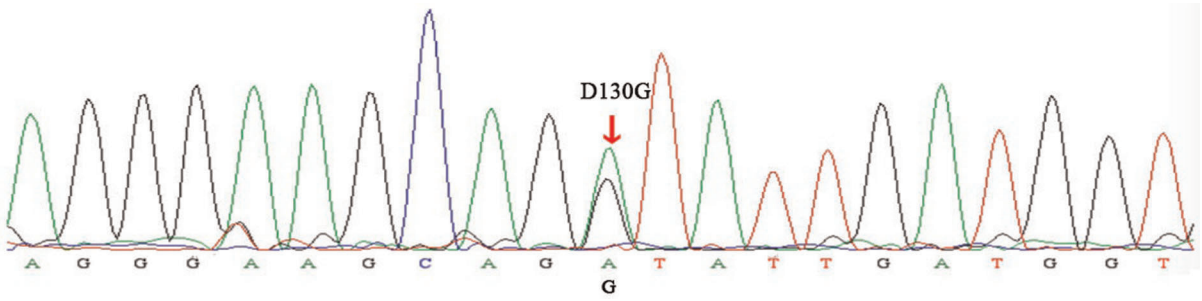

FIGURE 2
Sanger sequencing electropherogram. The variant (c.389A > G) demonstrated the replacement of a conserved aspartic acid residue at position 130 with glycine (p.D130G) in the *CALM2* gene (red arrow).

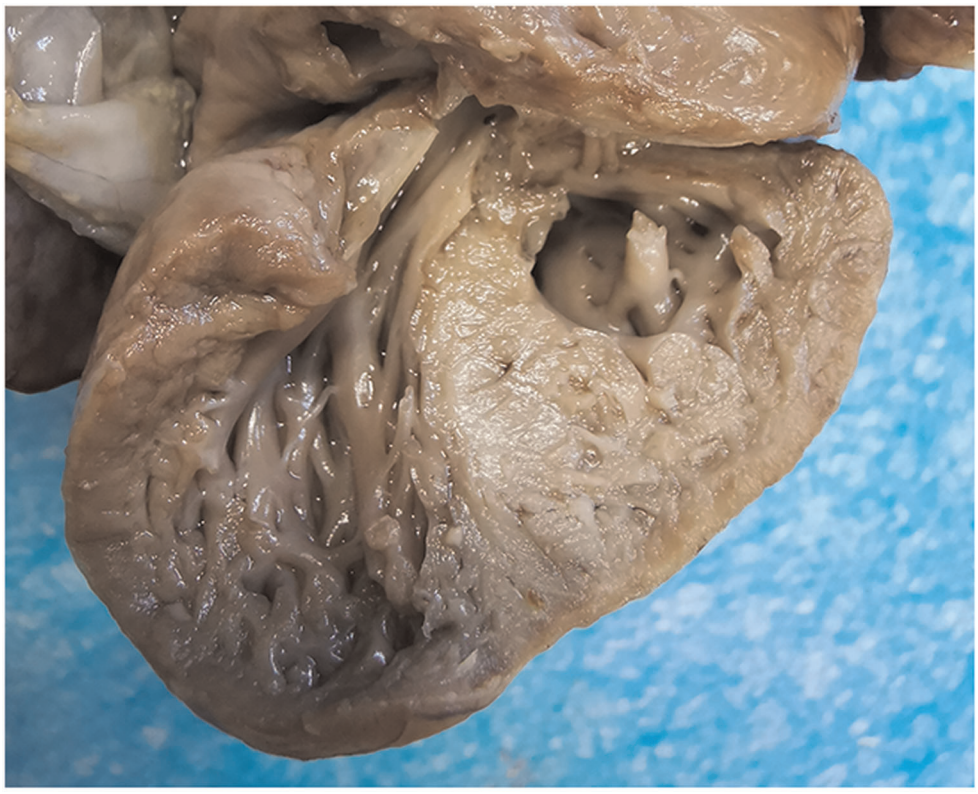

FIGURE 3
Dissected autopsy specimen. The specimen showed excessive trabeculae and deep intertrabecular recesses within the biventricular myocardium.

general population database (gnomAD, http://gnomad-sg.org) or the in-house control database.

Discussion

NCCM is a rare cardiomyopathy with various genotypic and phenotypic manifestations. It is categorized as a primary genetic cardiomyopathy by the American Heart Association and as an unclassified cardiomyopathy by the European Society of Cardiology (7). The diagnosis of NCCM is complicated in fetal life, and there is no uniform standard. At present, many scholars diagnose fetal NCCM by reference to pediatric or adult criteria, mainly using the N/C ratio. According to a study by Stöllberger et al. (8), the diagnostic criteria for NCCM by echocardiography during pregnancy are

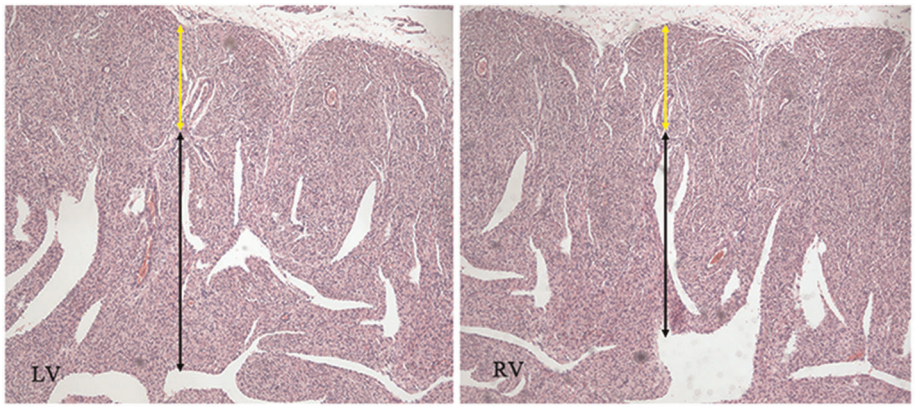

FIGURE 4
Histopathologic appearance of the myocardium at low magnification (hematoxylin and eosin, ×40). The images were compatible with non-compaction cardiomyopathy, with cardiomyocyte disarray in the non-compacted layer (black arrow) in opposition to regular cardiomyocytes in the compacted layer (yellow arrow).

as follows: at least four trabeculations protruding apically to the papillary muscle of the left ventricle visible in one imaging plane in end-diastole, a two-layered structure with epicardial compacted and endocardial noncompacted layers and an N/C ratio of ≥2, and perfusion of intraventricular blood into the intertrabecular spaces in color Doppler imaging. Fetal NCCM has its own specific imaging features. First, during development of the fetal cardiac structure, the N/C ratio of the myocardium in the normal fetus is much higher than that in a child or adult. Therefore, when the N/C ratio of the myocardium is about 2, we should be alert to the occurrence of NCCM and establish follow-up plans to observe the tendency of prominent trabeculations during the pregnancy. Second, because of the right ventricular dominance of the fetal circulation, fetal NCCM always involves both ventricles (9). By contrast, pediatric or adult NCCM most commonly occurs in the left ventricle; it rarely involves both ventricles, and isolated right ventricular NCCM is even rarer. Involvement of the right ventricle often implies a poor prognosis (10). In the published literature, most of the ultrasonic diagnostic criteria of right ventricular NCCM are based on the left ventricle; however, the right ventricle has more trabeculae, and its anatomical and morphological characteristics increase the difficulty of diagnosis of right ventricular NCCM. Fazio et al. (11) reported that the key to diagnosis of right ventricular NCCM is a significant increase of trabeculae in the right ventricle accompanied by dilation of this ventricle. The abnormal manifestations of the fetal right ventricle in the present case included a thin compacted layer, deep intertrabecular space, and dilated right ventricle. As noted by Fazio et al. (11), we consider that increased trabeculae within and enlargement of the right ventricle are the most important abnormalities for the diagnosis of fetal right ventricular NCCM and can provide instructive information for prenatal counseling.

NCCM in children and adults is always accompanied by arrhythmia. Kayvanpour et al. (12) found that the incidence of arrhythmias reached 61%, including conduction system diseases (26%), supraventricular tachycardia (17%), and sustained or non-sustained ventricular tachycardia (18%). Srivastava et al. (13) found that patients with NCCM had various electrocardiographic abnormalities, the most common of which were early repolarization and a prolonged QTc interval. Additionally, the types of arrhythmias were related to age. For example, Wolff-Parkinson-White syndrome and ventricular tachycardia were more common in children, and atrial fibrillation and other ventricular arrhythmias were more common in adults (13). However, prenatal diagnosis of fetal NCCM combined with arrhythmia has rarely been reported. We have herein presented the first case of fetal NCCM in both ventricles combined with sinus bradycardia. The normal fetal heart rate ranges from 120 to 160 bpm. Fetal bradyarrhythmia, which is defined as a heart rate of <110 bpm and mainly includes sinus bradycardia (16.9%) and AV block (38.2%) (14), is related to fetal hypoxia, abnormal heart structure, and maternal connective tissue disease. Sustained bradyarrhythmia can lead to cardiac function impairment manifesting as cardiac effusion in the fetus (15), as in the present case, suggesting a poor prognosis. Fetal echocardiography is the most commonly used method for diagnosing fetal arrhythmia. The AV interval is a key parameter for identifying the type of bradyarrhythmia. The normal fetal AV interval ranges from 112 to 130 ms (16). The AV interval of the fetus in this case was 133 ms; because it was <150 ms, it did not meet the diagnostic criteria for AV block (17). Therefore, the fetal arrhythmia type was

considered to be sinus bradycardia. Sinus bradycardia is found in 40% of cases of fetal long QT syndrome (LQTS) during the prenatal examination (18). The fetal findings combined with the WES findings of the family in this case demonstrated a new mutation in *CALM2*. Therefore, we highly suspected that the fetus had NCCM combined with LQTS. Fetal magnetocardiography is currently the most consistent and reliable technique for diagnosis of LQTS because it can provide a fetal electrocardiographic-like signal to definitively demonstrate QTc prolongation (19). However, because this advanced device was unavailable in the present case, we were unable to prove the presence of QTc prolongation using prenatal echocardiography. Additionally, because the parents chose to induce labor, we were unable to definitively determine whether the fetus had LQTS.

NCCM can be familial or sporadic and may be isolated or accompanied by other cardiac diseases. The etiology of NCCM is complex and still unclear. Although at least 40 gene mutations are reportedly associated with NCCM [e.g., *MYH7* and *PRDM16* (20–22)], few case reports of *CALM2* mutation in fetal NCCM have been published. A previous study demonstrated strong or definitive evidence for a causal relationship between *CALM2* mutation and atypical LQTS phenotypes, including marked sinus bradycardia or atrioventricular block as well as QT prolongation in infancy or early childhood (23). Limpitikul et al. (24) demonstrated that the potential mechanism of *CALM2* mutation-induced LQTS is a disruption of Ca^{2+}/calmodulin-dependent inactivation of L-type Ca^{2+} channels. Because the *CALM2* gene is involved in regulating ion channels, it may simultaneously contribute to cardiomyopathy and arrhythmia. Three published cases indicated that *CALM2* mutation might have contributed to LQTS accompanied by cardiomyopathy (one case of hypertrophic cardiomyopathy and two cases of left ventricular NCCM), indicating the variant positions in *CALM2* (c.396T > G; p.D132E, c.394G > C; p.D132H, and c395A > G; p.D132G) (25–27). Our case adds a report of a novel *CALM2* mutation (c.389A > G; p.D130G) in fetal NCCM combined with sinus bradycardia and detected by WES, providing more information regarding the relationship between the *CALM2* gene and fetal NCCM combined with arrhythmia. Considering our findings in combination with previously reported findings (25–27), we highly suspect that *CALM2* variants are simultaneous involved in cardiomyopathy and arrhythmia (especially LQTS). However, further research is required to confirm this hypothesis and elucidate the pathogenic mechanism.

In summary, prenatal ultrasound is very important to diagnose fetal NCCM. We should pay attention not only to abnormalities of myocardial morphology but also to the fetal heart rhythm. When prenatal ultrasound in the fetal period shows a dilated heart combined with increased trabeculae, especially in the right ventricle, fetal NCCM should be highly suspected. If the size of the heart and the N/C ratio progressively increase during ultrasound follow-up, genetic testing should be performed. Furthermore, in cases of fetal NCCM combined with arrhythmia, genetic testing is strongly recommended to provide more information for prenatal consulting and clinical application of precision medicine.

Data availability statement

The datasets presented in this study can be found in online repositories. The names of the repository/repositories and accession number(s) can be found in the article/ **Supplementary Material**.

Ethics statement

The studies involving human participants were reviewed and approved by Ethics Committee, West China Second Hospital, Sichuan University. The patients/participants provided their written informed consent to participate in this study.

Author contributions

XD and JC conceived the idea of presenting these clinical findings as a case report. SZ and LL curated the photographs and pathologic slides presented in the figures. WZ wrote the manuscript in discussion with XD. JC, QZ, and HL critiqued and revised the manuscript for quality. All authors contributed to the article and approved the submitted version.

Funding

This study was supported by the National Key R&D Program of China (2017YFC0211705, 2017YFC0113905), the Key R&D Program of Science and Technology Department of Sichuan Province (2019YFS0403, 19ZDYF1169), the Popularization and Application Project of the Sichuan Health and Family Planning Commission (17PJ415), and the Fundamental Research Funds for the Central Universities (SCU2022D022).

Acknowledgments

The authors are grateful to the patient for contributing the images in this article. The authors also thank Angela Morben, DVM, ELS, from Liwen Bianji (Edanz) (www.liwenbianji.cn), for editing the English text of a draft of this manuscript.

Conflict of interest

The authors declare that the research was conducted in the absence of any commercial or financial relationships that could be construed as a potential conflict of interest.

Publisher's note

All claims expressed in this article are solely those of the authors and do not necessarily represent those of their affiliated organizations, or those of the publisher, the editors and the reviewers. Any product that may be evaluated in this article, or claim that may be made by its manufacturer, is not guaranteed or endorsed by the publisher.

Supplementary material

The Supplementary Material for this article can be found online at: https://www.frontiersin.org/articles/10.3389/fped.2022.1012600/full#supplementary-material.

References

1. Finsterer J, Stollberger C, Towbin JA. Left ventricular noncompaction cardiomyopathy: cardiac, neuromuscular, and genetic factors. *Nat Rev Cardiol*. (2017) 14(4):224–37. doi: 10.1038/nrcardio.2016.207

2. Engberding R, Stöllberger C, Ong P, Yelbuz TM, Gerecke BJ, Breithardt G. Isolated non-compaction cardiomyopathy. *Dtsch Arztebl Int*. (2010) 107 (12):206–13. doi: 10.3238/arztebl.2010.0206

3. Sun H, Liu X, Hao X, Zhou X, Wang J, Han J, et al. Case report: biventricular noncompaction cardiomyopathy with pulmonary stenosis and bradycardia in a Fetus with KCNH2 mutation. *Front Genet*. (2022) 13:821226. doi: 10.3389/fgene.2022.821226

4. Kato K, Isbell HM, Fressart V, Denjoy I, Debbiche A, Itoh H, et al. Novel CALM3 variant causing calmodulinopathy with Variable expressivity in a 4-generation family. *Circ Arrhythm Electrophysiol*. (2022) 15(3):e010572. doi: 10.1161/CIRCEP.121.010572

5. Boczek NJ, Gomez-Hurtado N, Ye D, Calvert ML, Tester DJ, Kryshtal D, et al. Spectrum and prevalence of CALM1-, CALM2-, and CALM3-encoded calmodulin variants in long QT syndrome and functional characterization of a novel long QT syndrome-associated calmodulin missense variant, E141G. *Circ Cardiovasc Genet*. (2016) 9(2):136–46. doi: 10.1161/CIRCGENETICS.115.001323

6. Urrutia J, Aguado A, Muguruza-Montero A, Núñez E, Malo C, Casis O, Villarroel A. The crossroad of Ion channels and calmodulin in disease. *Int J Mol Sci*. (2019) 20(2):400. doi: 10.3390/ijms20020400

7. Chebrolu LH, Mehta AM, Nanda NC. Noncompaction cardiomyopathy: the role of advanced multimodality imaging techniques in diagnosis and assessment. *Echocardiography*. (2017) 34(2):279–89. doi: 10.1111/echo.13435

8. Stollberger C, Wegner C, Finsterer J. Fetal ventricular hypertrabeculation/noncompaction: clinical presentation, genetics, associated cardiac and extracardiac abnormalities and outcome. *Pediatr Cardiol*. (2015) 36(7):1319–26. doi: 10.1007/s00246-015-1200-y

9. Sun H, Hao X, Wang X, Zhou X, Zhang Y, Liu X, et al. Genetics and clinical features of noncompaction cardiomyopathy in the fetal population. *Front Cardiovasc Med*. (2020) 7:617561. doi: 10.3389/fcvm.2020.617561

10. Nappi L, Vasciaveo L, Sorrentino F, Scutiero G, Iannone P, Greco P. Fetal noncompaction cardiomyopathy and histologic diagnosis of spongy myocardium: case report and review of the literature. *Rev Bras Ginecol Obstet*. (2018) 40(11):722–5. doi: 10.1055/s-0038-1673677

11. Fazio G, Lunetta M, Grassedonio E, Gullotti A, Ferro G, Bacarella D, et al. Noncompaction of the right ventricle. *Pediatr Cardiol*. (2010) 31(4):576–8. doi: 10.1007/s00246-010-9652-6

12. Kayvanpour E, Sedaghat-Hamedani F, Gi WT, Tugrul OF, Amr A, Haas J, et al. Clinical and genetic insights into non-compaction: a meta-analysis and systematic review on 7598 individuals. *Clin Res Cardiol*. (2019) 108 (11):1297–308. doi: 10.1007/s00392-019-01465-3

13. Srivastava S, Yavari M, Al-Abcha A, Banga S, Abela G. Ventricular non-compaction review. *Heart Fail Rev*. (2021) 27(4):1063–76. doi: 10.1007/s10741-021-10128-3

14. Yuan SM. Fetal arrhythmias: diagnosis and treatment. *J Matern Fetal Neonatal Med*. (2020) 33(15):2671–8. doi: 10.1080/14767058.2018.1555804

15. Lingman G, Lundstrom NR, Marsal K. Clinical outcome and circulatory effects of fetal cardiac arrhythmia. *Acta Paediatr Scand Suppl*. (1986) 329:120–6. doi: 10.1111/j.1651-2227.1986.tb10398.x

16. Pan M, Zhang MX, Zhao BW, Mao YK, Peng XH, Yang Y, et al. Reference ranges and Z-scores of atrioventricular and ventriculoatrial time intervals in Normal fetuses. *Int J Cardiovasc Imaging*. (2021) 37(8):2419–28. doi: 10.1007/s10554-021-02217-z

17. Wojakowski A, Izbizky G, Carcano ME, Aiello H, Marantz P, Otaño L. Fetal Doppler mechanical PR interval: correlation with fetal heart rate,gestational age and fetal sex. *Ultrasound Obstet Gynecol*. (2009) 34(5):538–42. doi: 10.1002/uog.7333

18. Wacker-Gussmann A, Strasburger JF, Cuneo BF, Wakai RT. Diagnosis and treatment of fetal arrhythmia. *Am J Perinatol*. (2014) 31(7):617–28. doi: 10.1055/s-0034-1372430

19. Desai L, Wakai R, Tsao S, Strasburger J, Gotteiner N, Patel A. Fetal diagnosis of KCNQ1-variant long QT syndrome using fetal echocardiography and magnetocardiography. *Pacing Clin Electrophysiol*. (2020) 43(4):430–3. doi: 10.1111/pace.13900

20. Hoedemaekers YM, Cohen-Overbeek TE, Frohn-Mulder I ME, Dooijes D, Majoor-Krakauer DF. Prenatal ultrasound diagnosis of MYH7 non-compaction cardiomyopathy. *Ultrasound Obstet Gynecol*. (2013) 41(3):3369. doi: 10.1002/uog.12279

21. Nomura Y, Momoi N, Hirono K, Hata Y, Takasaki A, Nishida N, et al. A novel MYH7 gene mutation in a fetus with left ventricular noncompaction. *Can J Cardiol*. (2015) 31(1):103.e1–3. doi: 10.1016/j.cjca.2014.11.012

22. Delplancq G, Tarris G, Vitobello A, Nambot S, Sorlin A, Philippe C, et al. Cardiomyopathy due to PRDM16 mutation: first description of a fetal presentation, with possible modifier genes. *Am J Med Genet C Semin Med Genet*. (2020) 184(1):129–35. doi: 10.1002/ajmg.c.31766

23. Adler A, Novelli V, Amin AS, Abiusi E, Care M, Nannenberg EA, et al. An international, multicentered, evidence-based reappraisal of genes reported to cause congenital long QT syndrome. *Circulation*. (2020) 141(6):418–28. doi: 10.1161/CIRCULATIONAHA.119.043132

24. Limpitikul WB, Dick IE, Tester DJ, Boczek NJ, Limphong P, Yang W, et al. A precision medicine approach to the rescue of function on malignant calmodulinopathic long-QT syndrome. *Circ Res*. (2017) 120(1):39–48. doi: 10.1161/CIRCRESAHA.116.309283

25. Zahavich L, Tarnopolsky M, Yao R, Mital S. Novel association of a De Novo CALM2 mutation with long QT syndrome and hypertrophic cardiomyopathy. *Circ Genom Precis Med*. (2018) 11(10):e002255. doi: 10.1161/CIRCGEN.118.002255

26. Pipilas DC, Johnson CN, Webster G, Schlaepfer J, Fellmann F, Sekarski N, et al. Novel calmodulin mutations associated with congenital long QT syndrome affect calcium current in human cardiomyocytes. *Heart Rhythm*. (2016) 13 (10):2012–9. doi: 10.1016/j.hrthm.2016.06.038

27. Makita N, Yagihara N, Crotti L, Johnson CN, Beckmann BM, Roh MS, et al. Novel calmodulin mutations associated with congenital arrhythmia susceptibility. *Circ Cardiovasc Genet*. (2014) 7(4):466–74. doi: 10.1161/CIRCGENETICS.113.000459

frontiers | Frontiers in Cardiovascular Medicine

TYPE Case Report
PUBLISHED 30 November 2022
DOI 10.3389/fcvm.2022.1041039

OPEN ACCESS

EDITED BY
Alvise Guariento,
University of Toronto, Canada

REVIEWED BY
Luc Bruyndonckx,
University of Antwerp, Belgium
Claudia Cattapan,
University of Padua, Italy

*CORRESPONDENCE
Ingeborg Friehs
Ingeborg.Friehs@childrens.harvard.edu

†These authors share senior authorship

SPECIALTY SECTION
This article was submitted to Pediatric Cardiology, a section of the journal Frontiers in Cardiovascular Medicine

RECEIVED 10 September 2022
ACCEPTED 15 November 2022
PUBLISHED 30 November 2022

CITATION
Diaz-Gil D, Carreon CK, Silva-Gomez N, Benheim AE, Emani SM, del Nido PJ, Marx GR and Friehs I (2022) Case report: Active clinical manifestation of endocardial fibroelastosis in adolescence in a patient with mitral and aortic obstruction–histologic presence of endothelial-to-mesenchymal transformation.
Front. Cardiovasc. Med. 9:1041039.
doi: 10.3389/fcvm.2022.1041039

Case report: Active clinical manifestation of endocardial fibroelastosis in adolescence in a patient with mitral and aortic obstruction–histologic presence of endothelial-to-mesenchymal transformation

Daniel Diaz-Gil[1,2], Chrystalle Katte Carreon[3,4], Natalia Silva-Gomez[1], Alan E. Benheim[5], Sitaram M. Emani[1], Pedro J. del Nido[1], Gerald R. Marx[6†] and Ingeborg Friehs[1*†]

[1]Department of Cardiac Surgery, Boston Children's Hospital, Harvard Medical School, Boston, MA, United States, [2]Klinik für Kinderherzmedizin und Erwachsene mit angeborenen Herzfehlern, University Medical Center Hamburg-Eppendorf, Hamburg, Germany, [3]Cardiac Registry, Department of Cardiology, Pathology, and Cardiac Surgery, Boston Children's Hospital, Boston, MA, United States, [4]Department of Pathology, Boston Children's Hospital and Harvard Medical School, Boston, MA, United States, [5]Division of Cardiology, Inova L.J. Murphy Children's Hospital, Falls Church, VA, United States, [6]Department of Cardiology, Boston Children's Hospital, Harvard Medical School, Boston, MA, United States

This is the first description of active clinical manifestation of endocardial fibroelastosis (EFE) and remodeling of the endocardium *via* endothelial-to-mesenchymal transformation (EndMT) in an adolescent with Shone's variant hypoplastic left heart complex (HLHC) and a genetic heterozygous ABL1 variant. While EFE has not been typically associated HLHC or Shone's syndrome, in this patient flow alterations in the left ventricle (LV), combined with genetic alterations of intrinsic EndMT pathways led to active clinical manifestation of EFE in adolescence. This case emphasizes that new therapies for EFE might need to focus on molecular factors influenced by intrinsic and extrinsic stimuli of EndMT.

KEYWORDS

endocardial fibroelastosis, hypoplastic left heart complex, endothelial-to-mesenchymal transformation, ABL1, flow disturbance

Introduction

Hypoplastic left heart complex (HLHC) which also covers Shone's syndrome is a rare congenital heart disease comprised of severe obstructive lesions involving the left-sided inflow and outflow tracts (1, 2) with an incidence of 154–279 per million live births (3). In Shone's variant HLHC, the left ventricle (LV) is narrow but apex forming, the mitral valve (MV) can be stenotic due to annular hypoplasia or a parachute configuration, and the LV outflow tract (LVOT) shows multilevel obstructions. The spectrum of disease ranges from relatively mild to severe forms, and while supramitral fibroelastic membranes contributing to MV obstruction are common in this disease entity, LV endocardial fibroelastosis (EFE) has not been associated as a major factor in Shone's variant HLHC (4).

Based on clinical observation from the LV rehabilitation approach at Boston Children's Hospital, EFE involves the LV myocardium, contributing to LV systolic and diastolic dysfunction. Moreover, EFE is observed during surgery in multilevel obstructive lesions involving the left atrium, MV apparatus and LVOT. EFE is a thickened subendocardial layer of collagen and elastic, and occurs as early as during fetal development. Hypothetically, EFE can prevent normal growth and development of the LV but potentially might also contribute to the pathologic changes of the MV and LVOT and aortic valve. We have also recently reported that flow disturbances are associated with the remodeling of the endocardium through a process called endothelial-to-mesenchymal transformation (EndMT), which we have shown as an underlying root cause for EFE formation (5–7). EndMT is the phenotypical switch of endocardial endothelial cells to mesenchymal cells which is a normal developmental process during fetal heart morphogenesis giving rise to the septa and valves (8). Despite EFE being an early childhood disease, we present the case of an adolescent with active clinical manifestation of EFE through activation of EndMT in the entire LV cavity, MV and subaortic region at 14 years of age.

Case presentation

This male, Caucasian patient of Armenian descent presented at 2 days of age with Shone's variant anatomy, including MV stenosis, subaortic stenosis, a non-stenotic bicuspid aortic valve (right non-fusion), and aortic coarctation. At the referral hospital, the patient underwent a coarctectomy with end-to-end anastomosis in the newborn period, followed by several transcatheter interventions for recoarctation, resulting in coarctation recurrence, and the placement of multiple stents from the distal transverse arch to the thoracic descending aorta. He also underwent multiple catheter-based aortic balloon valvuloplasties for mild aortic valve stenosis. At 6 years of age, the patient required a surgical mitral valvuloplasty with separation of papillary muscles and resection of stenosis in the inter-chordal space in repair of a worsening mitral stenosis. Additionally, a septal myectomy was performed to relieve a muscular subaortic stenosis. After surgery, the patient had an uneventful recovery and returned to full activities with good stamina.

Whole-exome sequencing ruled out an underlying aortopathy (suggested due to the unusual aortic disease with extensive stenosis of the thoracic aorta requiring multiple stent placements), but demonstrated a heterozygous ABL1 variant (p.Pro329Arg (CCG > CGG): c.986 C > G in exon 6 on the ABL1 gene (NM_007313.2), ACMG/AMP classification as variant of uncertain significance). *In silico* analysis performed during whole exome sequencing supported that this missense variant has a deleterious effect on protein structure and function of ABL1. In addition, the patient's past medical history was significant for preterm birth, initially delayed milestones, short stature, dysmorphic facial features, cryptorchidism, webbed short fingers, narrow tapered palpebral fissures,– all features previously described in patients with similar heterozygous germline ABL1 variants, summarized as ABL1-associated congenital heart defects and skeletal malformation syndrome (9–11). Of note, the mutation was inherited from the father, who has no history of congenital heart disease, suggesting variability in penetrance.

At 13 years old, the patient presented with an asymptomatic aortic valve gradient of 55 mmHg, which was reduced to 30 mmHg *via* balloon valvuloplasty. The pulmonary capillary wedge pressure was elevated to 21 mm Hg with a mitral stenosis mean gradient of 9 mm Hg. In the following year, the patient reported a steady decrease in energy levels, accompanied by leg numbness, and limited stamina even after short periods of rest. The patient was referred to our institution, and echocardiographic and MRI imaging revealed global LV hypertrophy and dysfunction. Thickened amorphic tissue with bright signals from the base to LV apex consistent with a diagnosis of EFE were detected on the endocardial LV surface involving the MV and subaortic region. Marked thickening of the atrial surfaces of the anterior and posterior MV leaflets in the mid leaflet region prevented effective leaflet coaptation (**Figure 1**). There was LVOTO (peak gradient if 45 mmHg, mean gradient of 22 mmHg), from the subaortic region extending to the undersurface of the bicuspid aortic leaflets. At repeat catheterization, LV filling pressures were increased to 20 mmHg. On cardiac CT, severe in-stent stenosis along nearly the entire length of the stented descending aorta was seen. Overall, the patient's symptoms were attributed to an

Abbreviations: EFE, endocardial fibroelastosis; EndMT, endothelial-to-mesenchymal transformation; MV, mitral valve; LV, left ventricle; LVOT, left ventricular outflow tract; PCWP, pulmonary capillary wedge pressure; HLHS, hypoplastic left heart syndrome; HLHC, hypoplastic left heart complex.

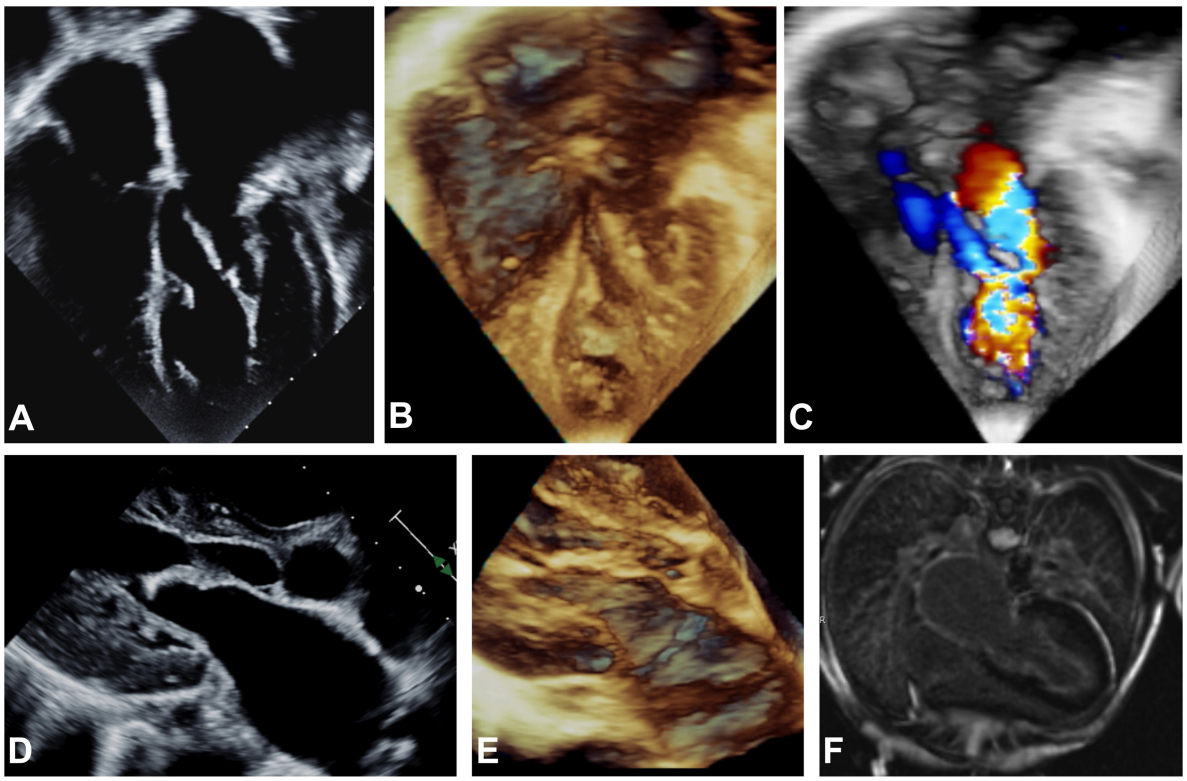

FIGURE 1
Echocardiographic apical 4-chamber view **(A–C)**, parasternal long axis **(D,E)** and MRI **(F)** imaging before EFE resection. 2D **(A,D)** and 3D **(B,C,E)** echocardiography showing hyperechogenic thickening of the endocardium on atrial, mitral valve, LV and LVOT level consistent with generalized EFE in the left sided structures of the heart is shown. Severe dilation of the left atrium can be noted. **(C)** Severe turbulences are detected by color Doppler in all left sided structures affected by EFE as compared to physiological color Doppler appearance in the right sided structures of the heart that are not affected by EFE. **(F)** Late gadolinium enhancement on endocardial level encapsulating all structures of the left atrium and ventricle is depicted.

inability to significantly increase his cardiac output due to inflow and outflow obstruction and decreased diastolic compliance due to EFE.

The patient underwent surgery consisting of a mitral valvuloplasty with surgical resection of the tethering attachments to the anterior and posterior leaflets, thinning of the leaflets with the removal of thickened amorphous tissue (presumed to be EFE), mobilization of the leaflets, and the anterior papillary muscle. Furthermore, tissue was resected from the entire LV, the subaortic region, and the aortic valve, accompanied by valvuloplasty and commissurotomy.

All resected tissues were comprised of paucicellular organized avascular collagen and elastin matrix, which is consistent with the histological picture of EFE (5, 6). Furthermore, pathological evaluation of the subaortic obstruction revealed fragments of endocardium-lined fibromyxoid tissue with scant attached myocardium. Additionally, immunofluorescence analysis of the resected EFE tissue from all areas showed a high number of cells expressing both endothelial and mesenchymal markers, indicative of active EndMT (**Figure 2**).

The immediate post-operative course was uneventful with only mild residual mitral stenosis (Doppler echo mean gradient 3–4 mmHg) and a residual gradient over the aortic valve (peak gradient 33 mmHg, mean gradient of 21 mmHg). At 3 months follow-up, B-type natriuretic peptide had normalized to 91 pg/ml from 827 pg/ml preoperatively. At 6 months follow-up, echocardiography showed a remaining mild LV hypertrophy with good systolic function, and mild valvular mitral and aortic stenosis with a mean gradient of 5–6 and 21 mmHg, respectively. A marked improvement in diastolic flow parameters was noted. The patient was doing well clinically without any apparent signs of congestive heart failure on his standard heart medication regimen. He now can exercise without limitations.

Discussion

This is the first description of active clinical manifestation of EFE and remodeling of the endocardium *via* EndMT in adolescence in an individual with longstanding congenital heart disease involving the MV, the subaortic region and the entire

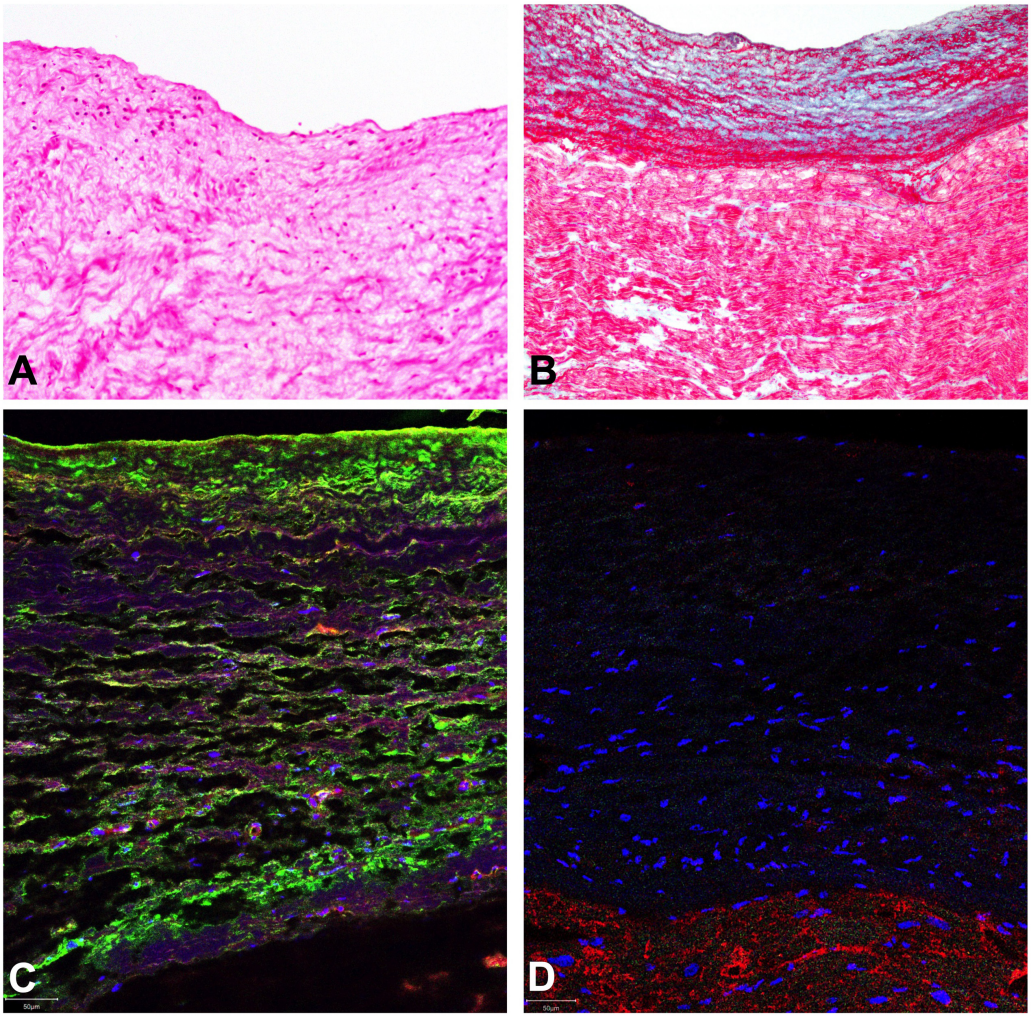

FIGURE 2
Representative histological evaluation of resected EFE tissue. Organized structured avascular collagen and elastin matrix with scarce cellularity, consistent with the histological picture of EFE is shown **(A)** H&E staining shows only sparse mononuclear likely mesenchymal stromal cells **(B)**. Masson's trichome stain displays a thickened subendocardium with multiple and often alternating layers of elastic fibers (red wavy profiles) and fibrous tissue (blue) with extension into the subjacent myocardium. **(C)** Double-staining of endocardial endothelial cells with VE-cadherin (red) and alpha-smooth muscle actin (green) were performed to detect EndMT. A representative section is shown. The majority of endocardial endothelial cells express both markers at the same time, indicating active EndMT. **(D)** Lack of predominant inflammatory invasion of EFE tissue is confirmed by negative immunofluorescence staining for CD45 (absence of green). Cardiomyocytes are counterstained with Troponin I (red).

LV endocardium, and no previous clinical evidence of EFE. EFE was visible immediately preoperatively on echocardiography and MRI, and confirmed by histological analysis of the resected tissue, showing active EndMT. This is a signature case, since it has been postulated that EFE manifests during the fetal stage and early childhood. In this case we have histological evidence of active EFE development and associated clinical manifestation in adolescence (4). While it cannot be ruled out that some level of EFE was already present earlier in the disease course, this patient presented with marked changes in clinical symptoms and LV function, which suggested an acute clinical manifestation reflecting either *de novo* development of acute progression in adolescence.

Endothelial-to-mesenchymal transformation can be induced by different stimuli including mechanical forces or inflammation (12). As we have previously shown hemodynamic alterations, primarily flow disturbances are directly associated with the induction of EndMT (5–7). Flow disturbances had been present in this patient since birth. To rule out inflammation as a potential stimulus for EndMT, we performed histological analysis of EFE tissue. As indicated in **Figures 2A,D**, there was no evidence of systemic infiltration of inflammatory cells which was supported by preoperative normal total and differential leukocyte counts.

In this case, we postulate that activation of EFE manifested in the context of disturbed LV inflow and outflow. Varying

degrees of altered flow patterns through the MV in combination with outflow tract obstructions have been suggested to contribute to the spectrum of critical AS to HLHS (AS/MS), with numerous studies showing that disturbed inflow through the MV is associated with the development of EFE (5, 7, 13, 14). Specifically, Sharland et al. (13) and Allan et al. (15) showed in the fetus that the initial intrauterine echocardiographic evaluation often displayed a pattern of reduced MV inflow while forward flow in the ascending aorta remained normal. Later in gestation when no antegrade flow was detected–through the MV or the aortic valve–a bright endocardial layer consistent with EFE was observed. These findings suggest that inflow disturbances caused by either MV abnormalities or increased LV filling pressures, are the underlying hemodynamic factors that are associated with EFE formation. Furthermore, the severity of the overall flow reduction and timespoints of such "insults" may play a role in ultimately developing into HLHS or–critical AS (16–18). Interestingly, in the presented patient, aortic and MV abnormalities and aortic coarctation were evident since birth. Reduction of recurrent aortic outflow tract gradients left a hemodynamic situation of MV stenosis with disturbed MV inflow and active clinical manifestation of EFE.

While the MV circumferences in patients with HLHS (AS/MS) or critical aortic stenosis may be just above or below the lower ranges of normal values, they are frequently dysplastic and stenotic, probably because of intrinsic alterations in EndMT regulation (19). In contrast, even though aortic valves are often small, they are also often formed normally (19). Furthermore, while no genetic abnormality is specific to HLHS or critical aortic stenosis, there is strong evidence supporting a genetic etiology, and certain implicated specific gene mutations like NOTCH1 play a crucial role in modulating EndMT (20–22). Not only was this patient's predominant intracardiac defect at birth a dysplasia of the MV but he was also diagnosed with a heterozygous germline missense ABL1 variant, which while being of uncertain significance, *in silico* analysis suggested has a deleterious effect on protein structure and function of ABL1. Although the protooncogene ABL1 is well known for being part of the fusion gene BCR*ABL1 in leukemic cells (23), inherited germline heterozygous mutations in ABL1 have only recently been found to cause congenital heart defects and skeletal malformations through an increase in ABL1 kinase activity (9–11). ABL1 kinase activity influences EndMT in the entire body through inactivation of the phosphatase and tensin homolog (PTEN) (24), a mechanism that has also been implicated in LV hypertrophy and non-compaction in response to biomechanical stress (25, 26). The combination of two hits—an intrinsic EndMT alteration through his underlying genetic mutation and distinct flow disturbances in adolescence potentially led to EFE formation, and we speculate that a similar two-hit hypothesis could also be the underlying mechanism behind the development and progression of EFE in patients with HLHS (AS/MS) / critical aortic stenosis spectrum disease.

In conclusion, this case emphasizes the likely multifactorial nature in development and persistence of EFE into adolescence. In this patient, presenting with distinct flow alterations in the LV, resembling well-described intrauterine patterns in patients with LV disease in the HLHS (AS/MS) / critical AS and Shone's spectrum, in combination with genetic alterations of intrinsic EndMT pathways, led to active clinical manifestation of EFE in adolescence. A deeper understanding of genetic and transcriptional factors influenced by intrinsic and extrinsic stimuli of EndMT might lead to new therapeutic strategies (e.g., through the usage of readily available pharmacotherapies like tyrosine kinase inhibitors) for the prevention of EFE and associated congenital heart defects.

Data availability statement

The raw data supporting the conclusions of this article will be made available by the authors, without undue reservation.

Ethics statement

Ethical review and approval was not required for the study on human participants in accordance with the local legislation and institutional requirements. Written informed consent to participate in this study was provided by the participants' legal guardian/next of kin. Written informed consent was obtained from the minor(s)' legal guardian/next of kin for the publication of any potentially identifiable images or data included in this article.

Author contributions

DD-G, GM, and IF were involved in the conceptualized of this case report. DD-G and IF designed the methodology, conducted the experiments, and wrote—original draft. DD-G and CC performed the experiments. DD-G, GM, PN, AB, and IF were responsible for clinical data acquisition. DD-G, CC, and IF performed the formal analyses. DD-G, CC, NS-G, AB, SE, PN, GM, and IF reviewed and edited the final draft. IF was responsible for the acquisition of funding. All authors contributed to the article and approved the submitted version.

Funding

This research was funded by IF: Additional Ventures–Single Ventricle Research Fund (SVRF); DD-G: Deutsche Forschungsgemeinschaft (DFG, German Research Found-

ation)–project number Di 2737/1-1; NS-G: German Cardiac Society (DGK).

Conflict of interest

The authors declare that the research was conducted in the absence of any commercial or financial relationships that could be construed as a potential conflict of interest.

Publisher's note

References

1. Shone JD, Sellers RD, Anderson RC, Adams P, Lillehei CW, Edwards JE. The developmental complex of "parachute mitral valve," supravalvular ring of left atrium, subaortic stenosis, and coarctation of aorta. *Am J Cardiol.* (1963) 11:714–25. doi: 10.1016/0002-9149(63)90098-5

2. Tchervenkov CI, Tahta SA, Jutras LC, Béland MJ. Biventricular repair in neonates with hypoplastic left heart complex. *Ann Thorac Surg.* (1998) 66:1350–7. doi: 10.1016/S0003-4975(98)00803-0

3. Hoffman JIE, Kaplan S. The incidence of congenital heart disease. *J Am Coll Cardiol.* (2002) 39:1890–900. doi: 10.1016/S0735-1097(02)01886-7

4. Shaddy RE. Fetal and perinatal cardiology. 10th ed. In: Allen HD, Driscoll DJ, Shaddy RE, Feltes TF editors. *Moss & adams' heart disease in infants, children, and adolescents*. Wolters Kluwer Health (2013). 154 p.

5. Weixler V, Marx GR, Hammer PE, Emani SM, del Nido PJ, Friehs I. Flow disturbances and the development of endocardial fibroelastosis. *J Thor Cardiovasc Surg.* (2020) 159:637–46. doi: 10.1016/j.jtcvs.2019.08.101

6. Weixler V, Kramer P, Lindner J, Murin P, Cho MY, Del Nido P, et al. Endothelial-to-mesenchymal transition as underlying mechanism for the formation of double-chambered right ventricle. *Pediatr Cardiol.* (2022) 43:1084–93. doi: 10.1007/s00246-022-02828-w

7. Oh NA, Hong X, Doulamis IP, Meibalan E, Peiseler T, Melero-Martin J, et al. Abnormal flow conditions promote endocardial fibroelastosis via endothelial-to-mesenchymal transition, which is responsive to losartan treatment. *JACC Basic Trans Sci.* (2021) 6:984–99. doi: 10.1016/j.jacbts.2021.10.002

8. von Gise A, Pu WT. Endocardial and epicardial epithelial to mesenchymal transitions in heart development and disease. *Circ Res.* (2012) 110:1628–45. doi: 10.1161/CIRCRESAHA.111.259960

9. Wang X, Charng W-L, Chen C-A, Rosenfeld JA, Al Shamsi A, Al-Gazali L, et al. Germline mutations in ABL1 cause an autosomal dominant syndrome characterized by congenital heart defects and skeletal malformations. *Nat Genet.* (2017) 49:613–7. doi: 10.1038/ng.3815

10. Bravo-Gil N, Marcos I, González-Meneses A, Antiñolo G, Borrego S. Expanding the clinical and mutational spectrum of germline ABL1 mutations-associated syndrome. *Medicine (Baltimore).* (2019) 98:e14782. doi: 10.1097/MD.0000000000014782

11. Chen C-A, Crutcher E, Gill H, Nelson TN, Robak LA, Jongmans MCJ, et al. The expanding clinical phenotype of germline ABL1-associated congenital heart defects and skeletal malformations syndrome. *Hum Mutat.* (2020) 41:1738–44. doi: 10.1002/humu.24075

12. Lurie PR. Changing concepts of endocardial fibroelastosis. *Cardiol Young.* (2010) 20:115–23. doi: 10.1017/S1047951110000181

13. Sharland GK, Chita SK, Fagg NL, Anderson RH, Tynan M, Cook AC, et al. Left ventricular dysfunction in the fetus: relation to aortic valve anomalies and endocardial fibroelastosis. *Heart.* (1991) 66:419–24. doi: 10.1136/hrt.66.6.419

14. Friehs I, Illigens B, Melnychenko I, Zhong-Hu T, Zeisberg E, Del Nido PJ. An animal model of endocardial fibroelastosis. *J Surg Res.* (2013) 182:94–100. doi: 10.1016/j.jss.2012.07.069

15. Allan LD, Sharland G, Tynan MJ. The natural history of the hypoplastic left heart syndrome. *Int J Cardiol.* (1989) 25:341–3. doi: 10.1016/0167-5273(89)90226-X

16. Chin AJ, Weinberg PM, Barber G. Subcostal two-dimensional echocardiographic identification of anomalous attachment of septum primum in patients with left atrioventricular valve underdevelopment. *J Am Coll Cardiol.* (1990) 15:678–81. doi: 10.1016/0735-1097(90)90645-6

17. Nowlen TT, Ayres NA, Kearney DL, Nihill MR, Grifka RG. Premature closure of the foramen ovale associated with aortic stenosis, left ventricular dilation with thrombus, and early mortality. *Am J Cardiol.* (2000) 85:1159–61. doi: 10.1016/s0002-9149(00)00718-9

18. Remmell-Dow DR, Bharati S, Davis JT, Lev M, Allen HD. Hypoplasia of the eustachian valve and abnormal orientation of the limbus of the foramen ovale in hypoplastic left heart syndrome. *Am Heart J.* (1995) 130:148–52. doi: 10.1016/0002-8703(95)90250-3

19. Smith A, Pozzi M, Anderson RH. The morphology of hypoplasia of the left heart [internet]. In: Anderson RH, Pozzi M, Hutchinson S editors. *Hypoplastic left heart syndrome*. London: Springer (2005).

20. Miao Y, Tian L, Martin M, Paige SL, Galdos FX, Li J, et al. Intrinsic endocardial defects contribute to hypoplastic left heart syndrome. *Cell Stem Cell.* (2020) 27:574–589e8. doi: 10.1016/j.stem.2020.07.015

21. Timmerman LA, Grego-Bessa J, Raya A, Bertrán E, Pérez-Pomares JM, Díez J, et al. Notch promotes epithelial-mesenchymal transition during cardiac development and oncogenic transformation. *Genes Dev.* (2004) 18:99–115. doi: 10.1101/gad.276304

22. Garg V, Muth AN, Ransom JF, Schluterman MK, Barnes R, King IN, et al. Mutations in NOTCH1 cause aortic valve disease. *Nature.* (2005) 437:270–4. doi: 10.1038/nature03940

23. Klein A, van Kessel AG, Grosveld G, Bartram CR, Hagemeijer A, Bootsma D, et al. A cellular oncogene is translocated to the *Philadelphia chromosome* in chronic myelocytic leukaemia. *Nature.* (1982) 300:765–7. doi: 10.1038/300765a0

24. Morotti A, Panuzzo C, Crivellaro S, Carrà G, Fava C, Guerrasio A, et al. BCR-ABL inactivates cytosolic PTEN through casein kinase II mediated tail phosphorylation. *Cell Cycle.* (2015) 14:973–9. doi: 10.1080/15384101.2015.1006970

25. Oudit GY, Kassiri Z, Zhou J, Liu QC, Liu PP, Backx PH, et al. Loss of PTEN attenuates the development of pathological hypertrophy and heart failure in response to biomechanical stress. *Cardiovasc Res.* (2008) 78:505–14. doi: 10.1093/cvr/cvn041

26. Tang VT, Arscott P, Helms AS, Day SM. Whole-exome sequencing reveals GATA4 and PTEN mutations as a potential digenic cause of left ventricular noncompaction. *Circ Geno Precis Med.* (2018) 11:e001966. doi: 10.1161/CIRCGEN.117.001966

frontiers | Frontiers in Cardiovascular Medicine

TYPE Case Report
PUBLISHED 20 December 2022
DOI 10.3389/fcvm.2022.1032519

OPEN ACCESS

EDITED BY
Cecile Tissot,
Clinique des Grangettes, Switzerland

REVIEWED BY
Toshihiro Tsuruda,
University of Miyazaki, Japan
Madjid Soltani,
University of Waterloo, Canada

*CORRESPONDENCE
Liliana Gozar
lili_gozar@yahoo.com
Simina-Elena Rusu Ghiragosian
simina_r88@yahoo.com

SPECIALTY SECTION
This article was submitted to Pediatric Cardiology, a section of the journal Frontiers in Cardiovascular Medicine

RECEIVED 30 August 2022
ACCEPTED 24 October 2022
PUBLISHED 20 December 2022

CITATION
Făgărăşan A, Gozar L, Ghiragosian S-ER, Murariu M, Pop M, Crauciuc A, Miclea D and Şuteu CC (2022) Severe early-onset manifestations of generalized arterial calcification of infancy (mimicking severe coarctation of the aorta) with *ABCC6* gene variant — Case report and literature review. *Front. Cardiovasc. Med.* 9:1032519. doi: 10.3389/fcvm.2022.1032519

Severe early-onset manifestations of generalized arterial calcification of infancy (mimicking severe coarctation of the aorta) with *ABCC6* gene variant — Case report and literature review

Amalia Făgărăşan[1,2], Liliana Gozar[1,2]*, Simina-Elena Rusu Ghiragosian[2]*, Mircea Murariu[1], Marian Pop[3,4], Andrei Crauciuc[1], Diana Miclea[5] and Carmen Corina Şuteu[1]

[1]Clinic of Pediatric Cardiology, Emergency Institute of Cardiovascular Diseases and Transplantation, Târgu Mureş, Romania, [2]Department of Pediatrics III, George Emil Palade University of Medicine, Pharmacy, Science, and Technology of Târgu Mureş, Târgu Mureş, Romania, [3]ME1 Department, George Emil Palade University of Medicine, Pharmacy, Science, and Technology of Târgu Mureş, Târgu Mureş, Romania, [4]Department of Radiology, Emergency Institute for Cardiovascular Diseases and Heart Transplant, Târgu Mureş, Romania, [5]Department of Medical Genetics, "Iuliu Hatieganu" University of Medicine and Pharmacy, Cluj-Napoca, Romania

Introduction: Generalized arterial calcification of infancy (GACI) is a rare cause of infantile heart failure and systemic hypertension with a poor prognosis, characterized by extensive calcification and proliferation of the intimal layer of large and medium sized arteries.

Case report: We present the first case report of successful surgical treatment of severe aortic arch obstruction by calcified plaques mimicking severe coarctation of the aorta and the outcome (of bisphosphonate therapy) in a newborn with GACI. Furthermore, we report the identification of a variant in ATP Binding Cassette Subfamily C, Member 6 (ABCC6) gene, possibly associated with severe early-onset manifestations of GACI.

Conclusion: This case report highlights the importance of considering GACI in an infant with heart failure, systemic hypertension, and evidence of increased echogenicity of the arterial vessels. We noted the favorable outcome in improving the aortic calcification in our patient after surgical treatment and bisphosphonates therapy. Early diagnosis and treatment improve the long-term prognosis. A better understanding of this rare genetic disease could lead to new therapeutic strategies.

KEYWORDS

GACI, infantile heart failure, systemic hypertension, infant, *ABCC6* gene

Introduction

We present a case of a newborn with early-onset manifestations of generalized arterial calcification of infancy (GACI-2) mimicking severe coarctation of the aorta (CoA), and the clinical evolution of the patient in the first 18-months of life. To our knowledge, this is the first case report of successful surgical treatment of the aortic arch in a child with GACI. Furthermore, this case contributes to enrich the literature with data on a homozygote variant in *ABCC6* gene as-sociated with severe GACI phenotype.

Case report

Introduction

Generalized arterial calcification of infancy (GACI) is an autosomal recessive condition characterized by extensive calcification and intimal proliferation of the large and medium arteries, including the aorta, coronary arteries, and renal arteries, leading to vascular stenosis (1, 2). The most frequent complications include severe systemic hypertension, heart failure, myocardial infarction, respiratory distress, and sudden death. The disease was first described in 1901 by Bryant and White (3). This genetic disorder is caused by mutation in ectonucleotide pyrophosphatase/phosphodiesterase 1 (*ENPP1*) gene (GACI-1) and by mutation in ATP-binding cassette, subfamily C, member 6 (*ABCC6*) (GACI-2), leading to decreased levels of inorganic pyrophosphate (PPi). Inorganic pyrophosphate prevents deposition of calcium hydroxyapatite crystal in the vessel wall (4).

Generalized arterial calcification of infancy is a rare genetic disorder with a poor prognosis. Data about this condition is mainly based on case reports. To date, approximately 300 cases of GACI have been re-ported, and an estimated frequency of 1/566.000 has been suggested (5, 6). Mortality rate is high in infancy, 55% of children with GACI die within the first 6 months of life due to rapid progression of arterial stenoses and heart failure (1).

We present a case of a newborn with early-onset manifestations of GACI-2 mimicking severe CoA, and the clinical evolution of the patient in the first 18-months of life. CoAo is a congenital narrowing of the proximal descending aorta located mostly after the emergence of the left subclavian artery, being considered as the fifth most common congenital heart disease. Studies show the rate of recoarctation varies from 3 to 15% (7, 8). To our knowledge, this is the first case report of successful surgical treatment of the aortic arch in a child with GACI. Furthermore, this case contributes to enrich the literature with data on a homozygote variant in *ABCC6* gene as-sociated with severe GACI phenotype.

Abbreviations: ABCC6, ATP-binding cassette, subfamily C, member 6; BP, blood pressure; BT, brachiocephalic trunk; CT, computed tomography; CoA, coarctation of the aorta; ENPP1, ectonucleotide pyrophosphatase/phosphodiesterase 1; FATHMM; GACI, generalized arterial calcification of infancy; LCCA, left common carotid artery; LSA, left subclavian artery; MTHFR, methylene-tetrahydro-folate-reductase mutations; PAI-1, plasminogen activator inhibitor 1; PGE1, prostaglandin E1; PDA, ductus arteriosus; PPi, inorganic pyrophosphate; rhENPP1-Fc protein, recombinant human (rh)ENPP1-Fc protein; SaO2, oxygen saturation; VUS, a variant of uncertain significance.

Case report – The history of this case without 80-81, 177

We report the case of an 18-day-old male newborn referred from the neonatal intensive care unit of a peripheral hospital to our tertiary center for management of a CoA with ductal dependent systemic blood flow. It was related negative medical family history, the absence of consanguineous relations and no abnormality on the prenatal ultrasound. The boy was born at 38 weeks of gestation *via* cesarean section (for placental pathology), with a birth weight of 3,380g, and APGAR score of 10 at 1 min.

In the third day of life, the newborn developed heart failure and severe hypertension and the echocardiography revealed severe CoA. The diagnosis was confirmed by computed tomography (CT). Intravenous infusions of prostaglandin E1 (PGE1) was started in dose of 0.05 microgram/kg/min for keeping the ductus arteriosus (PDA) open. In this condition was admitted in our center.

Presenting symptoms

The physical examination showed severe respiratory distress, a respiratory rate of 70 breaths per minute, cyanosis, with oxygen saturation on pulse oximetry (SaO2) of 85% in room air, tachycardia of 180 beats per minute, a grade III/IV systolic murmur with interscapulovertebral irradiation, weak pulse, a capillary refill time of 5 s, hepatomegaly, high systolic blood pressure (BP), ranging from 93 to 115 mmHg, and diastolic blood pressures between 40 and 50 mmHg (≥95th percentile for age); there was a significant difference in blood pressure between the upper and lower extremity (right upper limb BP 113/51 mmHg, left lower limb BP 64/31 mmHg).

Transthoracic echocardiography showed left ventricular hypertrophy with impaired systolic function (LV ejection fraction of 40%), severe pulmonary hypertension, hyperechogenicity and severe narrowing of the aortic arch and descending aorta, with a significant gradient of 90 mmHg (**Figures 1A,B**). The coronary arteries were normal (**Figure 1C**). Ductus arteriosus was patent, but restricted, requiring an increase in PGE1 dose.

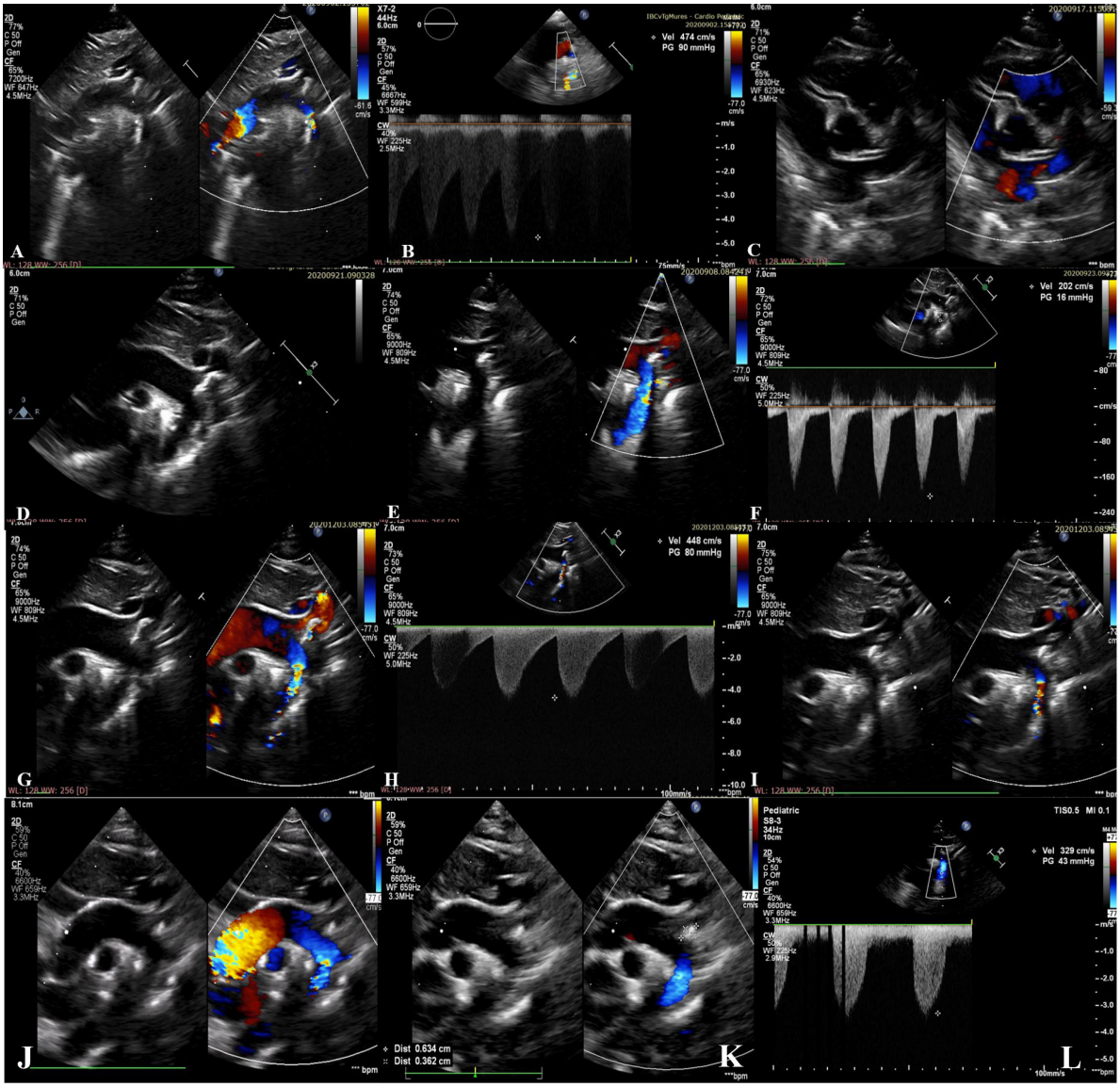

FIGURE 1
(A–C) Preoperative echocardiographic images from the neonatal period showing hyperechogenicity and severe narrowing of the aortic arch with a 2.5 mm diameter of the descending aorta lumen (gradient of 90mmHg) and normal coronary arteries; **(D–F)** postoperative echocardiographic images from the neonatal period showing the brightness and the abnormal echogenicity of the walls of the aortic arch and descending aorta and calcified residual masses at the level of the aortic arch extended to the brachiocephalic trunk, left common carotid artery, left subclavian artery, with laminar color Doppler flow in the descending aorta. Diameter of descending aorta lumen of 5.5 mm; **(G–I)** echocardiographic images at 3 months of age showing re-coarctation of the aorta with a significant gradient and the persistence of the aortic arch calcifications; **(J–L)** echocardiographic images at 18-months of age showing the regression of the aortic arch calcifications without obstruction, and mild left ventricular hypertrophy.

Therapeutic approach, postprocedural evolution

Due to hemodynamic instability, it was decided to perform the surgical repair of the CoA *via* lateral thoracotomy. Intraoperatively, after aortotomy, a calcified mass extended to the aortic arch, the left subclavian artery (LSA) and the left common carotid artery (LCCA) was detected and partially removed, and an end-to-end anastomosis was performed (Figure 2).

Postoperative hemodynamic evolution was favorable (LV ejection fraction of 65%), the inotropic therapy being stopped in the first postoperative day. Despite the progressive clinical improvement, without a difference in BP between the upper and lower extremity (right upper limb BP 90/46 mmHg, left lower limb BP 80/40 mmHg) his systemic BP remained

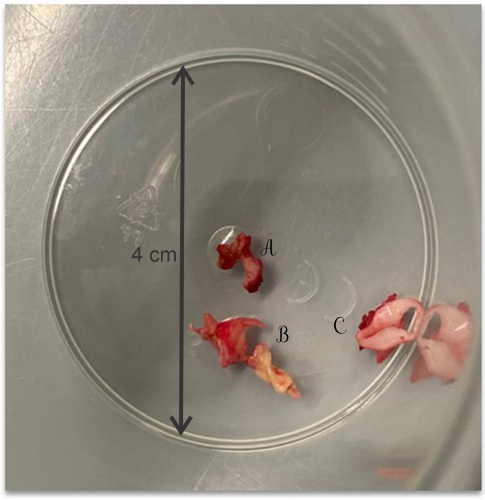

FIGURE 2
The calcified mass extracted intraoperatively from the left subclavian artery **(A)**, the aortic arch **(B)**, and the left common carotid artery **(C)**.

high (110–115 mmHg), and beta blocker therapy (Propranolol 1 mg/kg/day) was started. Postoperative echocardiography showed the brightness and the abnormal echogenicity of the walls of the aortic arch and descending aorta and calcified residual masses at the level of the aortic arch, with a 9 mm extension to the brachiocephalic trunk (BT), LCCA, LSA, with laminar color Doppler flow in the aorta (**Figures 1D–F**). The presence of ectopic calcification in the aorta was not appreciated preoperatively. Both preoperative ultrasound images and CT acquisitions were retrospectively reviewed (**Figure 3**).

Extended areas of increased echogenicity (compatible with calcifications) throughout the aortic arch extending into BT, LCCA, LSA, and descending aorta with severe narrowing of the aorta were noted (**Figures 3A,B**). To further elucidate the extent of the calcifications, whole-body CT scan was performed postoperatively, which detected diffuse areas of residual calcifications in the aortic arch, BT and LCCA without obstruction. No arterial calcifications were detected on the CT scan of the abdomen and head. Moreover, a histological exam of the calcified mass extracted intraoperatively was performed. This investigation highlighted a thickening of the vascular structure with fibrointimal proliferation and areas of nodular calcification and no histological appearance of thrombus. Parathyroid hormone, vitamin D3, calcium and phosphorus serum levels were normal (**Table 1**).

Genetic investigation

The combination of vascular hyperechogenicity, severe aortic calcification with critical obstruction of the aortic arch mimicking CoA, and arterial hypertension determined us to consider GACI as a possible underlying etiology. The whole exome sequencing using Illumina HiSeq PE150 platform and SureSelect Human All Exon V6 kit was performed. The analysis of the results revealed the homozygous variant genotype for c.*1896C > A* (p. His632Gln) in exon 15 of the *ABCC6* gene. Also, the sequencing data analysis did not reveal any mutation in *ENPP1* gene. Furthermore, the molecular screening for thrombophilia revealed: methylene-tetrahydro-folate-reductase mutations (*MTHFR*)-heterozygous genotype *c.1298A > C*, and plasminogen activator inhibitor 1 (*PAI-1*)- heterozygous 4G/5G polymorphism.

Pharmacotherapy and follow-up

Treatment with bisphosphonate was started. Zoledronic acid was administrated intravenously 0.025 mg/kg once every 3 months.

At the age of 3-months, his clinical course was complicated by aortic re-coarctation. The clinical exam revealed a grade III/IV systolic murmur with interscapulovertebral irradiation, bilateral absence of femoral pulse and a 20 mmHg BP difference between the upper and lower extremity (right upper limb BP 127/72 mmHg, left lower limb BP 105/60 mmHg). Echocardiography revealed a significant narrowing of the aortic isthmus (**Figures 1G–I**). CT scan confirmed the aortic re-coarctation and showed improvement of his residual aortic arch calcifications (**Figures 3C,D**). The infant underwent a prosthetic patch aortoplasty to enlarge the site of re-coarctation.

During the follow-up period, continuous monitoring with serial echocardiography was performed, emphasizing the reduction in size of aortic calcifications, especially at the level of BT. The child was re-admitted every 3 months for regular Zoledronic acid infusions. Antihypertensive medication was continued with regular blood pressure monitoring.

At the age of 18-months, the infant had normal growth and development; the BP was well controlled with Propranolol, without BP difference between the upper and lower extremity (right upper limb BP 100/61 mmHg, left lower limb BP 94/55 mmHg). Echocardiography showed that the vascular calcifications of the aortic arch and its branches were still present but were not progressing (**Figures 1J–L**), however, CT scan confirmed the regression of the aortic arch calcifications without stenosis (**Figures 3E,F**). There was no evidence of complications of his early calcification or of the bisphosphonate therapy.

Results and case interpretation

The newborn we report was not initially clinically suspected of having GACI, considering that the preoperative clinical manifestations overlapped with the clinical course of severe

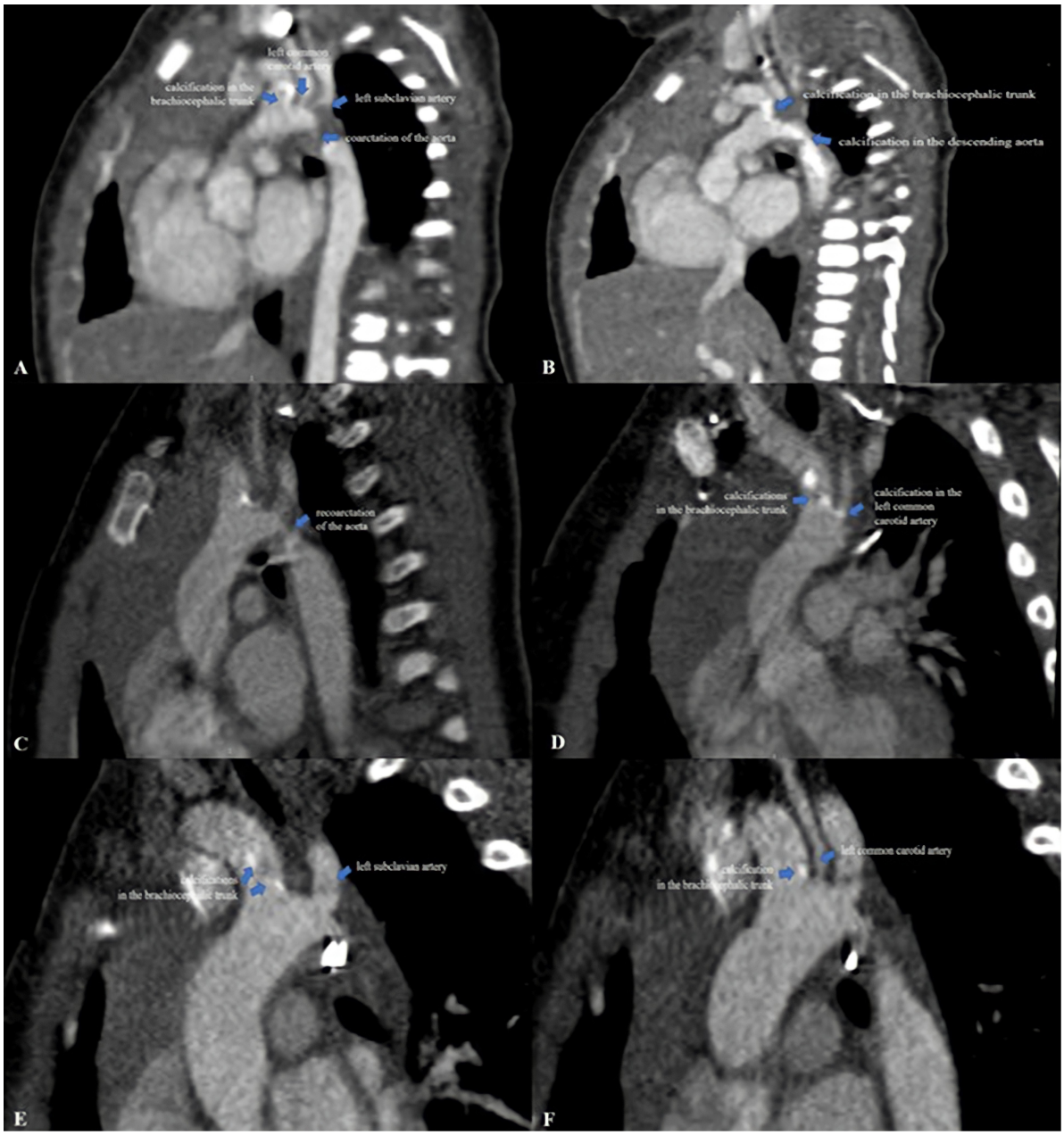

FIGURE 3
(A,B) Computed tomography images from the neonatal period showing extensive ectopic calcifications in the aortic arch, brachiocephalic trunk, left common carotid artery, left subclavian artery and descending aorta with severe narrowing of the aorta mimicking coarctation of the aorta. Note the brightness of the walls of the aortic arch and descending aorta; **(C,D)** computed tomography images at 3-months of age showing re-coarctation of the aorta and residual calcifications in the brachiocephalic trunk and left common carotid artery without obstruction; **(E,F)** computed tomography images at 18-months of age showing the regression of the aortic arch calcifications without stenosis.

CoA with restrictive PDA and systemic hypertension. Increased echogenicity of the aortic arch and its branches was not noted preoperatively by echocardiography and CT scan. Postoperatively, after the partial removal of the obstructive calcified plaque from the aortic arch, the increased echogenicity of the aortic arch and the residual calcifications could be much better appreciated by echocardiography. The combination of clinical features and extensive calcification of the aortic arch and its branches revealed on imaging and intraoperatively, together with histopathological findings and genetic testing confirmed the diagnosis of GACI-2 with severe early-onset manifestations. Although the main manifestations of GACI are widespread calcification of the aorta and its branches, including the aortic arch, the significant calcified plaques deposited in the aortic

10.3389/fcvm.2022.1032519

TABLE 1 The values of calcium and phosphate before and after bisphosphonate treatment.

Treatment	Calcium (mmol/L)	Phosphate (mmol/L)
Before treatment	2.72	2.17
After treatment	2.72	1.9

arch obstructing systemic flow and mimicking CoA presented in our case have not been previously described. Genetic testing of our patient revealed a variant in *ABCC6* gene reported in ClinVar database as a benign variant (9). This single nucleotide variant (SNV) is located in functional MRP6_HUMAN domain and, in a previous study, Le Saux et al. revealed that the missense mutations identified were considered pathogenic (10). The frequency of this SNV in European population is 0.4907, according to gnomAD database (11). This SNV identified determine, in 632 protein sequence, the substitution of glutamine with histidine, and according to UniProt database, this amino acid substitution is associated with pseudoxanthoma elasticum (PXE) (12). Furthermore, another study identified this SNV as a neutral (non-disease-causing) variant in patients with PXE (9). The analysis of the pathogenicity scores for *c.1896C > A* in prediction platforms established a benign predictor effect according to EIGEN, EIGEN PC, a tolerated prediction according to DEOGEN2, LIST-S2, SIFT, and a damaging prediction according to FATHMM. Therefore, the variant identified in our case is classified as a variant of uncertain significance (VUS) according to the American Collage of Medical Genetics Classification: PS1, PM1, PP2, PP5, BA1, BP4, BP6. Using applied bioinformatic tools it was performed *in silico* analysis based on algorithms which analyze the DNA and protein sequence substitution (Poly-Phen2, PhD-SNP, SNPs&Go). The functional effect of the identified SNV in our case was predicted to be benign. To our knowledge this variant has not previously been reported in association with GACI.

In our case, both the surgical treatment of the cardiovascular complication and the medical therapy with bisphosphonates had favorable outcomes; the patient successfully survived infancy without heart failure and with systemic hypertension under effective control. Zoledronic acid, a potent nitrogen(N)-containing-bisphosphonate, was administrated intravenously, 0.025 mg/kg once every 3 months, in accordance with the recommendations for use of bisphosphonates in pediatrics (13). At the time of this report, the patient is 18-months old, still under treatment with intravenously Zoledronic acid; CT scan and ultrasound showed a significant regression of aortic arch calcifications (0.5 mm from 9 mm at the level of BT) without stenosis. No side effects of long-term administration of bisphosphonates were detected.

Informed consent was obtained from the parents of the patient, and this case report was approved by the Ethics Committees of the Institute of Cardiovascular Diseases and Transplantation (permission number: 7718/14.10.2020).

Discussion

Ectopic mineralization is defined by the aberrant deposition of calcium-phosphate complexes in tissues, and particularly in blood vessels (14). Vascular calcification is a major cause of morbidity and mortality (15). The pathophysiology of the ectopic mineralization is poorly understood. In recent decades, improvements have been made in understanding the pathophysiological mechanisms, revealing that vascular calcification can be the consequence of both a high-calcium (Ca) and high-phosphorous (P) milieu and very well-organized biological processes, including an imbalance between osteochondrogenic signaling and anti-calcific events (15). Failure of anti-calcification processes due to loss or deficiency of mineralization inhibitors leads to vascular calcification (15). Inorganic pyrophosphate (PPi) is known as an endogenous inhibitor of biomineralization. Extracellular pyrophosphate is synthesized from extracellular ATP and has the role of preventing the formation and deposition of hydroxyapatite crystals. *ENPP1* and *ABCC6* are plasma membrane-associated proteins involved in PPi synthesis (4). *ENPP1* is the principal enzyme that generates PPi from ATP hydrolysis; *ABCC6* works upstream of *ENPP1* by mediating release of ATP (16). Mutations in the genes encoding these enzymes reduce the plasma concentration of PPi, resulting in reduced PPi (antimineralization factor)/Pi (inorganic phosphate: promineralization factor), which stimulates ectopic mineralization of the arterial vessels and other tissues (15). In children, there are two major prototypes of such disorders that associate spontaneous pathological arterial calcifications: PXE, a late-onset, slowly progressing disease with multisystemic clinical manifestations, and GACI, a more severe disease characterized by early-onset mineralization of the cardiovascular system.

Generalized arterial calcification of infancy is a rare autosomal recessive disorder characterized by congenital calcification of large and medium sized arteries. The calcification of arterial structures is initiated in the internal elastic lamina and extends into the intima and media, being accompanied by fibrous thickening of the intima, which causes luminal narrowing (17). There are two forms of GACI. In most cases (67%), causal mutations have been identified in the genes *ENPP1*(GACI-1) (1). There are many studies reporting the mutations in ENPP1 in patients with GACI (2, 4, 17–20). In 9% of cases, GACI results from biallelic inactivating variants in *ABCC6* (GACI-2) (1). Mutations in *ABCC6* typically cause PXE. Nitschke et al. studying 92 patients with severe, early-onset arterial calcification, identified biallelic pathogenic mutations in *ENPP1* in 62 patients and *ABCC6* mutations in 14 patients. Biallelic mutations in *ABCC6* were found in 8 cases of typical GACI that presented widespread calcifications of the aorta and coronary arteries; additionally, in six patients with critical GACI, monoallelic *ABCC6* mutations were detected. Thirteen different mutations in *ABCC6* were identified. Furthermore, it

has been suggested that there is a genotype-phenotype overlap between GACI and PXE (21). Ferreira et al. reported the results of clinical, laboratory and molecular evaluations of 20 subjects with GACI who survived infancy; they identified 16 biallelic *ENPP1* variants and 6 *ABCC6* variants; the patients with *ABCC6* variants did not differ in the frequency or location of ectopic calcification compared with those having *ENPP1* variants (1). Further evidence of genetic heterogeneity in the pathogenesis of GACI is based on identification of affected individuals who lack variants in either *ENPP1* or *ABCC6* (1, 21). While it is widely recognized that individuals with pathogenetic variants in *ENPP1* or *ABCC6* can manifest GACI, there is evidence that associateVUS with the GACI phenotype (22). Mahajan et al. reported two VUS located on chromosome *20q11.21* and *16p11.2* in a patient with GACI (22). In our case, the whole genome sequencing analysis revealed homozygous variant genotype for c.1896C > A of *ABCC6* gene. This SNV has been reported in *ABCC6* initially in 2001 as a neutral (non-disease-causing) variant in both heterozygous and homozygous states in a cohort of 122 patients with PXE (10). To our knowledge, this variant has not previously been reported in association with GACI phenotype.

Diagnosis of GACI is suspected based on clinical and imaging findings. A definitive diagnosis involves identification of variants in *ENPP1* or *ABCC6* and/or typical histopathological findings. The clinical spectrum of the disease varies widely. The most affected arteries are the aorta, coronary, pulmonary, cerebral, mesenteric, and renal arteries. Early-onset disease (48% of cases) presents variably with fetal distress, severe heart failure, respiratory distress, pulmonary hypertension, and systemic hypertension and refers to cases that occur in the fetal period or within 1 month of birth (6, 23). Presentation of late-onset disease (52% of cases) refers to cases where the onset is 1 month after birth and the clinical manifestations include respiratory failure, congestive heart failure, vomiting, feeding difficulties, irritability, failure to thrive, fever, hypertension, and edema (6, 23). Nearly half of all children with GACI are diagnosed during infancy (4, 24). Prenatal diagnosis is extremely rare and should be suspected when there is evidence of polyhydramnios or a history of early neonatal death or when increased echogenicity is observed along large vessels by fetal ultrasound (4, 25). A small number of prenatally diagnosed cases of GACI have been reported in the literature (26, 27). In our case, antenatal ultrasonography did not reveal any abnormalities.

Generalized arterial calcification of infancy should be considered in infants with signs of congestive heart failure, myocardial ischemia, severe systemic hypertension, respiratory failure (4, 28). The diagnosis involves high index of suspicion. Limited awareness of this disease and low suspicion by physicians make early diagnosis rare. Cases clinically suspicious for GACI can be confirmed with imaging studies, arterial biopsy, and genetic analysis (29). Imaging investigations are extremely useful in the clinical diagnosis of GACI by identifying increased echogenicity of arterial walls and vascular narrowing. While echocardiography is useful, it may not provide a definitive diagnosis and additional imaging techniques such as whole-body CT scan combined with CT angiography are usually necessary to assess the extent of calcifications and stenoses in the arteries. Several clinical reports have shown extensive calcifications and narrowing of the aortic arch and descending aorta, but no case developed severe obstruction (20, 22, 23). The severe phenotype of GACI mimicking CoA presented in our case have not been previously described.

The prognosis of GACI patients is poor, the greatest number of deaths occurring within the first 6 months; most infants die from severe, rapidly progressive heart failure or myocardial infarction. Only a few cases of survivors into later childhood or adulthood are reported (30–32). O'Brien et al. evaluated the lifelong impact of *ENPP1* deficiency and the early onset form of *ABCC6* deficiency from a patient or caregiver perspective and concluded that these morbidities are debilitating diseases with lifelong morbidity, including pain and impaired mobility, and those who are affected experience impairment of quality of life and psychosocial issues throughout life (33).

Early appropriate diagnosis would allow treatment and is associated with a higher survival rate. There are no guidelines for GACI treatment. In recent years, basic science has elucidated the molecular pathway and mechanisms involved in PXE, which has led to rapid advances in the development of many potential therapeutic options for PXE and GACI (34). The therapeutic solutions target various steps in the *ABCC6* pathway with the goal of either slowing or reversing the progression of the disease. Two main categories of therapeutic solutions have been proposed, most of them have been tested in pre-clinical animal models and a few early clinical trials. The first therapeutic strategy targets correction, replacement, or inhibition of dysfunctional genes/proteins [*ABCC6*, ectonucleotides (NPP1) and tissue non-specific alkaline phosphatase (TNAP)] (34). Nitschke et al. concluded that ENPP1 enzyme replacement by subcutaneous administration of the rhENPP1-Fc protein [recombinant human (rh)ENPP1-Fc protein] may influence vascular smooth muscle cells proliferation and may serve as an approach for effective prevention and treatment of arterial stenosis in GACI (35). The second therapeutic strategy targets direct inhibition of calcification *via* supplementation by various compounds: magnesium (inhibits the formation of apatite), vitamin K (correct for insufficient carboxylation of matrix gla protein), bisphosphonates (inhibit enzymes that utilize pyrophosphate), pyrophosphate (potent inhibitor of calcification, *ABCC6* modulates PPi production), phytic acid (inhibitor of calcification), sodium thiosulfate (approved for calciphylaxis) (34).

Bisphosphonates are PPi analogs and have been shown to decrease phosphate levels, increase parathormone levels and

cause stabile levels of calcium (36). Bisphosphonates have been used clinically for decades in treatment of osteoporosis, Paget's disease of bone, and osteogenesis imperfecta (34). The results of bisphosphonate therapy in GACI are variable, spontaneous resolution of calcifications on CT scan or echocardiography has occasionally been reported, but the long-term prognosis in survivors is not described (5, 37). In their retrospective study, Rutsch et al. reported that bisphosphonate therapy was associated with survival in 11 (65%) of 17 treated patients whereas 69% of the patients not treated with bisphosphonates died (38). Ramjan et al. reported complete resolution of arterial calcification with the long-term usage of bisphosphonates (39). Weingarten et al. recently reported the favorable therapeutic response in a case of GACI using an innovative therapeutic plan including bisphosphonate (Pamidronate), Acetazolamide (increase urinary excretion of phosphate) and Similac PM 60/40 (a low calcium and phosphate formula) (37). Yunfeng et al. reported the case of a preterm infant with GACI and concluded that the treatment with oral phosphonates is expected to improve the long-term prognosis (23).

There are two categories of bisphosphonates based on the presence of a non-nitrogenous or nitrogenous side chain. Etidronate is a non-nitrogen(N)-containing-bisphosphonate whose antiresorptive potency is at the lower end of the scale, while Pamidronate, Alendronate, Risedronate and Zoledronic acid are more potent N-containing-bisphosphonates. Furthermore, N-containing-bisphosphonates usually increase bone density, demonstrating a better antifracture efficacy (34). Etidronate has been used to treat GACI patients and early treatments improved GACI outcomes. Prolonged Etidronate use in GACI patients has been associated with severe skeletal toxicity, radiographic findings resembling osteoporosis or hypophosphatemia (40). It remains unclear whether bisphosphonates, Etidronate in particular, are associated with improved survival (41).

Zoledronic acid is being developed as an intravenous therapy and has the highest affinity for hydroxyapatite and the longest duration of action. Mixed results associated with Zoledronic acid treatment have been reported. Synetos et al. in an experimental model of aortic stenosis, concluded that the inhibition of aortic valve calcification by local delivery of Zoledronic acid was feasible and effective, without evident short-term complications (42). Cai et al. demonstrated that once-yearly Zoledronic acid did not affect progression of abdominal aortic calcification over 3 years in postmenstrual women with osteoporosis (43). The anti-calcification properties of Zoledronic acid for PXE have been reported in an *in vitro* series of experiments with primary fibroblasts (44). Intravenous Zoledronic acid or Pamidronate are the treatment of choice in patients with moderate-to-severe osteogenesis imperfecta (45). In our case, we opted for the treatment with Zoledronic acid considering the severe phenotype of the disease as well as the superior pharmacokinetics of this N-bisphosphonate, which is essential for optimal clinical outcomes and minimalization of the risk of adverse effects.

Deshpande et al. published the first report of successful mechanical support in a patient with GACI, additionally, over time with bisphosphonate therapy, there was a remarkable recovery of cardiac function (46). Giovannoni et al. reported an 18-month-old child with GACI and end-stage myocardial ischemia who underwent successful heart transplantation (47). Although Samyn et al. reported the first case of successful cardiac surgery in a child with severe pulmonary valve stenosis and GACI (48, 49), until now no one has reported surgical treatment for associated severe obstruction of the aortic arch in a newborn with GACI. In our case, both the surgical treatment of the cardiovascular complication and the medical therapy with Zoledronic acid had favorable outcomes. The patient successfully survived infancy with systemic hypertension under effective control, without bone or joint modifications, no signs of heart failure and significant regression of aortic arch calcifications on imaging.

Conclusion

Our case highlights the importance of considering GACI in an infant with heart failure, systemic hypertension, and evidence of increased echogenicity of the arterial vessels on imaging. Early diagnosis and treatment improve the long-term prognosis. We noted the favorable outcome in improving the aortic calcification in our patient after surgical treatment of the severe aortic arch obstruction by calcified plaques and bisphosphonates therapy. Furthermore, we report the identification of a variant in *ABCC6* gene, possibly associated with severe early-onset manifestations of GACI mimicking severe CoA. A better understanding of this rare genetic disease and further evidence of genetic heterogeneity both by identifying affected individuals who lack variants in either ENPP1 or ABCC6 and elucidating possible genes involved in this condition could lead to new therapeutic strategies.

Data availability statement

The original contributions presented in the study are publicly available. This data can be found at the European Nucleotide Archive, accession number: PRJEB57858.

Author contributions

CŞ: writing – original draft preparation. CŞ, LG, and AC: writing – review and editing. S-EG, MM, and MP: visualization. AF: supervision. DM: performing and interpreting genetic

testing. All authors read and agreed to the published version of the manuscript.

Conflict of interest

The authors declare that the research was conducted in the absence of any commercial or financial relationships that could be construed as a potential conflict of interest.

Publisher's note

References

1. Ferreira CR, Hackbarth ME, Ziegler SG, Pan KS, Roberts MS, Rosing DR, et al. Prospective phenotyping of long-term survivors of generalized arterial calcification of infancy (GACI). *Genet Med.* (2021) 2:396–407. doi: 10.1038/s41436-020-00983-0

2. Mulcahy CH, Mone F, McAuliffe FM, Mooney E, McParland P, Mc Mahon CJ. Antenatal diagnosis of idiopathic infantile arterial calcification (IIAC): a single centre experience and review of the literature. *J Cong Cardiol.* (2019) 3:1. doi: 10.1186/s40949-018-0022-1

3. Bryant JH, White WA. A case of calcification of the arteries and obliterative endarteritis associated with hydronephrosis in a child aged 6 months. *Guys Hosp Rep.* (1901) 55:17–28.

4. Attia TH, Abd Alhamed MM, Selim MF, Haggag MS, Fathalla D. Idiopathic arterial calcification of infancy: case report. *Pediatirc Radiol Radiol Case.* (2015) 9:32–40. doi: 10.3941/jrcr.v9i11.2622

5. Bulfamante GP, Carpenito L, Bragantini E, Graziani S, Bellizzi M, Bagowski CP, et al. Generalized arterial calcification of infancy type 1 (GACI1): identification of a novel pathogenic variant (c.1715T>C (p. Leu572Ser)). *Diagnostics (Basel).* (2021) 11:1034. doi: 10.3390/diagnostics11061034

6. Nitschke YV. *Generalized Arterial Calcification of Infancy*. (2019). Available online at: https://www.orpha.net/51608 (accessed April 2019).

7. Sadeghi R, Khodaei S, Ganame J, Keshavarz-Motamed Z. Towards non-invasive computational-mechanics and imaging-based diagnostic framework for personalized cardiology for coarctation. *Sci Rep.* (2020) 10:9048. doi: 10.1038/s41598-020-65576-y

8. Rafieianzab D, Abazari MA, Soltani M, Alimohammadi M. The effect of coarctation degrees on wall shear stress indices. *Sci Rep.* (2021) 11:12757. doi: 10.1038/s41598-021-92104-3

9. ClinVar. (2022) Available online at: https://www.ncbi.nlm.nih.gov/clinvar/variation/433247/ (accessed August 08, 2022)

10. Le Saux O, Beck K, Sachsinger C, Silvestri C, Treiber C, Göring HH, et al. A spectrum of ABCC6 mutations is responsible for pseudoxanthoma elasticum. Am J Hum Genet. 2001 Oct;69(4):749-64. Epub 2001 Aug 31. Erratum in: Am J Hum Genet;69(6):1413. *Erratum Am J Hum Genet.* (2001) 71:448. doi: 10.1086/323704

11. gnomAD. (2022). Available online at: https://gnomad.broadinstitute.org/variant/16-16278863-G-T?dataset=gnomad_r2_1 (accessed August 08, 2022).

12. UniProt. (2022). Available online at: https://www.uniprot.org/uniprotkb/O95255/entry (accessed August 08, 2022).

13. Baroncelli GI, Bertelloni S. The use of bisphosphonates in pediatrics. *Horm Res Paediatr.* (2014) 82:290–302. doi: 10.1159/000365889

14. Uitto J, Qiaoli L.). Vascular mineralization in Pseudoxanthoma elasticum. Etidro-nate to the rescue? *J Am Coll Cardiol.* (2018) 10:1127–9. doi: 10.1016/j.jacc.2018.01.018

15. Lee SJ, Jae-Han J. Vascular calcification-new insights into its mechanism. *Int J Mol Sci.* (2020) 21:1–32. doi: 10.3390/ijms21082685

16. Li Q, van de Wetering K, Uitto J. Pseudoxanthoma elasticum as a paradigm of heritable ectopic mineralization disorders. *Am J Pathol.* (2019) 189:216–25. doi: 10.1016/j.ajpath.2018.09.014

17. Yapıcıoğlu-Yıldızdaş H, Özbarlas N, Erdem S, Yılmaz MB, Özlü F, Büyükkurt S, et al. Two newborn babies with generalized arterial calcification of infancy, two new mutations. *Turkish J Pediatr.* (2016) 58:419–23. doi: 10.24953/turkjped.2016.04.013

18. Rutsch F, Ruf N, Vaingankar S, Toliat MR, Suk A, Höhne W, et al. Mutations in ENNP1 are associated with "idiopathic" in-fantile arterial calcification. *Nat Genet.* (2003) 34:379–81. doi: 10.1038/ng1221

19. Lorenz-Depiereux B, Schnabel D, Tiosano D, Häusler G, Strom TM. Loss-of-function ENPP1 mutations cause both generalized arterial calcification of infancy and autosomal-recessive hypophos-phatemic rickets. *Am J Hum Genet.* (2010) 86:267–72. doi: 10.1016/j.ajhg.2010.01.006

20. James CA, Powers S, Bloom DA, Maisels MJ. Generalized arterial calcification of infancy. *J Pediatr Neonatal Biol.* (2019).

21. Nitschke Y, Baujat G, Botschen U, Wittkampf T, du Moulin M, Stella J, et al. Generalized arterial calcification of infancy and pseudoxanthoma elasticum can be caused by mutations in either ENPP1 or ABCC6. *Am J Hum Genet.* (2012) 90:25–39. doi: 10.1016/j.ajhg.2011.11.020

22. Mahajan V, Sahni M, Dasgupta S, Amyn J, Jain SK (2019). Idiopathic Calcification of Infancy-case report, and re-view of literature. *J Pediatr Child Care.* 2:5.

23. Yunfeng L, Tongyan H, Jing W, Xiaomei T. Case report: a novel genetic mutation causes idio-pathic infantile arterial calcification in preterm infants. *Front Genet.* (2021) 12:763916. doi: 10.3389/fgene.2021.763916

24. Chong CR, Hutchins GM. Idiopathic infantile arterial calcification: the spectrum of clinical presentation. *Pediatric Dev Pathol.* (2008) 11:405–15. doi: 10.2350/07-06-0297.1

25. Donuru A, Kandula V, Oliver E, Saul D. Generalized arterial calcification of infancy. *Radiol Cardiothoracic Imaging.* (2020) 2:e190226. doi: 10.1148/ryct.2020190226

26. Nasrallah FK, Baho H, Sallout A. Prenatal diagnosis of idiopathic infantile arterial calcification with Hydrops fetalis. *Ultrasound Obstet Gynecol.* (2009) 34:601–4. doi: 10.1002/uog.7438

27. Gowda M, Popa D, Sagili H. Prenatal diagnosis of idiopathic infantile arterial calcification: a lethal heritable condition. *Austin J Clin Case Rep.* (2016) 3:1086. doi: 10.1007/s40556-016-0086-y

28. Li Q, Brodsky JL, Conlin LK, Pawel B, Glatz AC, Gafni RI, et al. Mutations in the ABCC6 gene as a cause of general ar-terial calcification in infancy- genotypic overlap with pseudoxanthoma elasticum. *J In-vest Dermatol.* (2014) 134:658–65. doi: 10.1038/jid.2013.370

29. Nael A, Siaghani PJ, Chen D, Romansky SG, Shane L. Idiopathic infantile arterial calcification: a possible cause of refractory cardiopulmonary failure in infancy. *Case Rep Pathol.* (2014) 2014:ID189850. doi: 10.1155/2014/189850

30. Ciana G, Trappan A, Bembi B, Benettoni A, Maso G, Zennaro F, et al. Generalized arterial calcification of infancy: two siblings with prolonged survival. *Eur J Pediatr.* (2006) 165:258–63. doi: 10.1007/s00431-005-0035-6

31. Patel M, Andronikou S, Solomon R, Sinclair P, McCulloch M. Idiopathic arterial calcification in childhood. *Pediatr Radiol.* (2004) 34:652–5. doi: 10.1007/s00247-004-1166-z

32. Van der Sluis IM, Boot AM, Vernooij M, Meradji M, Kroon AA. Idiopathic infantile arterial calcification: clinical presentation, therapy and long-term follow-up. *Eur J Pediatr.* (2006) 165:590–3. doi: 10.1007/s00431-006-0146-8

33. O'Brien C, Khursigara G, Huertas P, Leiro B, Molloy L, Nester C. Lifelong impact of ENPP1 deficiency and the early onset form of ABCC6 deficiency from patient or caregiver perspective. *PLoS One.* (2022) 17:e0270632. doi: 10.1371/journal.pone.0270632

34. Shimada BK, Pomozi V, Zoll J, Kuo S, Martin L, Le Saux O. ABCC6, pyrophosphate and ectopic calcification: therapeutic solutions. *Int J Mol Sci.* (2021) 22:4555. doi: 10.3390/ijms22094555

35. Nitschke Y, Yan Y, Buers I, Kintziger K, Askew K, Rutsch F. ENPP1-Fc prevents neointima formation in generalized arterial calcification of infancy through the generation of AMP. *Exp Mol Med.* (2018) 50:1–12. doi: 10.1038/s12276-018-0163-5

36. Omarjee L, Nitschke Y, Verschuere S, Bourrat E, Vignon MD, Navasiolava N, et al. Severe early-onset manifestations of pseudoxan-thoma elasticum resulting from the cumulative effects of several deleterious muta-tions in ENPP1, ABCC6 and HBB: transient improvement in ectopic calcification with sodium thiosulfate. *Br J Dermatol.* (2020) 183:367–72. doi: 10.1111/bjd.18632

37. Weingarten, AJ, Muller A, Langman C, Groner A. Novel and successful treatment of generalized ar-terial calcification of infancy in a patient with previously undescribed mutation in ENPP1. *Prog Pediatr Cardiol.* (2021) 66:101466. doi: 10.1016/j.ppedcard.2021.101466

38. Rutsch F, Böyer P, Nitschke Y, Ruf N, Lorenz-Depierieux B, Wittkampf T, et al. Hypophosphatemia, hyperphosphaturia, and bisphosphonate treatment are associated with survival beyond infancy in generalized arterial calcification of infancy. *Circ Cardiovasc Genet.* (2008) 1:133–40. doi: 10.1161/CIRCGENETICS.108.797704

39. Ramjan KA, Roscioli T, Rutsch F, Sillence D, Munns CF. Generalized arterial calcification of infancy: treatment with bisphosphonates. *Nat Rev Endocrinol.* (2009) 5:167–72. doi: 10.1038/ncpendmet1067

40. Otero JE, Gottesman GS, McAlister WH, Mumm S, Madson KL, Kiffer-Moreira T, et al. Severe skeletal toxicity from protracted etidronate therapy for generalized arterial calcification of infancy. *J Bone Miner Res.* (2013) 28:419–30. doi: 10.1002/jbmr.1752

41. Ziegler SG, Gahl WA, Ferreira CR. Generalized arterial calcification of infancy. In: Adam MP, Mirzaa GM, Pagon RA, et al. editors. *GeneRe-views® [Internet]*. Seattle, WA: University of Washington, Seattle (2014). p. 1993–2022.

42. Synetos A, Toutouzas K, Drakopoulou M, Koutagiar I, Benetos G, Kotronias R, et al. Inhibition of aortic valve calcification by local de-livery of zoledronic acid-an experimental study. *J Cardiovasc Transl Res.* (2018) 11:192–200. doi: 10.1007/s12265-018-9802-4

43. Cai G, Keen HI, Host LV, Aitken D, Laslett LL, Winzenberg T, et al. Once yearly zoledronic acid and change in abdominal aortic calcification over 3 years in postmenopausal women with osteoporosis: results from the HORIZON pivotal fracture trial. *Osteoporos Int.* (2020) 1:1741–7. doi: 10.1007/s00198-020-05430-z

44. Dabisch-Ruthe M, Kuzaj P, Götting C, Knabbe C, Hendig D. Pyrophosphates as a major inhibitor of matrix cal-cification in pseudoxanthoma elasticum. *J Dermatol Sci.* (2014) 75:109–20. doi: 10.1016/j.jdermsci.2014.04.015

45. Simm PJ, Biggin A, Zacharin MR, Rodda CP, Tham E, Siafarikas A, et al. Consensus guidelines on the use of bisphosphonate therapy in children and adolescents. *J Paediatr Child Health.* (2018) 54:223–33. doi: 10.1111/jpc.13768

46. Deshpande SR, Kasniya G, Cuadrado AR, Maher KO. Idiopathic infantile arterial calcification: a case report of successful extracorporeal membrane oxygenation support. *Int J Artif Organs.* (2016) 39:575–9. doi: 10.5301/ijao.5000544

47. Giovannoni I, Callea F, Travaglini L, Amodeo A, Cogo P, Secinaro A, et al. Heart transplant and 2-year follow up in a child with generalized arterial calcification of infancy. *Eur J Pediatr.* (2014) 173:1735–40. doi: 10.1007/s00431-014-2447-7

48. Samyn MM, Bick D, Humphrey JA, Gandy KL. Successful congenital heart surgery for a toddler with idiopathic infantile arterial calcification. *Pediatr Cardiol.* (2010) 31:1096–9. doi: 10.1007/s00246-010-9747-0

49. Abazari, MA, Rafieianzab D, Soltani M, Alimohammadi M. The effect of beta-blockers on hemodynamic parameters in patient-specific blood flow simulations of type-B aortic dissection: a virtual study. *Sci Rep.* (2021) 11:16058. doi: 10.1038/s41598-021-95315-w

frontiers | Frontiers in Cardiovascular Medicine

TYPE Case Report
PUBLISHED 06 January 2023
DOI 10.3389/fcvm.2022.1042631

OPEN ACCESS

EDITED BY
Sergei I. Bannykh,
Cedars-Sinai Medical Center,
United States

REVIEWED BY
Nikhil Agrawal,
The University of Texas Health Science Center at Houston, United States
Neelam Kaistha,
All India Institute of Medical Sciences, India

*CORRESPONDENCE
Jinlan Chen
✉ jinlanchen@csu.edu.cn

SPECIALTY SECTION
This article was submitted to Pediatric Cardiology, a section of the journal Frontiers in Cardiovascular Medicine

RECEIVED 12 September 2022
ACCEPTED 13 December 2022
PUBLISHED 06 January 2023

CITATION
Zhuang H, Xiang K, Gong S, Zhou Y and Chen J (2023) Cerebral aspergillosis after heart-lung transplantation in a child: Case report with 3-year follow-up and literature review.
Front. Cardiovasc. Med. 9:1042631.
doi: 10.3389/fcvm.2022.1042631

Cerebral aspergillosis after heart-lung transplantation in a child: Case report with 3-year follow-up and literature review

Huanwei Zhuang[1,3], Kun Xiang[1], Shuji Gong[1], Yangang Zhou[2] and Jinlan Chen[1]*

[1]Department of Cardiovascular Surgery, The Second Xiangya Hospital, Central South University, Changsha, China, [2]Department of Pharmacy, The Second Xiangya Hospital, Central South University, Changsha, China, [3]Department of Cardiac Surgery, Haikou Affiliated Hospital of Central South University Xiangya School of Medicine, Haikou, China

There are limited cases of heart-lung transplantation (HLT) in children worldwide owing to lack of donors, demanding surgical teamwork, and arduous post-operative management. Post-transplant management difficulties stem from the possible development of several post-operative complications, with infection being a common complication. Intracranial fungal infections are difficult to diagnose and prone to treatment delays because of their relatively insidious onset and atypical clinical presentation. Here, we present a case of a cerebral infection developed 3 months after HLT in a 10-year-old child, showing no positive results on conventional imaging or cerebrospinal fluid (CSF) examination and culture. On metagenomic next-generation sequencing of the cerebrospinal fluid, the causative organism was finally determined as *Aspergillus*. After administering 1-year anti-*Aspergillus* treatment, no recurrence of intracranial fungal infection was noted during the 3-year follow-up. This case illustrates the multifaceted diagnostic techniques for cerebral aspergillosis after HLT and shows the significance of dynamic monitoring of symptoms, such as headache, and of metagenomic sequencing results, trends in intracranial pressure and (1-3)-β-D-glucan levels for guiding diagnosis and treatment.

KEYWORDS

heart-lung transplantation, intracranial infection, *Aspergillus*, metagenomic next-generation sequencing (mNGS), voriconazole

1. Introduction

Heart–lung transplantation (HLT) is the only treatment for certain end-stage cardiopulmonary diseases so far. In 1968, Professor Cooley performed the first human HLT on a 2-month-old infant, who died of pulmonary insufficiency 14 h after the procedure (1). In recent years, the short- or long-term results of HLT have become increasingly more satisfactory due to improvements in donor organ preservation, surgical techniques, and postoperative management as well as advancements in immunosuppressive treatment. However, post-transplant rejection, infections, renal failure, tumors, and other postoperative complications continue to occur and adversely affect quality of life. Infections have become the most prevalent complication due to the administration of immunosuppressive drugs after transplantation. The most common site of infection is the lungs, but intracranial infections are the most insidious and are more challenging to diagnose and treat. Common pathogens that cause infection include bacteria, viruses, and fungi. Compared to invasion by bacteria and viruses, intracranial fungal infections are less common, with *Candida* spp. and *Aspergillus* spp. being predominant (2). However, diagnosing and treating intracranial fungal infections remain challenging in clinical neurology, and routine CSF examination and culture are often negative. The early application of metagenomic next-generation sequencing (mNGS) can help identify the pathogenic organism, ensuring the provision of appropriate treatment. The treatment of post-transplantation intracranial fungal infection includes reduction of immunosuppressive drugs, commencement of standardized medication, and long treatment courses. The monitoring of trends in symptoms, intracranial pressure, mNGS, and biochemical indicators in the CSF can help guide treatment and achieve more favorable outcomes.

2. Case description

Our patient was a 10-year-old girl with complex congenital heart disease identified at birth. Congenital heart malformations included single atrium, single ventricle (functionally a right ventricle), pulmonary artery stenosis, and a persistent left superior vena cava. The child underwent bidirectional Glenn shunt operation and total cavopulmonary connection in March 2010 and June 2013, respectively. Due to end-stage cardiopulmonary failure, the patient finally underwent *in situ* HLT in April 2019. The child was extremely unstable and needed extracorporeal membrane oxygenation (ECMO) when back to ICU from the operating theater, and suffered from functional impairment of multiple organs. When the clinical picture improved, she had bacterial pneumonia and viral septicemia. With the provision of support and protection of organ function as well as the adjustment of immunosuppressants and treatment with anti-infectives, the child fully recovered 2 months later. At 3 months postoperatively, the patient occasionally experienced self-resolving headaches. At that time, intracranial calcification was seen on cranial computed tomography with no other abnormalities. Two weeks later, the patient's headache worsened. A lumbar puncture revealed a CSF pressure of 380 mmH_2O. The CSF tested positive on Pan's test, but negative for *Cryptococcus neoformans* capsular antigen and ink staining, and negative on culture. Accordingly, a preliminary clinical diagnosis of intracranial infection was made.

Further cranial plain magnetic resonance imaging with enhancement, magnetic resonance angiography, and magnetic resonance venography revealed no significant abnormalities. During this period, repeated CSF culture was negative. But CSF manometry showed high levels, and CSF (1-3)-β-D-glucan was positive through G test, which suggested a high probability of an intracranial fungal infection. However, the causative organism was not identified. Testing of the CSF using mNGS revealed a high sequence number relating to *Aspergillus* species (mainly *Aspergillus niger*), thus confirming the diagnosis of cerebral aspergillosis. Regarding treatment, the prednisolone tablets were discontinued to reduce immunosuppression, and the antifungal voriconazole was given. After 4 weeks of voriconazole treatment, the child's headache symptoms did not resolve. There was no significant decrease in CSF pressure, and the patient had persistent positive G test results. A repeated mNGS check showed an increased sequence number of *A. niger*. As monotherapy was deemed ineffective, intravenous amphotericin B was added with supplemental intrathecal administration. After 8 weeks of treatment with voriconazole and amphotericin B, the child's headache gradually resolved and subsequently disappeared. The intracranial pressure gradually decreased to normal, the G test result turned negative, and repeated mGNS tests of the CSF became negative (see **Figure 1** for the specific treatment course). After a 12-week induction period, the amphotericin B was discontinued and maintenance therapy with oral voriconazole alone was administered for 1 year. At the end of the 3-year follow-up, the child had experienced no recurrence of the intracranial infection.

3. Discussion

With recent advancements in HLT and postoperative management, patient survival rates have improved significantly. The current 3-month, 1-year, 3-year, 5-year, and 10-year survival rates are 71, 63, 51, 44, and 31%, respectively (3). More complications are likely to occur associated with these higher survival rates. Possible graft-related complications include early graft dysfunction, acute allograft rejection, and heart graft vascular disease, while possible non-graft-related complications include infection, acute or chronic kidney injury, and malignancy (4).

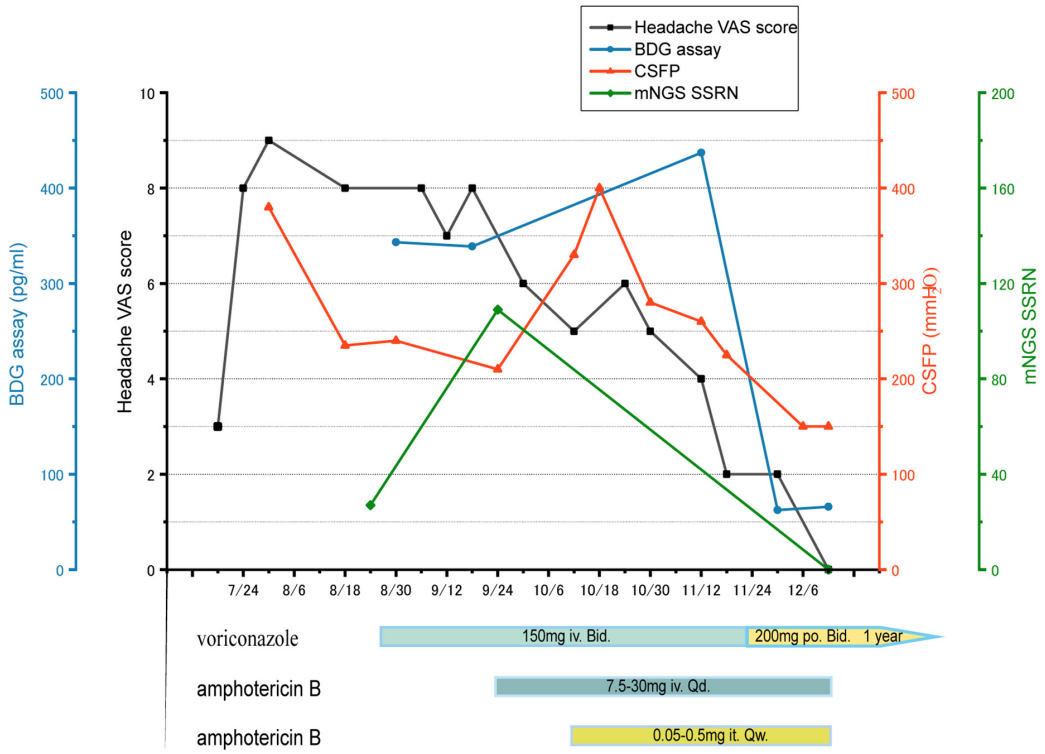

FIGURE 1
Headache VAS score (black), BDG assay (blue), CSFP (orange), mNGS SSRN (green). The treatment course: voriconazole iv for 4 weeks, but both of mNGS SSRN and CSFP increase, so intrathecal and intravenous amphotericin B were added, combined with voriconazole, for 8 weeks. Then voriconazole po for a year. VAS: visual analogue scale, BDG: (1-3)-β-D-glucan, CSFP: cerebrospinal fluid pressure, mNGS: metagenomic next-generation sequencing, SSRN: species-specific read number, iv: intravenous injection, po: *per os*, it: intrathecal injection.

The post-operative management of HLT in children poses great difficulty. Repeated preoperative cardiopulmonary failure may compromise extracardiac organs, including those that mediate immune function. This involvement, combined with the use of post-operative immunosuppressive agents, makes patients highly susceptible to infection. Postoperative infections that occur after solid organ transplantation are typically divided into three stages. Nosocomial infections comprise the majority of them in the early postoperative period, followed by opportunistic infections in the mid postoperative period and community-acquired infections in the late postoperative period (5). Pulmonary infection is the most common nosocomial infection, followed by urinary tract, hematologic, incisional, and intracranial infections. Intracranial infection is also more common after transplantation, and the responsible organisms are primarily bacteria (including even *Mycobacterium tuberculosis*), viruses, and fungi. Fungi that cause intracranial infections are invasive, the most common being caused by *Candida*, then *Aspergillus*, and other genera of fungi such as *Cryptococcus* (6–8). *Aspergillus* is a common causative organism of mycotic infections in humans, and most cases of cerebral aspergillosis are caused by *Aspergillus fumigatus* (6, 8).

Alexander et al. found additional induction immunosuppression, reoperation within 10 days of heart transplant, delayed chest closure and peri-transplant ventricular assist device (VAD) placement were associated with an increased risk of invasive fungal disease (IFD) (9). The risk factors for central nervous system (CNS) aspergillosis include neutropenia, systemic glucocorticoid treatment, mastoidectomy, spinal anesthesia, and paraspinal glucocorticoid injections (10). And risk factors for the development of intracranial fungal infections within 3 months post-transplantation include the use of vasoactive drugs, extended intensive care unit stay, renal failure requiring hemodialysis, and bacterial infection (11). In immunocompromised patients, the fungus often reaches the bloodstream through the respiratory tract and may disseminate to spread to the brain. Intracranial infection may also be caused by the fungus spreading through adjacent structures such as the sinuses, orbits, and mastoid process (12). Intracranial fungal infections in children are uncommon but can be fatal; hence, their early diagnosis and treatment are crucial.

Intracranial fungal infections can present as various clinical syndromes such as meningitis, encephalitis, brain abscess, and even rarely as stroke (7, 13). Clinical

symptoms include nausea, vomiting, headache, fever, confusion, and seizures (6, 14), but all are non-specific. Procedures such as microscopic examination, CSF culture, and histopathological examination of fungal pathogens constitute the gold standard for diagnosis (8, 15). However, CSF culture is time-consuming and has a low sensitivity, and specimens are often difficult to obtain for pathological examinations; thus, CSF analysis and imaging remain the basis for diagnosis. The presence of elevated pressure and protein levels along with decreased glucose levels in the CSF suggest an intracranial infection (13). These markers are important adjuncts to computed tomography and magnetic resonance imaging for the detection of infection and the monitoring of treatment.

Additional antigen analyses have been used to diagnose cerebral aspergillosis and monitor treatment efficacy. The substance (1,3)-β-D-glucan, which is detected using the G test, is a conserved component of the fungal cell wall. The test is indicated for the early diagnosis of all deep fungal infections except those caused by *Cryptococcus* and *Trichophyton,* but not for determining fungal infection type. The other substance of note is galactomannan detected using the GM test, which is primarily targeted for the early diagnosis of invasive aspergillosis. Its use is recommended by the Infectious Diseases Society of America for diagnosing aspergillosis. Polymerase chain reaction (PCR) of fungal-specific DNA is useful for diagnosing mycobacterial infections, but the results should be considered in conjunction with those of other tests and the clinical context (16). The current case showed only a strongly positive G test result of the CSF, suggesting an intracranial fungal infection. However, the child's GM test was negative. As infections caused by *Aspergillus* are often accompanied by a positive GM test, it was possible that antifungal therapy led to a false negative GM test result in this case. However, it is difficult for the conventional tests mentioned above to determine the causative organism; thus, more advanced testing techniques are needed.

The mNGS technology is a DNA sequencing technique that was developed from PCR and gene chips and belongs to a group of modern molecular diagnostic techniques. Since the first reported case of leptospirosis diagnosis using mNGS in 2014, mNGS has rapidly become a complementary test for various infections. Compared to traditional tests, mNGS is more effective at identifying CNS infections, with a positive rate of 57% (17). The combination of mNGS with traditional microbiological assays can significantly increase positive rates, especially in cases with difficult-to-grow fungi and low fungal culture loads. In mNGS detection, the thresholds of species-specific read number (SSRN) of different genera showing a positive result are inconsistent, with an SSRN $\geq$2 showing positive results for *Aspergillus*. In this case, the SSRN in the first mNGS test for *Aspergillus* was 27 and *A. niger* was 20, thus confirming its identity as the causative organism. During the treatment with voriconazole, mNGS was tested again and the SSRN of *A. niger* detected in the CSF reached 109. The increase in sequence number implied that the treatment was sub-optimal if not ineffective; thus, it was intensified by the addition of amphotericin B. At the end of the induction phase, no pathogenic organisms were detected during the final test, which shows the significance of mNGS for guiding treatment.

The diagnosis of cerebral aspergillosis is challenging, with only 55.9% of patients being diagnosed while still alive (10). The disease also has poor prognosis and high mortality rates. A review shows that Aspergillus meningitis has an ominous prognosis with a global case-fatality rate (CFR) of 72.1% but with a much better outcome among immunocompetent patients in whom a CFR of 63.5% was observed versus a 83% CFR registered among immunocompromised patients (10). So once diagnosed, a standardized and complete pharmacological treatment course is essential. Triazoles, particularly voriconazole, isavuconazole and posaconazole for invasive infections, and voriconazole or itraconazole for chronic infections, are the first line antifungal agents used to treat aspergillosis (18). The availability of both intravenous and different oral formulations of triazoles increases the therapeutic options. Voriconazole is the current treatment of choice for cerebral aspergillosis, while amphotericin B is reserved for voriconazole-intolerant or -refractory patients. The combination of the two is used as primary or remedial therapy for refractory aspergillosis. Once the induction period is over and the disease stabilizes, oral voriconazole may be administered for a year. In the current case, voriconazole administered intravenously for 4 weeks was ineffective; the child's headache was not relieved, the microorganisms persisted, and the intracranial pressure did not decrease. Hence, intrathecal and intravenous amphotericin B was added, starting at a low dose and gradually increasing to a maintenance dose. After 8 weeks of the above combination treatment, all the patient's symptoms and test results returned to normal; hence, the amphotericin B was discontinued and oral voriconazole was commenced. The patient experienced severe hypokalemia while receiving the amphotericin B. Daily monitoring and supplementation ensured safe treatment, and this case demonstrates the need for close monitoring of adverse effects during amphotericin B administration.

4. Conclusion

Cerebral aspergillosis, which is relatively rare after HLT, is clinically difficult to diagnose due to its insidious onset and low sensitivity of traditional detection methods. In addition to traditional detection methods, mNGS is recommended as early as possible as an adjunct for identifying the pathogenic organism. Once the diagnosis is confirmed, a standardized and long course of antifungal treatment should be administered.

The findings in this case showed that cerebral aspergillosis after transplantation in children is difficult to treat, as it requires combination voriconazole and amphotericin B and a long induction treatment period to achieve clearance of the microbial load. Closely observing the patient's clinical symptoms, using the G-test, and monitoring the intracranial pressure and mNGS during treatment may guide treatment and achieve satisfactory outcomes.

Data availability statement

The original contributions presented in this study are included in the article/supplementary material, further inquiries can be directed to the corresponding author.

Ethics statement

Written informed consent was obtained from the minor(s)' legal guardian/next of kin for the publication of any potentially identifiable images or data included in this article.

Author contributions

HZ and JC contributed to the conception and design of the study. HZ completed the data collection and wrote the first draft of the manuscript. HZ, JC, KX, SG, and YZ wrote the sections of the manuscript. All authors contributed to manuscript revision, read, and approved the submitted version.

Acknowledgments

We greatly acknowledge the contributions of specific colleagues, institutions, or agencies that aided the efforts of the authors.

Conflict of interest

The authors declare that the research was conducted in the absence of any commercial or financial relationships that could be construed as a potential conflict of interest.

Publisher's note

All claims expressed in this article are solely those of the authors and do not necessarily represent those of their affiliated organizations, or those of the publisher, the editors and the reviewers. Any product that may be evaluated in this article, or claim that may be made by its manufacturer, is not guaranteed or endorsed by the publisher.

References

1. Cooley D, Bloodwell R, Hallman G, Nora J, Harrison G, Leachman R. Organ transplantation for advanced cardiopulmonary disease. *Ann Thorac Surg.* (1969) 8:30–46. doi: 10.1016/s0003-4975(10)66405-3

2. Kidd S, Chen S, Meyer W, Halliday C. A new age in molecular diagnostics for invasive fungal disease: are we ready? *Front Microbiol.* (2019) 10:2903.

3. Kadakia S, Taghavi S, Jayarajan S, Ambur V, Wheatley G, Kaiser L, et al. Examining mortality and rejection in combined heart-lung transplantations. *Thorac Cardiovasc Surg.* (2017) 65:423–9. doi: 10.1055/s-0036-1597989

4. Potena L, Zuckermann A, Barberini F, Aliabadi-Zuckermann A. Complications of cardiac transplantation. *Curr Cardiol Rep.* (2018) 20:73. doi: 10.1007/s11886-018-1018-3

5. Alsaeed M, Husain S. Infections in heart and lung transplant recipients. *Crit Care Clin.* (2019) 35:75–93. doi: 10.1016/j.ccc.2018.08.010

6. Schwartz S, Kontoyiannis D, Harrison T, Ruhnke M. Advances in the diagnosis and treatment of fungal infections of the CNS. *Lancet Neurol.* (2018) 17:362–72.

7. Kunnathu Puthanveedu N, Lum J. Central nervous system infections after solid organ transplantation. *Curr Opin Infect Dis.* (2021) 34:207–16.

8. McCarthy M, Kalasauskas D, Petraitis V, Petraitiene R, Walsh T. Fungal infections of the central nervous system in children. *J Pediatric Infect Dis Soc.* (2017) 6:e123–33. doi: 10.1093/jpids/pix059

9. Rabin A, Givertz M, Couper G, Shea M, Peixoto D, Yokoe D, et al. Risk factors for invasive fungal disease in heart transplant recipients. *J Heart Lung Transplant.* (2015) 34:227–32. doi: 10.1016/j.healun.2014.09.036

10. Antinori S, Corbellino M, Meroni L, Resta F, Sollima S, Tonolini M, et al. *Aspergillus meningitis*: a rare clinical manifestation of central nervous system aspergillosis. Case report and review of 92 cases. *J Infect.* (2013) 66:218–38. doi: 10.1016/j.jinf.2012.11.003

11. Husain S, Camargo J. Invasive aspergillosis in solid-organ transplant recipients: guidelines from the American Society of Transplantation Infectious Diseases Community of Practice. *Clin Transplant.* (2019) 33:e13544. doi: 10.1111/ctr.13544

12. McCarthy M, Rosengart A, Schuetz A, Kontoyiannis D, Walsh T. Mold infections of the central nervous system. *N Engl J Med.* (2014) 371:150–60. doi: 10.1056/NEJMra1216008

13. Agnihotri S. Central nervous system opportunistic infections. *Semin Neurol.* (2019) 39:383–90. doi: 10.1055/s-0039-1687842

14. Giovane R, Lavender P. Central nervous system infections. *Prim Care.* (2018) 45:505–18. doi: 10.1016/j.pop.2018.05.007

15. McCarthy M, Walsh T. Molecular diagnosis of invasive mycoses of the central nervous system. *Expert Rev Mol Diagn.* (2017) 17:129–39. doi: 10.1080/14737159.2017.1271716

16. Patterson T, Thompson G III, Denning D, Fishman J, Hadley S, Herbrecht R, et al. Practice guidelines for the diagnosis and management of aspergillosis: 2016 update by the Infectious Diseases Society of America. *Clin Infect Dis.* (2016) 63:e1–60. doi: 10.1093/cid/ciw326

17. Xing X, Zhang J, Ma Y, He M, Yao G, Wang W, et al. Metagenomic next-generation sequencing for diagnosis of infectious encephalitis and meningitis: a large, prospective case series of 213 patients. *Front Cell Infect Microbiol.* (2020) 10:88. doi: 10.3389/fcimb.2020.00088

18. Cornely O, Alastruey-Izquierdo A, Arenz D, Chen S, Dannaoui E, Hochhegger B, et al. Global guideline for the diagnosis and management of mucormycosis: an initiative of the European Confederation of Medical Mycology in Cooperation with the Mycoses Study Group Education and Research Consortium. *Lancet Infect Dis.* (2019) 19:e405–21. doi: 10.1016/S1473-3099(19)30312-3

frontiers | Frontiers in Pediatrics

TYPE Case Report
PUBLISHED 09 January 2023
DOI 10.3389/fped.2022.1027177

OPEN ACCESS

EDITED BY
Pier Leopoldo Capecchi,
University of Siena, Italy

REVIEWED BY
John S. Kim,
University of Colorado Anschutz Medical Campus, United States
Cheng Wang,
Central South University, China

*CORRESPONDENCE
Zhi Chen
✉ eyxxgchenzhi@163.com

SPECIALTY SECTION
This article was submitted to Pediatric Cardiology, a section of the journal Frontiers in Pediatrics

RECEIVED 24 August 2022
ACCEPTED 12 December 2022
PUBLISHED 09 January 2023

CITATION
Wang Y, Zuo C, Wang X, Xiao Y, Liu Q and Chen Z (2023) Frequent torsades de pointes in a child with novel *AKAP9* mutation: A case report and literature review.
Front. Pediatr. 10:1027177.
doi: 10.3389/fped.2022.1027177

Frequent torsades de pointes in a child with novel *AKAP9* mutation: A case report and literature review

Yefeng Wang[1], Chao Zuo[1], Xiang Wang[1], Yunbin Xiao[1], Qiming Liu[2] and Zhi Chen[1]*

[1]Department of Cardiology, Hunan Children's Hospital, Changsha, China, [2]Department of Cardiology, Second Xiangya Hospital, Central South University, Changsha, China

Introduction: The aim of the present study is to report the diagnosis and treatment of a rare case of frequent torsades de pointes (Tdp) in a child with a novel *AKAP9* mutation. A 13-year-old girl suffered from repeated syncope and frequent Tdp. An electrocardiogram (ECG) showed frequent multisource premature ventricular contractions with the R-ON-T phenomenon. The QTc ranged from 410 to 468 ms. The genetic test indicated a heterozygous mutation, namely, c.11714T > C (p.M3905T), in the *AKAP9* gene, which is a controversial gene in long QT syndrome. After treatment with propranolol, recurrent syncope occurred, and the patient received an implantable cardioverter defibrillator (ICD). Due to frequent electrical storms at home, the child was additionally treated with propafenone to prevent arrhythmia. The antitachycardia pacing (ATP) function in the ICD was turned off, and the threshold of ventricular tachycardia (VT) assessment was adjusted from 180 beats/min to 200 beats/min. The patient was followed up for 12 months without malignant arrhythmia and electric shock.
Conclusion: Genetic testing may be a useful tool to determine the origin of channelopathy, but the results should be interpreted in combination with the actual situation. Rational parameter settings for the ICD and application of antiarrhythmic drugs can reduce the mortality rates of children.

KEYWORDS
torsades de pointes (TdP), long QT syndrome (LQTS), *AKAP9* gene, case report, implantable cardioverter defibrillator (ICD)

Introduction

Torsades de pointes (Tdp) is a life-threatening ventricular tachyarrhythmia characterized by a continuously changing QRS complex morphology, with the electrical axis twisting around the isoelectric line. Tdp is associated with a prolonged QT interval and may be preceded by T-wave alternans (1). Long QT syndrome (LQTS) is the most common hereditary ion channel disease in childhood, and it is characterized by Tdp, syncope, and sudden death. There are currently 17 genes known to cause LQTS, and their clinical manifestations are different (2). The present report discusses the diagnosis and treatment of a rare case of LQTS with a novel *AKAP9* mutation in a child, and it summarizes the relevant experience and literature analysis. The parents of

the child signed an informed consent, and this study was approved by the Medical Ethics Committee of the hospital (Hunan Children's Hospital, Changsha, China).

Case presentation

A 13-year-old girl was admitted to the hospital because of dizziness for 3 days and syncope twice. She experienced syncope first during school recess, which lasted for approximately 10 min, accompanied by salivation and urinary incontinence. She was immediately sent to the emergency department of a local hospital. During hospitalization, she suffered syncope for a second time, and she was then transported to our hospital by ambulance.

After admission, physical examination revealed that the child was conscious with a normal heart rate but an irregular

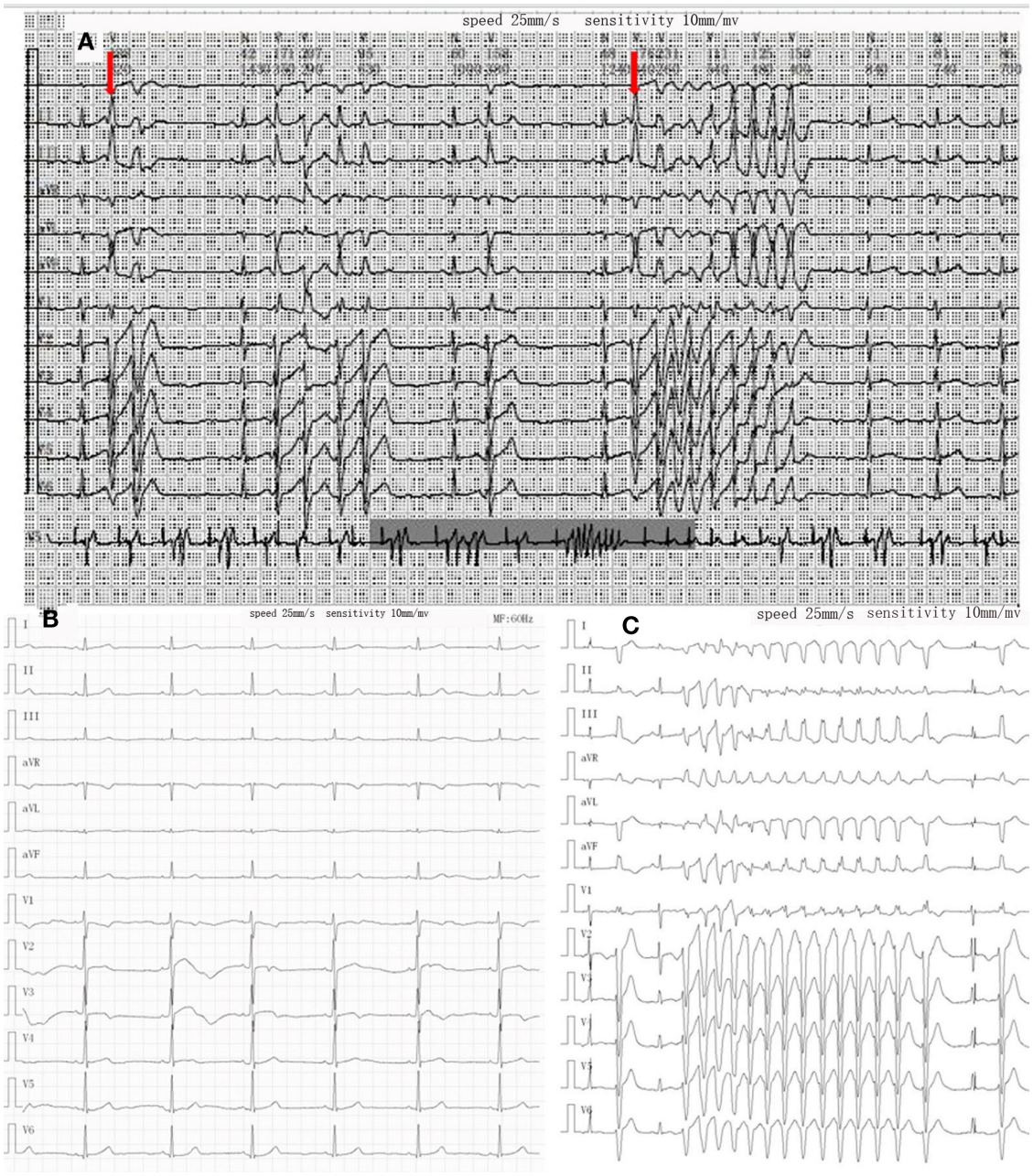

FIGURE 1
Changes in ECG during treatment. (**A**) Holter on admission showed R on T phenomenon (red arrow) and torsades de pointes. (**B**) After treatment of propranolol and magnesium sulfate, the QT interval was in the normal range, and no obvious ventricular premature beats were found. (**C**) Recurrence of torsades de pointes episode during oral propranolol.

heartbeat. Echocardiography showed normal left ventricular systolic function and a normal cardiac structure. Multiple bedside electrocardiograms (ECGs) showed frequent multisource premature ventricular contractions. Holter ECG showed frequent multisource premature ventricular contractions (43,729 beats/day, with some occurring in pairs and some occurring in doublet or triplet patterns) with the R-ON-T phenomenon and Tdp (**Figure 1A**). The QTc ranged from 410 to 468 ms. For treatment, the patient was administered an intravenous infusion of magnesium sulfate (0.5–1.0 mg/kg h) and potassium to maintain serum potassium concentration at 4.5–5 mmol/L. She received oral propranolol tablets (0.5 mg/kg) every 8 h. After 1 week of treatment, the child recovered and did not experience palpitations or dizziness in the hospital. An ECG showed that the premature ventricular contractions were significantly reduced and that no ventricular tachycardia (VT) occurred, and the QTc was 416 ms (**Figure 1B**). Occasionally, a biphasic T wave was observed in Lead V2 in this patient in sinus rhythm. Second-generation gene sequencing was performed after receiving approval by the Medical Ethics Committee and parental informed consent. As a result, a heterozygous mutation, namely, c.11714T > C (p.M3905T), in the *AKAP9* gene of the patient was detected, which was inherited from her mother (**Figure 2**), whose ECG was normal without QT prolongation and no history of syncope. This variant has not been previously described in the literature and has also not been previously reported in the Human Gene Mutation Database (HGMD). No other possible causative mutations were found, and no history of related genetic diseases was detected in the family.

After 9 months, the child suffered from syncope and convulsions again during housework. She was transferred to our hospital after cardiopulmonary resuscitation for 2 h. The ECG showed frequent multisource VT with Tdp (**Figure 1C**). Temporary subclavian pacing was given to the patient, and vasoactive drugs were used to maintain circulatory stability. Oral propranolol tablets were adjusted to 1 mg/kg every 8 h, and the patient received intravenous potassium and magnesium supplementation. The Holter ECG showed that the incidence of ventricular arrhythmia was 19,924 beats in 24 h with no occurrence of Tdp. Considering that the child had syncope after drug treatment, she was implanted with an implantable cardioverter defibrillator (ICD) under general

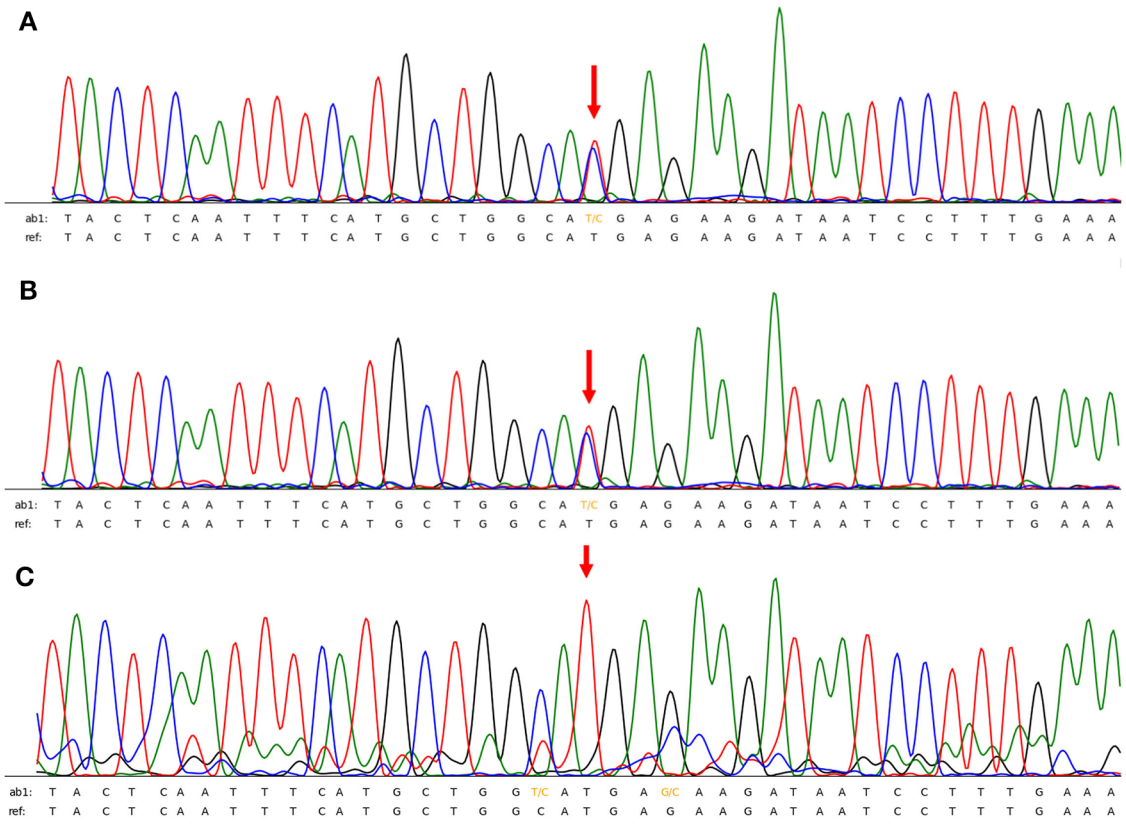

FIGURE 2
(**A**,**B**) the patient and her mother had a heterozygous mutation of *AKAP9* gene mutation of c.11714T > C (p.M3905T). (**C**) Her father had no relevant genetic mutations.

anesthesia after 7 days of stabilization (**Figure 3**). Her parents were informed that she needed activity restriction and exercise reduction.

Two weeks after discharge from the hospital, the patient developed obvious palpitations, fatigue, dizziness, and a sense of electric shock at night. Because she experienced several suspicious electric shock events, she was readmitted to our hospital. The bedside program control of the ICD confirmed that the child had multiple VT at home, and electrical cardioversion terminated the tachycardia after antitachycardia pacing (ATP) failed. In order to alleviate her anxiety, the ATP function was turned off, the VT judgment threshold was adjusted from 180 beats/min to 200 beats/min, and the energy of the first electric shock was lowered from 30 to 20 J. To reduce the incidence of ventricular arrhythmias, the patient was prescribed oral propafenone tablets (3 mg/kg) every 8 h. A repeated Holter ECG showed that the frequency of ventricular arrhythmias (3,387 beats/day) was significantly lower than before and that the ventricular pacing function was normal. The morphology of the T wave was normal in the lateral precordial leads. No malignant arrhythmia and electric shock events occurred during the 1-, 3-, and 6-month follow-ups. The child returned to school with restricted activities, and her parents were satisfied with the treatment provided.

Discussion

The diagnosis of LQTS is mainly based on electrocardiographic manifestations, clinical manifestations, and family history. A Schwartz score of ≥3.5 is considered for the diagnosis of LQTS (**Figure 4**) (2). In the present case, LQTS was diagnosed based on QT interval prolongation, history of Tdp, and syncope with stress. Based on the Schwartz scoring standard, the patient received a score of 6 points and met the diagnostic criteria of LQTS. Ion channel gene detection also aids in genotyping and guiding the treatment of LQTS (4). In the present case, we identified a heterozygous mutation, namely, c.11714T > C (p.M3905T), in *AKAP9*, which has not been reported in previous cases.

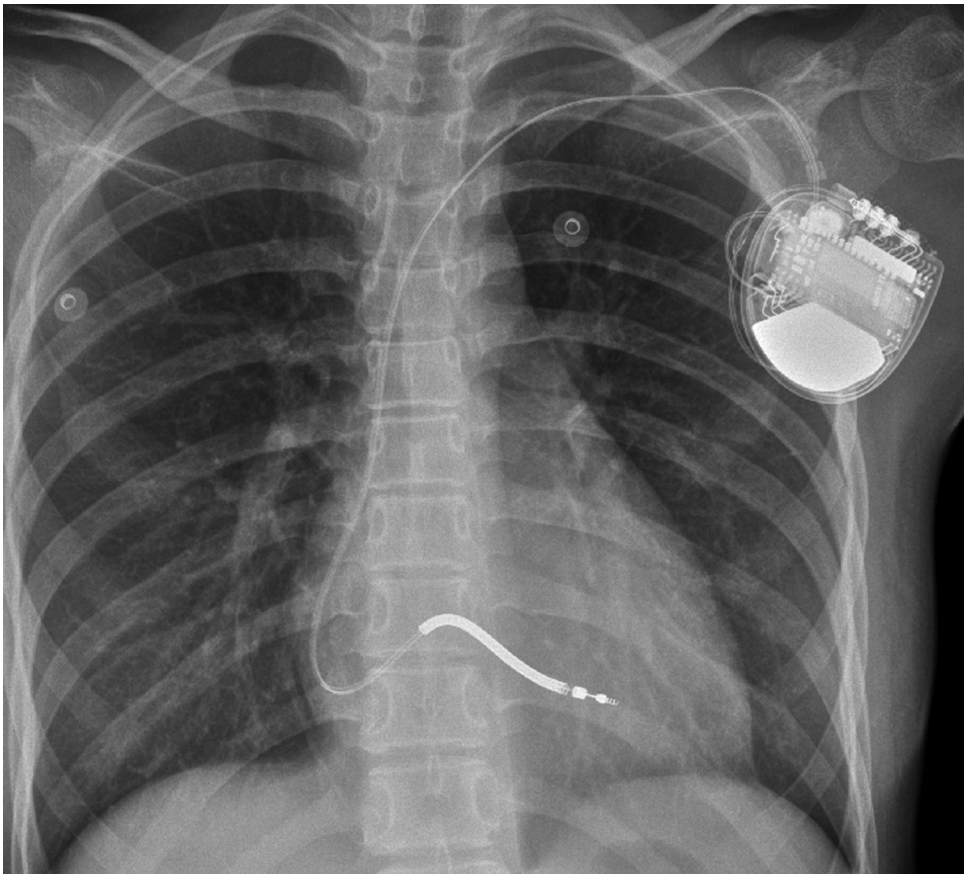

FIGURE 3
Chest x-ray after the implantation of the implantable cardioverter-defibrillator.

	Points
ECG findings	
QTc	
>480 ms	3
460–470 ms	2
450 (male) ms	1
4-min recovery QTc after exercise test ≥480 ms	1
Torsades de pointes	2
T-wave alternans	1
Notched T wave in 3 leads	1
Low heart rate for age	0.5
Clinical history	
Syncope	
With stress	2
Without stress	1
Congenital deafness	0.5
Family history	
A. Family members with definite LQTS	1
B. Unexplained sudden cardiac death <age 30 among immediate family members	0.5

FIGURE 4
Diagnostic criteria for long QT syndrome (LQTS) (the Schwartz score). Definite LQTS is defined by an LQTS score of ≥3.5 points.

Previous studies have named LQTS caused by *AKAP9* gene mutation as LQTS type 11. However, Adler et al. (5) analyzed a large sample and reported that among the 17 known genes that cause LQTS, only 3, namely, *KCNQ1*, *KCNH2*, and *SCN5A*, are clearly related to the occurrence of LQTS. Thus, it remains controversial whether *AKAP9* can cause LQTS. Previous studies on the *AKAP9* gene utilized a candidate gene approach compared with an unbiased genome-wide methodology used in this study. Recent studies have suggested that the protein encoded by the *AKAP9* gene is protein kinase A-anchored protein 9 (Yotiao protein) and that its function is mainly to act as a scaffold protein necessary for the assembly of several protein kinases and phosphatases on the centrosome and Golgi apparatus (6). The Yotiao protein forms a macromolecular complex with the voltage-gated potassium channel alpha subunit, Kv7.1 (also known as *KCNQ1*), and its associated beta subunit, KCNE1, which is responsible for the slow activation of delayed rectifier K+ currents and is a modifier of the clinical phenotype of LQTS (7, 8). The *AKAP9* gene not only alters QTc duration but also affects the risk and severity of cardiac events. In this case, the patient presented with frequent Tdp and multisource VT without significant QTc prolongation, which also indicated that the ECG manifestation of LQTS 11 was atypical but had a high degree of malignancy. However, the child's mother, who harbors the same heterozygous mutation in the *AKAP9* gene, had no LQTS-related symptoms, which suggested that *AKAP9*-associated LQTS is debatable, warranting further research to determine whether there are other unknown genes and influencing factors.

Treatments for LQTS include medication, implantable device therapy, and cardiac sympathetic denervation. Beta-blockers have been widely used as first-line drug therapy for congenital LQTS, and the mechanism of their antiarrhythmic

effect is to reduce or prevent the increase in cardiac transmural repolarization dispersion that occurs during intense sympathetic stimulation. However, if serious cardiovascular events still occur after an adequate dose of propranolol, an ICD or cardiac sympathetic denervation should be considered (3). Postoperative electrical storm is a common complication after ICD implantation in children, but the incidence in children is unknown. In adults, the incidence of electrical storm after ICD can be as high as 10%–60% (9), and it is mainly related to myocardial ischemia, electrolyte disturbance, sympathetic nerve excitation, and drugs (10). In this case, the child suffered from ICD electric shock during hyperbaric oxygen therapy as well as repeated electrical storms after painful stimulation and tension, which may have been related to sympathetic nerve excitation and the failure of beta-blockers to effectively control arrhythmia. Propafenone is a class Ic antiarrhythmic drug with strong membrane stability, competitive beta-receptor blockade, and calcium channel blockade, and it quickly interferes with sodium channels (11). In this case, the incidence of ventricular arrhythmias was significantly reduced after the addition of propafenone. However, attention should be paid to the children's QT interval and cardiac function to avoid cardiac insufficiency and prolongation of the QT interval when propafenone is combined with propranolol (12).

Currently, there is a lack of high-evidence guidelines or consensus on parameter settings for ICDs in children with cardiac channelopathies. For children with ICD implantation, especially when the diagnosis of cardiac channelopathies is clear and malignant arrhythmias have occurred in the past, the threshold for VT assessment in the ICD should not be lower than 188 beats/min or higher than the recorded VT (13). In this case, the VT threshold of the ICD was adjusted from 180 beats/min to 200 beats/min to avoid frequent electric shocks. The ATP function is recommended to reduce ICD discharge after ICD implantation in adults. However, in cardiac channelopathies, Tdp or ventricular fibrillation (VF) is the main attack and not monomorphic VT. Thus, in children with ATP and obvious symptoms of palpitations and anxiety, malignant arrhythmias are more like to occur. In the present case, after ATP function of the ICD was turned off, no electrical storm occurred again.

In conclusion, the diagnosis of LQTS in children needs to be combined with ECGs, clinical manifestations, and family history. Early genetic examination is helpful for typing and guiding treatment, but the genetic results need to be interpreted in combination with the actual situation. ICD implantation, as a means of preventing sudden death of children with cardiac syncope, can significantly reduce the sudden death rate. Rational parameter settings and application of antiarrhythmic drugs can reduce the mortality rates of children.

Data availability statement

The original contributions presented in the study are included in the article/supplementary material; further inquiries can be directed to the corresponding author.

Ethics statement

The studies involving human participants were reviewed and approved by the Medical Ethics Committee of Hunan Children's Hospital. Written informed consent to participate in this study was provided by the participants' legal guardian/next of kin.

Written informed consent was obtained from the individual(s), and minor(s)' legal guardian/next of kin, for the publication of any potentially identifiable images or data included in this article.

Author contributions

YW and CZ contributed to the conception and design of the study. CZ and XW organized the database and investigation. YX and QL performed the review and editing. YW wrote the first draft of the manuscript. All authors contributed to the article and approved the submitted version.

Funding

This study was funded by the Hunan Clinical Research Center for Children's Cardiovascular Diseases (No. 2021SK4019) and the General Guidance Project of Scientific Research Project of Hunan Provincial Health Commission (No. 202206012588).

Conflict of interest

The remaining authors declare that the research was conducted in the absence of any commercial or financial relationships that could be construed as a potential conflict of interest.

The reviewer CW declared a shared affiliation with the author QL to the handling editor at the time of review.

Publisher's note

References

1. Hsin-Ming L, Wei-Chieh T, Shuenn-Nan C. Immunosuppressant associated torsades de pointes after acute heart rejection in an 8-year-old boy. *Cardiol Young*. (2020) 30(8):1194–5. doi: 10.1017/S1047951120001602

2. Mizusawa Y, Horie M, Wilde AA. Genetic and clinical advances in congenital long QT syndrome. *Circ J*. (2014) 78(12):2827–33. doi: 10.1253/circj.cj-14-0905

3. Writing Committee M, Shah MJ, Silka MJ, Silva JNA, Balaji S, Beach CM, et al. PACES expert consensus statement on the indications and management of cardiovascular implantable electronic devices in pediatric patients. *Heart Rhythm*. (2021) 18(11):1888–924. doi: 10.1016/j.hrthm.2021.07.038

4. Schwartz PJ, Ackerman MJ, George Jr. AL, Wilde AAM. Impact of genetics on the clinical management of channelopathies. *J Am Coll Cardiol*. (2013) 62 (3):169–80. doi: 10.1016/j.jacc.2013.04.044

5. Adler A, Novelli V, Amin AS, Abiusi E, Care M, Nannenberg EA, et al. An international, multicentered, evidence-based reappraisal of genes reported to cause congenital long QT syndrome. *Circulation*. (2020) 141(6):418–28. doi: 10.1161/circulationaha.119.04313

6. de Villiers CP, van der Merwe L, Crotti L, Goosen A, George Jr. AL, Schwartz PJ, et al. AKAP9 is a genetic modifier of congenital long-QT syndrome type 1. *Circ Cardiovasc Genet*. (2014) 7(5):599–606. doi: 10.1161/circgenetics.113.000580

7. Bottigliero D, Monaco I, Santacroce R, Casavecchia G, Correale M, Guastafierro F, et al. Novel AKAP9 mutation and long QT syndrome in a patient with torsades des pointes. *J Interv Card Electrophysiol*. (2019) 56(2):171–2. doi: 10.1007/s10840-019-00606-y

8. Chen L, Kass RS. A-kinase anchoring protein 9 and IKs channel regulation. *J Cardiovasc Pharmacol*. (2011) 58(5):459–13. doi: 10.1097/fjc.0b013e318232c80c

9. Stiles MK, Fauchier L, Morillo CA, Wilkoff BL HRS/EHRA/APHRS/LAHRS focused update to 2015 expert consensus statement on optimal implantable cardioverter-defibrillator programming and testing. *Heart Rhythm*. (2019) 17(1): e220–8. doi: 10.1016/j.hrthm.2019.02.034

10. Vrints CJ. Management of out-of-hospital cardiac arrest and electric storm. *Eur Heart J Acute Cardiovasc Care*. (2018) 7(5):395–6. doi: 10.1177/2048872618791308

11. Harron DW, Brogden RN. Propafenone. A review of its pharmacodynamic and pharmacokinetic properties, and therapeutic use in the treatment of arrhythmias. *Drugs*. (1987) 34(6):617–47. doi: 10.2165/00003495-198734060-00001

12. Rosa M, Pappacoda S, D'Anna C, Di Mita O, Ponticiello E, Marzuillo P, et al. Ventricular tachycardia induced by propafenone intoxication in a pediatric patient. *Pediatr Emerg Care*. (2019) 35(9):e164–8. doi: 10.1097/pec.0000000000001346

13. Chen YW, Ji W, Zhu DQ, Li F. Efficacy and safety of implantable cardioverter-defibrillator implantation in pediatric tachycardia cases. *Zhonghua Er Ke Za Zhi*. (2020) 58(11):905–9. doi: 10.3760/cma.j.cn112140-20200408-00361

frontiers | Frontiers in Cardiovascular Medicine

TYPE Case Report
PUBLISHED 16 January 2023
DOI 10.3389/fcvm.2022.1095882

OPEN ACCESS

EDITED BY
Inga Voges,
University Medical Center Schleswig-Holstein, Germany

REVIEWED BY
Aliakbar Zeinaloo,
Tehran University of Medical Sciences, Iran
Attila Nemes,
University of Szeged, Hungary

*CORRESPONDENCE
Shiwei Yang
✉ jrdoctoryang@163.com

†These authors have contributed equally to this work

SPECIALTY SECTION
This article was submitted to Pediatric Cardiology, a section of the journal Frontiers in Cardiovascular Medicine

RECEIVED 11 November 2022
ACCEPTED 29 December 2022
PUBLISHED 16 January 2023

CITATION
Wang L, Lu P, Yin J, Xu K, Xiang D, Zhang Z, Zhang H, Zheng B, Zhou W, Wang C and Yang S (2023) Case report: Rare novel *MIPEP* compound heterozygous variants presenting with hypertrophic cardiomyopathy, severe lactic acidosis and hypotonia in a Chinese infant.
Front. Cardiovasc. Med. 9:1095882.
doi: 10.3389/fcvm.2022.1095882

Case report: Rare novel *MIPEP* compound heterozygous variants presenting with hypertrophic cardiomyopathy, severe lactic acidosis and hypotonia in a Chinese infant

Ling Wang[1†], Pengtao Lu[1†], Jie Yin[1†], Kangkang Xu[1], Dandan Xiang[1], Zhongman Zhang[1], Han Zhang[1], Bixia Zheng[2], Wei Zhou[2], Chunli Wang[2] and Shiwei Yang[1*]

[1]Department of Cardiology, Children's Hospital of Nanjing Medical University, Nanjing, China, [2]Nanjing Key Laboratory of Pediatrics, Children's Hospital of Nanjing Medical University, Nanjing, China

Background: Mitochondrial intermediate peptidase, encoded by the *MIPEP* gene, is involved in the processing of precursor mitochondrial proteins related to oxidative phosphorylation. Only a few studies have shown that mutations in *MIPEP* can cause combined oxidative phosphorylation deficiency-31 (COXPD31), an autosomal recessive multisystem disorder associated with mitochondrial dysfunction. We report herein a rare case of an 8-month-old boy in China with hypertrophic cardiomyopathy (HCM), severe lactic acidosis, and hypotonia caused by novel *MIPEP* compound heterozygous variants.

Methods: Trio-whole-exome sequencing and copy number variation sequencing were performed to identify mutated genetic loci. Sanger sequencing and quantitative real-time PCR were used to validate the candidate single nucleotide variants and copy number variants, respectively.

Results: The proband was an 8-month-old boy with HCM, severe lactic acidosis, and hypotonia who died 2 months after his first admission. Two novel compound heterozygous variants, c.1081T > A (p. Tyr361Asn) and a whole deletion (Ex1-19 del), were found in the *MIPEP* gene, which were inherited from his healthy parents respectively. Additionally, his mitochondria DNA copy number was significantly reduced.

Conclusion: We are the first to report a patient with rare *MIPEP* variants in China. Our findings expand the mutation spectrum of *MIPEP*, and provide insights into the genotype-phenotype relationship in COXPD31.

KEYWORDS

***MIPEP*, hypertrophic cardiomyopathy, mitochondrial disease, oxidative phosphorylation, combined oxidative phosphorylation deficiency-31**

Introduction

Mitochondrial diseases (MDs) are rare, with a prevalence of 5–12/100,000 (1). They are characterized by oxidative phosphorylation (OXPHOS) dysfunction caused by nuclear and/or mitochondrial DNA (mtDNA) variations (2–4). Approximately 20–40% of children with MDs develop cardiac manifestations, such as hypertrophic cardiomyopathy (HCM), dilated cardiomyopathy (DCM), arrhythmias, left ventricular non-compaction (LVNC), heart failure and sudden cardiac death (5–8), which are termed mitochondrial cardiomyopathy (MCM) (2, 4). Combined oxidative phosphorylation deficiency-31 (COXPD31) (OMIM: 617228) is an autosomal recessive mitochondrial disease caused by mutations in the *MIPEP* gene. It can manifest as LVNC, HCM, DCM, global developmental delay, severe hypotonia, seizures, cataracts, and abnormal movements (9, 10). The *MIPEP* gene spans 57 kb in the long arm of chromosome 13 (13q12.12) and consists of 19 exons (11). Mitochondrial intermediate peptidase (MIP), encoded by *MIPEP*, which localizes to the mitochondrial matrix, and participates in secondary cleavage processing for a specific class of nuclear-encoded precursor mitochondrial proteins mostly characterized by XRX(↓)(F/L/I)XX(T/S/G)XXXX(↓) (11–13). Pulman et al. (10) demonstrated that *MIPEP* variants impair the stability and abundance of OXPHOS complexes. Clinical reports of *MIPEP* variations have been exceedingly infrequent. We herein reported the first case of early-onset HCM, severe lactic acidosis, and hypotonia, caused by *MIPEP* variants in China.

Materials and methods

Whole-exome sequencing

Genomic DNA was extracted from the peripheral blood of the proband and his parents using a DNA isolation kit (Tiangen, China) according to the manufacturer's protocol. Following, the Genomic DNA was sheared into fragments and hybridized with the xGen Exome Research Panel v1.0 probe sequence capture array from IDT (Integrated Device Technology, USA) to enrich the exonic region. The enriched libraries were performed on an Illumina HiSeq XTen (Illumina, USA) platform. Variants with a minor allele frequency higher than 1% were filtered out. All identified variants were annotated using Genome Aggregation Database (gnomAD), 1000 Genomes Project (Chinese), dbSNP, and ExAC database. The candidate variants were further validated by Sanger sequencing and the pathogenicity of variants was evaluated according to the American College of Medical Genetics and Genomics (ACMG) criteria.

Copy number variation calling

Copy number variations detection and annotation: We use CANOE, CNVnator, DeviCNV, and ExomeDepth to detect CNVs from WES data, and all CNVs were annotated to obtain additional information about the population frequencies and possible effects. The population frequencies for CNVs were obtained from Database of Genomic Variants (DGV). To assess the inclusion of any established dosage-sensitive genes or regions and the possible impact on gene function, each CNV was evaluated against a select set of haploinsufficient and triplosensitive genes and genomic regions obtained from ClinGen and Database of Chromosomal Imbalance and Phenotype in Humans Using Ensembl Resource (DECIPHER).

Exon CNV analysis

The primer pair sequences are shown in **Supplementary Table 1**. Samples for quantitative real-time PCR(PT-qPCR) were assayed using the Takara SYBR Green with *ALB* genomic content used as

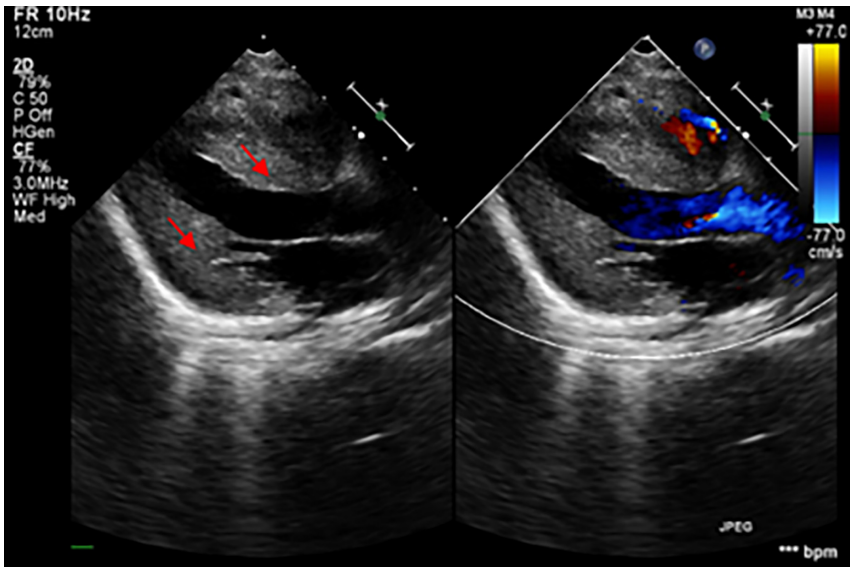

FIGURE 1
The echocardiogram demonstrated the thickening of the myocardium (the red arrows showed the hypertrophic interventricular septum and posterior wall of the left ventricle).

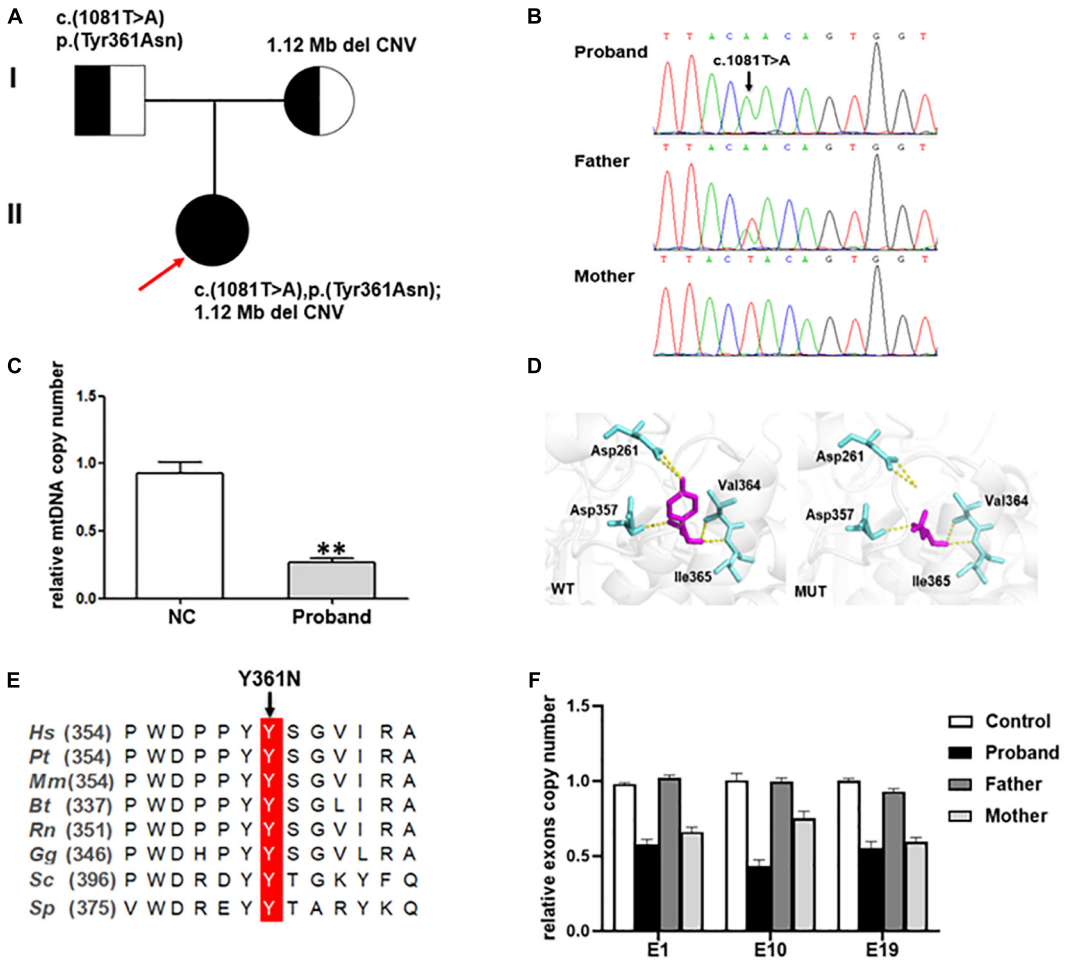

FIGURE 2
(A) Pedigree of the family reported in the present study. The arrow depicts the proband. The circles correspond to the women. The squares indicate the men. **(B)** Direct sequencing showing the novel missense variant c.1081T > A of the *MIPEP* gene. **(C)** The mtDNA copy numbers in healthy controls (n = 3) and the proband. A notable reduction in the mtDNA level was noted in the proband (NC, normal control, $^{**}P < 0.01$). **(D)** Structural visualization of the identified *MIPEP* missense alteration using Alpha Fold structure of the human *MIPEP* as a template (Identifier:AF-Q99797-F1). The variant site and the relevant residues were shown as sticks (the variant site is shown in magenta and the relevant residues are shown in aquamarine). The yellow dotted line represents the H-bond that connects the variant site with the residues. **(E)** Alignment of *MIPEP* orthologs in different species around the mutated amino acids residues. *Hs, Homo sapiens; Pt, Pan troglodytes; Mm, Macaca mulatta; Bt, Bos taurus; Rn, Rattus norvegicus; Gg, Gallus gallus; Sc, Saccharomyces cerevisiae S288C; Sp, Schizosaccharomyces pombe.* **(F)** *MIPEP* gene exons RT-qPCR analysis showed a heterozygous loss of exons 1, 10, and 19 in the proband and his mother.

an endogenous control for normalization of the data. The relative *MIPEP* gene expression was measured by subtracting the Ct values of the three exons (E1, E10, and E19) from the *ALB* gene, using the $2^{-\Delta\Delta Ct}$ method.

Mitochondrial DNA (mtDNA) copy number assay

The genomic DNA was isolated from the whole blood of the proband and 3 normal controls, respectively. Then, the mean mtDNA copy number was determined by RT-qPCR using SYBR Green Real-Time PCR Master Mix (Takara, Japan) in a 10 μl reaction volume, including 1.6 μl of primers, 1.0 μl of DNA, 5 μl of 2 × Taq Master Mix (Vazyme Biotech Co., Ltd., Nanjing, China), and 2.4 μl of ddH_2O. According to the instructions, the amplification cycles were as follows: 95°C for 30 s followed by 40 cycles of 95°C for 5 s, 60°C for 30 s and 72°C for 30 s. The melt curve stage includes 95°C for 10 s, 65°C for 5 s. By comparing the levels of mitochondrial DNA copy number (MT-ND2) versus nuclear DNA (18S), the relative levels of mtDNA copy numbers were assessed. Analyses were done in triplicates.

Results

Clinical presentation

The patient was an 8-month-old male, the only child of healthy unrelated Chinese parents, born full-term after normal pregnancy and delivery. He was admitted due to light coma and poor response to external stimuli. His vital signs were as follows: body temperature, 37°C; heart rate, 180/min; respiratory rate, 45/min; and blood pressure, 75/45 mmHg. He presented with respiratory distress associated with severe lactic acidemia (lactate, 17.7 mmol/L; pH, 7.138), requiring mechanical ventilation.

TABLE 1 The *MIPEP* gene variants in six unrelated patients from six unrelated families.

References	This case	Eldomery et al. (9)	Eldomery et al. (9)	Eldomery et al. (9)	Eldomery et al. (9)	Pulman et al. (10)
Patient ID	P1	P2	P3	P4	P5	P6
Age of onset	8M	5.5M	11 M	5 M	At birth	8M
Variants	p.Y361N; loss1 (Exon:1-19)	p.L582R; p.L71Q	p.L306F; p.E602*	p.K343E	p.H512D; 1.4-Mb deletion	p.L306F; p.A658Kfs*38
History of pregnancy and delivery	N	N	N	36 weeks gestation due to preterm labor	33 weeks gestation due to maternal preeclampsia and fetal decelerations	N
Family history	The farther with a history of tuberculous pleurisy	A paternal uncle with a history of supra-ventricular tachycardia and maternal great-aunt with early myocardial infarction (29 years of age)	An older brother had cataracts and infantile spasms and died unexpectedly at 14 months of age of unknown cause	The parents are first-degree cousins	His sister presented with cardiomyopathy in the immediate postnatal period and subsequently expired by 16 days of life	N
Electrocardiogram	N	Wolf-Parkinson-White syndrome	N	U	U	N
Echocardiography	HCM	LVNC	LVNC and DCM	HCM	HCM	N
Lactic acid (mmol/L)	17.7	3.2	U	11.1	8.9–10.4	2.2
Other features	Short penis, the testicles did not descend into the scrotum, could not sit by himself and had significant hypotonia	Wide mouth and bulbous nasal tip, tongue-thrusting, hypotonia with head lag, abnormal movements and dystonic posturing	Cataract, hypotonia, developmental delay and uncontrollable seizures	Long philtrum, opisthotonus and severe head lag when pulled to sit, microcephaly and seizures	Deep-set eyes, anteverted nares, depressed nasal bridge, midface hypoplasia, severe micrognathia, facial asymmetry, and an accessory palmar crease on the right hand	Developmental delay, global hypotonia, mild optic neuropathy and mild ataxia
Outcome	Died at 10 months	Alive at the age of 4.5 years old	Died at 2 years old	Died at 11 months	Died at 19 days	Alive at the age of 20 years old

P, patient; M, month; N, normal; U, unclear; HCM, hypertrophic cardiomyopathy; LVNC, left ventricular non-compaction; DCM, dilated cardiomyopathy.

His psychomotor development was delayed, and he could not sit unaided at 8 months due to global hypotonia. Notably, he had a short penis and undescended testicles. Echocardiography revealed the features suggesting HCM (**Figure 1**). Specifically, the posterior left ventricle wall was slightly thickened (6 mm) and the interventricular septum was primarily thickened (13.2 mm) (Z-scores were 3.29 and 21.83, respectively),[1] with mild left ventricular systolic dysfunction (left ventricular ejection fraction, 50%), there was minimal pericardial effusion with no abnormal valve morphology or motion. Brain magnetic resonance imaging showed abnormal signals on the bilateral thalamus and dorsal brainstem, strongly suggesting metabolic encephalopathy or inflammation. Furthermore, laboratory examinations showed markedly elevated plasma B-type natriuretic peptide (BNP) (2,613 pg/ml; upper limit of normal, 100 pg/ml) and slightly elevated liver enzyme levels [alanine transaminase (ALT), 121 U/L (reference, 0–41 U/L); aspartate transaminase (AST),105 U/L (reference,15–40 U/L)]. Urine creatinine and electrolyte levels were within normal ranges. Blood tests for genetic metabolic diseases revealed an abnormal increase in multiple acylcarnitine and 3-hydroxybutyrate levels. MD was then considered, and the patient was treated with high doses of coenzyme Q10, L-carnitine, vitamin B complex, etc. His blood PH value ultimately recovered to normal after a series of therapies, but lactic acid levels remained extraordinarily high (8–9 mmol/L). Finally, the boy's condition worsened and died 2 months after admission. All his family members had no similar conditions.

Genetic analysis

Genetic analysis revealed that the proband had two compound-heterozygous variants in *MIPEP* (NM_005932): a hemizygous variant c.1081T > A (p. Tyr361Asn) and a 1.12-Mb deletion (chr13:23777833-24895906) containing the entire gene (**Figures 2A, B**), neither of which has been previously reported.

The mtDNA content and alterations were associated with OXPHOS complex deficiency-related disease, which are the biomarker of mitochondrial function and may reflect the degree of mtDNA damage (14). We examined the mtDNA copy number from whole blood samples to indirectly estimate the function of *MIPEP* variants. And the result showed that the relative ratio of mtDNA copy number of the proband was significantly decreased by 71.5%, compared to that in the healthy controls ($p < 0.001$; **Figure 2C**).

1 http://zscore.chboston.org

Discussion

Here we reported a rare case with infantile-onset progressive cardiomyopathy and lactic acidosis. Genetic analysis identified a paternal missense variant c.1081T > A (p. Tyr361Asn) and a maternal hemizygous whole deletion (Ex1_19 del) in *MIPEP*, neither of which has been reported previously.

The c.1081T > A [p. (Tyr361Asn)] variant, absent from controls (1,000 Genomes, ExAC, gnomAD, and CNGB) (PM2), which was a missense variant in *MIPEP* involving a tyrosine-to-asparagine substitution at position 361. PolyPhen2, Mutation Taster and Provean predicted it as probably damaging, disease causing, and deleterious, respectively (PP3). According to ACMG, c.1081T > A (p. Tyr361Asn) was classified as a variant of uncertain significance (VUS) (PM2 + PP3). But the three-dimensional MIP molecular model showed this variant breaking its connection with aspartate at position 261 by H-bond, which destroyed the spatial structure of the protein (**Figure 2D**). Protein alignments also revealed the variant affected an amino acid highly conserved among species (**Figure 2E**). WES revealed that the patient and his mother may have a gene deletion (chr13:23777833-24895906), which involved eight genes (*MIPEP*, *SGCG*, *SACS*, *TNFRSF19*, *SPATA13*, *C1QTNF9*, *C1QTNF9B-AS1* and *C1QTNF9B*). Copy number analysis of three representative exons (E1, E10 and E19) was performed by RT-qPCR (**Figure 2F**) to verify the deletion detected by WES, and the results confirmed that the patient and his mother harbored the heterozygous deletion in *MIPEP* which was absent from controls (1000 Genomes, ExAC, gnomAD, and CNGB) (PM2). The deletion could have reduced MIP protein expression (PVS1), and it was classified as likely pathogenic (PVS1 + PM2) based on ACMG criteria. Moreover, the mtDNA copy number of the proband was significantly reduction comparing to that of healthy controls, suggesting that *MIPEP* may play a crucial role in regulating mitochondrial function. No variants in other MDs-related genes, such as *ACAD9*, *GTPBP3*, *NDUFV1*, *NCOA6*, *MMUT*, and *KARS1,* and the mtDNA were found in the proband. Therefore, the two variants were thought to cause the disease (15, 16).

To date, *MIPEP* variants have not been reported in Chinese patients. Only seven *MIPEP* variants in five patients have been reported worldwide, including five missense variants (p.Leu582Arg, p.Leu71Gln, p.Leu306Phe, p.Lys343Glu, p.His512Asp), one frameshift variant (p.Ala658Lysfs*38) and one deletion variant (1.4-Mb deletion, including the entire gene) (9, 10), all of which were inherited from their parents, following an autosomal recessive inheritance pattern. Four patients showed significant cardiac manifestations: 1 LVNC, 2 HCM, and 1 LVNC combined with DCM. Among them, three patients (75%) succumbed to progressive cardiac failure or sudden cardiac death before 2 years of age. Nevertheless, the patient with no cardiac symptoms who survived for more than 20 years (9, 10). Compared to the previous reports, the proband we reported had similar clinical presentations, such as cardiac abnormality, developmental delay, significant hypotonia, and lactic acidosis. Due to worsening condition even despite cocktail therapy, our patient died after 2 months treatment. The genetic and clinical information of all the patients are summarized in **Table 1**. These cases improved our awareness of COXPD31, and early recognition of MCM is essential to avoid heart failure and sudden cardiac death. Furthermore, identification of this severe early-onset condition expands the phenotypic spectrum associated with loss of MIP function, such as cardiomyopathy and other systemic impairments. Nowadays, most treatments for MCM could support and improve the quality of life to some extent. However, identifying an effective treatment modality remains difficult, owing to the heterogeneity of the disease.

Conclusion

We are the first to report a rare case of an 8-month-old boy in China with *MIPEP* variations who presented with HCM, severe lactic acidosis, and hypotonia. Genetic analysis revealed novel compound heterozygous variants c.1081T > A [p. (Tyr361Asn)] and a whole deletion (Ex1_19 del) in the *MIPEP* gene. Our findings expand the genetic spectrum of *MIPEP*-linked mitochondrial disease, and highlight the importance of an interrelationship between clinical and research for the identification of disease-associated genes.

Data availability statement

The original contributions presented in this study are included in the article/**Supplementary material**, further inquiries can be directed to the corresponding author.

Ethics statement

The studies involving human participants were reviewed and approved by the Institutional Ethical Committee of the Children's Hospital of Nanjing Medical University. Written informed consent to participate in this study was provided by the participants' legal guardian/next of kin. Written informed consent was obtained from the individual(s), and minor(s)' legal guardian/next of kin, for the publication of any potentially identifiable images or data included in this article.

Author contributions

LW edited the manuscript. PL contributed samples collection. JY and SY revised the manuscript. All authors contributed to the article and approved the submitted version.

Funding

This work was supported by the National Natural Science Foundation of China (81670284), the Medical Science and Technology Development Foundation of Jiangsu Commission of Health (ZD2021058), Research Project of Maternal and Child Health of Jiangsu Province (F202023), Medical Science and Technology Development Foundation of Nanjing Department of Health (ZKX20041), and Nanjing Medical Science and Technique Development Foundation (QRX17024).

Acknowledgments

We gratefully thank Dr. Di Cui [Chigene (Beijing) Translational Medical Research Center Co.] for her assistance in genetic analysis.

Conflict of interest

The authors declare that the research was conducted in the absence of any commercial or financial relationships that could be construed as a potential conflict of interest.

Publisher's note

All claims expressed in this article are solely those of the authors and do not necessarily represent those of their affiliated organizations, or those of the publisher, the editors and the reviewers. Any product that may be evaluated in this article, or claim that may be made by its manufacturer, is not guaranteed or endorsed by the publisher.

Supplementary material

The Supplementary Material for this article can be found online at: https://www.frontiersin.org/articles/10.3389/fcvm.2022.1095882/full#supplementary-material

References

1. Mazzaccara C, Mirra B, Barretta F, Caiazza M, Lombardo B, Scudiero O, et al. Molecular epidemiology of mitochondrial cardiomyopathy: a search among mitochondrial and nuclear genes. *Int J Mol Sci.* (2021) 22:5742. doi: 10.3390/ijms22115742

2. Imai-Okazaki A, Kishita Y, Kohda M, Mizuno Y, Fushimi T, Matsunaga A, et al. Cardiomyopathy in children with mitochondrial disease: prognosis and genetic background. *Int J Cardiol.* (2019) 279:115–21. doi: 10.1016/j.ijcard.2019.01.017

3. Kohda M, Tokuzawa Y, Kishita Y, Nyuzuki H, Moriyama Y, Mizuno Y, et al. A comprehensive genomic analysis reveals the genetic landscape of mitochondrial respiratory chain complex deficiencies. *PLoS Genet.* (2016) 12:e1005679.

4. Tokuyama T, Ahmed RE, Chanthra N, Anzai T, Uosaki H. Disease modeling of mitochondrial cardiomyopathy using patient-specific induced pluripotent stem cells. *Biology.* (2021) 10:981. doi: 10.3390/biology10100981

5. Meyers DE, Basha HI, Koenig MK. Mitochondrial cardiomyopathy: pathophysiology, diagnosis, and management. *Tex Heart Inst J.* (2013) 40:385–94.

6. El-Hattab AW, Scaglia F. Mitochondrial cardiomyopathies. *Front Cardiovasc Med.* (2016) 3:25. doi: 10.3389/fcvm.2016.00025

7. Brunel-Guitton C, Levtova A, Sasarman F. Mitochondrial diseases and cardiomyopathies. *Can J Cardiol.* (2015) 31:1360–76. doi: 10.1016/j.cjca.2015.08.017

8. Limongelli G, Masarone D, Pacileo G. Mitochondrial disease and the heart. *Heart.* (2017) 103:390–8. doi: 10.1136/heartjnl-2015-308193

9. Eldomery MK, Akdemir ZC, Vogtle FN, Charng WL, Mulica P, Rosenfeld JA, et al. MIPEP recessive variants cause a syndrome of left ventricular non-compaction, hypotonia, and infantile death. *Genome Med.* (2016) 8:106.

10. Pulman J, Ruzzenente B, Horak M, Barcia G, Boddaert N, Munnich A, et al. Variants in the MIPEP gene presenting with complex neurological phenotype without cardiomyopathy, impair OXPHOS protein maturation and lead to a reduced OXPHOS abundance in patient cells. *Mol Genet Metab.* (2021) 134:267–73. doi: 10.1016/j.ymgme.2021.09.005

11. Chew A, Buck EA, Peretz S, Sirugo G, Rinaldo P, Isaya G. Cloning, expression, and chromosomal assignment of the human mitochondrial intermediate peptidase gene (MIPEP). *Genomics.* (1997) 40:493–6. doi: 10.1006/geno.1996.4586

12. Hendrick JP, Hodges PE, Rosenberg LE. Survey of amino-terminal proteolytic cleavage sites in mitochondrial precursor proteins: leader peptides cleaved by two matrix proteases share a three-amino acid motif. *Proc Natl Acad Sci U.S.A.* (1989) 86:4056–60. doi: 10.1073/pnas.86.11.4056

13. Coenen MJ, Smeitink JA, Smeets R, Trijbels FJ, van den Heuvel LP. Mutation detection in four candidate genes (OXA1L, MRS2L, YME1L and MIPEP) for combined deficiencies in the oxidative phosphorylation system. *J Inherit Metab Dis.* (2005) 28:1091–7. doi: 10.1007/s10545-005-4483-y

14. Medeiros DM. Assessing mitochondria biogenesis. *Methods.* (2008) 46:288–94. doi: 10.1016/j.ymeth.2008.09.026

15. Bernier FP, Boneh A, Dennett X, Chow CW, Cleary MA, Thorburn DR. Diagnostic criteria for respiratory chain disorders in adults and children. *Neurology.* (2002) 59:1406–11. doi: 10.1212/01.wnl.0000033795.17156.00

16. Klopstock T, Priglinger C, Yilmaz A, Kornblum C, Distelmaier F, Prokisch H. Mitochondrial disorders. *Dtsch Arztebl Int.* (2021) 118:741–8. doi: 10.3238/arztebl.m2021.0251

frontiers | Frontiers in Cardiovascular Medicine

TYPE Case Report
PUBLISHED 25 January 2023
DOI 10.3389/fcvm.2022.1084170

OPEN ACCESS

EDITED BY
Hendrik Tevaearai Stahel,
Bern University Hospital, Switzerland

REVIEWED BY
Raymond N. Haddad,
Hôpital Necker-Enfants Malades, France
Neeraj Awasthy,
Max Healthcare, India

*CORRESPONDENCE
Radityo Prakoso
karajanh70@gmail.com

SPECIALTY SECTION
This article was submitted to Pediatric Cardiology, a section of the journal Frontiers in Cardiovascular Medicine

RECEIVED 31 October 2022
ACCEPTED 20 December 2022
PUBLISHED 25 January 2023

CITATION
Prakoso R, Sembiring AA, Hernisa L, Mendel B, Lelya O and Lilyasari O (2023) Case report: Right atrial appendage hybrid access to bailout a stuck stent from the inferior vena cava of a small child.
Front. Cardiovasc. Med. 9:1084170.
doi: 10.3389/fcvm.2022.1084170

Case report: Right atrial appendage hybrid access to bailout a stuck stent from the inferior vena cava of a small child

Radityo Prakoso[1]*, Aditya Agita Sembiring[1], Latifa Hernisa[2], Brian Mendel[1,3], Olfi Lelya[1] and Oktavia Lilyasari[1]

[1]Department of Cardiology and Vascular Medicine, Division of Pediatric Cardiology and Congenital Heart Disease, National Cardiovascular Center Harapan Kita, Universitas Indonesia, Jakarta, Indonesia, [2]Division of Pediatric and Congenital Heart Surgery, National Cardiovascular Centre of Harapan Kita, Universitas Indonesia, Jakarta, Indonesia, [3]Department of Cardiology and Vascular Medicine, Sultan Sulaiman Government Hospital, Serdang Bedagai, Sei Rampah, Indonesia

A three-month-old baby boy (5. 4 Kg) with pulmonary atresia, subaortic ventricular septal defect (VSD), and patent ductus arteriosus (PDA) was sent for ductal stenting from the femoral vein. The route to the PDA was extremely tortuous and the procedure was complicated with a stent stuck in the abdominal inferior vena cava (IVC). Transfemoral stent recapture was technically laborious and the stent was successfully recaptured across a 10-Fr right atrial appendage (RAA) hybrid access avoiding a cardiopulmonary bypass (CBP). The PDA was subsequently stented for the femoral artery with satisfactory clinical outcomes.

KEYWORDS

ductal stenting, inferior vena cava, patent ductus arteriosus, single ventricle, strutted stent

Introduction

The integrity and configuration of the stents can be easily disrupted with harsh manipulations making percutaneous interventions difficult and technically more complex. Strutted stents within the vessels are challenging scenarios for interventional cardiologists and can be associated with serious adverse events such as embolism, disintegration of the surrounding tissue, and vascular trauma (1, 2). There are currently no protocols for recapturing embolized strutted stents using percutaneous methods. Herein, we report and describe the use of the right atrial appendage (RAA) hybrid access as a bailout to safely remove a strutted stent from the abdominal inferior vena cava (IVC) of a small three-month-old baby boy.

Case illustration

A three-month-old boy (5.4 Kg) with severe cyanosis and diagnosed with type-II pulmonary atresia, subaortic 6.5 mm-large ventricular septal defect (VSD), and patent ductus arteriosus (PDA) with the saturation of only 40% was sent for femoral transvenous ductal stenting (DS). The case was discussed in a multidisciplinary meeting and DS was found more reasonable than surgical valvulotomy (Figure 1). From the right femoral vein, a 4-Fr 3.5 Judkins Right catheter was cannulated up to the PDA across the VSD. The PDA was pre-dilated with a 3.0 x 20 mm coronary balloon that was inflated to 6 atm (Figure 2A). A 0.035″ soft exchange wire was then positioned in the right pulmonary artery and a (6.0 x 38 mm) Dynamic vascular stent was delivered into position using the naked technique. It was technically impossible to push the stent inside the PDA because of the complex angulation (Figure 2B). The stent got stuck in the IVC upon retrieval (Figure 2C). We tried to push and pull the stent to verify that the stent is still on its wire track. Caval angiography was done to verify that the IVC was not damaged (Figure 2D). An urgent multidisciplinary decision was taken to remove the stent in the cath lab using a 10-Fr RAA hybrid access without cardiopulmonary bypass (CPB) support. The recapture of the stent was uneventfully performed using a 20 mm gooseneck snare (Figures 2E–G) and DS was successfully performed from the femoral artery with a (4.0 x 30 mm) Resolute Integrity stent that was inflated at 20 atm for 6 s (Figure 2H). Control angiography showed that the stent migrated toward the distal right pulmonary artery (Figures 2H, I). We decided to position a second stent because the PDA was not entirely covered. However, due to the complex PDA anatomy, it was technically difficult to overlap the first stent. We decided to abort our procedure since the PDA did not close at 3 months of age and the oxygen saturation had already risen to 94% (see Figure 2J). There were no vascular access complications. The follow-up was clinically satisfactory and the patient underwent Rastelli surgery age at 11 months with good outcomes.

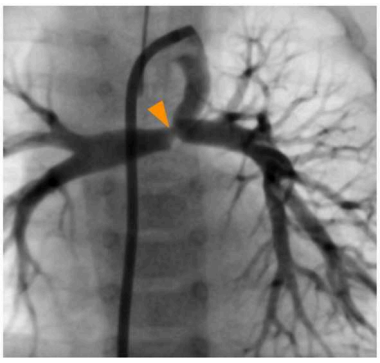

FIGURE 1
Ductal angiography showing the restricted pulmonary ductal (orange arrowhead) end and the absence of connection between the branch pulmonary arteries and the pulmonary artery trunk.

Discussions

Ductal stenting in critical congenital heart disease

The DS procedure is an essential cornerstone in the interventional treatment of newborns with pulmonary flow duct-dependent circulation (3). A 0.014 coronary wire with a radio-opaque tip was used to determine the size of the stent where the length of the lesion was compared to the wire's tip. In this small patient, we chose the naked method and the more complex transvenous approach to first implant a larger stent and second avoid the potential injuries on the femoral artery and acute limb ischemia (4). At the time of the intervention, we had no prior experience with the more direct approach from the carotid or axillary arteries through which a 5 or even a 6-Fr sheath can be safely used even in small kids (5). As the distal part of the PDA was constricted, we also performed balloon dilatation to assure the safety of the stent implantation (6).

Strutted stents in the abdominal inferior vena cava: Troubleshooting tactics

When we tried to retrieve the stent, the stent got stuck and strutted in the IVC. The stiffness of the Dynamic Vascular Stent and the rough maneuvering in the complex ductal loop may be to blame. Previous studies showed that coronary stent implantation in proximal segments of coronary arteries rather than distal ones may lead to dislodgement (7, 8). Its incidence ranges from 0.3 to 8% due to pre-mounting technologies and modern equipment (9). A limited number of reports described emergency surgical stent retrieval for entrapped coronary stents (8, 10). The majority of these cases are brought on by a balloon-stripped undeployed stent. This mechanism usually occurs due to constricted PDA, angulated lesions, short small stents, unexpanded stents, and manual handling of stents (11). The retrieving methods can be performed percutaneously, surgically, or a combination of both, which we used in this case. Percutaneous retrieval methods should be preferred if the patient's vital signs and clinical status are stable. Several retrieval methods are defined, including biliary forceps, twisted guide wires, multipurpose baskets, snares, and the small-balloon technique (12).

Extracting the stent through the RAA is a safe hybrid alternative but can be considered logistically challenging and there is a possibility of grazing the tricuspid valve, coronary

10.3389/fcvm.2022.1084170

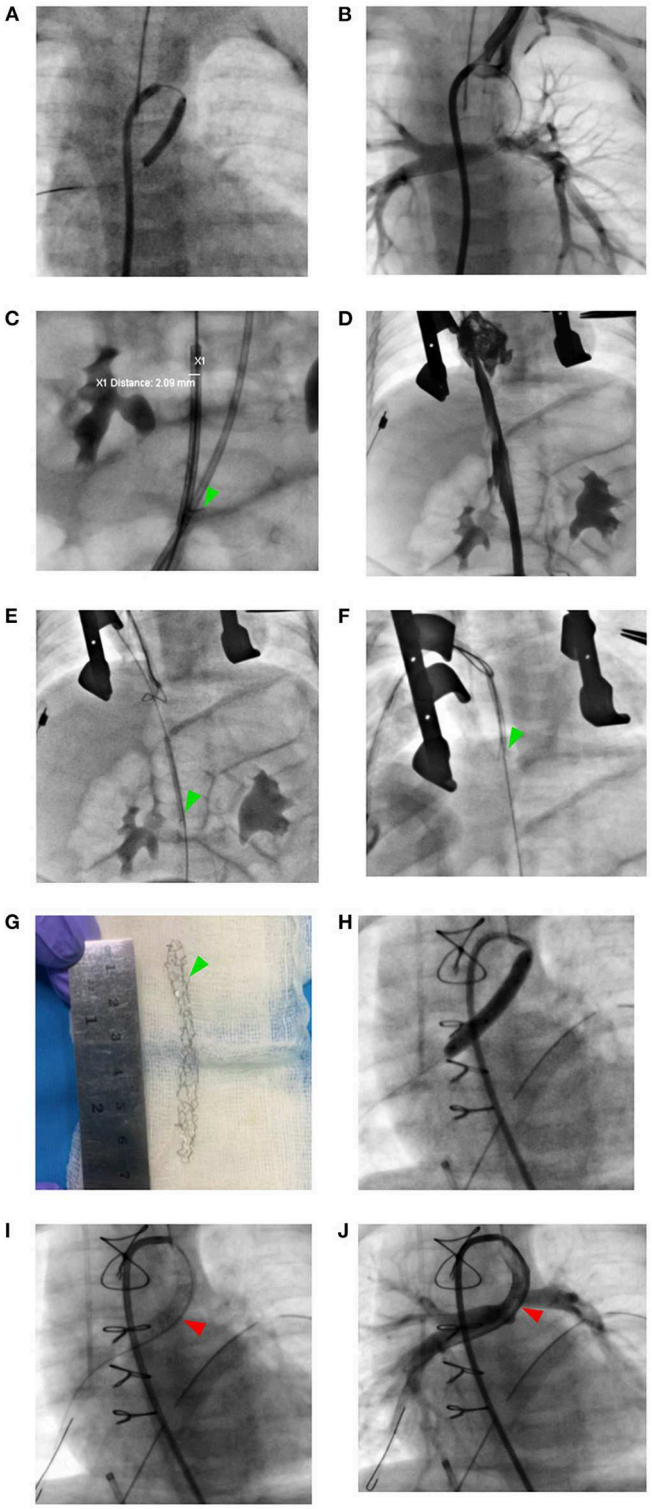

FIGURE 2
Stucked stent retrival strategy from the inferior vena cava and transarterial restenting the ductus arteriosus. **(A)** Ductal pre-dilation with an Ikazuchi coronary balloon 3.0 x 20 mm. **(B)** Failure to deliver the Dynamic vascular stent within the ductus arteriosus. **(C)** The stent strutted in the inferior vena cava (green arrowhead). **(D)** Caval angiography showing no vascular trauma. **(E–G)** Stent Evacuated through right atrial appendage hybrid access with 20 mm gooseneck snare. **(H, I)** Transarterial ductal restenting with Resolute Integrity 4.0 x 30 mm stent (red arrowhead). **(J)** Post-stenting ductal angiography.

sinus, and other surrounding structures (13). In this case, we tried to retrieve the stent by using a 90-gooseneck snaring system across an RAA hybrid access (13, 14). We decided to snare the stent through RAA access because transfemoral snaring would have certainly damaged the IVC or the femoral vein. Open abdominal surgery through the IVC was considered risky as air embolism can be detrimental in this case with an intracardiac shunt. Due to the IVC profundal location, surgical access to the clamp is also considered anatomically impossible with bad exposure to form purse-string sutures. Finally, the stent could be compressed and clamped when it is within the RAA, and damaged parts of the RAA could be surgically removed.

Conclusions

Strutted stent entrapment is a rare but serious complication of transcatheter stenting interventions. Hybrid access across the RAA can be a safe and effective bailout solution to retrieve a trapped stent from the IVC without cardiopulmonary bypass support.

Data availability statement

The original contributions presented in the study are included in the article/supplementary material, further inquiries can be directed to the corresponding author.

Ethics statement

Ethical review and approval was not required for the study on human participants in accordance with the local legislation and institutional requirements. Written informed consent to participate in this study was provided by the participants' legal guardian/next of kin. Written informed consent was obtained from the minor(s)' legal guardian/next of kin for the publication of any potentially identifiable images or data included in this article.

Author contributions

RP conceived the original idea of the manuscript. RP, AS, LH, and BM contributed in collecting the patient data and writing the main text of the paper. All authors discussed and agreed with the idea of the paper. The manuscript was proofread and accepted by all authors.

Acknowledgments

We would like to thank those who have supported us in the making of this study. We are especially grateful to the Department of Cardiology and Vascular Medicine, Faculty of Medicine Universitas Indonesia, as well as reviewers and editor, for their guidance and assistance in teaching the authors and for proof-reading this article.

Conflict of interest

The authors declare that the research was conducted in the absence of any commercial or financial relationships that could be construed as a potential conflict of interest.

Publisher's note

All claims expressed in this article are solely those of the authors and do not necessarily represent those of their affiliated organizations, or those of the publisher, the editors and the reviewers. Any product that may be evaluated in this article, or claim that may be made by its manufacturer, is not guaranteed or endorsed by the publisher.

References

1. Tongut A, Desai M, Peer SM, Yerebakan C. Emergency surgical stent retrieval following stent dislodgement during ductal stenting for hybrid palliation. *Interact CardioVasc Thorac Surg.* (2021) 32:825–7. doi: 10.1093/icvts/ivaa337

2. Ratnayaka K, Nageotte S, Moore J, Guyon P, Bhandari K, Weber R, et al. Patent ductus arteriosus stenting for all ductal-dependent cyanotic infants. *Circulation.* (2021). 14:e009520. doi: 10.1161/CIRCINTERVENTIONS.120.009520

3. Haddad RN, Hanna N, Charbel R, Daou L, Chehab G, Saliba Z. Ductal stenting to improve pulmonary blood flow in pulmonary atresia with intact ventricular septum and critical pulmonary stenosis after balloon valvuloplasty. Cardiol Young. (2019) 29:492–8. doi: 10.1017/S1047951119000118

4. Silva Marques J, Gonçalves C. Post-catheterisation arterial thrombosis in children – pathophysiology, prevention, and treatment. *Cardiol Young.* (2014) 24:767–73. doi: 10.1017/S1047951114000171

5. Bauser-Heaton H, Qureshi AM, Goldstein BH, Glatz AC, Nicholson GT, Meadows JJ, et al. Use of carotid and axillary artery approach for stenting the patent ductus arteriosus in infants with ductal-dependent pulmonary blood flow: a multicenter study from the congenital catheterization research collaborative. *Catheter Cardiovasc Interv.* (2020) 95:726–33. doi: 10.1002/ccd.28631

6. Cuculi F, Bossard M, Zasada W, Moccetti F, Voskuil M, Wolfrum M, et al. Performing percutaneous coronary interventions with predilatation using non-compliant balloons at high-pressure versus conventional semi-compliant balloons: insights from two randomised studies using optical coherence tomography. *Open Heart.* (2020) 7:e001204. doi: 10.1136/openhrt-2019-001204

7. Borhani S, Hassanajili S, Ahmadi Tafti SH, Rabbani S. Cardiovascular stents: overview, evolution, and next generation. *Prog Biomater.* (2018) 7:175–205. doi: 10.1007/s40204-018-0097-y

8. Sinha SK, Razi M, Thakur R, Jha J, Goel A, Mishra V, et al. Acute dislocation of fully deployed stent after use of non-compliant balloon: an enigma. *Folia Cardiol.* (2016) 11:222–5. doi: 10.5603/FC.2016.0035

9. Esenboga K. The stent was wriggled out in left main coronary: we tried many things and at the end retrieved it by snare. *Van Med Journal.* (2018) 25:253–6. doi: 10.5505/vtd.2018.02986

10. Alomar ME, Michael TT, Patel VG, Altomare C, Rangan B, Cipher D, et al. Stent loss and retrieval during percutaneous coronary interventions: a systematic review and metaanalysis. *J Invasive Cardiol.* (2013) 25:637–41.

11. Degirmenci H, Bakirci EM. Approach to coronary stent stripping. *MN Cardiology.* (2018) 25:87–92.

12. Porwal SC, Halkati PC, Patted SV, Joshi A. Successful deployment of a dislodged sirolimus- eluting stent with a small-balloon technique. *J Cardiol Cases.* (2013) 8:155–7. doi: 10.1016/j.jccase.2013.07.009

13. Hołda J, Słodowska K, Tyrak K, Bolechała F, Jasińska KA, Koziej M, et al. Topographical anatomy of the right atrial appendage vestibule and its isthmuses. *J Cardiovasc Electrophysiol.* (2020) 31:3199–206. doi: 10.1111/jce.14767

14. Yang Soon C, Chong E, Sangiorgi GM, A. challenging case of dislodged stent retrieval with the use of Goose neck snare kit. *Catheter Cardiovasc Interv.* (2010) 75:630–3. doi: 10.1002/ccd.22283

frontiers | Frontiers in Pediatrics

TYPE Case Report
PUBLISHED 26 January 2023
DOI 10.3389/fped.2022.1041728

OPEN ACCESS

EDITED BY
Cecile Tissot,
Clinique des Grangettes, Switzerland

REVIEWED BY
Tingliang Liu,
Shanghai Children's Medical Center, China
Juan Feng,
Shandong Provincial Hospital, China

*CORRESPONDENCE
Shujuan Li
✉ lishuj2@mail.sysu.edu.cn

SPECIALTY SECTION
This article was submitted to Pediatric Cardiology, a section of the journal Frontiers in Pediatrics

RECEIVED 11 September 2022
ACCEPTED 30 December 2022
PUBLISHED 26 January 2023

CITATION
Lin Y, Zhu L, Li X, Ba H, He X and Li S (2023) Stent implantation in severe aortic coarctation in a pediatric patient with Turner syndrome: Case report and literature review.
Front. Pediatr. 10:1041728.
doi: 10.3389/fped.2022.1041728

Stent implantation in severe aortic coarctation in a pediatric patient with Turner syndrome: Case report and literature review

Yuese Lin[1,2], Ling Zhu[1,2], Xuandi Li[1,2], Hongjun Ba[1,2], Xiufang He[1,2] and Shujuan Li[1,2]*

[1]Department of Paediatric Cardiology, Heart Center, The First Affiliated Hospital, Sun Yat-sen University, Guangzhou, China, [2]Key Laboratory on Assisted Circulation, Ministry of Health, Guangzhou, China

Background: Turner syndrome is a rare systemic disease and a significant proportion of these patients experience aortic coarctation. Selection of optimal therapy for aortic coarctation in patients with Turner syndrome is difficult due to the pathologic change of the systemic vessel.
Case presentation: We report one successful case of covered stent implantation for the treatment of severe native coarctation of the aorta in a 15-year-old patient with Turner syndrome weighing 36 kg. A covered stent was implanted in this patient. After the stent implantation, the peak systolic pressure gradient immediately decreased from 48 mmHg to 14 mmHg. The aortic diameter at the coarctation site increased from 3 mm to 10 mm after stenting. A femoral arterial complication occurred in this case, and we stabilized the situation finally.
Results: During a follow-up of 3 years, no restenosis of aortic coarctation was observed and the patient no longer experienced hypertension. The dissection of the right femoral artery remained stable.
Conclusion: A covered stent implantation for severe aortic coarctation in patients with Turner syndrome could be safe and effective. However, caution should be taken when using the technique to prevent complications.

KEYWORDS
aortic coarctation, Turner syndrome, stent implantation, covered stent, complications

Background

Although stent implantation for the treatment of native coarctation of the aorta (CoA) has been widely reported in older children, adolescents, and adults, limited data exist on the results in patients with Turner syndrome (1). We report one case of a covered Cheatam-platinum stent implantation in severe aortic coarctation in a patient with Turner syndrome. Although a femoral arterial complication occurred in this case, we finally stabilized the situation. During a follow-up of 3 years, the patient remained asymptomatic and normotensive, and the dissection of the right femoral artery remained stable.

Case presentation

A 15-year-old female patient was admitted to our hospital with a 12-year history of short stature and growth retardation. A physical examination on admission revealed that the weight and height of the patient was 36 kg and 1.37 m, respectively; both were less than three standard deviations of the same age. Special facial features of the patient were noted, including prominent posteriorly rotated auricles with looped helices, infraorbital skin creases,

10.3389/fped.2022.1041728

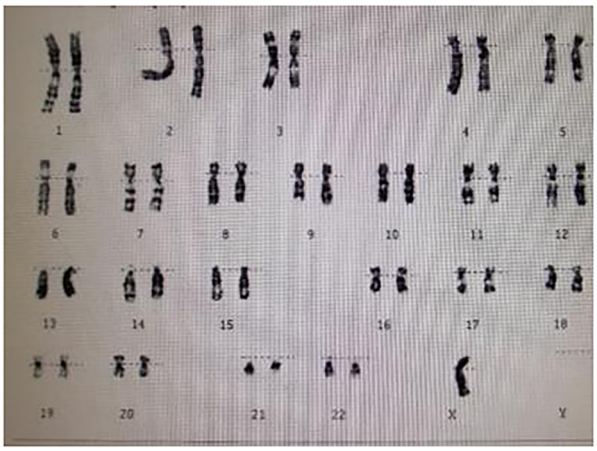

FIGURE 1
Karyotype analysis showing a pure 45, X karyotype.

and a mildly foreshortened mandible. Other characteristic signs, including a webbed neck, low posterior hairline, and lack of breast development, were also found. The cuff blood pressure in both arms was 160/100 mmHg, and in both legs 110/80 mmHg. A cardiac examination demonstrated a grade 2/6 systolic ejection murmur in the second and third left intercostal spaces radiating to the suprasternal fossa and back. The chest x-ray was unremarkable. An ECG indicated cardiac hypertrophy and an echocardiography examination revealed a severe native aortic coarctation with a peak pressure gradient of 60 mmHg by Doppler image. The aortic valve was normal, and no signs of bicuspid aortic valve, aortic root dilatation, and dissection were found by echo. Renal ultrasonography was normal, but no obvious uterine and ovarian structures were found using gynecological ultrasonography. In view of these findings, a karyotype analysis was performed, and the result was a complete loss of the second X chromosome, revealing she had a pure 45, X karyotype (**Figure 1**). Based on these examination results, the patient was diagnosed with Turner syndrome with a severe native aortic coarctation.

Further evaluations and examinations for cardiac malformation were performed. A CT scan showed a severe aortic coarctation just beyond the origin of the left subclavian artery (LSCA) (**Figure 2A**). At cardiac catheterization, under general anesthesia, the ascending aortic pressure was 138/85 mmHg and the descending aortic pressure was 90/72 mmHg. A descending aortogram confirmed a discrete lesion with a shelf-like in-folding and minimum diameter of 3 mm.

Due to the congenital dysplasia of the aortic wall and inherent vessel weakness in patients with Turner syndrome, and considering this was a case of severe aortic coarctation with the narrowest lesion being only 3 mm, we held a multidisciplinary team meeting for the case with surgeons and other colleagues to determine the appropriate choice of treatment. Finally, the interventional therapy of a covered stent implantation was considered to be suitable for this patient.

Interventions and results

After obtaining informed consent from the guardians, CoA stenting for the patient was performed very cautiously. Femoral arteriography showed that the diameters of both femoral arteries were similar, so we routinely picked the right femoral artery as the vessel access for stenting. The diameter of the aortic arch, thoracic aorta at the subclavian artery proximal to the coarctation site, and descending aorta at the level of the diaphragm were 11.0 mm,

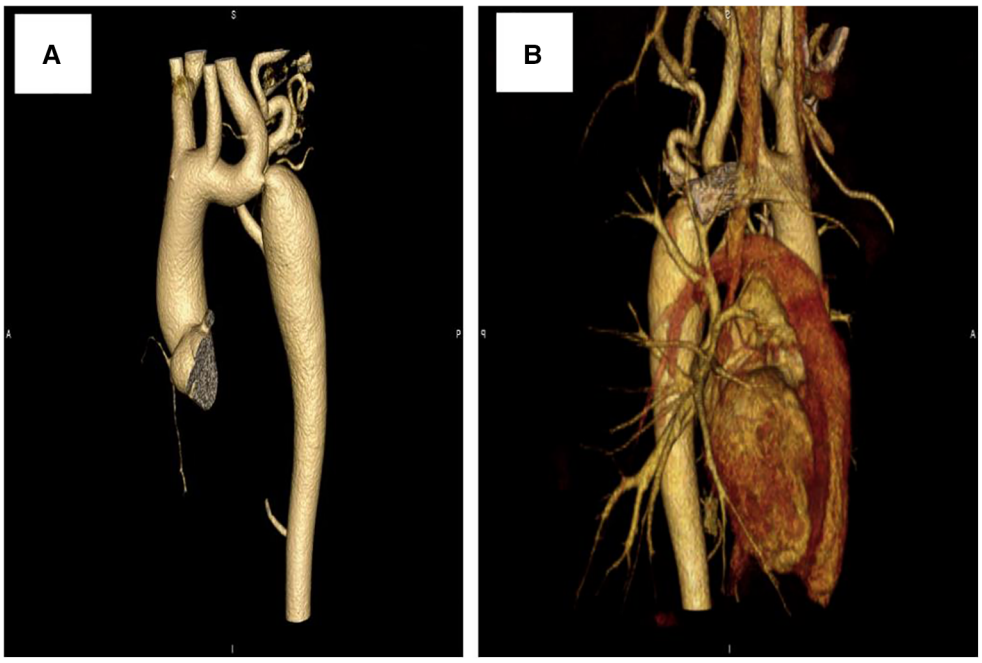

FIGURE 2
Computed tomography scan showing: (A) prior to stenting, (B) 3 years after stenting.

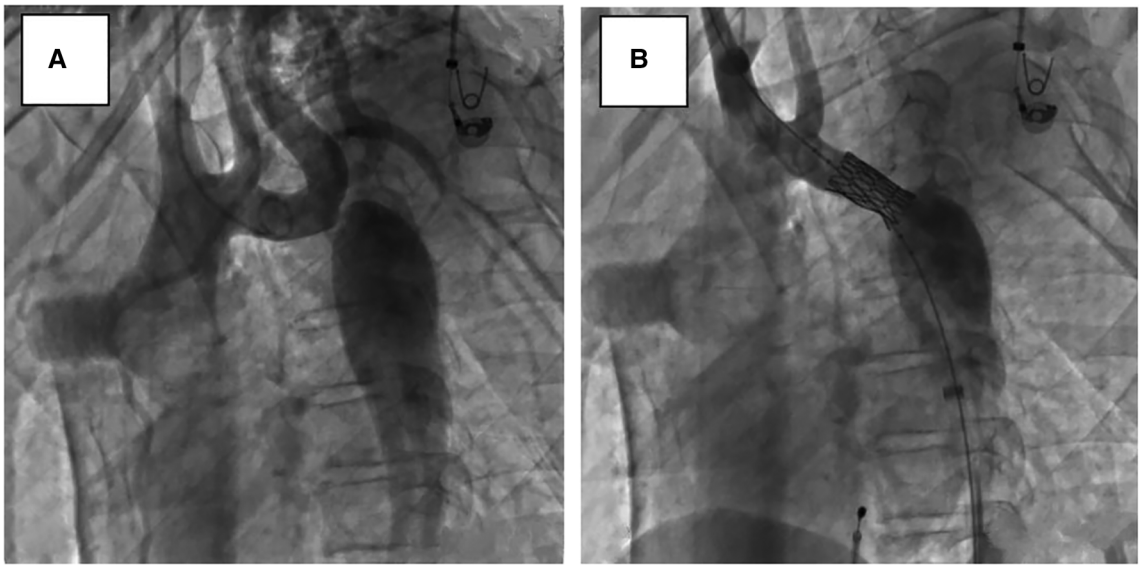

FIGURE 3
Lateral view, descending aortograms: (A) prior to stenting, (B) immediately after stenting.

11.8 mm, and 12.0 mm, respectively (Figure 3A). Therefore, we planned to expand the narrowest place to about 10 mm, which was not more than three times the diameter of the narrowest place and the diameter of the aortic arch, referring to the experiences and rules of stent implantation for severe CoA in the literature. A 22-mm-long covered Cheatam-platinum stent (NuMED, Hopkinton, NY, USA) mounted on a balloon in balloon catheter (NuMED), with a diameter of 12 mm and length of 25 mm, was implanted across the lesion through a 12-F delivery sheath. After stenting, the ascending aortic and descending aortic systolic pressure was 115 and 101 mmHg, respectively; the pressure gradient across the lesion decreased to 14 mmHg and a repeated descending aortogram showed that the diameter of the CoA increased to 10 mm, without angiographic evidence of an acute aneurysm formation (Figure 3B). However, 3 days after stenting, a CT scan showed a dissection of the right femoral artery (Figure 4A). Therapy with antihypertensive drugs and pain medication was initiated and the patient's condition stabilized. The case was discussed with colleagues from the department of vascular surgery. It was judged whether a stent implantation in the femoral artery would be a suitable treatment if the patient's condition deteriorated. Fortunately, during the next 2 weeks, the false lumen of the vessel did not widen further and perfusion of the right lower limb remained normal.

At a clinical follow-up visit 3 years after the stent implantation, the patient remained asymptomatic and normotensive, with a 10 mmHg gradient between upper and lower extremity blood pressures and a Doppler peak instantaneous gradient across the CoA of 15 mmHg by echocardiography. There was no evidence of aortic complications (Figure 2B) on CT scan and the dissection of the right femoral artery remained stable (Figure 4B). No signs of ischemia of the blood flow to the arterial side branches supplying

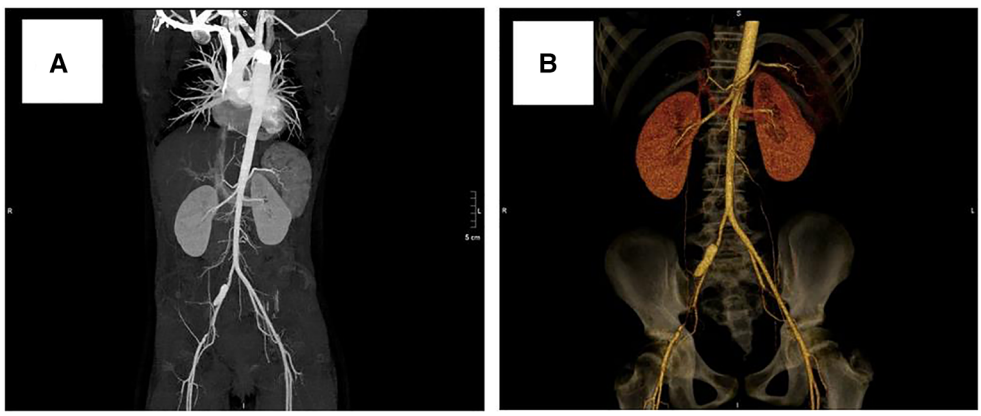

FIGURE 4
Computed tomography scan showing dissection of the right femoral artery: (A) 3 days after stenting, (B) 3 years after stenting.

the spinal cord and the left common carotid artery were observed during the follow-up.

Discussion

Turner syndrome occurs in about 1 of 2,500–3,000 live female births, and approximately one-third of these patients experience a cardiovascular malformation. It is reported that 75% of these lesions have been a CoA or a bicuspid aortic valve with or without stenosis (2, 3). General treatment options for a native CoA have been surgery, balloon angioplasty, and stent implantation, depending on the age and weight of the patients, morphology and anatomy of the obstructive vascular lesion, and the local medical technology.

Surgical repair is the traditional management for CoA and the first choice of treatment in neonates and infants aged less than 3 months. Surgery also remains the only treatment option when transcatheter therapies fail. However, in 1984, it was already noted that surgery for aortic coarctation carries greater risks in patients with Turner syndrome (4). Zanjani et al. (5) summarized that the operative mortality and aortic wall injury (dissection, aneurysm formation) rates were 11% and 30%, respectively, after surgical repair of CoA in patients with Turner syndrome, which were obviously higher than those in genetically normal patients and also the highest among the above three treatment methods. Due to the inherent vessel wall weakness, namely cystic medial necrosis of the aortic wall, surgical repair may not be an ideal treatment option for a CoA in patients with Turner syndrome.

Balloon angioplasty has become an alternative treatment strategy for native and recurrent coarctation after surgery for many decades, with a good success rate and safety profile (6). Zanjani et al. (5) reported that balloon dilatation of CoA in patients with Turner syndrome carried the lowest mortality and risks of aortic wall injury among the three treatment options, which were 0% and 2%, respectively. Although balloon dilatation of CoA has excellent short-term results in patients with Turner syndrome (7), a high rate of restenosis after balloon angioplasty (8) and potential complications, including aortic dissection, aortic rupture, and aneurysm formation (9), have generated controversy regarding its use. Furthermore, it may result in a structurally weakened area instead of reconstructing normal vessel wall histology after balloon angioplasty (10), which could be the pathologic basis for the formulation of aneurysms and vessel recoil, which can lead to a recurrent lesion.

In past decades, endovascular stenting has been a safe and effective alternative treatment strategy to surgery or angioplasty in children and adults (11, 12). The mortality and aortic wall injury rates after CoA stenting in patients with Turner syndrome were reported as 6.6% and 20%, respectively (4), clearly lower than surgical repair. Stenting has theoretical advantages over balloon angioplasty: it not only prevents vessel recoil and maintains the effect of stent dilation, but also reduces the risk of aneurysm formation by preventing excessive dilation of the blood vessels (10). Still, aortic dissection after the stenting for native CoA has been noted (13). Fejzic et al. (9) reported a case of a bare metal stent implantation in a teenage patient with Turner syndrome; fetal aortic dissection occurred after a second procedure to redilate the stent. The patient's mother had previously died, also due to a dissection of the ascending aorta. A histological examination of the mother's aortic tissue showed fragmentation of elastic fibers and cystic medial necrosis. Further genetic study of the DNA examination demonstrated evidence of a mutation in the fibrillin-1 gene, similar to the changes found in Marfan syndrome. Shahri et al. (14) reported an aortic dissection occurred in nine patients who had received stent implantation therapy. Due to this inherent vessel wall weakness (15), use of a covered stent may be an advisable alternative treatment option in the setting of Turner syndrome. Covered stents can not only reduce the degree of traumatic injury to the aortic wall but also cover the injured wall in the stented area, which is especially appropriate and safe when there has already been aneurysm formation. In addition, as the pediatric patient grows older and develops physically, restenosis may occur at the primary CoA. In view of the above considerations, we selected a covered stent for this case. On the one hand, the covered stent could protect the blood vessel better and reduce the risk of complications, which is particularly meaningful to the vascular situation of patients with Turner syndrome. On the other hand, if restenosis occurs in the patient during follow-up, a second procedure to redilate the stent could be applied.

The most common significant complications of stent implantation were aneurysm formation, aortic dissection, cerebrovascular accident, and femoral access vessel injury. Additional concerns regarding the use of covered stents focus on the potential compromise of blood flow to the arterial side branches, especially those supplying the spinal cord, the head, and left upper limb, which may cause severe ischemia. In our case, the site of the CoA was just beyond the origin of the LSCA. As the stent was positioned to cover the CoA site, it would cross the LSCA but did not affect the blood flow to the spinal cord and the left common carotid artery. A CT angiography scan before the procedure confirmed the side branches supply the LSCA by the cerebral artery ring. With regard to femoral access vessel injury, however, it would be another serious complication after arterial catheter interventions. Shahri et al. (14) also reported that a dissection occurred in the external femoral artery among the nine patients after stenting. During the stent implantation of the native CoA, the diameter of the balloon is chosen to be equal to that of the normal aorta (usually in the transverse arch) and not greater than the diameter of the aorta at the diaphragm. The diameter of the delivery sheath should be 2 F larger than the balloon, and it is difficult to crimp over a balloon with a diameter less than 8–9 F (16). In our case, the size of the delivery sheath was12 F, which may be somewhat related to the occurrence of the femoral artery complication. Turner syndrome is a systemic disease, similar to Marfan syndrome, and the pathologic change of cystic medial necrosis would affect the blood vessels in the whole body. Femoral arteriography of both femoral arteries, to pick up the appropriate vessel access for stenting and to choose a smaller delivery sheath as far as possible during the procedure, is beneficial to reduce the risk of femoral artery complications.

Selecting the optimal therapy for CoA in patients with Turner syndrome is difficult due to the pathologic change of systemic

vessel cystic medial necrosis. Although interventional treatment for CoA is a common treatment method and widely used in clinical practice nowadays, there are still limited data about the optimal choice for treatment, especially in patients with Turner syndrome. As we know, interventional therapy for severe aortic coarctation is challenging and somewhat difficult in clinical practice, especially when the pediatric patient has Turner syndrome. It not only increases the difficulty of the procedure itself, but also raises the risk of the operation, due to the inherent abnormality and weakness of the vascular wall. Taking into account the cases reported so far, stent implantation is not inferior to the other treatment methods with regard to mortality and vessel wall injury rates (5). Van den Hoven et al. (17) reported that adverse outcomes, such as aortic dissections, could occur in CoA in patients with Turner syndrome. However, there were only nine pediatric patients, and some adverse outcomes of cases were proved not to be related with the transcatheter procedure itself and no procedural complications were observed. A covered stent would be an interventional choice in the appropriate patient. Still, caution should be taken when using the technique and a larger population of pediatric patients is needed.

In conclusion, we presented a case of a successful covered stent implantation for the treatment of severe native CoA in a pediatric patient with Turner syndrome, with encouraging early and mid-term results, although not with a perfect outcome because of the femoral artery complication. A covered stent implantation could provide an alternative therapeutic option and could be safe and effective. However, vascular complications or adverse cardiac events may occur during the procedure and these should be handled cautiously. In addition, lifelong cardiovascular monitoring and follow-up for Turner syndrome is essential (1).

Data availability statement

The original contributions presented in the study are included in the article/Supplementary Material, further inquiries can be directed to the corresponding author/s.

Ethics statement

The studies involving human participants were reviewed and approved by the ethics committee of the First Affiliated Hospital, Sun Yat-sen University, Guangzhou, China. Written informed consent to participate in this study was provided by the participants' legal guardian/next of kin. Written informed consent was obtained from the individual(s), and minor(s)' legal guardian/next of kin, for the publication of any potentially identifiable images or data included in this article.

Author contributions

All authors listed have made a substantial, direct, and intellectual contribution to the work and approved it for publication. All authors contributed to the article and approved the submitted version.

Funding

This study was supported by the Natural Science Foundation of China (81900350).

Conflict of interest

The authors declare that the research was conducted in the absence of any commercial or financial relationships that could be construed as a potential conflict of interest.

Publisher's note

All claims expressed in this article are solely those of the authors and do not necessarily represent those of their affiliated organizations, or those of the publisher, the editors and the reviewers. Any product that may be evaluated in this article, or claim that may be made by its manufacturer, is not guaranteed or endorsed by the publisher.

References

1. Silberbach M, Roos-Hesselink JW, Andersen NH, Braverman AC, Brown N, Collins RT, et al. Cardiovascular health in turner syndrome: a scientific statement from the American Heart Association. *Circ Genom Precis Med.* (2018) 11:e000048. doi: 10.1161/HCG.0000000000000048

2. Morgan T. Turner syndrome: diagnosis and management. *Am Fam Physician.* (2007) 76:405–10. PMID: 17708142

3. Donadille B, Christin-Maitre S. Heart and Turner syndrome. *Ann Endocrinol (Paris).* (2021) 82:135–40. doi: 10.1016/j.ando.2020.12.004

4. Brandt B 3rd, Heintz SE, Rose EF, Ehrenhaft JL, Clark EB. Repair of coarctation of the aorta in children with Turner syndrome. *Pediatr Cardiol.* (1984) 5:175–7. doi: 10.1007/BF02427041

5. Zanjani KS, Thanopoulos BD, Peirone A, Alday L, Giannakoulas G. Usefulness of stenting in aortic coarctation in patients with the Turner syndrome. *Am J Cardiol.* (2010) 106:1327–31. doi: 10.1016/j.amjcard.2010.06.063

6. Hornung TS, Benson LN, McLaughlin PR. Interventions for aortic coarctation. *Cardiol Rev.* (2002) 10:139–48. doi: 10.1097/00045415-200205000-00002

7. Park Y, Sklansky MS, Shaughnessy RD, Kashani IA, Rothman A. Balloon dilatation of native aortic coarctation in two patients with turner syndrome. *Pediatr Cardiol.* (2000) 21:474–6. doi: 10.1007/s002460010114

8. Hernández-González M, Solorio S, Conde-Carmona I, Rangel-Abundis A, Ledesma M, Munayer J, et al. Intraluminal aortoplasty vs. Surgical aortic resection in congenital aortic coarctation. A clinical random study in pediatric patients. *Arch Med Res.* (2003) 34:305–10. doi: 10.1016/S0188-4409(03)00055-9

9. Fejzic Z, van Oort A. Fatal dissection of the descending aorta after implantation of a stent in a 19-year-old female with turner's syndrome. *Cardiol Young.* (2005) 15:529–31. doi: 10.1017/S1047951105001447

10. Kataoka K, Ozawa A, Inage A, Benson LN. Transcatheter repair of native coarctation in children with turner syndrome: three case reports and literature review. *Congenit Heart Dis.* (2006) 1:315–20. doi: 10.1111/j.1747-0803.2006.00054.x

11. Golden AB, Hellenbrand WE. Coarctation of the aorta: stenting in children and adults. *Catheter Cardiovasc Interv.* (2007) 69:289–99. doi: 10.1002/ccd.21009

12. Harrison DA, McLaughlin PR, Lazzam C, Connelly M, Benson LN. Endovascular stents in the management of coarctation of the aorta in the adolescent and adult: one year follow up. *Heart*. (2001) 85:561–6. doi: 10.1136/heart.85.5.561

13. Varma C, Benson LN, Butany J, McLaughlin PR. Aortic dissection after stent dilatation for coarctation of the aorta: a case report and literature review. *Catheter Cardiovasc Interv*. (2003) 59:528–35. doi: 10.1002/ccd.10548

14. Shahri HMM, Mortezaeian H, Firouzi A, Khajali Z, Birjandi H, Nezafati MH, et al. Safety of aortic coarctation treatment in patients with Turner syndrome: a single-country case series and literature review. *Ann Vasc Surg*. (2022) S0890-5096:00111-X. doi: 10.1016/j.avsg.2022.02.020

15. Bons LR, Van Den Hoven AT, Malik M, Van Den Bosch AE, McGhie JS, Duijnhouwer AL, et al. Abnormal aortic wall properties in women with turner syndrome. *Aorta (Stamford)*. (2020) 8:121–31. doi: 10.1055/s-0040-1714384

16. Cheatham JP. Stenting of coarctation of the aorta. *Catheter Cardiovasc Interv*. (2001) 54:112–25. doi: 10.1002/ccd.1249

17. van den Hoven AT, Duijnhouwer AL, Eicken A, Aboulhosn J, de Bruin C, Backeljauw PF, et al. Adverse outcome of coarctation stenting in patients with turner syndrome. *Catheter Cardiovasc Interv*. (2017) 89:280–7. doi: 10.1002/ccd.26728

frontiers | Frontiers in Pediatrics

TYPE Case Report
PUBLISHED 09 February 2023
DOI 10.3389/fped.2023.1063795

OPEN ACCESS

EDITED BY
Elena Cervi,
Great Ormond Street Hospital for Children NHS Foundation Trust, United Kingdom

REVIEWED BY
Zipu Li,
Qingdao Women and Children's Hospital, China
Fu Lijun,
Shanghai Children's Medical Center, China

*CORRESPONDENCE
Tao Wang
✉ tonywong121@163.com

†These authors have contributed equally to this work

SPECIALTY SECTION
This article was submitted to Pediatric Cardiology, a section of the journal Frontiers in Pediatrics

RECEIVED 07 October 2022
ACCEPTED 09 January 2023
PUBLISHED 09 February 2023

CITATION
Xu X, Liu M, Zhang Y, Wang J, Lei X, Wang J, Zhou Y and Wang T (2023) Case report: Catecholamine cardiomyopathy in children with neuroblastoma.
Front. Pediatr. 11:1063795.
doi: 10.3389/fped.2023.1063795

Case report: Catecholamine cardiomyopathy in children with neuroblastoma

Xiaoyan Xu[1†], Meiqi Liu[1†], Yanmin Zhang[1,2], Jie Wang[3], Xi Lei[1], Juanli Wang[1], Yafei Zhou[2] and Tao Wang[1*]

[1]Department of Cardiology, Xi'an Children's Hospital, Affiliated Children's Hospital of Xi'an Jiaotong University, Xi'an, China, [2]National Regional Children's Medical Center (Northwest), Key Laboratory of Precision Medicine to Pediatric Diseases of Shaanxi Province, Xi'an Key Laboratory of Children's Health and Diseases, Shaanxi Institute for Pediatric Diseases, Xi'an Children's Hospital, Affiliated Children's Hospital of Xi'an Jiaotong University, Xi'an, China, [3]Institute of Children's Diseases, Xi'an Children's Hospital, Affiliated Children's Hospital of Xi'an Jiaotong University, Xi'an, China

Introduction: Many endocrine diseases, such as neuroblastoma (NB), can be linked with acquired cardiomyopathy and heart failure. Neuroblastoma's cardiovascular manifestations are typically hypertension, electrocardiogram (ECG) changes, and conduction disturbances.

Case Presentation: A 5-year-old 8-month-old girl was admitted to the hospital with ventricular hypertrophy and hypertension (HT) and heart failure. She had no previous history of HT. On color doppler echocardiography, the left atrium and left ventricle were enlarged. The left ventricular ejection fraction (EF) was as low as 40%, and the ventricular septum and left ventricular free wall were thickened. The internal diameters of both coronary arteries were widened. Abdominal computed tomography scan (CT) demonstrated an 8.7 cm × 7.1 cm × 9.5 cm tumor behind the left peritoneum. In urine catecholamines analysis, free-norepinephrine (f-NE), free-dopamine (f-DA), free-normetanephrine (f-NMN), free-3-methoxytyramine (f-3MT), vanillylmandelic acid (VMA), and homovanillic acid (HVA) levels were all greater than the normal range for 24 h except free-metanephrine (f-MN) and free-epinephrine (f-E). Based on these findings, we diagnosed her as NB complicated by catecholamine cardiomyopathy manifested by hypertrophic cardiomyopathy (HCM). Oral metoprolol, spironolactone, captopril and amlodipine furosemide, and intravenously injected sodium nitroprusside and phentolamine were employed for treating HT. After the tumor resection, the blood pressure (BP) and urinary catecholamine levels were all restored. After a follow-up of 7 months, echocardiography indicated normalization of ventricular hypertrophy and function.

Conclusion: This is a rare report showing catecholamine cardiomyopathy in NB children. Tumor resection leads to a return to normal of the catecholamine cardiomyopathy manifested as HCM.

KEYWORDS

catecholamine cardiomyopathy, neuroblastoma, children, hypertrophic cardiomyopathy, hypertension

Introduction

Catecholamine-induced cardiomyopathy (CICMP), a rare, devastating, and difficult-to-treat complication of phaeochromocytoma-paraganglioma (PPGL), is common in pheochromocytoma (1), but uncommon in neuroblastoma (NB). PPGL is a catecholamine-producing neuroendocrine tumor arising from extra-adrenal pheochromocytoma in 80%–85% of the adrenal glands or the rest of the autonomic ganglia (2).

NB is one of the most common solid tumors in early childhood accounting for approximately 8% to 10% of all childhood malignancies (3). The prevalence is 11–13 per million children under 15 years of age, 65 per million children under 1 year of age, and 1 per million children between 10 and 14 years of age (4–6). The median age for diagnosis is 18 months, and 90% of which occurs in children under the age of 10 years (7). The location, size, invasion of the tumor, impact of catecholamine release, and symptoms brought on by the paraneoplastic syndrome are the primary determinants of clinical presentations (8). HT occurs in approximately 10% of patients with NB due to extension of the renal pedicle, compression of the renal parenchyma, catecholamine secretion, or activation of the renin-angiotensin system (9). Elevated levels of catecholamine metabolites can be found in 95% of NB patients, and used for the diagnosis, including catecholamines (dopamine [DA], epinephrine [E], norepinephrine [NE]), metanephrines (3-methoxytyramine [3-MT], metanephrine [MN], normetanephrine [NME]) and phenolic acids (vanillylmandelic acid [VMA], homo-vanillic acid [HVA]) (10–14). VMA and HVA are most commonly analyzed in the urine of patients with NB (15, 16).

Here, we present a case of catecholamine cardiomyopathy manifested with HCM in NB, explain the differential diagnosis, and clinical outcome.

Case description

A girl aged 5 years and 8 months was admitted to our hospital with ventricular hypertrophy. The child gained and lost weight gradually for more than a year. Five months ago, a heart murmur was discovered during a health check, and her transthoracic

TABLE 1 Laboratory data on admission in this subject.

Myocardial damage markers			Urine catecholamines		
CK (U/L)	39	24–229	f-E (ug/L)	7.67	—
CK-MB (U/L)	39↑	0–25	f-NE (ug/L)	1,361.6	—
hs-cTnT (pg/ml)	22.86↑	0–14	f-DA (ug/L)	3,366.89	—
BNP (pg/ml)	20932↑	<300	f-MN (ug/L)	7.25	—
Endocrinology markers			f-NMN (ug/L)	365.95	—
TSH (uIU/ml)	1.37	0.34–6	f-3MT (ug/L)	462.95	—
TT3 (ng/ml)	1.03↓	1.13–1.89	VMA ((ug/L)	112.19	—
TT4 (ug/dl)	9.18	4.02–13.3	HVA (ug/L)	160.39	—
FT3 (pg/ml)	3.34	1.71–4.87	24hUV (ml)	873	—
FT4 (ng/dl)	0.99	0.7–1.48	24h-f-E (ug/24 h)	6.7	0–20
Cortisol (ug/dl)	16.9	5.00–25.00	24h-f-NE (ug/24 h)	1,188.68↑	0–90
ACTH (pg/ml)	18.5	10.00–185.00	24h-f-DA	2,939.29↑	0–600
LH (mIU/ml)	0.02↓	0.07–2.77	(ug/24 h)		
FSH (mIU/ml)	0.07↓	0.14–5.55	24h-f-MN	6.33	0.0–42.5
Prolactin (ng/ml)	1.21↓	3.1–11.2	(ug/24 h)		
Estradiol (pg/ml)	<10↓	10–49	24h-f-NMN	319.47↑	0.0–57.1
Progesterone (ng/ml)	1.2↑	0–0.99	(ug/24 h)		
Testosterone	<0.45	0.03–0.69	24h-f-3MT	404.16↑	0.0–63.8
(nmol/L)			(ug/24 h)		
HCG-β (mIU/ml)	<1.2	0–3	24h-VMA	97.94↑	0.0–10.0
Aldosterone (pg/ml)	515.6↑	98–275	(ug/24 h)		
ET (pg/ml)	48.91	43.22–58.38	24h-HVA (ug/24 h)	140.02↑	0.0-7.5
ANP (pg/ml)	311.11↑	50–150	Cancer markers		
Ang-II (pg/ml)	172.96↑	10–30	AFP (ng/ml)	2.64	0.89–8.78
			CEA (ng/ml)	16.32↑	0-6.2

BNP, brain natriuretic peptide; hs-cTnT, high-sensitive cardiac troponin T; CK, creatine kinase; CK-MB, creatine kinase isoenzymes; TSH stands for thyroid-stimulating hormone; TT3 stands for total triiodothyronine; TT4 stands for total thyroxine; FT3 stands for free triiodothyronine; LH stands for luteinizing hormone; FSH for follicle-stimulating hormone; HCG for human chorionic gonadotropin; ET for endothelin; and ACTH for adrenocorticotropic hormone; LH, luteinizing hormone; FSH, follicle-stimulating hormone; HCG-β, human chorionic gonadotropin-β; ET, endothelin; ANP, atrialnatriureticpeptide; Ang-II, angiotensin-II; f-E, free-epinephrine; f-NE, free-norepinephrine; f-DA, free-dopamine; f-MN, free-metanephrine; f-NMN, free-normetanephrine; f-3MT, free-3-methoxytyramine; VMA, vanillylmandelic acid; HVA, homovanillic acid; 24 h UV, 24 h urine volume; AFP, alpha-fetoprotein; CEA, carcinoembryonic antigen.

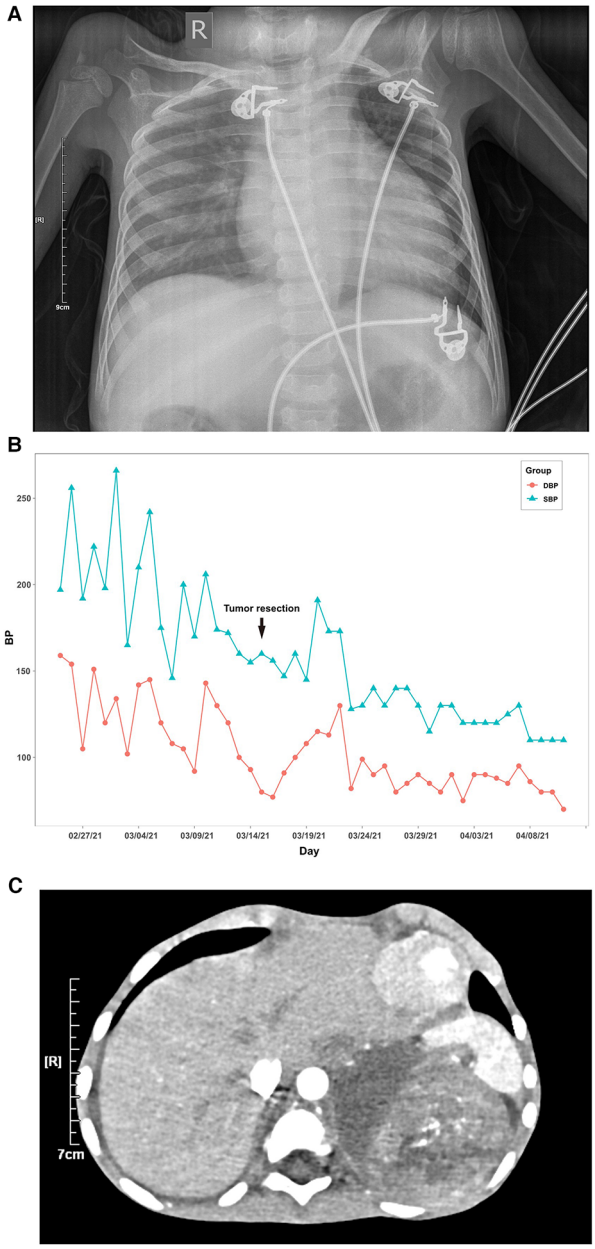

FIGURE 1
Blood pressure value, chest x-ray and abdominal computed tomography (CT) scan of the patient. (A) Line chart of the patient's daily maximum systolic and diastolic blood pressure. (B) In chest x-ray, the scattered patches revealed increased density and right pleural effusion, and the cardiac shadow was enlarged. (C) In the abdominal computed tomography (CT) scan, there was a right pleural effusion and a soft tissue density mass shadow behind the left peritoneum measuring 8.7 cm × 7.1 cm × 9.5 cm, with a CT value of approximately 28–46 HU. Internal density was varied, with calcified density shadow in certain areas. One possibility is neuroblastoma. The pressure is on the left kidney and spleen.

echocardiography revealed left ventricular hypertrophy without affecting the left heart's systolic function. Thus, she was diagnosed with nonobstructive hypertrophic cardiomyopathy (HCM), and began treatment with nutritional therapy. About 3 days before admission, she developed shortness of breath, decreased activity tolerance, and an increased heart rate, with no symptoms of cyanosis, dizziness, headache, nausea, or vomiting. She also had no family history of tumor, diabetes, HT, dyslipidemia, or endocrine disorders. The child gained and lost weight gradually for more than a year.

Her height, weight, and body mass index were 98 cm, 14 kg and 14.6 kg/m^2, respectively. Blood pressure (BP), pulse rate, respiratory frequency, and temperature were 170/135 mmHg, 130 beats/min, 47 beats/min, and 36.1°C. She had tachypnea and a dilated suprasternal fossa. Auscultation reveals attenuated bronchovesicular lung sounds in the right lung's basal region. A Class III/6 systolic murmur was heard in the 2–4 intercostal space at the left sternal margin. The abdomen was slightly distended, and a mass was felt in the upper abdomen's middle and left side, 10 cm below the xiphoid process and 2 cm below the left rib.

In myocardial markers, creatine kinase isoenzymes (CK-MB), high-sensitive cardiac troponin T (hs-cTnT), and brain natriuretic peptide (BNP) levels were elevated (**Table 1**). The ECG revealed a rapid atrial autonomic rhythm, biventricular hypertrophy, ST-T changes, and a prolonged QT interval (**Supplementary Figure S1**). In chest x-rays and computed tomography (CT) scans revealed an enlarged heart shadow, and the right pleural effusion [**Figure 1A**, **Supplementary Figure S2**]. Transthoracic echocardiography revealed that the left atrium and ventricle were both enlarged. Left ventricular ejection fraction (EF) was about 40%, and the ventricular septum and free wall of the left ventricle were thickened in general. The internal diameters of the bilateral coronary arteries were widened, with the left main coronary artery diameter of 4.1 mm and the right main coronary artery diameter of 3.0 mm (**Figure 2A,B**).

Her maximum systolic blood pressure (SBP) surpassed 160 mmHg and her maximum diastolic blood pressure (DBP) surpassed 100mmHg for up to 10 days after admission (**Figure 1B**). In relevant laboratory tests, her thyroid function, cortisol, and adrenocorticotrophic hormone (ACTH) revealed no abnormality. Aldosterone, atrial-natriuretic-peptide (ANP), and angiotensin-II (Ang-II) levels all increased. Except for f-MN and f-E, catecholamine concentrations in children's urine increased significantly, including f-NE, f-DA, f-NMN, f-MT, VMA, and HVA. Her symptoms, signs, and laboratory tests were all consistent with catecholamine cardiomyopathy diagnosis criteria (17).

Following the abnormal physical examination of her abdomen, we further performed an abdominal CT examination, which indicated an 8.7 cm × 7.1 cm × 9.5 cm mass shadow with low density behind the left peritoneum (**Figure 1C**). And her carcinoembryonic antigen (CEA) level was high (**Table 1**). On the 12th day, the child had a retroperitoneal tumor puncture biopsy. On the 19th day, the left retroperitoneal NB was resected. The detailed pathological findings of biopsy (**Figure 3A,B**) and resection both supported the diagnosis (**Figure 3C,D**). As a result, the child was diagnosed with NB complicated by catecholamine cardiomyopathy manifesting as HCM.

The treatment comprised anti-heart failure, anti-hypertension, and surgical therapy. **Figure 1A** depicts the BP changes during the entire treatment period. Her BP was still considerably raised six hours after admission, and it showed no signs of lowering. Therefore, we stopped the milrinone infusion and oral spironolactone tablets, and kept treating refractory hypertension

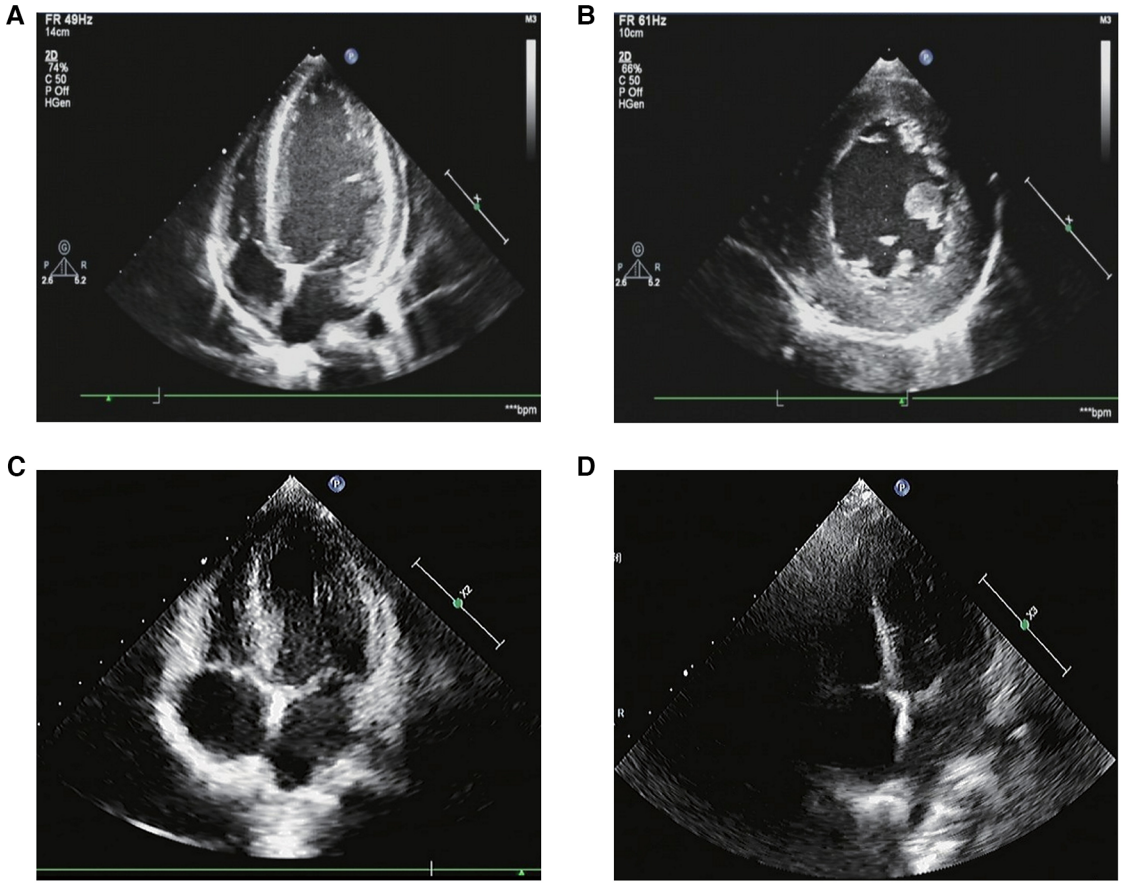

FIGURE 2
The transthoracic echocardiography. (A,B) The transthoracic echocardiography before the tumor resection. (1) The left atrium and ventricle were both enlarged. The ventricular septum and left ventricular free wall were generally thickened. The thicker left ventricular free wall was situated in the middle of the lateral wall, measuring about 14 mm in thickness, while the thicker ventricular septum was situated in the basal segment of the anterior septum, measuring about 12 mm in thickness. The estimated ejection fraction (EF) was about 40%. (2) Both of the bilateral coronary arteries' internal diameters were increased, with the left main coronary artery's diameter measuring 4.1 mm and the right main coronary artery's diameter measuring 3.0 mm. (3) A fluid dark area was observed in the pericardial cavity, 8 mm in the right ventricular sidewall and 4 mm in the apex. (C) The transthoracic echocardiography 3 months after the tumor resection. The left ventricle was mildly enlarged. The left ventricular wall was slightly thickened. The thicker left ventricular free wall was situated in the middle of the lateral wall, measuring about 9.5 mm in thickness, while the thicker ventricular septum was situated in the basal segment of the anterior septum, measuring about 10.6 mm in thickness. The systolic function of the left ventricle was normal. (D) The transthoracic echocardiography 7 months after the tumor resection. The measured values of the internal diameters of each atrioventricular cavity were normal. Each chamber wall's thickness and movement were both typical. The systolic function of the left ventricle was normal.

with the vasodilator sodium nitroprusside and the adrenergic α blocker phentolamine for 10 days. During this period, SBP was up to 266 mmHg and DBP was up to 159 mmHg. Amlodipine, in combination with sodium nitroprusside and phentolamine, was used to stabilize BP before tumor resection, followed by captopril and sodium nitroprusside. On the 27th day, we stopped the sodium nitroprusside, and switched to furosemide, spironolactone, metoprolol tartrate, captopril, and amlodipine tablets for 15 days. Then BP was sustained at 110–130/70–100 mmHg, and the values of catecholamines in urine were all returned to normal (**Supplementary Table S1**). After a subsequent follow-up of 3 months, her transthoracic echocardiography showed that the left ventricular wall became thinner than before, and left ventricular systolic function returned to normal (**Figure 2C**). After 7 months, her transthoracic echocardiography and hs-cTnT values were restored (**Figure 2D**). This implied that the catecholamine cardiomyopathy induced severe decline in heart function had been reversed.

Discussion

This case reported on a child who had catecholamine cardiomyopathy manifested as HCM in the retroperitoneal NB, which was gradually reversible after tumor resection. Most of the reported cases of cardiomyopathy were dilated cardiomyopathy (DCM) with heart failure (18–23), but unusual in NB. HT occurs in about 10% of NB cases (24). Left ventricular hypertrophy is seldom associated with NB (9), and HCM like changes are even rarer, with only 1 reported case in a 4.5-year-old child with sudden death (25). Among the reported DCM cases, urinary catecholamine excretion was elevated in all patients, but HT was present in only a few patients. This proved that myocardial injury and adrenergic receptor downregulation are caused by excessive catecholamine production rather than HT (18–23). This case also demonstrated that, prior to surgery, neither anti-hypertensive nor anti-heart failure treatments were beneficial to the child's condition. Chronic

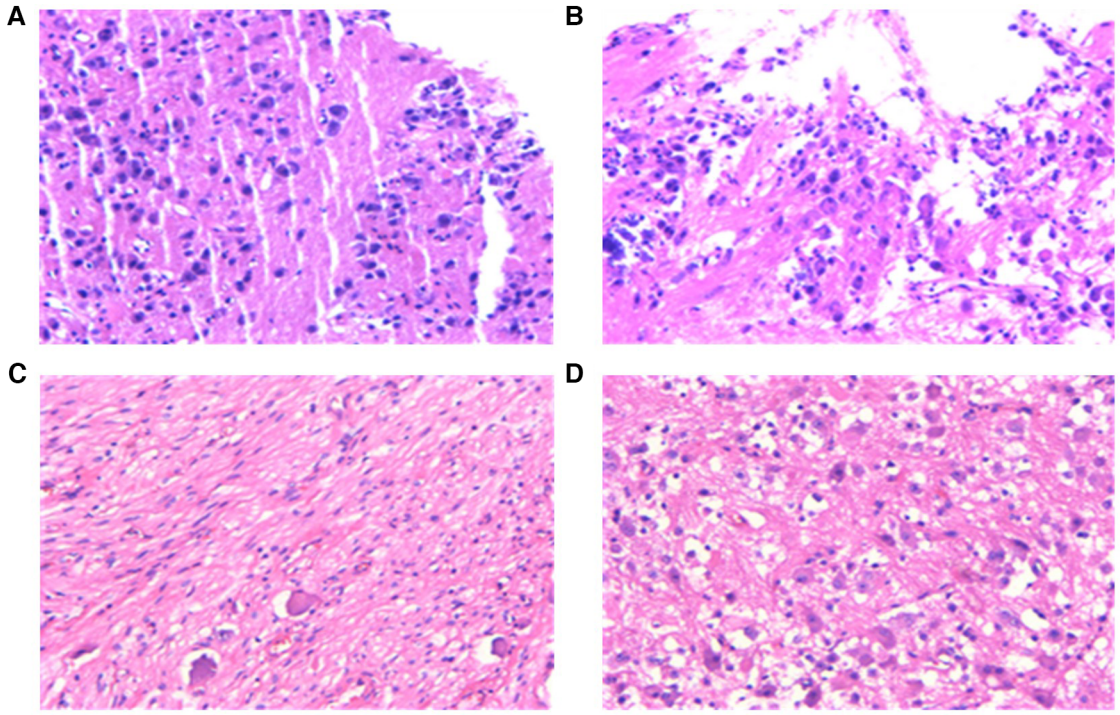

FIGURE 3
Pathological examination results. (A,B), pathology of a puncture biopsy specimen from a retroperitoneal tumor: Neuroblasts distributed in sheets were seen against the background of nerve fibers. The morphology was compatible with developed neuroblastoma with localized calcification, and the pathological diagnosis showed clear extrusion deformation of histiocytes. (C,D), pathology of biopsy specimen after surgical resection of tumor: (1) morphology was consistent with neuroblastoma (differentiated) with focal calcification. (2) retroperitoneal adrenal neuroblastoma (differentiated) with focal calcification, MKI < 2%. 3) tumor tissue was found in lymph nodes (aside from renal vein) (6/7). Tumor tissue was found in lymph nodes (aside from the abdominal aorta) (2/2). No tumor cells were discovered in lymph nodes (0/1) and (0/1).

catecholamine exposure can down-regulate cardiac β -adrenergic receptors, resulting in the loss of myofibrils, which results in cardiomyopathy and heart failure (26). Numerous factors contribute to the pathogenesis of cardiomyopathies, such as catecholamine-induced vasoconstriction and coronary vasospasm, chronic tachycardia myopathy brought on by an overactive sympathetic nervous system, adverse adrenergic receptor downregulation, free radical production, and encouragement of calcium influx into the sarcolemma (2, 27).

Catecholamine excess status has been linked to the pathogenesis of multiple cardiomyopathies, including tachycardia-associated cardiomyopathy, HCM, DCM, and Takotsubo cardiomyopathy (TCM) (17, 28–30). The results of chest radiography, electrocardiography, echocardiography, and invasive cardiac studies are crucial in the diagnosis of catecholamine cardiomyopathy (17). In this case, transthoracic echocardiography revealed left atrial and left ventricle enlargement, diffuse thickening of the interventricular septum and left ventricular free wall, and decreased LVEF. The chest radiograph revealed heart enlargement, ECG revealed changes in ST-T and QT interval prolongation, and 24 h urinary catecholamine metabolites were markedly elevated. These all fit the diagnostic criteria for catecholamine cardiomyopathy manifested as HCM. Echocardiography results confirm the distinction between DCM and HCM, with the former exhibiting no significant hypertrophy. Both HCM and DCM can progress to heart failure in the later stages of the disease, which manifests as tachypnea, dyspnea, hyperhidrosis, decreased activity tolerance, pulmonary edema, and reduced EF. As a result, this child began with ventricular hypertrophy and hypertension and progressed to heart failure, which also coincided with the points.

DCM and HCM are treated differently. Angiotensin converting enzyme inhibitors (ACEI), diuretics, digoxin, and nutritional agents have been used in all reported cases of DCM. However, as the loss of left ventricular volume may exacerbate the development of ventricular gradient, diuretics and digoxin should be avoided in HCM. Beta blockers and calcium antagonists, for example, are drugs that promote left ventricular filling. Metoprolol used in this case also controlled catecholamine-induced tachyarrhythmia (31). ACEI, such as captopril, exert the anti-hypertensive effect by directly blocking angiotensin II, and also reduce the severity of intraventricular obstruction and left ventricular hypertrophy (32). Therefore, the level of heart failure, outflow tract obstruction, and renal vascular compression should be taken into account while adjusting anti-hypertensive therapy. However, for catecholamine cardiomyopathy, the most critical treatment remains resection of the catecholamine-secreting NB (33). One of the most important targeted medications used to treat neuroblastoma is anthracyclines, although studies have shown that they have considerable cardiotoxicity (34). It should be initially avoided in this subject. A combination of various chemotherapeutic medications and the proper anti-hypertensive medications could be used to treat the patient's HT and heart failure in this

scenario. Anthracyclines can be considered at a later stage to maximize therapeutic effectiveness.

The child in this case developed coronary dilatation, but certain previous research showed that the coronary usually had no major disease (17, 35, 36). Catecholamine cardiomyopathy and coronary artery dilatation are understudied. Large coronary arteries have a significant proportion of α receptors mediating contraction, whereas small coronary arteries are almost entirely equipped with β receptors (β1 subclass) mediating relaxation (37). Acute excessive adrenergic stimulation causes excessive stimulation of the β1 adrenergic receptor, leading to increased cardiac oxygen demand and hypoxia in specific areas, which may contribute to coronary artery vasospasm (38, 39). Thus, we hypothesized that this could be related to coronary artery dilatation.

Catecholamine cardiomyopathy in NB is rare, thus early recognition of the complication is important for diagnosis and treatment. Cardiomyopathy may also occur in the absence of HT due to the direct effect of catecholamine on the myocardium. Therefore, throughout the course of treatment, BP monitoring and cardiovascular assessment should be actively improved, with a focus on cardiac problems connected to NB.

This case remains limited. First, while urine catecholamine metabolites were found, plasma catecholamine metabolites were not. Second, the mechanism of catecholamine cardiomyopathy complicated by coronary artery dilatation requires further investigation. Third, we did not conduct a genetic test on this patient, and it will be refined during a later follow-up to provide more insight into the pathogenesis of catecholamine cardiomyopathy.

Conclusion

We experienced a case of catecholamine cardiomyopathy in NB manifested with HCM. After tumor resection, catecholamine cardiomyopathy normalized. This case extremely important for clinicians in the early detection and treatment of special cardiomyopathy.

Data availability statement

The raw data supporting the conclusions of this article will be made available by the authors, without undue reservation.

Ethics statement

The studies involving human participants were reviewed and approved by Xi'an children's hospital's Medical Ethics Committee. Written informed consent to participate in this study was provided by the participants' legal guardian/next of kin. Written informed consent was obtained from the individual(s), and minor(s)' legal guardian/next of kin, for the publication of any potentially identifiable images or data included in this article.

Author contributions

XX & ML: writing original draft, review and editing. YZ: revising the manuscript for important intellectual content. JW: providing funding support. XL: collecting the data. JW & YZ: review and editing. TW: review, editing and final approval. XX and ML contributed equally to this paper. All authors contributed to the article and approved the submitted version.

Funding

This research was sponsored by the National Natural Science Foundation of China, 82300399.

Acknowledgments

We acknowledge the strong support of the Department of Cardiology of Children's Hospital affiliated with Xi'an Jiaotong University. We also thank editors and proofreaders for their help.

Conflict of interest

The authors declare that the research was conducted in the absence of any commercial or financial relationships that could be construed as a potential conflict of interest.

Publisher's note

Supplementary material

The Supplementary Material for this article can be found online at: https://www.frontiersin.org/articles/10.3389/fped.2023.1063795/full#supplementary-material.

References

1. Varghese RT, John AM, Paul TV. Catecholamine induced cardiomyopathy in pheochromocytoma. *Indian J Endocrinol Metab*. (2013) 17:733–5. doi: 10.4103/2230-8210.113771

2. Kumar A, Pappachan JM, Fernandez CJ. Catecholamine-induced cardiomyopathy: an endocrinologist's perspective. *Rev Cardiovasc Med*. (2021) 22:1215–28. doi: 10.31083/j.rcm2204130

3. Nakagawara A, Li Y, Izumi H, Muramori K, Inada H, Nishi M. Neuroblastoma. *Jpn J Clin Oncol*. (2018) 48:214–41. doi: 10.1093/jjco/hyx176

4. Hsieh MH, Meng MV, Walsh TJ, Matthay KK, Baskin LS. Increasing incidence of neuroblastoma and potentially higher associated mortality of children from nonmetropolitan areas: analysis of the surveillance, epidemiology, and end results database. *J Pediatr Hematol/Oncol*. (2009) 31:942–6. doi: 10.1097/MPH.0b013e3181bcc809

5. Xie L, Onysko J, Morrison H. Childhood cancer incidence in Canada: demographic and geographic variation of temporal trends (1992-2010). *Health Promot Chronic Dis Prev Can*. (2018) 38:79–115. doi: 10.24095/hpcdp.38.3.01

6. Kaatsch P, Steliarova-Foucher E, Crocetti E, Magnani C, Spix C, Zambon P. Time trends of cancer incidence in European children (1978-1997): report from the automated childhood cancer information system project. *Eur J Cancer*. (2006) 42:1961–71. doi: 10.1016/j.ejca.2006.05.014

7. London WB, Castleberry RP, Matthay KK, Look AT, Seeger RC, Shimada H, et al. Evidence for an age cutoff greater than 365 days for neuroblastoma risk group stratification in the children's oncology group. *J Clin Oncol*. (2005) 23:6459–65. doi: 10.1200/JCO.2005.05.571

8. Colon NC, Chung DH. Neuroblastoma. *Adv Pediatr*. (2011) 58:297–311. doi: 10.1016/j.yapd.2011.03.011

9. Madre C, Orbach D, Baudouin V, Brisse H, Bessa F, Schleiermacher G, et al. Hypertension in childhood cancer: a frequent complication of certain tumor sites. *J Pediatr Hematol Oncol*. (2006) 28:659–64. doi: 10.1097/01.mph.0000212995.56812.bb

10. Hoehner JC, Gestblom C, Hedborg F, Sandstedt B, Olsen L, Påhlman S. A developmental model of neuroblastoma: differentiating stroma-poor tumors' progress along an extra-adrenal chromaffin lineage. *Lab Invest*. (1996) 75:659–75. PMID: 8941212

11. LaBrosse EH, Comoy E, Bohuon C, Zucker JM, Schweisguth O. Catecholamine metabolism in neuroblastoma. *J Natl Cancer Instit*. (1976) 57:633–8. doi: 10.1093/jnci/57.3.633

12. Brodeur GM, Pritchard J, Berthold F, Carlsen NL, Castel V, Castelberry RP, et al. Revisions of the international criteria for neuroblastoma diagnosis, staging, and response to treatment. *J Clin Oncol*. (1993) 11:1466–77. doi: 10.1200/JCO.1993.11.8.1466

13. Verly IR, van Kuilenburg AB, Abeling NG, Goorden SM, Fiocco M, Vaz FM, et al. Catecholamines profiles at diagnosis: increased diagnostic sensitivity and correlation with biological and clinical features in neuroblastoma patients. *Eur J Cancer*. (2017) 72:235–43. doi: 10.1016/j.ejca.2016.12.002

14. Maris JM. Recent advances in neuroblastoma. *N Engl J Med*. (2010) 362:2202–11. doi: 10.1056/NEJMra0804577

15. Barontini de G, Bergadá C, Becú L. Significance of catecholamine excretion in the follow-up of sympathoblastomas. *Cancer*. (1971) 27:228–32. doi: 10.1002/1097-0142(197101)27:1<228::AID-CNCR2820270132>3.0.CO;2-F

16. Peaston RT, Weinkove C. Measurement of catecholamines and their metabolites. *Ann Clin Biochem*. (2004) 41:17–38. doi: 10.1258/000456304322664663

17. Kassim TA, Clarke DD, Mai VQ, Clyde PW, Mohamed Shakir KM. Catecholamine-induced cardiomyopathy. *Endocr Pract*. (2008) 14:1137–49. doi: 10.4158/EP.14.9.1137

18. Singh HR, Paules M, Forbes TJ, Zilberman MV. Reversible dilated cardiomyopathy and neuroblastoma. *J Pediatr*. (2005) 147:271. doi: 10.1016/j.jpeds.2004.12.030

19. Rosti L, Festa P, Corbetta C. Rapid reversal of dilated cardiomyopathy following removal of neuroblastoma. *Cardiol Young*. (1999) 9:519–21. doi: 10.1017/S1047951100005473

20. Joseph T, Olivier B, Magnier S, Brugières L, Casasoprana A. Cardiomyopathy induced by catecholamines in neuroblastoma. *Arch Pediatr*. (1997) 4:32–5. doi: 10.1016/S0929-693X(97)84303-5

21. Lee YH, Lee HD, Lee YA, Lee YS, Jung JA, Hwang GG, et al. Ganglioneuroblastoma presenting as dilated cardiomyopathy. *Arch Dis Child*. (2003) 88:162–4. doi: 10.1136/adc.88.2.162

22. Carlson P, Jefferies JL, Kearney D, Russell H. Refractory dilated cardiomyopathy associated with metastatic neuroblastoma. *Pediatr Blood Cancer*. (2010) 55:736–8. doi: 10.1002/pbc.22569

23. Kato M, Hirata S, Kikuchi A, Ogawa K, Kishimoto H, Hanada R. Neuroblastoma presenting with dilated cardiomyopathy. *Pediatr Blood Cancer*. (2008) 50:391–2. doi: 10.1002/pbc.21065

24. Duhil de Bénazé G, Iserin F, Durand P, Schleiermacher G, Orbach D. A dilated cardiomyopathy revealing a neuroblastoma: which link? *J Pediatr Hematol/Oncol*. (2016) 38:e251–3. doi: 10.1097/MPH.0000000000000659

25. Terbancea M, Pambuccian G, Goldis G. The sudden death of a 4 1/2-year-old child caused by hypertrophic obstructive cardiomyopathy owing to an abdominal neuroblastoma. *Acta Med Leg Soc*. (1986) 36:113–5. PMID: 2979142

26. Mäntysaari M, Kuikka J, Mustonen J, Tahvanainen K, Vanninen E, Länsimies E, et al. Measurement of myocardial accumulation of 123I-metaiodobenzylguanidine for studying cardiac autonomic neuropathy in diabetes mellitus. *Clin Auton Res*. (1996) 6:163–9. doi: 10.1007/BF02281904

27. Sardesai SH, Mourant AJ, Sivathandon Y, Farrow R, Gibbons DO. Phaeochromocytoma and catecholamine induced cardiomyopathy presenting as heart failure. *Br Heart J*. (1990) 63:234–7. doi: 10.1136/hrt.63.4.234

28. Redfield MM, Kay GN, Jenkins LS, Mianulli M, Jensen DN, Ellenbogen KA. Tachycardia-related cardiomyopathy: a common cause of ventricular dysfunction in patients with atrial fibrillation referred for atrioventricular ablation. *Mayo Clin Proc*. (2000) 75:790–5. doi: 10.4065/75.8.790

29. Jacob JL, da Silveira LC, de Freitas CG, Cêntola CA, Nicolau JC, Lorga AM. Pheochromocytoma with echocardiographic features of obstructive hypertrophic cardiomyopathy. A case report. *Angiology*. (1994) 45:985–9. doi: 10.1177/000331979404501113

30. Fleckenstein A, Janke J, Döring HJ, Pachinger O. Ca overload as the determinant factor in the production of catecholamine-induced myocardial lesions. *Recent Adv Stud Card Struct Metab*. (1973) 2:455–66. PMID: 4806979

31. Zampieri M, Argiro A, Marchi A, Berteotti M, Targetti M, Fornaro A, et al. Mavacamten, a novel therapeutic strategy for obstructive hypertrophic cardiomyopathy. *Curr Cardiol Rep*. (2021) 23:79. doi: 10.1007/s11886-021-01508-0

32. Li J, Wu Z, Zheng D, Sun Y, Wang S, Yan Y. Bioinformatics analysis of the regulatory lncRNA-miRNA-mRNA network and drug prediction in patients with hypertrophic cardiomyopathy. *Mol Med Rep*. (2019) 20:549–58. doi: 10.3892/mmr.2019.10289

33. Whittle SB, Smith V, Doherty E, Zhao S, McCarty S, Zage PE. Overview and recent advances in the treatment of neuroblastoma. *Expert Rev Anticancer Ther*. (2017) 17:369–86. doi: 10.1080/14737140.2017.1285230

34. Armenian S, Bhatia S. Predicting and preventing anthracycline-related cardiotoxicity. *Am Soc Clin Oncol Educ Book Am Soc Clin Oncol Annu Meeting*. (2018) 38:3–12. doi: 10.1200/EDBK_100015

35. Tuğ T, Özdemir N, Bulut V, Karaoğlu A, Muz MH. A case of pheochromocytoma manifested as noncardiogenic pulmonary edema. *Turk J Med Sci*. (1999) 29:71–4. Corpus ID: 70698311

36. Ma RC, Yip GW, Chow CC, Cockram CS. A woman with recurrent cardiac ischemia without coronary artery disease. *CMAJ*. (2007) 176:171–3. doi: 10.1503/cmaj.060291

37. Moreland RS, Bohr DF. Adrenergic control of coronary arteries. *Fed Proc*. (1984) 43:2857–61. PMID: 6386528

38. Santos JRU, Brofferio A, Viana B, Pacak K. Catecholamine-induced cardiomyopathy in pheochromocytoma: how to manage a rare complication in a rare disease? *Horm Metab Res*. (2019) 51:458–69. doi: 10.1055/a-0669-9556

39. Rona G, Kahn DS, Chappel CI. Studies on infarct-like myocardial necrosis produced by isoproterenol: a review. *Rev Can Biol*. (1963) 22:241–55. PMID: 14143355

frontiers | Frontiers in Pediatrics

TYPE Case Report
PUBLISHED 23 February 2023
DOI 10.3389/fped.2023.1051041

OPEN ACCESS

EDITED BY
Cecile Tissot,
Clinique des Grangettes, Switzerland

REVIEWED BY
Emanuele Micaglio,
IRCCS San Donato Polyclinic, Italy
Andrea Vergara,
University of Campania Luigi Vanvitelli, Italy

*CORRESPONDENCE
Jelena Hubrechts
jelena.hubrechts@saintluc.uclouvain.be

SPECIALTY SECTION
This article was submitted to Pediatric Cardiology, a section of the journal Frontiers in Pediatrics

RECEIVED 22 September 2022
ACCEPTED 25 January 2023
PUBLISHED 23 February 2023

CITATION
Hubrechts J, Vô C, Boulanger C, Carkeek K and Moniotte S (2023) Atrial fibrillation in a pediatric patient caused by an unusual malignant etiology: A case report.
Front. Pediatr. 11:1051041.
doi: 10.3389/fped.2023.1051041

Atrial fibrillation in a pediatric patient caused by an unusual malignant etiology: A case report

Jelena Hubrechts[1]*, Christophe Vô[1], Cécile Boulanger[2], Katherine Carkeek[3] and Stéphane Moniotte[1]

[1]Division of Congenital and Pediatric Cardiology, Department of Pediatrics, University Hospital Saint-Luc, Brussels, Belgium, [2]Division of Pediatric Oncology, Department of Hemato-Oncology, University Hospital Saint-Luc, Brussels, Belgium, [3]Division of Neonatology, Department of Pediatrics, University Hospital Saint-Luc, Brussels, Belgium

This case report describes a 15-year-old patient with a known congenital malformation syndrome and immune deficiency, presenting with new-onset atrial fibrillation (AF) after a recent diagnosis of an intrathoracic mass. Transthoracic echocardiography showed a structurally and functionally normal heart and workup confirmed a primary diffuse large B-cell lymphoma, with pericardial and left atrial involvement on cardiac magnetic resonance imaging. Electrical cardioversion was successfully performed to convert the AF and chemotherapy was promptly started. Antiarrhythmic treatment was continued for 6 weeks, without recurrent AF. We discuss the pathogenesis of AF in the setting of malignancies as well as the management strategies of AF, mainly based on adult guidelines.

KEYWORDS

atrial fibrillation, child, lymphoma, cardiac involvement, pericardial invasion, cardioversion

Introduction

Atrial fibrillation (AF) is uncommon in children in the absence of congenital heart disease (1, 2). Epidemiological pediatric data are scarce and management is guided by studies performed in the adult population (3). The presence of AF in a young patient with a structurally normal heart requires a careful etiological workup. This case illustrates a rare malignant etiology of AF, an intrathoracic non-Hodgkin lymphoma with cardiac involvement, demonstrated on cardiac magnetic resonance imaging (MRI). To our knowledge, this is the first pediatric case described with new-onset AF caused by a neoplastic invasion of the left atrial wall.

Case description

A 15-year-old girl, diagnosed with Hay–Wells syndrome–like phenotype at birth, was hospitalized for persistent cough, fatigue, and a deteriorating general condition. Her syndromic clinical features at birth and in infancy included cleft lip, cleft palate, maxillary hypoplasia, patchy alopecia, ankyloblepharon filiforme adnatum, absent eyelashes, dystrophic nails, bilateral syndactyly of the second to the fourth toe, ectrodactyly of both thumbs, hyperkeratosis, and hypoplasia of external genitalia. Furthermore, her medical history was marked by severe growth failure, celiac disease, gastroesophageal reflux, and hypogammaglobulinemia. She had no history of cardiac symptoms nor signs prior to this admission and there was no known family history of AF.

A persistent pleural effusion, found and monitored on chest x-ray and positron emission tomography computed tomography (PET-CT) scan, was suggestive of a malignant intrathoracic process. Primary mediastinal non-Hodgkin lymphoma was confirmed at

anatomopathological analysis, with the definitive diagnosis of a stage III diffuse large B-cell lymphoma. Shortly after diagnosis and before starting chemotherapy and corticosteroids, the patient presented with acute onset chest discomfort and palpitations. A cardiac monitoring showed a heart rate varying between 200 and 220 beats per minute (bpm) with normal blood pressure for age. On electrocardiogram (ECG), AF was diagnosed, with a rapid ventricular response and incomplete right bundle branch block secondary to the fast heart rate (**Figure 1**). On previously performed transthoracic echocardiography (TTE), a small atrial septal defect–type secundum and normal biventricular dimensions and function were seen. Previous ECG was also normal with no signs of pre-excitation or early repolarization.

At the time of the acute AF, blood gas excluded electrolyte abnormalities. Hematologic analysis showed a hemoglobin level of 9 g/dl [Normal (N): 11–14.5 g/dL], hematocrit of 29% (N: 35%–47%), 3,000/mm^3, neutrophils (N: 1,700–5,700/mm^3) among 4,200/mm^3 of white blood cells (N 4,000–10,000/mm^3), and 489,000/mm^3 of platelets (N: 1,75,000–3,45,000/mm^3). Renal function and thyroid hormone levels were normal. Given her clinical state and hemodynamic tolerance, she was given an oral loading dose of amiodarone 800 mg/m^2. Within 6 h, her ventricular response rate had dropped to 180 bpm, but she remained in AF and not in sinus rhythm. Over the next few hours, the clinical signs of increasing pallor and hepatomegaly developed and her blood pressure decreased to 79/43 mmHg. TTE showed normal cardiac function [with an ejection fraction (EF) of 70% and a shortening fraction (SF) of 39%], without enlargement of the left heart structures and no mitral valve regurgitation.

TTE was completed with a transesophageal echocardiography in order to rule out the presence of an intracardiac thrombus. Due to clinical deterioration, she was sedated (with propofol), intubated, and ventilated prior to electrical cardioversion. She returned to sinus rhythm after one shock of 1 J/kg. Anticoagulation by low-molecular-weight heparin (tinzaparin, 4,500 UI/day subcutaneously) was started and discontinued after 24 h of persistent sinus rhythm, without continuation of oral anticoagulation.

Etiological investigation was completed by performing cardiac MRI, which showed tumoral invasion into the pericardium and the lateral wall of the left atrium (**Figure 2**). Repeat TTE could not reproduce this finding.

Neurological examination at all times (at presentation and following treatment) remained normal. Cerebral MRI 24 h post-AF onset ruled out both intracranial tumoral invasion and signs of ischemic stroke.

Chemotherapy was started 24 h after AF onset according to the Inter-B-NHL 2010 treatment protocol. Amiodarone in maintenance dosage (200 mg/m^2 1×/day orally) was continued for 6 weeks without any use of antiarrhythmic agents thereafter. There was no recurrence of AF in this patient.

Discussion

The incidence of AF in pediatrics is rare (prevalence <0.05% prior to the age of 30) and mainly documented in children with congenital heart disease, cardiomyopathy, inherited arrhythmias, hyperthyroidism, or post-open-heart surgery (2–4). Isolated AF, in the absence of underlying cardiovascular disease, represents less than 5% of all cases of AF, across all ages (1). Several risk factors for AF are described, such as hypertension, diabetes mellitus, obstructive sleep disorder, obesity, smoking, alcohol and drug use,

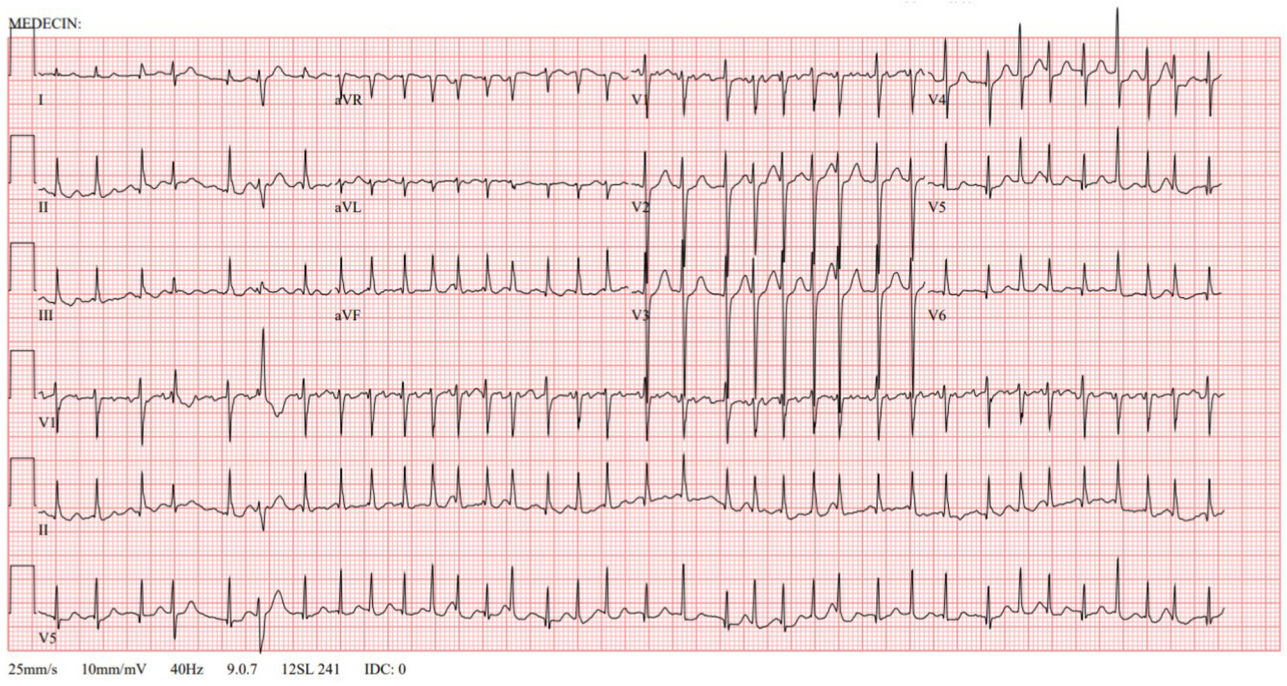

FIGURE 1
Electrocardiogram at onset. Atrial fibrillation with a rapid ventricular response. Incomplete right bundle branch block secondary to fast heart rate.

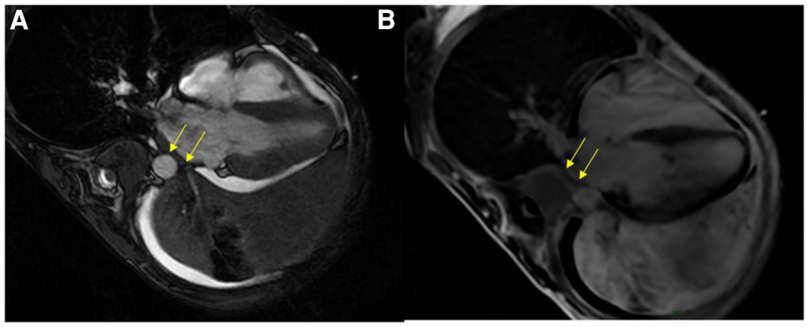

FIGURE 2
Cardiac MRI. SSFP four-chambers view showing the extensive tumoral process in the left pulmonary area coming into close contact with the left atrium, with paraneoplastic pleural and pericardial effusions (A); and likely tumoral invasion of the left atrial wall on the late-gadolinium-enhanced acquisition (B). MRI, magnetic resonance imaging; SSFP, steady-state free precession.

excessive exercise, hyperthyroidism, or positive family history. The patient in this case report had none of these known risk factors (3, 5).

The pathogenesis of AF is generally multifactorial, with electrical remodeling, structural remodeling, and inflammation (6, 7). Once initiated, AF alters the electrophysiologic properties of the atrial myocardium, responsible for the maintenance of the arrhythmia. Furthermore, the role of a susceptible atrial anatomical substrate, such as myocyte degeneration, activation of fibroblasts, and enhanced connective tissue deposition leading to interstitial fibroses, has been implicated in the physiology of the onset and maintenance of AF. The presence of AF has also been associated with an increased inflammatory burden.

Invasion of the malignant tumor into the atrial wall myocytes in this case, is considered an inflammatory burden, creating a susceptible atrial anatomical structure, with the underlying milieu of the systemic proinflammatory state of cancer. In the absence of other underlying extracardiac triggers such as hypertension, hyperthyroidism, pulmonary embolism, viral infection, sepsis, or drug overdose, we considered the non-Hodgkin lymphoma with neoplastic invasion of the pericardium and the left atrial wall as the etiology AF in our patient.

The association between various cancers and AF has been described, justified by the abovementioned pathophysiological mechanisms of proinflammatory markers in both AF and cancer (8, 9). A large cohort study in a Danish population found that patients with new-onset AF had a markedly increased probability of neoplasia within 3 months following AF diagnosis, and that moreover, AF was strongly associated with metastatic cancer (10). Conversely, a recent meta-analysis suggests that patients with newly diagnosed cancer have a significantly increased risk of AF during the first 3-months of follow-up (9). Hospitalization costs, length of stay, and mortality rates are higher in cancer patients with AF than in those without AF. With regard to different cancer subtypes, in patients under the age of 65 years, AF has the highest association with lung cancer, followed by multiple myeloma and non-Hodgkin lymphoma (such as in our patient) (8).

Primary cardiac lymphoma is rare, and secondary cardiac involvement is even rarely reported. Usually, cardiac involvement is a late manifestation of lymphoma with median onset at 20 months after initial diagnosis, and often diagnosed at autopsy (11). The right side of the heart seems to be more often involved than the left and typically associated features include superior vena cava syndrome, pericardial effusion, and lymphatic return obstruction. Various arrhythmias can occur, including AF, atrioventricular block, and ventricular tachycardia (12).

Diagnostic modalities include CT and MRI, with contrast-enhanced MRI resulting in superior quality images to identify the morphology, location, and extent of intrathoracic masses (13).

Pediatric cases are very poorly described in the literature, and this patient reported is most likely the youngest to date reported with AF caused by pericardial and left atrial wall invasion of a non-Hodgkin lymphoma. Very few similar adult cases have been described (12, 14).

An added feature of note in this case is that during infancy, she was diagnosed with a Hay–Wells syndrome–like phenotype (15). The ankyloblepharon-ectodermal defects-cleft lip/palate (AEC) syndrome or Hay–Wells syndrome (MIM #106260) was first reported in 1976 (16). Hay–Wells syndrome belongs to a large, heterogeneous group of ectodermal dysplasia that affects the embryonic development of ectodermal tissues: hair, nails, teeth, sweat glands, and skin (17, 18). This very rare genetic condition is caused by a heterozygous mutation of the tumor protein p63 (TP63) gene, located on chromosome 3q28. Exome sequencing in our patient revealed *de novo* heterozygous variants in CHUK, PTGER4, and IFIT2. The variant in CHUK appeared to be most relevant for the AEC-like phenotype. CHUK is a direct target gene of p63 and encodes a component of the IKK complex that plays a key role in NF-κB pathway activation (15).

As in most of the classic Hay–Wells patients, dermatological features were predominant in our patient. Cardiac features are extremely rare in these patients, with only ventricular septum defects and persistent ductus arteriosus described (19). No cardiac arrhythmias nor tumor development (such as lymphoma) have been reported in the literature linked to the syndrome. We did not consider her underlying genetic condition as the cause for her malignancy or AF.

With regard to the early workup in AF, early-stage cardiomyopathy and inherited ventricular arrhythmias should be ruled out/excluded. Rare channelopathies associated with AF in children include Brugada syndrome, long QT syndrome, and short QT syndrome. Baseline 12-lead ECG is a basic yet essential

screening tool in the diagnosis and has high value in establishing prognosis and orienting further therapy (3). In our patient, a 12-lead ECG taken earlier was carefully examined using the Bazett formula, and no case for channelopathy was made out.

AF can also be associated with organized supraventricular tachycardia such as atrioventricular reentrant tachycardia degenerating into AF. Patients with accessory pathways have a much higher incidence of AF than the general population, especially with manifest accessory pathways (Wolff–Parkinson–White syndrome), but it has also been reported in patients with concealed accessory pathways (20).

AF is strongly associated with heart failure, even in the early stages of cardiomyopathy, and therefore (21), diastolic function on TTE should be carefully examined. Structural changes, however, may be delayed and develop later depending on the management, control, and re-occurrence of arrhythmias (3). In this case, TTE remained normal during follow-up.

Importantly, our patient did not receive any treatment in the form of anthracyclines, monoclonal antibodies such as ibrutinib, or other oncological treatments at the onset of AF. These medications are all considered risk factors for cardiovascular events (22–24).

In the current literature, treatment strategies for AF in children are not well defined. In general, rate control is often sufficient to resolve AF-related symptoms; however, rhythm-control strategies should always be considered in children. There is no robust evidence for the best choice of pharmacological agents offered for rate control, and the current practice includes the use of beta-blockers, calcium channel blockers, other antiarrhythmic drugs such as amiodarone or combination therapies.

Conversion to sinus rhythm by antiarrhythmic drugs is observed in approximately 50% in adults (7), and due to our patient's initial hemodynamic stability, we initially chose this strategy, in the knowledge that amiodarone appears to be more effective than sotalol in restoring sinus rhythm (25, 26). Pharmacological cardioversion also has the benefit of not requiring a fasting state or sedation.

In our patient, due to the inefficacy of pharmacological cardioversion and her worsening clinical state with hypotension, synchronized electrical cardioversion was subsequently the most appropriate procedure to rapidly establish sinus rhythm and avoid further clinical deterioration. Electrical cardioversion was performed despite the risk of stroke in non-anticoagulated patients (7) because it is indeed a quicker procedure and a more effective treatment of choice in hemodynamically compromised patients. It can be performed safely under sedation with intravenous midazolam and/or propofol. Continuous cardiorespiratory monitoring is essential.

Thromboembolism is a known complication of AF. The structural and functional changes of the atrial myocardium and stasis of blood generate a prothrombotic milieu. Anticoagulation is usually indicated in order to prevent stroke, although it remains controversial as there is a lack of pediatric recommendations. In adults, various risk scores exist to guide long-term anticoagulation decisions, such as the CHA2DS2-VASc score [congestive heart failure, hypertension, age ≥75 (doubled), diabetes, stroke (doubled), vascular disease, age 65–74, and sex (female)] recommended by the European Society of Cardiology (ESC) (7). Our patient was covered with low-molecular-weight heparin in view of electrical cardioversion, from the time of the procedure until 24 h thereafter. Continuous monitoring showed no recurrence of AF, and additional oral anticoagulation was not proposed in our patient, in accordance with adult guidelines (1, 7, 27).

The recurrent risk of AF is described between 15% and 39% after a first episode of isolated AF (4, 28). According to different case cohorts, age, male sex, obesity, and duration of the initial episode of AF were associated with a higher risk of recurrence. Throughout the treatment and follow-up of the patient's oncological condition, no recurrence was seen on monitoring. The indication for long-term antiarrhythmic therapy for AF has to be carefully balanced and weighed up, with negative AF-related symptoms on the one hand vs. the possible adverse effects on the other. Informed patient preference also plays a role (7). In cases of non-cardiac conditions associated with AF, the treatment of the underlying condition is crucial, as first-line therapy and (29) prognosis rely strongly on the underlying condition, but the lymphoma stage in our patient was unfortunately unfavorable.

In case of the recurrence of AF our patient, an electrophysiology study should be considered because other forms of supraventricular tachycardia that may trigger AF should be excluded (2, 29). Further future pediatric studies on this topic are needed in order to establish more specific guidelines on the management of AF in young patients. This study highlights the importance of clinical workup, examinations, and investigations to search for the cause of every new onset of AF in a pediatric patient.

Conclusion

In young patients presenting with AF, with no prior history or findings of cardiac abnormalities, the investigative workup for determining etiology is vital. Oncological conditions, and especially intrathoracic or cardiac malignant lesions, are rare but a part of the differential diagnosis of new-onset AF, as demonstrated by this case report of a 15-year-old girl with non-Hodgkin lymphoma. Cardiac MRI is a helpful diagnostic tool and electrical cardioversion is a rapid and effective treatment option. Further pediatric studies are needed to establish clear management guidelines for isolated AF in pediatric populations.

Data availability statement

The original contributions presented in the study are included in the article/Supplementary Material, further inquiries can be directed to the corresponding author.

Author contributions

JH collected data, conceived and designed the analysis, and drafted the initial manuscript. CV conceived and designed the analysis. CB referred the patient, provided follow-up, and collected data. KC drafted the manuscript. SM provided the figures and

performed the analysis. All authors contributed to the article and approved the submitted version.

Conflict of interest

The authors declare that the research was conducted in the absence of any commercial or financial relationships that could be construed as a potential conflict of interest.

Publisher's note

References

1. Kopecky SL, Gersh BJ, McGoon MD, Whisnant JP, Holmes DR Jr., Ilstrup DM, et al. The natural history of lone atrial fibrillation. A population-based study over three decades. *N Engl J Med*. (1987) 317(11):669–74. doi: 10.1056/NEJM198709103171104

2. Ceresnak SR, Liberman L, Silver ES, Fishberger SB, Gates GJ, Nappo L, et al. Lone atrial fibrillation in the young—perhaps not so "lone"? *J Pediatr*. (2013) 162(4):827–31. doi: 10.1016/j.jpeds.2012.09.016

3. Gourraud JB, Khairy P, Abadir S, Tadros R, Cadrin-Tourigny J, Macle L, et al. Atrial fibrillation in young patients. *Expert Rev Cardiovasc Ther*. (2018) 16(7):489–500. doi: 10.1080/14779072.2018.1490644

4. El-Assaad I, Al-Kindi SG, Saarel EV, Aziz PF. Lone pediatric atrial fibrillation in the United States: analysis of over 1500 cases. *Pediatr Cardiol*. (2017) 38(5):1004–9. doi: 10.1007/s00246-017-1608-7

5. Kannel WB, Wolf PA, Benjamin EJ, Levy D. Prevalence, incidence, prognosis, and predisposing conditions for atrial fibrillation: population-based estimates. *Am J Cardiol*. (1998) 82(8A):2N–9N. doi: 10.1016/s0002-9149(98)00583-9

6. Kourliouros A, Savelieva I, Kiotsekoglou A, Jahangiri M, Camm J. Current concepts in the pathogenesis of atrial fibrillation. *Am Heart J*. (2009) 157(2):243–52. doi: 10.1016/j.ahj.2008.10.009

7. Hindricks G, Potpara T, Dagres N, Arbelo E, Bax JJ, Blomström-Lundqvist C, et al. 2020 ESC guidelines for the diagnosis and management of atrial fibrillation developed in collaboration with the European Association for Cardio-Thoracic Surgery (EACTS): the task force for the diagnosis and management of atrial fibrillation of the European Society of Cardiology (ESC) developed with the special contribution of the European Heart Rhythm Association (EHRA) of the ESC. *Eur Heart J*. (2021) 42(5):373–498. doi: 10.1093/eurheartj/ehaa612 Erratum in: *Eur Heart J*. (2021) **42**(5):507; *Eur Heart J*. (2021) **42**(5):546–7; and Eur Heart J. (2021) **42**(40):4194.

8. Zubair Khan M, Gupta A, Patel K, Abraham A, Franklin S, Kim DY, et al. Association of atrial fibrillation and various cancer subtypes. *J Arrhythm*. (2021) 37(5):1205–14. doi: 10.1002/joa3.12589

9. Yuan M, Zhang Z, Tse G, Feng X, Korantzopoulos P, Letsas KP, et al. Association of cancer and the risk of developing atrial fibrillation: a systematic review and meta-analysis. *Cardiol Res Pract*. (2019) 2019:8985273. doi: 10.1155/2019/8985273

10. Ostenfeld EB, Erichsen R, Pedersen L, Farkas DK, Weiss NS, Sørensen HT. Atrial fibrillation as a marker of occult cancer. *PLoS One*. (2014) 9(8):e102861. doi: 10.1371/journal.pone.0102861

11. Petersen CD, Robinson WA, Kurnick JE. Involvement of the heart and pericardium in the malignant lymphomas. *Am J Med Sci*. (1976) 272(2):161–5. doi: 10.1097/00000441-197609000-00005

12. Yang HC, Liao JN, Hsiao LT, Yu WC, Chen SA. An unusual etiology for a 37-year-old man with paroxysmal atrial fibrillation and termination pause. *JACC Case Rep*. (2021) 3(1):165–8. doi: 10.1016/j.jaccas.2020.10.031

13. O'Mahony D, Peikarz RL, Bandettini WP, Arai AE, Wilson WH, Bates SE. Cardiac involvement with lymphoma: a review of the literature. *Clin Lymphoma Myeloma*. (2008) 8(4):249–52. doi: 10.3816/CLM.2008.n.034

14. Hirabayashi T, Tanabe M, Onishi K, Tanigawa T, Kitamura T, Yamada N, et al. Cardiac malignant lymphoma with atrial arrhythmias. *Int J Cardiol*. (2007) 114(2):E42–4. doi: 10.1016/j.ijcard.2006.07.214

15. Khandelwal KD, Ockeloen CW, Venselaar H, Boulanger C, Brichard B, Sokal E, et al. Identification of a de novo variant in CHUK in a patient with an EEC/AEC syndrome-like phenotype and hypogammaglobulinemia. *Am J Med Genet A*. (2017) 173(7):1813–20. doi: 10.1002/ajmg.a.38274

16. Hay RJ, Wells RS. The syndrome of ankyloblepharon, ectodermal defects, and cleft lip and palate: an autosomal dominant condition. *Br J Dermatol*. (1976) 94(3):277–89. doi: 10.1111/j.1365-2133.1976.tb04384.x

17. Fete M, van Bokhoven H, Clements SE, McKeon F, Roop DR, Koster MI, et al. International research symposium on ankyloblepharon-ectodermal defectscleft lip/palate (AEC) syndrome. *Am J Med Genet A*. (2009) 149A(9):1885–93. doi: 10.1002/ajmg.a.32761

18. Rinne T, Brunner HG, van Bokhoven H. p63-associated disorders. *Cell Cycle*. (2007) 6(3):262–8. doi: 10.4161/cc.6.3.3796

19. *Online Mendelian inheritance in man, OMIM®*. Baltimore, MD: Johns Hopkins University (2022). MIM Number: 106260. Available at: https://omim.org/ (Accessed December 2, 2009).

20. Chen M, Feng X, Sun J, Wang Q, Zhang P, Wang J, et al. Risk factors responsible for atrial fibrillation development between symptomatic patients with concealed or manifest atrioventricular accessory pathways. *Int J Cardiol Heart Vasc*. (2015) 7:69–75. doi: 10.1016/j.ijcha.2015.02.010

21. Maisel WH, Stevenson LW. Atrial fibrillation in heart failure: epidemiology, pathophysiology, and rationale for therapy. *Am J Cardiol*. (2003) 91(6A):2D–8D. doi: 10.1016/s0002-9149(02)03373-8

22. Diamond A, Ayyappan S, Cao S, Tashtish N, Boughan K, Cooper B, et al. Risk factors for cardiovascular events and mortality in patients diagnosed with diffuse large B-cell lymphoma and treated with anthracyclines. *Hematol Oncol*. (2022) 40:626–36. doi: 10.1002/hon.3034

23. Palazzo AG, Zizza A, Nuzzo M, Urciuoli C, Scardia S, Romano A, et al. Atrial fibrillation with aberrant ventricular conduction after receiving bamlanivimab/etesevimab: a case report. *Curr Med Res Opin*. (2022) 38(7):1055–7. doi: 10.1080/03007995.2022.2081450

24. Caldeira D, Alves D, Costa J, Ferreira JJ, Pinto FJ. Ibrutinib increases the risk of hypertension and atrial fibrillation: systematic review and meta-analysis. *PLoS One*. (2019) 14(2):e0211228. doi: 10.1371/journal.pone.0211228

25. Vijayalakshmi K, Whittaker VJ, Sutton A, Campbell P, Wright RA, Hall JA, et al. A randomized trial of prophylactic antiarrhythmic agents (amiodarone and sotalol) in patients with atrial fibrillation for whom direct current cardioversion is planned. *Am Heart J*. (2006) 151(4):863.e1–6. doi: 10.1016/j.ahj.2005.09.009

26. Singh BN, Singh SN, Reda DJ, Tang XC, Lopez B, Harris CL, et al. Sotalol amiodarone atrial fibrillation efficacy trial (SAFE-T) investigators. Amiodarone versus sotalol for atrial fibrillation. *N Engl J Med*. (2005) 352(18):1861–72. doi: 10.1056/NEJMoa041705

27. You JJ, Singer DE, Howard PA, Lane DA, Eckman MH, Fang MC, et al. Antithrombotic therapy for atrial fibrillation: antithrombotic therapy and prevention of thrombosis, 9th ed: American College of Chest Physicians Evidence-Based Clinical Practice Guidelines. *Chest*. (2012) 141(2 Suppl):e531S–75S. doi: 10.1378/chest.11-2304

28. Mills LC, Gow RM, Myers K, Kantoch MJ, Gross GJ, Fournier A, et al. Lone atrial fibrillation in the pediatric population. *Can J Cardiol*. (2013) 29(10):1227–33. doi: 10.1016/j.cjca.2013.06.014

29. January CT, Wann LS, Alpert JS, Calkins H, Cigarroa JE, Cleveland JC Jr., et al. 2014 AHA/ACC/HRS guideline for the management of patients with atrial fibrillation: a report of the American College of Cardiology/American Heart Association Task Force on practice guidelines and the heart rhythm society. *J Am Coll Cardiol*. (2014) 64(21):e1–76. doi: 10.1016/j.jacc.2014.03.022

frontiers | Frontiers in Pediatrics

TYPE Case Report
PUBLISHED 01 March 2023
DOI 10.3389/fped.2023.1059685

OPEN ACCESS

EDITED BY
Estela Azeka,
University of São Paulo, Brazil

REVIEWED BY
Francesco Bianco,
Azienda Ospedaliero Universitaria Ospedali Riuniti, Italy
Kei Yamamoto,
National Center For Global Health and Medicine, Japan

*CORRESPONDENCE
Paola Di Filippo
✉ difilippopaola@libero.it

†These authors have contributed equally to this work

SPECIALTY SECTION
This article was submitted to Pediatric Cardiology, a section of the journal Frontiers in Pediatrics

RECEIVED 01 October 2022
ACCEPTED 06 February 2023
PUBLISHED 01 March 2023

CITATION
Di Filippo P, David D, Attanasi M, Rossi N and Chiarelli F (2023) Case report: Increased troponin level in 125 children during COVID-19. Front. Pediatr. 11:1059685.
doi: 10.3389/fped.2023.1059685

Case report: Increased troponin level in 125 children during COVID-19

Paola Di Filippo*†, Daniela David†, Marina Attanasi, Nadia Rossi and Francesco Chiarelli

Department of Pediatrics, University of Chieti, Chieti, Italy

Introduction: Increase in cardiac biomarkers during Coronavirus disease 2019 (COVID-19) was frequent regardless of the presence of myocarditis and multisystem inflammatory syndrome in children (MIS-C). Several studies described MIS-C, but few papers evaluated cardiac manifestations in children with SARS-CoV-2 infection without MIS-C and investigated the role of troponin in absence of electrocardiogram (ECG) and echocardiographic alterations. The aim of this case series is to describe the cardiac manifestations during COVID-19 in children, trying to explain the meaning of laboratory findings during COVID-19, especially of increased troponin.

Materials and methods: We conducted a retrospective case series of children aged <18 years admitted at the Department of Pediatrics, University of Chieti, for SARS-CoV-2 infection between 1st March 2020 and 31th July 2022. All patients with documented SARS-CoV-2 infection underwent a laboratory evaluation at admission. Children with increased troponin I and/or BNP underwent electrocardiographic and echocardiographic exams.

Results: 125 children were admitted for SARS-CoV-2 infection to our Department of Pediatrics, of whom 17 (13.6% of cases) with different patterns of cardiac involvement. Specifically, 5 subjects (4.0% of admitted children) were diagnosed as MIS-C and 12 children (9.6%) manifested a cardiac involvement in terms of increased troponin with or without ECG and echocardiography anomalies. Troponin, C-reactive protein, procalcitonin and BNP values resulted higher in patients with MIS-C compared to patients without MIS-C. Furthermore, patients with MIS-C had higher neutrophils and lower lymphocytes compared to patients without MIS-C. ECG abnormalities were found in 4/5 patients with MIS-C and in 2/12 patients without MIS-C. Echocardiographic anomalies were found in all patients with MIS-C, especially in terms of valve regurgitation and ejection fraction reduction and in 2/12 patients without MIS-C, especially in terms of pericardial effusion. Despite high troponin levels, children presented a favorable clinical evolution.

Conclusion: The increase in troponin level in children with COVID-19 could also be due to respiratory causes or a massive inflammatory state. In our case series, patients with increased troponin associated to COVID-19 presented a favorable clinical course with clinical and laboratory remission almost always within 7 days.

KEYWORDS

MIS-C, SARS-CoV-2, cardiac involvement, children, troponin

Abbreviations

COVID-19, coronavirus disease 2019; MIS-C, multisystem inflammatory syndrome in children; IL, interleukin; CDC, centers for disease control; KD, Kawasaki disease; MRI, magnetic resonance imaging; PCR, polymerase chain reaction; WBC, white blood cells; PLT, platelet count; Hb, hemoglobin; CRP, C-reactive protein; PCT, procalcitonin; BNP, brain natriuretic peptid; WHO, World Health Organization; ECG, electrocardiogram; AV, atrioventricular; CAVC, complete atrioventricular canal.

1. Introduction

At the onset of the Coronavirus disease 2019 (COVID-19) outbreak, children were marginally involved, accounting for 1.7% of cases, and considered mostly asymptomatic carrier cases (1). During the following epidemic waves, an increasing number of children exposed to COVID-19 developed a multisystem inflammatory syndrome in children (MIS-C), defined on May 14, 2020, by the Centers for Disease Control (CDC) with a Health Alert Network (1, 2). Although COVID-19 mostly showed a favorable prognosis in children, MIS-C was characterized by an overwhelming inflammatory activation, with clinical similarities with Kawasaki disease (KD) including cardiac involvement (3).

SARS-CoV-2 mainly affects the upper respiratory tract. Nevertheless, the virus can damage other tissue than lung through a direct injury or an indirect one caused by the release of proinflammatory cytokines (4). An exaggerated inflammatory response triggered by the cytokine storm could cause a multi-organ involvement (5). A higher risk of severity and mortality was described in patients with underlying cardiovascular morbidity (6).

The incidence of MIS-C is not clear, but some estimates showed that MIS-C occurs in 5.1 out of 1,000,000 person-months in individuals under the age of 21 years (7). Cardiac involvement was frequently described in children with MIS-C, with myo-pericardial inflammation, coronary dilatation or aneurysm and arrhythmias (8). The mechanism of myocardial dysfunction in MIS-C is still unclear, but possible causes include acute myocarditis, post-viral immunological reaction, and systemic inflammatory response syndrome (2). The pathophysiology of MIS-C includes a sequence of events. Firstly, neutrophils infiltrate vessel walls causing acute necrotizing arteritis and an aneurysm within the coronary artery. Macrophages and T-cell lymphocytes accumulate in the damaged vessel wall, initiating a chronic form of vasculitis, with proliferation of myofibroblasts and risk for coronary artery stenosis. In the early acute phase, myocardial edema characterizes myocarditis before evidence of an aneurysm, with possibly transient left ventricular dysfunction that can lead to cardiovascular shock (4).

In literature, clinical and laboratory data mostly derived from clinical cases. In a case series of 20 critically ill children admitted for shock, fever and SARS-CoV-2 infection between 15th and 27th April 2020, the authors found an acute myocarditis with a mean left ventricular ejection fraction of 35% and high troponin level (269 ng/ml). The first symptoms before admission were intense abdominal pain and fever for 6 days and all children showed increased inflammation indexes (9).

In a French prospective study including 21 children and adolescents with features of KD admitted between 27 April and 11 May 2020, Toubiana et al. (10) found evidence of recent SARS-CoV-2 infection in 19 (90%) subjects. The authors observed myocarditis in 16 (76%) patients, with a median left ventricular ejection fraction rate of 42%, increased troponin I and B-type natriuretic peptide in 81% and 78% patients respectively, and pericardial effusion in 48% of enrolled children. Interestingly, all 21 patients presented noticeable gastrointestinal symptoms and high levels of inflammatory markers during the early stage of disease.

Furthermore, in a multicenter case series of 183 children with MIS-C, a wide clinical spectrum was found. All patients presented with fever, 63.9% gastrointestinal symptoms, and 43.2% presented with shock. Inotropic support, mechanical ventilation, and extracorporeal membrane oxygenation were indicated in 39.3%, 23.5%, and 2.2% patients, respectively (11).

An increased volume, a diastolic dysfunction and a reduced ejection fraction of the left ventricle were frequently found during echocardiographic exam. On imaging examinations, Magnetic Resonance Imaging (MRI) findings often showed late gadolinium enhancement, native T1 and T2 enhancement, and pericardial enhancement (9). These data suggest that SARS-CoV-2 can cause myocarditis, myocardial ischemia, and heart failure in a significant percentage of infected patients (12).

Children with COVID-19 myocarditis showed higher C-reactive protein levels, variable clinical features, need for shorter inotropic therapy and faster recovery of the left ventricular systolic function compared to patients with non-COVID-19 myocarditis (13).

The management of acute MIS-C patient includes cardiac support, immunomodulation, and antiplatelet/anticoagulant treatments (14). Whittaker et al. (15) documented cardiac involvement with left ventricular dysfunction on echocardiography and troponin elevation in 62% and 66% of children with MIS-C, respectively.

The aim of this case series is to describe the cardiac manifestations during COVID-19 in children, trying to explain the meaning of laboratory findings during COVID-19, especially of increased troponin.

2. Materials and methods

We conducted a retrospective case series of all children aged <18 years admitted at the Department of Pediatrics, University of Chieti, for SARS-CoV-2 infection between 1st March 2020 and 31th July 2022. Written informed consent was obtained from the minor's legal guardian for the publication of any potentially identifiable images or data included in this article. We reviewed the medical records of children who needed hospitalization to collect clinical, laboratory, imaging and echocardiographic findings and data about COVID-19 vaccination history. The time between onset of symptoms and admission and days of hospitalization were also recorded.

SARS-CoV-2 was diagnosed at the admission using reverse-transcriptase polymerase chain reaction (PCR) on nasopharyngeal and/or oropharyngeal swab samples. Serological test for SARS-CoV-2 antibodies detection was performed in children without active infection.

Clinical evaluation included physical examination and vital signs. Main clinical symptoms at onset, including fever, mucocutaneous involvement, presence of nonsuppurative laterocervical lymphadenopathy, conjunctivitis, and

gastrointestinal, respiratory, cardiovascular and neurologic symptoms were also collected.

All patients with documented SARS-CoV-2 infection underwent a laboratory evaluation at admission, including blood cell count with white blood cells (WBC, 10^3/mmc), platelet count (PLT, 10^3/mmc) and hemoglobin (Hb, g/dl); C-reactive protein (CRP, mg/L) and procalcitonin (PCT, mg/ml); troponin I (pg/ml) and brain natriuretic peptid (BNP, pg/ml), transaminases (U/L), ferritin (ng/ml), D-dimer (ng/ml). According to our Laboratory Unit, the upper limit of serum troponin level is 15.2 pg/ml and of BNP is 100 pg/ml.

Children with increased troponin I and/or BNP underwent electrocardiographic and echocardiographic exams. Electrocardiogram (ECG) data, including abnormal PR and QT intervals and ST- and T-wave changes, were recorded. Echocardiography findings were considered, including left ventricular ejection fraction, assessment of coronary arteries, and pericardial effusion.

Cardiac involvement is defined according to World Health Organization (WHO) definition as the presence of myocardial dysfunction, pericarditis, valvulitis, or coronary abnormalities (including findings on echocardiogram or elevated levels of troponin/BNP) (16). Patients with cardiac involvement were included in the analysis and divided into two groups: SARS-CoV-2 patients with and without MIS-C. According to WHO criteria, MIS-C was diagnosed in children and adolescents 0–19 years of age with fever >3 days with evidence of SARS-CoV-2 infection and exclusion of other obvious microbial cause and increased inflammation markers and two the following criteria: (a) Rash or bilateral non-purulent conjunctivitis or muco-cutaneous inflammation signs (oral, hands or feet); (b) Hypotension or shock; (c) cardiac involvement; (d) Evidence of coagulopathy (by prothrombin time, partial thromboplastin time, elevated d-Dimers); (e) Acute gastrointestinal problems (diarrhea, vomiting, or abdominal pain) (16).

In children with MIS-C, usual etiologic causes of acute myocarditis were screened, including testing of a large panel of non-SARS-CoV-2 viruses in blood, as Epstein–Barr virus, Cytomegalovirus, Parvovirus B19, Coxsackievirus, Echovirus. Other causes of infection were also excluded testing culture of urine, stool, and nasopharyngeal swabs and detection of Mycoplasma, Adenovirus, Influenza and Parainfluenza virus antibodies.

Information about need for oxygen, intravenous immunoglobulins, antiplatelet/anticoagulant treatments and inotropic support was collected. The clinical evolution including admission to Intensive Care Unit or death was also considered.

Continuous data was expressed as median and range 5%–95%. Categorical data was presented as numbers and percentages. Mann-Whitney *U* test was performed to compare characteristics between two groups. The statistical significance level was $p < 0.05$. SPSS version 25.0 for Windows (IBM, Armonk, NY, USA) and STATA/IC 15.1 (StataCorp. 2017. Stata *Statistical Software: Release 15*. StataCorp LLC. College Station, TX, USA) were used to perform statistical analysis.

3. Results

One hundred twenty five children were admitted for SARS-CoV-2 infection to our Department of Pediatrics. Seventeen children (13.6% of cases) showed different patterns of cardiac involvement. Specifically, 5 subjects (4.0% of admitted children) were diagnosed as MIS-C with a median age of 8.8 years (5%–95% CI 1.8–16.0); three were male (60.0%). Twelve children (9.6% of total cases) with a median age of 0.2 years (5%–95% CI 0.1–5.4, male 50%) manifested a cardiac involvement in terms of increased troponin with or without ECG and echocardiography anomalies, and showing no diagnostic criteria for MIS-C (**Figure 1**). Other etiologic causes of acute myocarditis (Epstein–Barr virus, Cytomegalovirus, Parvovirus B19, Coxsackievirus, Echovirus) resulted negative in children with MIS-C.

Children with MIS-C were older compared to children without MIS-C (8.8 vs. 0.2 years, $p < 0.001$). Patients without MIS-C were mainly infants (11/12 patients, 91.6% of cases), mostly within the first 3 months of life. The child with the highest troponin level (710 picogram/ml) was a 2-month-old infant with a minimal pericardial effusion detected by echocardiography that did not require any intervention. In this case, troponin level gradually decreased fluctuating after approximately 70 days, while increased troponin values in other patients became normal after about a week.

Nine patients (9/108, 8.3%) among children without cardiac involvement and one patient (1/17, 5.9%) with increased troponin levels were previously vaccinated for SARS-CoV-2.

Children with MIS-C presented fever (100% of cases), rash (80.0%), diarrhea (80.0%), conjunctivitis (60.0%), dyspnea (40.0%), mucositis (40.0%) and neurologic symptoms (lethargy, headache, confusion in 40.0% of patients). In patients without MIS-C, clinical characteristics ranged from fever (66.7% of patients), tachypnea (50.0%), cough (41.7%), diarrhea and weight loss (8.3%), headache (8.3%) and tachycardia (8.3%). Patients with MIS-C showed higher troponin levels compared to patients without MIS-C [201.6 (35.5–6638.0) vs. 65.5 (18.3–710.0)] but the difference was not statistically significant ($p = 0.328$). C-reactive protein [158.6 (89.7–109.4) vs. 3.5 (0.2–38.5); $p < 0.0001$], procalcitonin [4.1 (0.04–55.3) vs. 0.2 (0.01–1.4); $p = 0.048$], and BNP [410.0 (82.4–3352.0) vs. 24.7 (0–564.2); $p = 0.008$] values were higher in patients with MIS-C compared to patients without MIS-C. Values of WBS are similar between the two groups [12.8 (5.4–18.3) vs. 9.7 (2.9–19.5); $p = 0.442$], but patients with MIS-C had higher neutrophils [10.7 (CI 4.1–15.5) vs. 2.1 (0.6–7.1); $p = 0.002$] and lower lymphocytes [1.4 (0.7–2.2) vs. 6.7 (1.7–10.9); $p = 0.002$] compared to patients without MIS-C.

Aspartate aminotransferase [28.0 (20.0–156.0) vs. 49.0 (25.0–574.0); $p = 0.377$], alanine aminotransferase [21.0 (19.0–350.0) vs. 43.0 (21.0–406.0); $p = 0.377$], ferritin [378.0 (283.8–524.8) vs. 784.5 (186.4–1755.0); $p = 0.247$] and D-dimer [1.2 (0.5–10.2) vs. 0.9 (0.6–1.5); $p = 0.524$] were not significantly different between the two groups.

ECG abnormalities were found in 4/5 patients (80.0%) with MIS-C (**Table 1**), while in patients with increased troponin and without MIS-C 2/12 patients (16.7%) showed ECG abnormalities:

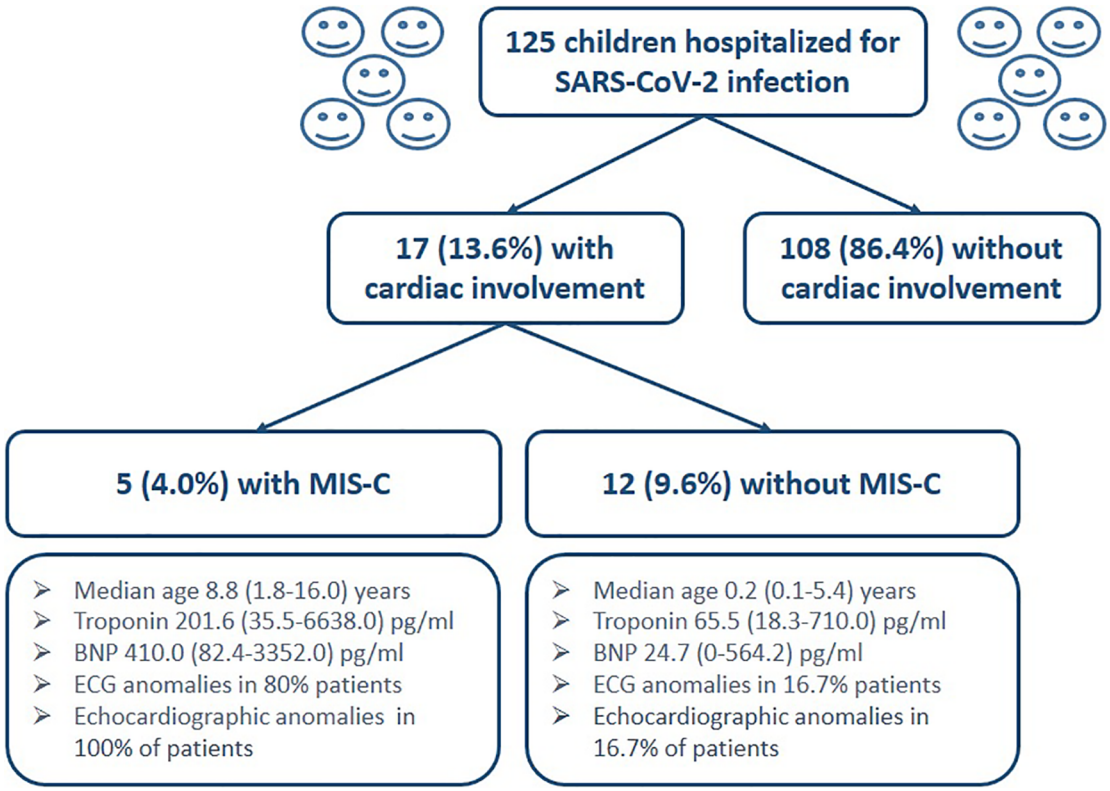

FIGURE 1
Flow-chart of children enrollment with main laboratory, electrocardiographic and echocardiographic findings in the two groups.

a patient with ventricular repolarization (VR) abnormalities and one with sinus tachycardia (Table 2).

Echocardiographic anomalies were found in all patients with MIS-C, especially in terms of valve regurgitation and ejection fraction reduction (Table 1). Conversely, echocardiographic anomalies were found in 2/12 patients (16.7%), especially in terms of pericardial effusion (Table 2).

One patient (20.0%) in the MIS-C group and one patient (8.3%) in the group without MIS-C were transferred to the Pediatric Intensive Care Unit. None of the 17 patients presented sequelae. None of the 17 patients died, but a patient in the whole group of infected children (1/125, 0.8%) died because of respiratory failure. The patient had Down syndrome and congenital heart disease (subaortic ventricular defect and patent foramen ovale with pulmonary hypertension, previously surgically corrected).

4. Discussion

In this case series, cardiac involvement was detected in 13.6% (17/125) and MIS-C in 4.0% (5/125) of hospitalized children with a recent history of COVID-19 or acute COVID-19. All the patients with MIS-C showed increased troponin level, while 12 children (9.6% patients) with current SARS-CoV-2 infection presented increased troponin levels. Despite high troponin level, only 2/12 patients had ECG anomalies and 3/12 echocardiographic ones.

In literature, several studies described MIS-C and the role of troponin increase as a marker of myocardial damage was widely reported (17–19). Otherwise, few papers evaluated cardiac manifestations in children with SARS-CoV-2 infection without MIS-C and investigated the role of troponin in absence of ECG and echocardiographic alterations. Noteworthy, increase in cardiac biomarkers during COVID-19 was frequent regardless of the presence of myocarditis, especially in the phase of severe systemic inflammation and acute respiratory distress syndrome and quantitatively associated with poor outcome (20). Indeed, an increase in cardiac biomarkers was found in up to 27% of COVID-19 patients (21).

In a single-center retrospective observational study of 759 children with increased troponin levels over an 11-year period, the authors found that this laboratory finding was associated mostly to cardiac diseases. Nevertheless, increased troponin resulted also in drug or carbon monoxide intoxication, bronchopneumonia, asthma, sepsis, septic shock, and systemic inflammatory response syndrome and hypotension or hypovolemia (22). Therefore, Yoldas et al. (22) showed that troponin elevation could be caused also by non-cardiac disease.

We speculated that the frequent increased troponin levels in children with COVID-19 could not be due to viral infection of the heart. Indeed, in a study including COVID-19 patients increased troponin levels were not correlated with left ventricular

10.3389/fped.2023.1059685

TABLE 1 Clinical, laboratory and cardiac findings and oxygen need of 5 patients with MIS-C.

Patient	1	2	3	4	5
Age (years)	12.5	6.7	1.8	8.8	16.0
PCR for SARS-CoV-2 on naso/oro-pharyngeal swab	Negative	Negative	Negative	Negative	Negative
Serological test for SARS-CoV-2	Positive	Positive	Positive	Positive	Positive
Clinical characteristics	Fever, rash, dyspnea, diarrhea	Fever, rash, dyspnea, diarrhea	Fever, rash, diarrhea, conjunctivitis, mucositis, lethargy	Fever, conjunctivitis, mucositis, headache, confusion	Fever, rash, rhinitis, diarrhea
Weeks after the positive SARS-CoV-2 swab	4	3	4	4	4
Days between onset of symptoms and admission	4	2	6	7	7
Days of hospitalization	17	12	1 before PICU	12	16
WBC (x 10^3/μl)	5.4	9.2	18.3	14.4	12.8
N Ratio (%)	76.6	84.3	85.0	75.7	83.8
CRP (mg/L) Nv < 5	166.3	89.7	308.4	158.6	98.0
PCT (ng/ml) Nv < 0.5	4.1	8.9	55.3	1.3	0.04
Troponin (pg/ml) Nv 0.0–15.2	211.9	201.6	35.5	56.7	6638.0
BNP (pg/ml) Nv < 100	240.8	2926.0	3352.0	410.0	88.4
Echocardiographic findings	Mild to moderate mitral regurgitation, EF 55%	Mild tricuspid regurgitation, moderate mitral regurgitation, EF 60%	Left ventricular function at lower limit of normal, EF 50%	Slight reduction in EF (50%)	Minimal mitral and tricuspid regurgitation, EF 55%
ECG	Bradycardia First degree atrioventricular block	Low atrial ectopic rhythm QT interval prolongation	Normal	Sinus bradycardia	Incomplete right bundle branch block
Oxygen need	No	No	No	No	No

Children with MIS-C were older compared to children without MIS-C (8.8 vs. 0.2 years, $p < 0.001$). All patients had a negative swab and positive serology for SARS-CoV-2; the infection dated back to 3–4 weeks ago in all 5 cases. Regarding clinical findings, children with MIS-C presented fever (100% of cases), rash (80.0%), diarrhea (80.0%), conjunctivitis (60.0%), dyspnea (40.0%), mucositis (40.0%) and neurologic symptoms (lethargy, headache, confusion in 40.0% of patients). Regarding cardiac findings in patients with MIS-C, troponin levels resulted increased in all patients and ranged from 35.5 to 6638.0 pg/ml; BNP levels resulted increased in 4 patients (80.0%) and ranged from 82.4 to 3352.0 pg/ml; echocardiographic anomalies were found in all patients, especially in terms of valve regurgitation and ejection fraction reduction; ECG abnormalities were found in 4 patients (80.0%). Furthermore, all patients presented neutrophilia and inflammation indices were increased in almost all patients with MIS-C: CRP was increased in all patients and PCT in 4 patients (80.0%). WBC, white blood cells; N, neutrophil; Hb, hemoglobin; PLTs, platelets; CRP, C-reactive protein; Nv, normal values; PCT, procalcitonin; BNP, brain natriuretic peptid; EF, ejection fraction; MRI, magnetic resonance imaging; ECG, electrocardiogram; O_2, oxygen.

dysfunction, but with right ventricular one. These findings suggested that increased troponin was due to acute right ventricular overload secondary to parenchymal or vascular lung disease resulting in subendocardial damage of the right ventricular myocardium (23). However, respiratory distress was not significant in our 12 patients with troponin increase, such that only one required oxygen. Therefore, in children infected and without myocarditis, the increase in troponin could be mostly related to the intense inflammatory state (22).

Otherwise, another hypothesis could be that very mild myocarditis, not evident on ECG and echocardiogram findings, resulted only in troponin increase. Tunçer et al. (24) reported that a mild myocarditis evolved with complete recovery without complications, albeit elevated troponin levels. ECG anomalies were detected in 93%–100% of children with myocarditis in retrospective studies; therefore, a myocarditis without ECG alterations was described rarely (25–27). We speculated that mild cardiac involvement with no clinical significance could be detected only by laboratory tests.

Comparing patients with and without MIS-C, we found higher troponin level in patients with MIS-C, although not significantly. Furthermore, we found significant higher levels of neutrophils, C-reactive protein, procalcitonin and BNP and significant lower values of lymphocytes in patients with MIS-C compared to patients without MIS-C. Similarly, in a recent study with 233 children with MIS-C and 102 with COVID-19, patients with MIS-C had significant higher levels of troponin, BNP and C-reactive protein and lower lymphocytes compared with COVID-19 children (28). We suggested that these laboratory findings could help the physician to differentiate patients with MIS-C. Particularly, BNP seems to be a promising severity index. In a recent metanalysis including 24 studies comprised of 2,583 COVID-19 patients and 1,613 MIS-C patients, the authors suggested that BNP was the key cardiac marker that showed differences between patients with MIS-C/non-severe COVID-19 and between patients with severe/non-severe MIS-C. The authors found that other markers, such as troponin and transaminases, did not exhibit notable differences in indicating cardiac injury between patients with MIS-C and COVID-19 (29).

In our study population, ECG abnormalities were found in 80% of patients with MIS-C and 16.7% of patients without MIS-C. In literature, arrhythmic manifestations were described in a wide range of patients (from 7% to 60%) with MIS-C (14). The most frequently described ECG anomalies were non-specific anomalies of ventricular repolarization, prolongation of the QT interval and premature atrial or ventricular beats (14). First and second degree atrioventricular (AV) blocks and atrial fibrillation were also reported (8, 30). In literature, less information were reported

TABLE 2 Clinical, laboratory and cardiac findings and oxygen need of 12 patients with increased troponin levels without MIS-C.

Patient	1	2	3	4	5	6	7	8	9	10	11	12
Age (years)	0.2	5.4	0.1	0.3	0.2	0.1	0.1	0.2	0.2	0.7	0.2	0.2
PCR for SARS-CoV-2 on naso/oro-pharyngeal swab	Positive	Positive	Positive	Positive	Positive	Positive	Positive	Positive	Positive	Positive	Positive	Positive
Clinical characteristics	Cough Tachypnea	Haedache Tachycardia	Fever	Fever Cough	Fever Tachypnea	Fever Cough Tachypnea	Fever Diarrhea Weight loss	Cough Tachypnea	Fever Tachypnea Perioral cianosis	Fever Cough Tachypnea	Irritability	Fever
Days between onset of symptoms and admission	3	7	1	5	4	1	2	8	2	4	1	3
Days of hospitalization	6	10	5	6	3 before PICU	4	4	24	3	9	16	3
WBC (x 10^3/μl)	7.09	8.00	7.39	8.41	12.19	2.93	13.02	8.86	14.35	11.13	15.62	6.99
N Ratio (%)	61.7	41.6	19.8	12.4	11.2	22.2	16.8	14.0	15.0	63.8	27.9	33.6
CRP (mg/L) Nv < 5	0.36	20.31	0.96	0.11	2.52	6.68	1.89	0.17	4.53	38.50	0.91	6.77
PCT (ng/ml) Nv < 0.5	n.a.	0.26	0.17	0.07	0.08	0.71	0.46	0.04	1.00	0.13	0.18	0.16
Troponin (pg/ml) Nv 0.0–15.2	96.1	137.7	54.9	18.3	53.6	142.4	62.0	710.0	20.9	196.0	67.0	36.2
BNP (pg/ml) Nv < 100	n.a.	<10	19.1	<10	13.9	30.2	11.3	52.2	n.a.	564.2	82	91.5
Echocardiographic findings	Normal	Normal	Normal	Mild pericardial effusion	Normal	Normal	Normal	Pericardial effusion	Normal	Normal (past surgery for CAVC type C)	Normal	n.a.
ECG	Normal	Sinus tachycardia	Normal	Normal	Normal	Normal	Normal	Normal	Normal	Repolarization abnormalities	Normal	Normal
Oxygen need	No	No	No	No	No	No	No	No	No	Low-flow O2 for 1 day	No	No

Patients without MIS-C were mainly infants (11/12 patients, 91.6% of cases), mostly within the first 3 months of life. All patients had a positive swab for SARS-CoV-2. Clinical findings in patients without MIS-C ranged from fever (66.7% of patients), tachypnea (50.0%), cough (41.7%), diarrhea and weight loss (8.3%), headache (8.3%) and tachycardia (8.3%). Regarding cardiac findings in patients with increased troponin levels and without MIS-C, troponin levels ranged from 18.3 to 710.0 pg/ml. The child with the highest troponin was a 2-month-old infant with a minimal pericardial effusion detected by echocardiography that did not require therapy. In this case, troponin level gradually decreased fluctuating after approximately 70 days, while increased troponin values in other patients became normal after about a week. BNP levels resulted increased in 1 patient (8.3%) and ranged from 0 to 564.2 pg/ml; echocardiographic anomalies were found in 2/12 patients (16.7%), especially in terms of pericardial effusion; ECG abnormalities were found in 2/12 patients (16.7%), a patient with ventricular repolarization abnormalities and one with sinus tachycardia. Furthermore, neutrophilia was less frequent compared to subjects with MIS-C, as well as inflammation indices were less frequently and deeply elevated: CRP was increased in 4 patients (33.3%) and PCT in only one patient (8.3%). WBC, white blood cells; N, neutrophil; Hb, hemoglobin; PLTs, platelets; CRP, C-reactive protein; Nv, normal values; PCT, procalcitonin; BNP, brain natriuretic peptid; ECG, electrocardiogram; CAVC, complete atrioventricular canal; O_2, oxygen.

10.3389/fped.2023.1059685

regarding ECG changes in children with troponin elevation without MIS-C. In the 12 children without MIS-C, we found no ECG changes that were clinically significant: one reported only sinus tachycardia and the other ventricular repolarization. Furthermore, the latter was a child with a history of previous surgery for complete atrioventricular canal.

Echocardiography has a key role for the diagnosis and monitoring of myocarditis (31). In our study population, echocardiographic anomalies were found in all patients with MIS-C (especially in terms of valve regurgitation and ejection fraction reduction), confirming the key role of this tool in the diagnosis of MIS-C. Echocardiographic anomalies were also found in 16.7% of patients without MIS-C, especially in terms of pericardial effusion, probably indicating very mild pericarditis. In literature, cardiac complications occurred in approximately 30% of infected children and in nearly all those with MIS-C (2). In a study including 294 children with active or previous SARS-CoV-2 infection, of which 46 with MIS-C, the most frequent echocardiographic change was pericardial effusion, followed by left ventricular systolic dysfunction, while coronary abnormalities occurred in about one third of patients with MIS-C (2).

The lack of MRI data in patients with cardiac involvement is a limitation in this case series. Indeed, cardiac MRI is the gold standard for the quantitative evaluation of ventricular systolic function and it could detect myocardial edema. Verification of myocarditis in patients with acute cardiac syndromes but normal coronary arteries or with atypical symptoms is one of its greatest challenges in clinical practice (32).

Regarding clinical evolution, in our population one patient in the MIS-C group and one patient in the group without MIS-C were transferred to a Pediatric Intensive Care Unit. However, the clinical evolution was favorable for all patients with complete clinical remission; none of the 17 patients presented sequelae or died. In literature, a mortality rate of 1% in children with MIS-C after adequate treatment was reported (33). In a large meta-analysis of 42 studies including 275,661 children without comorbidities and 9,353 children with comorbidities, a mortality rate of 0.03% in children without comorbidities and of 1.5% in children with pre-existing comorbidities was found (34). In our study population, a patient in the whole group of infected children (1/125, 0.8%) died because of respiratory failure. The patient had Down syndrome and congenital heart disease (subaortic ventricular defect and patent foramen ovale with pulmonary hypertension, previously surgically corrected).

5. Conclusion

We found a 4% prevalence of MIS-C in subjects hospitalized for COVID-19 and a 9.6% prevalence of troponin elevation in patients infected without MIS-C. Additionally, children with MIS-C were older, had higher neutrophils, inflammation indexes, troponin and BNP levels and lower lymphocytes compared to children without MIS-C.

This case series is one of the few investigating the role of troponin in SARS-CoV-2 infected children without MIS-C. The significance of troponin increase not associated to ECG and echocardial anomalies is not yet clear. Surely, it must be kept in mind that the increase in troponin level can also occur in case of right ventricle overload due to respiratory causes or in case of a massive inflammatory state. However, this increase could also be caused by a very slight myocardial damage, not detectable on ECG and echocardiogram. In our case series, patients with increased troponin associated to SARS-CoV-2 infection presented a favorable clinical course with clinical and laboratory remission almost always within 7 days.

Nevertheless, follow-up of children with cardiac involvement associated to SARS-CoV-2 infection remains to be clarified. It is not clear whether a control echocardiogram is necessary in all patients with increased troponin. Larger multicenter studies to better define the incidence and characteristics of cardiac involvement associated to SARS-CoV-2 infection in children are needed. Finally, being a novel entity, long-term studies are needed to better define evolution and prognosis of this disease in children.

Data availability statement

The original contributions presented in the study are included in the article/Supplementary Material, further inquiries can be directed to the corresponding author.

Ethics statement

Ethical review and approval was not required for the study on human participants in accordance with the local legislation and institutional requirements. Written informed consent to participate in this study was provided by the participants' legal guardian/next of kin. Written informed consent was obtained from the minor's legal guardian for the publication of any potentially identifiable images or data included in this article.

Disclosure

All authors disclose no personal or financial support or author involvement with organizations with financial interest in the subject. All authors contributed equally to this manuscript and approved the final version and its submission to the journal. The author reports no conflicts of interest in this work. All authors disclose no prior presentation of study data as an abstract or poster.

Author contributions

PDF wrote sections of the manuscript, reviewed the manuscript and created figure and tables. DD collected data and wrote the first draft of the manuscript. MA performed statistical analysis. NR

conceived the study and collected participants. FR reviewed the manuscript.

Conflict of interest

The authors declare that the research was conducted in the absence of any commercial or financial relationships that could be construed as a potential conflict of interest.

Publisher's note

References

1. CDC COVID-19 Response Team. Coronavirus disease 2019 in children - United States, February 12-April 2, 2020. *Morb Mortal Wkly Rep*. (2020) 69(14):422–6. doi: 10.15585/mmwr.mm6914e4

2. Cantarutti N, Battista V, Adorisio R, Cicenia M, Campanello C, Listo E, et al. Cardiac manifestations in children with SARS-COV-2 infection: 1-year pediatric multicenter experience. *Children*. (2021) 8(8):717. doi: 10.3390/children8080717

3. Soumya RS, Unni TG, Raghu KG. Impact of COVID-19 on the cardiovascular system: a review of available reports. *Cardiovasc Drugs Ther*. (2021) 35(3):411–25. doi: 10.1007/s10557-020-07073-y

4. Abi Nassif T, Fakhri G, Younis NK, Zareef R, Al Amin F, Bitar F, et al. Cardiac manifestations in COVID-19 patients: a focus on the pediatric population. *Can J Infect Dis Med Microbiol*. (2021) 2021:5518979. doi: 10.1155/2021/5518979

5. van Doremalen N, Bushmaker T, Morris DH, Holbrook MG, Gamble A, Williamson BN, et al. Aerosol and surface stability of SARS-CoV-2 as compared with SARS-CoV-1. *N Engl J Med*. (2020) 382(16):1564–7. doi: 10.1056/NEJMc2004973

6. Tan W, Aboulhosn J. The cardiovascular burden of coronavirus disease 2019 (COVID-19) with a focus on congenital heart disease. *Int J Cardiol*. (2020) 309:70–7. doi: 10.1016/j.ijcard.2020.03.063

7. Dufort EM, Koumans EH, Chow EJ, Rosenthal EM, Muse A, Rowlands J, et al. Multisystem inflammatory syndrome in children in New York state. *N Engl J Med*. (2020) 383:347–58. doi: 10.1056/NEJMoa2021756

8. Di Filippo P, Raso M, Cacciatore M, Patacchiola R, Renda G, Rossi N, et al. Case report: mitral valve involvement and first-degree atrial-ventricular block in two patients with multisystem inflammatory syndrome in children. *Front Pediatr*. (2021) 9:676934. doi: 10.3389/fped.2021.676934

9. Grimaud M, Starck J, Levy M, Marais C, Chareyre J, Khraiche D, et al. Acute myocarditis and multisystem inflammatory emerging disease following SARS-CoV-2 infection in critically ill children. *Ann Intensive Care*. (2020) 10(1):69. doi: 10.1186/s13613-020-00690-8

10. Toubiana J, Poirault C, Corsia A, Bajolle F, Fourgeaud J, Angoulvant F, et al. Kawasaki-like multisystem inflammatory syndrome in children during the COVID-19 pandemic in Paris, France: prospective observational study. *Br Med J*. (2020) 369:m2094. doi: 10.1136/bmj.m2094

11. Bautista-Rodriguez C, Sanchez-de-Toledo J, Clark BC, Herberg J, Bajolle F, Randanne PC, et al. Multisystem inflammatory syndrome in children: an international survey. *Pediatrics*. (2021) 147(2):e2020024554. doi: 10.1542/peds.2020-024554

12. Fried JA, Ramasubbu K, Bhatt R, Topkara VK, Clerkin KJ, Horn E, et al. The variety of cardiovascular presentations of COVID-19. *Circulation*. (2020) 141 (23):1930–6. doi: 10.1161/CIRCULATIONAHA.120.047164

13. Vukomanovic VA, Krasic S, Prijic S, Ninic S, Minic P, Petrovic G, et al. Differences between pediatric acute myocarditis related and unrelated to SARS-CoV-2. *Pediatr Infect Dis J*. (2021) 40(5):e173–8. doi: 10.1097/INF.0000000000003094

14. Sperotto F, Friedman KG, Son MBF, VanderPluym CJ, Newburger JW, Dionne A. Cardiac manifestations in SARS-CoV-2-associated multisystem inflammatory syndrome in children: a comprehensive review and proposed clinical approach. *Eur J Pediatr*. (2021) 180(2):307–22. doi: 10.1007/s00431-020-03766-6

15. Whittaker E, Bamford A, Kenny J, Kaforou M, Jones CE, Shah P, et al. Clinical characteristics of 58 children with a pediatric inflammatory multisystem syndrome temporally associated with SARS-CoV-2. *J Am Med Assoc*. (2020) 324(3):259–69. doi: 10.1001/jama.2020.10369

16. World Health Organization. Multisystem inflammatory syndrome in children and adolescents with COVID-19: Scientific brief (2020). Available at: https://www.who.int/publications/i/item/multisystem-inflammatory-syndrome-in-children-and-adolescents-with-covid-19 (Accessed July 25, 2022).

17. Cui Y, Tian M, Huang D, Wang X, Huang Y, Fan L, et al. A 55-day-old female infant infected with 2019 novel coronavirus disease: presenting with pneumonia, liver injury, and heart damage. *J Infect Dis*. (2020) 221(11):1775–81. doi: 10.1093/infdis/jiaa113; Erratum in: J Infect Dis. 2020;222(3):519.

18. Li Y, Guo F, Cao Y, Li L, Guo Y. Insight into COVID-2019 for pediatricians. *Pediatr Pulmonol*. (2020) 55(5):E1–4. doi: 10.1002/ppul.24734

19. Su L, Ma X, Yu H, Zhang Z, Bian P, Han Y, et al. The different clinical characteristics of corona virus disease cases between children and their families in China - the character of children with COVID-19. *Emerg Microbes Infect*. (2020) 9 (1):707–13. doi: 10.1080/22221751.2020.1744483

20. Kurz DJ, Eberli FR. Cardiovascular aspects of COVID-19. *Swiss Med Wkly*. (2020) 150:w20417. doi: 10.4414/smw.2020.20417

21. Guo T, Fan Y, Chen M, Wu X, Zhang L, He T, et al. Cardiovascular implications of fatal outcomes of patients with coronavirus disease 2019 (COVID-19). *JAMA Cardiol*. (2020) 5(7):811–8. doi: 10.1001/jamacardio.2020.1017

22. Yoldaş T, Örün UA. What is the significance of elevated troponin I in children and adolescents? A diagnostic approach. *Pediatr Cardiol*. (2019) 40(8):1638–44. doi: 10.1007/s00246-019-02198-w

23. Szekely Y, Lichter Y, Taieb P, Banai A, Hochstadt A, Merdler I, et al. Spectrum of cardiac manifestations in COVID-19: a systematic echocardiographic study. *Circulation*. (2020) 142(4):342–53. doi: 10.1161/CIRCULATIONAHA.120.047971

24. Tunçer T, Varol F, Coşkun Ş, Güzel B, Güven Ş, Çam H. Patterns of myocardial involvement during COVID-19 pandemic; from newborn to adolescents. *J Curr Pediatr*. (2021) 19:319–27. doi: 10.4274/jcp.2021.83798

25. Durani Y, Egan M, Baffa J, Selbst SM, Nager AL. Pediatric myocarditis: presenting clinical characteristics. *Am J Emerg Med*. (2009) 27(8):942–7. doi: 10.1016/j.ajem.2008.07.032

26. Freedman SB, Haladyn JK, Floh A, Kirsh JA, Taylor G, Thull-Freedman J. Pediatric myocarditis: emergency department clinical findings and diagnostic evaluation. *Pediatrics*. (2007) 120(6):1278–85. doi: 10.1542/peds.2007-1073

27. Chang YJ, Chao HC, Hsia SH, Yan DC. Myocarditis presenting as gastritis in children. *Pediatr Emerg Care*. (2006) 22(6):439–40. doi: 10.1097/01.pec.0000221346.64991.e7

28. Godfred-Cato S, Abrams JY, Balachandran N, Jaggi P, Jones K, Rostad CA, et al. Distinguishing multisystem inflammatory syndrome in children from COVID-19, kawasaki disease and toxic shock syndrome. *Pediatr Infect Dis J*. (2022) 41 (4):315–23. doi: 10.1097/INF.0000000000003449

29. Zhao Y, Patel J, Huang Y, Yin L, Tang L. Cardiac markers of multisystem inflammatory syndrome in children (MIS-C) in COVID-19 patients: a meta-analysis. *Am J Emerg Med*. (2021) 49:62–70. doi: 10.1016/j.ajem.2021.05.044

30. Deza Leon MP, Redzepi A, McGrath E, Abdel-Haq N, Shawaqfeh A, Sethuraman U, et al. COVID-19-associated pediatric multisystem inflammatory syndrome. *J Pediatric Infect Dis Soc*. (2020) 9(3):407–8. doi: 10.1093/jpids/piaa061

31. Dancea AB. Myocarditis in infants and children: a review for the paediatrician. *Paediatr Child Health*. (2001) 6(8):543–5. doi: 10.1093/pch/6.8.543

32. Friedrich MG, Marcotte F. Cardiac magnetic resonance assessment of myocarditis. *Circ Cardiovasc Imaging*. (2013) 6(5):833–9. doi: 10.1161/CIRCIMAGING.113.000416

33. Acevedo L, Piñeres-Olave BE, Niño-Serna LF, Vega LM, Gomez IJA, Chacón S, et al. Mortality and clinical characteristics of multisystem inflammatory syndrome in children (MIS-C) associated with COVID-19 in critically ill patients: an observational multicenter study (MISCO study). *BMC Pediatr*. (2021) 21(1):516. doi: 10.1186/s12887-021-02974-9

34. Frenkel LD, Gomez F, Bellanti JA. COVID-19 in children: pathogenesis and current status. *Allergy Asthma Proc*. (2021) 42(1):8–15. doi: 10.2500/aap.2021.42.200104

frontiers | Frontiers in Cardiovascular Medicine

TYPE Case Report
PUBLISHED 03 March 2023
DOI 10.3389/fcvm.2023.1105381

OPEN ACCESS

EDITED BY
Inga Voges,
University Medical Center Schleswig-Holstein, Germany

REVIEWED BY
Rika Kawakami,
CVPath Institute, United States
Michal Odermarsky,
Skåne University Hospital, Sweden

*CORRESPONDENCE
Shiwei Yang
✉ jrdoctoryang@163.com

†These authors have contributed equally to this work

SPECIALTY SECTION
This article was submitted to Pediatric Cardiology, a section of the journal Frontiers in Cardiovascular Medicine

RECEIVED 22 November 2022
ACCEPTED 17 February 2023
PUBLISHED 03 March 2023

CITATION
Lu P, Chen J, Chen M, Wang L, Xiang D, Yin J and Yang S (2023) Case report: A rare homozygous variation in the *ENPP1* gene, presenting with generalized arterial calcification of infancy in a Chinese infant.
Front. Cardiovasc. Med. 10:1105381.
doi: 10.3389/fcvm.2023.1105381

Case report: A rare homozygous variation in the *ENPP1* gene, presenting with generalized arterial calcification of infancy in a Chinese infant

Pengtao Lu†, Jinglong Chen†, Mei Chen†, Ling Wang, Dandan Xiang, Jie Yin and Shiwei Yang*

Department of Cardiology, Children's Hospital of Nanjing Medical University, Nanjing, China

Generalized arterial calcification of infancy (GACI) is a rare genetic disease characterized by arterial calcifications or stenoses and hypertension. GACI is caused by mutations in the *ENPP1* or *ABCC6* genes, and it often causes intrauterine or early infancy death. Here, we report a case of rare GACI caused by a homozygous variation in *ENPP1*, in a Chinese infant initially presenting with hypertension. The proband was an 8-month-old boy with *in utero* tricuspid valve calcification, presenting with hypertension at birth. Enhanced computed tomography revealed extensive arterial calcification. Genetic testing identified a homozygous variation in *ENPP1* (c.783C > G *p*.Y261X), which led to the diagnosis of GACI. This mutation has been reported in only three Chinese patients, which all initially presented with hypophosphatemic rickets rather than GACI. This case enriches the clinical and genetic spectrum of *ENPP1* mutations and reminds us that GACI should be considered in an infant presenting with hypertension and extensive arterial calcification, and that genetic testing should be performed.

KEYWORDS

generalized arterial calcification of infancy, ENPP1, early-onset of hypertension, arterial calcification, ectopic mineralization

Introduction

Generalized arterial calcification of infancy (GACI, OMIM 208,000), is a rare autosomal recessive disorder caused by mutations in the *ENPP1* (ectonucleotide pyrophosphatase 1) or *ABCC6* (ATP-binding cassette subfamily C member 6) genes (1,2). GACI is characterized by the deposition of calcium hydroxyapatite in the arteries, skin, and eyes, leading to severe arterial calcification and hypertension; GACI may cause intrauterine or early infant death. GACI is usually treated using bisphosphonates; however, their efficacy is still uncertain. Herein, we report a case of rare GACI in a Chinese infant who initially presented with hypertension and arterial calcification caused by homozygous variation in the *ENPP1* gene.

Clinical presentation

The proband was an 8-month-old boy admitted to our hospital for hypertension, hypertrophic cardiomyopathy (HCM), and heart failure. Physical examination revealed abnormal vital signs: a heart rate of 180 BPM, a respiratory rate of 46 breaths/min, and a

blood pressure of 180/105 mmHg. An electrocardiogram showed sinus tachycardia and left ventricular hypertrophy. Laboratory examinations revealed hypophosphatemia (serum phosphate level of 0.94 mmol/L, normal range 1.5–2.3 mmol/L) and hypocalcemia (serum calcium level of 1.05 mmol/L, normal range 2.25–2.75 mmol/L). Other laboratory results for hereditary and metabolic disorders were negative. Echocardiography revealed hypertrophy of the ventricular wall, with a left ventricular ejection fraction of 62%. Doppler ultrasound revealed bilateral extensive calcification of the renal arteries. Enhanced CT further revealed extensive calcification of the iliac arteries, renal arteries, and abdominal aorta, without bone abnormalities (**Figure 1**).

The patient is the second son of healthy non-consanguineous Chinese parents. Prenatal concerns discovered on ultrasound included tricuspid valve calcification, fetal HCM, and hydrops fetalis. No abnormality was found in other prenatal investigations. This patient was delivered by emergency caesarean section at 32 weeks of gestation because of an abnormal fetal heart rate. At birth, he presented with neonatal asphyxia, intracranial hemorrhage, shortness of breath, and cyanosis, for which he received ventilator management. The patient developed severe hypertension in the first few hours of life, and echocardiography showed myocardial hypertrophy with no other cardiac structural abnormality. After symptomatic treatment, the patient's condition improved, but the hypertension persisted, and he was discharged from the local hospital on captopril.

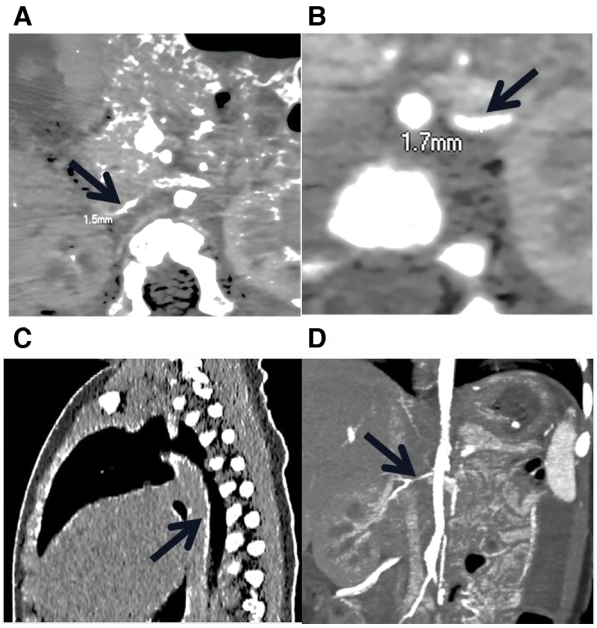

FIGURE 1
Low-dose, enhanced CT of the child with GACI caused by a homozygous variation in *ENPP1*. (**A**) and (**B**) stenosis of bilateral iliac artery; the thinnest parts of the left and right iliac arteries are 1.7 mm and 1.3 mm wide, respectively. (**C**) The black arrow indicates the presence of calcification in the descending aorta, thoracic aorta, and abdominal aorta. (**D**) The black arrow indicates the stenotic right renal artery.

During the follow-up, the patient still had hypertension and his condition had deteriorated. He was admitted to our hospital at the age of 8 months due to severe pneumonia and sepsis, and was placed on ventilator and treated with antibiotics and blood pressure reduction. However, his condition worsened, and the hypertension was resistant to triple therapy (nicardipine, metoprolol, and captopril). Eventually, the child died of heart failure and respiratory failure a week after admission, before bisphosphonates could be used. GACI was suspected, and whole exome sequencing was subsequently performed after obtaining the consent of the child's parents. Genomic DNA was extracted from the peripheral blood of the patient and his parents. Whole-exome sequencing was performed in the proband using IDT (Integrated Device Technology, United States) and the x-Gen Exome Research Panel v1.0 whole-exome capture cores. Variants were annotated using the Genome Aggregation Database (gnomAD), 1,000 Genomes Project (Chinese), dbSNP, and the ExAC database. The candidate variants were further validated by Sanger sequencing in the proband and his parents, and the pathogenicity of variants was evaluated according to the American College of Medical Genetics and Genomics (ACMG) criteria. The patient's grandfather, grandmother, and brother were all healthy and refused to accept genetic testing.

Genetic testing revealed a rare homozygous mutation in the *ENPP1* (c.783C > G Y261X) gene, which was inherited from his parents (**Figure 2A, B**). This mutation was located in exon 7 of *ENPP1*, and Provean and Mutation-based bioinformatics analysis suggested that this variant was likely a pathogenic mutation. No mutation was identified in the *ABCC6* gene. Based on the clinical and genetic characteristics, this patient was finally diagnosed with GACI.

Discussion

GACI is a rare but life-threatening disease, secondary to *ENPP1* (75%) or *ABCC6* (9%–10%) mutations (3). To date, only approximately 250 cases of GACI have been reported, with vascular calcification being the earliest and most prominent feature, which is often considered the most significant factor in morbidity and mortality (4). GACI can occur prenatally and has a mortality of approximately 55%; however, many children who died *in utero* and shortly after birth have not been included in this figure, giving an overestimation of the survival rate (5).

Inorganic pyrophosphate (PPi) is a potent calcification inhibitor that acts as a physiological "water softener" by preventing the formation and growth of hydroxyapatite crystals, and *ENPP1* forms adenosine monophosphate and PPi by hydrolyzing extracellular adenosine triphosphate (6). Lack of *ENPP1* results in decreased extracellular PPi, which is linked to ectopic calcification, particularly in the elastic layer of the endovascular lining, cartilage, and other soft tissues. A decrease in plasma PPi levels to almost zero has been suggested to be a potential cause of vascular calcification in GACI (7). A retrospective study by Ferreira et al. found a possible genotype-phenotypic correlation in 55 patients with GACI in a multicenter

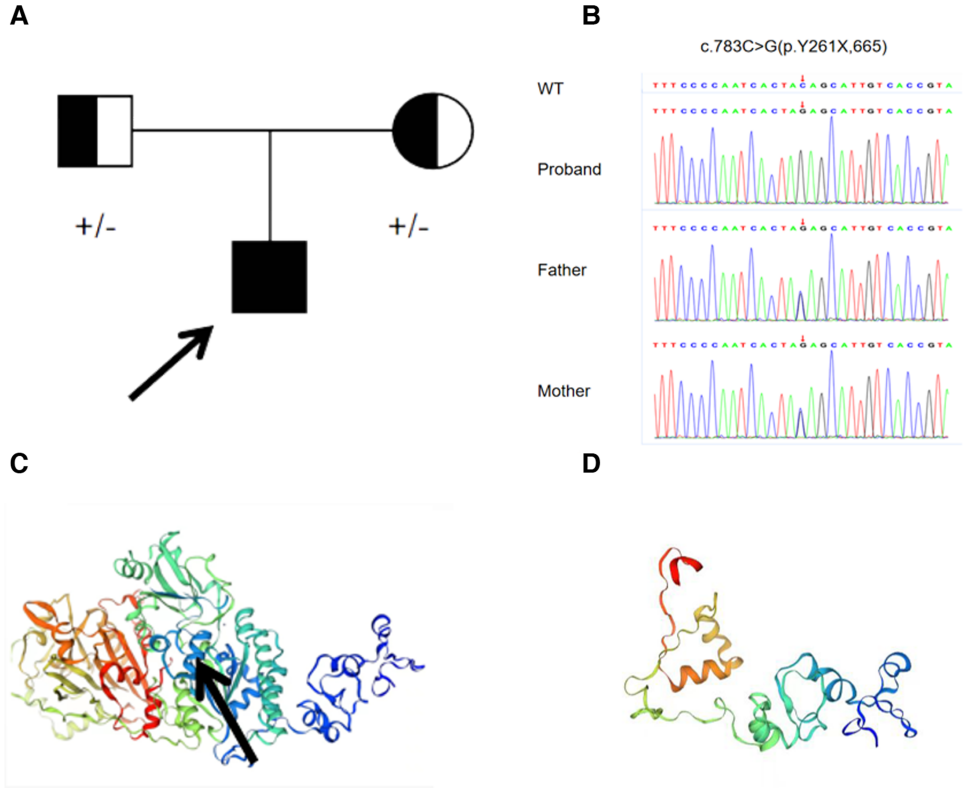

FIGURE 2
(A) family history of the proband. (B) Sanger sequencing revealed a homozygous mutation (c.783C > G *p*.Y261X) of *ENPP1* in the proband boy, originating from his parents. (C) Normal protein structure; the black arrow represents the mutation site. (D) Structure of the mutated protein.

genetics study: *p*.Pro305Thr in *ENPP1* was related to infant death in five cases, but there was no significant genotype-phenotypic correlation in the other subjects (8). Nitschke et al. found no variants of *ENPP1* or *ABCC6* in 22 patients in a retrospective analysis of 92 patients, implying that other genes may be involved in the onset of the disease.

Chong et al. reported 161 patients with GACI, of which 48% developed the condition *in utero* or in the first few hours of life, namely, "early onset," and 52% developed the condition after birth (median 3 months), namely, "late-onset" (9). The most common presentations of "early-onset" GACI included fetal hydrops, polyhydramnios, and fetal distress, while "late-onset" GACI was usually asymptomatic *in utero*, but presented with cardiovascular disease, respiratory distress, hypertension, and feeding difficulties after birth. Early-onset GACI commonly affects the hepatic arteries (81%), aorta (80%), and pulmonary arteries (67%), whereas late-onset GACI predominantly affects the coronary arteries (88%), renal arteries (55%), and pulmonary arteries (49%). Nitschke et al. (10) retrospectively analyzed 92 cases of GACI that had been tested for *ENPP1* and *ABCC6* and found that calcification may involve extravascular sites, including the myocardium, pancreas, liver, and kidneys, resulting in multi-organ dysfunction. However, the aforementioned studies were conducted in multiple centers without standardized data collection, limiting the development of consistent management strategies for GACI due to critical knowledge gaps.

The most reported therapy is bisphosphonates, whose efficacy has not been fully confirmed and for which clinical trials are not feasible. *ENPP1* substitution is a potential therapy. *ENPP1*-Fc replacement can prevent vascular calcification and reduce mortality in mice with *ENPP1* variants (11), as well as lower the blood pressure and improve heart function. Against this backdrop, prospective and longitudinal studies on the natural history of GACI are urgently needed to treat arterial calcification to prevent early mortality.

Our patient, presenting with *in utero* hydrops fetalis, tricuspid valve calcification, neonatal asphyxia, intracranial hemorrhage at birth, refractory hypertension, HCM after birth, and extensive calcifications of the bilateral iliac arteries, renal arteries, and abdominal aorta, conformed to "early-onset" GACI. Genetic testing revealed a homozygous variation in *ENPP1* (c.783C > G). This variation results in the deletion of the *ENPP1* protein from the 261 amino acid, Y261X, in the pathogenic form of PVS1, according to ACMG (**Figures 2C,D**). The mutation has been reported in only three Chinese patients, one with a homozygous variation in *ENPP1* (c.783C > G) and the other two with compound heterozygous mutations (12). Interestingly, the clinical phenotype of all three patients was hypophosphatemic rickets, a skeletal mineralization disorder characterized by excessive renal excretion of phosphorus, resulting in hypophosphatemia, rather than GACI. This phenomenon was also found in the study of Rutsch et al., in which the proband had GACI caused by a homozygous variation in

c.2320C > T; however, his father, who had the same homozygous variation, grew up with HR, not GACI (13). This suggests the diversity of the clinical phenotypes in *ENPP1* mutations.

In conclusion, GACI has early-onset symptoms and a very poor prognosis, and early diagnosis of GACI is very important. This report enriches the clinical and genetic spectrum of GACI. Clinicians should suspect GACI when children develop hypertension or vascular calcification soon after birth (median time 3 months). Imaging tests, such as magnetic resonance imaging and computed tomography, as well as genetic testing should be performed.

Data availability statement

The original contributions presented in the study are included in the article/Supplementary Material, further inquiries can be directed to the corresponding author.

Ethics statement

The studies involving human participants were reviewed and approved by Ethics Committee of children's Hospital Affiliated to Nanjing Medical University. Written informed consent to participate in this study was provided by the participants' legal guardian/next of kin. Written informed consent was obtained from the participant/patient(s) for the publication of this case report.

Author contributions

PL edited the manuscript. JC and MC contributed to data collection. LW prepared the figures. SY revised the paper. All authors contributed to the article and approved the submitted version.

Funding

This work was supported by the Medical Science and Technology Development Foundation of Jiangsu Commission of Health [grant number ZD2021058], the Research Project Maternal and Child Health of Jiangsu Province [grant number F202023], and the Medical Science and Technology Development Foundation of Nanjing Department of Health [grant number ZKX20041].

Conflict of interest

The authors declare that the research was conducted in the absence of any commercial or financial relationships that could be construed as a potential conflict of interest.

Publisher's note

All claims expressed in this article are solely those of the authors and do not necessarily represent those of their affiliated organizations, or those of the publisher, the editors and the reviewers. Any product that may be evaluated in this article, or claim that may be made by its manufacturer, is not guaranteed or endorsed by the publisher.

References

1. Ruf N, Uhlenberg B, Terkeltaub R, Nürnberg P, Rutsch F. The mutational spectrum of *ENPP1* as arising after the analysis of 23 unrelated patients with generalized arterial calcification of infancy (GACI). *Hum Mutat.* (2005) 25(1):98. doi: 10.1002/humu.9297

2. Guimarães S, Lopes JM, Oliveira JB, Santos A. Idiopathic infantile arterial calcification: a rare cause of sudden unexpected death in childhood. *Patholog Res Int.* (2010) 2010:185314. doi: 10.4061/2010/185314

3. Kawai K, Sato Y, Kawakami R, Sakamoto A, Cornelissen A, Mori M. Generalized arterial calcification of infancy (GACI): optimizing care with a multidisciplinary approach. *J Multidiscip Healthc.* (2022) 15:1261–76. doi: 10.2147/JMDH.S251861

4. Boyce AM, Gafni RI, Ferreira CR. Generalized arterial calcification of infancy: new insights, controversies, and approach to management. *Curr Osteoporos Rep.* (2020) 18(3):232–41. doi: 10.1007/s11914-020-00577-4

5. Ferreira CR, Kintzinger K, Hackbarth ME, Botschen U, Nitschke Y, Mughal MZ. Ectopic calcification and hypophosphatemic rickets: natural history of *ENPP1* and *ABCC6* deficiencies. *J Bone Miner Res.* (2021) 36(11):2193–202. doi: 10.1002/jbmr.4418

6. Orriss IR, Arnett TR, Russell RG. Pyrophosphate: a key inhibitor of ineralisation. *Curr Opin Pharmacol.* (2016) 28:57–68. doi: 10.1016/j.coph.2016.03.003

7. Ralph D, Nitschke Y, Levine MA, Caffet M, Wurst T, Saeidian AH. *ENPP1* Variants in patients with GACI and PXE expand the clinical and genetic heterogeneity of heritable disorders of ectopic calcification. *PLoS Genet.* (2022) 18 (4):e1010192. doi: 10.1371/journal.pgen.1010192

8. Ferreira CR, Hackbarth ME, Ziegler SG, Pan KS, Roberts MS, Rosing DR. Prospective phenotyping of long-term survivors of generalized arterial calcification of infancy (GACI). *Genet Med.* (2021) 23(2):396–407. doi: 10.1038/s41436-020-00983-0

9. Chong CR, Hutchins GM. Idiopathic infantile arterial calcification: the spectrum of clinical presentations. *Pediatr Dev Pathol.* (2008) 11(5):405–15. doi: 10.2350/07-06-0297.1

10. Nitschke Y, Baujat G, Botschen U, Wittkampf T, du Moulin M, Stella J. Generalized arterial calcification of infancy and pseudoxanthoma elasticum can be caused by mutations in either *ENPP1* or *ABCC6*. *Am J Hum Genet.* (2012) 90 (1):25–39. doi: 10.1016/j.ajhg.2011.11.020

11. Albright RA, Stabach P, Cao W, Kavanagh D, Mullen I, Braddock AA. *ENPP1*-Fc Prevents mortality and vascular calcifications in rodent model of generalized arterial calcification of infancy. *Nat Commun.* (2015) 6:10006. doi: 10.1038/ncomms10006

12. Liu ZQ, Chen XB, Song FY, Gao K, Qiu MF, Qian Y, et al. [Homozygous ectonucleotide pyrophosphatase/phosphodiesterase 1 variants in a girl with hypophosphatemic rickets and literature review]. *Zhonghua Er Ke Za Zhi.* (2017) 55 (11):858–61. Chinese. doi: 10.3760/cma.j.issn.0578-310.2017.11.014

13. Rutsch F, Ruf N, Vaingankar S, Toliat MR, Suk A, Höhne W. Mutations in *ENPP1* are associated with 'idiopathic' infantile arterial calcification. *Nat Genet.* (2003) 34(4):379–81. doi: 10.1038/ng1221

frontiers | Frontiers in Cardiovascular Medicine

TYPE Case Report
PUBLISHED 15 March 2023
DOI 10.3389/fcvm.2023.1083188

OPEN ACCESS

EDITED BY
Alvise Guariento,
University of Toronto, Canada

REVIEWED BY
Junbao Du,
Peking University, China
Paolo Compagnucci,
Marche Polytechnic University, Italy

*CORRESPONDENCE
Zipu Li
✉ apuqd@sina.com

SPECIALTY SECTION
This article was submitted to Pediatric Cardiology, a section of the journal Frontiers in Cardiovascular Medicine

RECEIVED 28 October 2022
ACCEPTED 17 February 2023
PUBLISHED 15 March 2023

CITATION
Wang B, Shan G, Bing Z, Zhang Q, Xing Q and Li Z (2023) Giant right atrium in a child with dilated cardiomyopathy: A case report. Front. Cardiovasc. Med. 10:1083188. doi: 10.3389/fcvm.2023.1083188

Giant right atrium in a child with dilated cardiomyopathy: A case report

Benzhen Wang[1], Guangsong Shan[1], Zhen Bing[1], Qi Zhang[2], Quansheng Xing[1] and Zipu Li[1]*

[1]Heart Center, Qingdao Women and Children's Hospital, Qingdao University, Qingdao, China, [2]Department of Radiology, Qingdao Women and Children's Hospital, Qingdao University, Qingdao, China

Dilated cardiomyopathy (DCM) is one of the leading causes of heart failure in children with diverse clinical characteristics. To date, DCM with a giant atrium as the first manifestation is rare and has not been reported in previous literature. We report a case of a male infant born with a significantly enlarged right atrium. Due to worsened clinical symptoms and the risk of arrhythmias and thrombosis, we performed the surgical reduction of the right atrium. Unfortunately, DCM and a progressive re-enlargement of the right atrium appeared during midterm follow-up. The mother's echocardiogram also suggested DCM, and the patient was eventually considered for a diagnosis of familial DCM. This case may expand the clinical spectrum of DCM and reminds us of the importance of good follow-up of children with idiopathic dilatation of the right atrium.

KEYWORDS

heart failure, right atrium, cardiomyopathy, pediatrics, cardiac surgery

Introduction

Dilated cardiomyopathy (DCM) is one of the leading causes of heart failure in children with complex etiologies and diverse clinical manifestations (1). Marked enlargement of the right atrium (RA) as the initial presentation of DCM has not been reported. Herein, we report an infant born with a giant right atrium and developed DCM during midterm follow-up.

Case report

We report the case of a male infant born from cesarean section after a normal pregnancy, with an Apgar score of 10/10 at 1st and 5th minutes, respectively. His mother was a 28-year-old, healthy, Gesta 2 para 2 woman who was presented for an obstetric ultrasound at 30 weeks of gestational age. An enlargement of the right atrium was noted. No other fetal anatomic abnormalities were detected. After birth, the case was admitted to the cardiac intensive care unit at the Qingdao Women and Children's Hospital. Family medical history was normal.

Heart rate, respiratory rate, blood pressure, and oxygen saturation on room air were normal on admission. No cyanosis, heart murmurs, wheezing, or hepatomegaly were present. Blood gas analysis, routine test, and liver and renal function were normal. The patient's and his mother's erythrocyte sedimentation rate, antinuclear antibodies, and extractable nuclear antigens were negative. N-terminal pro-brain natriuretic peptide reached 2,035 pg/mL (reference ranges <125 pg/mL). Transthoracic echocardiogram

10.3389/fcvm.2023.1083188

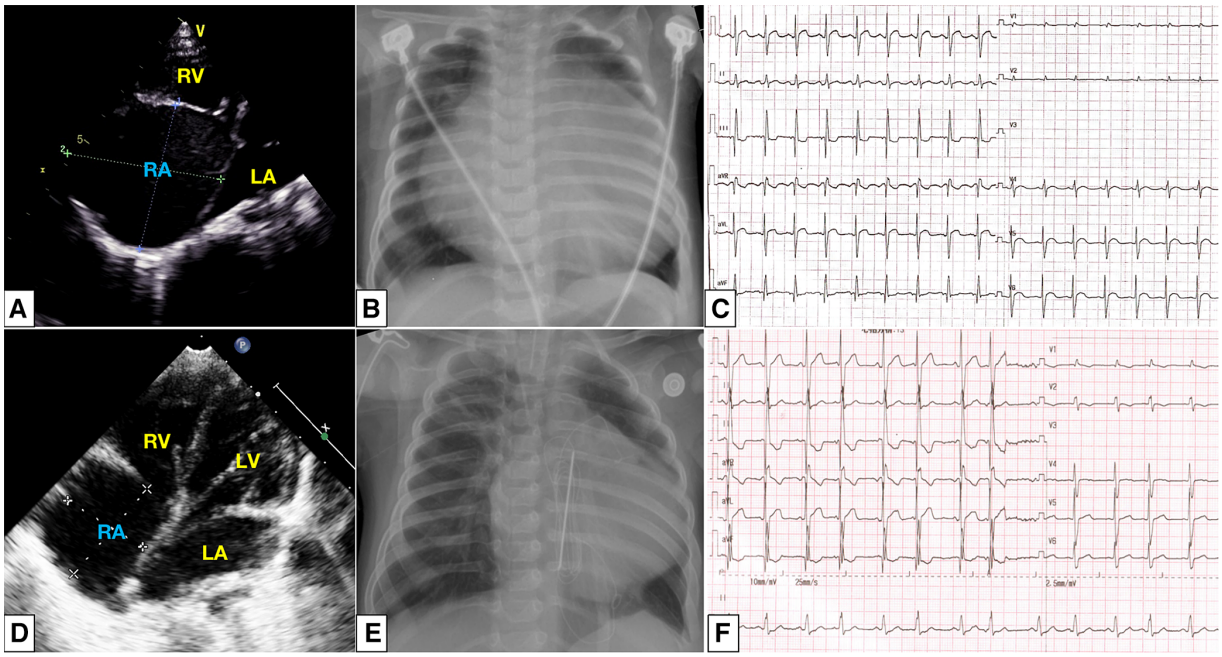

FIGURE 1
At initial presentation: a dilated right atrium was noted in apical four-chamber view (A); chest radiography showed cardiomegaly with a CTR of 80% (B); electrocardiograph showed sinus tachycardia, right axis deviation, and incomplete right bundle branch block (C). After surgical reduction, a slightly enlarged right atrium and intact atrial septum (D), CTR decreased to 0.61 (E), and the atrial premature beat was detected (F). CTR, cardiothoracic ratio;

(TTE) showed a giant RA (50 mm × 48 mm) with normal right and left ventricular volumes, a 15 mm secundum atrial septal defect (ASD), the tricuspid annulus was 14 mm, slight tricuspid regurgitation, a pulmonary arterial systolic pressure (PASP) of 45 mmHg, and left ventricular ejection fraction (LVEF) of 65% (Figure 1A). The chest x-ray showed an enlarged heart, and the

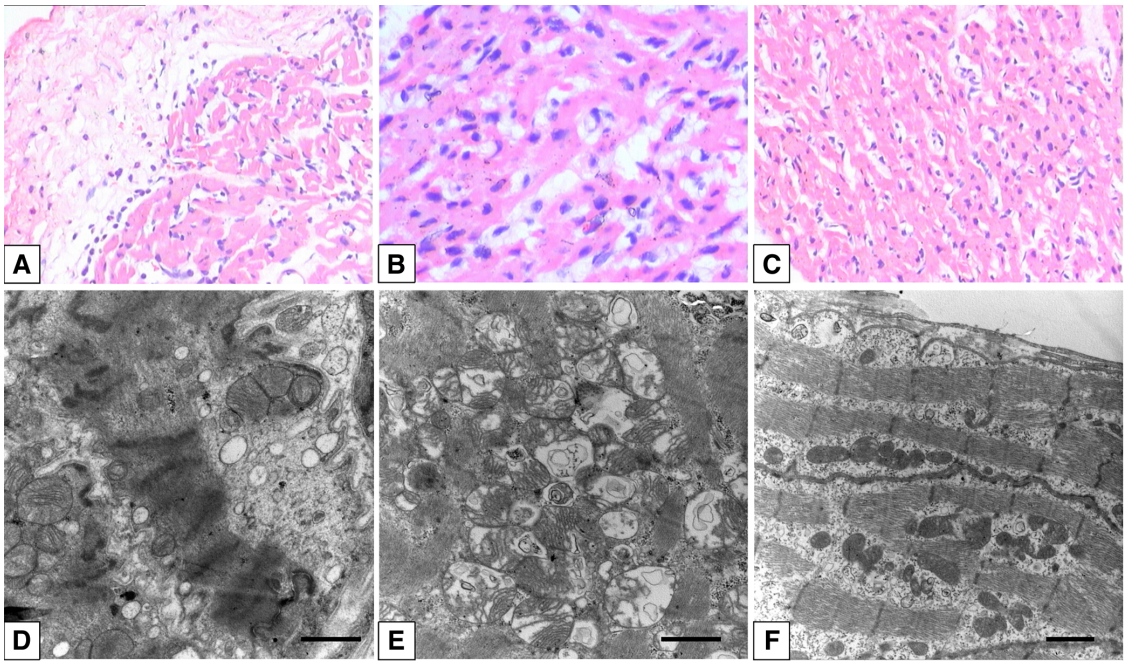

FIGURE 2
H&E staining showing the pathological changes in myocardial tissues of the right atrium (A), right ventricle (B), and left atrium (C). TEM shows damage to myofibrils and mitochondria in the right atrium (D), right ventricle (E), and left atrium (F). Scar bar: 1 μm. Magnification: ×25,000 and ×20,000. TEM, transmission electron microscopy.

cardiothoracic ratio (CTR) reached about 0.80 (Figure 1B). Electrocardiograph showed sinus tachycardia, right axis deviation, and right bundle branch block (Figure 1C). Computed tomography angiography indicated abnormalities similar to TTE. After extensive discussion, the initial diagnosis we considered was idiopathic dilatation of the right atrium (IDRA). The patient was discharged and followed up regularly every month in the clinic.

Clinical symptoms worsened during the patient's follow-up, such as feeding difficulty, shortness of breath, and growth retardation. Considering the possibility of compression caused by the enlarged RA and the risk of arrhythmias and thrombosis, we performed the surgical reduction of RA at 3 months with consent obtained from the parents. Transesophageal echocardiography and intraoperative findings confirmed the diagnosis of giant RA and ASD. Resection of extensive RA wall and atrioseptopexy were performed. At surgery, biopsies of the RA wall, right ventricle (RV) and left atrium (LA) revealed unspecific inflammatory cell infiltration and various degrees of focal myocardial hypertrophy and degeneration (Figures 2A–2C). Transmission electron microscopy (TEM) demonstrated damage to myofibrils and mitochondria, with a blurring of mitochondrial cristae (Figures 2D–2F). The patient recovered sufficiently post-operation. Repeat TTE showed a slightly enlarged RA, intact atrial septum, and normal LVEF (Figure 1D). Chest x-ray revealed a decreased CTR as 0.61 (Figure 1E). At 1-year follow-up, there was a progressive enlargement of the RA (Figures 3A,B), and the patient remained asymptomatic except for growth retardation. Unexpectedly, TTE

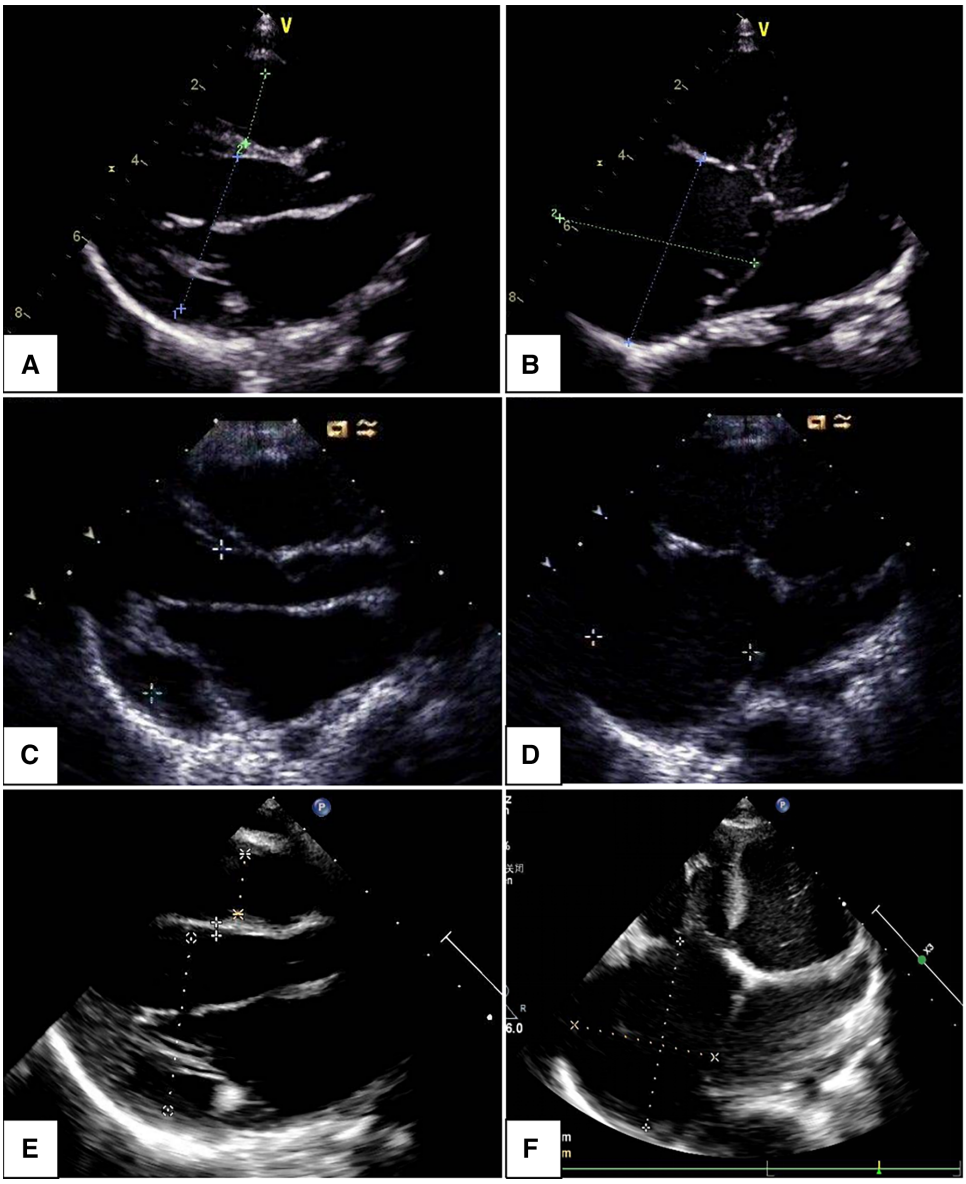

FIGURE 3
Changes in echocardiogram with follow-up time: parasternal long axis view indicated left ventricular end-diastolic dimension increased within 1, 2, and 5 years (A,C,E); apical four-chamber view showed an enlarged right atrium, the changes were not significant within 1, 2, and 5 years (B,D,F).

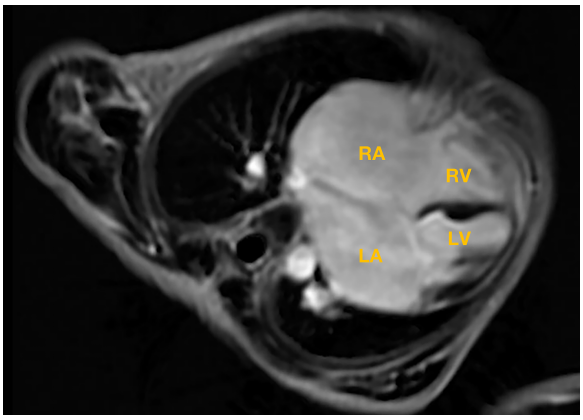

FIGURE 4
Cardiac magnetic resonance showed an enlarged right atrium, left atrium, and left ventricle; no typical manifestations of ventricular myocardial fibrosis were detected. RA, right atrium; LA, left atrium; RV, right ventricle; LV, left ventricle.

2 years after epilepsy surgery demonstrated an enlarged left ventricle (LV) with a left ventricular end-diastolic diameter (LVEDD) of 40 mm, a giant RA (52 mm × 39 mm), a normal PASP of 20 mmHg, and reduced LVEF of 55% (**Figures 3C,D**). Anti-heart failure therapy was administered, including captopril, diuretics, metoprolol, and acetylsalicylic acid. The patient had a good condition at 5 years post-operation. The size of the RA and LV did not change significantly, and the LVEF was about 50% (**Figures 3E,F**). Cardiac magnetic resonance (CMR) showed cardiomegaly at the expense of the right atrium with a decreased LVEF of 45% and no typical manifestations of ventricular myocardial fibrosis (**Figure 4**).

A genetic study showed a heterozygous missense *Pkp2* variant (c.2380T > G; OMIM: 609040; SCV 002576312) related to arrhythmogenic right ventricular cardiomyopathy (ARVC) (**Supplementary material S1**). Further Sanger sequencing indicated that his mother presented the same variant in *Pkp2*; the variant was classified as a variant of uncertain significance according to the American College of Medical Genetics and Genomics (ACMG) guidelines. Although his mother was asymptomatic, her echocardiography showed an enlarged LA and LV (LVEDD 55 mm), mild to moderate mitral regurgitation, and reduced LVEF (48%) without other cardiac structural defects. Then, the mother was diagnosed with DCM, and the diagnosis of familial DCM was established based on the patient's and his mother's features.

Discussion

Giant RA is considered to be of congenital origin in the absence of conditions such as congenital heart disease, pulmonary arterial hypertension, or tricuspid valve disease. IDRA is the most common disease mentioned in recent years due to a marked enlarged right atrium, a congenital anomaly with unknown etiology reported in fetuses, infants, children, and adults (2–4). Most patients are asymptomatic, and the most common symptoms are palpitations, dyspnea, and syncope caused by atrial tachyarrhythmias (2). The diagnosis of IDRA is usually established with fetal echocardiography and transthoracic echocardiography, and CT or CMR may be beneficial for a definitive diagnosis (2–4). According to prenatal and postnatal imaging features, IDRA should be considered as the primary disorder in our case. It is important to note that IDRA may be accompanied by congenital heart defects consisting of ASD (5). Our case also has a large secundum ASD, which could have contributed to the enlargement of RA. However, the recurrence of atrial enlargement after surgical repair of ASD suggests that the effect of ASD on giant RA is limited. The postnatal management of asymptomatic patients with IDRA remains controversial. Indications for surgical reduction of RA in children with IDRA have included right atrial thrombus and atrial arrhythmias, as well as others, such as progressive dilatation of the RA, concern about airway compression, and severe tricuspid insufficiency suspected as Ebstein's anomaly (6). So far, many studies suggest that the long-term outcomes of patients post-surgery are also contradictory. Although many cases demonstrate that surgery may indeed relieve symptoms associated with IDRA, some children still suffer the recurrent attack of giant RA (4, 6). Unfortunately, the situation of our case also suggests that the surgical indications for children with IDRA should be more strictly controlled.

In patients with cardiomyopathy, huge atria are commonly seen in restrictive cardiomyopathy (RCM), leading to a significant atrial pressure increase due to limited ventricular diastolic function and progressive atrial enlargement (7). The morphological definition of RCM is based on imaging features demonstrating non-hypertrophied, non-dilated ventricles, with marked bi-atrial enlargement (7). Nevertheless, the findings are not consistent with the characteristics of RCM in this case but with the features of DCM, such as LV dilation and poor cardiac systolic function.

Endomyocardial biopsy (EMB) is the gold standard method for diagnosing acute or chronic inflammatory heart diseases and enables the identification of the underlying etiology of cardiac inflammation (8, 9). Although there are no structural or functional changes in the heart chambers except RA in the early stage of the disease in our case, it is worth noting that the histological findings of damage to LA and RA were present. On the other hand, early involvement of the LV cannot be ruled out despite the absence of an LV biopsy. With the evidence of inflammatory cell infiltration, the probability of inflammatory disorders in the myocardium should still be considered (10).

The diagnosis of familial DCM is confirmed when two or more first-degree relatives have "idiopathic" DCM and/or unexplained death at a young age, and there could be an underlying genetic etiology (11). The pathogenesis of genetically mediated DCM has been associated with genes that encode components of the cytoskeleton, sarcomeric proteins, and nuclear envelope proteins (12). Recently, *Pkp2* gene, encoding components of desmosomes, has also been associated with different inherited cardiac conditions, including ARVC and Brugada syndrome (13). Few studies have suggested that *Pkp2* can also lead to DCM and left ventricular non-compaction (LVNC) (14). However, these associations do not prove causality between *Pkp2* and DCM in

our case, and further research should be conducted on the variant we detected.

In summary, DCM with a giant atrium as the first manifestation is an uncommon complex condition. Although the etiology remains unclear, a key factor should contribute to this unique phenotype. This case also reminds us of the importance of good follow-up of children with IDRA, including those after surgery. Further follow-up is needed for this case and his mother to evaluate the prognosis of this phenotype in DCM.

Data availability statement

The original contributions presented in the study are included in the article/Supplementary Material, further inquiries can be directed to the corresponding author.

Ethics statement

The studies involving human participants were reviewed and approved by the ethics committee of Qingdao Women and Children's Hospital. Written informed consent to participate in this study was provided by the participants' legal guardian/next of kin.

Author contributions

BW, GS, and ZB acquired the clinical data. QX performed the cardiac surgery. QZ performed the radiological analyses. BW and GS interpreted the data and drafted the manuscript. ZL contributed to the clinical design and study concept, and revised the manuscript. All authors contributed to the article and approved the submitted version.

Conflict of interest

The authors declare that the research was conducted in the absence of any commercial or financial relationships that could be construed as a potential conflict of interest.

Publisher's note

Supplementary material

The Supplementary Material for this article can be found online at: https://www.frontiersin.org/articles/10.3389/fcvm.2023.1083188/full#supplementary-material.

References

1. Price JF. Congestive heart failure in children. *Pediatr Rev.* (2019) 40:60–70. doi: 10.1542/pir.2016-0168

2. Hofmann SR, Heilmann A, Häusler HJ, Dähnert I, Kamin G, Lachmann R. Congenital idiopathic dilatation of the right atrium: antenatal appearance, postnatal management, long-term follow-up and possible pathomechanism. *Fetal Diagn Ther.* (2012) 32:256–61. doi: 10.1159/000338661

3. Wagner N, Kagan KO, Abele H, Hoopmann M, Kaulitz R, Hofbeck M. Fetal idiopathic dilatation of the right atrium. *Ultraschall Med.* (2011) 32:81–2. doi: 10.1055/s-0028-1109998

4. Walter C, Bartrons J, Gómez O, Caffarena JM, Carretero JM. Idiopathic dilatation of the right atrium: a not so benign entity. *Cardiol Young.* (2020) 30:919–22. doi: 10.1017/S1047951120001353

5. Venugopalan P, Jain R. Accidental detection of a giant right atrial aneurysm in an asymptomatic infant. *Acta Cardiol.* (2002) 57:125–7. doi: 10.2143/AC.57.2.2005384

6. Forbes K, Kantoch MJ, Divekar A, Ross D, Rebeyka IM. Management of infants with idiopathic dilatation of the right atrium and atrial tachycardia. *Pediatr Cardiol.* (2007) 28:289–96. doi: 10.1007/s00246-006-0012-5

7. Muchtar E, Blauwet LA, Gertz MA. Restrictive cardiomyopathy: genetics, pathogenesis, clinical manifestations, diagnosis, and therapy. *Circ Res.* (2017) 121:819–37. doi: 10.1161/CIRCRESAHA.117.310982

8. Tschöpe C, Ammirati E, Bozkurt B, Caforio ALP, Cooper LT, Felix SB, et al. Myocarditis and inflammatory cardiomyopathy: current evidence and future directions. *Nat Rev Cardiol.* (2021) 18:169–93. doi: 10.1038/s41569-020-00435-x

9. Li B, Lento PA, Pan S. Inflammatory cardiomyopathy: case-based review on clinical presentation, diagnosis, and management. *Cardiol Rev.* (2021) 29:230–7. doi: 10.1097/CRD.0000000000000369

10. Heymans S, Eriksson U, Lehtonen J, Cooper LT. The quest for new approaches in myocarditis and inflammatory cardiomyopathy. *J Am Coll Cardiol.* (2016) 68:2348–64. doi: 10.1016/j.jacc.2016.09.937

11. Peters S, Johnson R, Birch S, Zentner D, Hershberger RE, Fatkin D. Familial dilated cardiomyopathy. *Heart Lung Circ.* (2020) 29:566–74. doi: 10.1016/j.hlc.2019.11.018

12. Khan RS, Pahl E, Dellefave-Castillo L, Rychlik K, Ing A, Yap KL, et al. Genotype and cardiac outcomes in pediatric dilated cardiomyopathy. *J Am Heart Assoc.* (2022) 11:e022854. doi: 10.1161/JAHA.121.022854

13. Novelli V, Malkani K, Cerrone M. Pleiotropic phenotypes associated with *Pkp2* variants. *Front Cardiovasc Med.* (2018) 5:184. doi: 10.3389/fcvm.2018.00184

14. Ramond F, Janin A, Di Filippo S, Chanavat V, Chalabreysse L, Roux-Buisson N, et al. Homozygous *Pkp2* deletion associated with neonatal left ventricle noncompaction. *Clin Genet.* (2017) 91:126–30. doi: 10.1111/cge.12780

frontiers | Frontiers in Cardiovascular Medicine

TYPE Case Report
PUBLISHED 23 March 2023
DOI 10.3389/fcvm.2023.1093563

OPEN ACCESS

EDITED BY
Mingxing Xie,
Huazhong University of Science and Technology, China

REVIEWED BY
Do Tin,
Ho Chi Minh City Medicine and Pharmacy University, Vietnam
Xiangbin Pan,
Chinese Academy of Medical Sciences and Peking Union Medical College, China

*CORRESPONDENCE
Sisca Natalia Siagian
✉ sisca.ped.car@gmail.com

SPECIALTY SECTION
This article was submitted to Pediatric Cardiology, a section of the journal Frontiers in Cardiovascular Medicine

RECEIVED 09 November 2022
ACCEPTED 03 March 2023
PUBLISHED 23 March 2023

CITATION
Siagian SN, Prakoso R, Mendel B, Hazami Z, Putri VYS, Zulfahmi, Sakti DDA and Kuncoro AS (2023) Transesophageal echocardiography-guided percutaneous closure of multiple muscular ventricular septal defects with pulmonary hypertension using single device: A case report.
Front. Cardiovasc. Med. 10:1093563.
doi: 10.3389/fcvm.2023.1093563

Transesophageal echocardiography-guided percutaneous closure of multiple muscular ventricular septal defects with pulmonary hypertension using single device: A case report

Sisca Natalia Siagian[1]*, Radityo Prakoso[1], Brian Mendel[1,2], Zakky Hazami[3], Valerinna Yogibuana Swastika Putri[1], Zulfahmi[1], Damba Dwisepto Aulia Sakti[1] and Ario Soeryo Kuncoro[4]

[1]Department of Cardiology and Vascular Medicine, Division of Pediatric Cardiology and Congenital Heart Disease, National Cardiovascular Centre Harapan Kita, Universitas Indonesia, Jakarta, Indonesia, [2]Department of Cardiology and Vascular Medicine, Sultan Sulaiman Government Hospital, Serdang Bedagai, Indonesia, [3]Department of Cardiology and Vascular Medicine, National Cardiovascular Centre Harapan Kita, Universitas Indonesia, Jakarta, Indonesia, [4]Department of Cardiology and Vascular Medicine, Division of Non-Invasive Diagnostic and Cardiovacular Imaging, National Cardiovascular Centre Harapan Kita, Universitas Indonesia, Jakarta, Indonesia

Background: Surgery is typically used to correct challenging ventricular septal defects (VSDs), such as VSD with pulmonary hypertension and multiple defects. In this case report, we would like to highlight the feasibility of multiple defects VSD closure with single device percutaneously using zero-fluoroscopy technique.
Case presentation: A 7-year-old child was referred with the main symptom of shortness of breath. She started experiencing repeated respiratory tract infections, feeding issues, and failure to thrive at the age of six months. Her body weight was only 18 kg. TEE revealed several muscular VSD with 2–3 mm and 12 mm diameters, 3 mm spacing between VSD, L to R shunt, AR (-), and TR mild with septal leaflet tricuspid prolapse. Following right heart catheterization (Qp:Qs 3.5, PVRi 5.23WUmsq, PVR 4.55 WU, PVR/SVR 0.16), we made the decision to correct the defect using an Amplatzer Septal Occluder (AGA) No. 16 mm using transjugular method. Full device deployment was successfully performed with several episodes of PVC storm and severe bradycardia. One and a half years after the procedure, her TVG dropped to only 18 mmHg, her visible indicators of PH subsided, and the PA dilator treatment was discontinued. Her body weight had increased to 28 kg, and she had no complaints.
Conclusions: Our experience demonstrated that percutaneous closure of multiple VSD with a single device is possible, even with pulmonary hypertension.

KEYWORDS

echocardiography-guided, muscular VSD, pulmonary hypertension, single device, transjugular

1. Introduction

Surgery is typically used to correct ventricular septal defects (VSDs), particularly in challenging cases like those involving individuals with pulmonary hypertension and multiple defects. In recent years, muscular VSD found in locations that are challenging for surgeons to reach are often treated with transcatheter percutaneous closure. However, multiple defects are often repaired using multiple devices and are typically guided by fluoroscopy (1, 2). Eliminating radiation exposure during procedure is crucial since fluoroscopy effects are cumulative and raise serious issues, especially in the younger population (3). In this case report, we would like to highlight the feasibility of multiple defects VSD closure with single device using zero-fluoroscopy technique.

2. Case description

A 7-year-old child was referred with the main symptom of shortness of breath one year prior to admission. She started experiencing repeated respiratory tract infections, feeding issues, and failure to thrive at the age of six months, although she was not bluish. She received a pulmonary TB diagnosis and had 9 months of therapy. She continued to report having dyspnea, and an echocardiogram showed that she had multiple muscular VSDs with a left-to-right shunt and pulmonary hypertension with a total diameter of 1–1.4 cm. The results of a physical examination revealed a heart rate of 115 beats per minute, a respiratory rate of 21 breaths per minute, and a room air oxygen saturation of 98%. Her height was 122 cm, and her body weight was 18 kg. Regular first and second heart sounds were audible during auscultation, as well as a loud intensity holosystolic murmur grade 3/6 in the lower left sternal border. The patient had a D-shaped LV and severe PH with a TVG of 69 mmHg and a transVSD gradient of 15 mmHg.

We chose to use the jugular vein approach to accomplish percutaneous transcatheter VSD closure. Preprocedural 98%; patient underwent general anesthesia. The patient was intubated using ETT No. 5.5% and 30% FiO2. 100% post-intubation saturation TEE revealed several muscular VSD with 2–3 mm and 12 mm diameters, 3 mm spacing between VSD, L to R shunt, AR (-), and TR mild with septal leaflet tricuspid prolapse. (**Figure 1A**). The decision was made to catheterize the right heart. The right femoral artery of the patient was punctured, and the patient then inserted a 4F sheath, heparin 1.000 IU, and MP sidehole 5F catheter. The right jugular vein was punctured; the MP sidehole was 5F and the sheath 6F was used. Following right cardiac catheterization (Qp:Qs 3.5, PVRi 5.23WUmsq, PVR 4.55 WU, PVR/SVR 0.16), we made the decision to correct the defect using an Amplatzer Septal Occluder (AGA) No. 16 mm using transjugular method. Through the muscular VSD, a 5F MP sidehole diagnostic catheter was introduced under the direction of transesophageal echocardiography (TEE). A 5F MP sidehole diagnostic catheter was introduced under the direction of transesophageal echocardiography (TEE) from SVC, RA, RV and LV through muscular VSD (**Figures 1B–D**). Using 0.035″ Amplatzer stiff wire, we change to 8F delivery sheath (**Figure 1E**). Full device deployment was successfully performed with several episodes of PVC storm and severe bradycardia (**Figures 1F–H**). Echocardiography evaluation showed no complications before, during, and after deployment of the occluder device (**Figure 1H**). Her symptoms and appetite steadily improved a week after the operation. She was able to engage in moderately intensive activities three months after the treatment without experiencing any discomfort.

Her TVG was 60 mmHg and 50 mmHg six months and one year after the procedure, respectively, with still visible evidence of PH. However, 1.5 years after the procedure, her TVG dropped to only 18 mmHg, her visible indicators of PH subsided, and the PA dilator treatment was discontinued. Her body weight had increased to 28 kg, and she had no complaints. The patient's ECG showed sinus rhythm during our most recent clinic visit.

3. Discussions

3.1. Management of ventricular septal defect with pulmonary hypertension

The care of patients with PAH-CHD depends heavily on behavioral change and identification of relevant risk factors. According to knowledge provided, patients with PAH-CHD who are functional class III begin treatment with the endothelin receptor antagonist bosentan (class I, level of evidence B). In contrast to placebo, bosentan significantly improved exercise capacity, haemodynamics, and functional class in the BREATHE-5 (Bosentan Randomised Trial of Endothelin Antagonist-5) trial and its long-term open label extension research, regardless of the location of septal defects (4–6).

In patients with PAH-CHD, sildenafil therapy has been demonstrated to enhance exercise capacity, Borg dyspnoea score, functional class, quality of life, and hemodynamics. When symptoms persisted despite taking the maximum amount of medication, as we did in this patient, right cardiac catheterization should be carried out to determine whether shunt closure is appropriate (4, 6).

The ESC (European Society of Cardiology) 2022 guidelines recommend shunt closure in individuals with a pulmonary-systemic flow ratio greater than 1.5:1 based on estimated pulmonary vascular resistance. When PVR is less than 3 WU and when PVR is between 3 and 5 WU, VSD closure is advised. After thorough assessment in a specialized facility, shunt closure may be taken into consideration in patients with PVR > 5 WU (6). As a result, we chose to treat on this patient's VSD.

3.2. Strategy for multiple ventricular septal defect closure

The apical, central, or outflow regions of the interventricular septum are the most common locations for muscular ventricular septal defects (VSDs). Up to 20% of VSDs in babies are muscular VSDs, which can have several occurrences and take on a "Swiss cheese" appearance (1, 2, 7). The VSD in our instance

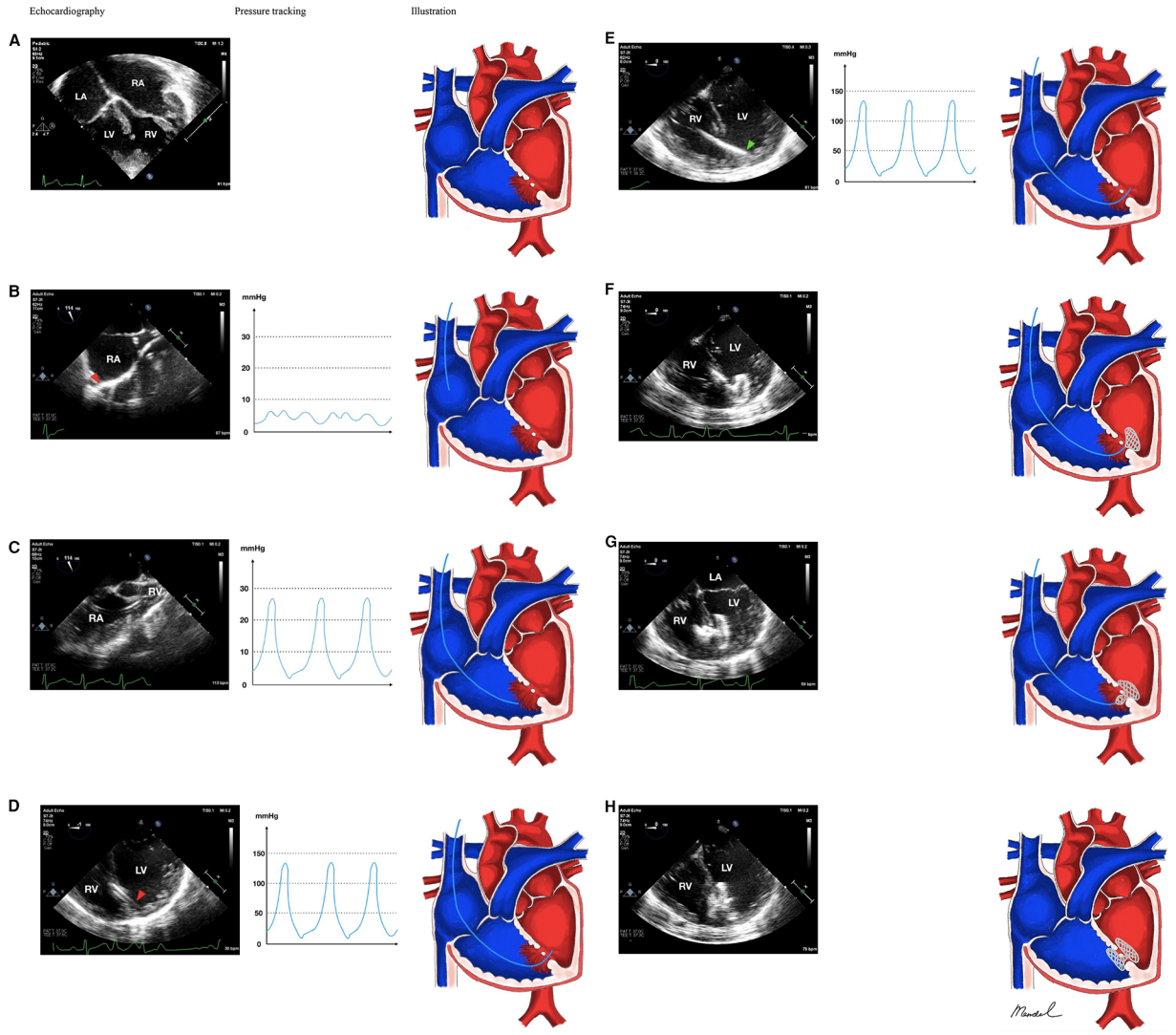

FIGURE 1
Antegrade jugular vein approach in multiple-defect muscular VSD closure with pulmonary hypertension. (**A**) Multiple VSD. (**B**) 5F sidehole Multipurpose catheter was directed from SVC towards RA. (**C**) Catheter was then directed towards RV. (**D**) The catheter successfully crossed from RV into LV. (**E**) With the assistance of 0.035" Amplatzer stiff wire, the catheter was changed with 8F delivery sheath. (**F**) The Amplatzer device occluder (AGA) No 16 mm was delivered and one of the disc was deployed in the LV side, (**G**) and RV side. (**H**) Device stowed in place; *Red arrowhead showed the position of the catheter, green arrowhead showed the position of the delivery sheath. Notes: VSD, ventricular septal defect; SVC, superior vena cava; RV, right ventricle; LV, left ventricle; RA, right atrium; LA, left atrium.*

was situated mid-apical. In our institution, surgery is typically used as a method of multiple VSD defect repair. However, it was determined during the surgical discussion that the defect could be closed percutaneously. We are only authorized to use one device per interventional operation at our hospital due to legislation. There is no agreement on the maximum diameter at which a single device could close numerous VSD faults at the moment. For atrial septal defects, If the distance between defects is smaller than 0.5 or 0.7, only one device needs to be used (2).

As the abnormalities in the IVS are more posteriorly positioned, we attempted to operate through the jugular vein route to reduce curvature of the delivery sheath and eliminate resistance across the septum. This patient's jugular vein technique also provided a more direct route to the problem. It is also possible to approach the deficiency from the transfemoral side, although this method carries a higher risk because it is more complicated, sinuous, and difficult to traverse to the mid-apical position of the defect.

Delivered through the sheath, the multipurpose catheter and guidewire was then moved to the right ventricle *via* the tricuspid valve and readjusted with its top facing the VSD. The guidewire was gently moved and adjusted to the left ventricle *via* the VSD utilizing transesophageal echocardiography (TEE)-guided only. Since the patient was young and just 18 kg in weight, the 5F sheath expander needed to be removed gradually while the sheath was inserted into the conduit to prevent heart injury. To prevent harming nearby intracardiac structures, the sheath shouldn't be put straight and should instead be inserted about 3 to 5 cm deep.

Patients with perimembranous VSD utilize a different type of closure device than those with muscular VSD. For this patient, we utilized the Amplatzer Septal Occluder (AGA) No. 16 mm device because a sufficient size for a muscular VSD device was not available at the time of the procedure. We also chose Amplatzer Septal Occluder (AGA) since the retention disc is larger and could cover both defects with a 3 mm gap. We chose device no. 16 mm since there were two defects, and we expect that the device will cover both defects as well as the gap between them.

It is challenging to complete the closure process for a patient who has a defect adjacent to the apex since the insertion of the occluder necessitates the catheter bevel. Hemolysis that is brief and self-contained has been demonstrated by (8) Santos et al. (2018). Both perimembranous and muscular VSD that were treated with Amplatzer Septal Occluder (AGA) had a lower risk of total AV block (9); however, in our instance, some PVC storms and severe bradycardia transiently occurred after the defect closure. We suspected that several PVC storms and bradycardia episodes in our patient were caused by pulmonary hypertension rather than by the device. As we know, the most common arrhythmia complications caused by device closure are AV block and bundle branch block. We also saw no conduction abnormalities until the current follow-up, so we believe the issues were not caused by the device.

Patients with numerous VSDs frequently experience residual shunt because a proper occluder size is necessary to completely cover the defect. As a result, the type and placement of the occlusion should be carefully chosen based on the specific circumstances. After the treatment, our patient, however, displayed no symptoms of a residual shunt. Our post-procedural echocardiogram also revealed that the mitral and tricuspid valves were not damaged, as predicted when we selected and estimated the distance between the device, and the interventricular septum that would be covered by the device.

3.3. Feasibility of transesophageal echocardiography-guided closure

Even though ALARA (as low as reasonably achievable) principle is used, it would be preferable to completely eliminate radiation exposure risks for both the operators and the patient. In our facility, the technique would be carried out initially without any fluoroscopy, or if the echocardiography window was insufficient intraprocedurally, the technique would be converted to the standardized fluoroscopy process (1, 3, 10, 11).

As far as we know, fluoroscopy may cause certain long-term, delayed negative effects, particularly in children and newborns. Over the years, there have been more reports of skin injuries, such as redness, necrosis, and ulceration, which can be painful and disabling. There has also been an increase in the likelihood of developing neoplasms, radiation-induced cataracts, and hair loss (3).

In this instance, the finding of the VSD from the jugular approach is simple and is followed by a cross to the LV to close the defect after the patient has been intubated and is being seen with TEE. In our scenario, a fluoroscopy-guided operation is also possible, but since there are two defects, a TEE could provide a superior image. With TEE, we could instantly see the position and visualize it. Therefore, if there were multiple defects, we would prefer to advise using TEE directed. The shape and diameter of the VSD may be estimated with precision using TEE. When employing TEE, the danger of oesophageal trauma and erosion should be taken into account (1, 3, 10, 11).

4. Conclusions

Our experience demonstrated that percutaneous closure with a single device is possible to carry out successfully even in multiple VSD defects accompanied by pulmonary hypertension. However, the cardiac team should think about a more direct strategy to lower the danger and they should pick the patient carefully in which patient with multiple defects should be done percutaneously or surgically.

Data availability statement

The original contributions presented in the study are included in the article/Supplementary Material, further inquiries can be directed to the corresponding author/s.

Ethics statement

Ethical review and approval was not required for the study on human participants in accordance with the local legislation and institutional requirements. Written informed consent to participate in this study was provided by the participants' legal guardian/next of kin. Written informed consent was obtained from the individual(s), and minor(s)' legal guardian/next of kin, for the publication of any potentially identifiable images or data included in this article. Written informed consent was obtained from the participant/patient(s) for the publication of this case report.

Author contributions

SNS and RP: conceived the original idea of the manuscript, and all authors discussed and agreed with the idea of the paper. BM, ZH, VYSP and Z: contributed in collecting the patient data and writing the main text of the paper. The manuscript was proofread and accepted by all authors. All authors contributed to the article and approved the submitted version.

Acknowledgments

We would like to thank those who have supported us in the making of this study. We are especially grateful to the Department of Cardiology and Vascular Medicine, Faculty of Medicine Universitas

Indonesia, for their guidance and assistance in teaching the authors about research methodology and for proof-reading this article.

Conflict of interest

The authors declare that the research was conducted in the absence of any commercial or financial relationships that could be construed as a potential conflict of interest.

Publisher's note

References

1. Mendel B, Laurentius A, Ulfiarakhma D, Prakoso R. Safety and feasibility of transesophageal echocardiography in comparison to transthoracic echocardiography-guided ventricular septal defect percutaneous closure: an evidence-based case report. *World Heart J.* (2020) 12:199–207.

2. Felice H, Chandran S, Bhamra-Ariza P, Brecker H Transcatheter closure of multiple defects of the atrial septum: technique and follow-up. *Int J Clin Med.* (2015) 06(09):591–6. doi: 10.4236/ijcm.2015.69079

3. Siagian SN, Prakoso R, Putra BE, Kurniawati Y, Lelya O, Sembiring AA, et al. Echocardiography-guided percutaneous patent ductus arteriosus closure: 1-year single center experience in Indonesia. *Front Cardiovasc Med.* (2022) 9:2–7. doi: 10.3389/fcvm.2022.885140

4. D'Alto M, Mahadevan VS. Pulmonary arterial hypertension associated with congenital heart disease,". *Eur Respir Rev.* (2012) 21(126):328–37. doi: 10.1183/09059180.00004712

5. Mendel B, Christianto C, Angellia P, Holiyono I, Prakoso R, Siagian SN. Reversed potts shunt outcome in suprasystemic pulmonary arterial hypertension: a systematic review and meta-analysis. *Curr Cardiol Rev.* (2022) 18(6):95–103. doi: 10.2174/1573403X18666220509203335

6. Humbert M, Kovacs G, Hoeper MM, Badagliacca R, Berger RM, Brida M, et al. ESC/ERS guidelines for the diagnosis and treatment of pulmonary hypertension. *Eur Heart J.* (2022) 43(38):3618–731. doi: 10.1093/eurheartj/ehac237

7. Wang S, Ouyang W, Liu Y, Zhang F, Guo G, Zhao G, et al. Transcatheter perimembranous ventricular septal defect closure under transthoracic echocardiographic guidance without fluoroscopy. *J Thorac Dis.* (2018) 10 (9):5222–31. doi: 10.21037/jtd.2018.08.03

8. Santos RAP, Guedes H, Marques L, Lourenco C, Silva JC, Pinot P. Transcatheter closure of a traumatic VSD with an ASD occluder. *Arq Bras Cardiol.* (2018) 111(2):223–5.

9. Carminati M, Butera G, Chessa M, Drago M, Negura D, Piazza L. Transcatheter closure of congenital ventricular septal defect with amplatzer septal occluders. *Am J Cardiol.* (2005) 96(12A):52l–8l. doi: 10.1016/j.amjcard.2005.09.068

10. Bu H, Yang Y, Wu Q, Jin W, Zhao T. Echocardiography-guided percutaneous closure of perimembranous ventricular septal defects without arterial access and fluoroscopy. *BMC Pediatr.* (2019) 19:302. doi: 10.1186/s12887-019-1687-0

11. Mendel B, Faris Amin B, Prakoso R. Potency of non-fluoroscopy guided patent ductus arteriosus closure: a case report. *SN Comprehensive Clin Med.* (2021) 3 (12):2665–72. doi: 10.1007/s42399-021-01062-4

Frontiers in
Cardiovascular Medicine

Innovations and improvements in cardiovascular treatment and practice

Focuses on research that challenges the status quo of cardiovascular care, or facilitates the translation of advances into new therapies and diagnostic tools.

Discover the latest Research Topics

See more →

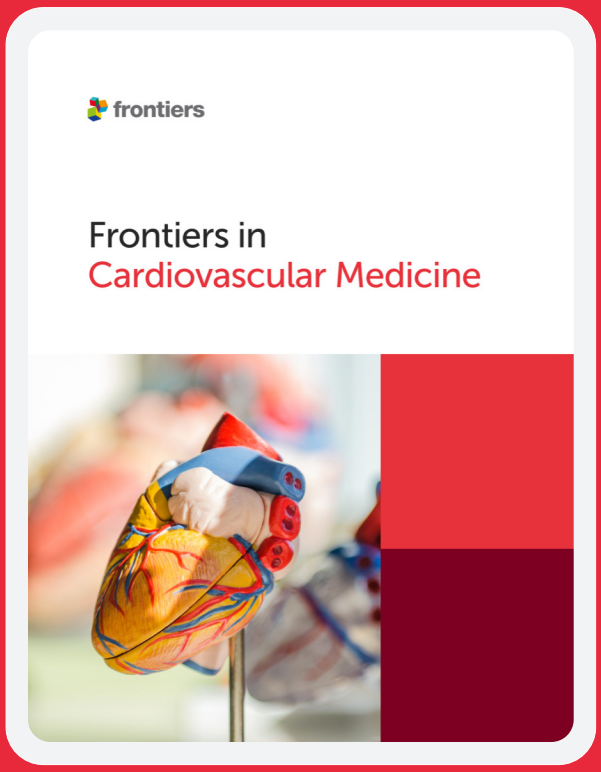

Frontiers

Avenue du Tribunal-Fédéral 34
1005 Lausanne, Switzerland
frontiersin.org

Contact us

+41 (0)21 510 17 00
frontiersin.org/about/contact